LEABHARLANN CHOLÁISTE NA TRÍONÓIDE, BAILE ÁTHA CLIATH | TRINITY COLLEGE LIBRARY DUBLIN
Ollscoil Átha Cliath | The University of Dublin

Terms and Conditions of Use of Digitised Theses from Trinity College Library Dublin

Copyright statement

All material supplied by Trinity College Library is protected by copyright (under the Copyright and Related Rights Act, 2000 as amended) and other relevant Intellectual Property Rights. By accessing and using a Digitised Thesis from Trinity College Library you acknowledge that all Intellectual Property Rights in any Works supplied are the sole and exclusive property of the copyright and/or other IPR holder. Specific copyright holders may not be explicitly identified. Use of materials from other sources within a thesis should not be construed as a claim over them.

A non-exclusive, non-transferable licence is hereby granted to those using or reproducing, in whole or in part, the material for valid purposes, providing the copyright owners are acknowledged using the normal conventions. Where specific permission to use material is required, this is identified and such permission must be sought from the copyright holder or agency cited.

Liability statement

By using a Digitised Thesis, I accept that Trinity College Dublin bears no legal responsibility for the accuracy, legality or comprehensiveness of materials contained within the thesis, and that Trinity College Dublin accepts no liability for indirect, consequential, or incidental, damages or losses arising from use of the thesis for whatever reason. Information located in a thesis may be subject to specific use constraints, details of which may not be explicitly described. It is the responsibility of potential and actual users to be aware of such constraints and to abide by them. By making use of material from a digitised thesis, you accept these copyright and disclaimer provisions. Where it is brought to the attention of Trinity College Library that there may be a breach of copyright or other restraint, it is the policy to withdraw or take down access to a thesis while the issue is being resolved.

Access Agreement

By using a Digitised Thesis from Trinity College Library you are bound by the following Terms & Conditions. Please read them carefully.

I have read and I understand the following statement: All material supplied via a Digitised Thesis from Trinity College Library is protected by copyright and other intellectual property rights, and duplication or sale of all or part of any of a thesis is not permitted, except that material may be duplicated by you for your research use or for educational purposes in electronic or print form providing the copyright owners are acknowledged using the normal conventions. You must obtain permission for any other use. Electronic or print copies may not be offered, whether for sale or otherwise to anyone. This copy has been supplied on the understanding that it is copyright material and that no quotation from the thesis may be published without proper acknowledgement.

Ursodeoxycholic Acid – A Molecular Modulator of the Inflammation-Carcinoma Sequence in the Oesophagus?

A thesis submitted for the degree of Doctor of Philosophy (PhD)

by

David Prichard

University of Dublin, Trinity College

2011

Co-Supervisors:

Dr Aideen Long,

Department of Clinical Medicine,

Trinity College Dublin,

Dublin 2.

Prof. Dermot Kelleher,

Department of Clinical Medicine,

Trinity College Dublin,

Dublin 2.

TRINITY COLLEGE
2 5 SEP 2012
LIBRARY DUBLIN

Thesis 9617

I. Declaration

I declare that this thesis has not been submitted as an exercise for a degree at this or any other university and it is entirely my own work.

I agree to deposit this thesis in the University's open access institutional repository or allow the library to do so on my behalf, subject to Irish Copyright Legislation and Trinity College Library conditions of use and acknowledgement.

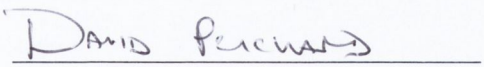

David Prichard

October 2011

II. Acknowledgements

As the end of this PhD approaches, there are many people I wish to thank.

Aideen Long and Dermot Kelleher (My supervisors) are at the top of the list. I have to thank Aideen for being of constant support for three years. Her friendly open door policy made the day to day work easier. Her positivity saved me from a nervous breakdown more than once. Dermot Kelleher recruited me for this research, opening the door for me to a world of research. For that I have to thank him. However, when he told me that it was the hardest thing that I would ever do, he undersold it; for that, I might not forgive him!

Every experiment in this thesis has been helped by the people I worked with in the lab and each one deserves a big Thank You. Anne-Marie Byrne (aka "Golgi") was my mentor for three years. She taught me the basics of science, educated me in scientific methodology and critiqued every experiment I performed. As the PhD progressed and the stress got worse, she was always there with encouragement and a smile. Shane Duggan gets a thank you for being a great source of help whenever anything to do with the microarray went wrong. That was frequently and took a lot of his time. Mike Freeley (aka "The Western God") was a help every single day. I have never met anybody so dedicated to his work. Any questions regarding experimental technique were answered with patience and tolerance. On the days I had to run out of the lab, Mike was always there to help finish an experiment. Every bad day was made easier by Mike's dreadful sense of humour. Dara Dunican (aka "Mr Science") taught me so much about science. Every idea I had was improved by talking to Dara. No matter how much I read about bile acids, the oesophagus, cell adhesion or nuclear steroid receptors, Dara knew more and steered me in the right direction. No matter how much I learnt about experimental techniques, Dara refined my knowledge and improved my understanding. Ruchika Sharma (aka "The Bile Acid Queen") worked on UDCA with me. As she finished her PhD (in depression) and I started mine, she helped me understand what was important to know about bile acids and what wasn't. Hopefully I helped her in return. Jennifer Conroy deserves special thanks for putting up with me when I was trying to break her precious confocal microscope. Jen's empathy as we finished our PhDs together made finishing this tome easier! If only I had been able to diagnose her "medical problems" as well as she diagnosed my microscopy issues! Seonadh O'Leary has to get a thank you for stealing my chair and never letting me use her equipment! Despite that, she always made me smile!

Everybody else in the lab pitched in, helped out and made me laugh. Thank you Sarah Mullins, Fran Quilty, Cormac McKenna, Denise Triglia, Seow-Theng Ong, Murat Kirca, Finbar MacCarthy,

Antje Hoff, Emily Bennett, Sinead Phipps, Anthony Davies, Ann Atzberger and everybody else from whom I begged, borrowed, stole, grovelled or harassed during the past three years.

Special thanks have to go to my family who have put up with my constant absence and neglect during the last three years.

Niamh Collins helped me through a large part of this research. For so much of the time she made the world a better place by just being part of my life. I know that she empathises with the misery involved in, and challenge of undertaking, a PhD. For the help she gave me I thank her.

Finally, I have to thank Molecular Medicine Ireland for my introduction to science. Their recruiting process was a challenge, their education was exceptional and their tolerance of my late replies to their emails was appreciated.

To absolutely everybody who helped and taught me I say thank you.

III. Abstract

Background

Gastro-oesophageal reflux disease (GORD) is a prevalent disease, affecting up to 20% of the western population. In up to 10% of these patients Barrett's Oesophagus (BO) will exist. This metaplastic epithelium carries a risk of developing into oesophageal adenocarcinoma (OAC). BO and OAC have a negligible hereditary component; they are environmental diseases with GORD representing the most significant risk factor for both. The refluxate of GORD is predominantly comprised of acid and bile acids (BAs). The acid component of GORD has been successfully targeted pharmacologically. Despite this, the incidence of BO and OAC has risen steadily over the last three decades. BAs remain the untreated component. Research has shown that BAs are pro-inflammatory, pro-apoptotic and carcinogenic molecules. Increasing exposure of the oesophagus to BAs correlates with an increasing risk of erosive oesophagitis, BO and OAC. Epidemiological studies have confirmed BAs as carcinogens in the oesophagus. Thus, there is a need for a safe and effective therapeutic which targets BA-induced toxicity in the oesophagus.

Ursodeoxycholic acid (UDCA) has been shown to modulate the inflammatory, apoptotic and carcinogenic effects of hydrophobic BAs such as deoxycholic acid (DCA). UDCA can attenuate the pro-inflammatory and pro-apoptotic mechanisms (COX-2, ROS, etc) induced by BAs. UDCA has also been demonstrated to activate the glucocorticoid receptor (GR) – a potent anti-inflammatory transcription factor. The UDCA-GR interaction appears to induce *trans*-repression without significantly inducing *trans*-activation. GR mediated t*rans*-repression inhibits the functions of pro-inflammatory transcription factors such as NF-κB and AP-1. *Trans*-activation is thought to be responsible for the undesirable effects associated with the GR.

Specific Objectives

The objective of this PhD was to investigate whether UDCA may be of therapeutic use in the modulation of BA-induced inflammation and apoptosis and in the oesophagus.

Results

Inflammation and apoptosis induced by BAs are activated through similar pathways. Modulation of BA-induced apoptosis may therefore also reflect modulation of inflammation in normal squamous epithelium and *vice versa*. We demonstrate that UDCA exerts less cellular toxicity than DCA in the HET-1A cell line representing normal squamous epithelium. DCA induces both apoptosis and autophagy. Pre-treatment, but not co-treatment, with UDCA reduces levels of DCA-induced apoptosis (levels of cleaved PARP and mitochondrial depolarisation), but does not reduce the total amount of DCA-induced cell death (as determined by an MTT and a nuclear count assay). Our

findings are most consistent with UDCA pre-treatment reducing levels of apoptosis but at the expense of increasing levels of necrosis.

From data identified in research regarding the effect of DCA and UDCA on cell death, we identified that DCA induces a loss of adhesion in the HET-1A cell line. We confirmed that DCA induces a reversible loss of adherence in a dose dependent fashion. Loss of adhesion appeared predominantly specific for the extracellular matrix protein vitronectin. Consistent with this finding, a reversible reduction in the surface expression of integrin α_V (ITGAV) was induced by DCA. This is mediated through impaired endocytic recycling. These findings are mediated discreetly of apoptosis. Confirming the *in vivo* validity of these findings, the fluorescent intensity of ITGAV at the inter-cellular junctions of explanted oesophageal tissue was reduced by exposure to DCA. QH cells (representing BO) resisted the effect of DCA on cell detachment and ITGAV. UDCA neither reduced nor enhanced the effects of DCA on cell adhesion or ITGAV expression, suggesting that it does not modulate this pathway. These findings suggest a new mechanism through which BAs can increase the risk of erosive oesophagitis and BO in GORD patients. They also suggest a previously unidentified pathway which could be targeted in a prophylactic or therapeutic fashion.

In the final part of this research, we investigated the gene role of UDCA and the GR in modulating oesophageal inflammation. GORD-induced chronic inflammation is a crucial driver of oesophageal carcinogenesis. We demonstrate that the GR is expressed throughout the normal-BO-OAC sequence. However, the GR is expressed at a much greater level in squamous epithelium than in BO. UDCA induces nuclear translocation of the GR in oesophageal cell lines without inducing *trans*-activation. Using micro-array based experiments we demonstrate that UDCA induces a gene expression profile discrete from both DCA and Dexamethasone (Dex), but which also exhibits similarities to both. This suggests that this hydrophilic BA has both properties to activate the GR as well as exerting effects similar to the hydrophobic DCA. As UDCA shares structural similarities to DCA and Dex, it may exert structure-function properties of both. The genes most up-regulated by UDCA were those associated with ER stress suggesting that this BA has the potential to be pro-apoptotic in the oesophageal cell line HET-1A. Yet the magnitude of the ER stress gene induction was significantly lower than that induced by DCA. These findings suggest that UDCA not only exerts less cytotoxicity than DCA, but also has the potential to modulate the GR in the HET-1A cell line.

Conclusion

UDCA pre-treatment reduces apoptosis, but not total cell death, induced by DCA in the HET-1A cell line. UDCA can modulate the GR in oesophageal cell lines. The expression of this transcription factor in limited in the oesophagus, potentially allowing preferential targeting of squamous epithelium above that of BO. UDCA treatment induces a gene expression profile which

has similarities to both DCA and Dex. Therefore, UDCA administration could reduce inflammation in the oesophagus through displacement of hydrophobic BAs and potentially through activation of the GR. The novel finding that DCA mediates a reduction in adhesion in oesophageal cells suggests a new pathway which could be targeted therapeutically to treat GORD.

IV. Contents

I. Declaration ..... **i**

II. Acknowledgements ..... **iii**

III. Abstract ..... **v**

IV. Contents ..... **ix**

V. Figures ..... **xv**

VI. Tables ..... **xxi**

VII. Abbreviations ..... **xxiii**

Title: Ursodeoxycholic Acid – A Molecular Modulator of the Inflammation-Carcinoma Sequence in the Oesophagus? **1**

1. Introduction **3**

1.1. Summary of Research Background 5

1.2. Gastro-Oesophageal Reflux Disease, Barrett's Oesophagus and Oesophageal Adenocarcinoma 7

1.2.1. Gastro-Oesophageal Reflux Disease 7

1.2.2. Barrett's Oesophagus 8

1.2.3. Oesophageal Adenocarcinoma 9

1.3. The Pathology of Gastro-Oesophageal Reflux Disease 10

1.3.1. The Pathogenesis of GORD 10

1.3.2. Duodenogastro-Oesophageal Reflux 12

1.4. Molecular Aspects of Bile Acids and Bile Acid Pathology 15

1.4.1. Bile Salt Physiology 15

1.4.2. The Physico-Chemical Properties of Bile Acids 15

1.4.3. Cell Death; Apoptosis, Necrosis and Autophagy 18

1.4.4. Bile Acid Induced Inflammation and Pathology in the Oesophagus 21

1.5. The Protective Role of Ursodeoxycholic Acid 24

1.6. Summary 28

1.7. Research Aims 30

2. Ursodeoxycholic Acid Reduces Deoxycholic Acid Induced Apoptosis, but not Total Cell Death, in an Oesophageal Cell Line **33**

2.1. Introduction 35

2.1.1. Bile Acids Induce Apoptosis Through Multiple Mechanisms. 35

2.1.2. UDCA Modulates the Apoptotic Pathways Activated by Hydrophobic Bile Acids *In Vitro* 36
2.1.3. UDCA Activates Pro-Survival Signalling Which Overcome Pro-Apoptotic Signals 40
2.1.4. UDCA Exerts an Anti-Apoptotic Effect through the Glucocorticoid Receptor 42
2.1.5. Summary 42
2.2. Aims 44
2.3. Methods 45
2.3.1. Cell Lines, Culture and the Quantification of Cell Concentrations 45
2.3.2. Proliferation and Viability Assays 45
2.3.3. Cell Cycle Analysis 53
2.3.4. Flow Cytometric Determination of Mitochondrial Membrane Potential 54
2.3.5. Flow cytometric Analysis of Quantity and Mechanism of Cell Death. 55
2.3.6. Analysis of Poly ADP Ribose Polymerase (PARP) and LC3 cleavage by Western blotting 57
2.3.7. Determination of Oesophageal Explant Viability by Lactate Dehydrogenase Estimation 58
2.3.8. Statistics 59
2.4. Results 61
2.4.1. Ursodeoxycholic Acid Reduces the Toxic Effects of Deoxycholic Acid in HUH-7 Cells Consistent with the Published Scientific Literature. 61
2.4.2. DCA and UDCA Reduce Proliferation in the HET-1A Cell Line Without Altering Cell Cycle Progression 65
2.4.3. The Lethal Effects of the Hydrophobic Bile Acid DCA are not Attenuated by Pre-Treatment or Co-Treatment with the Hydrophilic BA UDCA in the Oesophageal Cell Line HET-1A 69
2.4.4. UDCA Pre-Treatment, but not Co-Treatment, Reduces the Levels of Cleaved Poly-ADP-Ribose Polymerase (PARP) 77
2.4.5. UDCA Pre-Treatment does not Reduce the Magnitude of Mitochondrial Depolarisation Induced by DCA. 79
2.4.6. UDCA does not Reduce the Magnitude of Apoptosis Induced by DCA Exposure 81
2.4.7. DCA Stimulation Increases Autophagy in HET-1A Cells 89
2.4.8. 300μM Bile Acids have no Toxic Effect on Biopsy Explants of Healthy Oesophageal Tissue. 91
2.5. Discussion 93
2.6. Conclusions 96

3. Deoxycholic Acid Modulates Cell Adhesion in a Mechanism Discreet From Apoptosis 97

3.1. Introduction 99
3.1.1. Cell Adhesion 99
3.1.2. Integrin-Mediated Cell Attachment and Pro-Survival Signalling 99
3.1.3. Integrin-Mediated Cell Detachment 100
3.1.4. The Endocytic Recycling Pathway 101

3.1.5. Integrin Expression within the Oesophagus 102
3.2. Aims 103
3.3. Methods 104
3.3.1. Cell Lines and Culture 104
3.3.2. Time lapse Live Cell Light Microscopy 104
3.3.3. Adherence Assays 104
3.3.4. Detachment and Re-Adherence Assays 108
3.3.5. Analysis of Cell Surface Integrin Expression Using Flow Cytometry 108
3.3.6. Visualization of ITGAV Expression in Human Oesophageal Tissue Using Immunofluorescence Microscopy 109
3.3.7. Analysis of Levels of Expression of ITGAV, Cleaved PARP and LC3 by Western Blotting. 110
3.3.8. Visualisation of Rab5 and Rab11 and Co-Localization with ITGAV in HET-1A Cells using Immunofluorescent Microscopy 111
3.4. Results 113
3.4.1. DCA Stimulation Rapidly Induces a Loss of Adhesion in A Dose Dependent Fashion, Hours Prior to the Onset of Apoptosis. 113
3.4.2. DCA, but not UDCA, Induces a Loss of Adherence, Which is Modulated Distinctly from Apoptosis 120
3.4.3. DCA Induces a Specific Loss of Adhesion to the ECM Proteins Vitronectin and Laminin in HET-1A Cells 124
3.4.4. Integrin α_V, the Vitronectin Receptor is Present on HET-1A Cells and is Expressed on a Variety of Oesophageal Tissues 126
3.4.5. DCA, but not Other BAs, Reversibly Modulates the Surface Expression of Integrin α_V on HET-1A Cells 129
3.4.6. DCA Induces a Reduction in the Surface Expression of the Alpha Integrins 4, 5 and V, but not 3 or 4, on HET-1A Cells Which is not Attenuated by UDCA 138
3.4.7. ITGAV Co-localises with Rab5 and Rab11 Positive Vesicles. 142
3.4.8. DCA Treatment Impairs Endosomal Processing as Determined by Rab5 and Rab11 Morphology 142
3.4.9. DCA Reduces the Expression of ITGAV in Oesophageal Tissue Explants Exposed to DCA 146
3.4.10. ITGAV is Upregulated in Peri-Ulcerated Regions of Rat Oesophagus which have Undergone Oesophago-jejunostomies 146
3.4.11. In the QH Cell Line Cell Death Occurs Without Inducing a Loss of Adhesion and Surface Expression of ITGAV is Unaffected by DCA Treatment. 149
3.5. Discussion 152
3.6. Conclusion 157

4. UDCA Induces a Discrete Gene Signature Which Has Limited Concordance With DCA or Dex 159

4.1. Introduction 161
4.1.1. Nuclear Steroid Receptors 161
4.1.2. The Glucocorticoid Receptor 162
4.1.3. Expression and Physiology of the GR in Human Tissues 164
4.1.4. Inflammation in the Oesophagus 165
4.1.5. UDCA and the Glucocorticoid Receptor 166
4.2. Aims 168
4.3. Methods 169
4.3.1. Cell Lines and Culture 169
4.3.2. Analysis of Glucocorticoid Receptor Expression by Western Blotting in Oesophageal Cells 169
4.3.3. Analysis of Glucocorticoid Receptor mRNA Expression in Oesophageal Cells by RT-PCR 170
4.3.4. Immunohistochemical Staining of GR in Paraffin Embedded Oesophageal Biopsies. 171
4.3.5. Nuclear Translocation of the Glucocorticoid Receptor 174
4.3.6. GR *Trans*-activation Assay 177
4.3.7. Microarray Data Experiment and Analysis. 178
4.4. Results 183
4.4.1. Glucocorticoid Receptor α, but not GRβ, is Expressed in Oesophageal Cell Lines representing the Normal - BO - OAC Sequence 183
4.4.2. UDCA Stimulation Induces Nuclear Translocation of the GR 187
4.4.3. Stimulation of HET-1A and SKGT-4 Cells with UDCA Does Not Result in *Trans*-Activation of the GR. 196
4.4.4. The Genes Expression Profile Induced by UDCA Shares Similarities With Those Induced by Dexamethasone and DCA 198
4.4.5. UDCA Pre-Treatment Inhibits DCA-Induced Expression of IL-8 239
4.5. Discussion 241
4.6. Conclusion 246

5. Discussion of Research and Conclusions 247

5.1. The Role of BAs in Inflammation and Carcinogenesis in the Oesophagus 249
5.2. The Need for a New Therapeutic for the Treatment of GORD. 250
5.3. UDCA 251
5.4. UDCA Reduces DCA-Induced Apoptosis but does not Reduce the Total Magnitude of DCA-Induced Cell Death 252
5.5. DCA Modulates Adhesion Molecules 254
5.6. UDCA Induces a Discrete Gene Signature Which Has Limited Concordance With DCA or Dex 256
5.7. Conclusion 258

6. Appendix 1: Supplemental Data from Chapter 2 259

6.1. List of Figures 261

7. Appendix 2: Supplemental Data from Chapter 3 283

7.1. List of Figures 285

8. Appendix 3. Supplemental Data from Chapter 4. 289

8.1. List of Figures 291

8.2. List of Tables 291

8.3. Quality and Quantity of mRNA Used for the Micro-Array Experiment 293

8.4. Microarray Probesets Remaining after Data Refinement 296

8.5. Genes with the Largest Alterations in Expression induced by UDCA, Dex or DCA. 298

8.6. Overlapping Gene Profiles Induced by Treatment with UDCA, Dex and DCA. 302

8.7. Intensity Values of Probeset Pairs for Genes Chosen for Validation 315

9. Appendix 4: Protocols, Reagents and Equipment Used 319

9.1. Cell Lines, Cell Culture and Cell Passage 321

9.1.1. Cell lines 321

9.1.2. Cell Culture and Cell Passage 323

9.1.3. Freezing Cells for Storage 324

9.2. Sodium Dodecyl Sulphate Polyacrylamide Gel Electrophoresis (SDS-PAGE) (based on the Atto gel electrophoresis system) 325

9.3. Western blotting (based on the Atto semi-dry technique) 329

9.4. Immunofluorescence Staining Protocol (PFA fixation) 333

9.5. Immunofluorescent Staining of Paraffin Embedded Tissue. 335

9.6. Protocol for Real Time Polymerase Chain Reaction 337

9.7. Reagents and Suppliers 339

9.8. Antibodies and Suppliers 341

9.9. Equipment and Suppliers 342

10. References 343

V. Figures

Figure 1–1: Macroscopic images and haematoxylin and eosin stained biopsy samples of normal squamous epithelium, Barrett's oesophagus and oesophageal adenocarcinoma 5

Figure 1–2: The yearly incidence of OAC relative to its incidence in 1975 (Thick black line) and the relative increase in incidence of other cancers.. 9

Figure 1–3: Protective mechanisms of the oesophageFrom Guillem; Digestive Diseases and Science: 2005. 12

Figure 1–4: The toxic potential of gastric and duodenal refluxate is dependent on the local environment during a reflux episode. Mucosal injury is represented by the heavyset boxes. 16

Figure 1–5: The toxic effects of DCA and UDCA on cellular function and the established mechanisms of UDCA's cyto-protective properties. 25

Figure 2–1: Images of HET-1A (A) and HCT116 (B) cells used to determine cell counts after BA treatment 48

Figure 2–2: The effect of various concentrations of DMSO on nuclear count after 24 hours treatment 49

Figure 2–3: The effect of various concentrations of DMSO on MTT conversion after 24 hours treatment. No concentration of DMSO studied significantly reduced viability as determined by an. 52

Figure 2–4: Representation of DNA histogram acquired during flow cytometric analysis of cell cycle. 53

Figure 2–5: The effect of UDCA in modulating DCA induced cell death in the HUH-7 cell line.. 63

Figure 2–6: UDCA pre-treatment prior to 300μM DCA treatment for 48 hours reduces the expression of cleaved PARP in the HUH-7 cell line but co-treatment enhances the expression..... 64

Figure 2–7: DCA and UDCA reduce the proliferation of HET-1A cells in a dose and time dependent fashion.. 66

Figure 2–8: The effect of DCA treatment on HET-1A cell viability after four hours UDCA pre-treatment as determined by a nuclear count assay normalised to untreated cells... 72

Figure 2–9: The effect of DCA treatment on HET-1A cell viability after four hours UDCA pre-treatment as determined by an MTT assay normalised to untreated cells 73

Figure 2–10: The effect of DCA treatment on HCT116 cell viability after four hours UDCA pre-treatment as determined by a nuclear count assay normalised to untreated cells.. 74

Figure 2–11: The effect of DCA treatment on HCT116 cell viability after four hours UDCA pre-treatment as determined by an MTT assay normalised to untreated cells 75

Figure 2–12: Bland-Altman plots of the differences between the 4 hour pre-treated matrices and the 18 hour pre-treated matrices for nuclear counts (A) and MTT assays (B) 76

Figure 2–13: UDCA pre-treatment, but not co-treatment, can reduce DCA induced cleavage of PARP 78

Figure 2–14: Mitochondrial depolarization induced by DCA in the HET-1A cell line is not significantly modulated by UDCA pre-treatment 80

Figure 2–15: The effect of UDCA and DCA co-treatment (A) and 4 hours UDCA pre-treatment prior to DCA (B) on the nuclear area of HET-1A cells 83

Figure 2–16: UDCA does not reduce apoptosis induced by DCA as determined by TUNEL based flow cytometry 85

Figure 2–17: DCA induces a significant increase in cell death after 12 hours exposure as determined by AV / PI based flow cytometry 87

Figure 2–18: UDCA does not reduce apoptosis induced by DCA as determined by AV/PI based flow cytometry 88

Figure 2–19: The effect of DCA and UDCA on LC3 I and II expression in HET-1A cells. 90

Figure 2–20: LDH release from oesophageal explants after 24 hours treatment with various bile acids 92

Figure 3–1: A representation of the endocytotic integrin recycling pathway 102

Figure 3–2: The relationship between Calcein AM and HET-1A cell number per well. 107

Figure 3–3: Difference between viability as estimated by the cell count and the MTT assay is greatest at higher BA concentrations and at earlier time-points in the four hour pre-treatment experiment 115

Figure 3–4: Live Cell Imaging of HET-1A Cells during Exposure to 300μM DCA or 300μM UDCA demonstrated a rounded phenotype in the 300μM DCA treated cells beginning minutes after exposure 117

Figure 3–5: Live Cell Imaging of HET-1A Cells During Exposure to 300μM DCA or 300μM UDCA for 24 Hours. 118

Figure 3–6: Live Cell Imaging of HCT116 Cells During Exposure to 300μM DCA or 300μM UDCA for 24 Hours 119

Figure 3–7: DCA (A) but not UDCA (B) treatment reduces the adherence of HET-1A cells to uncoated plastic. In combined treatments 300μM UDCA does not modulate the loss of adherence induced by 300μM DCA 121

Figure 3–8: DCA induces detachment of adherent HET-1A cells in a dose dependent fashion and a proportion of these detached cells can re-adhere 123

Figure 3–9: Adherence of HET-1A cells to the ECM proteins vitronectin and laminin is reduced by DCA treatment 125

Figure 3–10: ITGAV is expressed in cell lines representing normal – BO – OAC sequence. The expression of ITGAV is greatest in QH Cells representing BO 127

Figure 3–11: Immunofluorescent staining demonstrates that ITGAV is expressed in oesophageal squamous epithelium, Barrett's Oesophagus, oesophageal adenocarcinoma, and squamous cell carcinoma of the oesophagus 128

Figure 3–12: DCA stimulation reduces the surface expression of ITGAV on HET-1A cells in a dose dependent fashion 131

Figure 3–13: ITGAV intensity in HET-1A cells is reduced in un-permeabilised cells but not in permeabilised cells after BA treatment.. 132

Figure 3–14: DCA, but not other hydrophobic and hydrophilic BAs, reduces the surface expression of ITGAV.. 133

Figure 3–15: The effect of DCA and low pH (A) and STS (B) on the surface expression of ITGAV in the HET-1A cell line.. 134

Figure 3–16: Bile acid treatment does not reduce total cellular expression of ITGAV.. 135

Figure 3–17: The surface expression of ITGAV on HET-1A cells returns to baseline after removal of the DCA stimulus.. 137

Figure 3–18: The surface expression of Integrins α_5, α_6 and α_V, but not α_3 or α_4, is reduced by treatment with DCA. UDCA has no effect on surface expression in isolation or in combination with DCA 139

Figure 3–19: The changes in median fluorescent intensity in integrins α_3, α_4, α_5, and α_6, and α_v after treatment with 300μM DCA, UDCA or a combination of the two. 140

Figure 3–20: Difference between intensity histograms of integrins α_3, α_4, α_5, and α_6 and α_v after treatment with 300μM DCA, UDCA or a combination of the two.. 141

Figure 3–21: ITGAV co-localises with Rab5 and Rab11 in untreated cells in the HET-1A cell line.. 144

Figure 3–22: DCA treatment results morphological changes in Rab5 and Rab11 positive vesicles consistent with a dysfunction in endocytic recycling 145

Figure 3–23: DCA stimulation of oesophageal tissue explants results in a reduction in the mean intensity of immunofluorescent ITGAV staining 147

Figure 3–24: The intensity of ITGAV staining is higher in the upper oesophagus of anatomically unaltered rats than the lower oesophagus (A), however expression on ITGAV is higher in the peri-ulcerated area of the oesophagus relative to normal (B).. 148

Figure 3–25: DCA Induces a loss of viability in QH cells without inducing cell detachment. 150

Figure 3–26: DCA treatment does not induce a change in the total expression of ITGAV protein or surface expression of ITGAV in the QH cell line. 151

Figure 4–1: Mechanisms through which the GR exerts genomic effects 164

Figure 4–2: Optimization of immunohistochemical staining for the GR in oesophageal tissue. .. 173

Figure 4–3: Optimization of a high content assay for nuclear translocation of the GR demonstrates that Dex (a positive control) induces translocation of the GR to the Nucleus. 176

Figure 4–4: The expression of GR in oesophageal and colonic epithelium as determined by Western blotting (A) and RT-PCR (B). 185

Figure 4–5: IHC staining of oesophageal and colonic tissue demonstrating expression of GR in squamous epithelium and squamous cell cancer of the oesophagus but not in BO or colonic epithelium 186

Figure 4–6: UDCA is capable of inducing nuclear translocation of the GR in a dose and time dependent fashion in the HET-1A (A, B), QH (C, D), OE33 (E, F), SKGT-4 (G, H) and HCT116 (I, J) cell lines. 189

Figure 4–7: UDCA is capable of inducing translocating the GR to the nucleus in a dose dependent fashion. 191

Figure 4–8: UDCA is capable of inducing translocating the GR to the nucleus in a time dependent fashion. 192

Figure 4–9: DCA translocates the GR to the nucleus in the SKGT-4 cell line (B) but not the HET-1A cell line (A). 193

Figure 4–10: DCA does not induce nuclear translocation of the GR in a dose or time dependent fashion in HET-1A cells. 194

Figure 4–11: DCA induces nuclear translocation of the GR in a dose and time dependent fashion in SKGT-4 cells. 195

Figure 4–12: Neither UDCA nor DCA results in GR *trans*-activation in HET-1A (A) or SKGT-4 (B) cell lines.. 197

Figure 4–13: Absolute numbers of genes upregulated (A) and downregulated (B) by UDCA, Dex and DCA in the HET-1A cell lines after twelve hours treatment at $\alpha \leq 0.01$. 204

Figure 4–14: Absolute numbers of genes upregulated (A) and downregulated (B) by UDCA, Dex and DCA in the HET-1A cell lines after twelve hours treatment $\alpha \leq 0.05$ 205

Figure 4–15: Heatmap of clustered genes produced through hierarchical clustering using Euclidian averages of probeset intensities after treatment of HET-1A cells with DCA, UDCA or Dex for 12 hours ($p \leq 0.05$).. 207

Figure 4–16: Genes associated with ER stress are similarly modulated by DCA and UDCA in the HET-1A cell line. 208

Figure 4–17: Genes modulated by both UDCA and Dex in the HET-1A cell line which are associated with the GR as determined using IPA. 209

Figure 4–18: Absolute numbers of genes upregulated (A) and downregulated (B) by UDCA, Dex and DCA in the OE33 cell lines after twelve hours treatment at $\alpha \leq 0.05$ (A and B) and $\alpha \leq 0.01$ (C) 211

Figure 4–19: Heatmap of clustered genes produced through hierarchical clustering using Euclidian averages of probeset intensities after treatment of OE33 cells with DCA, UDCA or Dex for 12 hours ($p \leq 0.05$).. 212

Figure 4–20: Absolute numbers of genes upregulated (A) and downregulated (B) by UDCA, Dex and DCA in the HCT116 cell lines after twelve hours treatment at $\alpha \leq 0.05$ and $\alpha \leq 0.01$ (C) 214

Figure 4–21: Heatmap of clustered genes produced through hierarchical clustering using Euclidian averages of probeset intensities after treatment of HCT116 cells with DCA, UDCA or Dex for 12 hours 215

Figure 4–22: Heatmap of clustered genes after 12 hours treatment with UDCA ($p \leq 0.05$) in the HET-1A, OE33 and HCT116 cell lines. 217

Figure 4–23: Heatmap of clustered genes after 12 hours treatment with Dex ($p \leq 0.05$) in the HET-1A, OE33 and HCT116 cell lines. 218

Figure 4–24: Heatmap of clustered genes after 12 hours treatment with DCA ($p \leq 0.05$) in the HET-1A, OE33 and HCT116 cell lines. 220

Figure 4–25: ER stress genes classically associated with DCA stimulation demonstrated differential regulation in the OE33 cell line.. 221

Figure 4–26: Heatmap of clustered genes after 12 hours treatment with UDCA, Dex or DCA ($p \leq 0.05$) in cell lines HET-1A, OE33 and HCT116 cell lines..... 223

Figure 4–27: Expression levels of mRNA as determined by microarray probesets and as validated by PCR.. 232

Figure 4–28: Four hours UDCA pre-treatment prior to DCA exposure in HET-1A cells reduced DCA induced expression of IL-8 mRNA. HET-1A cells were grown until 80 – 90 %..... 240

Figure 6–1: The effect of DCA and UDCA co-treatment, with no pre-treatment, in the HET-1A cell line as determined by a nuclear count assay normalised to untreated cells. 263

Figure 6–2: The effect of DCA and UDCA co-treatment, with no pre-treatment, in the HET-1A cell line as determined by an MTT assay normalised to untreated cells..... 264

Figure 6–3: The effect of DCA and UDCA co-treatment, with no pre-treatment, in the HCT116 cell line as determined by a nuclear count assay normalised to untreated cells..... 265

Figure 6–4: The effect of DCA and UDCA co-treatment, with no pre-treatment, in the HCT116 cell line as determined by an MTT assay normalised to untreated cells.. 266

Figure 6–5: The effect of DCA, UDCA and 18 hours UDCA pre-treatment prior to DCA treatment in HET-1A cells as determined by a nuclear count assay normalised to untreated cells. 267

Figure 6–6: The effect of DCA, UDCA and 18 hours UDCA pre-treatment prior to DCA treatment in HET-1A cells as determined by an MTT assay normalised to untreated cells. 268

Figure 6–7: The effect of DCA, UDCA and 18 hours UDCA pre-treatment prior to DCA treatment in HCT116 cells as determined by a nuclear count assay normalised to untreated cells. 269

Figure 6–8: The effect of DCA, UDCA and 18 hours UDCA pre-treatment prior to DCA treatment in HCT116 cells as determined by an MTT assay normalised to untreated cells. 270

Figure 6–9: The effect of DCA, UDCA and 4 hours UDCA pre-treatment prior to co-treatment in HET-1A cells as determined by a nuclear count assay normalised to untreated cells. 271

Figure 6–10: The effect of DCA, UDCA and 4 hours UDCA pre-treatment prior to co-treatment in HET-1A cells as determined by an MTT assay normalised to untreated cells. 272

Figure 6–11: The effect of DCA, UDCA and 4 hours UDCA pre-treatment prior to co-treatment in HCT116 cells as determined by a nuclear count assay normalised to untreated cells. 273

Figure 6–12: The effect of DCA, UDCA and 4 hours UDCA pre-treatment prior to co-treatment in HCT116 cells as determined by an MTT assay normalised to untreated cells.. 274

Figure 6–13: The effect of DCA, UDCA and 18 hours 300μM UDCA pre-treatment prior to co-treatment with various doses of DCA in HET-1A cells as determined by a nuclear count assay normalised to untreated cells..... 275

Figure 6–14: The effect of DCA, UDCA and 18 hours of various concentrations of UDCA pre-treatment prior to co-treatment with 300μM DCA in HET-1A Cells as determined by a nuclear count assay normalised to untreated cells..... 275

Figure 6–15: The effect of DCA, UDCA and 18 hours 300μM UDCA pre-treatment prior to co-treatment with various doses of DCA in HET-1A cells as determined by an MTT assay normalised to untreated cells..... 276

Figure 6–16: The effect of DCA, UDCA and 18 hours of various concentrations of UDCA pre-treatment prior to co-treatment with 300μM DCA in HET-1A Cells as determined by an MTT assay normalised to untreated cells. 276

Figure 6–17: The effect of DCA, UDCA and 18 hours 300μM UDCA pre-treatment prior to co-treatment with various doses of DCA in HCT116 cells as determined by a nuclear count assay normalised to untreated cells.. 277

Figure 6–18: The effect of DCA, UDCA and 18 hours of various concentrations of UDCA pre-treatment prior to co-treatment with 300μM DCA in HCT116 cells as Determined by a nuclear count assay normalised to untreated cells..... 277

Figure 6–19: The effect of DCA, UDCA and 18 hours 300μM UDCA pre-treatment prior to co-treatment with various doses of DCA in HCT116 cells as determined by an MTT assay normalised to untreated cells..... 278

Figure 6–20: The effect of DCA, UDCA and 18 hours UDCA pre-treatment prior to co-treatment in HCT116 cells as determined by an MTT assay normalised to untreated cells..... 278

Figure 6–21: Bland-Altman plots of the differences between the 4 hour pre-treated matrices and the 18 hour-pre-treated matrices for cell counts (A) and MTT assays (B) in the HCT116 cell line.... 279

Figure 6–22: The effect of UDCA and DCA and 18 hours UDCA pre-treatment prior to DCA on the nuclear area of HET-1A cells. 280

Figure 6–23: The effect of UDCA and DCA co-treatment (A) and 4 hours UDCA pre-treatment prior to DCA (B) on the nuclear area of HCT116 cells..... 281

Figure 6–24: The effect of UDCA and DCA and 18 hours UDCA pre-treatment prior to DCA on the nuclear area of HCT116 cells. 282

Figure 7–1: Difference between viability as estimated by the cell count and the MTT assay is greatest at higher BA concentrations and at earlier time-points in the co-treatment experiment... 286

Figure 7–2: Difference between viability as estimated by the cell count and the MTT assay is greatest at higher BA concentrations and at earlier time-points in the 18 hour pre-treatment experiment. 287

Figure 8–1: Example of Control RNA ladder used to determine RINs for each RNA sample. 293

Figure 8–2: RIN and RNA concentration of each sample processed in duplicate during the micro-array experiment. 295

Figure 8–3: Micro-array probesets available for analysis after data refinement 297

VI. Tables

Table 1–1: Oesophageal pH and bile acid concentrations (μMol, median and inter-quartile range) in the oesophagus in health and disease. Nehra; Gut 1999. 13

Table 1–2: The critical micellar concentrations for a number of bile acids. Fini: J Lipid Res; 1987 17

Table 1–3: Protonation state of different bile acids at various pH. Fini: J Lipid Res; 1987 18

Table 2–1: The percentage of HET-1A cells in G0/G1, S and G2/M phase of the cell cycle after treatment with 300μM UDCA or 300μM DCA. 68

Table 4–1: The effect of data refinement on the absolute numbers of genes regulated by 200μM UDCA, 100nM Dex and 200μM DCA in the HET-1A, OE33 and HCT116 cell lines after twelve hours treatment 200

Table 4–2: Lists of genes similarly regulated by UDCA and Dex in the cell lines HET-1A, OE33 and HCT116 219

Table 4–3: An overview of changes in mRNA expression induced by DCA, UDCA or Dex in the microarray experiment (MA) and the changes identified using RT-PCR (PCR) 236

Table 4–4: Percentage of genes modulated by DCA or Dex which are similarly modulated by UDCA. 244

Table 4–5: Percentage of genes modulated by UDCA which are similarly modulated by Dex or DCA 244

Table 8–1: List of 25 Probesets with the greatest upregulation or down-regulation in response to UDCA. 299

Table 8–2: List of 25 Probesets with the greatest upregulation or down-regulation in response to Dex. 300

Table 8–3: List of 25 Probesets with the greatest upregulation or down-regulation in response to DCA. 301

Table 8–4: Genes Up-regulated by UDCA, Dex, DCA or both UDCA and Dex in the HET-1A Cell Line 303

Table 8–5: Genes Up-regulated by UDCA and DCA, DCA and Dex, or All Three of UDCA, Dex and DCA in the HET-1A Cell Line 304

Table 8–6: Genes Down-regulated by UDCA, Dex, DCA or both UDCA and Dex in the HET-1A Cell Line 305

Table 8–7: Genes Down-regulated by UDCA and DCA, DCA and Dex, or All Three of UDCA, Dex and DCA in the HET-1A Cell Line 306

Table 8–8: Genes Up-regulated by UDCA, Dex, DCA or both UDCA and Dex in the OE33 Cell Line 307

Table 8–9: Genes Up-regulated by UDCA and DCA, DCA and Dex, or All Three of UDCA, Dex and DCA in the OE33 Cell Line 308

Table 8–10: Genes Down-regulated by UDCA, Dex, DCA or both UDCA and Dex in the OE33 Cell Line 309

Table 8–11: Genes Down-regulated by UDCA and DCA, DCA and Dex, or All Three of UDCA, Dex and DCA in the OE33 Cell Line 310

Table 8–12: Genes Up-regulated by UDCA, Dex, DCA or both UDCA and Dex in the HCT116 Cell Line 311

Table 8–13: Genes Up-regulated by UDCA and DCA, DCA and Dex, or All Three of UDCA, Dex and DCA in the HCT116 Cell Line 312

Table 8–14: Genes Down-regulated by UDCA, Dex, DCA or both UDCA and Dex in the HCT116 Cell Line 313

Table 8–15: Genes Down-regulated by UDCA and DCA, DCA and Dex, or All Three of UDCA, Dex and DCA in the HCT116 Cell Line 314

Table 8–16: Micro-Array Intensity Values for Probeset Pairs of Validation Genes 316

Table 8–17: Micro-Array Intensity Values for Probeset Pairs of Validation Genes 317

Table 8–18: Micro-Array Intensity Values for Probeset Pairs of Validation Genes 318

Table 9–1: Cell Lines used in this research, Their origin and Growth Medium. 322

VII. Abbreviations

Abbreviation	Name
4-IBPA	4-Iodophenylboronic Acid
ADP	Adenosine Di-Phosphate
AP-1	Activator Protein 1
ATP	Adenosine Tri-Phosphate
AV	Annexin V
BA	Bile Acid
BCL-2	B Cell Lymphoma 2 Family of Proteins
BO	Barrett's Oesophagus
BSA	Bovine Serum Albumin
CA	Cholic Acid
Ca^{++}	Calcium
Caspase	Cysteinyl Aspartate-Specific Proteases
CDCA	Chenodeoxycholic Acid
cDNA	Complementary DNA
CDX-1	Caudal-Related Homeobox Transcription Factor 1
CDX-2	Caudal-Related Homeobox Transcription Factor 2
CMC	Critical Micellar Concentration
CMpH	Critical Micellar pH
COX-2	Cyclooxygenase 2
CyA	Cyclosporin A
DBD	DNA-Binding Domain
DCA	Deoxycholic Acid
DGOR	Duodeno-gastrooesophageal Reflux
DIS	Dilated Intercellular Spaces
DMSO	Dimethyl Sulphoxide
DNA	Deoxyribonucleic Acid
ECM	Extracellular Matrix
EDTA	Ethylenediaminetetraacetic acid
EGFR	Epidermal Growth Factor Receptor
EGTA	Ethylene Glycol Tetraacetic Acid
ER	Endoplasmic Reticulum
ER	Oestrogen Receptor
ERK	Extracellular-Signal-Regulated Kinases
FAC	Focal Adhesion Complex
FAK	Focal Adhesion Kinase
FasL	Fas Ligand
FasR	Fas Receptor
FCS	Fetal Calf Serum

FXR	Farnesoid X Receptor
GC	Glucocorticoid
GCA	Glycocholic Acid
GCDCA	Glycochenodeoxycholic Acid
GDCA	Glycodeoxycholic Acid
GORD	Gastro-Oesophageal Reflux Disease
GR	Glucocorticoid Receptor
GTP	Guanosine-5'-Triphosphate
GUDCA	Glyco-Ursodeoxycholic Acid
H^+	Acid / Hydrogen Ion
H2RA	H2 Receptor Antagonist
HBSS	Hanks Buffered Salt Solution
HCl	Hydrochloric Acid
HGD	High Grade Dysplasia
IFN-y	Interferon-γ
IL-6	Interleukin 6
IL-8	Interleukin 8
IP3	Inositol-Phosphate-3
IPA	Ingenuity Pathway Analysis
ITGAV	Integrin α_V
LBD	Ligand-Binding Domain
LC-3	Microtubule Associated Light Chain 3
LCA	Lithocholic acid
LDH	Lactate Dehydrogenase
LES	Lower Oesophageal Sphincter
LGD	Low Grade Dysplasia
MAPK	Mitogen Activated Protein Kinase
MMP	Matrix Metalloproteinases
MPT	Mitochondrial Permeability Transition Pore
mRNA	Messenger Ribonucleic acid
MTT	3-(4,5-Dimethylthiazol-2-yl)-2,5-diphenyltetrazolium bromide
MW	Molecular Weight
Na^+	Sodium
NF-κB	Nuclear Factor Kappa-Light-Chain-Enhancer of Activated B Cells
NSR	Nuclear Steroid Receptor
OAC	Oesophageal Adenocarcinoma
PARP	Poly-ADP-Ribose Polymerase
PBC	Primary Biliary Cirrhosis
PBS	Phosphate Buffered Saline
PCNA	Proliferating Cell Nuclear Antigen
PCR	Polymerase Chain Reaction
PFA	Paraformaldehyde
PHAsO	Phenylarsinine Oxide

PI	Propidium Iodide
PI3K	Phospho-Inositol 3 Kinase
pKa	Acid Dissociation Constant
PKC	Protein kinase C
PMSF	Phenylmethanesulfonylfluoride
PNRC	Peri-nuclear Recycling Compartment
PPI	Proton Pump Inhibitor
PR	Progesterone Receptor
PSC	Primary Sclerosing Cholangitis
RGD	arginine-glycine-aspartate
RIPA	Radioimmunoprecipitation assay
RNA	Ribonucleic Acid
RNS	Reactive Nitrogen Species
ROS	Reactive Oxygen Species
RT	Room Temperature
RT-PCR	Real Time Polymerase Chain Reaction
SBTI	Soybean Trypsin Inhibitor
SEM	Standard Error of the Mean
SiRNA	Specific Inhibitory RNA
SqCCA	Squamous Cell Carcinoma
STS	Staurosporine
TCA	Taurocholic Acid
TCDCA	Taurochenodeoxycholic Acid
TDCA	Taurodeoxycholic Acid
TGF-β	Transforming Growth Factor Beta
TLESR	Transient Lower Oesophageal Sphincter Relaxations
TMRM	Tetramethylrhodamine methyl ester
TNF	Tumour Necrosis Factor
TNF-R	TNF-Receptor
TOR	Target of Rapamycin
TRAIL	TNF-R Apoptosis Inducing Ligand
TUDCA	Tauro-Ursodeoxycholic Acid
TUNEL	Terminal Deoxynucleotidyl Transferase Nick-End Labelling
UDCA	Ursodeoxycholic Acid
V/V	Volume / Volume

Ursodeoxycholic Acid – A Molecular Modulator of the Inflammation-Carcinoma Sequence in the Oesophagus?

CHAPTER 1.

1. Introduction

1.1. Summary of Research Background

Reflux of gastric contents into the oesophagus is a physiological event that most frequently occurs after eating. As a result, 20% of the western population admit to symptoms of heartburn or regurgitation when questioned. Yet the majority of these individuals are never given the diagnosis of gastro-oesophageal reflux disease (GORD) and never develop complications from their reflux.

5-10% of the general population will have either frequent or severe reflux symptoms, impairing their quality of life. 10% of these patients will develop Barrett's Oesophagus (BO), a premalignant condition of the oesophagus. Depending on the degree of dysplasia present in BO (none, low grade or high grade), this metaplastic transformation carries a risk of developing oesophageal adenocarcinoma (OAC) 30 – 400 fold above that seen in the general population. Overall, just under 0.5% of individuals with BO will develop OAC each year making in the greatest risk factor for developing this cancer. However, predicting which GORD patients will progress to BO or OAC is impossible. American surveillance data has shown that the incidence BO is rising and the incidence of OAC in the western world has consistently increased by over ten percent per year during the last thirty years. Despite known risk factors and a known precursor lesion, OAC has the most rapidly increasing incidence of any cancer worldwide and a previously rare disease with a dismal prognosis is now becoming a major health concern.

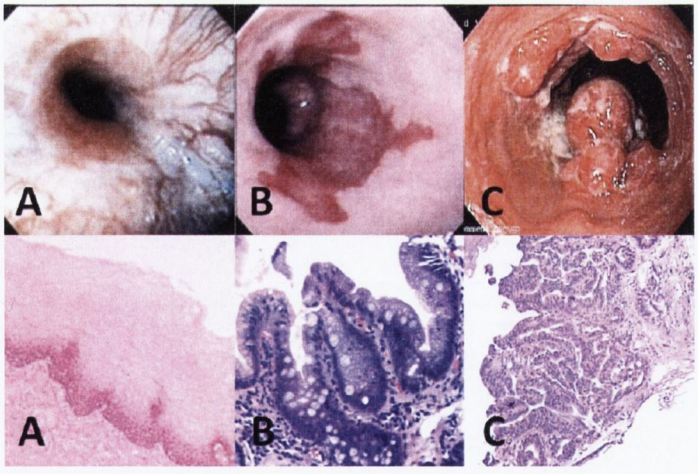

Figure 1–1: Macroscopic images (upper row) and haematoxylin and eosin stained biopsy samples (lower row) of normal squamous epithelium (A), Barrett's oesophagus (B) and oesophageal adenocarcinoma (C). Normal oesophageal epithelium is characterized by a stratified squamous phenotype (A). BO is characterized by columnar epithelium with mucin producing goblet cells (B). Adenocarcinoma is characterized by columnar epithelium in a tubulo-papillary architecture.

Classically, it was thought that acid reflux was the predominant aetiological factor for both BO and OAC. However, two clinical factors have led to a reappraisal of this theory. Firstly, effective acid suppressing medications such as H2 receptor antagonists (H2RA) and proton pump inhibitors (PPIs) have failed to halt the rising incidence of these diseases. In fact, there is no clinical evidence that the use of PPIs reduce the risk of developing OAC in the setting of BO. Secondly, once pathological reflux disease begins it can continue to disrupt the protective mechanisms of the oesophagus and perpetuate the disease despite adequate acid suppression. These findings have led to a re-evaluation of other reflux constituents in the pathogenesis of BO and OAC.

The majority of reflux episodes consist of mixed refluxate of gastric and duodenal components, rather than acid alone. Hydrochloric acid, pepsin and nitrogenous products (from partially digested food) comprise the gastric refluxate and bile acids (BAs) and pancreatic digestive enzymes comprise the duodenal component. These chemicals have the potential to cause cellular damage and many have mutagenic potential. Acid has been proven to be a significant aetiological factor in oesophageal inflammation and carcinogenesis but evidence is now accumulating that BAs have a major role in these pathways both independently and synergistically with acid.

While the role of BAs in oesophageal disease has not been universally accepted there is a growing volume of research indicating that they are pathological in every aspect of GORD. Clinical studies have demonstrated that BAs propagate the mechanical damage that results in reflux. Higher concentrations of BAs have been identified in the oesophagi of patients with BO or OAC than in healthy controls or GORD patients. Molecular research has shown BAs to be carcinogenic through both mutagenic and signalling mechanisms. Animal models have demonstrated that BAs are carcinogenic *in-vivo* and that BAs are essential prerequisites for the development of BO while acid (H^+) is not. Epidemiological studies have shown that BAs in oesophageal refluxate are independent risk factors for both BO and OAC. Taken all-together, this epidemiological, clinical and molecular research has demonstrated that BAs are a significant aetiological factor in the development of both BO and OAC.

PPIs have failed to prevent the rising incidence of BO and OAC and so another pharmacological therapy is needed to prevent or inhibit the progression of BO. Ursodeoxycholic acid (UDCA) has been shown to attenuate the toxic effects of hydrophobic BAs in the liver and in the colon. Consequently, it could potentially offer a therapeutic agent for the treatment of GORD; one that could safely be given to as large a cohort of society as PPIs in order to enhance our empiric treatment of a highly prevalent disease.

1.2. Gastro-Oesophageal Reflux Disease, Barrett's Oesophagus and Oesophageal Adenocarcinoma

1.2.1. Gastro-Oesophageal Reflux Disease

GORD is defined as "reflux of gastric contents into the oesophagus leading to oesophagitis, reflux symptoms sufficient to impair quality of life, or risk of long-term complications" [1]. By this definition, GORD is thought to affect 5 – 20% of the world's population and to result in considerable work related illness and impaired quality of life [2-3]. Among western populations, 25% of individuals report having heartburn at least once a month, 12% at least once per week, and 5% describe daily symptoms. In other geographical areas, the prevalence is thought to be lower [4]. These estimates suggest that GORD has a much higher prevalence in western society; a suggestion that reflects the higher incidence of GORD complications in this region.

The relationship between reflux episodes and symptoms is complicated, resulting from a balance between exposure to noxious stimuli (such as acid or bile) and visceral sensitivity that is unique for each individual. Patients with minimal chemical or volume reflux may have severe symptoms and patients with severe reflux may be asymptomatic. This was well demonstrated in a random sample of the Swedish adult population where reflux symptoms were reported by 40% but oesophagitis was diagnosed in only 16%. However, among those with oesophagitis, 37% had no reflux symptoms [5]. Because of this complexity, predicting the severity of disease and the risk of future complications from reported symptoms is impossible.

Prior to the advent of PPIs, the identification of oesophagitis during upper gastrointestinal endoscopy was highly specific (90–95%) for GORD but only had a sensitivity of 50% [4]. Currently, the sensitivity is lower as the use of PPIs has significantly reduced the incidence of oesophagitis. Inflammation on histological examination is seen in one-third of individuals who are symptomatic but who have normal endoscopic examination. The other two-thirds will have reflux symptoms but no macroscopic or microscopic evidence of pathological reflux or inflammation [6].

Whether symptomatic patients have oesophagitis or normal mucosa on endoscopy, the majority will be treated pharmacologically. Treatment is long-term and usually with a PPI but symptomatic benefit is often limited [4]. In patients with reflux symptoms without oesophagitis only one-third will symptomatically improve on therapy [7]. Similarly, in patients with oesophagitis, therapy may only resolve the symptoms in 30-40% [7]. Even when oesophagitis patients are fully compliant with prescribed PPI treatment, 50% will continue to have pathological levels of acid reflux. A higher percentage will continue to have BA reflux. Despite acid suppression therapy, GORD patients are often still at risk of complications such as BO and OAC. This may be because of the

ongoing BA exposure and PPIs may in fact be enhancing the carcinogenic potential of these molecules by raising the pH of the refluxate (See Section 1.4.2).

1.2.2. Barrett's Oesophagus

As a result of longstanding GORD, the squamous epithelium lining the distal oesophagus can undergo a phenotypic change which makes the oesophagus less susceptible to reflux induced damage. This transformation is most frequently (~90%) into BO or "incomplete intestinal metaplasia" where a villous and glandular epithelium, similar to that seen in the small intestine, develops [4, 8]. Multiple unproven theories exist as to the origin of this metaplasia but all theories agree that the GORD induced mucosal damage must occur to a significant depth so that atypical "regeneration" may begin. The first theory suggests that Barrett's cells arise from metaplastic transformation of stem cells present in the basal layer of the oesophageal epithelium. The second suggests that Barrett's cells arise from the columnar cells present in the oesophageal glands. The most recent theory hypothesises that the origin of BO is in residual embryological stem cells which are held in stasis in the adult epithelium [9-13]. No theory has, to date, been convincingly proven.

Studies estimate the overall prevalence of BO at 2.3% among people symptomatic with GORD and 1.2% in asymptomatic patients [5]. It is uncommonly detected in patients younger than 50 years but above this age threshold it is present in 1– 2% of patients referred for endoscopy [4]. However, these figures are imprecise and recent data suggests that the incidence of BO is rising in the western world [14]. Both epidemiological and animal studies suggest that acid reflux and duodeno-gastroesophageal reflux (DGOR) are the most significant risk factors for developing BO [8, 11, 15-22] and molecular research has shown that BAs may be more toxic at higher pH. Consequently, the widespread use of PPIs may be both helping and harming GORD patients.

Over time, BO may progress to the development of low (LGD) and high grade dysplasia (HGD) with consequent development of OAC. The incidence of LGD, HGD, and OAC in BO is estimated at 4 percent, 1 percent, and 0.5 percent per year in patients with BO. LGD is estimated to progress to HGD or OAC in 10-28% of patients over a five year period and among patients with HGD, the incidence of OAC may be as high as 59% over the same period [8]. This accounts for a 30 – 400 fold increase in risk of OAC above the general population [8, 23-24]. Because no current pharmacological therapy can sufficiently inhibit progression of BO, it has until recently been standard clinical practice to recommend an oesophagectomy in the setting of confirmed persistent HGD. Newer therapies such as radiofrequency ablation or cryotherapy are now offering localised therapy to treat Barrett's dysplasia. However, the long term success rate of these therapies have yet

to be proven and issues such as buried BO (the presence of residual BO beneath squamous epithelium) are of concern [25-26].

1.2.3. Oesophageal Adenocarcinoma

The lifetime risk for oesophageal adenocarcinoma is estimated to be 0.8% for men and 0.3% for women with an overall incidence in the US of 4.8 per 100,000 persons per year. However, in the western world the last few decades have seen increases in the incidence of this disease of over 450% in Caucasian males and 50% in black males. This increase has occurred at the same time as the incidence of squamous cell carcinoma of the oesophagus has decreased (Figure 1–2) [27-29].

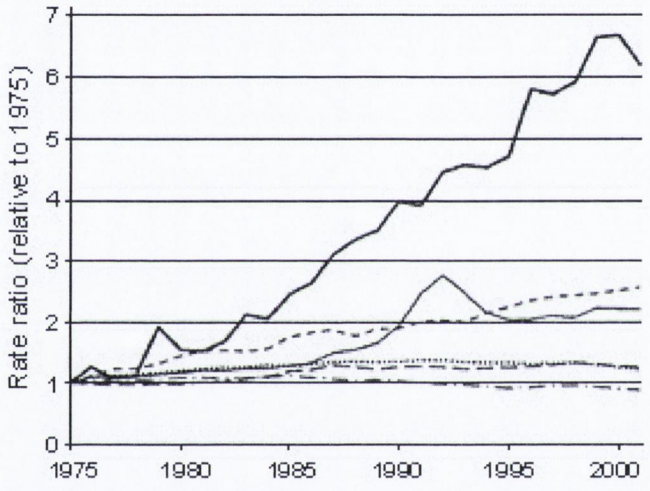

Figure 1–2: The yearly incidence of OAC relative to its incidence in 1975 (Thick black line) and the relative increase in incidence of other cancers (melanoma - dashed line and prostate – thin black line). NIH: *http://www.cancernet.gov* (Accessed 24th July 2011).

What *is* striking about OAC, other than the incidence data, is the predominance of environmental risk factors; genetics seem to exert little influence (a fact that is strongly supported by the rapidly changing incidence of disease). Three large population studies have shown no relationship between a family history of intestinal cancers and OAC [30-32] and while a rare hereditary form of BO and OAC exists, it is highly exceptional [31]. Among the environmental risk factors for OAC, BO and longstanding GORD appear to be the most significant. 60% of OAC arises in the presence of BO, a finding which would be expected in <1% of asymptomatic individuals and only 3–7% of patients with reflux symptoms and no BO [33]. In addition, more frequent, more severe, and longer-lasting symptoms of reflux are associated with a greater risk of OAC. However, 40% of patients who

develop OAC do not have BO and the severity and duration of reflux symptoms are similar in OAC cases with and without BO [8]. This highlights the significant independent role of GORD in the pathogenesis of OAC. Recently, DGOR was identified as a risk factor for OAC independently of BO and acid reflux, potentially explaining some of the risk associated with GORD despite acid suppression therapies [15]. Obesity (independently of GORD), age and a smoking history account for the majority of the remaining risk [33-38].

Despite known risk factors, fewer than 5% of patients are known to have BO before they are diagnosed with OAC, primarily because of the high prevalence of reflux symptoms and the poor correlation between symptoms and complications. As a result, 50% of OAC patients have either unresectable tumours or radiographically visible metastases at diagnosis [39-40]. The five-year survival rate exceeds 95 percent for operatively managed stage 0 disease but for more advanced disease, the prognosis is poor with five year survival ranging from 10 to 25% [23]. Patients with metastatic (stage IV) disease have a median survival of less than one year.

However, while OAC has a dire prognosis, even for an obese, smoking, aging male with severe reflux for many years (all the significant risk factors), the absolute risk remains low (1 in 600 population per year). Even the absolute risk of developing OAC in the setting of Barrett's is small in the absence of any dysplastic change (1 in 200 population per year). As only 2-3% of patients with BO die from OAC, and as the overall life expectancy is no different to age and gender matched members of the general population, the current epidemiology does not justify screening [40]. Yet, OAC represents a disease which occurs as a result of potentially modifiable environmental factors. Thus the incidence of OAC should be amenable to environmental or pharmacological modulation. However, while PPIs target acid production, weight reduction can be achieved and smoking can be ceased, no treatment is available to modify the risk of BAs in the oesophagus.

1.3. The Pathology of Gastro-Oesophageal Reflux Disease

1.3.1. The Pathogenesis of GORD

The oesophagus is primarily designed for the unidirectional passage of masticated material and fluid. Peristaltic waves, the intrinsic lower oesophageal sphincter (LES) and external pressure from the diaphragmatic crus synergise to prevent the reflux of gastric contents back into the oesophagus.

However, despite these mechanical barriers, reflux is a component of health [41]. *All* individuals have episodes of reflux into the oesophagus with the majority occurring within hours of eating.

It is impaired function of the LES that is thought to be the primary underlying pathology which results in physiological refluxate becoming pathological. 87% of physiological reflux episodes occur during transient lower oesophageal sphincter relaxation (TLESR) but only one third of TLESRs are associated with reflux episodes. Compared with healthy individuals, people with GORD do not have more TLESRs, but either initially have, or as a result of reflux develop, structural changes at the gastro-oesophageal junction which include a reduction in LES tone and a shortening of oesophagus [40, 42]. This results in an increased proportion of TLESRs being associated with reflux of gastric contents, and the oesophagus more frequently being exposed to refluxate [5, 6, 9, 10].

Reflux also affects the mechanical function of the oesophagus above the level of the LES resulting in defective clearance from the oesophagus. In healthy individuals reflux provokes an increase in oesophageal tone proximally which inhibits retrograde reflux and initiates peristalsis. In patients with GORD, an increase in oesophageal tone during reflux episodes is less common, there is a longer period until peristalsis is initiated and there is reduced amplitude and frequency of the peristaltic waves. This results in delayed clearance of the refluxate from the oesophagus [41, 43-45]. As these mechanical impairments become more pronounced, GORD becomes more established [4, 40].

The majority of refluxate contains a mixture of gastric and duodenal components; both of which have the potential to damage the oesophagus. The gastric components include H^+ and pepsin and the duodenal components include BAs and duodenal proteases. Pre-epithelial, epithelial and post-epithelial defences contribute to protecting the oesophagus from these stimuli (Figure 1–3). However, given enough time or a high enough concentration, any noxious stimuli in the oesophageal lumen can overcome these protective mechanisms, either in isolation or through synergistic mechanisms [11]. At this stage, mucosal damage, inflammation, ulceration or haemorrhage may occur.

Hydrogen ions attack the apical membrane of squamous cells but the epithelium is resistant to penetration unless the pH is <2. At this pH the ionic gradient can drive H^+ into the squamous cells but even then, Na^+/H^+ pumps clear H^+ back into oesophageal lumen. BAs damage the oesophageal mucus layer allowing H^+ direct contact with the squamous cells as well as increasing H^+ permeability into the cells by damaging the cellular membrane. The H^+ toxicity is further propagated when adhesion molecules between cells are damaged by proteases such as trypsin and pepsin. When this happens, the baso-lateral membranes which are less resistant to H^+ become exposed, the Na^+/H^+ pumps are overwhelmed and cellular toxicity and genetic damage occurs. If

the Na^+/H^+ pumps are successful in protecting cells, rebound alkalinisation can lead to cellular hyper-proliferation [11] which potentially propagates any mutagenic damage. BAs may independently result in mucosal damage as well. In their unconjugated or non-ionic form they can traverse the cellular membrane resulting in mitochondria damage, the release of free oxygen and nitrogen radicals and genetic damage. This may be of particular concern when rebound alkalinisation and epithelial proliferation occurs.

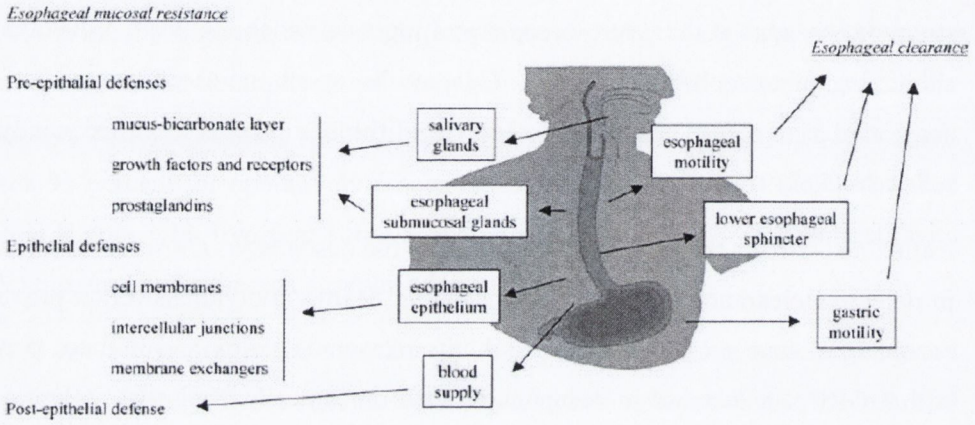

Figure 1–3: Protective mechanisms of the oesophageal mucosa against GORD induced injury. From Guillem; Digestive Diseases and Science: 2005.

Synergy between the gastric and duodenal components of refluxate exacerbates the epithelial damage induced by GORD. Bile refluxate alone does not usually result in mucosal damage and acid alone only usually causes it to a limited extent. Impaired mechanical function of the oesophagus is also more profound in cases of mixed type refluxate. Overall, patients with significant and prolonged mixed reflux have more severe mucosal and mechanical damage as well as a higher chance of developing complications as a result of GORD [42].

1.3.2. Duodenogastro-Oesophageal Reflux

It is only in the last two decades, as acid suppression therapy has failed to eliminate the sequelae of GORD that interest in oesophageal BA toxicity increased. With the development of new technologies capable of documenting BA in the oesophagus, mixed reflux (gastric and duodenal contents) was identified as the most common form of reflux event in the oesophagus. Subsequently, it was identified that increasing concentrations of BAs in the oesophagus were associated with a greater risk of inflammatory, metaplastic and neoplastic complications.

Initial investigations of mixed duodenogastro-oesophageal refluxate using aspiration technology and chromatographic analysis demonstrated the presence of bile in the oesophagi of healthy subjects as well as in patients with oesophageal disease [18, 20-22]. The majority of bile reflux occurred in the postprandial state both in healthy controls and in patients with reflux disease, a situation analogous to acid reflux. BA concentrations reached levels of almost 200μMol in the majority of patients with BO or severe oesophagitis and increasing levels of bile in the oesophagus (in DGOR alone or mixed reflux) correlated with more severe oesophageal disease (Table 1–1) [21-22]. This research identified that glycine conjugated forms of cholic acid, chenodeoxycholic and deoxycholic acids were the most common BAs in the refluxate. This composition reflected that seen in bile where the glycine conjugates are three times more common than taurine [20].

Group	*Normal*	*Minimal*	*Erosive*	*Barrett's oesophagus/stricture*
Primary bile acids				
Cholic acid	0 (0–8)	0 (0–99)*	34 (0–150)*	25 (0–126)*
Taurocholic acid	0 (0–8)	7 (0–67)*	21 (0–198)*	39 (4–131)†
Glycocholic acid	0 (0–6)	7 (0–102)*	21 (0–88)*	27 (0–95)*
Secondary bile acids				
Deoxycholic acid	0 (0–3)	0 (0–7)	2 (0–230)†	0 (0–282)†
Taurodeoxycholic acid	0 (0–0)	0 (0–0)	0 (0–157)†	5.5 (0–410)†
Glycodeoxycholic acid	0 (0–0)	0 (0–47)	2.5 (0–285)*	0 (0–72)
Taurolithocholic acid	0 (0–0)	0 (0–0)	0 (0–0)	6 (0–482)‡
Total bile acid concentration	0 (0–16)	14 (0–257)*	124 (6–1020)†	181 (30–820)†
Oesophageal pH				
% time pH<4	2.1 (0.9–12.1)	2.7 (1.3–5.9)	5.1 (3.6–12.1)	22.3 (10.0–46.0)‡
DeMeester acid score	11.1 (7.5–25.6)	12.5 (8.8–20.4)	20.2 (13.7–36.0)‡	43.3 (30.6–83.0)†

*p<0.05 versus normal; †p<0.05 versus normal and minimal; ‡p<0.05 versus normal, minimal, and erosive (Mann-Whitney U test)
0 = less than the limit of sensitivity (0.25 μmol/l).

Table 1–1: Oesophageal pH and bile acid concentrations (μMol, median and inter-quartile range) in the oesophagus in health and disease. Nehra; Gut 1999.

The development and validation of Bilitec™, a spectrophotometric method of identifying bilirubin in the oesophagus, increased our understanding of DGOR through greater ease of use and patient acceptance. Bilirubin measurement represents an indirect measurement of duodenal reflux into the oesophagus but correlates well with the presence of pancreatic enzymes and is regarded as representative of DGOR [46]. However, spectrophotometric assessment of DGOR has some limitations including a low sampling frequency and data loss due to meal artefacts [47-50]. Of particular concern is that the instrument underestimates bile reflux by at least 30% in an acidic medium (pH < 3.5) because of a shift in the bilirubin absorption wavelength as a result of dimerisation at this pH.

Spectrophotometric analysis with simultaneous pH monitoring confirmed that acid and bile reflux correlate well and that mixed reflux (pH <4 and absorbance > 0.14) accounts for the majority of

episodes, corroborating earlier aspiration data [51]. One study of 402 subjects demonstrated that 60% of patients with abnormal reflux had mixed profiles, 30% had acid reflux only and 13% had bile reflux only [42]. Another study demonstrated that among GORD patients, mixed reflux occurred in over 50% (31/53). In this group 70% of mixed refluxers had BO compared to 20% of acid refluxers and conversely, only 20% of mixed refluxers had normal oesophagus compared to 50% of acid refluxers. The same study reinforced that BA exposure increases across the spectrum of reflux disease, being higher in patients with OAC or BO than in patients with GORD alone [19-22]. The median BA exposure time per day in healthy individuals was 0.1% and in patients with Barrett's was 15%.

Further reinforcing the role of BAs in oesophageal disease are spectrophotometric studies performed on patients in the intensive care unit. In this cohort, one third develop gastric or oesophageal ulceration in the absence of medical hardware and despite adequate prophylactic acid suppression by intravenous PPI therapy. The use of Bilitec demonstrated significant bile reflux in these oesophagi [52].

Spectrophotometric studies have also given us insight as to why patients on PPIs may still have symptoms and are still at risk of developing GORD complications. Among GORD patients whose symptoms have not responded to PPI therapy, combined bile and pH monitoring has demonstrated that acid and bile reflux, in isolation or combined, continues in a significant proportion. Patients with persistent oesophagitis are more likely to have bile reflux or mixed reflux than acid reflux alone [53-54]. This may explain why GORD patients continue to develop complications despite "adequate" treatment with PPIs. This hypothesis is reinforced by evidence that post gastrectomy patients may still develop BO despite the absence of gastric acid. However, among these patients the degree of oesophageal mucosal injury may be minimal highlighting the role of acid-bile synergy in oesophageal inflammation [17, 55].

While these clinical studies have demonstrated that BAs are toxic in isolation, a decade of combined pH and bilirubin monitoring has now confirmed the association between increasing DGOR and the risk of BO and OAC at an epidemiological level. A recent multivariate analysis of over four hundred patients identified DGOR as an independent risk factor for both oesophagitis and BO. Interestingly though, only acid exposure was a predictive factor for severity of oesophagitis. This suggests that the association of DGOR with oesophagitis might reflect a threshold factor rather than a progressively increasing quantitative factor [15].

Finally, in animal models, it has been shown that surgically induced pathological BA exposure is significantly more likely to result in the genesis of columnar lined oesophagus and adenocarcinoma than acid exposure in the presence or absence of a tumour promoter [56-59]. This research also demonstrated that BAs were carcinogens and not simply tumour promoters. Reinforcing the

hypothesis that acid suppression may enhance the toxicity of BAs, in the presence of a tumour promoter acid protected against BA induced OAC in a rat model [58].

1.4. Molecular Aspects of Bile Acids and Bile Acid Pathology

1.4.1. Bile Salt Physiology

Bile salts are synthesised in hepatocytes as primary BAs (cholic acid and chenodeoxycholic acid) and are subsequently conjugated with either glycine or taurine and then secreted into the hepatic collecting systems. They are either transiently stored in the gallbladder or secreted into the intestinal lumen to perform their physiological functions. The majority of BAs are reabsorbed in the terminal ileum but some progress to the colon. Here bacterial metabolism can de-conjugate or de-hydroxylate the BAs. Further reabsorption occurs in the colon so that <3% of BAs are excreted in the faeces.

Classically, BAs were regarded as having two essential functions; facilitating lipid and fat soluble vitamin absorption and excretion of bilirubin and cholesterol. However, identification of nuclear steroid receptors (NSR), G-protein coupled transmembrane receptors and membrane transporters whose primary ligands are BAs has shown us that BAs have a role in lipid homeostasis, endocrine signalling and trophic effects on intestinal epithelial cells [60-65]. None of these functions appear to physiologically relevant to the oesophagus. The expression of the transmembrane G-protein coupled receptor TGR5/M-BAR appears to be highest on intestinal endocrine cells and it has been postulated that it may play a role in the release of glucagon, cholecystokinin or other paracrine mediators [61, 66-70]. The BA transmembrane transporter appears to be predominantly expressed in the ileum and liver suggesting that they facilitate transport of BAs through the enterohepatic cycle. Neither TGR5 or the BA transporter is expressed in the oesophagus [71].

1.4.2. The Physico-Chemical Properties of Bile Acids

The complex chemical properties of BAs make these molecules difficult to study. The difficulty for researchers lies in mimicking the refluxate that exists *in vivo* during mixed reflux events. In physiological systems a BA can exist in a number of forms; an insoluble protonated acid, a simple soluble protonated acid or its anion, a simple micelle, a constituent of a mixed micelle or, as an insoluble salt. Each form exerts a different toxicity profile but the form in which an individual BA

exists depends on its solubility, concentration, the influence of other amphipathic molecules and the local pH (Figure 1–4) [72]. Early experiments investigating the injurious effects of various duodenal components on rabbit oesophageal mucosa demonstrated this effectively [73-74].

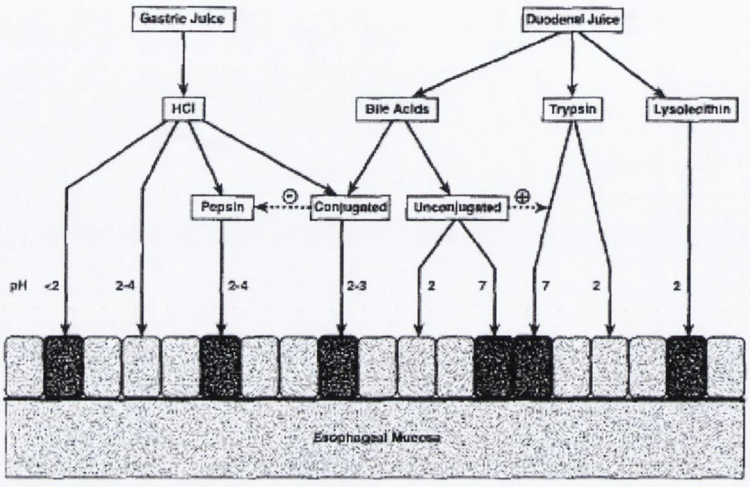

Figure 1–4: The toxic potential of gastric and duodenal refluxate is dependent on the local environment during a reflux episode. Mucosal injury is represented by the heavyset boxes.

Concentration, ionisation and phase can all be influenced by factors such as pH, the presence of other BAs or amphipathic molecules or lipids. In the oesophagus, refluxate pH is a primary determinant of the BA toxicity (Figure 1–4). In general the higher the pH of the solution, the more ionised the BAs will become. While more likely to form micelles at high pH, they are less likely to traverse cellular membranes in their ionised form. Conversely at low pH, most BAs are protonated and can traverse cellular membranes. At the extreme end of the spectrum, when the pH is <2 it is thought that BAs form complexes (possibly dimers) and irreversibly precipitate out of solution, negating their toxicity.

BA solubility depends on conjugation, hydroxylation, pH and temperature. Taurine conjugated BAs are strong acids freely soluble in water in either their ionised or un-ionised form [19]. Unconjugated and glycine conjugated BAs are poorly soluble in water. However, their solubility increases as the number of hydroxyl groups in the BA rises from one to three; the saturation concentration of UDCA in water is 9μMol/L, of deoxycholic acid (DCA) is 28μMol/L and of cholic acid (CA) is 283μMol/L [75]. Concentrations rise until the critical micellar concentration (CMC, the lowest concentration of BAs at which micelles will begin to form) is reached and micelles begin to form. After this point, further BAs become incorporated into micelles, while the concentration of monomeric BAs remains constant. As a result, above this concentration, BAs

exhibit both detergent and signalling effects. Estimated values for the CMCs for different BAs in isolation are shown in (Table 1–2) [75].

Bile Acid	CMC (mMol/L)
CA	11
TCA	6
GCA	10
CDCA	4
DCA	3

Table 1–2: The critical micellar concentrations for a number of bile acids. Fini: J Lipid Res; 1987

In general, hydrophobic BAs have lower CMCs. However, all CMCs are influenced by the presence of other amphipathic or lipophilic molecules and the concentration and type of surrounding cations (H^+ or Ca^{++} for example). In fact, the CMC may be reduced to half its monomeric value in the presence of lipophilic or amphipathic molecules [72]. *In vivo,* mixed micelles contain multiple BAs, phosphotidylcholines (a major amphipathic species), partly ionised fatty acids and monoglycerides. All of these contributing factors are thought to lower the *in vivo* CMC to a level much lower than that estimated based on chemical research.

The concentration of hydrogen ions (pH) in any solution also affects the solubility and CMC of individual bile acids. As a result of conjugation, the dissociation constants (pKa), reflecting the strength of the acids (and their pH dependent solubility), are estimated range from 3.79 to 5.03 at 25 degrees Celsius in water [76]. Unfortunately, the pKa of most BAs were derived before an understanding of micellar aggregates and maxima concentrations was refined. As a result, different pKa are reported in the literature for the same BAs. However, as the pH rises, a greater proportion of BAs become ionised and at a certain pH the anion concentration will pass the CMC. This pH value is the critical micellar pH (CMpH) and is defined as the lowest pH which ensures a sufficiently high concentration of the ionised form to create micelles. However, if the pH falls too low, conjugated BAs are likely to precipitate from the solution in the protonated form. Despite this, micelles are reasonably resistant to rapid pH changes; the presence of both charged and uncharged groups existing within the micelle provides stability and rapid pH changes do not immediately result in disaggregation of the micelles or precipitation of these molecules.

When the concentration and pH effects are viewed together, we see that the CMC must be lower than the solubility for the given BA at a given pH value. For glycine or taurine conjugates, this is not a problem at intestinal pH (6-8) or in aqueous solutions. Unconjugated acids with less ionic potential have much lower solubility and as a result are only found in very low concentrations (< 2% of the total BA pool) where they exist as monomers in solution or as components of mixed micelles.

While these factors make *in vivo* estimation of BA toxicity difficult to evaluate, we can at least evaluate whether BAs are predominantly protonated or ionised at pHs that exist in the oesophagus during refluxate episodes. At concentrations below the CMC, this will determine the predominant toxicity of the BAs as protonated BAs are more likely to have the potential to traverse the cell membrane than the ionised BAs (Table 1–3) [77].

Bile acid in refluxate	pH		
	<= 3	4	>= 5
CA (pKa 5.02)	Protonated	Protonated	Ionised
TCA (pKa 1.4)	Ionised	Ionised	Ionised
GCA (pKa 3.88)	Protonated	Ionised	Ionised
DCA (pKa 5.02)	Protonated	Protonated	Ionised
TDCA (pKa 1.4)	Ionised	Ionised	Ionised
GDCA (pKa 3.88)	Protonated	Ionised	Ionised

Table 1–3: Protonation state of different bile acids at various pH. Fini: J Lipid Res; 1987

As a result of the complex chemical and phase properties of BAs (and the different toxicities exerted by each), small experimental alterations may have profound effects on experimental findings. Endless variations of these are possible to generate for experiments, but *in vivo*, these are likely to vary from minute to minute. This makes *in vitro* imitation of DGOR and mixed reflux difficult.

1.4.3. Cell Death; Apoptosis, Necrosis and Autophagy

Cell death occurs in one of three ways: apoptosis, necrosis or autophagy. BAs may induce all three. At low concentrations hydrophobic BAs induce apoptosis [78-80] while at higher doses, they can induce necrosis.[81-83]. At concentrations which induce apoptosis, BAs have been similarly shown to induce autophagy [84].

1.4.3.1. Apoptosis

Apoptosis is a process of programmed cell death designed to prevent the uncontrolled release of intracellular components. It can be triggered by any stimulus which tells the cell to activate apoptotic machinery. The activation of this machinery may occur through an intrinsic pathway, an extrinsic pathway, or an endoplasmic reticulum (ER) stress pathway.

The intrinsic or mitochondrial pathway of apoptosis may be triggered by several forms of intracellular stress, including oxidative stress and DNA damage, all of which may be caused by BAs.[85-88] These signals converge on the mitochondria and result in membrane permeabilization and depolarization.[89-91] This results in the release of apoptogenic proteins such as cytochrome *c*, second mitochondria-derived activator of caspases (Smac) and apoptosis-inducing factor (AIF), amongst others. These activate the cysteinyl aspartate-specific proteases (caspases). Initiator caspases which are activated first (e.g. caspase-8 or 9) activate effector caspases (e.g., caspase-3 or 7), which cleave a wide array of cellular substrates resulting in cell death.[92-93] Two major pathways have been proposed for release of caspase activating proteins from mitochondria. The first is the opening of the mitochondrial permeability transition (MPT) pore on the inner mitochondrial membrane which results in mitochondrial depolarization. This may occur in response to exposures such as Ca^{++}, inorganic phosphate, alkaline pH, or reactive oxygen species (ROS). The second is associated with the formation of specific release channels in the outer mitochondria membrane by members of the B-cell lymphoma-2 (Bcl-2) family of proteins. Pro-apoptotic members (Bax, Bak and Bad) form oligomeric complexes within the outer mitochondrial membrane, allowing mitochondrial depolarization and the subsequent release of cytochrome c. However, this pathway is balanced by anti-apoptotic Bcl-2 family members such as Bcl-2 which inhibit the function of pro-apoptotic members through unclear mechanisms..[89-91, 94-95].

The extrinsic apoptotic pathway or "classical death receptor pathway" is initiated by trans-membrane death receptors. These include the TNF family of receptors including TNF-R1 and R2, TRAIL and FAS.[96] Activation of these receptors results in recruitment and activation of caspase 8 which in turn activates the effector caspases.[92-93] Caspase 8 may also cleave the Bcl-2 family member Bid to release an active truncated fragment, which activates the mitochondrial apoptotic pathway.[97-99]

The ER pathway occurs as a result of chronic ER stress leading to disordered cellular homeostasis and protein misfolding which activates the unfolded protein response. This results in activation of members of the Bcl-2 family which act on the mitochondria. The concomitant release of ER calcium accentuates the subsequent activation of pro-apoptotic cascade.[100-101] BAs can rapidly induce ER stress genes suggesting that they may induce ER stress.[102-103] Furthermore, it has been postulated that the detergent activity of DCA can, via phospholipase C activation and inositol

triphosphate, promote Ca^{++} from the ER, which can result in the activation of caspases and the induction of apoptosis. The release of Ca^{++} may be further enhanced by the ionophore ability of DCA.[104]

Whichever pathway activates apoptosis, the biochemical processes result in characteristic morphological changes prior to death. These changes include membrane blebbing, cell shrinkage, fragmentation of the nuclei, chromatin condensation, and chromosomal DNA fragmentation.

1.4.3.2. Necrosis

Necrosis is a form of un-programmed traumatic cell death in which intra-cellular components are released from the dying cell in an uncontrolled manner [105]. This may occur either because the insult was too acute to allow activation of the apoptotic machinery or because the insult was too great to allow the energy dependent processes necessary for apoptosis to occur. Therefore, it is similar insults which induce either apoptosis or necrosis and the severity or intensity of the insult which determines the outcome.

Similar to apoptosis, necrosis has a specific morphological pattern, albeit one that is more diverse that that seen in apoptosis. These features include early cell membrane permeablalisation, dilation of organelles, ribosomal dissociation from the E and nuclear disintegration [105-106].

1.4.3.3. Autophagy

Autophagy is a process where the cells own components are degraded through the cells own lysosomal machinery [107]. It is a mechanism through which a starving cell promotes survival by the reallocation of nutrients from non-essential to essential processes. The most common form of autophagy involves the formation of a bi-layer membrane around a targeted region of the cell to form an autophagosome. This isolates the contents from the cytoplasm. The resultant vesicle fuses with a lysosome, to form an autophagolysosome in which the contents are degraded.

Autophagy can be driving by a number of stimuli including starvation, cellular detachment, cell damage and repair, infection or as a mechanism of cell death. In the case of starvation or cellular detachment, autophagy leads eventually to apoptosis.

During autophagy, autophagolysosomes can be identified by staining for the protein Microtubule associated protein 1 light chain 3 (LC3). However, it is important to determine between activation of autophagy and failure of protease function which can lead to an accumulation of LC3 suggestive of autophagy. This will be further explained in subsequent chapters .

1.4.4. Bile Acid Induced Inflammation and Pathology in the Oesophagus

The squamous epithelium of the oesophagus lacks sufficient protective mechanisms to deal with recurrent exposure to BAs such as that seen in GORD. As a result, BAs can injure oesophageal cells through membranous and intracellular mechanisms, resulting in inflammatory mucosal damage and carcinogenic consequences.

At the level of the cell membrane, BAs may cause damage through detergent mechanisms or through inappropriate cell signalling. At concentrations above the CMC, BAs solubilise cell membranes, resulting in the release of membrane phospholipids and cholesterol and the generation of reactive ion species [108-109]. However, this mechanism is unlikely to explain the majority of BA toxicity in the oesophagus. BAs concentrations in the oesophagus rarely reach the CMC, and animal studies have shown significant mucosal barrier disruption occurs at concentrations below the level at which membrane solubilization occurs [110-111]. One particularly interesting finding is the presence of dilated intercellular spaces (DIS) between epithelial cells of the oesophagus when reflux occurs, even non-erosive reflux [112-113]. This could potentially allow refluxate to penetrate deeper into the mucosa, allowing access to the basal layer stem cells, enhancing the risk of mutagenic change in these cells.

At concentrations below the CMC, lipophilic BAs can incorporate themselves into the phospholipid bilayer of the cell membrane resulting in increased membrane fluidity and potentially causing alterations in cellular interactions and exosomal and endosomal functions [114-115]. These lipophilic BAs in the phospholipid bilayer can also interact with the intramembranous region of transmembrane receptors, causing inappropriate activation or deactivation and dysregulation of cell signalling. The Ras and the Mitogen Activated Protein Kinase (MAPK) pathways have been shown to be activated in this fashion [116-118].

Some BAs may traverse the cell membrane, where they can activate inflammatory pathways or exert mutagenic effects. Unconjugated BAs, which are usually protonated, may cross the cell membrane with relative ease as a result of their lipophilic properties. Conjugated BAs however (which account for the vast majority of the circulating pool), are predominantly ionised and cannot readily traverse membranes without a membrane transporter. However, the state of protonation of BAs, and thus the ability to traverse the cellular membrane, is heavily influenced by pH; unionized (protonated) forms predominate at acidic pH for taurine-conjugated BAs (pKa 1.9) and at neutral pH for unconjugated BAs (pKa 5.1). Once BAs are internalised, they become ionised and trapped inside the cells [119-120] where increasing intracellular concentrations have been shown to correlate with increasing mucosal damage [110-111].

Through these mechanisms, BAs can induce inflammatory, apoptotic and carcinogenic influence in oesophageal cells. The carcinogenic potential of BAs has been demonstrated to work through both

mutagenic and non-genotoxic mechanisms. Mutagenesis appears to result from the generation of reactive ions as well as direct BA genotoxicity. The non-genomic carcinogenic effects are mediated through gene expression alteration affected by epigenetic modulation as well as stimulation of inflammatory and pro-oncogenic proteins [121].

DCA has been shown to induce oxidative stress and genotoxicity in oesophageal cell lines through the generation of reactive oxygen species (ROS) [86]. In non-oesophageal cell lines, BAs have been shown to also generate reactive nitrogen species (RNS) [66]. The detergent effect of BAs releases arachadonic acid which is acted on by cyclooxygenase or lipoxygenase to release ROS during the formation of prostaglandins and leukotrienes. At levels insufficient to damage cellular membranes, intracellular BAs induce ROS through mitochondrial damage-induced leakage. ROS cause oxidative DNA damage and replication errors but also inactivate mismatch repair mechanisms potentiating this damage [66]. The p53 mutation, found in one third of BO and over ninety percent of OAC, frequently occurs as a result of oxidative damage and suggests that ROS are a likely carcinogen in OAC [122-123].

Significant genotoxicity has been demonstrated in HET-1A cells (representing normal oesophageal epithelium) exposed to BAs at pH 7. This was measured by the comet assay testing for DNA strand breaks. The same effect was seen at pH 4 without BAs, but no further toxicity was seen when BAs and low pH were used in combination. Over shorter exposure times, more similar to that seen in most episodes of reflux, DNA damage occurred without significant loss of cellular viability [88]. Significant chromosomal damage has also been seen with BAs. In the OE33 cell line (OAC) and KYSE30 (squamous cell carcinoma (SqCCa)) DCA at 50μMol in neutral pH induced the formation of micronuclei, indicating genotoxicity. Other BAs (taurocholic acid (TCA), glycocholic acid (GCA), taurodeoxycholic acid (TDCA) and glycodeoxycholic acid (GDCA)) had no effects, presumably because these are predominantly ionised at neutral pH. In acidic pH DCA again increased numbers of micronuclei but only at higher concentrations [86].

Some of the strongest evidence for the role of BAs in the molecular genesis of BO comes from research relating to caudal-related homeobox transcription factors 1 and 2 (CDX 1 and 2). These factors are thought to be regulators of differentiation necessary for the appropriate generation of intestinal mucosa. CDX-2 has been shown to be present in all cases of BO and in some cases of reflux oesophagitis [124]. Validated microarray studies have demonstrated that upregulation of CDX2 results in the expression of proteins more associated with intestinal mucosa and the suppression of proteins associated with squamous epithelium [121, 125-127]. BA exposure can independently induce upregulation of CDX2 in oesophageal cells in a dose and time dependent fashion through upregulation of pro-inflammatory signalling such as NF-κB [128-130]. In animal studies, low pH or BAs upregulate CDX2 after prolonged exposure [121, 125]. In normal

oesophageal cells exposed to pulsed low pH, a BA cocktail, or both, the CDX2 promoter can be demethylated and the expression of CDX mRNA can increase significantly as a result. This effect is attenuated in the presence of a methylating agent [121, 128-129].

BAs can also exert carcinogenic properties through inappropriate activation of other pro-inflammatory and pro-oncogenic signalling pathways. Chenodeoxycholic acid (CDCA) and its conjugates can stimulate cyclo-oxygenase-2 (COX-2) expression in SqCCa cells and as the pH changes from 7.3 to 6.5 the toxicity increases, consistent with the pH approaching CDCA's pKa and a greater proportion of molecules becoming protonated. Interestingly, inhibitors of the inositol-phophate-3 (IP3) kinase pathway and the MAPK/ERK pathway inhibited the increase in COX-2 levels, suggesting that this effect may be mediated through BA interactions at the membrane rather than the genetic level [131]. The activation of receptors by BAs via intra-membranous interaction has been demonstrated in a variety of cell lines outside of the oesophagus [116-118].

At the transcriptional level, work using OE21 (SqCCa), OE33 (OAC) and TE-7 (OAC) cell lines demonstrated that C-myc is upregulated in the presence of both low pH and BAs but not when either is present in isolation. C-myc is a proto-oncogene that has been shown to be upregulated in 50% of BO and in 90% of OAC [132]. NF-κB and interleukin-8 (IL-8) are also upregulated in OE33 cells exposed to BAs. This has been demonstrated using array studies (validated using RT-PCR) and through the measurement of NF-κB dependent genes [85, 133]. Other genes associated with BO have been shown to be altered by exposure to BAs (DCA), however, no validation was performed on these [133].

Once BO has been established the expression of numerous inflammatory mediators such as NF-κB, interleukin-6 (IL-6), IL-8 and COX-2 becomes constitutive [133-136]. However proliferative signalling is also upregulated in a predictable pattern. β-Catenin concentration is frequently raised resulting in increased levels of c-myc and cyclin D. These proteins are involved in the final steps in a number of pathways including the Ras/Raf/MAPK pathway which prevents the APC gene from inhibiting cellular proliferation [132-133, 137-138]. Loss of the control of cellular proliferation may be further compounded by the reduction in Transforming Growth Factor β (TGF-β) signalling [139]. Reflecting this, there is an increase in proliferative markers including Proliferating Cell Nuclear Antigen (PCNA) and Ki-67. p53 may be switched off early in BO, possibly due to increased levels of anterior gradient 2 protein, which compounds further oxidative DNA damage occurring as a result of ongoing H^+ and BA exposure [86, 122, 140-143]. A number of these signalling pathways are ones altered by BAs.

While the research described above suggests that BAs are a component of the inflammation-metaplasia-carcinoma sequence in the oesophagus, there are a number of confounding factors which must be taken into account:

- BAs are a heterogeneous group of moieties which are present in varying concentrations, phases, conjugations and ionisation potentials in DGOR. This makes research into the effects of reflux components, either as individual components or synergistically, difficult to perform, difficult to compare and difficult to translate into clinical research as innumerable variations of refluxate constituents exist, each of which may exert a level of toxicity from none to gross.
- Extrapolation from and corroboration with intestinal cell lines derived from outside of the oesophagus may not be feasible as the oesophageal epithelium is squamous where the remainder of the intestinal epithelium is columnar.
- Animal models differ from humans significantly and may not be a valid representation. While the animal forms of BAs promote mutagenesis and carcinogenesis in the intestinal tract, the composition and concentration of BAs in the refluxate and the reflux events themselves are rarely similar to that seen in humans [51, 66].

These factors combine to make the literature relating to GORD, BO and OAC difficult to interpret.

1.5. The Protective Role of Ursodeoxycholic Acid

UDCA is a secondary BA derived from CDCA through bacterial action in the colon. In healthy physiology UDCA and its conjugates (GUDCA and TUDCA) comprise roughly 2% of the circulating BA pool [144-145]. It differs from CDCA in that the hydroxyl group in the seven position is in the β conformation, rendering UDCA more hydrophilic than other BAs. Whether as a result of this, or otherwise, UDCA has a significantly less potent toxicity profile than other BAs.

While remaining an amphipathic molecule capable of forming micelles, UDCA lacks the aggressive cellular toxicity of other BAs. In humans and *in vitro* models, UDCA at concentrations of up to 500 μMol displays little potential for cell-membrane damage or the destruction of subcellular organelles [146-147]. However, above 500μMol UDCA becomes toxic to human cells in a fashion similar to other BAs.

Surprisingly UDCA has been shown to have anti-apoptotic, anti-inflammatory and immunomodulatory effects on various cell and tissue types. In particular, it been shown to abrogate the inflammatory and genotoxic effect of other BAs. It has demonstrated some therapeutic effect in treating cholestatic diseases of the liver such as primary biliary cirrhosis (PBC) and primary

sclerosing cholangitis (PSC). There is also clinical and animal evidence to suggest that UDCA may inhibit the adenoma-carcinoma sequence in both healthy and chronically inflamed colonic mucosa [148-150].

When first used to treat cholestatic liver diseases, it was thought that the therapeutic effect was exerted through a choleresis and through displacement of more hepatotoxic BAs from the circulating pool. Oral administration of supplementary UDCA (8-10mg/Kg) results in competitive displacement of hydrophobic BA from the circulating BA pool and results in UDCA levels rising to almost 50% of the total biliary BA concentration. This most likely occurs through competitive displacement of hydrophobic BAs from BA transporters in the terminal ileum [151-153].

However, it is now accepted that the therapeutic effects are also mediated through pathways that promote cell survival and modulate inflammatory responses. Research primarily using hepatic and colonic cell-lines, reflecting tissues in which BAs are known to induce pathology, have demonstrated that UDCA may have a role in reducing BA induced inflammation and mutagenicity by preventing the generation of ROS and RNS [154-156]. Furthermore, UDCA can prevent apoptosis through modulation of mitochondrial depolarisation, pro-apoptotic signalling and pro-survival signalling [156-158]. These functions appear to be mediated through a variety of both intra- and extra-cellular pathways including membrane effects, cell signalling, receptor activation and transcriptional activity (Figure 1–5).

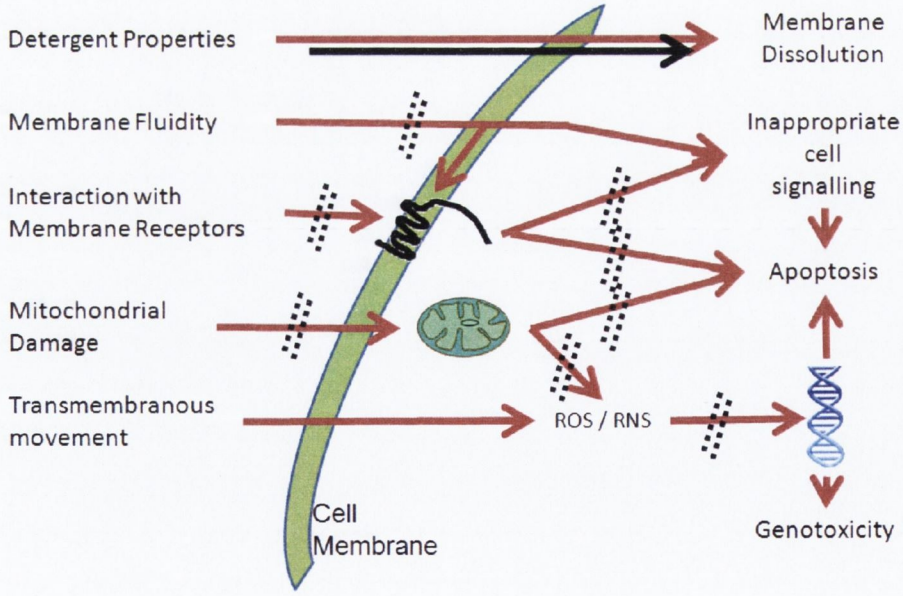

Figure 1–5: The toxic effects of DCA and UDCA on cellular function (Solid Red and Black lines) and the established mechanisms of UDCA's cyto-protective properties (Dashed Black lines). Each of these may have variable contribution in different BA-induced disorders.

The anti-apoptotic effects of UDCA are medicated through both the intrinsic and extrinsic apoptotic pathways. Toxic BA exposure can activate the intrinsic mitochondrial pathway of apoptosis through oxidative stress, DNA damage, and protein misfolding. Initiation of this pathway results in mitochondrial membrane depolarization through either opening of the mitochondrial permeability transition pore (MPT) on the inner mitochondrial membrane or by formation of specific release channels in the outer mitochondria membrane. Depolarization results in the release of apoptogenic proteins which activate the cysteinyl aspartate-specific proteases (Caspases). These cleave a wide array of cellular substrates and consequently cause cell death [159-160]. UDCA can inhibit both MPT opening and release channel formation, reducing BA induced "intrinsic" apoptosis [161-162]. The extrinsic pathway of apoptosis is activated through membranous "death receptors". UDCA has been shown to partially inhibit this pathway, possibly by its direct effects at the mitochondrial membrane [98].

UDCA may also inhibit apoptosis through mechanisms other than direct interaction with the mitochondria. In hepatocytes, UDCA can activate the MAPK pathway survival signal. In human colon cancer cells UDCA has been shown to inhibit DCA induced apoptosis through modulation of Epidermal Growth Factor Receptor (EGFR)/Raf-1/ERK signalling in a fashion that is not overcome with increasing DCA concentrations [116]. In primary rat hepatocytes UDCA activates the phosphoinositide-3-kinase (PI3K) survival pathway which protects against mitochondrial controlled apoptosis [163]. UDCA prevents apoptosis through inhibiting p53 induced transcription of Bax but the mechanism through which this works currently remains unknown [164].

The anti-inflammatory effects seen with UDCA appear to result from two different processes. One is through modulation of the pro-inflammatory signalling mechanisms that are upregulated by cell stress such as that caused by BAs. Experiments on hepatic and colonic cell lines have shown that UDCA can modulate many of the signalling pathways that BAs upregulate in the oesophagus. DCA has been shown to increase the expression of COX-2 in colonic cell lines through the ras/MAPK-p38 dependent pathway. UDCA inhibits this [117, 165]. In hepatic cell lines, UDCA induces production of anti-oxidants, potentially mitigating BA damage occurring as a result of ROS production [154-155], and UDCA itself does not appear to induce significant upregulation of ROS [68]. UDCA has been shown to inhibit Nuclear Factor κ Light Chain Enhancer of Activated B Cells (NF-κB) and Activator Protein 1 (AP-1) DNA binding and the upregulation of NF-κB dependent genes in colonic cell lines [166]. Interestingly, in this paper, the same results were seen in OE33 cells, an oesophageal cell line.

The second potential anti-inflammatory mechanism of UDCA is activation of the glucocorticoid receptor (GR). This may also prevent cellular apoptosis. UDCA can promote GR/chaperone

dissociation at a site outside of the normal ligand binding domain, inducing nuclear translocation [167-168]. The interaction appears to enhance the *trans*-repressive and inhibitory attributes of the GR without resulting in significant *trans*-activation [116, 167, 169-171]. Both cell line and animal models have demonstrated that the UDCA-GR interaction can inhibits apoptosis and suppress pro-inflammatory signalling such as Interferon-γ (IFN-y) induced HLA-DRA gene expression and NF-κB function, although not as effectively as glucocorticoids (GCs) [167, 172].

These experiments provide the basis for a hypothesis regarding the potential therapeutic role of UDCA in the oesophagus, where BAs have been shown to be pro-inflammatory and genotoxic. However, the majority of experiments have either used cells of hepatic or colonic origin or cell lines unrelated to the human gastrointestinal tract (COS7, CV-1 and HeLa [169], Rat Hepatocytes [167], IM1 and CHO [171], and T98G human glioblastoma cell line [173]) to study UDCA mediated cell signalling and the interaction between UDCA and the GR. Furthermore, all of the experiments studying the UDCA-GR interaction have either used plasmid over-expression of the GR or artificial reporter constructs to assess response to treatment. Whether these findings will translate to oesophageal cell lines or tissue has yet to be seen.

Despite the lack of molecular research regarding the effects of UDCA on oesophageal cells, one small clinical trial has been undertaken to assess the potential therapeutic benefit of UDCA in the oesophagus. In a cross-over trial design, Bozicas *et al* treated a group of BO patients with either a PPI or with a PPI in conjunction with UDCA in an attempt to prevent progression to dysplasia or OAC. While the trial showed no benefit of UDCA administration, it was underpowered (n=11) and probably of too short a duration to demonstrate benefit (t = 6 months on UDCA) [151]. Irrespective of this trial, the effect, or lack, of UDCA in preventing progression in BO would not imply that it could not prevent progression of normal mucosa to BO.

1.6. Summary

GORD represents a highly prevalent disease in western society with complex symptomatology, potentially lethal complications and, currently, poor treatment outcomes. While PPIs have dramatically altered the natural history of inflammatory GORD complications such as oesophagitis, ulcerations or strictures, they have failed to impact on the incidence of BO or OAC.

Research and therapeutic strategies have, until now, been targeted at preventing damage induced by acid. However, BAs have been identified as both synergistic and independent aetiological agents in the generation of BO and OAC. Repetitive exposure to a variety of forms of acid and bile reflux over a prolonged period is likely to result in either recurrent acute cellular destruction and healthy proliferative recovery or, the development of apoptosis resistant cells with genetic and protein alterations and a high carcinogenic potential.

The role of H^+ in the genesis of BO and OAC has been well studied; however, the role of BAs in this process is still a relatively novel concept. Evidence is accumulating supporting this hypothesis as a result of clinical, epidemiological, animal and molecular studies.

At the clinical level it has been demonstrated that:

- Acid suppression fails to inhibit the genesis of BO and OAC *in vivo,*
- BAs are a major components of human oesophageal refluxate,
- DGOR continues when acid refluxate has been neutralised,
- Greater exposure of the oesophagus to mixed reflux and DGOR correlates with increasing mechanical impairment of oesophageal function, increasing severity of inflammatory mucosal damage and the a higher likelihood of BO, and,
- Epidemiological studies have shown that DGOR is an independent risk factor for oesophagitis, BO and OAC.

Basic scientific research has shown that BAs:

- Are essential for metaplastic transformation of the oesophagus and that this effect is enhanced through the simultaneous exposure of acid,
- Have carcinogenic potential through mutagenic mechanisms, and,
- Induce the expression of pro-inflammatory and stress genes which over a prolonged period are likely to have a role in oesophageal mutagenesis and carcinogenesis.

Despite the precise aetiology of BO remaining unclear, molecular, clinical and epidemiological evidence has associated BAs with the pathogenesis of GORD and with a greater risk of developing BO and OAC. While acceptance of the toxic role of BAs in the genesis of BO and OAC remains controversial, the evidence is accumulating.

However, our therapeutic agents for targeting DGOR are limited. Our best therapy for GORD, including DGOR, remains the PPIs, but the absence of low pH is not sufficient to prevent development of BO or progression to OAC. Nor do we have sensitive or specific biomarkers to identify which GORD patients are at risk of developing these complications. Furthermore, the high prevalence of GORD and the relatively low risk of progression to complications or death from this disease means that screening for BO and OAC is not cost-effective.

There is crucial need to identify a cost effective and safe prophylactic agent that could be given to all GORD patients to reduce the incidence of BO and the risk of progression to OAC. Targeting BA toxicity, early in the course of GORD, may be a potential way to prevent these complications as well as reducing the symptomatic burden of the disease in general.

UDCA has been shown to ameliorate the inflammatory and apoptotic effects of more toxic BAs in the biliary system and large intestine. It protects against apoptosis medicated by both the "intrinsic" mitochondrial and the "extrinsic" death receptor pathways. It down-regulates the activity of signalling pathways such as AKT and MAPK and can inhibit pro-inflammatory transcription factors such as NF-κB and AP-1. Molecular research has shown these pathways to be active in the oesophagus and this suggests UDCA may have a beneficial effect in preventing BA toxicity in the oesophagus. The few published studies relating to the effects of UDCA on cell signalling in oesophageal cells support this hypothesis.

If UDCA is shown to provide anti-inflammatory signalling through the GR in the oesophagus, it potentially offers an anti-apoptotic or anti-inflammatory drug without the systemic GC side effects that are thought to result from genomic *trans*-activation [168-169]. If UDCA attenuates the genotoxic effects of more toxic BAs, either through suppression of chronic inflammatory carcinogenic signalling or through direct mitigation of mutagenicity, then it may be of use both in the treatment of GORD and possibly in the prevention of BO and OAC.

However, our understanding of the genomic, transcriptional and proteomic mechanisms of action of this molecule in the oesophagus is limited.

1.7. Research Aims

The role of BAs in inflammatory and neoplastic diseases in the oesophagus has been conclusively proven. There is a large body of scientific literature regarding the ability of UDCA to mediate anti-apoptotic effects and to reduce carcinogenic effects of hydrophobic BAs such as DCA.

Therefore, the aims of this research were:

- To investigate whether UDCA can modulate apoptosis and cell death in the oesophageal cell line HET-1A. Inflammation and apoptosis induced by BAs are closely related. Therefore modulation of one is likely to reflect modulation of the other.

- To investigate the role of DCA in modulating cell adhesion in the HET-1A cell line. Loss of adhesion is likely to contribute to the risk of erosions and ulcerations in the oesophagus as well as the risk of re-epithelialisation with BO. The role of DCA in reducing adhesion research strand occurred during experiments investigating the role of UDCA in modulating DCA-induced apoptosis.

- To investigate expression of the GR in the oesophagus and to determine whether UDCA can modulate this transcription factor in this tissue.

- To identify the complete profile of genes modulated by UDCA in oesophageal cells using gene array technology and to compare them to:

    - the gene profile modulated by DCA and Dexamethasone
    - genes known to be involved in the normal-BO-OAC sequence

Experimental Approach

1. The first part of this research investigated whether UDCA ccould modulate DCA-induced apoptosis and cell death in the oesophageal cell line HET-1A representing normal oesophageal epithelium. High content analysis tools (InCell Technology, nuclear counts, nuclear area analysis and MTT assays) were used to screen four BA concentrations (0,

100μM, 300μM and 500μM) at three time-points (four, eight and twenty-four hours) in order to determine whether UDCA can attenuate the cytotoxic effects of DCA. Subsequent investigations as to the mechanism of cell death were performed using Western blotting and flow cytometry.

2. In the second part of this research the role of DCA in modulating adhesion in oesophageal cells was investigated. General and specific adhesion assays were used to demonstrate that DCA induced a loss of adhesion in HET-1A cell lines. Re-adhesion and Western Blotting was used to demonstrate that modulation of adhesion occurred independently of apoptosis. Flow cytometry and immunofluorescent techniques were used to investigate the effect of DCA on the surface expression of a variety of integrins. Immunofluorescent staining of paraffin embedded explanted oesophageal biopsies was used to investigate whether DCA modulated the expression of integrins *in-vivo.*

3. In the third part of this research, the expression of the GR in oesophageal cell lines was characterised using Western blotting and real-time PCR. GR expression was confirmed *in vivo* by immunohistochemical staining of paraffin embedded oesophageal biopsy samples. The ability of UDCA to modulate the GR in oesophageal cell lines was investigated using high content analysis techniques (InCell), trans-activation and trans-repression assays.

4. The final part of this research investigated the gene expression profile induced by UDCA, DCA and Dexamethasone in oesophageal cells. The HET-1A cell line (representing undifferentiated normal oesophageal squamous cells) and the OE33 cell line (derived from OAC which had arisen from BO) were used as the cellular models. Gene expression profiles were determined using micro-array technology. Comparison between the profiles induced by UDCA and Dexamethasone, and UDCA and DCA elucidated similarities in the effects of these different cholesterol-based compounds in oesophageal cells. Comparison was also performed with a gene array already performed in the Institute of Molecular Medicine, TCD, which has identified a cohort of genes involved in the normal-BO-OAC sequence. RT-PCR was used to validate genes of interest identified during the array analysis. In theory, these were genes associated with inflammation, endoplasmic reticulum stress and apoptosis.

Chapter 2.

2. Ursodeoxycholic Acid Reduces Deoxycholic Acid Induced Apoptosis, but not Total Cell Death, in an Oesophageal Cell Line

2.1. Introduction

BAs are amphipathic derivatives of cholesterol synthesised in hepatocytes, secreted into the intestine and recycled to the liver through the entero-hepatic cycle. The polar nature of these molecules that confers the ability to form physiologically essential detergent micelles also potentiates their role as highly pathological entities. Consequently, the concentration and conjugation of BAs are tightly regulated [63-64, 174-178]. However, experimental models have demonstrated that significant cellular toxicity also occurs at concentrations below that at which BAs form micelles. The complex physico-chemical properties of BAs in conjunction with the inherently labile conditions of the intestine *in vivo*, makes BA toxicity in healthy physiology difficult to predict [72]. In dysregulated BA physiology, or pathological situations where high concentrations of BAs exist in the liver or intestine, BA-induced toxicity is almost guaranteed. This may be mediated through inflammation [131, 133], inappropriate cell signalling [116-118, 132], carcinogenesis [66, 85-86, 88, 133], or cell death [179-183].

In the oesophagus *in vivo*, levels of apoptosis correlate with the severity of oesophagitis [184]. While this is likely to occur as a result of low pH and BAs in DGOR, BAs have been shown to induce apoptosis in oesophageal cell lines and in cultures of primary oesophageal epithelial cells [185-186]. Rat models have been used to demonstrate that BAs induce significant levels of apoptosis in the oesophagus of rats who had undergone an oesophagoduodenostomy. In this group, glutathione levels were increased and the authors suggested that apoptosis and the consequent oesophagitis may be mediated by free radicals (ROS and RNS) [187]. The ability of BAs to induce free radicals in oesophageal cell lines has been demonstrated elsewhere [85-86, 188]. Althoug other forms of cell death have not been studied *in vivo*, these findings suggest that BAs induce either inflammation or apoptosis, possibly in a dose dependent fashion. As BO cells are more resistant to apoptosis, it is likely that selective pressure induced by DGOR allows BO to develop at the expense of apoptosis sensitive squamous epithelium. Therefore, modulation of BA-induced apoptosis may also reflect modulation of inflammation in normal squamous epithelium.

2.1.1. Bile Acids Induce Apoptosis Through Multiple Mechanisms.

At high concentrations hydrophobic BAs have been shown to induce necrosis [81-83]. At lower concentrations they appear to induce apoptosis through activation of three pathways: the intrinsic pathway, the extrinsic pathway, and the endoplasmic reticulum (ER) stress pathways [78-80].

The intrinsic pathway of apoptosis is triggered by several forms of intracellular stress, including oxidative stress and DNA damage [85-88]. These signals converge on the mitochondria, where they induce membrane permeabilization and depolarization [89-91]. This occurs through the opening of the MPT on the inner mitochondrial membrane or through formation of specific release channels in the outer mitochondrial membrane by members of the B-cell lymphoma-2 (Bcl-2) family of proteins. Loss of the mitochondrial membrane potential causes the release of apoptogenic proteins which activate the initiator caspases such as caspase-8 or 9. These subsequently activate effector caspases (e.g., caspase-3 or 7), which cleave a wide array of cellular substrates resulting in cell death [92-93].

The extrinsic apoptotic pathway is initiated by trans-membrane death receptors. These include the Tumour Necrosis Factor (TNF) family of receptors including TNF-R1 and R2, TRAIL and Fas [96]. Activation of these receptors results in recruitment and activation of caspase 8 which in turn activates the effector caspases [92-93]. Caspase 8 may also cleave the Bcl-2 family member Bid to release an active truncated fragment, which activates the mitochondrial apoptotic pathway [97-99].

The ER pathway of apoptosis is activated through chronic cellular stress leading to disordered cellular homeostasis and protein misfolding. This activates the unfolded protein response which results in activation of pro-apoptotic members of the Bcl-2 family. The concomitant release of ER calcium accentuates the subsequent activation of pro-apoptotic cascades [100-101]. BAs can rapidly induce ER stress genes suggesting that they may induce ER stress [102-103]. Furthermore, it has been postulated that the detergent activity of DCA can, via phospholipase C activation and inositol triphosphate, promote Ca^{++} release from the ER, which can result in the activation of caspases and the induction of apoptosis [104].

2.1.2. UDCA Modulates the Apoptotic Pathways Activated by Hydrophobic Bile Acids *In Vitro*

Despite significant pathology associated with BAs, few therapeutic agents are available to modulate these diseases. UDCA has been used therapeutically in the western world for last three decades to treat cholestatic diseases of the liver such as PBC. Apoptosis of hepatocytes and biliary epithelial cells is well documented in these diseases and the role of UDCA as an anti-apoptotic agent *in vitro* has been demonstrated by numerous groups [189-193]. The anti-apoptotic effects of UDCA can be modulated through four primary mechanisms: protection of the mitochondria, inhibition of pro-apoptotic signalling, activation of pro-survival signalling, and activation of the GR.

2.1.2.1. UDCA Modulates Mitochondrial Depolarisation Induced by DCA

Modulation of mitochondrial mediated apoptosis by UDCA has been shown to occur through at least three distinct mechanisms: inhibition of the MPT, modulation of the Bcl-2 family of proteins and through maintaining functional oxidative phosphorylation in the presence of BAs.

2.1.2.1.1. UDCA Modulates the Mitochondrial Permeability Transition Pore

Initial studies by Botla *et al* and Rodriguez *et al* regarding BA-induced mitochondrial apoptosis demonstrated that exposure of primary rat hepatocytes to DCA resulted in a dose and time dependent increase in apoptosis [82, 156, 194]. This research identified MPT formation as a mechanism through which hydrophobic BAs induced apoptosis. UDCA, in isolation, did not induce apoptosis. Pre-treatment of cells with UDCA (from 5 to 60 minutes) inhibited MPT activation, reduced mitochondrial swelling and depolarisation, and reduced the release of cytochrome c induced by Phenylarsinine Oxide (PhAsO, an MPT inducer) and hydrophobic BAs. The induction of apoptosis by agents other than BAs (TGF-β, okadaic acid, Anti-Fas antibody) was found to be similarly targeted by UDCA [194-196]. The protective effect of UDCA was concentration dependent up to a critical threshold of 500uM [194-195]. Interestingly, UDCA prevented hydrophobic BA-induced apoptosis to a greater extent than cyclosporin A (CyA, an MPT inhibitor) suggesting that this molecule modulated apoptosis through mechanisms other than just modulation of the MPT [82, 156, 194]. Finally, it was demonstrated that other hydrophilic BAs, such as hyocholic acid, failed to exhibit similar protective effects suggesting that the cyto-protective effects were specific to UDCA [81-82, 156, 197].

2.1.2.1.2. UDCA Induces Alteration in the Expression of the Bcl-2 Family of Proteins

It was subsequently identified that UDCA also modulates the expression of the Bcl-2 family of proteins. However, this data less consistently and less convincingly demonstrates the anti-apoptotic benefit of UDCA. Rodriguez *et al* demonstrated that in hepatocytes isolated from Sprague-Dawley rats fed chow supplemented with DCA, UDCA or the combination, Bcl-XL (an anti-apoptotic member of the Bcl-2 family) expression was increased by both UDCA and UDCA/DCA feeding. However, expression of Bad (a pro-apoptotic Bcl-2 family member) was seen to increase two-fold after exposure to DCA but five-fold after exposure to the combination of UDCA and DCA. Levels of expression of Bax and Bcl-2 remained unchanged. Within isolated mitochondrial fractions levels of these proteins were similarly variable [156]. In a similar experiment, modulation of the Bcl-2 proteins by UDCA was similarly demonstrated by Oyama *et al.* However, in this model there were no changes in the levels of Bcl-XL, Bcl-Xs or Bcl-2 [198]. In cell culture UDCA prevented upregulation of Bax induced by DCA, okadaic acid or TGF-β [156, 194-196].

Despite these *in vitro* findings, studies of primary human hepatocytes have failed to demonstrate alterations in Bcl-2 expression on exposure to UDCA [199]. Even if the *in vitro* results were consistent, in *Bax*-/- cells DCA still induced apoptosis and UDCA pre-treatment still reduced BA-induced apoptosis [200]. This suggests that the magnitude of *Bcl*-2 family alterations in UDCA mediated cytoprotection is limited. Furthermore, BA-induced apoptosis still occurs rapidly in the presence of a protein synthesis inhibitor (cyclohexamide) suggesting that protein synthesis is not necessary for DCA induced apoptosis [201].

2.1.2.1.3. UDCA May Prevent BA Induced Dysfunction of Oxidative Phosphorylation

BAs also induce mitochondrial depolarization through inhibition of oxidative phosphorylation. DCA, CDCA and lithocholic acid (LCA) have been shown to impair the function of complexes I, III and IV of the electron transport chain while the function of complex II remains unaffected. Consequently, these BAs have consistently been shown to inhibit state-3 mitochondrial respiration (adenosine di-phosphate (ADP)-stimulated oxygen consumption) in a dose-dependent manner and may increase state-4 respiration (the oxygen consumption by isolated mitochondria using a particular substrate in the absence of ADP and poisons or inhibitors) [81, 197, 202]. This results in a reduction in intra-cellular adenosine tri-phosphate (ATP), failure of ATP-dependent Ca^{++} homeostasis and consequently, cell death [81, 203-204].

In isolation, UDCA concentrations less than 100μM do not appear to impair oxidative metabolism but higher doses (300μM) result in effects similar to other BAs: decreased state-3 oxidation rates and respiratory control ratios (the ratio of state-3: state-4 respiration) of numerous respiratory substrates. However, low dose UDCA (30μM) demonstrated protective effects in the setting of BA exposure, inhibiting the CDCA- or LCA-induced reduction in state-3 oxidation [83, 202]. Conversely, 300μM UDCA in combination with CDCA or LCA demonstrated greater impairment of state-3 respiration, greater ATP depletion and increased levels of cytochrome c release than the individual BAs in isolation. Correspondingly, the combination treatment resulted in greater cellular death [83, 197].

The loss of UDCA cyto-protection at higher concentrations suggests a dose related phenomenon. However, in similar experiments also using rat hepatocytes, lower dose combinations of UDCA and CDCA (50uM each) resulted in enhanced cell death over either in isolation, as determined by LDH assay. Interestingly, in the co-treatment experiment, reduced levels of apoptosis were seen in a nuclear morphology-based assay. The apoptotic markers caspase-9 and PARP cleavage were similarly lower in the UDCA/CDCA co-treated group than in the CDCA treated group. Necrotic cell death was felt to account for the discordance in findings and the authors hypothesised that UDCA-enhanced mitochondrial respiratory dysfunction could prohibit ATP-dependent caspases from exerting their functional effects, switching apoptosis to necrosis and therefore reducing the

levels of apoptotic markers [203]. However the switch into necrosis was speculation and the authors made no reference to other forms of cell death (i.e. autophagy) in their research.

2.1.2.2. Inhibition of Pro-Apoptotic Death Receptor Signalling (Fas) by UDCA

Pro-apoptotic death receptors are members of the TNF family of cell membrane receptors. Regarding BAs, the most studied is the Fas Receptor (FasR, CD95). FasR activation occurs *in vivo* through the interaction of Fas ligand (FasL) with trimerized membranous FasR [98, 205]. When stimulated, this activates the activator caspases -8 and -10 resulting in the activation of executioner caspases. In the majority of cells, including hepatocytes, amplification of this pro-apoptotic death receptor signal by mitochondria is needed to induce apoptosis [206]. The cleavage of Bid by caspase 8 is one mechanism through which mitochondrial recruitment occurs [96, 207-209].

Research regarding the role of mitochondria in BA-induced apoptosis suggested that FasR was utilized in the process [79, 158]. BA stimulation (CDCA, glycol-chenodeoxycholic acid (GCDCA) and DCA) can result in the oligomerization and activation of FasR in the absence of exogenous FasL resulting in caspase-8 activation, mitochondrial depolarization and subsequently apoptosis [79, 158, 210]. The absence of FasR, or the presence of a dominant negative (DN) Fadd or DN c-Flip-s (downstream mediators of FasR function) abolished BA-induced apoptosis to baseline levels in certain cell lines, even in the presence of pro-apoptotic signalling modifications [79, 158, 210]. However, higher DCA concentrations still induced apoptosis, suggesting that apoptosis also occurs in a death receptor independent mechanism [79, 211].

UDCA modulates both BA and FasL-induced FasR-mediated apoptosis. It can reduce anti-Fas-antibody (a surrogate activator of FasR) induced apoptosis in hepatocytes by over 80% [194]. Treatment with UDCA (<100μM), TUDCA (<400μM), and surprisingly tauro-chenodeoxycholic acid (TCDCA, <200μM), also inhibited apoptosis induced by co-culture of hepatocytes with mouse fibroblasts expressing trimerized FasL (a more physiological stimulus), although to a lesser magnitude than that seen with FasR antibodies [157]. In these experiments [157, 180], UDCA did not affect the levels of FasR expression or trimerisation although other authors have demonstrated significantly increased membrane expression of FasR in response to GCDCA in cells containing BA transporters [212-213].

In other studies using cells expressing a BA transporter, GCDCA was capable of inducing Fas induced activation of caspase 8 and the subsequent release of cytochrome c, while TCDCA was not. However, inhibition of PI3K resulted in TCDCA activating apoptotic and mitochondrial machinery. This suggests that TCDCA simultaneously stimulates pro-survival mechanisms which overcome the pro-apoptotic FasR signalling [214-215] (See Section 2.1.3).

In contrast to these *in vitro* findings, in a rat model fed UDCA supplemented chow, there was no reduction in apoptosis after hepatocytes were isolated and exposed to fibroblasts expressing trimerized FasL. Whether this suggests that the protective effects of UDCA are transient or whether cytoprotection will not work *in vivo* remains unclear. While FasR is not indispensable for inducing BA-induced apoptosis, the presence of a functioning receptor greatly enhances BA induced apoptosis in a fashion that is not only mediated by *Bid*-induced mitochondrial depolarization, but also by p53 [79, 84, 211, 216].

2.1.2.3. Inhibition of Intra-Cellular Pro-Apoptotic Signalling (p53)

Activation of the pro-apoptotic transcription factor p53 occurs as a result of cellular stress or DNA damage, both of which may be BA-induced. Once activated, it modulates both the intrinsic and extrinsic pathways of apoptosis at multiple levels. Mitochondrial depolarisation induced by p53 can be inhibited by CyA suggesting MPT activation. Pro-apoptotic p53 signalling is also mediated through direct activation and increased expression of members of the Bcl-2 family including Bax, Bid, Puma and Noxa. The extrinsic apoptotic pathway is modulated by p53 through increased expression of death receptors concurrently with increased expression of their activating ligands [217-219].

When TGF-β is used as an apoptotic stimulus UDCA and TUDCA pre-treatment can reduce p53-mediated expression of Bax, caspase activation and the magnitude of the apoptotic response. The mechanisms for this were varied. UDCA inhibited nuclear translocation of p53 and DNA binding by preventing the dissociation of mdm-2 from p53 [164]. Pre-treatment also inhibited E2F mediated increases in p53 expression seen after TGF-β exposure [196].

Fewer studies have investigated the role of this molecule in BA-induced apoptosis and conflicting evidence exists regarding the effects of BAs on p53 expression or subcellular localization [84, 181, 199].

2.1.3. UDCA Activates Pro-Survival Signalling Which Overcome Pro-Apoptotic Signals

Pro-survival signalling mechanisms which are activated by UDCA and which modulate apoptosis have been extensively studied. Both hydrophobic and hydrophilic BAs activate EGFR through intra-membranous activation of the receptor [79, 158]. This results in downstream signalling through the p42/44 MAPK (Ras-Raf-MEK-ERK), p38 MAPK, and PI3K dependent (Akt-mammalian Target of Rapamycin (mTOR) and -Protein kinase C (PKC)) pathways [154, 220-226]. These pathways can promote cell survival and proliferation. Activation of the JNK MAPK

signalling pathway is less consistently demonstrated although it has been shown in some models to occur through FasR or TGR5 [215, 227-228].

The p42/44 survival pathway is activated by BAs in cells of hepatic and colonic origin [79, 116, 158, 220-221, 226, 229]. Low doses of DCA, CDCA and UDCA that had little effect on apoptosis induced significant apoptosis after inhibition of MEK1/2 or ERK or in the presence of a DN ERK [158, 221]. Surprisingly, in the presence of the MEK1/2 inhibitor PD98059 DCA increased the level of apoptosis from 3% to 20%, but UDCA increased levels of apoptosis to 55%. Corresponding increases in caspase levels and PARP cleavage suggested that this was apoptosis mediated death [158]. Interestingly, functional EGFR has been shown to be involved in FasR activation and the FasR has been shown to activate the p42/44 pathway [215, 230].

Other authors have shown ERK over-expression reduced the levels of apoptosis seen with DCA stimulation [221] and that ERK1/2 inhibition (UO126) resulted in a similar loss of cytoprotection in the presence of TUDCA [226]. Similar pro-survival effects have been seen with the p38 pathway where inhibition of p38 by SB203580 in hepatocytes abrogated the protective effect of TUDCA [221, 226].

Activation of the PI3K (and the downstream Akt and PKC) pathway by EGFR is similarly modulated by BAs and influences UDCA mediated cytoprotection. Akt activates NF-κB and phosphorylates Bad, preventing it from inactivating the anti-apoptotic proteins Bcl-2 and Bcl-XL [231]. PI3K-mediated activation of PKC enzymes, particularly PKCζ, promoted cell survival and proliferation [232]. However, PI3K activation by BAs appears specific, with TCDCA, but not GCDCA, resulting in activation. Furthermore, downstream signalling of PI3K by BAs appears selective; TCDCA activates PI3K but not Akt [223]. However, expression of constitutively active PI3K prevented BA induced apoptosis and PI3K inhibition enhanced the apoptotic potential of BAs in rat hepatocytes, but to a lesser magnitude than inhibition of ERK [79, 158, 223].

In colonic epithelial cell lines (HCT116) different observations regarding EGFR have been reported. Perhaps the greatest is that inhibition of EGFR with ZD1839, an EGFR tyrosine kinase inhibitor, prevented DCA-induced apoptosis suggesting that pro-apoptotic signalling is mediated through this receptor in this model, possibly through the FasR as discussed above. UDCA itself failed to activate EGFR in the colonic system but pre-treatment still inhibited DCA-induced EGFR activation and the downstream ERK and AP-1 activation [116]. Interestingly though, in the HCT116 cell line, both UDCA and DCA activated Akt in a PI3K dependent fashion [225]. UDCA pre-treatment prevented DCA-induced apoptosis and reduced the levels of caspase -3, -8, -9 and cleaved PARP. However, UDCA mediated cytoprotection was only apparent after a minimum of 10 hours pre-treatment and was transient with levels of DCA induced apoptosis being equal after 18 hours whether UDCA pre-treatment had been administered or not. Similar findings have been

reported elsewhere [233]. The anti-apoptotic effect was abolished with a DN Akt and inhibition of PI3K again transformed UDCA into a cytotoxic agent in its own right [225].

2.1.4. UDCA Exerts an Anti-Apoptotic Effect through the Glucocorticoid Receptor

The GR is an NSR involved in modulating inflammation, growth, development, metabolism and apoptosis [234-235]. Activation of this receptor can inhibit the function of pro-inflammatory and pro-apoptotic transcription factors such as AP-1 and NF-κB through a process called *trans*-repression [173, 236-238]. UDCA stimulation induces nuclear translocation of the GR and can induce *trans*-repression although the mechanism of GR-UDCA interaction remains unclear [168-169, 171, 239].

The anti-apoptotic effects of UDCA have been shown to be modulated partially through the GR. In studying the protective effects of UDCA in reducing TGF-β induced apoptosis, Sola *et al* demonstrated that UDCA induced nuclear translocation of the GR and prevented TGF-β induced suppression of GR expression at both the mRNA and protein level [239]. Small Interfering RNA (SiRNA) mediated knockdown of the GR reduced the protective effects of UDCA. Furthermore, GR knockdown prevented the increased levels of E2F induced by TGF-β stimulation, as well as the E2F suppression seen with UDCA in isolation as was discussed above in section 2.1.2.3 [196, 239]. However, whether this transcription factor has a role in the UDCA mediated modulation of BA-induced apoptosis has not been investigated.

2.1.5. Summary

BAs are amphipathic cholesterol derivatives with a potentially high level of toxicity. However, the toxicity is dependent on the individual BA and the specific tissue [185, 216]. Consequently, these molecules have been implicated in the aetiology of a variety of inflammatory, metabolic and neoplastic diseases. In the oesophagus apoptosis has been shown to increase with increasing severity of oesophagitis and in oesophageal cell lines BAs have been shown to induce significant levels of apoptosis [184-187].

The majority of the scientific literature suggests that UDCA mediates a reduction in both basal and stimulated levels of apoptosis in cell models of disease. The mechanisms through which UDCA has been shown to reduce apoptosis are diverse and include mitochondrial protection, activation of pro-survival signalling, modulation of p53 signalling and activation of the GR. These pathways appear to be activated simultaneously and to interact extensively with each other.

However, any potential anti-apoptotic effect offered by UDCA is complex and is influenced by numerous factors. The protection offered by UDCA may be dependent on a certain minimum duration of pre-treatment. Some research has demonstrated that co-treatment is sufficient to exert protection while other research has demonstrated that ten hours pre-treatment with UDCA prior to DCA alone is required to exert protection. Some research has demonstrated a pro-apoptotic effect of UDCA at low concentrations and it is generally agreed that UDCA is pro-apoptotic at high concentrations. This may be the case in our series of experiments in the HET-1A cell line where there was a reduction in proliferation without an apparent alteration in cell cycle progression. However, protective effects are not simply dependent on concentration and duration of pre-treatment. For example, UDCA co-treatment may actually increase the intracellular concentration of a hydrophobic BA *in vivo* while still exerting a protective effects [82, 194].

While the majority of the published scientific literature suggests that UDCA is a non-specific inhibitor of apoptosis, the potential anti-apoptotic effects of UDCA can be difficult to elicit and are not guaranteed. In the majority of research demonstrating either effect (beneficial of harmful) of UDCA, numerous complementary models have often been used to investigate the mechanism of cell death, making the conclusions difficult to dismiss.

2.2. Aims

BAs have been demonstrated to have a role in the aetiology of oesophagitis, BO and OAC. They have been demonstrated to be pro-inflammatory and pro-apoptotic in oesophageal tissues. Despite their documented pathology, no therapeutic agents exist to modulate their toxicity in the oesophagus.

UDCA offers a potential candidate to modulate BA toxicity in the oesophagus. As apoptosis is often induced by inflammatory pathways and inflammation can occur as a result of the activation of apoptotic machinery, UDCA could potentially target both pathways. Despite this, no research to date has investigated the therapeutic potential of UDCA in modulating BA-induced cell death in the oesophagus.

Thus, the aims of this chapter were:

- To investigate the toxicity profiles of UDCA and DCA in the HET-1A oesophageal cell line.
- To investigate whether UDCA could modulate DCA induced cell death in the oesophageal cell line HET-1A and,
- To determine a concentration range at which UDCA may exert protective effects,
- To determine the optimal temporal treatment strategy to elicit an anti-apoptotic effect of UDCA in oesophageal cell lines,
- To determine the mechanism through which UDCA exerts any potential anti-apoptotic effects.
- To validate any *in vitro* findings in explanted oesophageal tissue.

2.3. Methods

2.3.1. Cell Lines, Culture and the Quantification of Cell Concentrations

2.3.1.1. Cell lines and culture

The HET-1A [240], HCT116 [241] and HUH-7 [242-243] cell lines were used for these experiments. These cell lines represent normal squamous epithelium of the oesophagus, colonic adenocarcinoma and human hepatoma cells respectively. The origin of these cells and the rationale for their use is explained in Section 9.1.1. Cells were grown in appropriate media: Bronchial Epithelium Basal Medium (BEBM, Lonza, Allendale, NJ, USA), McCoy's 5A Medium (Gibco, Billings, MT, USA) and Dulbecco's Modified Eagle Medium (DMEM, Gibco, Billings, MT, USA) respectively. Cells were cultured in cell culture flasks at 37°C in 5% CO_2 until 80-90% confluent. To passage cells, the cells were washed twice in buffered salt solutions (Hanks Buffered Salt Solutions (HBSS, Sigma, St. Louis, MO, USA) or phosphate buffered saline (PBS, Sigma, St. Louis, MO, USA)), trypsinised in 0.05% trypsin containing EDTA (Gibco, Billings, MT, USA) for 3-5 minutes until cells detached from plastic, harvested with either soybean trypsin inhibitor (SBTI, Gibco, Billings, MT, USA) or complete medium (containing 10% foetal calf serum (FCS), Gibco, Billings, MT, USA) and subsequently centrifuged for 3 minutes at 1100rpm. The supernatant was discarded and the cell pellet loosened by gentle agitation. The cells were either re-seeded in a fresh cell culture flask or counted in order to seed cells for experimental use.

2.3.1.2. Cell Counting

Cell concentrations were determined using a bright-line haemocytometer (Hausser Scientific, Horsham, P.A., USA) in conjunction with the exclusion dye 0.4% trypan blue (Sigma, St. Louis, MO, USA) to exclude non-viable cells. 20µL of medium containing cells was diluted in 180µL trypan blue and mixed well. The mixed cell suspension was injected into the haemocytometer underneath the cover slip. The volume of fluid under each 4X4 counting chamber was $0.1mm^3$. The number of cells was calculated as average / mm^3 X 10 (dilution in trypan blue) X 10^4 (overall multiplication factor: $X10^5$).

2.3.2. Proliferation and Viability Assays

Proliferation of a cell population represents a balance between two competing factors: cell replication and cell death [244]. If the rate of replication exceeds that of cell death the number of

cells will increase, and if the rate of cell death exceeds replication the cell population will decrease. While replication occurs solely through mitosis in the case of somatic eukaryotic cells, cell death may occur through apoptosis, necrosis or autophagy [245-246], each with its own characterised molecular and macroscopic phenotype [106]. For example, necrosis is associated with cellular swelling and disruption of the plasma membrane in the early phases, while in apoptosis morphological changes including nuclear condensation and membrane blebbing occur. However, clear cut morphological changes are often only seen in the late stages of cell death and interpretation of these changes is highly operator dependent [105, 247]. If a stimulus modifies the rate of either mitosis or death, a change in the rate of proliferation will occur relative to that of untreated cells. Consequently, techniques which quantify viable cell number directly or through other mechanisms such as metabolic activity represent a simple tool for screening the effects of numerous chemicals on cell populations. However, each is subject to biases and limitations.

2.3.2.1. Immunofluorescent Nuclear Counting and Nuclear Area Estimation

2.3.2.1.1. Background

Nuclear count, representing cell count, is a crude technique in an era when numerous mechanisms of cell death are understood and in which molecular tools allow detailed investigation of stages and mechanisms of cell death [247]. However, automated nuclear counts offer a facile way of screening large numbers of treatments to develop an understanding both temporal and relative toxicology. The simplicity of this assay overcomes the potential pitfall of trying to analyse the morphological features associated with different forms of cell death.

Despite the positive aspects of this simple technique, inherent deficits also exist. Nuclear counts do not differentiate between healthy and dying cells. Furthermore the fraction of dead or dying cells may be underestimated as these cells often lose adherence and are removed during the staining process. Conversely, the fraction of healthy cells may also be underestimated as healthy cells may also be lost during processing

Despite these caveats, we reasoned that given the relatively long doubling time of HET-1A cells and HUH-7 cells (32-48 hours and 47-51 hours respectively), simple cell counts would represent a method of assessing BA toxicity and total cell death, whether through apoptosis, necrosis or autophagy [240, 242-243, 248]. The faster doubling time of the HCT-116 cell line (21 hours) meant that proliferation would represent a greater variance within this system [241].

2.3.2.1.2. Experimental Methods

For growth curves, HET-1A cells were seeded at a density of 7.5 X 10^3 cells/200μL in a Nunc 96-well plate. Cells were allowed to adhere to the well base overnight. The medium was replaced with

complete fresh medium containing 0, 100μM, 300μM or 500μM concentrations of DCA or UDCA (Sigma, St. Louis, MO, USA). At each treatment time-point, half the medium was removed and replaced with 8% paraformaldehyde (PFA) in PBS at 37°C. After 15 minutes at 37°C, the media and PFA were aspirated and the cells were gently washed with PBS. Nuclei were stained with 1:2000 Hoechst 33342 (Invitrogen, Carlsbad, CA, USA) for 15 minutes at room temperature (RT) and then washed twice with PBS at RT. Using the GE InCell Analyser 1000 (GE Healthcare, Wauwatosa, WI, USA) the number of cells, based on the number of nuclei in four 10X magnification fields per well were counted and the values averaged. All treatments were performed in duplicate wells and each experiment was performed at least three times.

To investigate the effects of UDCA on DCA induced cell death, cells were seeded at 7.5 X 10^3 cells per well in a Nunc 96-well plate and left to adhere overnight. At the appropriate time point prior to DCA treatment (0, 4 or 18 hours), all media was replaced with fresh complete medium containing 100, 300 or 500μM UDCA. Wells not requiring pre-treatment had media removed and replaced with fresh media. 1μM staurosporine (STS) was used as a positive control to induce apoptosis and cell death. At t0, after the pre-treatment duration, the media was aspirated and replaced with media containing 0, 100, 300 or 500μM DCA, alone or in combination with appropriate concentrations of UDCA, to establish matrices of UDCA pre-treatment and DCA treatment concentrations. For nuclear counting, cell were stained and imaged as described above (Figure 2–1). This provided information on cell number as well as nuclear geometry. Cell counts were normalised to the untreated control for each time-point. Again, all treatments were performed in duplicate wells and each experiment was performed at least three times.

Prior to performing the BA experiments, the effects of various concentrations of dimethyl sulphoxide (DMSO, Sigma, St. Louis, MO, USA), reflecting the vehicle concentrations for each of the BA concentrations, on cell survival was investigated. DMSO itself can be toxic to cell lines and so it was necessary to estimate the contribution of this to the toxicity seen with BAs. This demonstrated that only at concentrations of 0.20% and 0.32% DMSO (V/V), equivalent to a total BA concentration of 600μM or above, did DMSO induce a significant reduction in viability (to 62% and 60% respectively) relative to untreated cells (Figure 2–2).

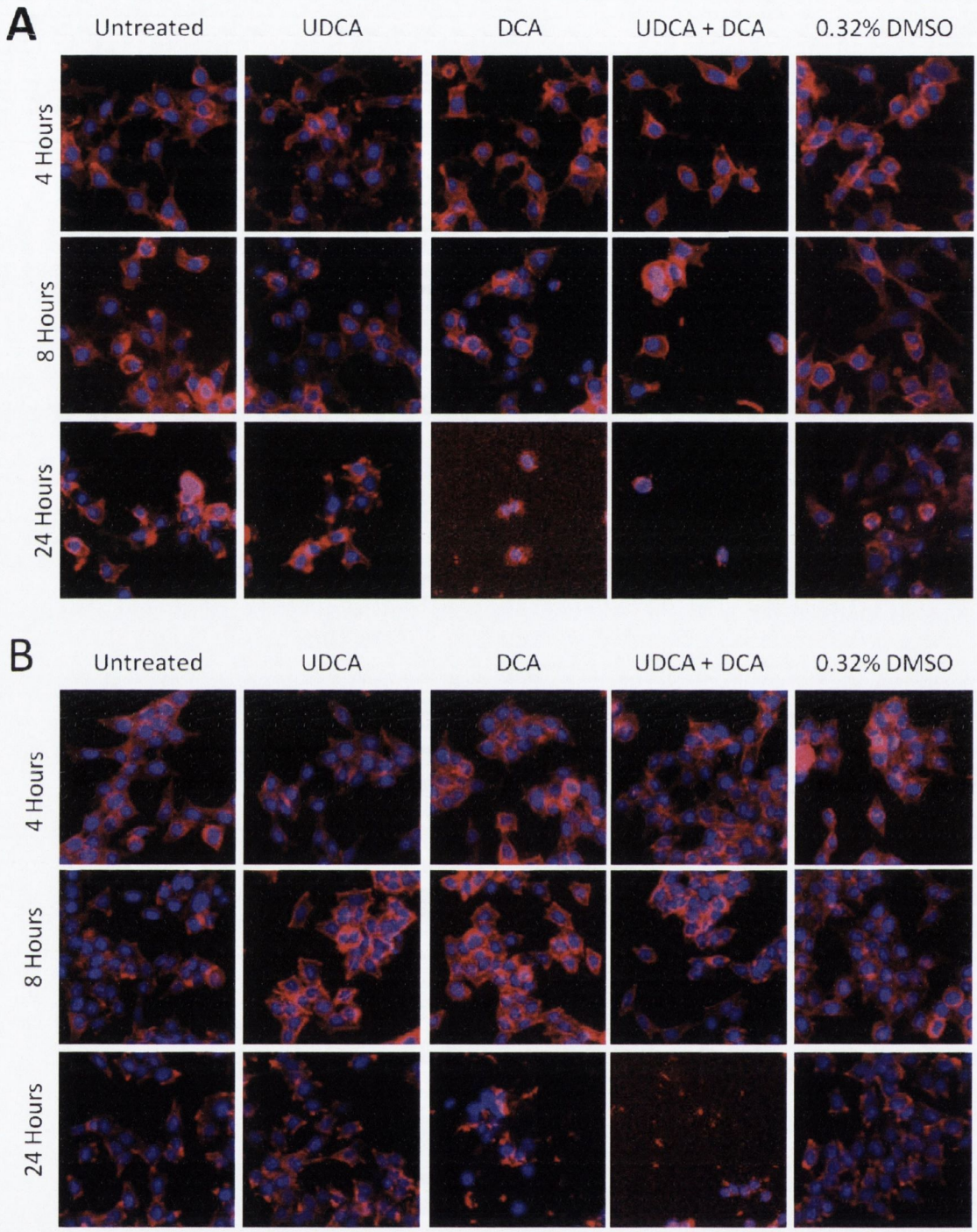

Figure 2–1: Images of HET-1A (A) and HCT116 (B) cells used to determine cell counts after BA treatment. Cells were seeded and treated with BAs as described above. After fixing and staining, images were acquired using the InCell 1000. Cell counts were performed using the GE InCell Analysis Software. Red; Phalloidin (Actin stain), Blue: Hoechst (Nuclear Stain).

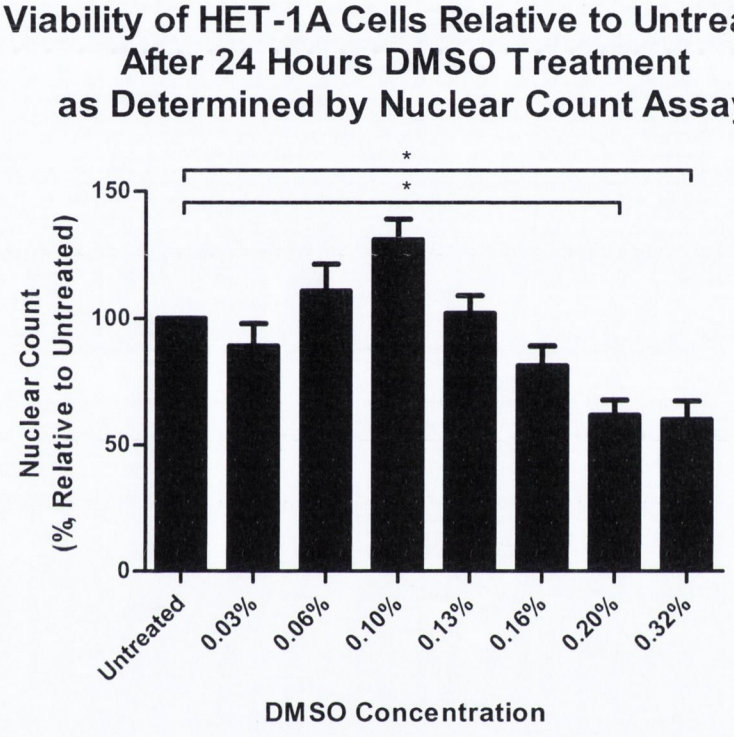

Figure 2–2: The effect of various concentrations of DMSO on nuclear count after 24 hours treatment. High concentrations of DMSO (0.2% and 0.32%) reduce cell viability as determined by a nuclear count assay. Cells were seeded in 96-well plates at a concentration of 7.5 X 10^3 cells per well and allowed to adhere for 24 hours. The medium was then replaced with fresh complete medium containing DMSO. After 24 hours the cells were fixed with 4% PFA for 15 minutes. The nuclei were stained with Hoechst and images were acquired using the GE InCell Analyser 1000. The number of cells, based on the number of nuclei in four 10X magnification fields per well were counted and the values averaged. Data is represented as Mean and SEM of N = 3. * denotes ANOVA $p < 0.05$.

2.3.2.2. MTT Assay

2.3.2.2.1. Background

The MTT assay is a colorimetric assay measuring the activity of an enzyme which converts 3-(4,5-Dimethylthiazol-2-yl)-2,5-diphenyltetrazolium bromide to purple water-insoluble formazan [249]. The addition of a DMSO allows solubilization of the water insoluble formazan. Quantification is achieved by measuring absorbance at a wavelength of 570nM in a spectrophotometer. The assay was initially designed to assess cellular proliferation but it has now become accepted as a measure of cell viability and is frequently used as a screening tool to assess the cytotoxicity of compounds.

Again however, this simple assay is subject to functional issues. Firstly, agents which effect mitochondrial function can reduce conversion of MTT to formazan. When first designed, the site of MTT reduction was thought to solely be within the mitochondria. As such, the assay was thought to assess the activity of mitochondrial dehydrogenases, reflecting mitochondrial function and thus the number of viable cells. Consequently, factors affecting the mitochondrial function, such as medium overconsumption or cellular over-confluence, were thought to have significant effects on this assay. More recent research suggests that greater than half of MTT is reduced within the cytosol or in cellular compartments other than the mitochondria [250-251]. Therefore, agents toxic to the mitochondria bias the results, but to not completely invalidate them. Similarly to the nuclear count assay, we reasoned that MTT conversion would be a reasonable representation of cell death given the short duration of treatment and the relatively slow proliferative rate the cell lines used in this research.

2.3.2.2.2. Experimental Method

Cells were seeded at a density of 7.5 X 10^3 cells/200uL of media in a Nunc 96-well plate. The cells were allowed to adhere overnight. All media was gently removed and fresh media added containing the appropriate concentration of UDCA for pre-treatment. Wells not requiring pre-treatment had media removed and replaced with fresh media. After the pre-treatment duration, all media was again removed gently and replaced with fresh media with supplements and BAs (DCA and /or UDCA) as in the nuclear count experiments. Three hours prior to the designated time-point, 20uL of 2.5mg/mL MTT (Sigma, St. Louis, MO, USA) was added to each well to allow sufficient conversion of the fomazan salt prior to the end of the experiment. At each time-point, all media was removed gently and the cells and crystals were dissolved by the addition of 100uL of DMSO. The plates were gently agitated for 30mins to allow complete dissolution of formazan crystals and subsequently the absorbance at 570nM was read using a BioTek ELx800 absorbance micro-plate reader (BioTek, Winooski, VT, USA). Background absorbance estimated in wells containing

DMSO alone was subtracted from the readings and all measurements were normalised to the untreated control for the time-point.

Again, prior to performing the BA experiments, the effects of various concentrations of DMSO, reflecting the vehicle concentrations for each of the BA concentrations, on cell survival were investigated. This demonstrated that at no concentration did DMSO significantly reduce the viability of HET-1A cells after 24 hours exposure (Figure 2–3).

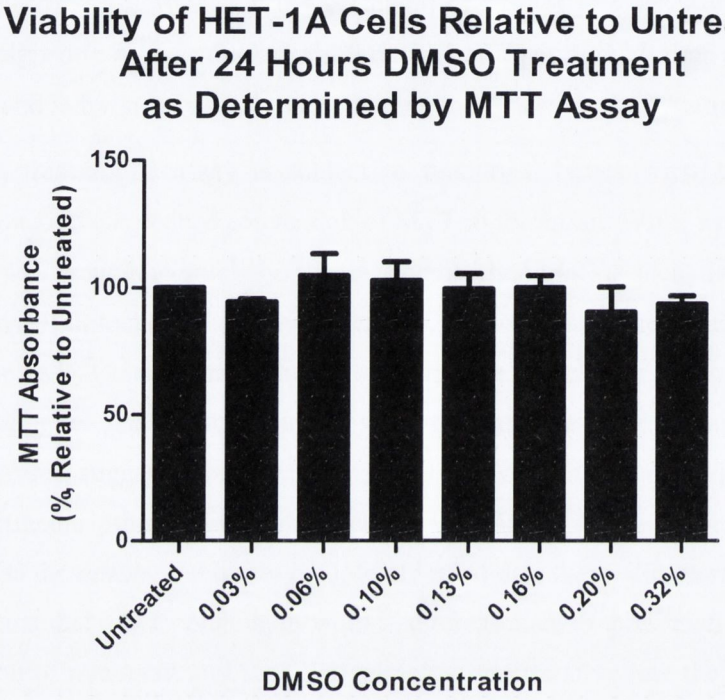

Figure 2–3: The effect of various concentrations of DMSO on MTT conversion after 24 hours treatment. No concentration of DMSO studied significantly reduced viability as determined by an MTT assay. Cells were seeded in 96-well plates at a concentration of 7.5 X 10^3 cells per well and allowed to adhere for 24 hours. The medium was then replaced with fresh complete medium containing DMSO. Three hours before the end of the treatment, (after 21 hours treatment) 20ul of 2.5mg/ml MTT was added to each well. After 24 hours the medium was gently aspirated and the formazan crystals dissolved in DMSO. Absorbance at 570nM was determined using a plate reader and values normalized to untreated cells. Data is represented as Mean and SEM of N = 3.

2.3.3. Cell Cycle Analysis

2.3.3.1. Background

The rate of cellular proliferation is partially determined by how fast cells progress through a mitotic cycle. Resting or quiescent cells reside in the G0 phase of the cell cycle until induced to progress through G1, S and M phases by growth factors, cyclins or mitogens. Each phase is characterised by predictable localisation of subcellular structures, the activation of mitotic machinery and the relative number of chromosomes. In order to produce two daughter cells, the quantity of DNA doubles during the S phase as the strands are replicated. When duplication is complete, the cell is tetraploid, containing twice as much DNA as a diploid cell.

Assuming that the cells in culture contain 44 autosomes and two sex chromosomes, the cells in G0/G1 phase are diploid, cells in the M phase are tetraploid and cells in the S phase contain a quantity of DNA varying between diploidy and tetraploidy. Thus, the intensity of DNA staining in a diploid cell should be half that of a tetraploid cell. For hypo-diploid or hyper-diploid cells the theory of relative fluorescence still holds true (Figure 2–4).

Thus, staining of DNA and the measurement of the relative intensity of DNA staining in a population of cells allows estimation of the proportion in each phase of the cell cycle. In rapidly dividing cells, the analysis of cell cycle can be enhanced through cell cycle synchronisation in the population of cells, through growth factor restriction of pharmacological methods. However, in our experiments, due to the slow proliferative rate of the cells, this technique was not employed and unsynchronised populations were studied.

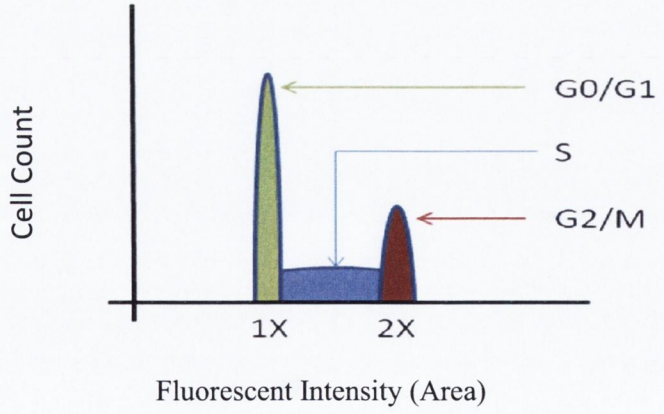

Figure 2–4: Representation of DNA histogram acquired during flow cytometric analysis of cell cycle.

2.3.3.2. Experimental Methodology

HET-1A cells were seeded at a concentration of 2 X 10^5 in Nunc 6-well plates and allowed to adhere overnight. Media was replaced with fresh complete BEBM containing no BA, 300μM UDCA or 300μM DCA. After twenty-four or forty-eight hours the media was removed and discarded. Cells were enzymatically detached using trypsin-EDTA. The cells were collected and spun at 1100rpm for 3 minutes. The cells were resuspended in 0.5mls PBS and the suspension added to 4.5mls of 70% ethanol on ice. The cells were maintained in the fixative/permeabalizer for 2 hours. To stain the DNA, the ethanol suspension was spun at 1100rpm to pellet the cells. The ethanol supernatant was removed and the cells re-suspended in 5mls PBS. This was re-spun at 1100 rpm for 5 minutes. The supernatant was removed and the cells were resuspended in propidium iodide containing RNAse (BD Biosciences, Franklin Lakes, NJ, USA) for 30 minutes at 37°C. The cells were washed and the intensity area determined using flow cytometry (Beckman Coulter Cyan ADP 9 Colour, Brea, CA, USA). DNA intensity histograms were analysed using FCS Express (De Novo Software, CA, USA).

2.3.4. Flow Cytometric Determination of Mitochondrial Membrane Potential

2.3.4.1. Background

Oxidative Phosphorylation and the production of ATP, the major source of energy for energy dependent cellular processes, occur in the mitochondria. The generation of an electric potential between the inner and outer mitochondrial space occurs as a result of hydrogen ion transport. This in turn allows the formation of energy rich phosphate bonds in ATP. This provides energy to drive cellular processes.

Disruption of the mitochondrial membrane potential induces apoptosis or necrosis and occurs in response to apoptotic stimulation. DCA and other BAs have been shown to induce the MPT, resulting in a reduction in mitochondrial membrane potential and the initiation of apoptosis. UDCA has been shown to attenuate this in a fashion similar to cyclosporin A, an MPT inhibitor [82, 252].

Tetramethylrhodamine methyl ester (TMRM) is a cell permeable dye which accumulates in mitochondria. Although at high concentrations, it may be toxic to mitochondrial respiration, at low concentration, it selectively stains mitochondria proportionally to the mitochondrial membrane potential.

2.3.4.2. Experimental Method

HET-1A cells were seeded at a density of $2x10^5$ cells per well in a Nunc 6-well plate and allowed to adhere overnight. The cells were treated for 4 hours with BAs, vehicle, or PhAsO as a positive control. 30 minutes prior to the end of the treatment period, TMRM (Invitrogen, Carlsbad, CA, USA) was added to each well to give a final concentration of 100nM. Simultaneously, the fluorescent exclusion dye Hoechst 33358 (Invitrogen, Carlsbad, CA, USA) was added to give a final dilution of 1:2000. At the end of the treatment period, the medium and detached cells were aspirated, placed in tubes for flow cytometry spun at 1500rpm for 5 minutes to pellet the cells. Concurrently, the adherent cells were enzymatically detached using trypsin-EDTA. When the cells were detached, the trypsin was neutralised with SBTI and the enzymatically detached cells added to the pelleted cells in the flow cytometry tube. Data was acquired using a Beckman Coulter Cyan flow cytometer, and cells which stained positive for Hoechst 33358 (dead cells) were excluded from the analysis.

2.3.5. Flow cytometric Analysis of Quantity and Mechanism of Cell Death.

2.3.5.1. Background

Numerous flow cytometry methods have been optimised to investigate the mechanism of cell death. Phosphatidylserine is a phospholipid component located on the inner side of the cell membrane in healthy cells. Early in apoptosis this loses its membrane polarity and is found on the external side of the membrane. It is regarded as an early marker of apoptosis. Annexin V (AV), an endogenous protein, binds to and can be used to identify phosphatidylserine [253]. Exclusion dyes such as Hoechst 33358 or Propidium Iodide (PI) are excluded from cells that have an intact and functional plasma membrane. In late apoptosis or necrosis the membrane becomes unable to exclude these dyes from the cell and they bind to DNA. Combining staining for phosphatidylserine (using AV) and an exclusion dye allows differentiation of early apoptosis, late apoptosis and necrosis. However, detergents, such as BAs, or proteases such as trypsin have the potential to damage the cellular membrane potentially resulting in false positive results from this assay.

A potentially more sensitive method for determining apoptosis alone is the terminal deoxynucleotidyl transferase nick-end labelling (TUNEL) method [254-255]. A late feature of apoptosis is the cleavage of DNA into 300kD fragments and subsequently into 50kD fragments. This occurs as a result of caspase dependent activation of nucleases. Labelling these DNA breaks using FITC labelled-deoxyuridine triphosphate (dUTP) and terminal deoxynucleotidyl transferase (TdT) allows fluorescent identification of these DNA breaks. However, in cells that have suffered severe DNA damage false positives may occur. This method appears not to be as susceptible to

detergent effects as other assays and more accurately reflects apoptosis rather than apoptosis in combination with necrosis [256-258].

2.3.5.2. Experimental method

Cells were seeded at a density of 2 X 10^5 cells per well in a Nunc six well plate. Cells were allowed to adhere overnight. The media was aspirated gently and replaced with fresh media or fresh media with UDCA to pre-treat. After pre-treatment period, the media was aspirated gently and replaced with media containing DCA, UDCA or a combination of the two. After treatment, the media was aspirated gently and stored. 0.5mL of 0.05% Trypsin EDTA was added to each well and the plate was incubated at 37°C until the cells were no longer adherent to the plate (2-3 mins). The cells were aspirated and added to the previously removed supernatant. The wells were washed with PBS and this was also added to the supernatant. The trypsin was neutralised with 0.5mL of SBTI.

2.3.5.2.1. Annexin V – Propidium Iodide Method

The cells were spun at 300g for 5 minutes, the supernatant removed from the pellet by gentle aspiration and the cells re-suspended in 1mL of PBS. The cells were again centrifuged at 300g for 5 minutes. The cells were re-suspended in 100uL of annexin V binding buffer. 5uL of Annexin V (AV, IQ Products, Groningen, Netherlands) was added to each 100uL of cell suspension and the cells were incubated for 15 mins on ice in the dark. Subsequently the cells were washed and 1:1000 PI (Sigma, St. Louis, MO, USA) added just prior to flow cytometric analysis (Beckman Coulter Cyan ADP 9 Colour, Brea, CA, USA).

2.3.5.2.2. Terminal Deoxynucleotidyl Transferase Nick-End Labelling - Propidium Iodide Method

Cells were fixed and stained according to the instructions provided for the Apo-Direct kit (BD Biosciences, Franklin Lakes, NJ, USA). Briefly, cells were suspended in 1mL 1% PFA on ice for one hour. The suspension was centrifuged at 300g for 5 minutes. The cells were washed twice in 5mL of PBS. The cells were re-suspended in 1mL of ice cold 70% ethanol and were stored overnight at -20°C until staining. The cells were centrifuged at 300g for 5 mins and re-suspended in 1mL wash buffer. This step was repeated again. The cells were incubated for 1 hour at 37°C with DNA labelling solution (containing reaction buffer, TdT enzyme and FITC-dUTP). The cells were spun and rinsed twice with rinse buffer. The pellet was re-suspended in 0.3mL of PI-RNAse staining buffer and incubated for 30 minutes in the dark. Cell staining was analysed by flow cytometry (Beckman Coulter Cyan ADP 9 Colour, Brea, CA, USA).

2.3.6. Analysis of Poly ADP Ribose Polymerase (PARP) and LC3 cleavage by Western blotting

2.3.6.1. Poly ADP Ribose Polymerase (PARP)

Located in the cell nucleus, the primary function of PARP is to identify and target repair machinery to single strand DNA breaks. Activation occurs in response to multiple inducers of DNA damage. Inactivation is performed through cleavage by caspase-3 or caspase-7 resulting in the formation of cleavage products of 85kDa and 24kDa molecular weights. The 24kDa product contains the DNA biding domain of the enzyme which can still bind to DNA damage sites, preventing the binding of un-cleaved PARP and the initiation of further repair attempts. During apoptosis, the activation of high levels of caspases results in the formation of large quantities of cleaved PARP, of which the 85kDa fraction is readily detectible.

2.3.6.2. LC-3

Microtubule associated protein 1 light chain 3 (LC3) is a marker of autophagy. The identification of a mechanism of cell death independent of apoptosis and necrosis led to the identification of autophagy, a process in which cellular components undergo auto-degradation. During autophagy, double membrane structures engulf organelles, to form autophagosomes, and subsequently fuse with lysosomes, to form the autophagolysosomes in which the organelle is degraded. This process may be used by any cell to induce cell death or to promote survival through the recycling of subcellular components to repair essential cellular processes or to provide energy.

During autophagy, cytoplasmic LC3-I (18kDa) is recruited to the autophagolysosome and undergoes cleavage near the c-terminal end resulting in the formation of a 16kDa fraction. Thus by monitoring the conversion of LC3-1 to LC3-II it is possible to monitor the induction of autophagy. However, interpretation of LC3 conversion is difficult as the relative levels of LC3-I and LC3-II depend on both recruitment and degradation of the protein. Thus, for appropriate interpretation, the lysosomal protease inhibitor pepstatin A (Sigma, St. Louis, MO, USA) is used to prevent degradation. This allows an understanding of the relative contribution of recruitment and degradation to the process of LC3-I and LC3-II level alteration.

2.3.6.3. Experimental Method

Protein expression was determined using Western blotting (A complete protocol is available in Appendix 4). Cells were seeded in 6-well plates and allowed to adhere and grow until 80-90% confluent. The cells were stimulated with BAs or controls for appropriate durations. At the end of the stimulation, the media was aspirated, placed in a centrifuge tube and spun at 100rpm for five minutes to pellet the detached cells. The pellet was gently disaggregated by flicking. To both the

centrifuged cells and the plate wells, 40uL of Radioimmunoprecipitation assay (RIPA) buffer containing fresh protease inhibitors (PMSF, Leupeptin, and Sodium Orthovanadate (Sigma, St. Louis, MO, USA)) was added and the cells incubated on ice for 30 minutes. The lysed cells were collected and pooled in the respective centrifuge tube, after which the lysate was sonicated to ensure complete cellular disruption and to further lyse nuclear fragments remaining in the lysis buffer.

Quantification of the protein concentration in the lysate was performed using the Pierce BCA Protein Assay Kit (Thermo Fischer Scientific, Waltham, MA, USA).

After quantification of concentration, equal concentrations of protein were diluted to 20uL volume with dH_2O. 7uL of 4X Llamelli Buffer was added and the lysate boiled at 95°C for 5 minutes. The tube was then cooled on ice and centrifuged to collect the evaporated fluid. 25uL of each sample was loaded into SDS-PAGE electrophoresis gels. Due to the significantly different MWs of the protein studied, a 10% gel was used for the PARP immunoblots, and a 15% gel for the LC-3 immunoblots. 10% gels were run for 60 minutes and 15% gels for 30 minutes at 200 volts and 40 millamps using a Consort E865 electrophoresis power supply (Consort, Turnhout, Belgium). The protein was subsequently transferred to PVDF membrane using a semi-dry technique. For high MW proteins 60 minutes transfer was used and for low MW proteins, 30 minutes.

After transfer, the membrane was blocked for 60 minutes in 5% dried milk powder in 0.1% TBST. The membrane was then incubated in 5% dried milk powder in TBST containing primary antibody at a concentration of 1:1000 with gentle agitation overnight at 4°C. Mouse-anti-human PARP antibody was supplied by Promega (Madison, WI, USA) and mouse anti-human LC3 by Nanotools (Clone 5F10, Nanotools, Teningen, Germany). After primary incubation, the membrane was washed 3 times for 5 minutes in 0.1% TBST to remove residual primary antibody. The membrane was then incubated with 1:2000 HRP linked secondary antibody in 5% dried milk powder for 60 minutes at RT. The membrane was washed 3 times for 5 minutes in TBST and then incubated with 4-Iodophenylboronic Acid (4-IBPA) based ECL. Western blots were developed using the Agfa Curex CP1000 (Agfa, Mortsel, Belgium).

2.3.7. Determination of Oesophageal Explant Viability by Lactate Dehydrogenase Estimation

2.3.7.1. Background

Lactate dehydrogenase (LDH) is an enzyme present at high concentrations in the cytosolic compartment of all cells. LDH that is released into medium suggests a loss of cell membrane

integrity. This usually occurs during cell death, whether occurring through apoptosis or necrosis. Therefore an estimation of the released LDH relative to intracellular LDH can be used as a means to estimate cytotoxicity induced by various stimuli.

Released LDH is used to catalyze the reduction of NAD^+ to NADH and H^+ by oxidation of lactate to pyruvate. Subsequently, diaphorase uses the formed NADH and H^+ to catalyze the reduction of a tetrazolium salt (INT) to formazan. The absorbance of this salt at 490-520nM is read using a microplate reader. Correlation with a standard curve is required to estimate the actual LDH concentration present in a sample.

2.3.7.2. Experimental Method

An LDH Cytotoxicity Assay Kit (Cayman Chemicals, Ann Arbor, MN, USA) was used to determine LDH release from oesophageal tissue explants after exposure to BAs.

With the patient's consent, biopsies were acquired during gastroscopy from the endoscopy department in St James Hospital. Ethics approval had previously been provided by the hospital ethics committee. 6 biopsies were taken from each of five patients, who were undergoing gastroscopy for non-oesophageal indications including coeliac screening, investigation of abdominal pain, etc. Biopsies were taken only from patients with macroscopically normal oesophagi. The samples were placed in medium and incubated at 37°C for 4 hours. Each individual explant sample was then exposed to complete medium, or medium containing 0.2% DMSO, 300μM UDCA, 300μM DCA, the combination of 300μM UDCA and 300μM DCA or 300μM UDCA pre-treatment prior to 300μM DCA.

After 24 hours stimulation, 100μL of supernatant was aspirated and the tissue in the remaining medium was mechanically homogenised, triton-X added to a final concentration of 0.1% and the explant cells sonicated to release all of the intracellular LDH.

LDH concentrations in the 100μL supernatant pre- and post-tissue disruption were established using the LDH cytotoxicity Kit and an estimate of the proportion of total LDH released by BA treatment was determined.

2.3.8. Statistics

For parametrically distributed data statistical analysis was performed using Analysis of Variance (ANOVA). *Post-hoc* analysis to determine significance between treatments was performed using Dunnett's test for normalised data and Tukey's test for non normalised data. For the MTT and nuclear count data, a two way ANOVA was used to investigate the influence of both time and BA concentration on cell viability. In all cases, a two-tailed α of < 0.05 was considered significant.

For comparisons between the nuclear count and MTT assays Bland-Altman plots were used. Comparison between two methods designed to measure the same parameter will often lead to a high degree of correlation (using Pearson's Correlation coefficient or the Coefficient of Determination) and a small amount of variance by virtue of the bias that high measurements in one assay will correlate with high measurements in another assay and low measurements will correlate with low measurements. This inherent bias can lead to overestimation of the similarity of two techniques. What is more important to understand in comparing assays is an understanding of any constant or predictable bias between the two assays and the variability between the two reported results. Ideally, two genuinely similar assays should demonstrate minimal constant bias and limited variance.

The Bland-Altman plot provides a graphic representation of these factors [259-260]. In the Bland-Altman Plot used in this research, the mean results of two assays ([A+B]/2) is plotted on the *x* axis and the absolute difference between the assays ([A-B]) is plotted on the *y* axis. Using the mean value of the assays provides an estimate of the real absolute value by assuming that neither assay is precisely correct in its measurement. The mean difference between the assays and the mean difference +/- 2SD of the difference between the assays (limits of agreement of the assays) are plotted against the *y* axis. This allows direct visualisation of the mean difference, the variance of the difference between the two systems and whether there is a change in the variance between the systems at different mean measurements.

2.4. Results

2.4.1. Ursodeoxycholic Acid Reduces the Toxic Effects of Deoxycholic Acid in HUH-7 Cells Consistent with the Published Scientific Literature.

One of the most extensively researched and established effects of UDCA is that of preventing apoptosis in hepatocytes. The anti-apoptotic properties of UDCA have been demonstrated in attenuating the apoptotic effects of not only hydrophobic BAs but also other toxic chemicals such as ethanol and okadaic acid and apoptosis inducers such as TGF-β. However, the protective effect is not ubiquitous, and frequently the experimental design is poorly specified. Researchers have simultaneously exposed cells to UDCA and DCA and demonstrated protective effects, while others have found that pre-treatment is needed to elicit this effect. Research in colonocytes has further clouded the issue, demonstrating that different durations of pre-treatment may be needed to illicit protective effects [116, 225].

To establish that the anti-apoptotic model was reproducible in our laboratory we first investigated whether UDCA could prevent cell death induced by the hydrophobic BA DCA in HUH-7 cells. Cells were treated with various doses of DCA and UDCA, alone or in combination, with or without UDCA pre-treatment. After 48 hours, a nuclear count assay demonstrated that 100μM DCA had reduced the normalised nuclear count to 58.76% (95% CI: 20.11% to 97.41%, $p < 0.05$) and 300μM DCA to 42.26% (95% CI: 25.95% to 58.58%, $p < 0.01$) relative to untreated cells (Figure 2–5A). Both short duration (four hours) and long duration (eighteen hours) pre-treatment with 300μM UDCA prior to 100μM DCA prevented a reduction in nuclear count below that of the untreated control (80.86%, 95% CI: 32.03% to 129.07% and 86.28%, 95% CI: 41.47% to 131.10% respectively). 4 hours pre-treatment with UDCA prior to 48 hours exposure to 300μM DCA again reduced the toxicity of DCA.

In view of confusion in the literature regarding whether UDCA treatment is continued in conjunction with an apoptotic stimulus, we also treated HUH-7 cells with a combination of UDCA and DCA. 300μM UDCA pre-treatment followed by co-treatment of cells with UDCA and either 100μM or 300μM DCA did not consistently demonstrate a beneficial effect. 300μM UDCA in conjunction with 100μM DCA increased the reduction in nuclear count above that of 100μM DCA alone, to 42.26% (95% CI: 25.95% to 58.58%). This enhanced toxicity was seen with all combinations, except 4 hours 300μM UDCA pre-treatment followed by co-treatment with 100μM DCA. This combination demonstrated a non-significant reduction in the toxicity of 100μM DCA (mean diff 12.26 ± 16.69, $p = 0.440$).

A similar pattern was seen in the MTT assay after 48 hours treatment with 100μM DCA, with co-treatment enhancing the toxicity above that of DCA treatment, however, no salvage of cell death induced by either 100 or 300μM DCA was identified (Figure 2–5B).

Finally, in order to confirm that a reduction in apoptosis was accounting for the reduction in cell death we performed immunoblots to examine the relative expression of cleaved PARP in the 300μM DCA treatment group. Compared to 300μM DCA, there was lower expression cleaved PARP in the 300μM UDCA pre-treatment group but greater expression in the 300μM co-treatment group suggesting that pre-treatment was reducing and co-treatment enhancing the levels of apoptosis (Figure 2–6).

These findings were consistent with the published literature regarding the effect of UDCA in reducing apoptosis and total cell death.

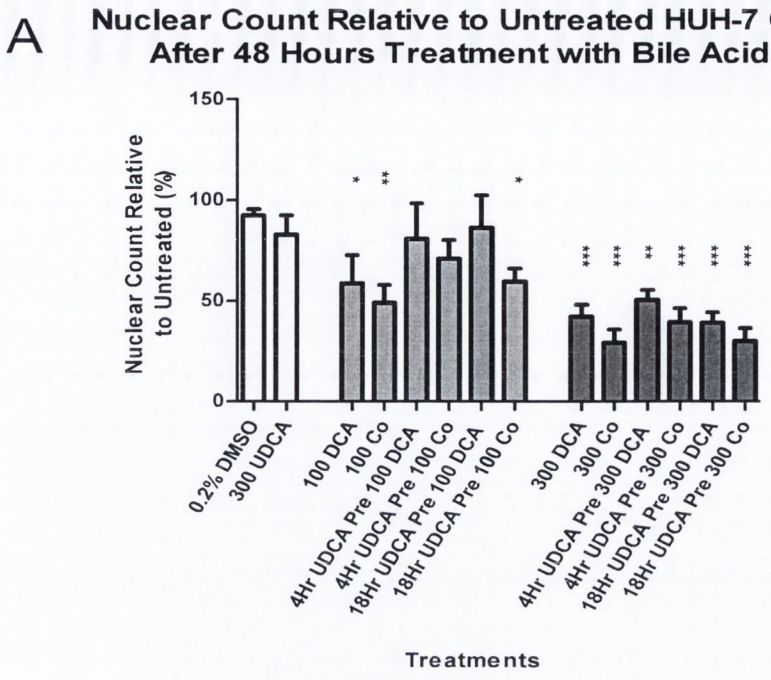

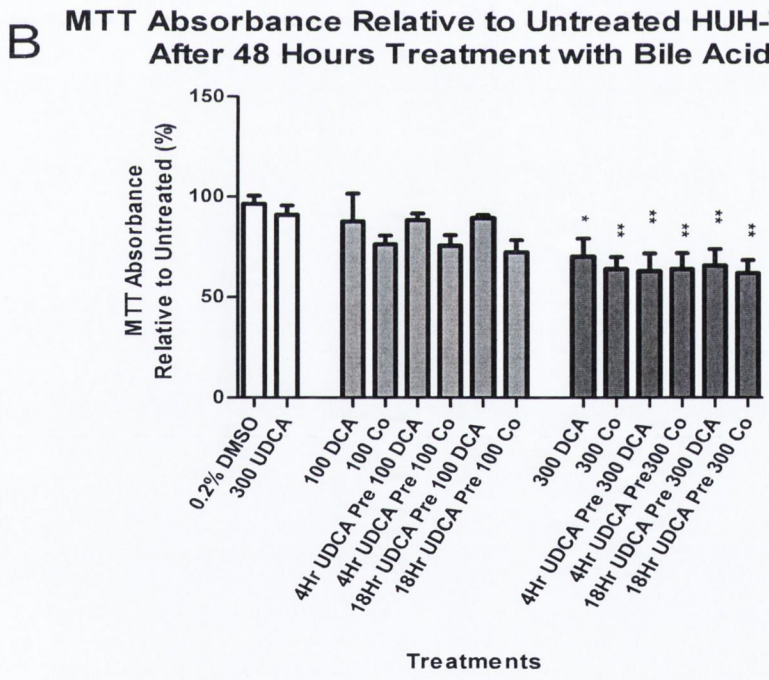

Figure 2–5: The effect of UDCA in modulating DCA induced cell death in the HUH-7 cell line. HUH-7 cells were treated with a DCA in isolation or in combination with UDCA, with or without UDCA pre-treatment, for 48 hours. At this time, cells were either fixed and stained with Hoechst for nuclear counts (A), or treated with MTT (B), in order to determine the relative viabilities. The number of cells was normalised to those untreated. Mean results and SEM of N=4. Comparative analysis was performed using one-way ANOVA. * denotes $p < 0.05$, ** $p < 0.01$ and *** $p < 0.001$ compared to untreated cells.

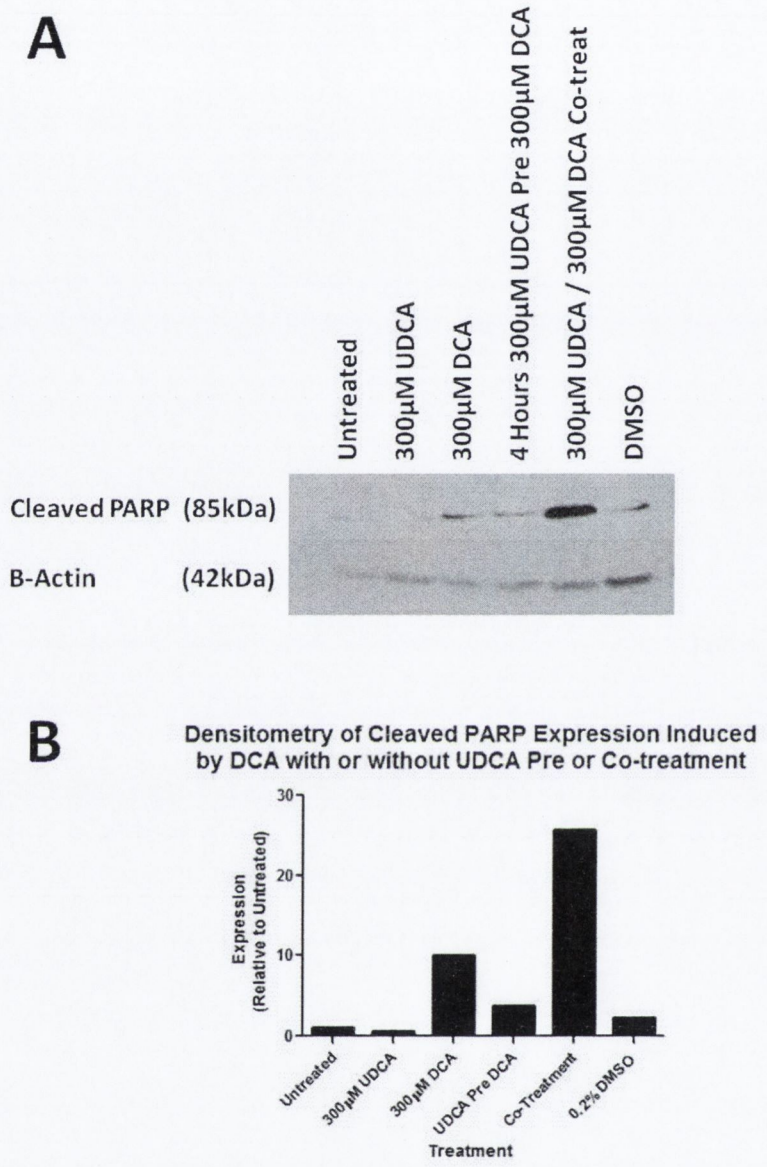

Figure 2–6: UDCA pre-treatment prior to 300µM DCA treatment for 48 hours reduces the expression of cleaved PARP in the HUH-7 cell line but co-treatment enhances the expression. HUH-7 cells were seeded at a density of 1 X 10^5 cells/well in a Nunc 6 well plate and allowed to adhere overnight. They were subsequently treated with DCA in isolation, or in combination with UDCA for 48 hours, with or without four hours UDCA pre-treatment. At this time, cells were lysed in RIPA buffer and immunoblotting for cleaved PARP was performed. A representative example of the three replicates is shown above (A) with its associated densitometry (B).

2.4.2. DCA and UDCA Reduce Proliferation in the HET-1A Cell Line Without Altering Cell Cycle Progression

2.4.2.1. DCA and UDCA Inhibit HET-1A Proliferation in a Dose and Time Dependent Fashion

We next established the toxicity profile of DCA and UDCA in the HET-1A cell line using a nuclear count assay (Figure 2–7). This demonstrated that in our system HET-1A cells were proliferating with a doubling time of 23.5 +/- 4 hours. 100μM UDCA repressed the doubling time to 28.8 hours and 300μM completely inhibited proliferation. 500μM UDCA and DCA at 100, 300 or 500μM concentrations resulted in a reduction in cell viability to a level below that of the initial seeding density. After 12 hours exposure, 500μM DCA had significantly reduced cell numbers below that of the untreated group. By 24 hours, cell counts in all treatments except for 100μM UDCA were significantly reduced below that of the untreated cells.

The finding that UDCA at low doses (300μM) was itself inducing a reduction in viability was surprising. High doses of this BA have been documented as toxic but the threshold for toxicity in numerous cell lines is considered to be above 500μM. However, at lower concentrations, UDCA has been shown to induce cell cycle arrest. Therefore, we next investigated whether 300μM UDCA, which was completely abolishing proliferation, was inducing cell cycle arrest.

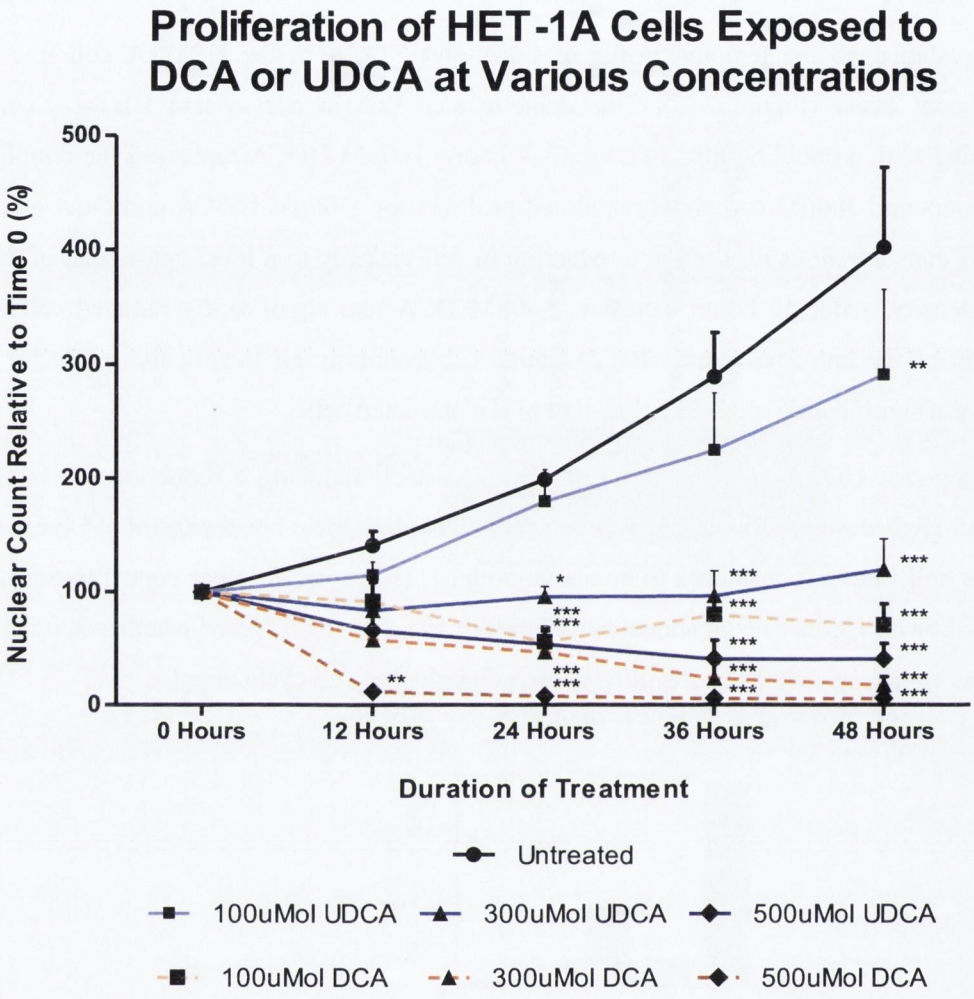

Figure 2–7: DCA and UDCA reduce the proliferation of HET-1A cells in a dose and time dependent fashion. HET-1A cells were seeded at a density of 7.5 X 10^3 cells/well in a Nunc 96 well plate and allowed to adhere overnight. The medium was replaced with complete fresh medium containing BAs. At each time-point the cells were fixed with PFA, and the nuclei were subsequently stained with Hoechst. Using GE InCell Analyser, the nuclei, representing cells, in four 10X magnification fields were counted. The number of cells was normalised to the 0 hour time-point. The graph shows mean and SEM of N=3. Comparative analysis was performed using two-way ANOVA. ** denotes $p < 0.01$ and *** denotes $p < 0.001$ relative to untreated cells.

2.4.2.2. Neither UDCA nor DCA Effect Cell Cycle Progression in the HET-1A Cell Line.

300μM is a frequently used concentration of UDCA in cell culture based research. This concentration is generally not considered toxic, but in our models had completely inhibited proliferation of the HET-1A cell line. Due to the slow proliferative rate, it was not felt to be possible to synchronise the cell culture as over 24 hours would have been needed in the presence of a pharmacological inhibitor of cell cycle or through serum starvation. Consequently, unsynchronised cell populations were used to investigate the effects of BAs in modulating the HET-1A cell cycle.

The experiment demonstrated that 300μM UDCA had no significant effect on the proportion of cells in G0/G1, S or G2/M phase of the DNA histogram after 24 or 48 hours treatment (Table 2–1). This suggested that the reduction in viability seen with UDCA nuclear count assay was due to cell death rather than interference with cell cycle progression. DCA similarly had no effect on cell cycle progression at 24 hours. After 48 hours exposure, DCA appeared to induce a reduction in S phase and an increase in G2 phase of the cell cycle. However, these results must be interpreted with significant caution as high levels of cell death led to poor quality DNA histograms with poor definition of cell cycle phase by the analysis software.

		G1 Phase		S Phase		G2 Phase	
		Mean	SEM	Mean	SEM	Mean	SEM
24 Hours	Untreated	39.5	4.9	51.6	1.4	8.9	5.1
	UDCA	43.2	7.8	45.5	8.4	11.4	2.8
	DCA	37.7	4.8	54.6	3.2	7.7	2.3
48 Hours	Untreated	31.9	3.3	59.7	7.1	8.4	4.0
	UDCA	46.1	4.3	48.9	3.2	5.0	1.2
	DCA	*47.9*	*14.3*	*26.7*	*10.7*	**25.4*	*9.9*

Table 2–1: The percentage of HET-1A cells in G0/G1, S and G2/M phase of the cell cycle after treatment with 300μM UDCA or 300μM DCA. Cells were seeded at 2 X 10^5 cells in a Nunc 6 well plate and allowed to adhere overnight. The medium was replaced with medium containing BAs. At the relevant time points the media was removed and discarded, and the cells enzymatically detached from the cell base. The cells were stained with PI containing RNAse. DNA histograms were acquired using a Beckman Coulter flow cytometry. Mean results and SEM of N=3. Data was analyzed using one way ANOVA. * denotes $p < 0.05$ compared to untreated time-point control.

2.4.3. The Lethal Effects of the Hydrophobic Bile Acid DCA are not Attenuated by Pre-Treatment or Co-Treatment with the Hydrophilic BA UDCA in the Oesophageal Cell Line HET-1A

Having established a model of protection in the HUH-7 cell line consistent with that published in the scientific literature, and explored proliferation and cell cycle alteration in the HET-1A cell line in response to BAs, we next undertook to research whether UDCA could modulate the lethal effect of DCA in HET-1A cells. This was in order to determine whether the demonstrated protective effects of UDCA in mesothelial cell lines (HUH-7) and columnar epithelium of the GI tract (HCT116) would extend to the squamous epithelium of the oesophagus. While research in cell lines representing hepatocytes, colonocytes and other tissues has demonstrated that UDCA can attenuate apoptosis induced by hydrophobic BAs, and DCA in particular, the majority of research has investigated a reduction in apoptosis rather than an absolute reduction in viability. Only infrequently have researchers used LDH assays or MTT assays to investigate the effect of UDCA in modulating cell death induced by hydrophobic BAs. The effects of UDCA in modulating the effects of DCA in the oesophagus or in oesophageal cells have not been investigated to date.

To investigate whether UDCA could modulate the toxic effect of DCA in the HET-1A cell line we used two complementary assays: nuclear counts and MTT assays. Based on the results of the proliferation assay, two short duration time-points (4 and 8 hours) and one long time-point (24 hours) were used to investigate the potential protective effects. As the protective effects of UDCA in some cell lines have been shown to be overcome at high concentrations, treatments matrices were established using all combinations of 0μM, 100μM, 300μM and 500μM of UDCA and DCA. However, investigation of the protective effects of UDCA was further complicated by the fact that the literature is often unclear as to whether UDCA treatment should be continued during hydrophobic BA treatment. Consequently, the following experiments were performed for each of the matrices:

- No pre-treatment prior to UDCA and DCA co-treatment
- Four hours UDCA pre-treatment prior to DCA treatment
- Four hours UDCA pre-treatment prior to UDCA and DCA co-treatment, and,
- Eighteen hours UDCA pre-treatment prior to DCA treatment or UDCA and DCA co-treatment. Smaller matrices were performed for these conditions given our findings that UDCA was itself reducing proliferation in the HET-1A cell lines and the finding in the HUH-7 cell line that pre-treatment followed by co-treatment was significantly reducing cell counts.

The experiments were simultaneously performed in the colorectal cell line HCT116 as this represents an epithelial cell line in which UDCA has been previously, although not consistently, been shown demonstrate protective effects against DCA-induced apoptosis [116, 182, 201, 225].

In each experiment, in both assays, and in both the HET-1A and the HCT116 cell lines, DCA induced a reduction in viability in a dose and time dependent fashion (both ANOVA $p < 0.001$).

Figure 2–8 and Figure 2–9 demonstrate the effect of 4 hours UDCA pre-treatment prior to DCA stimulation in nuclear count and MTT assays in the HET-1A cell line. Figure 2–10 and Figure 2–11 demonstrate the same experiment in the HCT116 cell line. In the HET-1A cell line, the viability for 100μM, 300μM and 500μM DCA in the nuclear count assay, relative to untreated cells, after 24 hours exposure was 62.3% (SEM 2.6%, $p < 0.001$), 42.8% (SEM 5.2%, $p < 0.001$) and 8.03% (SEM 1.9%, $p < 0.001$) respectively. In the MTT assay, the viability was 68.3% (SEM 5.4%, $p < 0.05$), 44.0% (SEM 7.2%, $p < 0.001$) and 14.5% (SEM 6.2%, $p < 0.001$) respectively. 500μM DCA induced a significant reduction in viability after 4 hours in the nuclear count but not in the MTT assay.

For UDCA, the respective viability relative to untreated cell was 88.5% (SEM 3.5%, NS), 59.1% (SEM 4.2%, $p < 0.001$) and 27.47% (SEM 5.5%, $p < 0.001$) in the nuclear count assay and 103.8% (SEM 4.4%, NS), 97.6% (SEM 5.4%, NS) and 90.27% (SEM 4.8%, NS) in the MTT assay. Similar to DCA, 500μM UDCA induced a significant reduction in viability after 4 hours in the nuclear count but not in the MTT assay. The reduction in viability seen at the lower concentrations of UDCA was such that it could represent either a reduction in proliferation or a small increase in cell death. As cell cycle alterations had been out-ruled in earlier experiments, it appears likely that this reduction in viability is a consequence of cell death.

DCA exerted a similar effect in the HCT-116 cell line although the magnitude of the reduction in viability was less profound (Figure 2–10 and Figure 2–11).

300μM and 500μM DCA UDCA pre-treatment prior to DCA consistently reduced the cell viability below that of DCA alone in the nuclear count assay ($p < 0.001$) but had no significant effect in the MTT assay. In the nuclear count assay 100μM UDCA did not significantly reduce viability below that of DCA alone but neither did it enhance survival.

In none of the other experimental designs did UDCA protect against DCA induced cell death (See Appendix 1). Neither co-treatment of UDCA with DCA nor four or eighteen hours UDCA pre-treatment prior to DCA or combination treatment attenuated the DCA induced reduction in cell viability. In the nuclear count assays UDCA pre-treatment consistently reduced counts to a level below that of DCA, while in the MTT assay, only 18 hours pre-treatment enhanced the toxicity. In

the HCT116 cell line only 500μM UDCA enhanced the toxicity of DCA in the nuclear count assay. In the MTT assay, no significant differences were seen.

The relatively minor toxicity of UDCA alone is likely to account for a proportion of the observed decline in viable cells. This factor must be always be taken into account for the 500μM concentration which independently exerts a notable reduction in viability at 4 and 8 hours. However, for 100 and 300μM UDCA this appears to be a significant factor only in cells pre-treated for 18 hours. Consistent with this hypothesis, there is a significant generalised reduction in viability between cells pre-treated for 4 hours and 18 hours with UDCA in both the HET-1A and the HCT116 cell line. Using Bland-Altman plots to explore the difference, we found that in the nuclear count experiment, the values in the 18 hours pre-treatment were on average 11.4% lower than in the 4 hour pre-treatment experiments (one-sample t-test $p < 0.001$, 95% CI of diff: -5.8% to -17.1%). In the MTT assay, the reduction was 20.1% ($p < 0.0001$, 95% CI of diff: 15.6% to 26.4%,

Figure 2–12). In the HCT116 cell line, the nuclear count demonstrated a reduction of 16.7% ($p < 0.0001$, 95% CI of the diff: 11.1% to 22.2%) and the MTT a reduction of 20.9% ($p < 0.0001$, 95% CI of the diff: -15.0% to -26.8%) (See Appendix 1). Despite similar absolute differences, again it was noted that the nuclear count assay demonstrated significantly lower values than those seen in the MTT assay.

These finding taken together demonstrate that UDCA has no effect in ameliorating the total toxicity of DCA in HET-1A cells. In fact, UDCA may enhance the toxicity of the hydrophobic BA at high doses. At lower doses, a discrepancy exists between the MTT and nuclear counts assays. That the longer duration pre-treatment significantly reduced the overall viability as demonstrated by the comparative Bland-Altman plots, confirmed the finding of earlier experiments that UDCA inhibited proliferation in the HET-1A cell line.

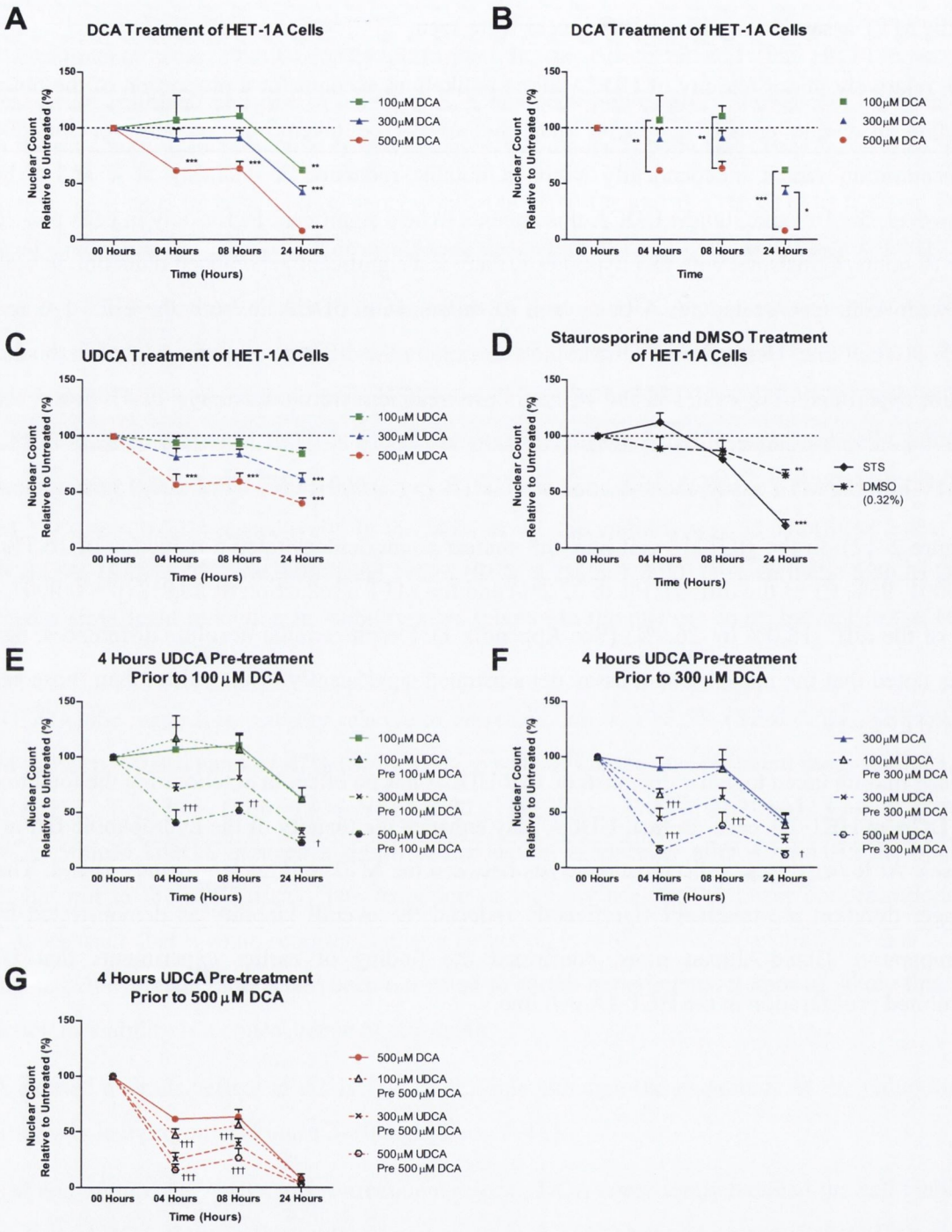

Figure 2–8: The effect of DCA treatment on HET-1A cell viability after four hours UDCA pre-treatment as determined by a nuclear count assay normalised to untreated cells. DCA induced a time (A) and dose (B) dependent reduction in viability. UDCA stimulation reduced viability but to a lesser degree than DCA (C). 0.32% DMSO vehicle, equivalent to the highest vehicle concentration used, and the positive control STS reduced viability at 24 hours only (D). UDCA pre-treatment prior to DCA reduced nuclear count below that of DCA alone at all concentrations studied (E - G). Results are mean and SEM of N=3. Analysis was performed using two-way ANOVA. */† denotes $p < 0.05$, **/†† denotes $p < 0.01$ and ***/††† denotes $p < 0.001$ compared to untreated cells. * = relative to untreated and † = relative to DCA alone.

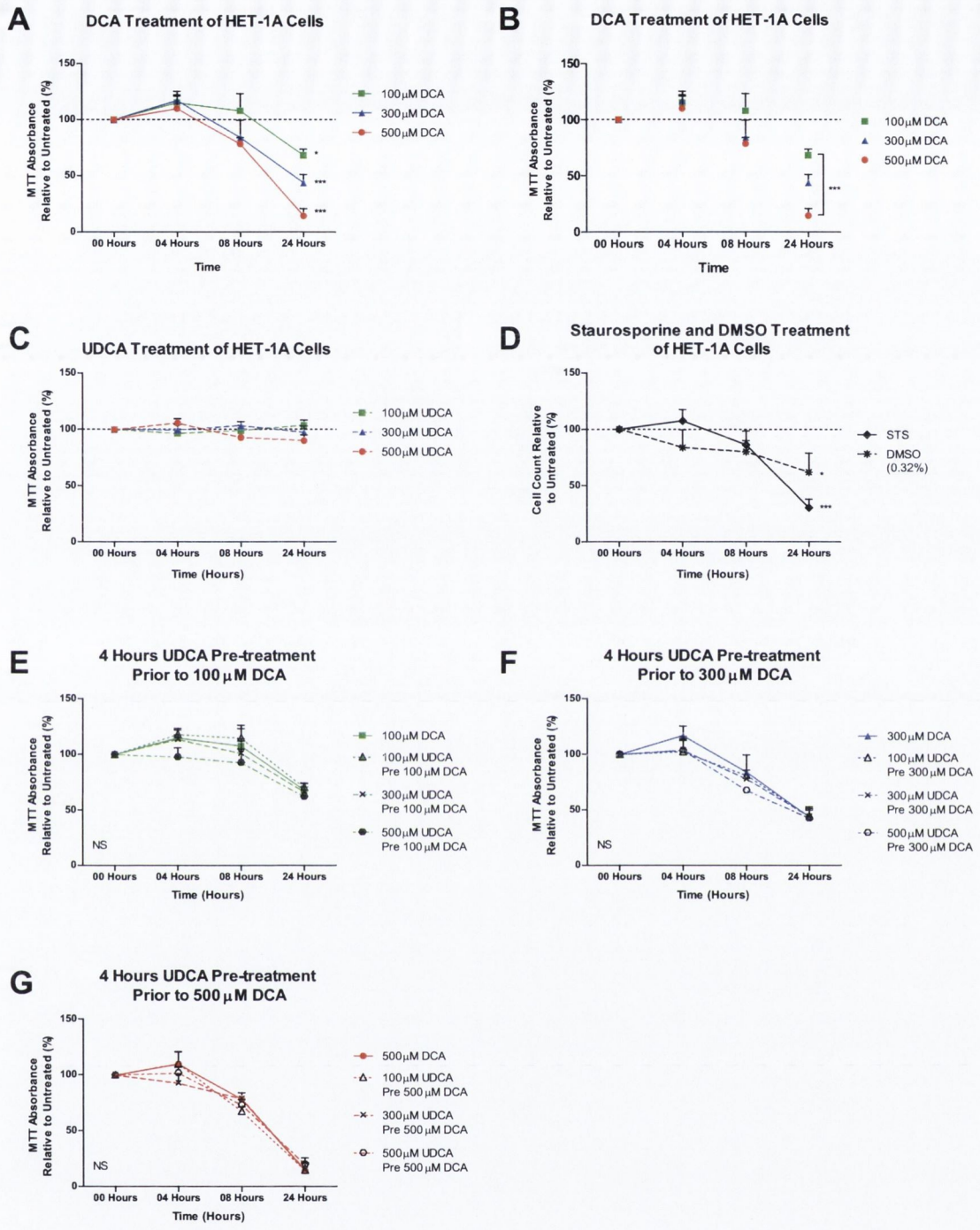

Figure 2–9: The effect of DCA treatment on HET-1A cell viability after four hours UDCA pre-treatment as determined by an MTT assay normalised to untreated cells. DCA induced a time (A) and dose (B) dependent reduction in viability. UDCA stimulation reduced viability but to a lesser degree than DCA (C). 0.32% DMSO vehicle, equivalent to the highest vehicle concentration used, and the positive control STS reduced viability at 24 hours only (D). UDCA pre-treatment prior to DCA reduced nuclear count below that of DCA alone at all concentrations studied (E - G). Results are mean and SEM of N=3. Analysis was performed using two-way ANOVA. */† denotes $p < 0.05$, **/†† denotes $p < 0.01$ and ***/††† denotes $p < 0.001$ compared to untreated cells. * = relative to untreated and † = relative to DCA alone.

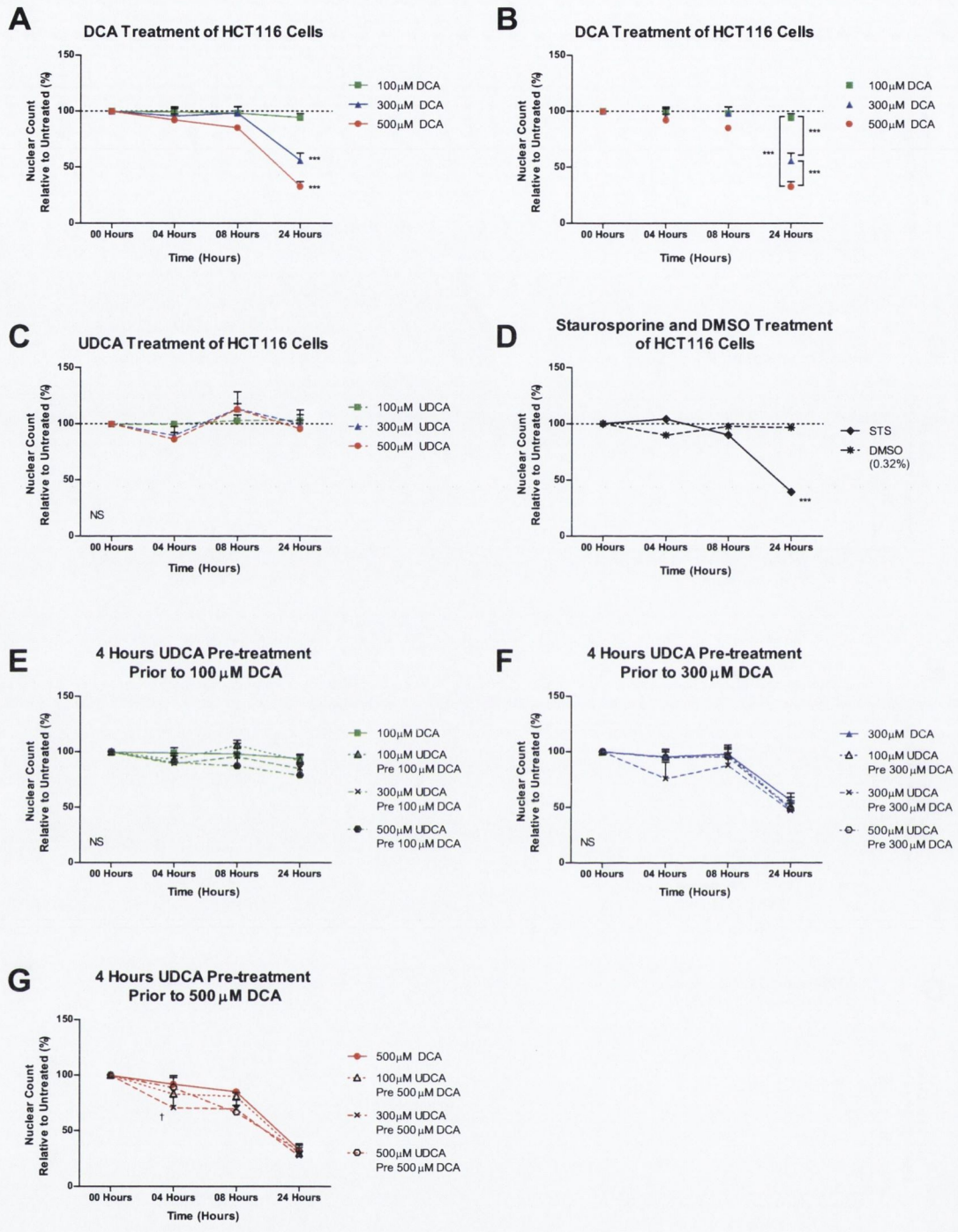

Figure 2–10: The effect of DCA treatment on HCT116 cell viability after four hours UDCA pre-treatment as determined by a nuclear count assay normalised to untreated cells. DCA induced a time (A) and dose (B) dependent reduction in viability. UDCA stimulation reduced viability but to a lesser degree than DCA (C). 0.32% DMSO vehicle, equivalent to the highest vehicle concentration used, and the positive control STS reduced viability at 24 hours only (D). UDCA pre-treatment prior to DCA reduced nuclear count below that of DCA alone at all concentrations studied (E - G). Results are mean and SEM of N=3. Analysis was performed using two-way ANOVA. */† denotes $p < 0.05$, **/†† denotes $p < 0.01$ and ***/††† denotes $p < 0.001$ compared to untreated cells. * = relative to untreated and † = relative to DCA alone.

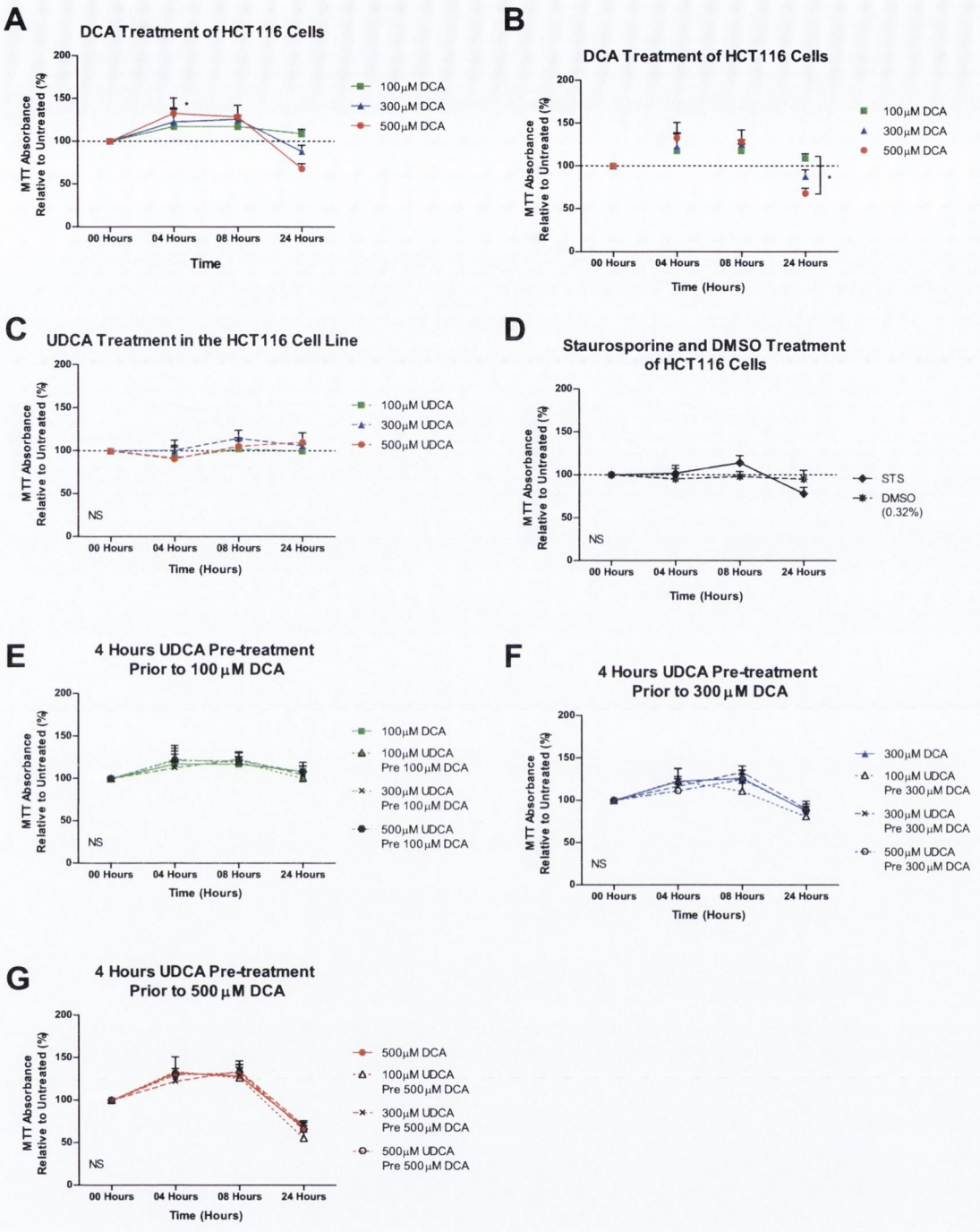

Figure 2–11: The effect of DCA treatment on HCT116 cell viability after four hours UDCA pre-treatment as determined by an MTT assay normalised to untreated cells. DCA induced a time (A) and dose (B) dependent reduction in viability. UDCA stimulation reduced viability but to a lesser degree than DCA (C). 0.32% DMSO vehicle, equivalent to the highest vehicle concentration used, and the positive control STS reduced viability at 24 hours only (D). UDCA pre-treatment prior to DCA reduced nuclear count below that of DCA alone at all concentrations studied (E - G). Results are mean and SEM of N=3. Analysis was performed using two-way ANOVA. */† denotes $p < 0.05$, **/†† denotes $p < 0.01$ and ***/††† denotes $p < 0.001$ compared to untreated cells. * = relative to untreated and † = relative to DCA alone.

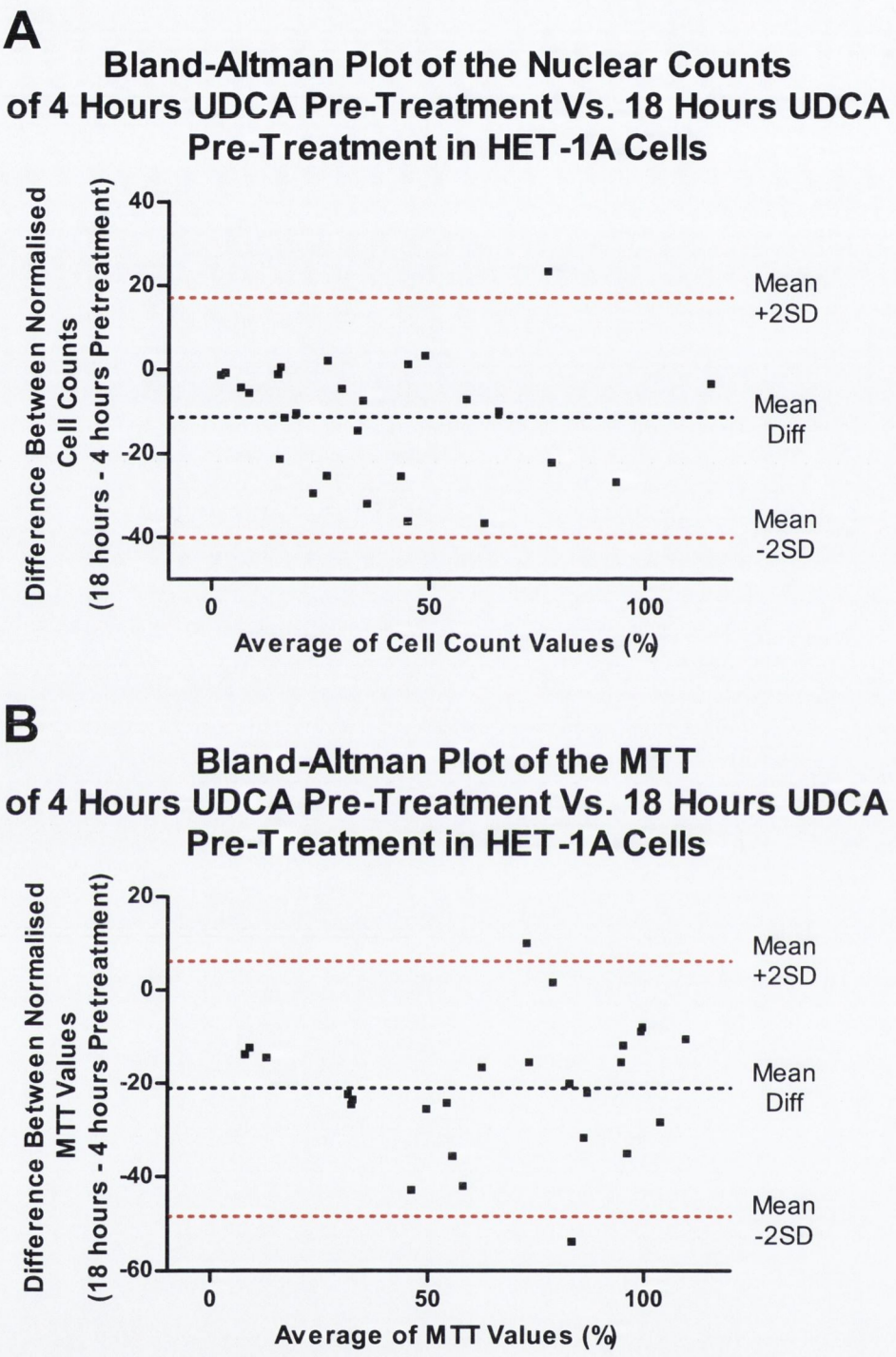

Figure 2–12: Bland-Altman plots of the differences between the 4 hour pre-treated matrices and the 18 hour pre-treated matrices for nuclear counts (A) and MTT assays (B). In both assays, the values in the 4 hour pre-treatment group are consistently higher than in the 18 hour pre-treatment group.

2.4.4. UDCA Pre-Treatment, but not Co-Treatment, Reduces the Levels of Cleaved Poly-ADP-Ribose Polymerase (PARP)

The MTT and nuclear count assays has provided an estimate of cell viability but had not investigated the mechanism through which cells were dying. Concurrently with the MTT and nuclear count assays immunoblotting was performed to detect cleaved PARP, a marker of apoptosis (as discussed in Section 2.3.6). DCA was first demonstrated to induce PARP cleavage in a dose dependent manner (Figure 2–13A). After 4 hours stimulation, 300 and 500μM DCA induced the expression of cleaved PARP, suggesting that DCA was inducing apoptosis.

We next investigated whether UDCA could modulate the cleavage of PARP induced by 300μM DCA exposure. Co-treatment increased the levels of cleaved PARP above that seen with DCA alone (Figure 2–13B). However, pre-treatment reduced the level of expression of cleaved PARP below that induced by DCA, suggesting a reduction in the levels of apoptosis induced by DCA (Figure 2–13C). This was a surprising finding given the increased reduction in nuclear count seen with UDCA pre-treatment prior to DCA exposure. It suggested that cells exposed to UDCA prior to DCA were dying through a mechanism other than apoptosis.

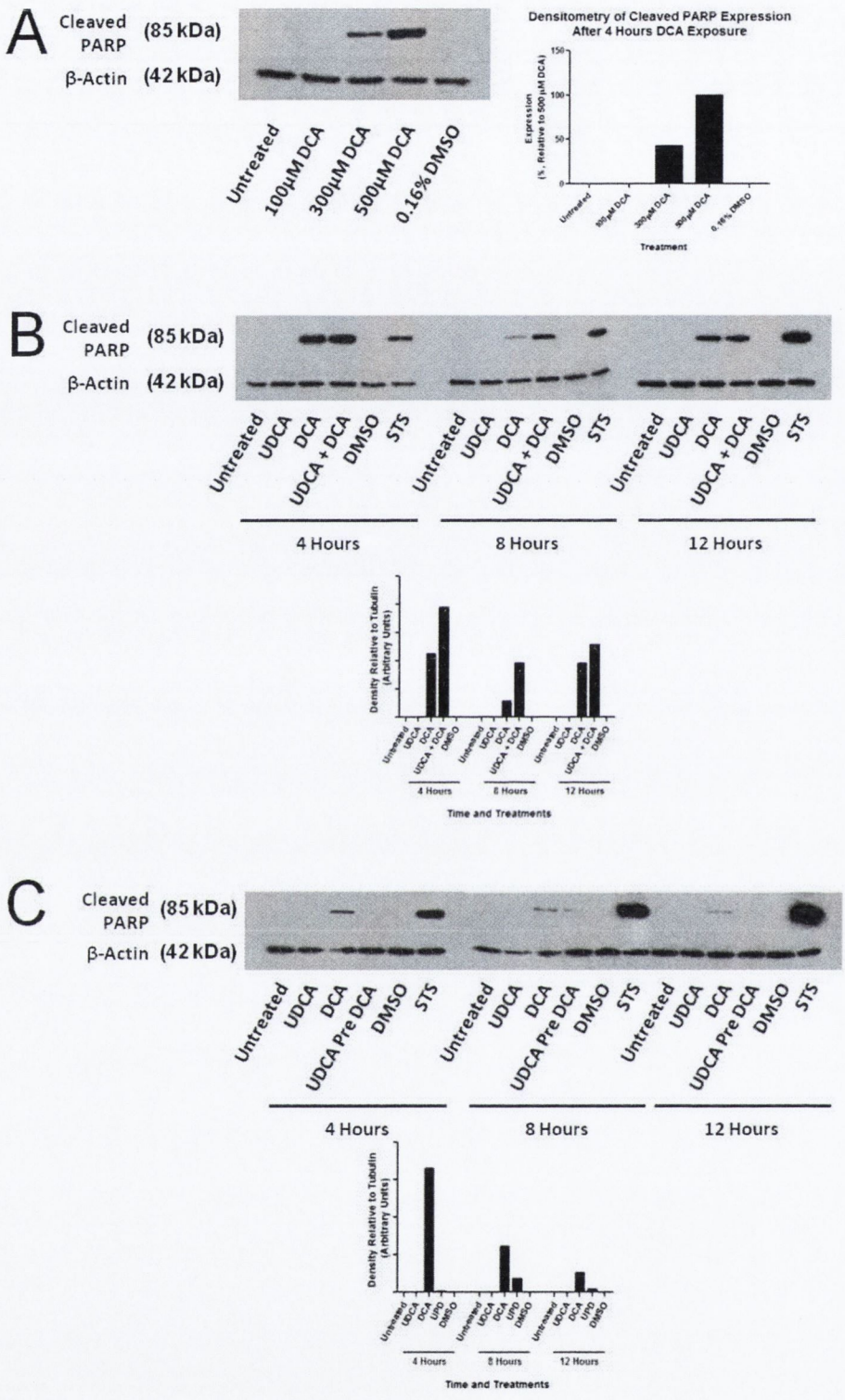

Figure 2–13: UDCA pre-treatment, but not co-treatment, can reduce DCA induced cleavage of PARP. DCA induces cleavage of PARP in a dose dependent fashion (A). Co-treatment (B) does not reduce the levels of cleaved PARP seen after DCA exposure while four hours pre-treatment does (C). A representative example of Western Blotting and densitometry of three experiments are shown. Protein loading is equalised within time-point and not across complete experiments.

2.4.5. UDCA Pre-Treatment does not Reduce the Magnitude of Mitochondrial Depolarisation Induced by DCA.

DCA has been demonstrated to induce mitochondrial depolarisation through activation of the MPT. Depolarization of mitochondria results in apoptosis or necrosis depending on the severity of the mitochondrial dysfunction. With increasing mitochondrial dysfunction, there is thought to be an inability to provide sufficient energy to complete the energy-dependent apoptotic processes and thus secondary necrosis occurs.

We next investigated whether DCA induced mitochondrial depolarization in the HET-1A cell line. 300μM DCA induced significant mitochondrial depolarization after four hours stimulation (Figure 2–14). Similar to the findings with PARP cleavage, UDCA pre-treatment reduced the level of mitochondrial depolarization, although not significantly ($p = 0.053$), while co-treatment enhanced the percentage of cells with mitochondrial depolarization. This suggested that either UDCA pre-treatment prior to DCA protected against mitochondrial depolarization and potentially against apoptosis, or that UDCA pre-treatment resulted in necrosis and a greater number of cells were excluded from the analysis, thus biasing the result downwards.

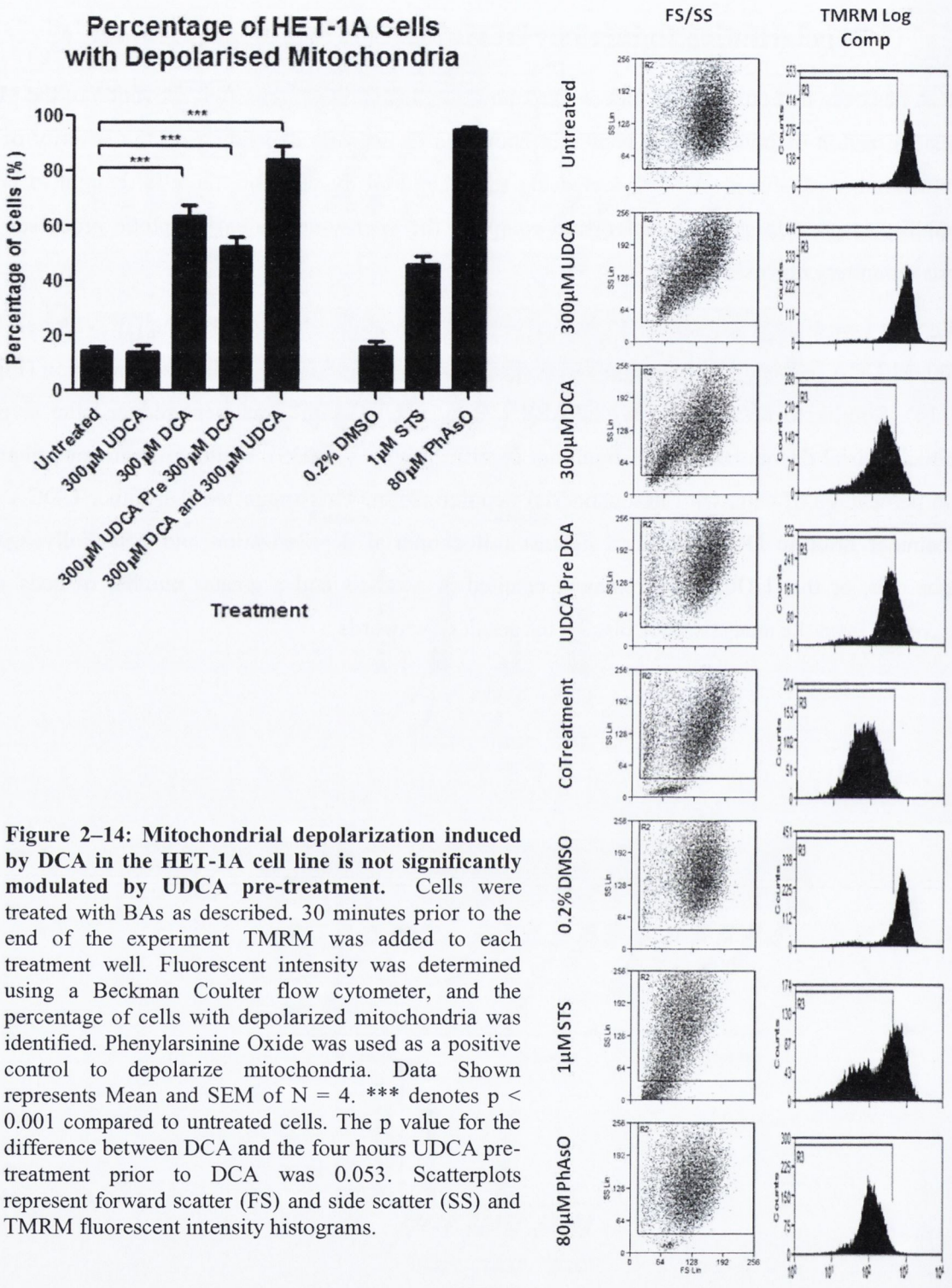

Figure 2–14: Mitochondrial depolarization induced by DCA in the HET-1A cell line is not significantly modulated by UDCA pre-treatment. Cells were treated with BAs as described. 30 minutes prior to the end of the experiment TMRM was added to each treatment well. Fluorescent intensity was determined using a Beckman Coulter flow cytometer, and the percentage of cells with depolarized mitochondria was identified. Phenylarsinine Oxide was used as a positive control to depolarize mitochondria. Data Shown represents Mean and SEM of N = 4. *** denotes $p < 0.001$ compared to untreated cells. The p value for the difference between DCA and the four hours UDCA pre-treatment prior to DCA was 0.053. Scatterplots represent forward scatter (FS) and side scatter (SS) and TMRM fluorescent intensity histograms.

2.4.6. UDCA does not Reduce the Magnitude of Apoptosis Induced by DCA Exposure

The enhanced loss of viability in the HET-1A cell line induced by UDCA in the nuclear count assays was at odds with the findings that UDCA pre-treatment prior to DCA reduced expression of cleaved PARP, and trended toward a reduction in mitochondrial depolarization induced by DCA. However, the value of multiple assays in investigating apoptosis has recently been highlighted [247]. Although, the PARP and TMRM experiments had suggested that cells may be dying through a mechanism other than apoptosis, it was necessary to confirm these findings regarding the reduction in apoptosis prior to assuming that UDCA was altering the mechanism of cell death induced by DCA. Precedent for this exists as research has suggested that UDCA may switch apoptosis to necrosis in epithelial and hepatocyte models [203]. To further elucidate how UDCA was modulating DCA induced cell death, the following assays were used:

- Nuclear area, representing the nuclear condensation which occurs during the late phase of apoptosis, following BA treatment was measured. In this case, re-analysis of the high content analysis of nuclear count data was performed.
- TUNEL-PI based flow cytometry.
- AV-PI based flow cytometry to differentiate apoptosis from necrosis.

2.4.6.1. UDCA does not Prevent Nuclear Condensation Induced by DCA Exposure.

Nuclear area analysis was performed using data previously acquired in the nuclear count assays. In the co-treatment experiment, general linear model ANOVA demonstrated that nuclear area was significantly reduced with time ($p < 0.001$), DCA concentration ($p < 0.001$) and UDCA concentration ($p < 0.001$, Figure 2–15A), The individual effect of 100, 300 and 500μM DCA was to reduce nuclear area by 5.19%, 15.25% and 22.02% respectively. The equivalent concentrations of UDCA reduced nuclear area by 1.48% ($p=0.85$), 4.11% ($p<0.001$), and 4.58% ($p<0.001$) respectively. These findings were consistent with the nuclear count assay, the MTT assay and the PARP blots in that UDCA and DCA individually reduced viability and induced apoptosis.

In the 4 hours UDCA pre-treatment prior to DCA exposure experiment, nuclear area was reduced significantly with increasing time ($P < 0.0001$) and DCA concentration ($P < 0.001$, Figure 2–15B). 100, 300 and 500μM DCA reduced nuclear area, compared to untreated cells, by 4.5% ($p<0.001$), 7.5% ($p<0.001$) and 13.3% ($p<0.001$) respectively. However in this experiment, the effect of

UDCA was not found to be significant ($p = 0.683$). Similarly in the 18 hours pre-treatment prior to DCA exposure, UDCA had no significant effect on nuclear area ($p = 0.287$, Appendix 1). These findings suggest that UDCA appears to enhance the toxicity of DCA when used in combination, but has minimal toxic effect when used to pre-treat prior to DCA stimulation.

Similar results regarding time and DCA concentration were found in HCT116 cell line (Appendix 1). However, in these experiments, UDCA stimulation never had a significant effect on nuclear area.

Nuclear area analysis is however subject to significant bias by virtue of the fact that it only assesses cells still attached to the well base. Dead or dying cells which have lost adherence prior to, or during, the fixing and staining process are excluded, resulting in lower estimates of toxicity. In an attempt to overcome this, we next investigated apoptosis induced by 300μM DCA in the HET-1A cell line using TUNEL / PI based flow cytometry.

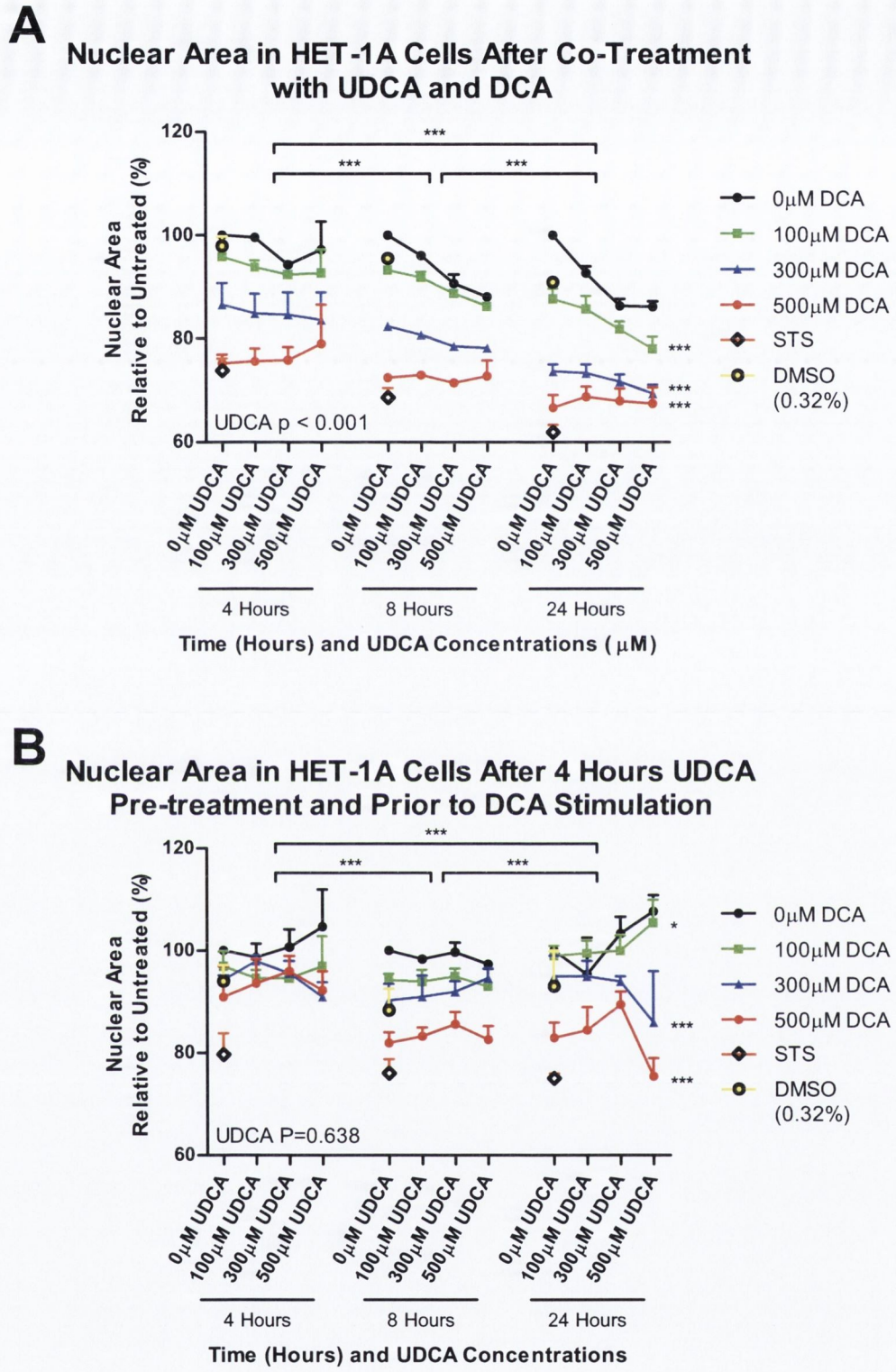

Figure 2–15: The effect of UDCA and DCA co-treatment (A) and 4 hours UDCA pre-treatment prior to DCA (B) on the nuclear area of HET-1A cells. The GE InCell analyser was used to investigate the mean area of Hoechst stained nuclei after BA treatment. Mean and SEM of N=3. Comparative analysis was performed using general linear model ANOVA. * denotes $p < 0.05$ and *** denotes $p < 0.001$ compared to untreated cells.

2.4.6.2. UDCA does not Reduce DCA-Induced Apoptosis as Determined by TUNEL Based Flow Cytometry

Similar to nuclear area analysis, the TUNEL assay detects only late apoptotic events (as discussed in section 2.3.5). However, as both attached and detached cells are included in the analysis, TUNEL is a more robust experimental model for analysing apoptosis. However, we first investigated whether DCA or UDCA could induce an increase in TUNEL positive cells after 4, 8 or 12 hours exposure (Figure 2–16A). While 8 hours DCA stimulation demonstrated an increase in TUNEL positive cells, this increase was not significant (Mean diff 6.0%, 95% CI of diff: 8.8% to -20.7%) due to the large variance at this time-point. After 12 hours DCA exposure the percentage of TUNEL positive cells increased from 4.9% (95% CI: 3.4% to 6.4%) to 21.8% (95% CI: 16.0% to 27.5%, Mean Diff 18.8%, 95% CI of diff: 5.6% to 32.0%, $p < 0.01$). In this system an increase in TUNEL positive cells was also seen with UDCA treatment although this failed to reach significance (Mean diff 3.3%, 95% CI of diff: 16.5% to -9.9%).

As only the 12 hour time-point demonstrated a significant increase in the number of TUNEL positive cells in the time-course study, we investigated whether UDCA could modulate the effect of DCA after this duration of exposure (Figure 2–16B). Baseline levels of TUNEL positive cells were 6.6% (95% CI: 0.04% to 12.7%). DCA again significantly increased the rate of apoptosis to 28.4% (Mean diff 21.9%, 95% CI of Diff: 0.8% to 42.9%, $p < 0.05$) while UDCA itself increased levels of apoptosis to 15.6% (95% CI: 9.4% to 21.8%, NS from untreated). UDCA pre-treatment prior to DCA had no effect in reducing DCA-induced apoptosis (Mean diff. from DCA -0.3%, 95% CI of diff -25.8 to 25.3, p = NS). Interestingly UDCA prior to co-treatment slightly reduced levels of apoptosis to 17.9% (Mean diff from DCA 10.6%, 95% CI of the diff: -17.1% to 38.1%, p = NS). However, this was also not significantly different from untreated (Mean diff from untreated 11.3%, 95% CI of diff: 12.3% to 34.9%).

These findings further confounded an understanding as to how UDCA was modulating DCA induced cell death. While co-treatment increased cleavage of PARP after 12 hours exposure, in the TUNEL assay, co-treatment reduced the proportion of TUNEL positive cells, although not significantly below that of DCA alone. Furthermore, UDCA pre-treatment prior to DCA had reduced PARP cleavage, but had no effect on the proportion of TUNEL positive cells.

These varying results failed to clarify the mechanism of cell death induced by DCA. Consequently, AV / PI based flow cytometry was used to further attempt to clarify the effect of UDCA in modulating DCA induced apoptosis and cell death in HET-1A cells.

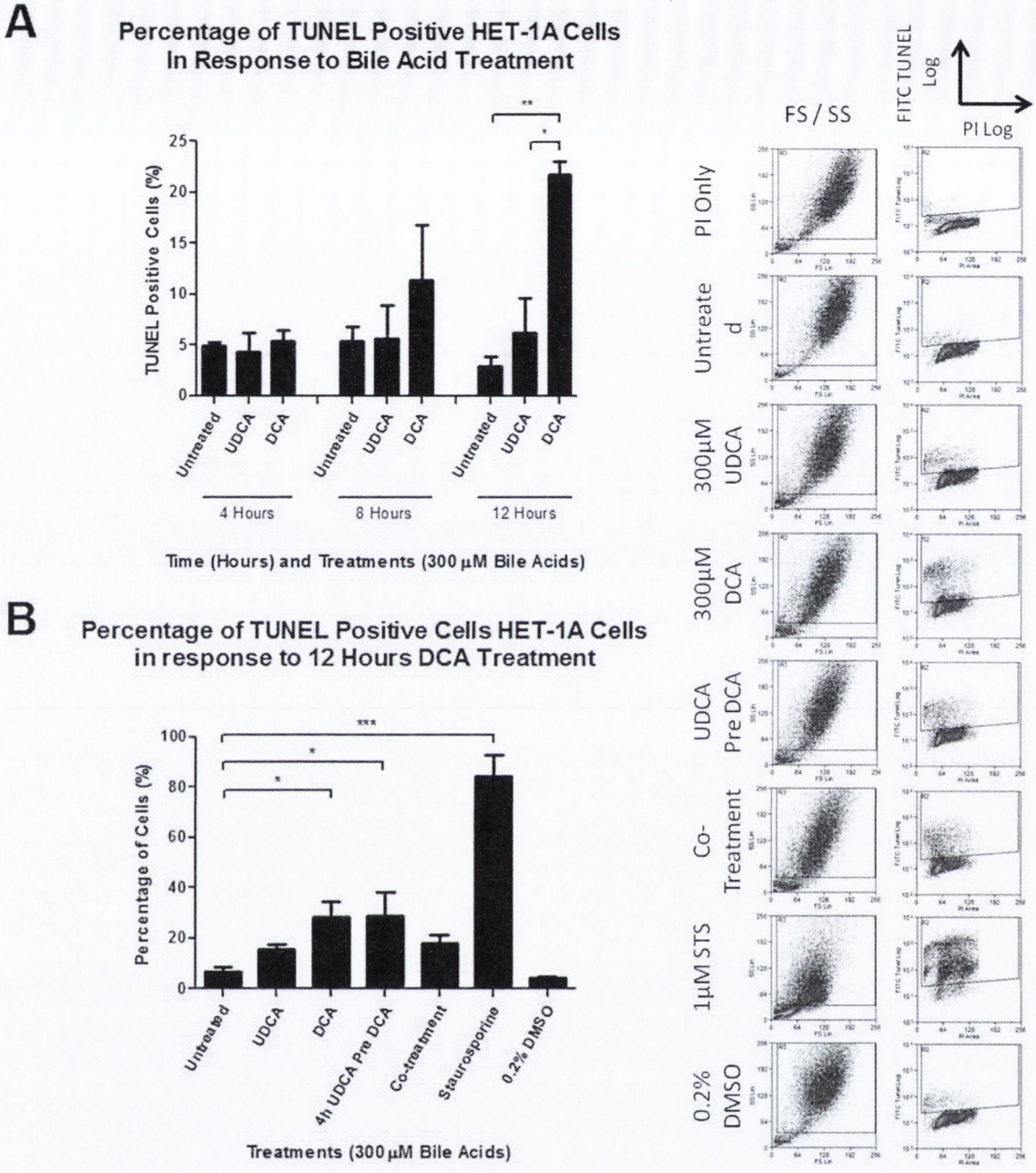

Figure 2–16: UDCA does not reduce apoptosis induced by DCA as determined by TUNEL based flow cytometry. A) The effect of 300µM DCA and 300µM UDCA at 4, 8 and 12 hour time-points. The representative scattergraphs demonstrate the 12 hour time-point. B) The effect of UDCA in modulating DCA induced TUNEL positivity after 12 hours treatment. After BA stimulation, at the relevant time points, the media was removed spun at 1500rpm to pellet the detached cells. The remaining cells were enzymatically detached from the cell base and pooled with the detached cells. All cells were stained with TUNEL and PI. Mean and SEM of N=3. Data was analyzed using one way ANOVA. * denotes $p < 0.05$, ** denoted $p < 0.01$ and *** denotes $p < 0.005$ relative to untreated cells. Scatterplots represent forward scatter (FS) and side scatter (SS) and, PI Log Vs. FITC-dUTP Log.

2.4.6.3. UDCA does not significantly alter the mechanism of DCA-induced cell death as determined by Annexin V / PI Based Flow Cytometry.

Phosphatidylserine is located on the internal plasma membrane in healthy cells. However, early in the apoptotic programme, it becomes expressed on the external plasma membrane. AV binds to phosphatidylserine in a Ca^{++} dependent manner and thus when cells are positive for this marker, they are considered to be in an early apoptotic phase. PI can only enter cells to bind to DNA in those cells in which plasma membrane integrity has been lost. Thus, PI positivity represents a late apoptotic or necrotic marker.

A time-course study of the effects of 300μM DCA and 300μM UDCA on cell death in HET-1A cells demonstrated a high background level of cell death with 22.6% (95% CI: 11.0% to 32.2%) of untreated cells demonstrating positivity for PI, AV, or both (Figure 2–17). There was no significant increase in cell death at 4 or 8 hours exposure, similar to the findings in the TUNEL assay, the nuclear count assay and the MTT assay. Treatment with 300μM DCA was only seen to significantly increase the number of AV and/or PI positive cells to 32.8% (95% CI: 27.6% to 38.0%) after 12 hours exposure. Individually however, there was no significant increase in the level of early apoptosis (AV + only), late apoptosis (AV + / PI +) or necrosis (PI + only).

At the 12 hour time-point only (Figure 2–18), the number of AV and/or PI positive cells was found to increase significantly from 17.4% (95% CI: 9.9% to 24.8%) to 41.9% (95% CI: 33.1% to 50.7%, Mean Diff 18.2%, $p < 0.001$). 300μM UDCA in isolation had no significant effect on levels cell death. Neither UDCA pre-treatment prior to DCA or co-treatment altered the proportion of dying cells from that seen with DCA alone. In this model, DCA only significantly increased the proportion of necrotic cells. Conversely, co-treatment significantly reduced this back to baseline levels. However, co-treatment instead increased the levels of early apoptotic ($p < 0.05$) and late apoptotic cells (p = NS) above that of baseline. UDCA pre-treatment prior to DCA significantly increased the percentage of necrotic cells but did not significantly increase the proportion of early or late apoptotic cells.

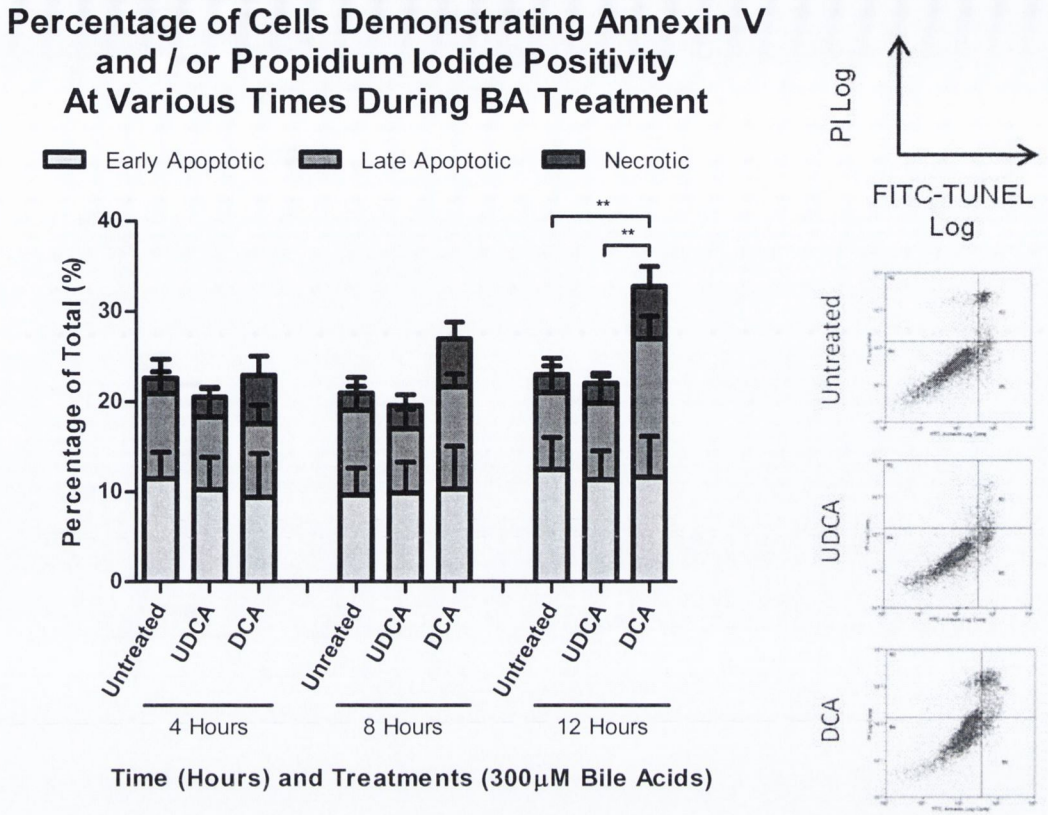

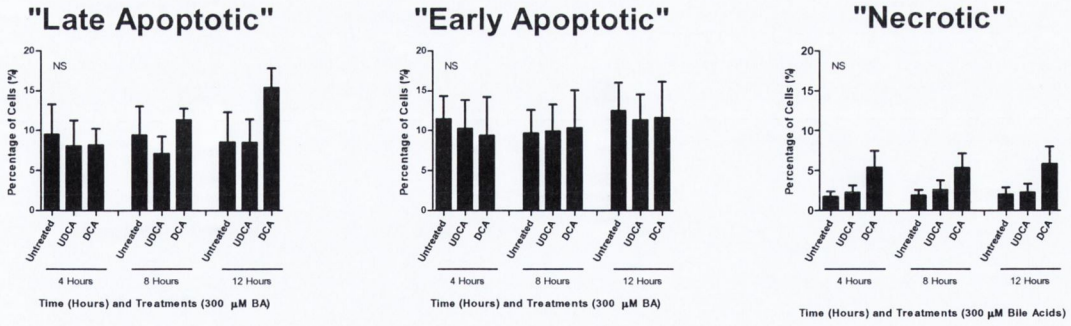

Figure 2–17: DCA induces a significant increase in cell death after 12 hours exposure as determined by AV / PI based flow cytometry. After 300μM BA stimulation, at the relevant time points, the media was removed spun at 1500rpm to pellet the detached cells. The remaining cells were enzymatically detached from the cell base and pooled with the detached cells. All cells were stained with AV and PI. Mean and SEM of N=3. Data was analyzed using one way ANOVA. ** denotes $p < 0.01$ compared to untreated cells. Scatterplots demonstrate FITC-AV Log Vs. PI Log.

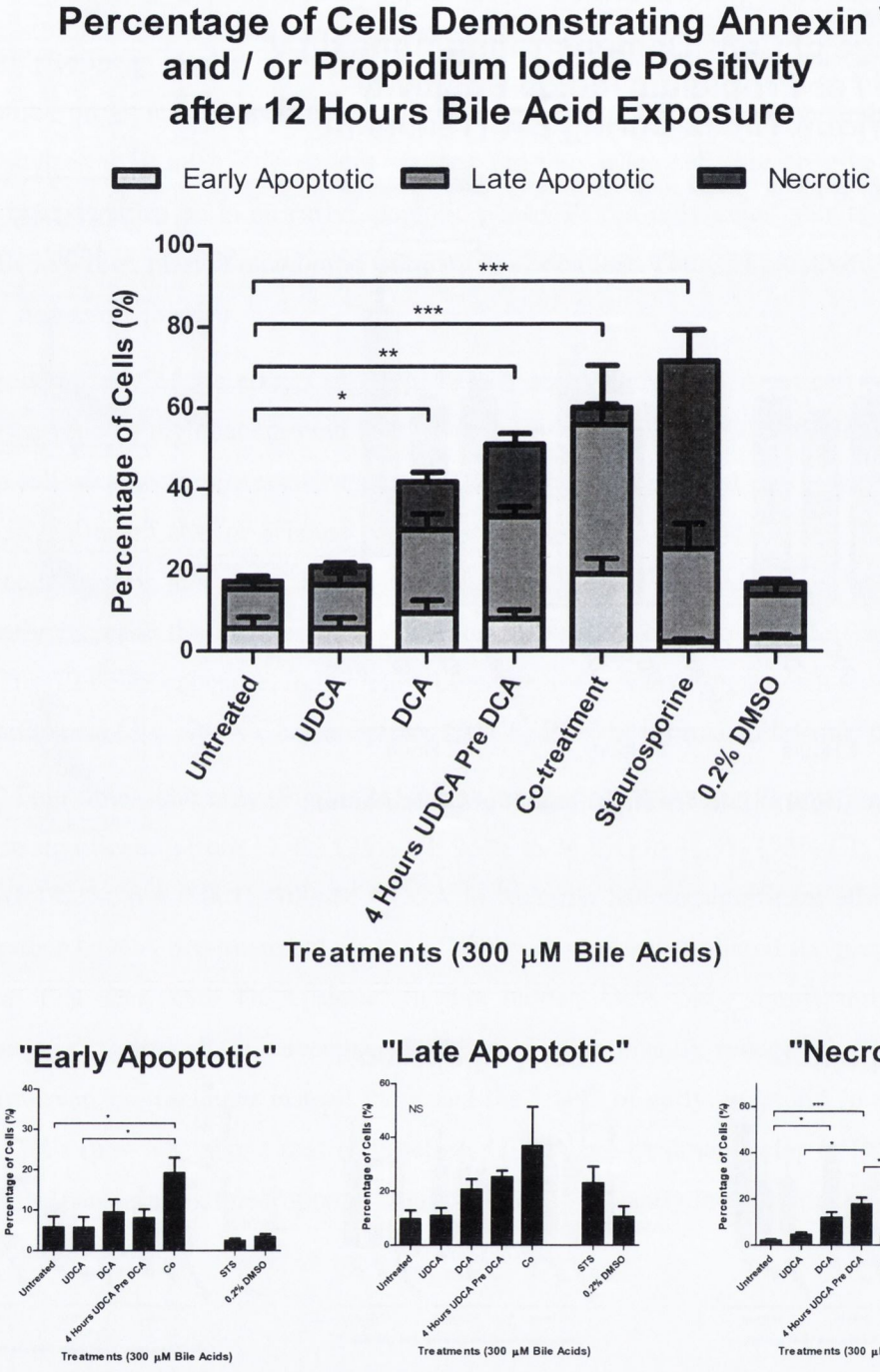

Figure 2–18: UDCA does not reduce apoptosis induced by DCA as determined by AV/PI based flow cytometry. After 300μM BA stimulation, at the relevant time points, the media was removed and spun at 1500rpm to pellet the detached cells. The remaining cells were enzymatically detached from the cell base and pooled with the detached cells. All cells were stained with AV and PI. Mean and SEM of N=3. Data was analyzed using one way ANOVA. * denotes $p < 0.05$, ** denoted $p < 0.01$ and *** denotes $p < 0.005$ relative to untreated cells.

2.4.7. DCA Stimulation Increases Autophagy in HET-1A Cells

DCA stimulation induces apoptosis in HET-1A. However, modulation of apoptosis by UDCA had proven unpredictable. In the majority of assays, UDCA co-treatment appeared to significantly enhance the toxic effects of DCA. Experimental results had provided contradictory findings regarding the effect of UDCA pre-treatment in modulating DCA induced apoptosis and cell death. While some markers of DCA-induced apoptosis (cleaved PARP and TMRM) were reduced by UDCA pre-treatment, the nuclear count assay and the AV / PI analysis suggested that total cell death was being increased by this treatment strategy. These findings taken together suggested that UDCA pre-treatment was enhancing cell death, while possibly reducing levels of apoptosis in cells exposed to DCA.

However, given the lack of consistent results regarding a reduction in apoptosis, the role of autophagy, a potential third mechanism of cell death, in this system was investigated by visualising processing of the microtubule associated protein LC3 by Western blotting. The rationale for this has been explained in Section 2.3.6.

We first investigated the role of DCA and UDCA in inducing autophagy. Cells were treated with DCA, UDCA, DMSO equivalent, or rapamycin (a positive control for autophagy) for four hours and then 5μg/ml of the lysosomal protease inhibitor pepstatin was added and the cells incubated for a further four hours. The pepstatin control is used to differentiate autophagy from failed lysosomal degradation in the autophagolysosome. This experiment demonstrated that DCA increased levels of LC3-II above that of untreated in the HET-1A cells. Pepstatin further enhanced the levels of LC3-II suggesting that this was indeed autophagy (Figure 2–19A).

We next investigated the effects of increasing concentrations of DCA on inducing autophagy. This demonstrated a consistent induction of LC3-II by 100 and 300μM DCA. 500μM DCA induced an increase in LC3-II expression which was intermittently greater than that seen with 300μM (Figure 2–19B).

Co-treatment and 4 hours pre-treatment experiments were again repeated to investigate the effects of UDCA in modulating DCA induced autophagy. In the co-treatment experiment, the addition of UDCA to DCA had an unpredictable effect on the conversion of LC3-I to LC3-II, with unpredictable increases or reductions in seen at each time-point around the DCA level (Figure 2–19C).

Interestingly, UDCA pre-treatment consistently reduced the induction of LC3-II after 4 hours stimulation, but by 12 hours, had increased the levels (Figure 2–19D).

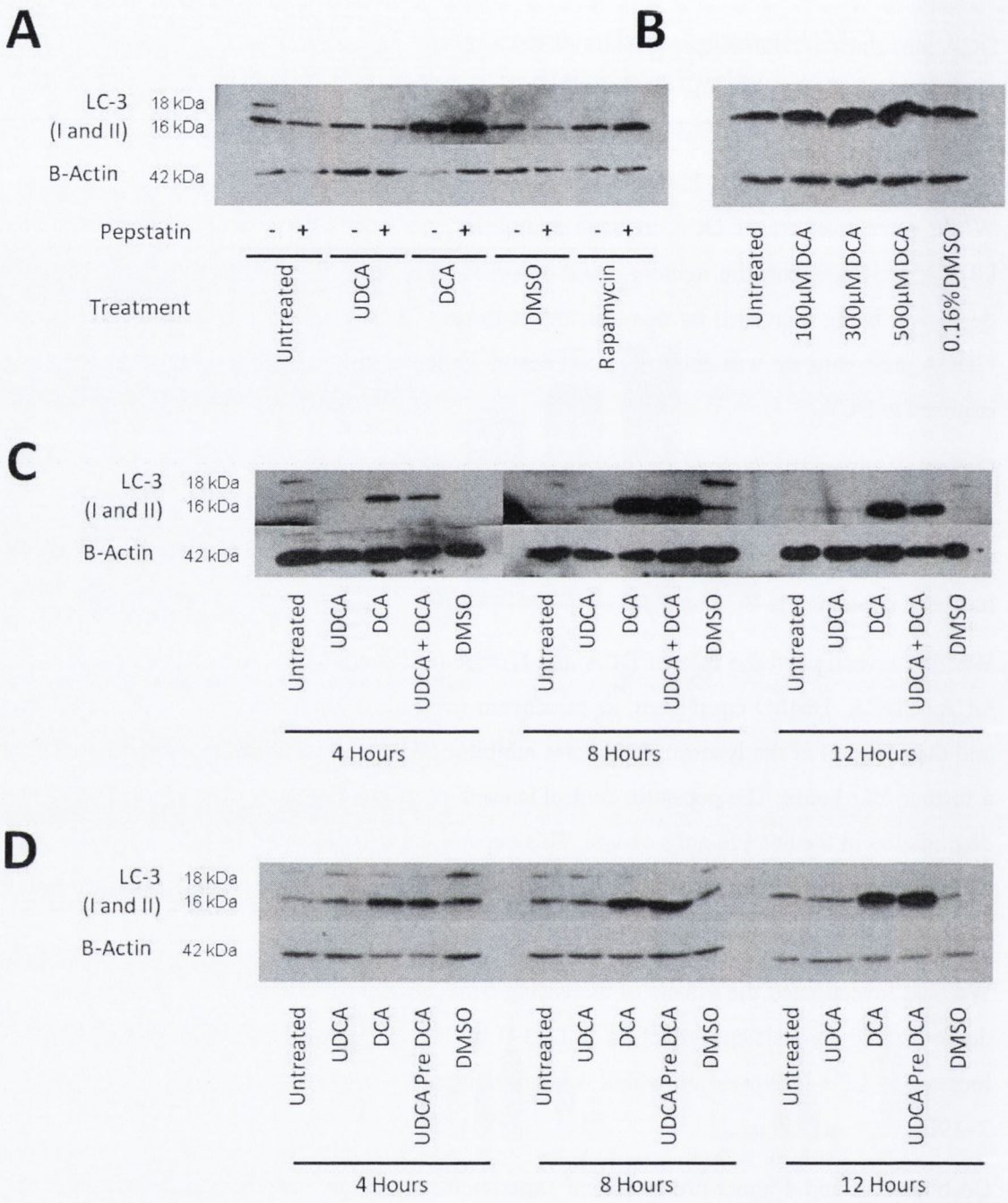

Figure 2–19: The effect of DCA and UDCA on LC3 I and II expression in HET-1A cells. 300µM DCA but not 300µM UDCA induces a conversion of LC3-I to LC3-II the HET-1A cells, which is increased by pepstatin suggesting autophagy in (A). This occurs in a dose dependent fashion (B). UDCA unpredictably modulated the conversion of LC3-1 to LC3-II (C and D). A representative example of three experiments is shown above. Protein loading is equalised within time-point and not across complete experiments

2.4.8. 300μM Bile Acids have no Toxic Effect on Biopsy Explants of Healthy Oesophageal Tissue.

Finally, to investigate the effects of BAs on human oesophageal tissue, we used explanted oesophageal tissue. With the patient's consent, biopsies were acquired during gastroscopy from the endoscopy department in St James Hospital. Ethics approval had previously been provided by the hospital ethics committee. 6 biopsies were taken from each of five patients, who were undergoing gastroscopy for non-oesophageal indications including coeliac screening, investigation of abdominal pain, etc. Biopsies were taken only from patients with macroscopically normal oesophagi. The samples were placed in medium and incubated at 37°C for 4 hours. An individual explant sample was then exposed to complete medium, or BAs in isolation or combination as in previous experiments. After 24 hours 100μL of supernatant was aspirated and the tissue in the remaining medium was mechanically homogenised, triton-X added to a final concentration of 0.1% and the cells sonicated to release all of the intracellular LDH.

Comparison of the proportion of LDH released compared to total LDH demonstrated no significant difference the untreated cells and any BA treatments (Figure 2–20). This suggested that at these concentrations, BAs exert no significant toxicity on explanted tissue.

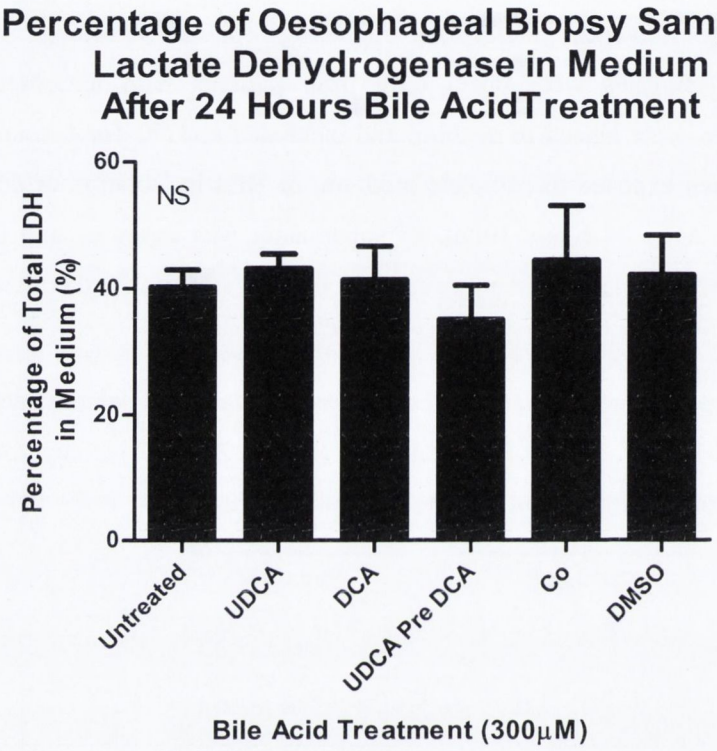

Figure 2–20: LDH release from oesophageal explants after 24 hours treatment with various bile acids. Explanted oesophageal biopsy samples were cultured in medium 199 with BAs, with or without UDCA pre- or co-treatment. After 24 hours 100μL of medium was aspirated prior to the disruption of the explant to release the intracellular LDH. The ratio of the released to total LDH was calculated. Results represent mean and SEM of N = 5.

2.5. Discussion

BO represents the greatest risk factor for OAC [33, 38]. However, little is understood about the transformation of normal squamous oesophageal epithelium into BO. Three primary hypotheses exist as to the aetiology of this pre-malignant epithelium [11]. The first is that BAs and low pH damage DNA, causing mutagenic change in the basal epithelial stem cells resulting in a metaplastic transformation of the squamous epithelium into columnar epithelium [261-263]. The second hypothesis suggests that columnar epithelium of the oesophageal glands re-epithelise the oesophageal basement membrane from which the squamous epithelium has been denuded as a result of chemical or mechanical stress [264-266]. The final and most recent hypothesis is that Barrett's epithelium arises from embryological stem cells which remain quiescent in the oesophageal epithelium until they can re-adhere to the basement membrane. Once adherent, this cellular population proliferation and expands to form BO [13]. The one feature common to the three hypotheses is that there must be substantial erosion of the squamous epithelium of the oesophagus to allow re-epithelialisation with columnar epithelium.

Both low pH and BAs in oesophageal refluxate have been shown to be toxic to squamous oesophageal epithelial cells, through the induction of inflammation, apoptosis and necrosis [187-188, 267]. Increasing volume of reflux in the oesophagus has been shown to correlate with the more severe disease phenotype and increasing levels of apoptosis in the oesophagus are seen in increasingly severe oesophageal disease [20-22]. Hydrophobic BAs such as DCA induce apoptosis through numerous mechanisms including mitochondrial dysfunction, generation of reactive oxygen and nitrogen species, DNA damage and through indirect activation of membrane death receptors. Both mitochondrial depolarisation and direct effects of BAs on the cell membrane release reactive ion species into the cytoplasm [82, 85-86, 156, 194-195]. Therefore inflammation and apoptosis are closely linked entities which occur in response to BAs. Thus, modulation of apoptosis is likely to also represent modulation of inflammation in the oesophagus.

Reducing BA-induced inflammation and apoptosis in the oesophagus could therefore prevent erosive oesophagitis and protect against re-epithelisation of the oesophagus with BO. UDCA has been shown to modulate BA-induced apoptosis in numerous cell lines. The most well established of these is hepatocytes [162]. UDCA protects mitochondria from depolarisation by inhibiting activation of the MPT, and prevents against the generation of free radicals [82, 116, 156-157, 194-195, 225]. Therefore UDCA is likely to attenuate BA-induced inflammation as well as apoptosis. Consequently the aim of the research in this chapter was to identify whether UDCA could modulate DCA induced cell death in the oesophageal cell line HET-1A.

Our initial findings using the HUH-7 hepatoma cell line mimicked results previously demonstrated in the literature. UDCA pre-treatment, but not co-treatment, not only reduced the cleavage of PARP in HUH-7 cells, but also reduced cell death as determined by a nuclear count assay. These findings, although not exact replications of previously performed experiments, verified the protective effects of UDCA in a hepatocellular cell line. However, experiments regarding the modulation of DCA-induced cell death by UDCA in the oesophageal cell line HET-1A produced more complex results.

Both DCA and UDCA inhibited proliferation of the HET-1A cell line as determined by nuclear count assay, although DCA had a significantly more profound effect than UDCA. As neither DCA nor UDCA induced cell cycle arrest in HET-1A cells (although this has previously been shown to occur in hepatocytes and colonocytes in response to UDCA [182, 199, 268-269]), it suggested that the reduction in cellular proliferation induced by both BAs was due to an increase in cell death.

The ability of UDCA to modulate DCA-induced cell death was next investigated using MTT and nuclear count assays as they represented simple high-throughput assays to investigate multiple pre-treatment, co-treatment, concentration and time-point experimental designs. In the majority of the experiments, concentration matrices were established ranging from 0 to 500 μmol of DCA and UDCA. In none of the experimental designs investigated or experimental technique used did UDCA reduce DCA-induced cell death in the HET-1A cell line. Even at the lower concentrations of DCA, no protective benefit was identified. In fact, in the nuclear count assays, UDCA appeared to synergistically enhance DCA toxicity. However, the validity of this particular result is questionable as demonstrated in Chapter 3. Therefore, UDCA does not reduce the magnitude of cell death induced by DCA in the oesophageal cell line HET-1A.

However, neither the nuclear count nor MTT assay was capable of elucidating the mechanism of cell death: apoptosis, necrosis, or autophagy. This was investigated using multiple techniques as recommended by Galluzzi *et al* [247]. Research presented in this chapter suggests that UDCA pre-treatment was capable of reducing markers of apoptosis such as mitochondrial depolarisation and PARP cleavage in the HET-1A cell line. This has been demonstrated by other authors in different cell lines [82, 156, 194-195, 225]. Co-treatment increased both the cleavage of PARP and the magnitude of mitochondrial depolarisation above that seen with DCA alone.

Other markers of apoptosis induced by DCA including nuclear condensation, DNA fragmentation and phosphatidylserine expression were not reduced by UDCA pre-treatment. However, the specificity of the TUNEL assay in differentiating between apoptosis, necrosis and autophagy has been questioned, especially as apoptosis converts to secondary necrosis *in vitro.* Similar arguments have been made regarding AV/PI based flow cytometry [256, 270-272]. A reduction in TUNEL or AV/PI positive cells may therefore not have been identified even though there was a reduction in

apoptosis. The identification that STS was inducing "necrosis" (AV-, PI+) in this assay adds credence to this argument.

As PARP cleavage was the most specific marker of apoptosis used in this research it suggests that UDCA pre-treatment is reducing DCA-induced apoptosis in the HET-1A cell line. However, as measures of total cell death (i.e. including apoptosis, autophagy and necrosis) are unaffected by this treatment strategy, it suggests that other mechanisms of cell death are being upregulated while apoptosis is downregulated.

DCA induced autophagy in a dose dependent fashion in the HET-1A cell line. The effect of UDCA in modulating DCA-induced autophagy was erratic. UDCA co-treatment unpredictably modulated levels of LC3 conversion. However, pre-treatment consistently reduced the levels of LC3-II below that induced by DCA alone at four hours but increased levels of LC3-II above that of DCA after 12 hours treatment.

Taken together, the findings presented in this chapter suggest that UDCA pre-treatment is likely to result in a reduction in DCA-induced apoptosis and autophagy in the HET-1A cell line, but at the expense of an increase in necrosis. The induction of necrosis by DCA, in the presence or absence of UDCA, has been demonstrated by other authors. Utanahora *et al* and Benz *et al* demonstrated that after prolonged of exposure to UDCA, or with high concentrations of UDCA, markers of apoptosis decreased while cell death increased. They suggested that an increase in necrosis could account for both of these phenomena [179, 233]. Similarly, in the setting of BA treatment, concentrations of UDCA shown to be protective by some authors have been demonstrated to be toxic to the mitochondria by others. An increase in mitochondrial toxicity has been hypothesised to result in an energy deficit of such magnitude that that the energy dependent apoptotic pathway cannot be executed [203-204, 273]. It is suggested that this may switch apoptosis into necrosis.

However, the concentrations of BAs used to treat the HET-1A cell line, while physiologically plausible, had no effect on the viability of oesophageal explants. Therefore, we cannot say with certainty what the effect of a reduction in apoptosis may have on oesophageal cell survival *in vivo*. The identification that UDCA pre-treatment reduced DCA-induced mitochondrial depolarisation suggests this strategy may reduce the quantity of ROS and RNS induced by BA exposure. If this were to occur in oesophageal tissue, it could potentially reduce the pro-inflammatory signalling induced by these agents. Failing this, the toxicity exerted by UDCA in this research was consistently less than that exerted by DCA. Therefore, displacement of hydrophobic BAs by oral administration of UDCA could potentially reduce the magnitude of the inflammatory and apoptotic effects of DGOR, resulting in a reduction in the risk of erosive oesophagitis and BO.

2.6. Conclusions

The aims of this chapter were:

- To investigate the toxicity profiles of UDCA and DCA in the oesophageal cell line HET-1A
- To investigate whether UDCA could modulate DCA-induced cell death in the oesophageal cell line HET-1A
- To determine a concentration range at which UDCA may exert protective effects
- To determine the optimal temporal treatment strategy to elicit an anti-apoptotic effect of UDCA in oesophageal cell lines
- To determine the mechanism through which UDCA exerts any potential anti-apoptotic effects
- To validate any findings in oesophageal explants

In concordance with the published literature we demonstrated that DCA induced cell death in a dose and time dependent fashion. Interestingly, we also identified that UDCA resulted in a reduction in proliferation in the HET-1A cell line in a dose and time dependent fashion. This occurred without an alteration in cell cycle progression suggesting that UDCA was inducing cell death in a dose dependent fashion.

We next investigated whether UDCA could attenuate DCA-induced cell death in the HET-1A cell line. Short duration UDCA pre-treatment (4 hours) reduced markers of DCA-induced apoptosis. It also transiently reduced autophagy in this cell line. Co-treatment increased markers of apoptosis. However, general markers of cell survival (viability, proliferation and cell death) did not demonstrate that UDCA induced a reduction in DCA-induced cell death. The most likely explanation for this is that DCA induces apoptosis, necrosis and autophagy in the HET-1A cell line and that UDCA treatment alters the mechanism of DCA-induced cell death, rather than reducing it. As prolonged (twenty-four hours) exposure of explanted tissue to 300μM DCA had no significant effect on viability, whether these *in-vitro* findings will translate to the *in-vivo* setting remains unknown.

Chapter 3.

3. Deoxycholic Acid Modulates Cell Adhesion in a Mechanism Discreet From Apoptosis

3.1. Introduction

3.1.1. Cell Adhesion

Cell adhesion to extra-cellular matrix (EMC) proteins and to other cells is required for the maintenance of functional tissue in the human body. This is facilitated by multiple families of adhesion molecules (cadherins, selectins, the immunoglobulin superfamily and integrins) which allow inter-cellular binding and adhesion to basement membranes. Without this variety of cell adhesion molecules organogenesis during embryological development, tissue repair, proliferation and cell survival would not be possible [274-276]. Adhesion to ECM proteins is mediated primarily through hetero-dimeric proteins called integrins, comprised of one α and one β subunit [274, 277-279]. Expression of the more restricted subunit of a hetero-dimeric pair determines the total number of complete integrin units expressed on a cell surface [280-282]. Eighteen identified α subunits and eight β subunit variably interact and have been identified as forming at least 24 hetero-dimers which demonstrate different specificity for ECM proteins [283]. Both subunits contribute to the specificity of the hetero-dimeric pair, but the specificity of each hetero-dimeric integrin pair is low and they often bind to multiple ECM proteins. For example, only eight integrin heterodimers have been shown to bind to the arginine-glycine-aspartate (RGD) protein motif sequence found on the ECM proteins such as fibronectin, vitronectin and some collagens [284-285]. Similarly, multiple integrin heterodimers can bind to the same ECM protein. For example, integrins including $\alpha_V\beta_3$, $\alpha_V\beta_5$, $\alpha_8\beta_1$ and, $\alpha_{IIb}\beta_3$ can bind to the ECM protein vitronectin with varying affinity [286].

3.1.2. Integrin-Mediated Cell Attachment and Pro-Survival Signalling

The overall strength of interaction between integrins and ECM proteins or other cells is termed avidity and is influenced by integrin affinity and valency [287]. Affinity represents the strength of interaction between a single integrin heterodimer and a ligand and is influenced by the conformational shape of an integrin [287-289]. Three predominant affinity states are thought to exist for each integrin heterodimer: a low affinity inactive state, a partially conformationally active state and high affinity active state [287]. This has been particularly well demonstrated using electron microscopy of the $\alpha_V\beta_3$ integrin [290]. Transition between these states is determined by cytoplasmic signalling ("inside-out" signalling) including concentrations of divalent cations (calcium, magnesium and manganese), interaction with adaptor proteins and cytoskeletal proteins (talins, kindlins and filamins) and through interaction with kinases (such as Focal Adhesion Kinase

(FAK) and Integrin Linked Kinase) [287-288, 291]. "Outside-in" signalling, induced through integrin binding to ligand, may also affect integrin affinity. Valency represents the cell surface receptor density or diffusivity. Higher densities of integrin heterodimer expression strengthen the interaction between integrins and ligands. This can be modulated by total integrin expression, the clustering of integrins into micro-clusters or focal adhesion complexes (FACs), or the ability of integrins to diffuse around a membrane to strengthen the cell ligand interaction [287-288].

Binding of integrins to ligands produces "outside-in" signalling, activating pro-survival signalling. While the cytoplasmic domain of integrins is not equipped with enzymatic machinery, it interacts with numerous adaptor proteins and enzymes (such as FAK or Src) which activate downstream pathways such as MAPK [278-279, 292]. These are primarily activated at FACs. Without survival signalling appropriate to a specific cell type, apoptosis is induced in order to prevent re-adhesion and growth of a particular cell type in an incorrect tissue or location. In neoplastic cells, dysregulation of adhesion signalling is often seen, allowing escape from this mechanism of apoptosis induction. For example, while integrin α_V (ITGAV) has infrequently been seen in epithelial cells, its upregulation has been shown to play a role in metastasis of neoplasia arising from these cells [293-296]. It also has a demonstrated role in neoplastic angiogenesis [297]. Classically, attachment of cells was thought to be essential for survival [298-299]. However, the loss of cell adhesion to basement membrane ECMs does not irreversibly induce apoptosis. Cells which have reduced adherence or which have detached have been shown to upregulate autophagocytic pathways to promote survival until they can either re-adhere, or until a sufficient amount of time has passed, at which stage apoptosis is induced [300-301].

3.1.3. Integrin-Mediated Cell Detachment

Detachment of cells is an complex procedure, which has been best characterised in leukocytes due to their highly dynamic migratory function. Detachment of cells may occur through either controlled release of ligand by the integrin, through "ripping" in which the integrin, still attached to the ligand, is released from the cells, or through enzymatic degradation of the ligand [302].

Conformational shape change of the integrins modulates its affinity for ligand and can result in detachment of integrin from ECM. This is again mediated by the presence of divalent ions such as calcium, and also by direct (although poorly characterised) intracellular signalling [302-304]. As affinity is reduced, mechanical stresses on the cell can overcome the integrin-ligand force and result in separation of the two proteins. However, if the integrins are still in a high affinity state mechanical forces may result in a controlled or uncontrolled release of the integrin from the cell. In the controlled mechanism the integrin is detached from the structural components at the

cytoplasmic level. In the uncontrolled mechanism, the integrin is torn away from the cell. In both, an integrin trail is left behind migrating cells [302].

While both epithelial and mesenchymal cells synthesise and secrete ECM proteins, they also produce and secrete matrix metalloproteinases (MMP) which degrade ECM proteins and have a role in invasion and metastasis [305-306]. Degradation of the ligand results in separation of the cell from the ECM. After ECM proteins are fragmented by MMPs, FACs disassemble, and the integrin hetero-dimers are endocytosed with ECM fragments. During this process, the two are separated and the integrins are re-expressed after endocytotic recycling [302, 307].

3.1.4. The Endocytic Recycling Pathway

Removal of a receptor from the cell surface occurs through the formation of membrane pits frequently associated with either clathrin or caveolin – proteins which mediate endocytosis. The pits bud to form intracellular vesicles called early endosomes. This usually occurs in response to receptor activation. In order to reduce pressure on protein synthesis machinery, the majority of these receptors are recycled to the cell surface rather than being degraded [308-309]. Depending on the environmental conditions, this may either occur through a fast or slow endosomal loop [310]. These recycling loops are modulated by Rab proteins, a family of Guanosine-5'-Triphosphateases (GTPases) which modulate membrane trafficking, vesicle formation and movement, and membrane fusion. In the fast loop, endosomes are cycled rapidly in a Rab4 dependent fashion, close to the plasma membrane to a different part of the cell membrane where they are re-expressed on the cell surface. In the long loop, the endosomes are trafficked in a Rab11 dependent fashion through the peri-nuclear recycling compartment (PNRC) prior to being re-packaged and again transferred to the cell membrane [308-310]. Alternately, the endosomal contents may either reside in storage vesicles ready for membrane expression or may be targeted for lysosomal degradation (

Figure 3–**1**).

Endocytosis of integrins can occur through either clathrin dependent or independent mechanisms [311]. Determination of which of these energy dependent mechanisms of invagination and endocytosis an integrin will enter into is primarily dependent on which receptors the integrin is in close proximity to. For instance, ITGAV is internalised in a clathrin dependent mechanism when it is in close association with EGFR but through a clathrin independent mechanism when in association with fibronectin [307, 312-313].

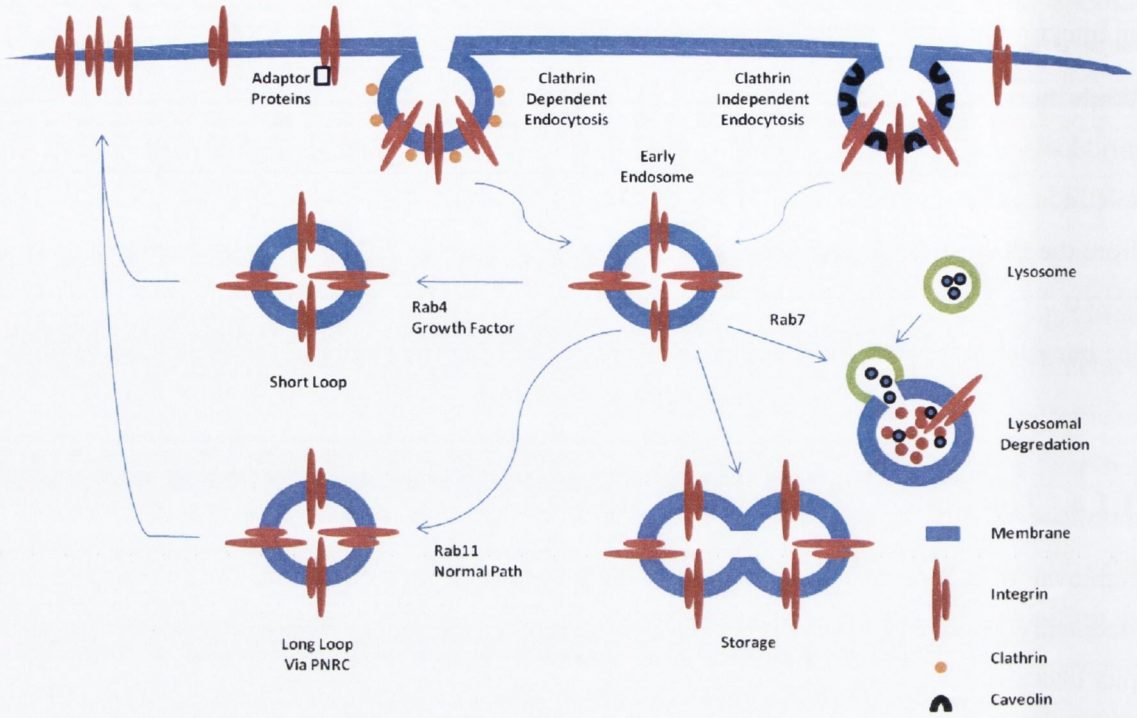

Figure 3–1: A representation of the endocytotic integrin recycling pathway. During integrin recycling internalization can occur through either a clathrin dependent, caveolae dependent or a clathrin and caveolar independent mechanism. Early endosomes express Rab5 and then Rab4 if they cycle via the short (fast) sub-membranous loop, or Rab11 if they cycle via the long (slow) loop which passes through the PNRC. Otherwise integrins may either be stored internally or lysosomally degraded (Rab7 associated).

3.1.5. Integrin Expression within the Oesophagus

Within the oesophagus, the expression of integrins has been poorly characterised. Integrin α_2, α_3, α_6, and α_V have been demonstrated as present throughout the oesophageal epithelium, with the greatest expression seen in the basal cell layers [262, 314]. The expression of these integrins varies throughout the normal-BO-OAC sequence. For example, ITGAV has been shown to be highly expressed in SqCCa of the oesophagus [315]. However, in squamous epithelium the expression of ITGAV has been less consistently demonstrated; studies have demonstrated conflicting results regarding the expression of this molecule [262, 314, 316]. However, the apparent upregulation of this integrin in tumours and in the associated angiogenesis has led to the clinical trials investigating the use of ITGAV inhibitors as therapeutic agents to treat oesophageal neoplasia [297, 317-318].

3.2. Aims

Increasing exposure of the oesophagus to BAs has been shown to correlate with the risk of erosive oesophagitis, BO and OAC [18, 20-21]. Despite the lack of a definitive aetiology regarding BO the general consensus is that significant denudation of the squamous epithelium is required to allow re-epithelialisation with BO [11]. The toxicity of BAs and low pH has been thought to be the primary mechanism regarding the erosions seen in erosive reflux disease. The addition of the proteases trypsin and pepsin is thought to perpetuate the toxicity of the refluxate. Yet interestingly, BAs have been shown to inhibit protease function [319].

While researching cell death induced by DCA in the HET-1A cell line, and its potential modulation by UDCA, a predictable discordance was identified between the results generated by the MTT and nuclear count assays (See Section 3.4.1). If this discrepancy were simply due to the washing and staining processes involved in the nuclear count assay, then the discrepancy would have been constant between treatments, especially at the earlier time-points when viability was relatively unaffected.

Given the predictable discrepancy between the MTT and the cell count assay, we hypothesised that DCA and UDCA were inducing a reduction in adherence in the HET-1A cell line. A reduction in integrin expression, induced by BAs, could reduce adhesion of oesophageal squamous epithelium to the ECM proteins in the basement membrane.

Thus the aims of this chapter were:

- To characterise the effect of BAs (with particular focus on DCA) on the adherence of HET-1A oesophageal cells to ECM components,
- To investigate whether any BA-mediated loss of adhesion was due to alterations in the expression or function of a broad range of adhesion molecules or was specific to a certain subset,
- To investigate whether any BA-mediated loss of adhesion was occurring as a result of apoptosis, or whether it was occurring through a specific mechanism independent of cell death, and,
- To investigate the potential validity of this hypothesis *in-vivo*.

3.3. Methods

3.3.1. Cell Lines and Culture

The HET-1A [240], QH [320], SKGT-4 [321], HCT116 [241], and HUH-7 [242-243] cell lines were used for these experiments. These lines represent normal squamous epithelium of the oesophagus, non-dysplastic BO, Barrett's derived OAC, colonic adenocarcinoma and human hepatoma cells respectively. The origin of these cells and the rationale for their use is explained in Section 9.1.1. QH cells were grown in BEBM with supplements and 5% FCS and SKGT-4 cells were grown in RPMI 1640 with 10% FCS. The media used for other cell lines and the culture methodology have previously been explained (Section 2.3.1).

3.3.2. Time lapse Live Cell Light Microscopy

3.3.2.1. Background

Time-lapse live cell microscopy allows repeated imaging of specific cell populations to evaluate dynamic changes over a prolonged period of time without manipulation or environmental alteration of the experimental setup. The use of fixed cell imaging to evaluate cell death is limited by the morphological changes induced by the fixing and staining process, the disintegration of dead cells and the removal of dead or dying cells which have lost adherence. However, the absence of fluorescent labelling limits the study to morphological assessments only.

3.3.2.2. Experimental Methodology

Cells were seeded at 7.5 X 10^3 cells / well in a Nunc-96 well plate and left to adhere overnight. At t0 the media was aspirated and replaced with media containing individual BAs. Time lapse live cell imaging was performed using the IncuCyte live cell imaging system (Essen Biosystems, Ann Arbour, MI) with images taken every 30 minutes for a 24 hour period.

3.3.3. Adherence Assays

3.3.3.1. Background

Adherence of cells to a basement requires the binding of membrane based proteins to a ligand. After initial contact, the adhesive strength is reinforced by spreading of the cell on the basement

enhancing the contact area between the cell and the structure to which it is attached [274]. Thus spherical cells in media transition to polygonal adherent cells in cell culture. The strength of adherence of a cell to a basement membrane is determined by the expression of a variety of cell adhesion molecules on the cell surface and the presence of ECM ligands appropriate to the expressed cell adhesion molecules.

3.3.3.2. Experimental Method

3.3.3.2.1. General Adherence Assay

Cells were allowed to grow to 80-90% confluence in cell culture flasks (approximately 48 hours after seeding). The cells were then dissociated from the flasks by gentle scraping. The cells were collected, centrifuged at 1100 rpm for 5 minutes, the supernatant discarded and the cells re-suspended in complete medium. To determine the ability of cells to adhere to plastic (broad adhesive capacity), the cells were seeded at 3 X 10^4 cells per well in 100µL of medium in black Nunc 96-well plates. 100µL of medium containing BAs was added to each well. Cells were allowed to adhere for two hours. The medium was gently aspirated and the wells gently washed twice with PBS. 100µL of medium containing 2.5µM Calcein AM (Biotium, Hayward, CA, USA) was added to each well and the plate incubated in the dark for one hour at 37°C. Calcein AM is a cell permeable non-fluorescent compound. In live cells Calcein AM is hydrolyzed by esterase into a green fluorescent anion which is trapped intra-cellularly. The green fluorescence was read using a Victor luminometer (Perkin Elmer, Waltham, MA, USA).

Demonstration of the relationship between Calcein AM concentration and HET-1A cell count is shown in

Figure 3–2. This demonstrated that at a constant cell number there was a linear relationship between Calcein AM concentration and fluorescence up to a concentration of 5µM. Similarly, using a constant concentration of Calcein AM, there was an adequately linear concentration between cell number and fluorescence.

3.3.3.2.2. Adherence to Specific ECM Proteins

To measure the adherence of cells to specific ECMs, cell adhesion was determined as per the protocol of the Millicoat™ ECM screening kit (Millipore, Billerica, MA, USA). Briefly, ECM proteins were rehydrated and cells were seeded and treated as described above. Cells were left to adhere for two hours. The media was gently aspirated and the plate washed three times with PBS containing Ca^{2+} and Mg^{2+}. 100µL of 0.2% crystal violet (Sigma, St. Louis, MO, USA) in 10% ethanol was added to each well and left to incubate for 5 minutes at RT. The stain was gently

aspirated and the wells washed gently three times with PBS. 100μL of solubilization buffer (50/50 mixture of 0.1M NaH_2PO, pH 4.5 and 50% ethanol) was added to each well and the plate gently shaken at room temperature for 10 minutes, until the cell-bound stain was completely solubilized. The absorbance at 570nM was determined using a BioTek ELx800 absorbance microplate reader (BioTek, Winooski, VT, USA).

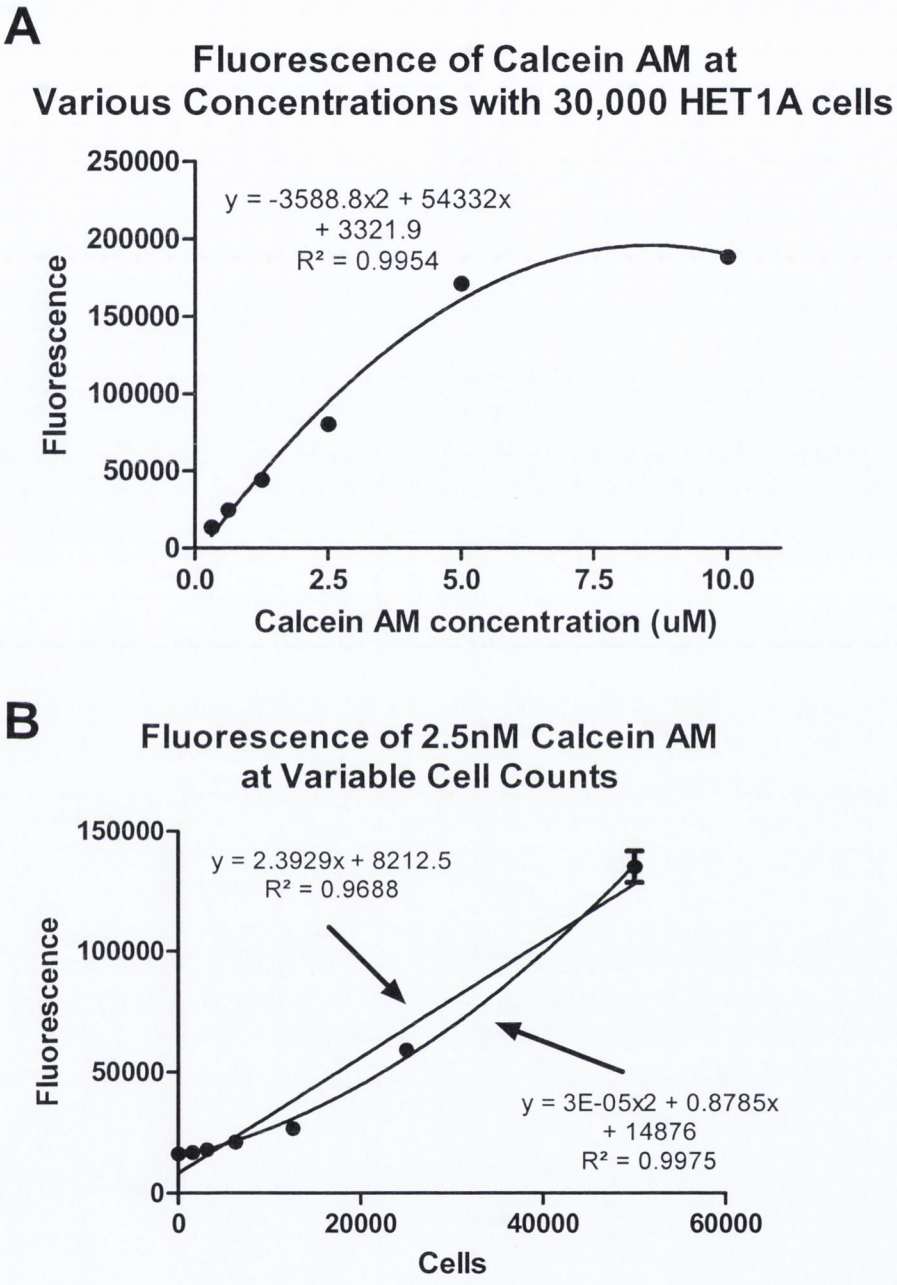

Figure 3–2: The relationship between Calcein AM and HET-1A cell number per well. The fluorescence of Calcein AM demonstrated a linear relationship with increasing concentration up to a concentration of 5μM (A). Fluorescence of Calcein AM demonstrated an approximately linear relationship with HET-1A cell number per well, although in fact a quadratic curve demonstrated a slightly better fit (B). Data shown represents mean and SEM of N=2.

3.3.4. Detachment and Re-Adherence Assays

3.3.4.1. Background

Detachment of cells from a basement membrane occurs through a variety of mechanisms, some controlled and others un-controlled [302-304]. Apoptosis and cell death is known to induce a loss of adherence of cells. DCA had been shown to induce a loss of adhesion in the HET-1A cell line in a dose dependent fashion. However, it had also been shown to induce cell death in a dose and time dependent fashion. Thus we next investigated whether cells which had detached in response to DCA were capable of re-adherence and spreading after removal of the DCA stimulus.

3.3.4.2. Experimental Method

The ability of detached cells to re-adhere to plastic was measured using an MTT assay (See Section 2.3.2.2). Cells were seeded at $2x10^5$ cells per well in 12-well plates and allowed to adhere overnight. The cells were treated for two hours with DCA or vehicle control. After treatment the medium was aspirated and the wells washed twice with the aspirated medium to ensure capture of all detached cells. The well was then washed twice with fresh medium to dilute out the DCA or vehicle control. 1ml of fresh medium was then placed in the wells. The aspirated supernatant was spun at 1800rpm for 4 minutes to pellet the cells. The pellet washed twice with fresh warm medium to dilute out the DCA or vehicle control. The pellet was re-suspended in 1ml of fresh medium and the cells replaced in an unused well in the 12-well plate. After 24 hours, images were acquired to demonstrate re-adherence and cell spreading on the plastic surface. Subsequently 100μL of 2.5mg/mL MTT added to each well and two hours later, the medium was gently aspirated and the formazan crystals dissolved in 200μL DMSO. 100μL of DMSO was aspirated and placed in a 96-well plate and the absorbance at 570nM read using a plate reader.

3.3.5. Analysis of Cell Surface Integrin Expression Using Flow Cytometry

3.3.5.1. Background

The role of integrins and the mechanisms through which surface expression of these molecules is modulated has been explained above (Section 3.1). in order to investigate the expression of integrin sub-families on the epithelial cell line HET-1A in the presence or absence of BAs, flow cytometry of immunofluorescently stained cells was used. Live cells were un-fixed and un-permeabilised so that only surface integrins were immunofluorescently labelled.

3.3.5.2. Experimental Method

Cells were seeded in T25 cell culture flasks and allowed to grow until 89-90% confluent. The media was gently removed and replaced with media containing the sodium salts of DCA or UDCA (Sigma, St. Louis, MO, USA and EMD Chemicals, Gibbstown, NJ, USA respectively) or vehicle control (DMSO). The cells were incubated for 2 hours at 37°C. The cells were dissociated by gentle scraping. All cells were collected and centrifuged at 1100rpm for 5 minutes at 4°C and the supernatant discarded. Blocking was performed in 1mL of a 50/50 mixture of FBS and wash buffer (2% FBS in PBS) for 5 minutes at 4°C. The cells were centrifuged and washed in wash buffer twice at 4°C. The supernatant was gently aspirated, leaving 100μL of wash buffer. Anti-integrin antibody (α_3/ α_4/ α_5/ α_6; BD Biosciences, Franklin Lakes, NJ, USA, α_v; Merck, Whitehouse Station, NJ, USA, and Santa Cruz Biotechnology Inc, Santa Cruz, Ca, USA) was added and the cells re-suspended by vortexing. The cells were left to incubate for 30 minutes in the dark at RT at 4°C. 1mL of wash buffer was added, the cells centrifuged and the wash step repeated. For antibodies directly labelled with fluorophore, the cells were re-suspended in 300μL wash buffer and analysed using flow cytometry. For those antibodies not directly labelled, the cells were incubated with (1:500) Alexa Fluor fluorescent secondary antibodies (Invitrogen, Carlsbad, CA, USA) for 30 minutes in the dark at 4°C. Cells were then washed and centrifuged twice, re-suspended in 300μL wash buffer and analysed using flow cytometry (Beckman Coulter Cyan ADP 9 Colour, Brea, CA, USA).

Comparison of the intensity data was undertaken using two methods. The first was direct statistical comparison of the mean intensity values. The second is comparison of the percentage difference in intensity histograms. These two complementary methods were used to demonstrate the robustness of the data.

3.3.6. Visualization of ITGAV Expression in Human Oesophageal Tissue Using Immunofluorescence Microscopy

3.3.6.1. Experimental Method

In order to determine in-vivo expression in ITGAV in oesophageal tissues (Rat and Human), immunofluorescent staining was performed on 4-μm formalin-fixed, paraffin-embedded tissue sections. A full protocol is available in Appendix 4. Paraffin embedded samples of squamous epithelium (N=12), BO (N=9), OAC (N=3) and SqCCa (N=2) were kindly provided by the Departments of Surgery and Histopathology in St James' Hospital. Paraffin embedded rat oesophagi were kindly provided by Dr James Murphy from work he had previously performed [322]. To investigate the effects of BAs on human oesophageal tissue, biopsies of healthy

squamous oesophageal tissue was acquired, with the patient's consent, during gastroscopy in the endoscopy department in St James Hospital. Ethics had previously been approved by the hospital ethics committee. Six biopsies were taken from each of five patients, placed in medium containing no DCA, 300μM DCA or 500μM DCA and incubated at 37°C for 2 hours. These were subsequently fixed and embedded in paraffin blocks.

Prior to staining, each slide was de-paraffinized and rehydrated by sequential immersion in xylene (2 X 5 minutes) 100% ethanol (2 X 5 minutes), 70% ethanol (2 X 5 minutes), and distilled water (2 X 5 minutes). Antigen retrieval to unmask protein epitopes altered during formalin fixation and paraffin embedding was performed using a sodium citrate based heat retrieval method in which rehydrated sections were treated for 10 minutes in sodium citrate buffer in a low-pressure pressure-cooker. After 10 minutes, the sections were transferred to fresh warm sodium citrate buffer and allowed to cool to RT (30 minutes). The sections were transferred to 0.1% PBST. Blocking was performed with 5% normal goat serum (Sigma, St. Louis, MO, USA) in PBS for one hour at RT. The tissue was then incubated with primary antibody (anti-ITGAV, 1:100, BD Biosciences) overnight at 4°C in a humidity chamber. The tissue was washed twice for 5 minutes in baths of PBST and was then incubated with secondary antibody (1:500, Alexa fluor 488 Goat Anti-Mouse, Invitrogen) and Hoechst (1:2000, Hoechst 44432, Invitrogen) in PBS for one hour at RT in a humidity chamber. The tissue was washed twice for 5 minutes in baths of PBST to remove excess secondary antibody. Finally, coverslips were mounted using aqueous mounting medium (Sigma, St. Louis, MO, USA). Images were acquired using a Zeiss LSM510 laser confocal microscope using a 63X oil immersion objective.

3.3.7. Analysis of Levels of Expression of ITGAV, Cleaved PARP and LC3 by Western Blotting.

3.3.7.1. Experimental Method

The experimental methodology for performing Western blotting for cleaved PARP and LC3 has been explained previously in section 2.3.6 and a full protocol is presented in Appendix 4.

For ITGAV, the same experimental protocol was used, except that cells were incubated with mouse anti-human ITGAV (1:500, Santa Cruz Biotechnology Inc, Santa Cruz, Ca, USA) overnight at 4°C.

3.3.8. Visualisation of Rab5 and Rab11 and Co-Localization with ITGAV in HET-1A Cells using Immunofluorescent Microscopy

3.3.8.1. Background

Endocytic recycling loops are modulated by Rab GTPases. These proteins modulate membrane trafficking, vesicle formation and movement, and membrane fusion. Early endosomes represent the earliest definitive vesicles seen after budding of an invaginated pit from the cell membrane. Early endosomes are associated with Rab5. In the fast recycling loop endosomes are cycled rapidly in a Rab4 dependent fashion. In the long loop, the endosomes are trafficked in a Rab11 dependent fashion through the PNRC prior to being re-packaged and again transferred to the cell membrane. Endosomal vesicles targeted for lysosomal degradation are associated with Rab7 [308-310]. For this research, we chose to study whether ITGAV associated with Rab5 or Rab11. Co-localization would suggest that ITGAV was undergoing endocytic recycling.

3.3.8.2. Experimental method

A full immunofluorescent staining protocol is available in Appendix 4. Glass bottomed Matrix 96-well plates (Thermo Fischer Scientific, Waltham, MA, USA) were treated with 50µL poly-l-lysine (Sigma, St. Louis, MO, USA) for one hour at 37 °C. Coating of wells with this positively charged homopolymer allows greater adherence of cells to the glass plate. After 30 minutes at 37°C the poly-l-lysine was removed and the wells washed twice with 200µL PBS. HET-1A cells were seeded at a density of $5X10^4$/well and allowed to adhere overnight. After treatment with BAs, fixation was performed with 4% PFA for 15 minutes at 37°. The cells were then permeabilized with 0.1% PBST for 5 minutes at RT and then washed twice with 200µL PBS. Blocking was performed for 30 minutes at RT with 5% bovine serum albumin (BSA) in PBS. Cells were incubated with rabbit anti-Rab5 (1:100, Santa Cruz Biotechnology Inc, Santa Cruz, Ca, USA), rabbit anti-Rab11 antibody (1:100, Zymed Laboratories, San Francisco, CA, USA) or a rabbit IgG isotype control (1:100, Zymed Laboratories, San Francisco, CA, USA) for one hour at RT. The cells were washed twice with 200µL PBS. The cells were then incubated with AlexaFluor-586-conjugated anti-rabbit secondary antibody (1:500, Invitrogen, Carlsbad, CA, USA) for 60 minutes at RT. The cells were washed twice with 200µL PBS and incubated with mouse anti-ITGAV (1:100 BD Biosciences, Franklin Lakes, NJ, USA) or non-specific mouse IgG antibody (1:100, Zymed Laboratories, San Francisco, CA, USA) for 60 minutes at RT and then washed twice with 200µL PBS. Cells were then incubated with AlexaFluor-488-conjugated anti-mouse secondary antibody (1:500, Invitrogen, Carlsbad, CA, USA) for 60 minutes at RT. Finally, nuclei were labelled with Hoechst 33342 (1:2000, Invitrogen, Carlsbad, CA, USA) for 15 minutes at RT.

Images were acquired using a Zeiss LSM510 laser confocal microscope using a 63X oil immersion objective.

For analysis of Rab5 or Rab11 vesicle morphology, the GE InCell was used. After image acquisition, vesicle size and number were determined using GE InCell Analyser algorithms (granularity and sub-cellular organelles) optimized for the Rab staining.

3.4. Results

3.4.1. DCA Stimulation Rapidly Induces a Loss of Adhesion in A Dose Dependent Fashion, Hours Prior to the Onset of Apoptosis.

While UDCA failed to inhibit DCA-induced apoptosis in the HET-1A cell line, the significant discordance between the MTT and the nuclear count assays remained of concern. Investigation of the difference using Bland-Altman plots demonstrated mean differences in the HET-1A cell line of 2.6% (95% CI of Diff: -2.0% to 7.1%, $p = 0.265$), -29.0% (95% CI of Diff: -21.3% to -36.7%, $p < 0.0001$) and -19.1% (95% CI of Diff: -12.0% to -26.3%, $p < 0.0001$) in the co-treatment, and the four and eighteen hour UDCA pre-treatment experiments respectively (Figure 3–3A). In the HCT116 cell line the values were -8.4% ($p < 0.05$), -20.7% ($p < 0.0001$) and -21.9% ($p < 0.0001$) respectively (Figure 3–3A and Appendix 2). However, the Bland-Altman plots demonstrated a large amount of variance in the system without a predictable pattern.

Further evaluation of the difference between the assays demonstrated that the greatest discrepancy in the HET-1A cell line was at early time-points. At these time-points there appeared to be a greater difference with increasing concentrations of DCA and UDCA (Figure 3–3B). This suggested that there was a predictable discrepancy between the two assays, which was not seen in the Bland-Altman plots. Using multiple linear regression, we next demonstrated that the discrepancy could be modelled. For the UDCA pre-treatment prior to DCA experiments in the HET-1A line, the discrepancy between the two assays could be predicted using the following equation (where the difference was the percentage difference between the remaining viable cells (Based on the MTT assay):

$$\text{Difference} = 6.29 - 0.227*\text{Time} - 0.117*\text{UDCA} - 0.0543*\text{DCA}$$

$$R^2 = 76.7\%, \text{SD} = 14.263.$$

In this model, the effect of time was not significant ($p = 0.345$), however, the effects of DCA and UDCA were both significantly influencing the difference between the assays ($p < 0.001$ for both).

When the absolute values were modelled, time was an inversely proportional predictor and DCA lost its significance predicting the difference between the nuclear count and the MTT assay. However, when the 24 hour time-point was removed from the analysis the effect of DCA again became significant. This likely represents the fact that at higher concentrations of DCA at longer exposure time-points, there is too little absolute difference between the normalised nuclear count and the MTT values as a consequence of the majority of cells having died.

The difference between the nuclear counts and the MTT assay could be similarly modelled for the HTC116 cell line:

$$\text{Difference} = 26.9 - 1.56*\text{Time} - 0.0246*\text{UDCA} - 0.0769*\text{DCA}$$

$$R^2 = 69.7\%, \text{SD} = 14.148.$$

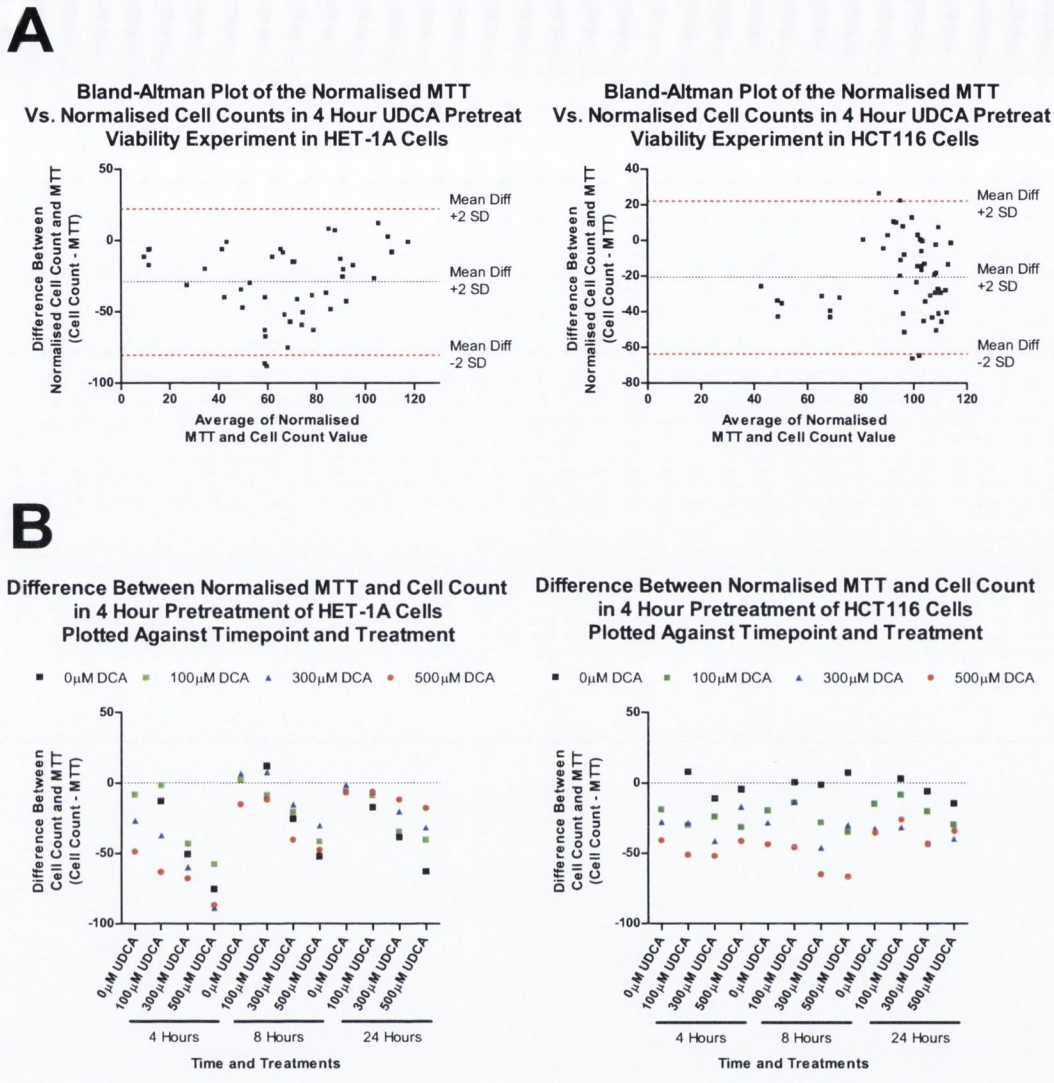

Diff = 6.29 - 0.227*Time - 0.117*UDCA - 0.0543*DCA
R2 = 76.7%, SD = 14.263.

Diff = 26.9 - 1.56*Time - 0.0246*UDCA - 0.0769*DCA
R2 = 69.7%, SD = 14.148.

Figure 3–3: Difference between viability as estimated by the cell count and the MTT assay is greatest at higher BA concentrations and at earlier time-points in the four hour pre-treatment experiment. The mean normalised viability of the MTT experiments for each treatment was subtracted from the same treatment normalised viability as measured by the nuclear count. Data represents the difference between the mean values of the three experiments. The Bland-Altman plots demonstrate that HET-1A cells exhibit a wide variety of viabilities while the HCT116 cell line remains viable in the majority of time-points and treatments. However, the Bland-Altman plots demonstrated a large limit of agreement between the two assays as demonstrated by the red dashed lines marking +/- 2SD from the mean difference. Plotting the difference between the assays against treatment and time demonstrated a predictable pattern in the HET-1A cell line with difference being predicted by DCA concentration, UDCA concentration and time.

We hypothesised that the predictable discrepancy reflected a loss of adherence in the cells after BA treatment resulting in a greater loss of cells during the fixing and staining process for the nuclear count assay. Had the discrepancy only been due to the greater number of washing steps in the nuclear count assay, we hypothesised that the difference between the assays would have been a similar proportion of viable cells after all treatments.

To investigate this further we performed live cell imaging of the HET-1A and HCT116 cell lines exposed to 300μM UDCA or DCA (Figure 3–4, Figure 3–5, and Figure 3–6). This demonstrated that DCA induced a rounded phenotype in the HET-1A cell line that was seen within after less than 120 minutes of exposure. In the HCT116 cell line, no noticeable phenotypic changes occurred until 8 to 12 hours after exposure to DCA. Apoptotic features did not occur in either cell line until hours after the development of this rounded phenotype. UDCA had no significant effect on cell morphology at up to 24 hours.

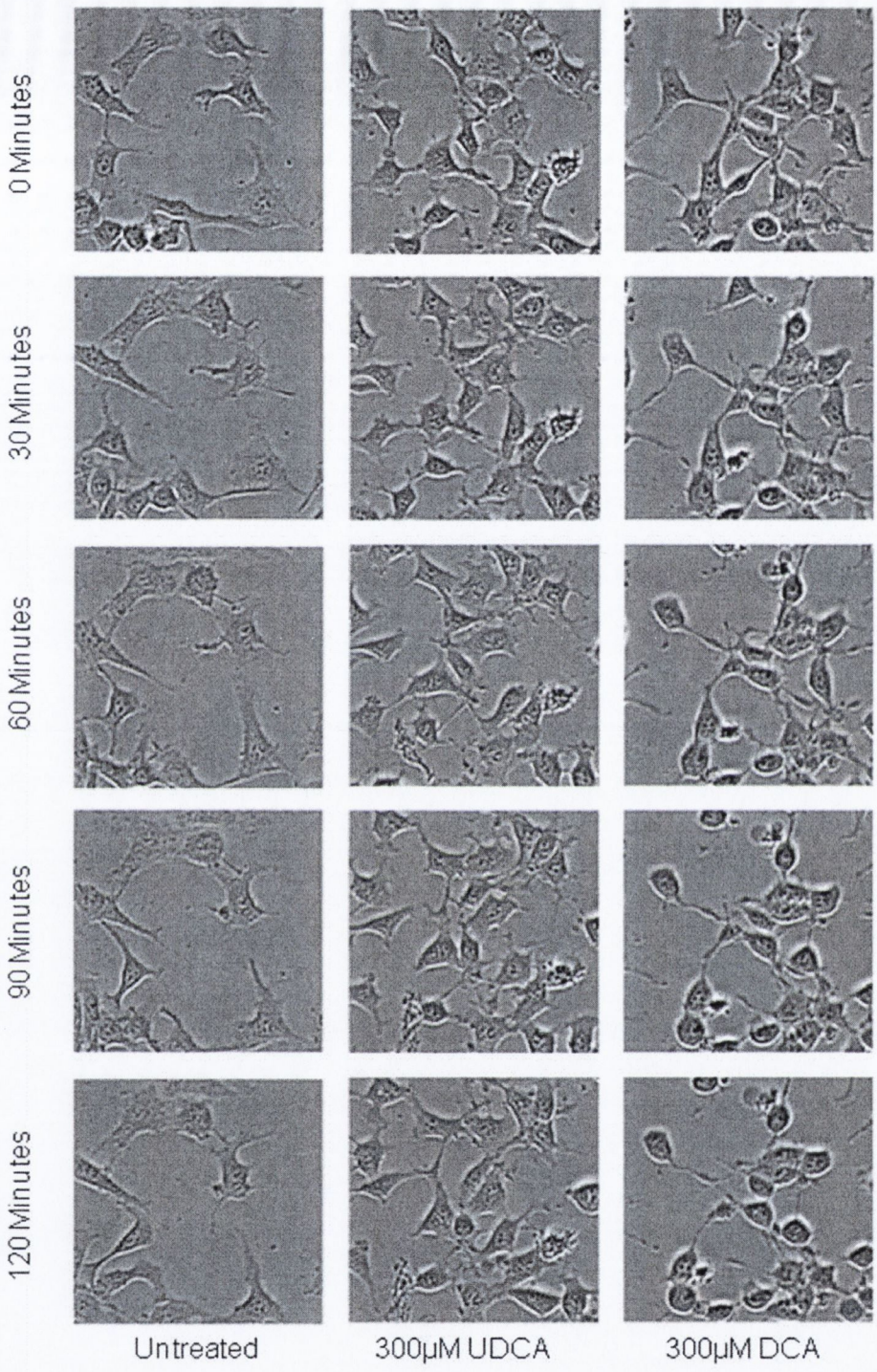

Figure 3–4: Live Cell Imaging of HET-1A Cells during Exposure to 300µM DCA or 300µM UDCA demonstrated a rounded phenotype in the 300µM DCA treated cells beginning minutes after exposure. Cells were seeded at 7.5 X 10^3 cells / well in a Nunc-96 well plate and left to adhere overnight. At t0 the media replaced with media containing 300µM DCA or 300µM UDCA. Time lapse live cell imaging was performed every 30 minutes for a 24 hours period using the IncuCyte live cell imaging system.

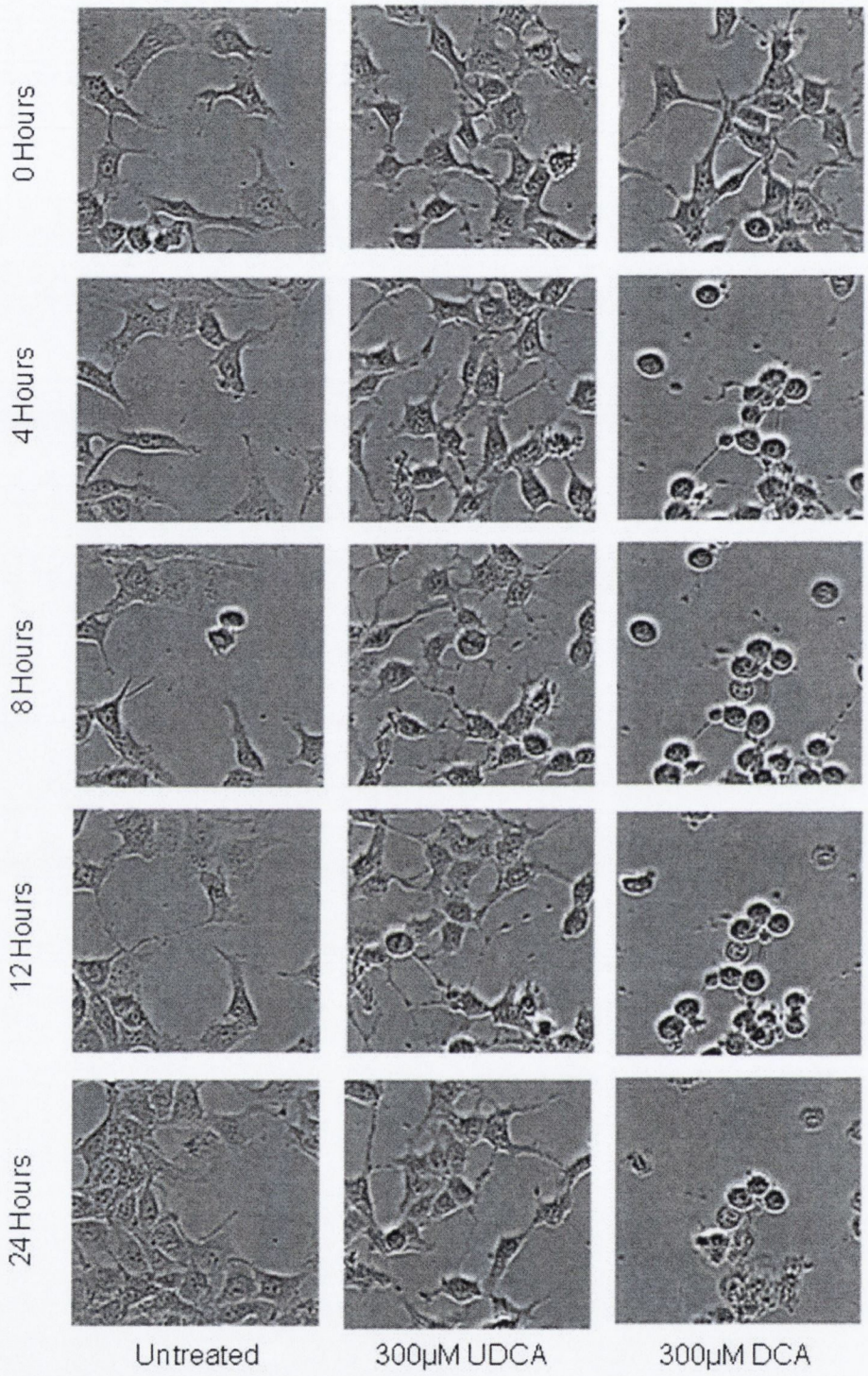

Figure 3–5: Live Cell Imaging of HET-1A Cells During Exposure to 300µM DCA or 300µM UDCA for 24 Hours. Cells were seeded at 7.5 X 10^3 cells / well in a Nunc-96 well plate and left to adhere overnight. At t0 the media replaced with media containing 300µM DCA or 300µM UDCA. Time lapse live cell imaging was performed every 30 minutes for a 24 hours period using the IncuCyte live cell imaging system.

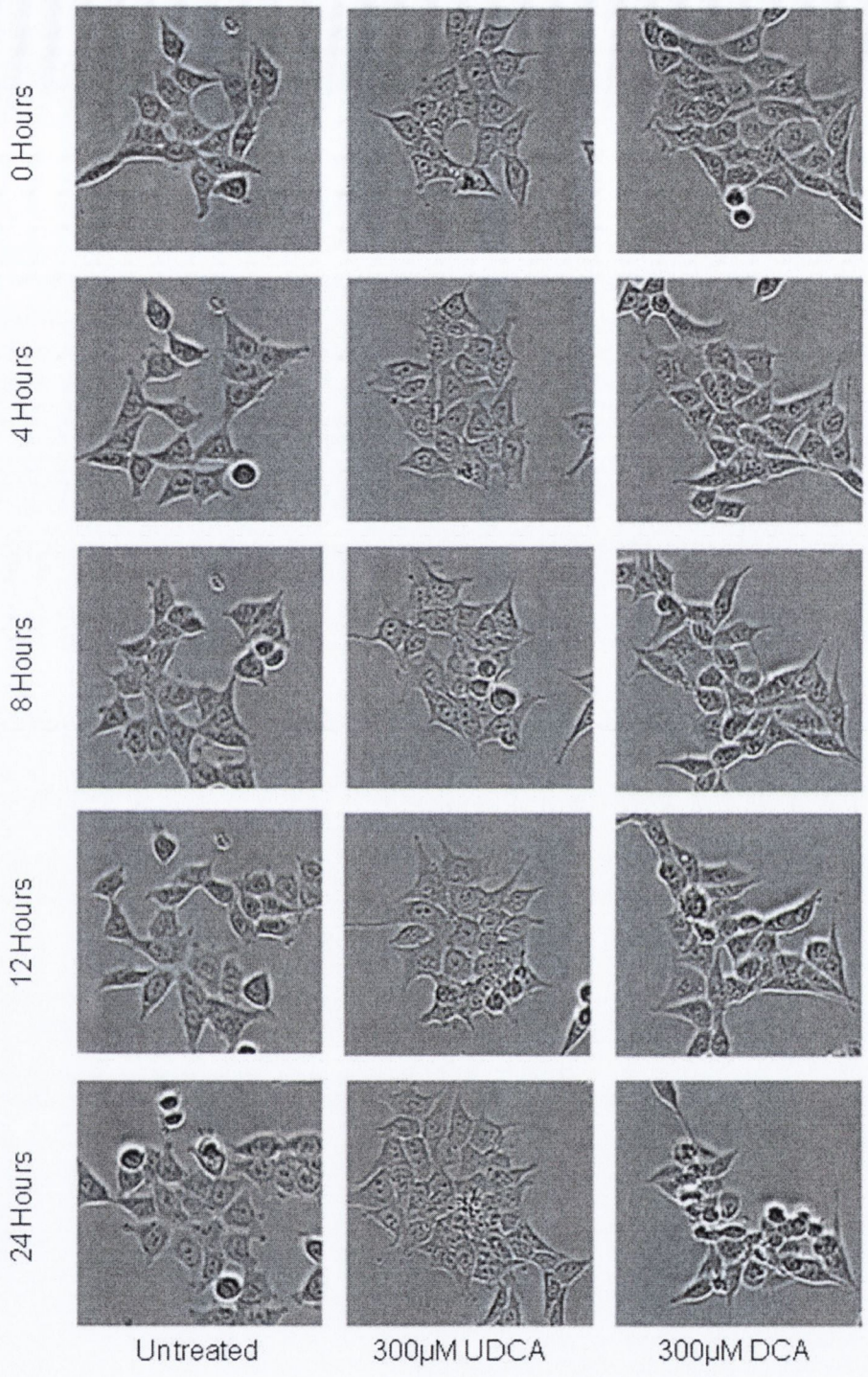

Figure 3–6: Live Cell Imaging of HCT116 Cells During Exposure to 300µM DCA or 300µM UDCA for 24 Hours. Cells were seeded at 7.5 X 10^3 cells / well in a Nunc-96 well plate and left to adhere overnight. At t0 the media replaced with media containing 300µM DCA or 300µM UDCA. Time lapse live cell imaging was performed every 30 minutes for a 24 hours period using the IncuCyte live cell imaging system.

3.4.2. DCA, but not UDCA, Induces a Loss of Adherence, Which is Modulated Distinctly from Apoptosis

3.4.2.1. DCA, but not UDCA Prevents Adhesion of HET-1A Cells to a Plastic Surface in a Dose Dependent Fashion

To investigate whether the BAs were indeed modulating adhesion in a dose dependant fashion, adhesion assays were performed on uncoated plastic surfaces. DCA prevented adhesion in a dose dependent fashion (ANOVA $p < 0.001$, Figure 3–7A). UDCA in combination with DCA did not enhance or reduce the effect of DCA on adhesion. In isolation, UDCA itself had no effect on adhesion at concentrations of up to 600μM, although low dose UDCA appeared to increase the adherence in a non significant manner at lower concentrations. At a concentration of 37.5μM UDCA, $p = 0.08$.

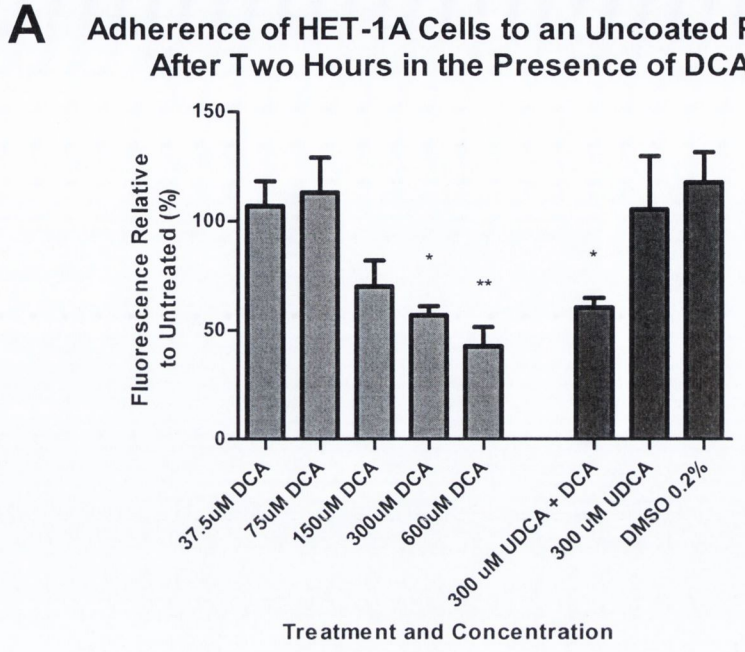

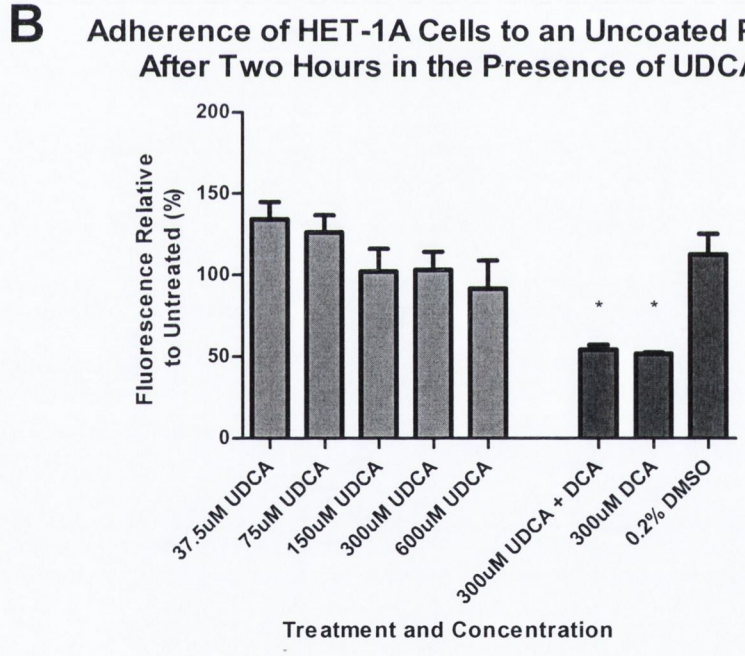

Figure 3–7: DCA (A) but not UDCA (B) treatment reduces the adherence of HET-1A cells to uncoated plastic. In combined treatments 300μM UDCA does not modulate the loss of adherence induced by 300μM DCA. Cells were non-enzymatically dissociated from growth flasks and seeded at 3 X 10^4 cells per well in medium containing BAs. Two hours later the media was aspirated, the wells washed three times gently with PBS. 2.5nM Calcein AM in fresh medium was added and one hour later, the fluorescence was read at λ = 535nM. Mean and SEM for N=4. * denotes $p < 0.05$ and ** denotes $p < 0.01$ when compared to the untreated control.

3.4.2.2. DCA Induces a Detachment of Adherent HET-1A Cells but These Cells are Capable of Re-adhering.

Previous authors have suggested that the loss of adherence which occurs in the setting of BA exposure is a consequence of the activation of apoptotic machinery and represents an irreversible process along the pathway to cell death. To determine whether this was the case in the DCA-induced loss of adherence, we investigated whether DCA could induce detachment of attached cells and if so, whether cells which had lost adherence were capable of surviving and re-adhering when the BA stimulation was removed.

As per previous experiments regarding viability in HET-1A cells treated with DCA, increasing concentrations of DCA induced greater amounts of cell death. Two hours exposure to 100μM, 300μM and 500μM of DCA reduced total viability to 101.5% (95% CI 77.2% to 125.8%), 67.5% (95% CI 50.5% to 84.5%, $p < 0.01$) and 41% (95% CI 20.3% to 61.7%, $p < 0.001$) respectively (Figure 3–8A). DMSO induced no significant reduction in viability. Of the remaining viable cells, 10.6% (95% CI 0.5% to 20.8%) of untreated and 15.0% (95% CI 4.2% to 68.2%) of DMSO-treated had been moved to the new well as a result of the experimental process. When treated with DCA this increased to 20.6% (95% CI -3.7% to 45.0%), 33.9% (95% CI -0.1% to 67.93%) and 43.9% (95% CI 10.9% to 76.9%, $p < 0.001$ relative to untreated moved) for 100, 300 and 500μM respectively (Figure 3–8B).

Imaging demonstrated that the majority of cells that had detached had re-adhered to the well base during the 24 hours after treatment. A phenotype consistent with apoptotic cells was seen in both treated and untreated wells, and not solely in those cells which had been become detached (and subsequently re-adhered) after DCA treatment (Figure 3–8C).

These findings suggest that while DCA is inducing cell death in a dose dependent fashion, at least some of the detached cells are capable of surviving and re-adhering. The increasing percentage of viable cells present in the supernatant seeded well are concordant with the adherence data from previous experiments (Figure 3–7A) but also suggests that while the magnitude of cell death increased in both the unmoved and moved cells with increasing concentrations of DCA, some of these cells are capable of surviving, re-adhering and proliferating again.

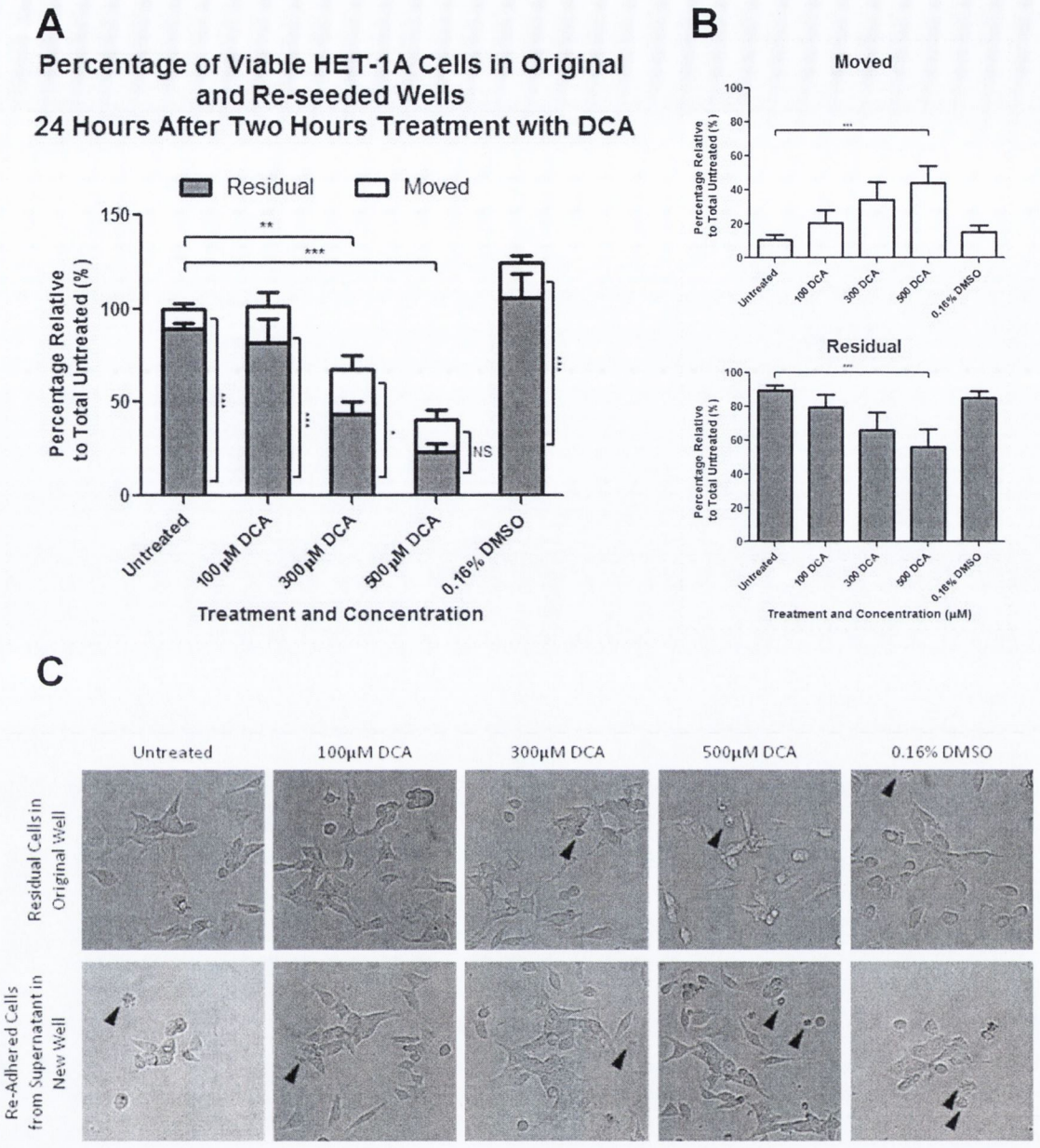

Figure 3–8: DCA induces detachment of adherent HET-1A cells in a dose dependent fashion and a proportion of these detached cells can re-adhere. DCA induced a dose dependent reduction in cell viability (A). DCA also induced a dose-dependent detachment of cells from the uncoated plastic, and these cells were capable of re-adherence and spreading after removal of the DCA stimulus (A, B and C). Apoptotic cells were present in all wells (C, arrowheads). Cells were seeded at in 12-well plate and allowed to adhere overnight. After treatment for two hours with DCA or vehicle control the medium and detached cells were aspirated. Residual cells were washed twice and 1ml of fresh medium was placed in the wells. The originally aspirated medium was spun to pellet the cells. The treatment medium was aspirated and the pellet washed twice with fresh warm medium. The pellet was re-suspended in 1ml of medium and the cells placed in a clean well in the 12 well plate. After 24 hours, images were acquired and subsequently 100uL of 2.5mg/mL MTT added to each well. After two hours the medium was gently aspirated and formazan crystals dissolved in 200μL DMSO. The absorbance at 570nM read using a plate reader. * and ** denote $p < 0.01$ and 0.001 respectively.

3.4.3. DCA Induces a Specific Loss of Adhesion to the ECM Proteins Vitronectin and Laminin in HET-1A Cells

We next investigated whether the reduction in adhesion was specific for any ECM protein. Using plates pre-coated with ECM proteins, we repeated the adhesion assay. The binding of untreated HET-1A cells to the ECM proteins was relatively homogeneous except for binding to vitronectin which demonstrated approximately 70% of the adhesion of the other ECM proteins ($p < 0.05$). DMSO vehicle (0.2%) itself induced a significant reduction in adherence to fibronectin and a non-significant reduction to other ECM proteins (Figure 3–9A).

With DCA stimulation, a loss of adherence of 23%, 20% and 9% (relative to DMSO control) was seen to collagen I, collage IV and fibronectin but these failed to reach significance. A reduction of 14.3% to laminin (95% CI of diff 27.2% to 1.4%, $p < 0.05$) and 88% to vitronectin (95% CI of diff 122.3% to 53.6%, $p < 0.001$) was seen with 300μM DCA (Figure 3–9B).

UDCA in isolation significantly increased adherence above that of DMSO control on fibronectin (22.7%, 95% CI of diff: 43.1% to 2.3%, $p < 0.05$) but this increase failed to reach significance on the other ECM proteins (greater adherence of 11.6%, 23.3%, 2.4% and 22.8% respectively). On vitronectin UDCA reduced the loss of adherence induced by DCA ($p < 0.01$) although on all other ECM proteins, the reduction in adherence was less in the UDCA and DCA co-treatment than in DCA alone.

These findings suggested that there was indeed a reduction in adherence which was not mediated solely through an induction of apoptotic machinery. Furthermore, these findings suggested that UDCA may be able to modulate the DCA-induced loss of adherence, at least on vitronectin.

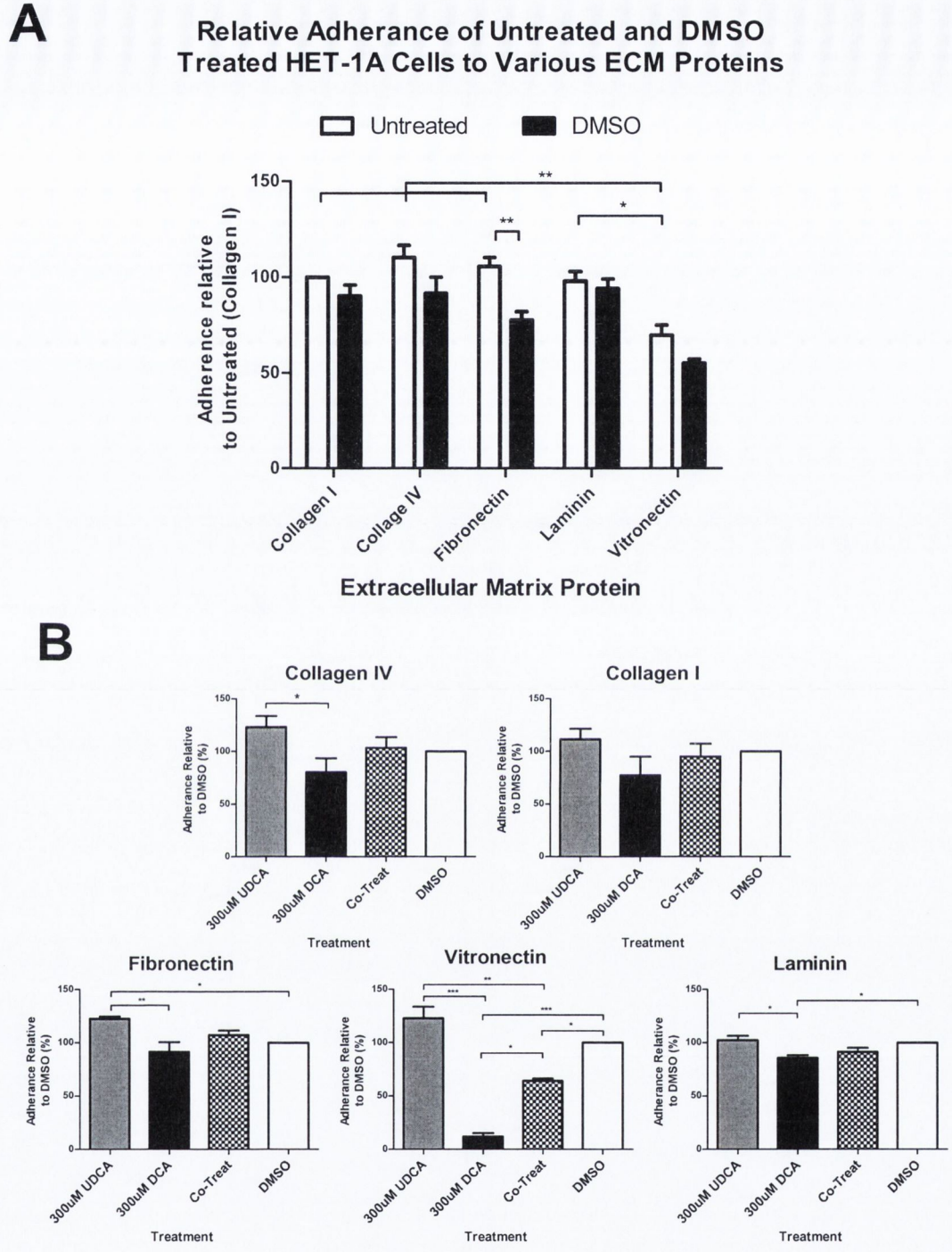

Figure 3–9: Adherence of HET-1A cells to the ECM proteins vitronectin and laminin is reduced by DCA treatment. Adherence of HET-1A cells to ECM proteins is equivocal except for a lower level of adherence to vitronectin, and 0.2% DMSO results in a minor loss of adherence to all ECM proteins but specifically to Fibronectin (A). Relative to DMSO, 300μM DCA stimulation results in a reduction in adherence to vitronectin and 300μM UDCA increases adherence to fibronectin (B). UDCA reduced Cells were seeded at 3 X 10^4 cells per well in medium containing BAs. Two hours later the media was aspirated, the wells washed gently three times with PBS. The remaining cells were stained with crystal violet for 5 minutes and then washed with PBS. The cells were dissolved and the absorbance from each well read at 540nM. Mean and SEM for N=3. * denotes $p < 0.05$. ** denotes $p < 0.01$ and *** denotes $p < 0.001$ when compared to DMSO control.

3.4.4. Integrin α_V, the Vitronectin Receptor is Present on HET-1A Cells and is Expressed on a Variety of Oesophageal Tissues

Binding of cells to ECM proteins is mediated through a variety of trans-membrane proteins, the most important of which are the integrins. While the binding of integrin heterodimers to ECM proteins is promiscuous, the affinity of specific integrins may be greater for some specific ECMs than others. ITGAV demonstrates significant affinity for vitronectin. As the greatest reduction in adhesion was seen on vitronectin, we next chose to investigate whether this protein (ITGAV) was expressed in HET-1A cells and in human oesophageal tissue.

Western Blotting for the 125kDa protein ITGAV demonstrated its presence in a variety of cell lines representing the normal - BO - OAC sequence. The greatest level of expression was seen in the QH cell line representing BO (Figure 3–10).

Next, using immunofluorescent staining of endoscopically acquired samples of normal squamous epithelium, BO and OAC, we demonstrated that ITGAV is expressed in human tissue (N=6). SqCCa of the oesophagus was used as a positive control (N=2) for ITGAV as this cancer has demonstrated significant expression of this protein [316] (Figure 3–11). In the normal squamous epithelium, ITGAV is expressed on the cell membrane but with the greatest expression being seen in the basal layers of the epithelium. The expression of ITGAV in SqCCa was similarly located diffusely around the cell membrane. In BO ITGAV was predominantly expressed on the basal surface of the epithelial cells. In OAC ITGAV was often similarly polarised toward one side of the cells.

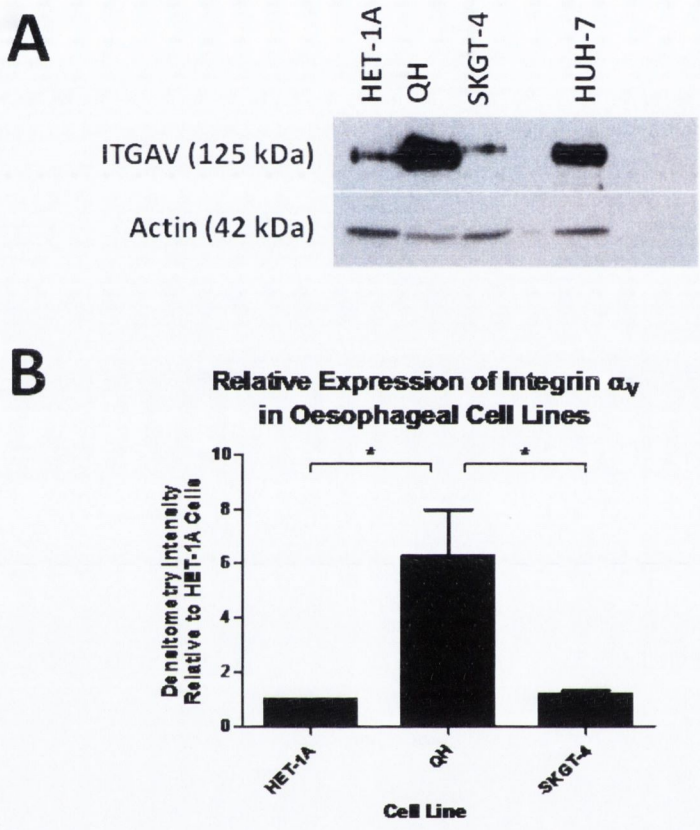

Figure 3–10: ITGAV is expressed in cell lines representing normal – BO – OAC sequence. The expression of ITGAV is greatest in QH Cells representing BO. Untreated cells were lysed in RIPA buffer and Western blotting performed using a mouse anti-human ITGAV antibody (BD Biosciences). A representative blot is shown (A). Densitometry was performed on the blots and the mean and SEM of N=3 is shown (B). * denotes $p < 0.05$.

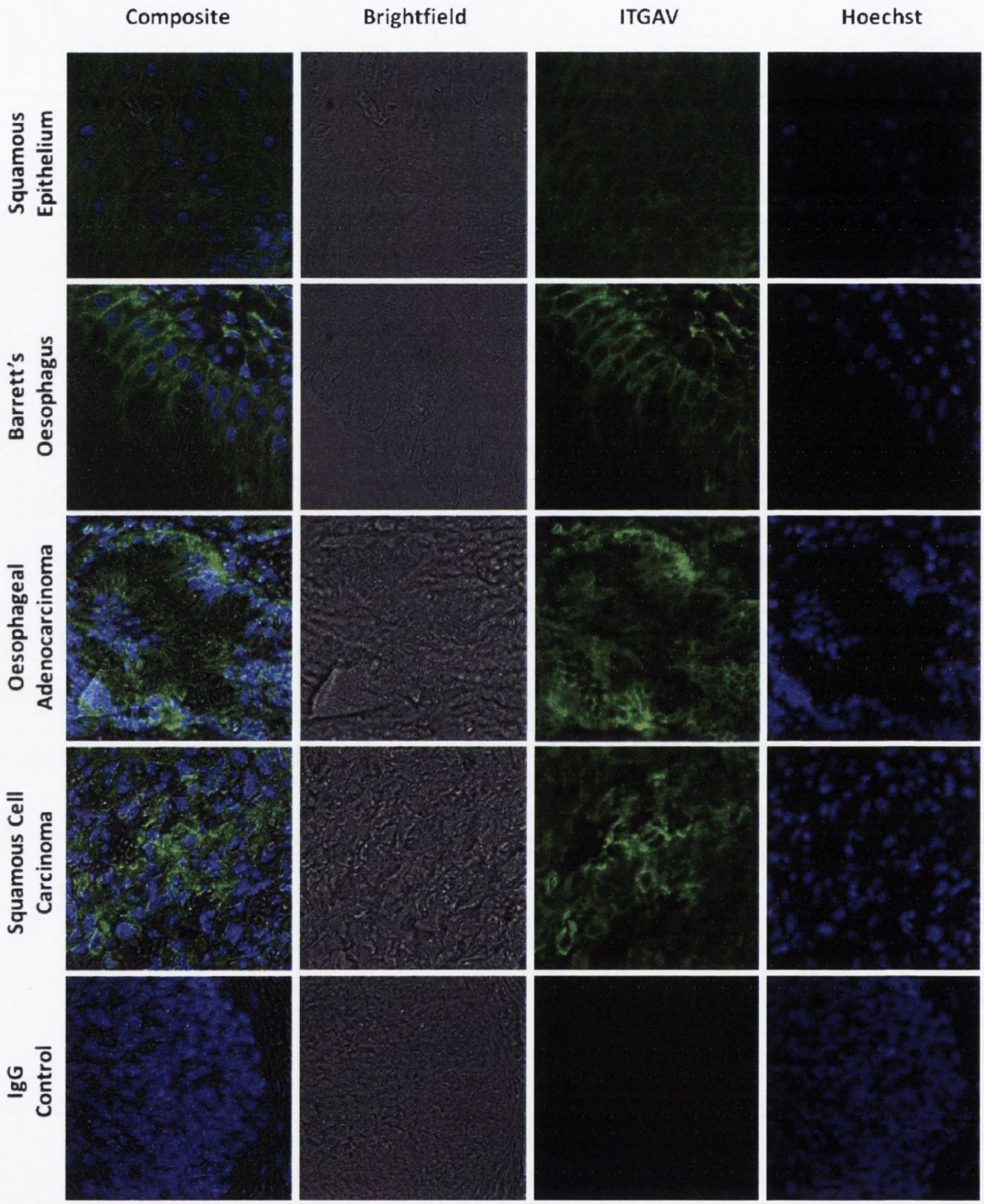

Figure 3–11: Immunofluorescent staining demonstrates that ITGAV is expressed in oesophageal squamous epithelium, Barrett's Oesophagus, oesophageal adenocarcinoma, and squamous cell carcinoma of the oesophagus. 4μM paraffin embedded tissue sections were de-paraffinized and rehydrated and antigen retrieval performed using a heat based sodium citrate technique. Staining was performed using mouse anti-human ITGAV (BD Biosciences) and a FITC labelled anti-mouse secondary. A non-specific mouse IgG was used as a negative control. Images were acquired using a Zeiss LCM 510 confocal microscope. Squamous cell carcinoma of the oesophagus was used as a positive control.

3.4.5. DCA, but not Other BAs, Reversibly Modulates the Surface Expression of Integrin α_V on HET-1A Cells

3.4.5.1. Stimulation with DCA, but not other BAs, Results in a Reduction in the Surface Expression of ITGAV on HET-1A Cells

We next investigated whether DCA was modulating the cell surface expression of ITGAV. We first assessed whether DCA altered the surface expression of ITGAV on HET-1A cells using immunofluorescent staining for ITGAV (SC-9969, P2W7 clone, Santa Cruz Biotechnology Inc, Santa Cruz, Ca, USA) and flow cytometry. DCA reduced surface expression in a dose dependent fashion after two hours exposure. 100, 300 and 500μM DCA reduced the median surface expression of ITGAV by 2.8% (95% CI of Diff: -11.72 to 17.25), 24.2% (95% CI of Diff: 9.753 to 38.72) and 33.2% (95% CI of Diff: 18.72 to 47.69) respectively (Figure 3–12). This corresponded to a differences between the ITGAV histograms of 2.2% (95% CI of Diff: -7.509 to 11.87), 14.4% (95% CI of Diff: 4.551 to 23.93) and 24.6% (95% CI of Diff: 14.95 to 34.33) respectively. These findings were confirmed using a second antibody directed against a second epitope on the extra-cellular domain of ITGAV (17E6 clone, Merck, Whitehouse Station, NJ, USA, data not shown). This suggests that the reduction in ITGAV staining is a reduction in surface expression of ITGAV rather than a conformational shape change of the integrin which could prevent the antibody binding to a specific epitope.

These findings were further confirmed using immunofluorescent staining and imaging. Cells were seeded and allowed to adhere to a 96-well plate and subsequently treated with BA or vehicle for two hours. After treatment, wells were either permeabilised (for measurement of total cellular ITGAV expression) or left un-permeabilised (for measurement of cell surface ITGAV expression) prior to staining. Images were acquired using GE InCell 1000 technology and analysis of ITGAV intensity performed using InCell analysis software. Similar to the data acquired using flow cytometry, 300μM DCA, but not UDCA, reduced ITGAV expression in the un-permeabilised cells (Figure 3–13). The reduction in intensity was less than that seen in the flow cytometry experiments. One possibility for this is that cells which had detached due to a reduction in adhesion molecules may have been lost during the staining process. Consequently, there is likely to be an upward bias in the reduction in intensity seen in the InCell as compared to the flow cytometric quantification. Cells which had been permeabilised demonstrated approximately 40% greater intensity than un-permeabilised cells and BA treatment induced no alterations in mean cellular intensity.

We next investigated whether other BAs could induce a reduction in ITGAV. Cells were treated with 300μM of DCA, taurochenodeoxycholic acid (TCDCA) or UDCA. Exposure of adherent cells to UDCA or TCDCA did not demonstrate a significant reduction in median ITGAV intensity as

determined using flow cytometry (Figure 3–14). The respective reductions in median intensity were 43.0% (95% CI: 21.5 to 64.6 %, $p<0.05$ relative to untreated), 3.8% (95% CI: -17.8% to 25.3%, p = NS) and -0.3 (95% CI: -21.9 to 21.2%, p = NS). The difference in ITGAV intensity histograms, compared to DMSO vehicle were 32.1% (95% CI: 21.3% to 42.8%, $p < 0.001$), 3.3% (95% CI: -7.4% to 14.1%, p = NS) and 1.9% (95% CI: -8.9 to 12.6%, p = NS) for 300μM DCA, TCDCA and UDCA.

3.4.5.2. A Decrease in pH Does Not Affect the Surface Expression of ITGAV on HET-1A Cells Either Alone or in Conjunction with DCA

As the predominant exposure of the oesophagus to BAs occurs in conjunction with acid, we next lowered the pH of the medium to 7 using HCl. HET-1A cells exposed to normal medium or medium at pH 7, with or without 300μM DCA. The lower pH had no effect on the surface expression of ITGAV either alone or in conjunction with 300μM DCA (Figure 3–15A).

3.4.5.3. The Apoptosis Inducer Staurosporine does not Reduce Surface Expression of ITGAV in HET-1A Cells

We next treated cells with 1μM STS for two hours in order to induce apoptosis. Apoptosis did not reduce the surface expression of ITGAV (Figure 3–15B), adding further strength to the hypothesis that detachment and apoptosis are discretely mediated entities.

3.4.5.4. The DCA Induced Reduction in Surface Expression of ITGAV in HET-1A Cells is not a Result of a Reduction in Total cellular Expression of the Integrin

Finally, to confirm high content analysis (InCell) data that that there was no reduction in total cellular expression of ITGAV in response to DCA (Figure 3–13), western blotting was used. Combined lysates of adherent and detached cells, after treatment with DCA, UDCA or the combination, demonstrated no difference in total ITGAV expression (Figure 3–16A).

There was also no difference in total ITGAV expression between adherent and detached cells. This was despite a significant increase in the expression in cleaved PARP (suggesting apoptosis) in the DCA-treated detached cells and an increase in LC3-II (suggesting autophagy) in DCA-treated non-detached cells (Figure 3–16B).

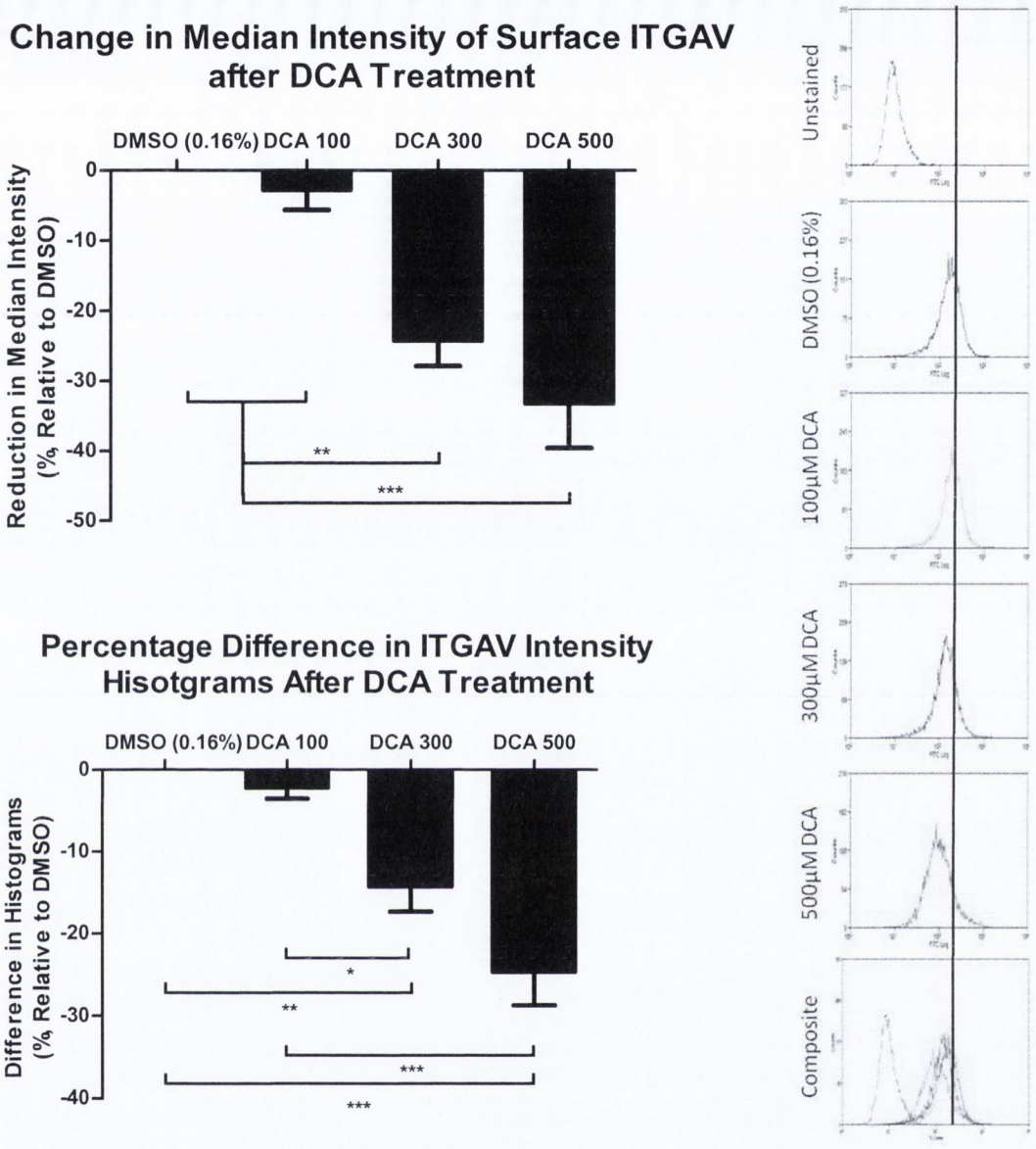

Figure 3–12: DCA stimulation reduces the surface expression of ITGAV on HET-1A cells in a dose dependent fashion. Cells were seeded at 2 x 10^5 cells per well in a Nunc 6-well plate and left to adhere overnight. After treatment for two hours with DCA, the cells were mechanically detached from the well base using a cell scraper and placed in a flow cytometry tube and incubated. Cells were stained using 1:100 ITGAV for 30 minutes at 4°C and then with a 1:500 FITC labeled anti-mouse secondary (Santa Cruz). Intensity readings were acquired using a Beckman Coulter Cyan Flow Cytometer. Mean and SEM of N = 3. * denotes $p < 0.05$, ** denotes $p < 0.01$ and *** denotes $p < 0.001$. Identical findings were found with the 17E6 clone anti-ITGAV antibody (Merck).

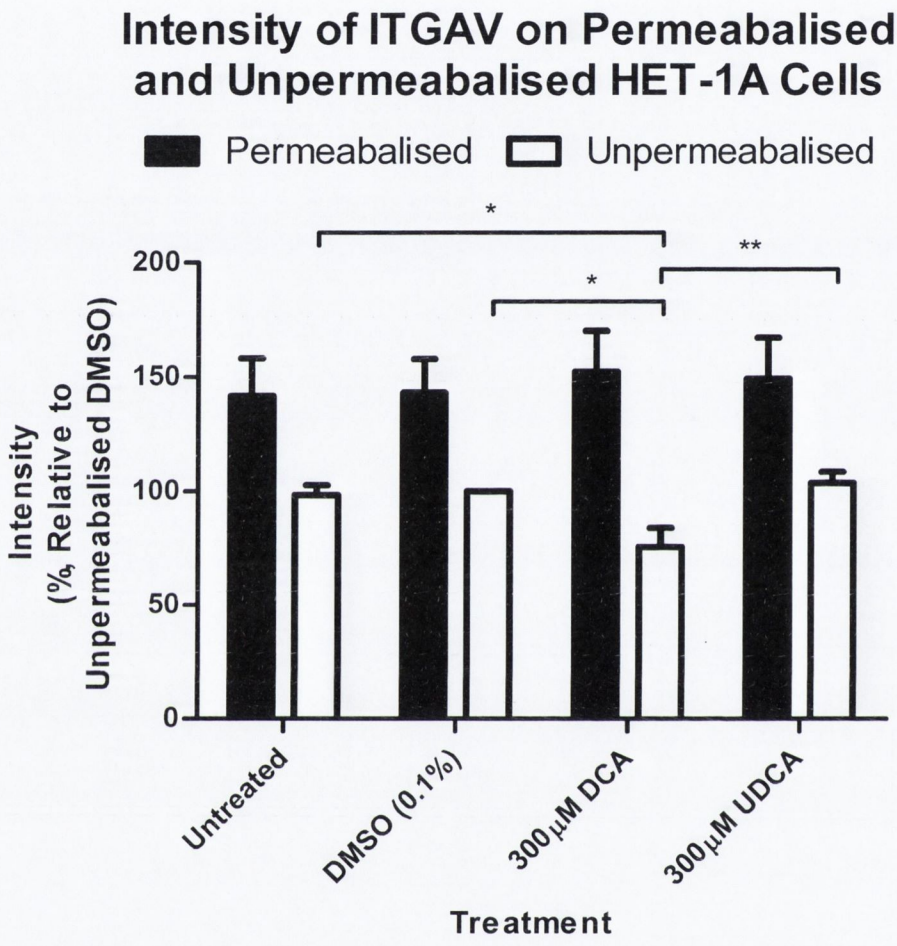

Figure 3–13: ITGAV intensity in HET-1A cells is reduced in un-permeabilised cells but not in permeabilised cells after BA treatment. Cells were seeded at 2 x 10^4 cells per well and allowed to adhere overnight. The cells were treated with BAs for two hours and then fixed with 4% PFA. After fixation, the cells in half the treated wells were permeabilised using 0.1% PBST. The cells were then blocked with 5% BSA for 30 minutes and stained with 1:250 anti-ITGAV antibody (Santa-Cruz) for 1 hour and the 1:500 FITC labelled anti-mouse secondary antibody. Images were acquired using GE InCell 1000 and cell ITGAV intensity analysed using GE InCell analyser software. * and ** denote $p < 0.05$ and 0.01 respectively.

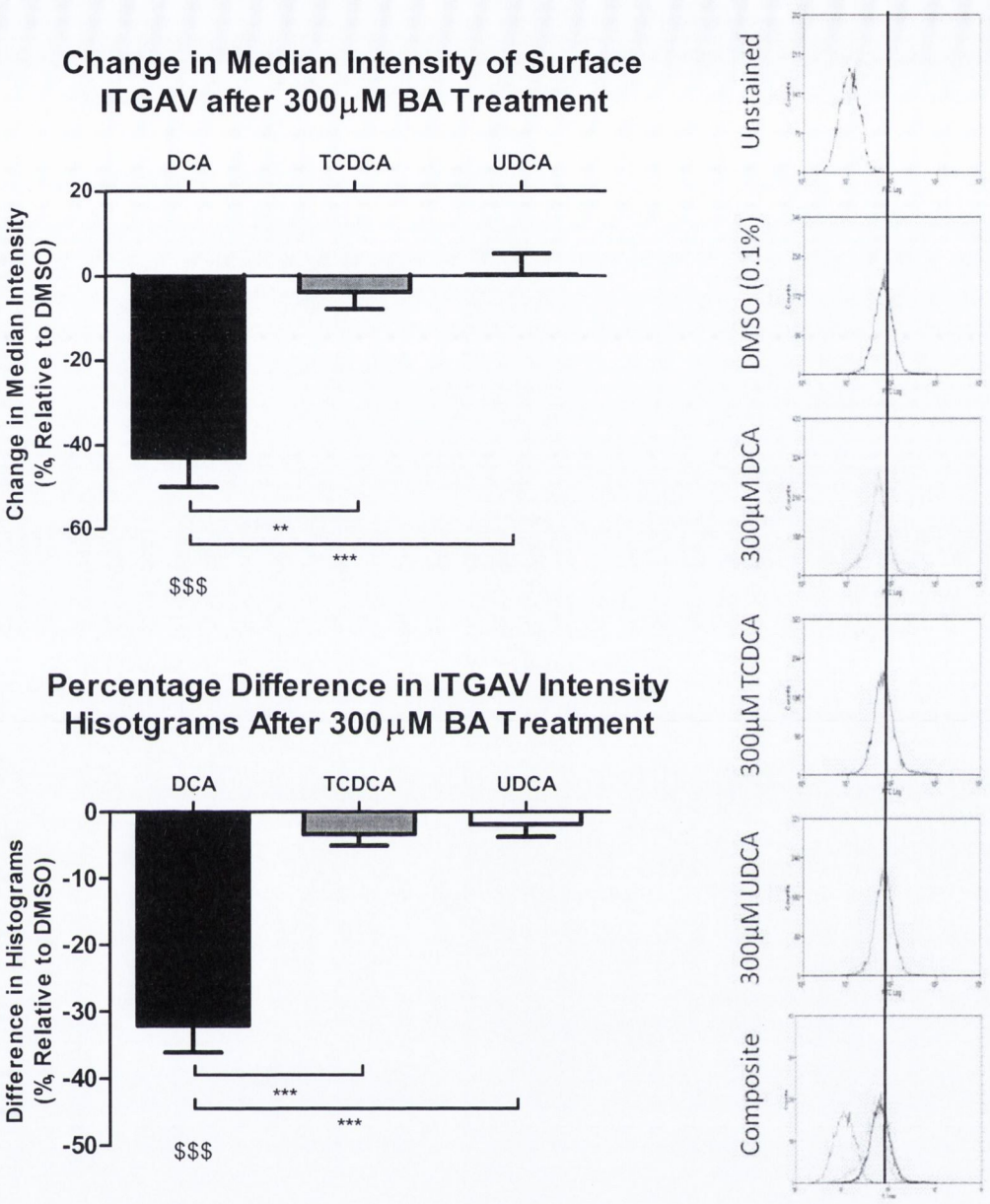

Figure 3–14: DCA, but not other hydrophobic and hydrophilic BAs, reduces the surface expression of ITGAV. Cells were seeded at 2 x 10^5 cells per well in a Nunc 6-well plate and left to adhere overnight. After treatment for two hours with BAs, the cells were mechanically detached from the well base using a cell scraper and placed in a flow cytometry tube. Cells were stained using 1:100 mouse anti-human ITGAV (Santa-Cruz) for 30 minutes at 4°C and then with a 1:500 FITC labeled anti-mouse secondary. Intensity readings were acquired using a Beckman Coulter Cyan Flow Cytometer. Mean and SEM of N = 3. ** denotes $p < 0.01$, *** / $$$ denote $p < 0.001$. $$$ = relative to 0.1% DMSO.

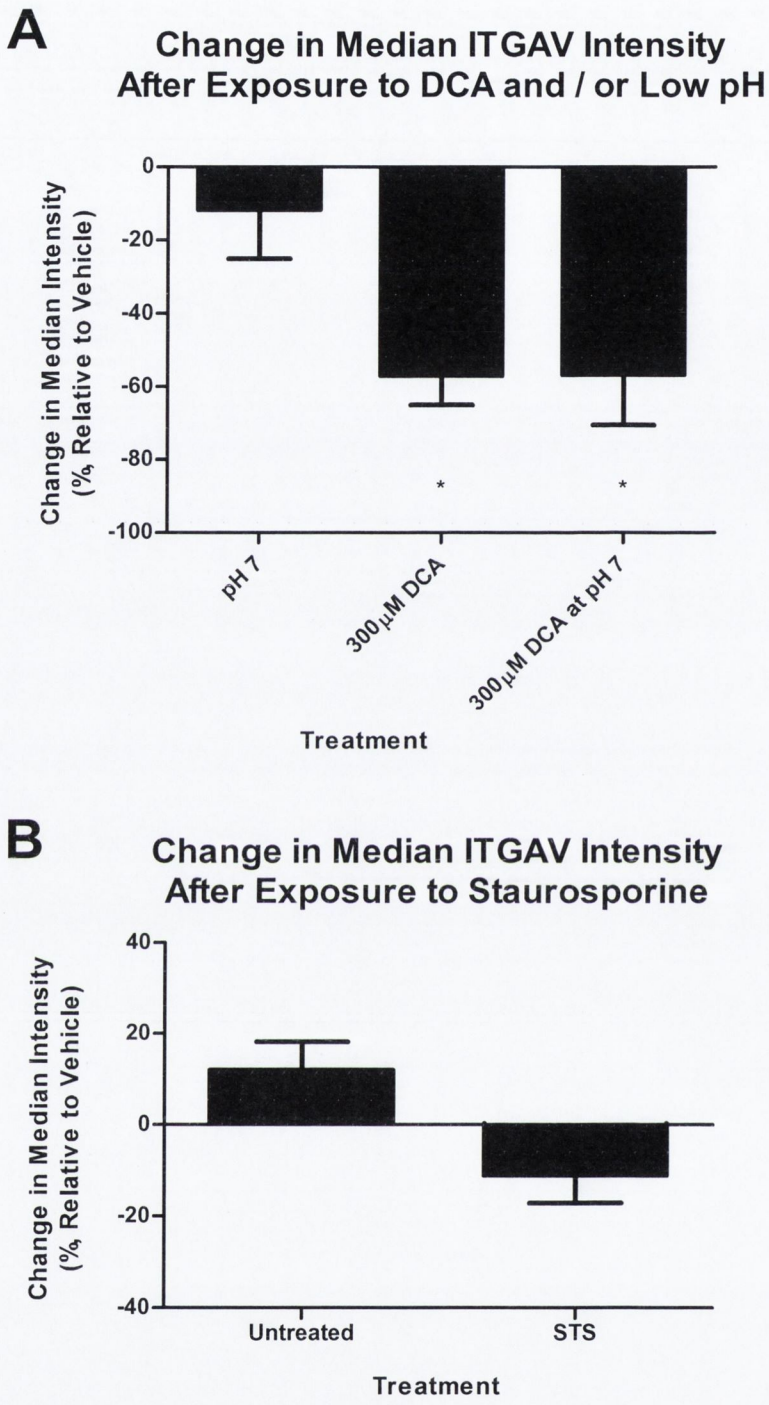

Figure 3–15: The effect of DCA and low pH (A) and STS (B) on the surface expression of ITGAV in the HET-1A cell line. Cells were exposed to chemicals (STS, DCA, medium at pH 7 or DCA in medium at a pH of 7) for two hours. Cells were subsequently detached and stained using a mouse anti-human ITGAV antibody (Santa Cruz). Intensity was measured using flow cytometry. Data represents mean and SEM of N = 3. * denotes $p < 0.05$ relative to DMSO control.

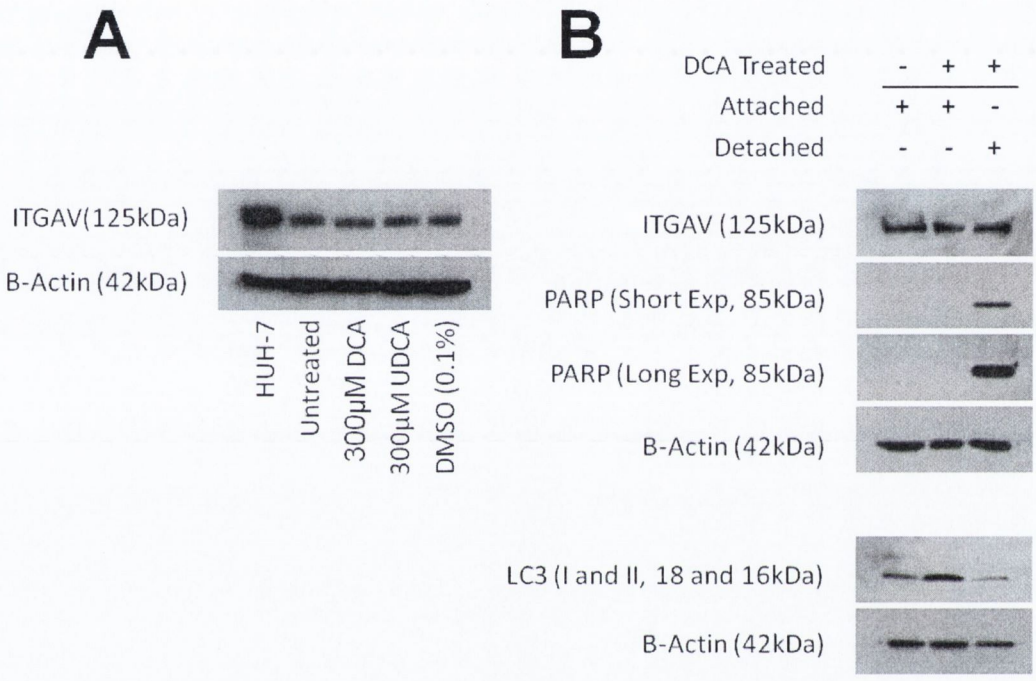

Figure 3–16: Bile acid treatment does not reduce total cellular expression of ITGAV. Cells treated with 300μM DCA, 300μM UDCA or vehicle for two hours showed no difference in expression of ITGAV (A). ITGAV protein is not differentially expressed between the attached and detached cells (B) despite differential expression of the apoptotic and autophagocytic proteins cleaved PARP and LC3. Representative examples of three experiments are shown.

3.4.5.5. After Removal of the DCA Stimulus the Expression of Integrin α_V Returns to Baseline Levels

Cells exposed to DCA, especially those which had detached, had demonstrated an increased expression of cleaved PARP, suggestive of increased levels of apoptosis (Figure 2–13 and Figure 3–16B). However, at least some of these cells were capable of re-adherence and survival (Figure 3–8). These findings demonstrated that of the detached cells, some were not undergoing apoptosis, suggesting that ITGAV expression was being modulated independently of apoptosis. Therefore we next investigated whether the surface expression of ITGAV would return to baseline after removal of the DCA stimulus.

Cells were treated with 300μM DCA for two hours to induce a reduction in the surface expression of ITGAV. The media and detached cells were removed and the remaining attached cells were washed twice with fresh media in order to dilute out the DCA. The detached cells were spun at 1500rpm for 5 minutes to pellet the cells. The DCA containing medium was aspirated and the cells washed twice fresh warmed media. The cells were re-suspended in fresh complete medium and replaced in the original well. After a variable recovery period the cells were mechanically detached, stained for ITGAV and expression determined using flow cytometry (Figure 3–17).

DCA stimulation of HET-1A cells resulted in a reduction in the surface expression of ITGAV as previously demonstrated. After six hours recovery, there was an increase in surface expression of ITGAV above that of the DCA treated cells and by twelve hours, the surface expression had almost returned to baseline untreated levels.

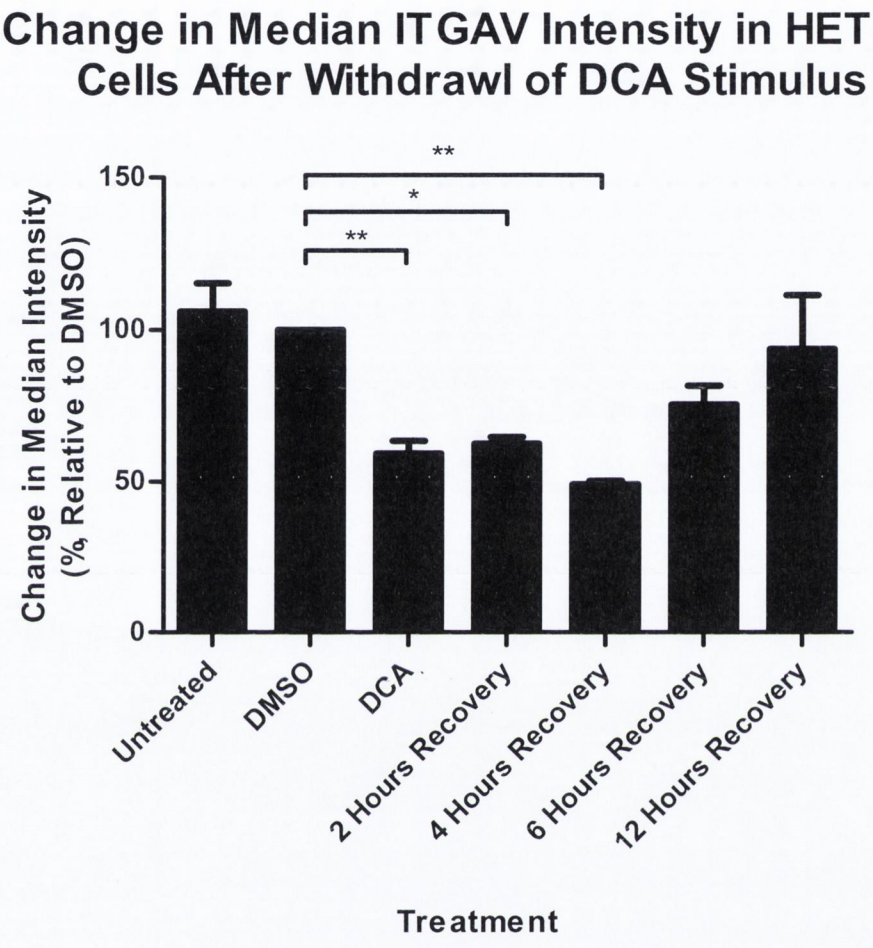

Figure 3–17: The surface expression of ITGAV on HET-1A cells returns to baseline after removal of the DCA stimulus. HET-1A cells were treated with 300μM DCA for two hours and then washed with fresh complete medium to remove the DCA. After a variable recovery period (2 – 12 hours), the cells were detached and stained with mouse anti-human ITGAV (Santa Cruz) and fluorescent intensity determined using flow cytometry. Results are mean and SEM of N=3. * denotes $p < 0.05$ and ** denotes $P < 0.01$.

3.4.6. DCA Induces a Reduction in the Surface Expression of the Alpha Integrins 4, 5 and V, but not 3 or 4, on HET-1A Cells Which is not Attenuated by UDCA

As DCA had almost exclusively prevented adherence to vitronectin and had been shown to modulate the surface expression if ITGAV, we next investigated whether the effect was specific to ITGAV and whether any DCA-induced alterations in surface expression could be modulated by UDCA. HET-1A cells were treated for 2 hours with 300μM DCA, UDCA or a combination of the two and stained using PE-labelled antibodies directed against integrins α_3, α_4, α_5 and α_6 and a mouse anti ITGAV antibody (Santa Cruz) in combination with a FTIC labelled secondary antibody (Invitrogen) to stain for ITGAV. The median intensities of integrin α_3 and α_4 did not change significantly (7.0%, 95% CI of Diff: -11.33 to 25.31 and -8.6%, 95% CI of Diff: -36.35 to 19.06). The median intensities of α_5 and α_6 and α_v were reduced by 29.3% (95% CI of Diff: 16.3% to 42.3%, $p < 0.001$ relative to DMSO vehicle control), 28.1% (95% CI of Diff: 18.7 to 37.4, $p < 0.001$) and 32.6% (95% CI of Diff: 18.5% to 46.6, $p < 0.001$). 300μM UDCA had no effect on the surface expression of the integrins either in isolation or in conjunction with DCA (Figure 3–18, Figure 3–19, and Figure 3–20).

There was no significant difference between the reductions in surface expression of α_5 and α_6 and α_v. Despite a similar reduction in these three integrins, it is only ITGAV that has a specific affinity for the ECM vitronectin. However, integrin α_5 exhibits specificity for other RGD containing ECM proteins and α_6 exhibits a specificity for laminin [283, 286]. Adhesion to the ECM protein laminin had been slightly, and significantly, reduced after DCA treatment as demonstrated in Figure 3–9.

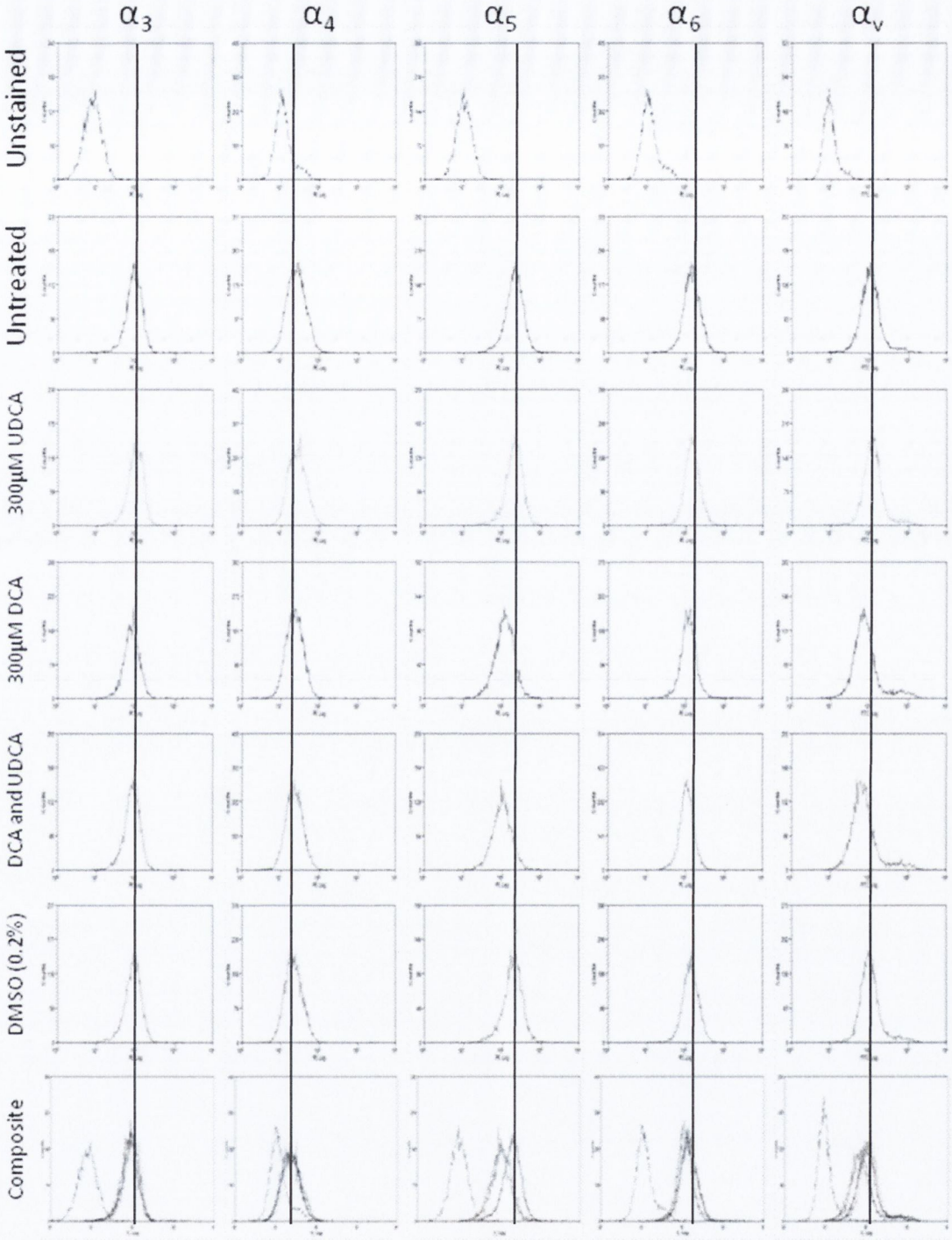

Figure 3–18: The surface expression of Integrins α_5, α_6 and α_V, but not α_3 or α_4, is reduced by treatment with DCA. UDCA has no effect on surface expression in isolation or in combination with DCA. HET-1A cells were treated with 300μM DCA, 300μM UDCA or a combination of the two. The cells were detached and fluorescently stained for the relative α integrins. Intensity was determined using flow cytometry. A representative set of histograms from 3 experiments is shown.

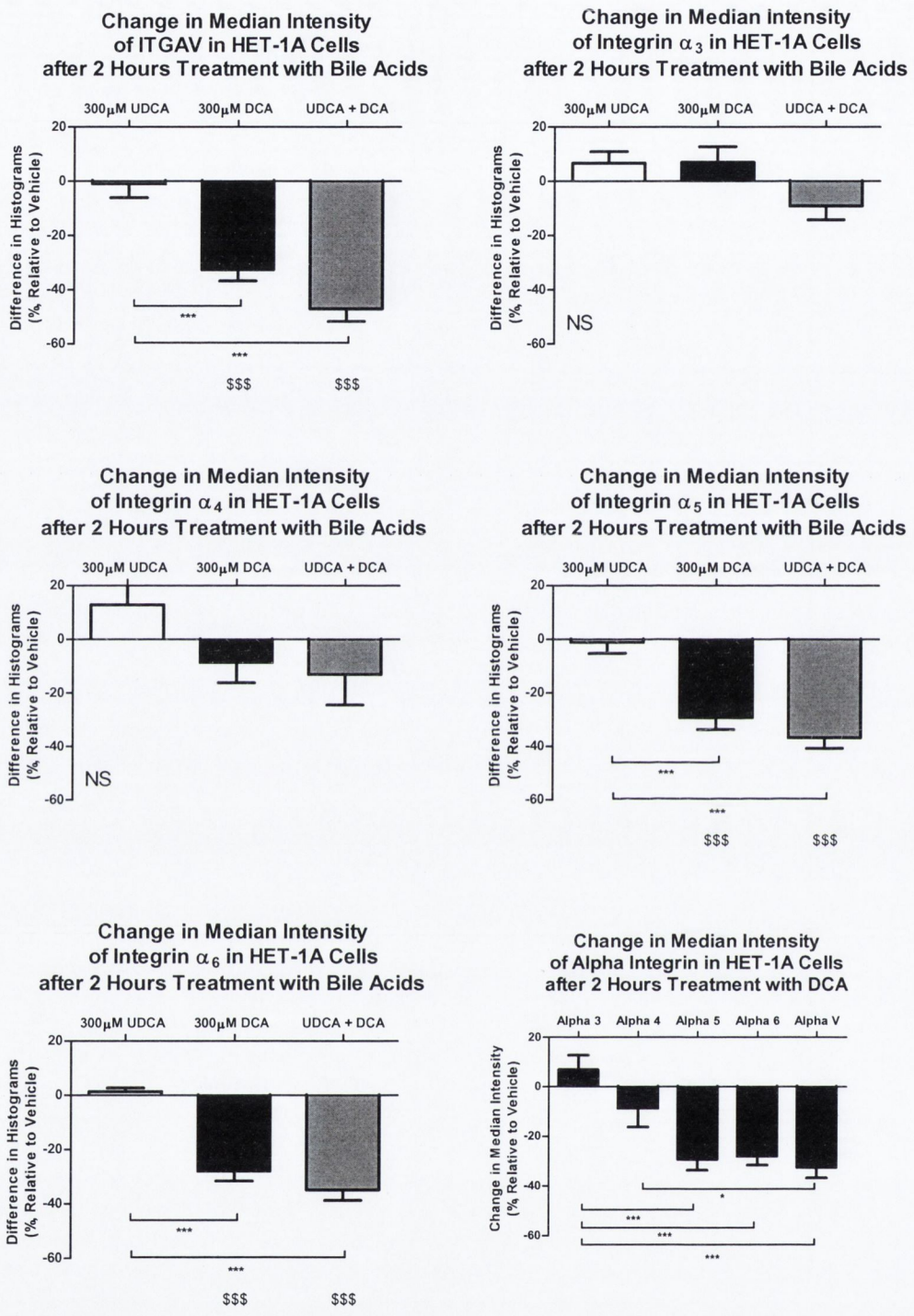

Figure 3–19: The changes in median fluorescent intensity in integrins α_3, α_4, α_5, and α_6, and α_v after treatment with 300μM DCA, UDCA or a combination of the two. Mean and SEM for N=6. * denotes $p < 0.05$. ** denotes $p < 0.01$ and *** / $$$ denotes $p < 0.001$. $$$ demonstrates significance when compared to DMSO control.

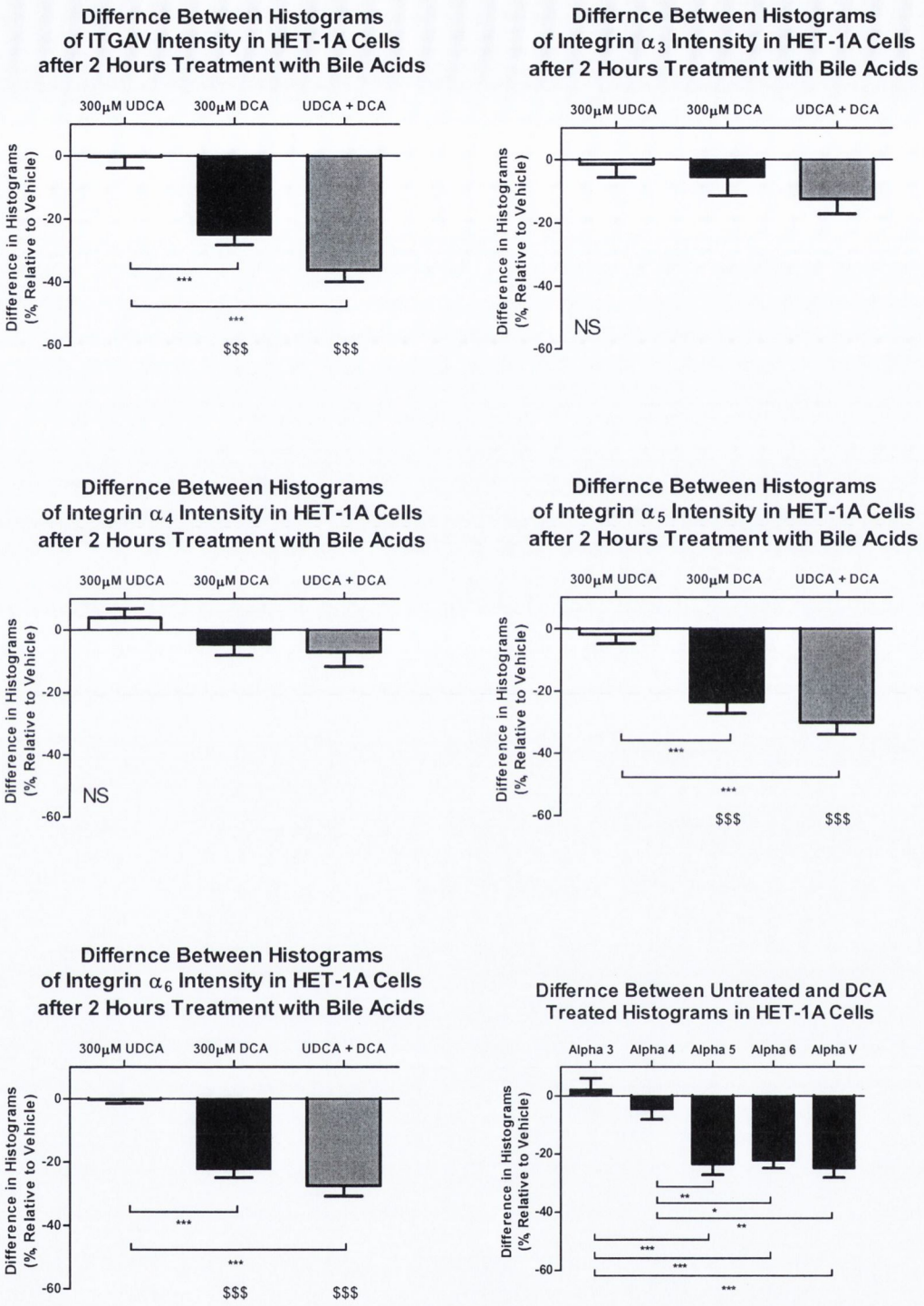

Figure 3–20: Difference between intensity histograms of integrins α_3, α_4, α_5, and α_6 and α_v after treatment with 300μM DCA, UDCA or a combination of the two. Mean and SEM for N=6. * denotes $p < 0.05$. ** denotes $p < 0.01$ and *** / $$$ denotes $p < 0.001$. $$$ demonstrates significance when compared to DMSO control.

3.4.7. ITGAV Co-localises with Rab5 and Rab11 Positive Vesicles.

A reduction in the surface expression of ITGAV without a reduction in the total levels of ITGAV suggested that the integrin was being internalised. Endocytotic recycling of integrins is a well documented phenomenon. Endocytic recycling of integrin α_5, α_6 and ITGAV has been demonstrated to occur through the long endosomal recycling loop. Therefore, to investigate whether internalisation and recycling accounted for the reduction in surface expression, we next attempted co-staining of ITGAV with Rab5 and Rab11 (Figure 3–21). In HET-1A cells, ITGAV co-localized with both Rab5 (an early endosomal marker) and Rab11 (a late endosomal marker in the long recycling loop) suggesting that it is undergoing endocytic recycling.

3.4.8. DCA Treatment Impairs Endosomal Processing as Determined by Rab5 and Rab11 Morphology

We next investigated the effect of DCA stimulation on endosomal function. Alterations in the morphology of Rab5 and Rab11 positive vesicles have been shown to correlate with endosomal maturation. Changes in mean vesicle size can be associated with hyper-activation or dysfunction of endosomal trafficking [323-324]. As demonstrated by Rink *et al*, endosomal processing has been identified as a dynamic process involving fusion of numerous small endosomes into larger vesicular structures which migrate towards the cell centre. Interestingly fusion of vesicles is only transiently associated with an increase in Rab intensity. Excess Rab appears to dissociate from the vesicular structure to maintain a steady surface density of this GTPase [323]. During this process Rab GTPases dissociate from the vesicles and are replaced by other Rab GTPases. Different Rabs are associated with different stages of the endocytic recycling pathways. For example, Rab5 is associated with early endosomes, Rab11 with late endosomes and Rab7 with endosomes targeted for lysosomal degradation.

After serum starvation for one hour and subsequent treatment of HET-1A cells with DMSO or DCA immunofluorescent staining for Rab5 and Rab11 was performed. High content analysis using InCell Technology demonstrated findings consistent with DCA impairing endosomal processing (Figure 3–22). DMSO treatment reduced the number of Rab vesicles and increased the mean vesicular size. These findings could be consistent with the reactivation of endocytosis after serum starvation with fusion of endocytosed vesicles into larger structures [323-324]. Conversely, DCA treatment increased the number of Rab5 and Rab11 positive vesicles but reduced the mean vesicular size relative to DMSO. The increase in the number of Rab11 positive vesicles corresponded with an increase in the total vesicular area, despite a reduction in mean vesicular size, perhaps suggesting a genuine increase in the number of late endocytotic vesicles. For Rab5, there

was an increase in the number of vesicles but with a reduction in the vesicular size and no alteration in total vesicular area. These findings suggest that after DCA treatment endosomes are failing to fuse into larger endosomes.

Surprisingly, despite the alterations in vesicular size and number, the mean vesicular intensity remained constant consistent with the work published by Rink *et al* (see above) [323]. As impairment of Rab function would have prevented dissociation of Rabs from the vesicular surface, this finding might suggest that impaired endosomal functioning seen with DCA is not a consequence of either reduced cellular GTP or direct Rab GTPase impairment

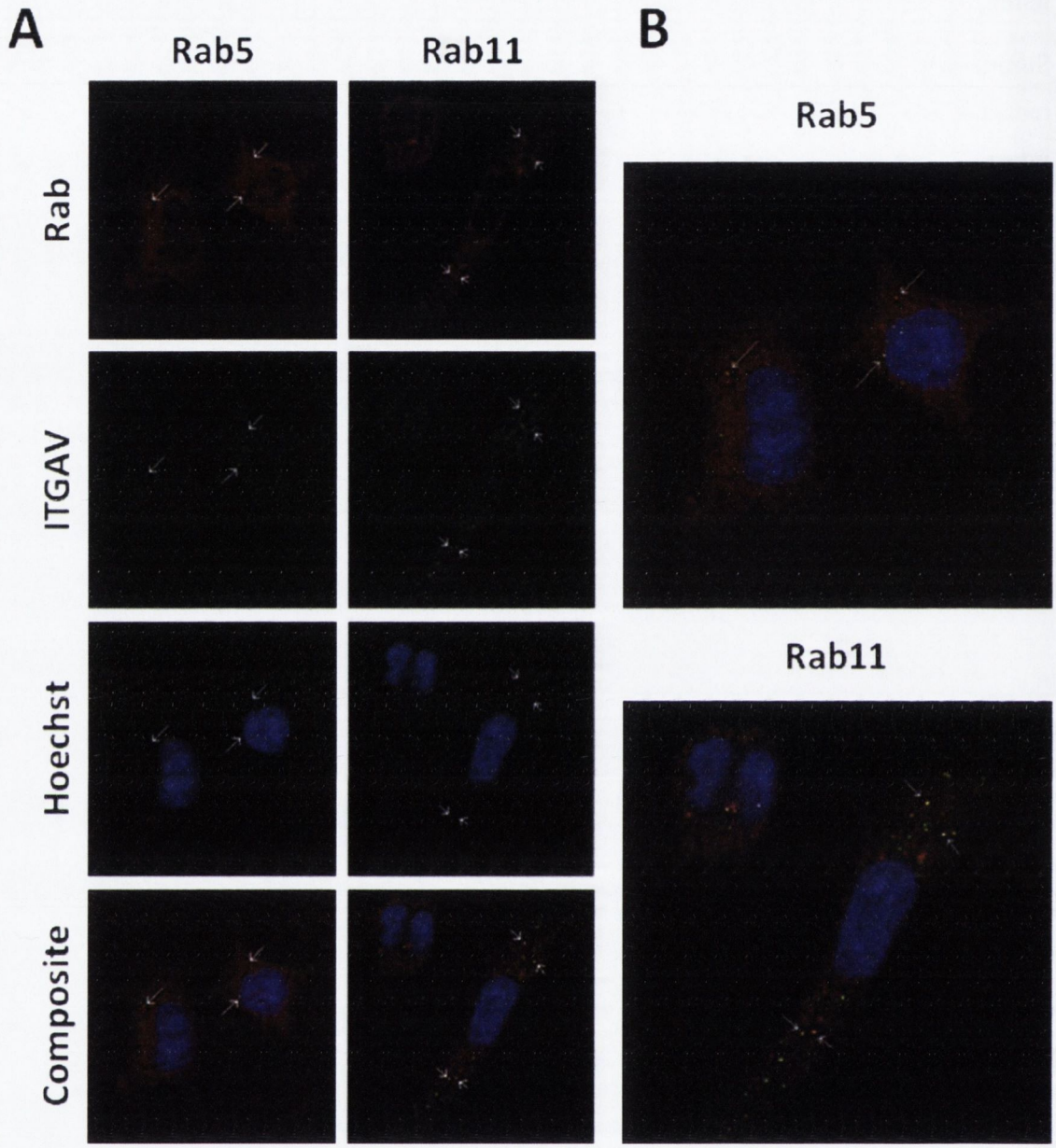

Figure 3–21: ITGAV co-localises with Rab5 and Rab11 in untreated cells in the HET-1A cell line. HET-1A cells were seeded at a density of $3X10^4$ cells per well in a chamber slide coated with poly-L-lysine to prevent cell detachment. Cells were fixed with 4% PFA and stained with ITGAV (BD Biosciences) and either Rab5 (Santa Cruz) or Rab11 (Zymed Laboratories) antibodies. Images were acquired using a Zeiss 510 confocal microscope. Images are representative of three experiments. (A) Separated channels and composite image and (B) higher power composite image of (A). White arrows demonstrate co-localisation of Rab and ITGAV.

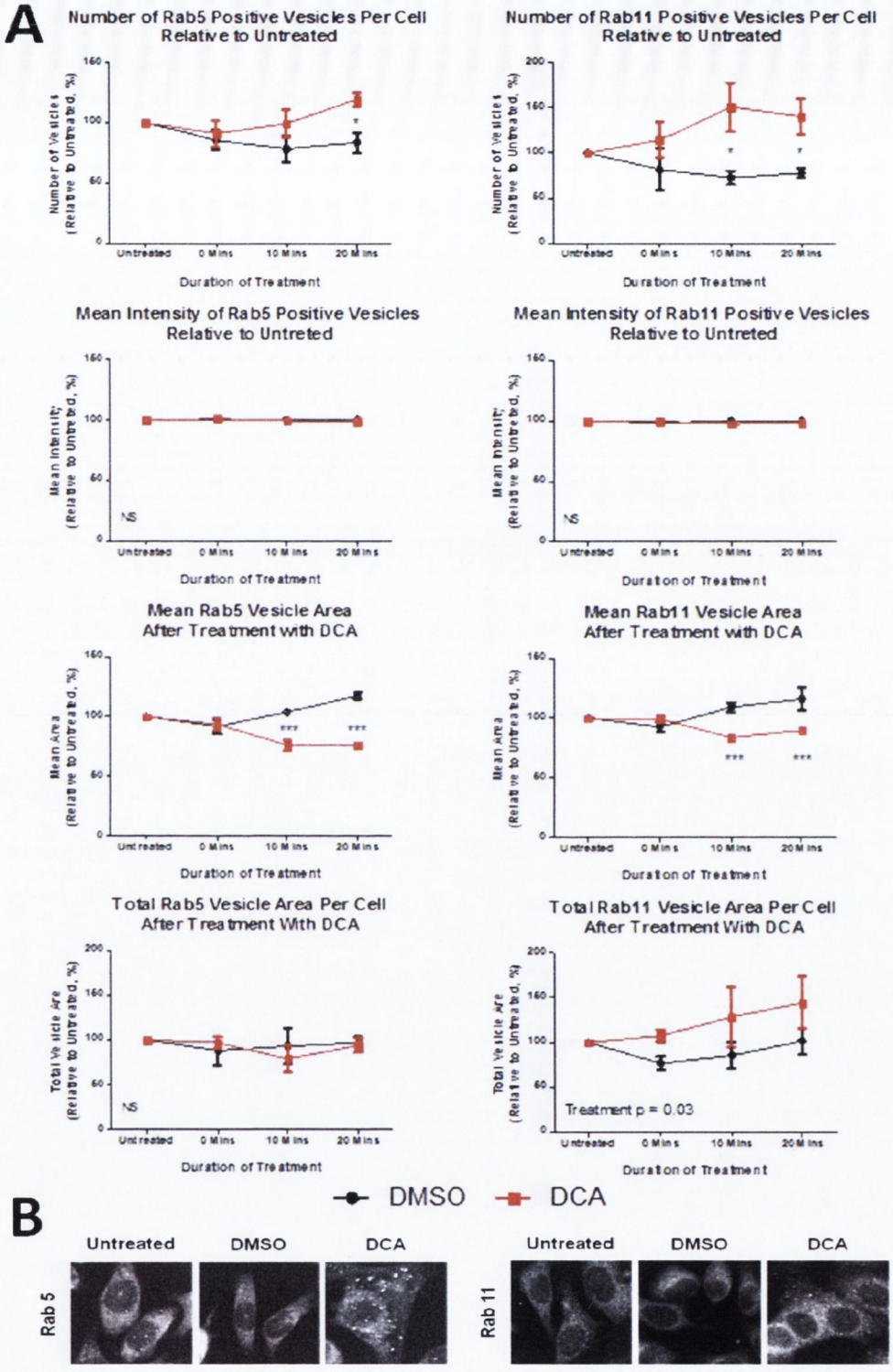

Figure 3–22: DCA treatment results morphological changes in Rab5 and Rab11 positive vesicles consistent with a dysfunction in endocytic recycling. Cells were treated with 300μM DCA or 0.1% DMSO. At the relative time-point cells were fixed with 4% PFA and co-stained with ITGAV and either anti-Rab5 or anti-Rab11 antibody. Data shown (A) is mean and SEM of N=3. * denotes $p < 0.05$ and *** denotes $p < 0.001$. A representative set of Rab staining images acquired during high content analysis are shown (B).

3.4.9. DCA Reduces the Expression of ITGAV in Oesophageal Tissue Explants Exposed to DCA

In order to determine whether our *in vitro* experiments would translate to the *in vivo* setting, we used tissue explants to investigate whether DCA induced a reduction in the expression of ITGAV. Biopsy samples exposed to DCA for two hours were fixed and paraffin embedded. Images were acquired using a Zeiss 510 confocal microscope and the mean fluorescent intensity in the green channel determined using the Zeiss software. Analysis demonstrated a reduction in the mean intensity of ITGAV staining after 500μM DCA treatment although this failed to reach statistical significance ($p=0.056$, Figure 3–23).

3.4.10. ITGAV is Upregulated in Peri-Ulcerated Regions of Rat Oesophagus which have Undergone Oesophago-jejunostomies

To further investigate the effects of BAs in the *in-vivo* setting we next stained the oesophagi of rats which had been exposed to high levels of oesophageal refluxate. Previously in this department, a rat model was established in order to attempt to generate an animal model of BA reflux in order to generate BO [322]. Oesophago-jejunostomies were established and although no BO was generated, severe hyperkeratinisation and ulceration was seen in the surgery group. Rats which had not been surgically altered were used as a control group.

In healthy non-surgically altered oesophagus the expression of ITGAV was higher in the proximal oesophagus than in the distal. This may represent a higher level of BA exposure in the distal oesophagus, although this remains hypothetical.

Within the surgically altered group, the expression of ITGAV was increased in the peri-ulcerated areas but not increased in hyper-keratinised areas (Figure 3–24). This might suggest increased expression of ITGAV in response to a wound, although again this remains speculation.

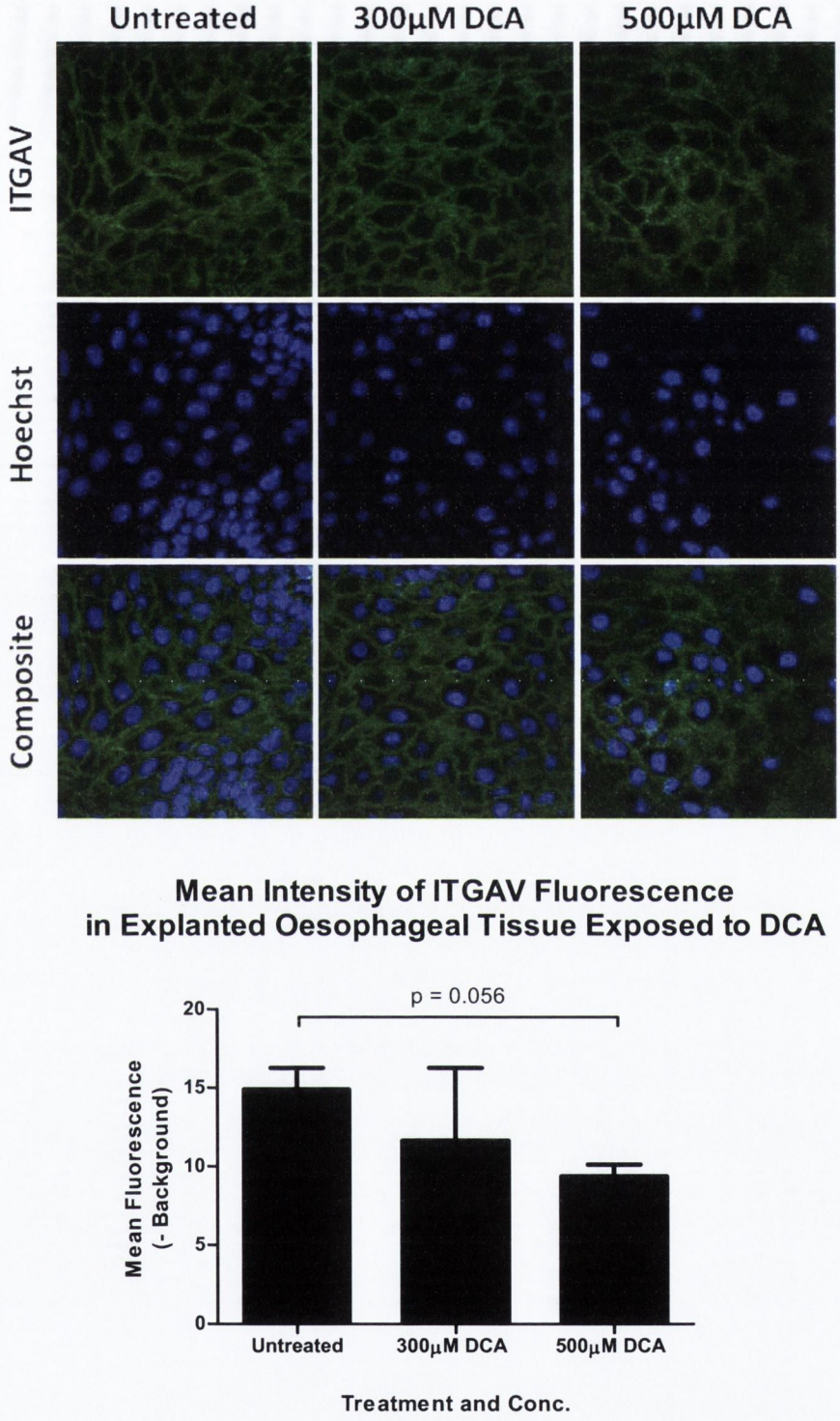

Figure 3–23: DCA stimulation of oesophageal tissue explants results in a reduction in the mean intensity of immunofluorescent ITGAV staining. Tissue explants were exposed to DCA for two hours, fixed and embedded. 4μM thick slices were cut, deparaffinised, and stained with primary anti-ITGAV antibody and subsequently alexafluor 488 secondary antibody. Images were acquired using a Zeiss 510 confocal microscope. Images are representative of five samples. Data represents mean and SEM of N=5. Intensity measurements represent the mean of the median intensities of ITGAV immunofluorescence.

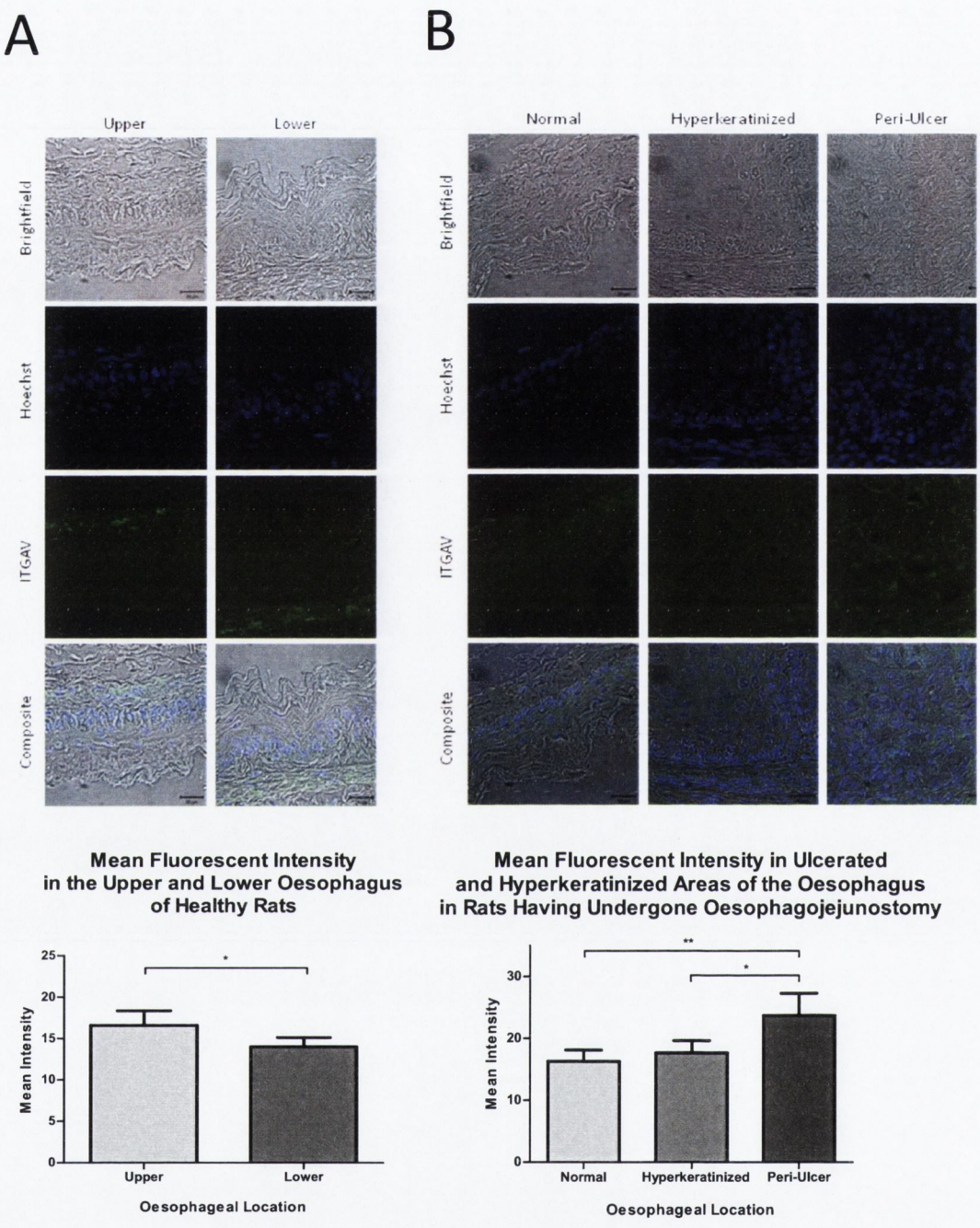

Figure 3–24: The intensity of ITGAV staining is higher in the upper oesophagus of anatomically unaltered rats than the lower oesophagus (A), however expression on ITGAV is higher in the peri-ulcerated area of the oesophagus relative to normal (B). Paraffin embedded oesophagus from rats with unaltered anatomy and oesophago-jejunostomies was stained for ITGAV. Eight unaltered rats and eight surgically altered rats oesophagus survived the staining process and was available for imaging. Images were acquired using a Zeiss 510 confocal microscope. Intensity measurements represent the mean intensities of ITGAV immunofluorescence. * and ** denote $p < 0.05$ and < 0.01 respectively.

3.4.11.In the QH Cell Line Cell Death Occurs Without Inducing a Loss of Adhesion and Surface Expression of ITGAV is Unaffected by DCA Treatment.

DCA exposure had induced a loss of adhesion and reduction in the surface expression of integrins in HET-1A cells and squamous oesophageal epithelium. We hypothesised that *in-vivo*, this could not only promote a loss of adhesion, but also a reduction in integrin mediated pro-survival signalling in normal oesophageal tissue. This could increase the risk of erosive oesophagitis and ulceration and therefore the risk of re-epithelialisation with Barrett's epithelium. Consequently, we hypothesised that BO would be more resistant to detachment and the alterations in the surface expression of integrins.

To investigate this, we repeated the detachment assay, flow cytometric assessment of surface expression of ITGAV and immune-blotting for total ITGAV protein expression in the QH cell line representing BO.

The viability of QH cells was reduced in a dose dependent fashion after two hours exposure to DCA, similar to that seen in the HET-1A cell line (Figure 3–8). However, in the QH cell line, either no cells detached, or, cells which did detach were not capable of re-attachment and survival (Figure 3–25).

Similar to the HET-1A cell line, DCA treatment did not induce a change in the total expression of ITGAV protein. However, in the QH cell line flow cytometric assessment of the surface expression of ITGAV demonstrated that 300μM DCA did not alter surface expression of ITGAV (Figure 3–26).

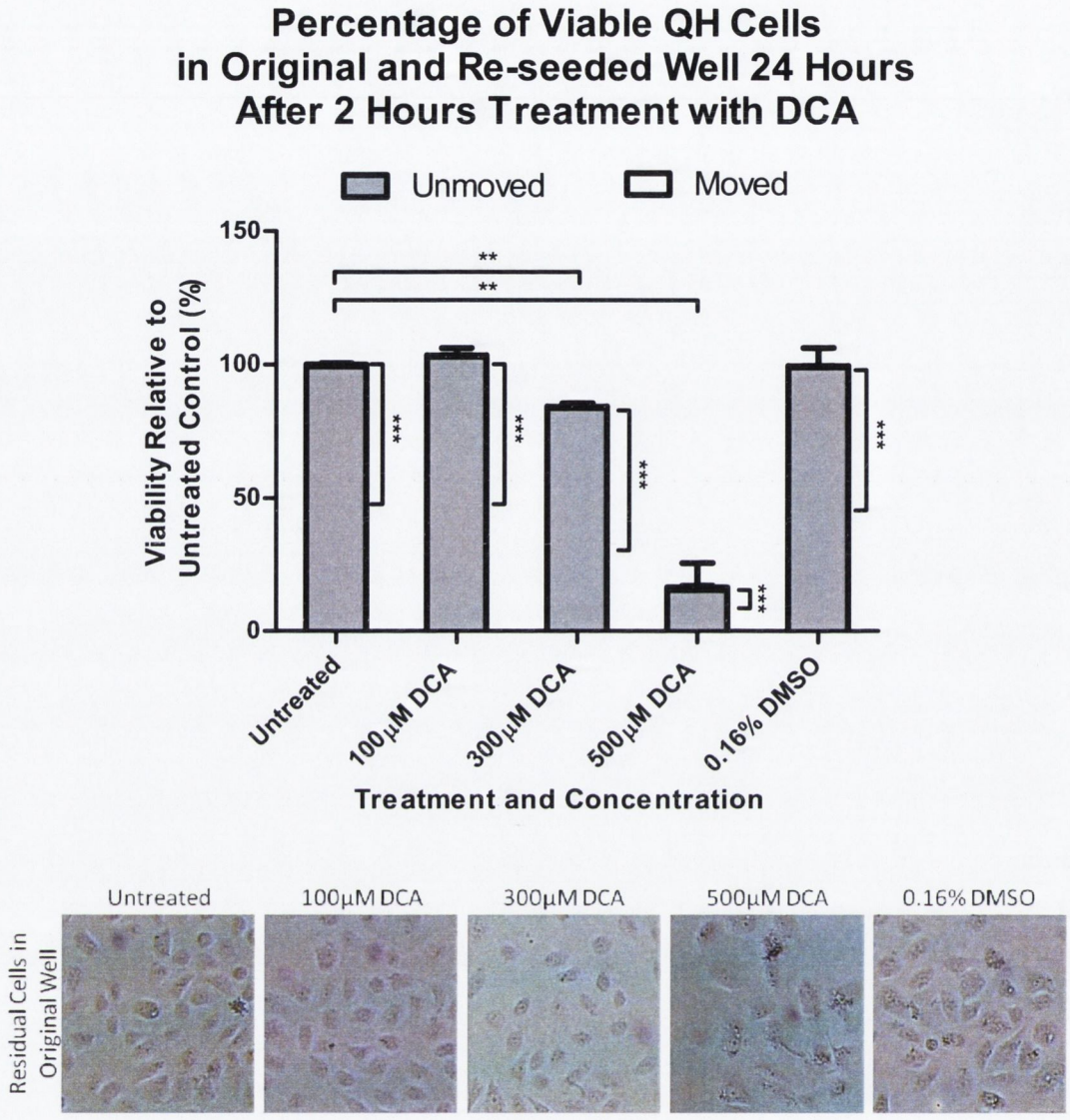

Figure 3–25: DCA Induces a loss of viability in QH cells without inducing cell detachment. DCA induced a dose dependent reduction in cell viability but no detached and re-adhered cells were identified. QH Cells were seeded at $2x10^5$ cells per well in 12-well plates and allowed to adhere overnight. The cells were treated for two hours with DCA or vehicle control. After treatment the medium was aspirated and the wells washed twice with the medium. The well was washed twice with fresh medium and 1ml of fresh medium was placed in the wells. The supernatant and cells were spun at 1800rpm for 4 minutes to pellet the cells. The treatment medium was aspirated and the pellet washed twice with fresh warm medium. The pellet was re-suspended in 1ml of medium and the cells replaced in a clean well in the 12-well plate. After 24 hours, images were acquired and 100uL of 2.5mg/mL MTT added to each well. After two hours the medium was gently aspirated and MTT crystals dissolved in 200μL DMSO. 100μL of DMSO was placed in a 96-well plate and the absorbance at 570nM read using a plate reader. ** and *** denote $p < 0.01$ and < 0.001 respectively.

A

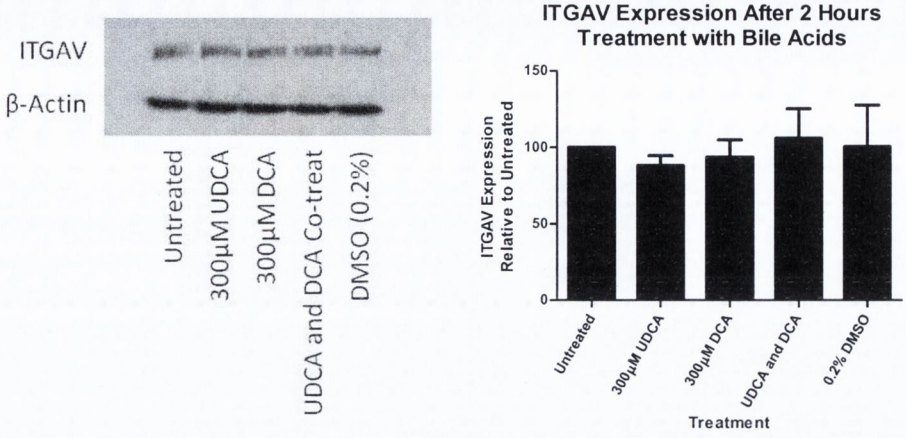

B

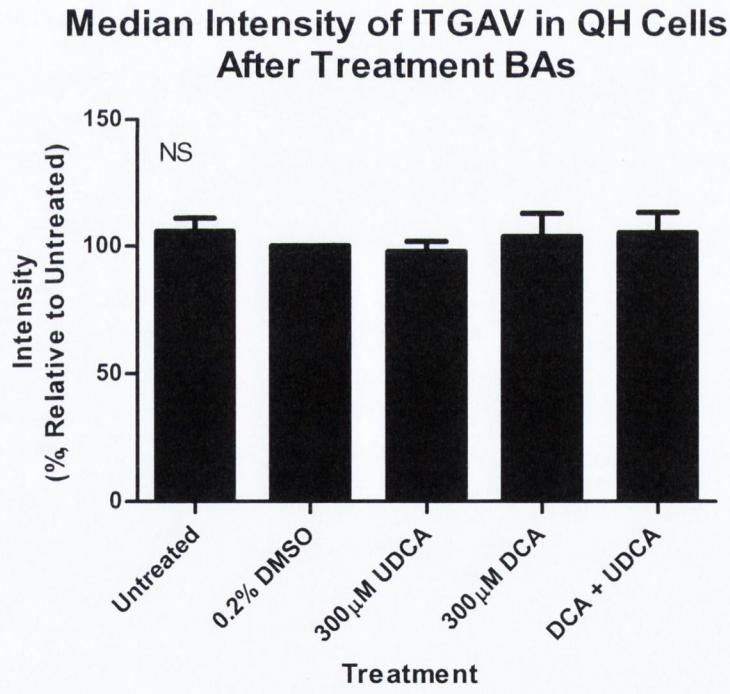

Figure 3–26: DCA treatment does not induce a change in the total expression of ITGAV protein or surface expression of ITGAV in the QH cell line. Western blotting (and densitometry) of RIPA lysed cells demonstrated no change in total expression of ITGAV protein (A). Flow cytometric assessment of surface expression of ITGAV is not altered by treatment with BAs relative to DMSO vehicle (B).

3.5. Discussion

The hypothesis researched in this chapter was that DCA was inducing a loss of adhesion of HET-1A cells. This premise was derived from viability experiments presented in Chapter 2 (Section 2.4.3) and Appendix 1. In these experiments viability as determined by a nuclear count assay was consistently lower than viability as assessed by an MTT assay. As the experimental method for nuclear counting involved a greater number of wash steps than the experimental method for the MTT assay, we hypothesised that adhesive strength in HET-1A cells may be reduced by DCA treatment. Re-analysis of the nuclear count and MTT assays demonstrated that that the discrepancy between the two assays was proportional to BA concentration at any given time-point. This difference was predictable and could be modelled using multiple linear regression techniques (See Section 3.4.1 and Appendix 2).

Consistent with the hypothesis, live cell imaging demonstrated that cells were "rounding up" after exposure to DCA. This rounded phenotype was identified hours prior to the identification of an apoptotic phenotype (membrane blebbing, nuclear fragmentation, etc). UDCA had little visible effect on cellular morphology. Strengthening the hypothesis that this phenotype was related to detachment, an adhesion assay demonstrated that DCA, but not UDCA, reduced adhesion to uncoated plastic in a dose dependent fashion after only two hours exposure (Figure 3–7). However, attachment and detachment are differently modulated processes. Therefore, we further demonstrated that DCA could induce detachment of adherent HET-1A cells (Figure 3–8).

However, these experiments did not exclude apoptosis as the sole cause of impaired adhesion. Certainly, these processes are closely linked. Apoptosis can result in cell detachment and prolonged detachment of cells has been shown to induce apoptosis in a phenomenon called anoikis [325]. However, prior to the irreversible activation of apoptosis in detached cells, autophagy has been shown to be upregulated, and this is postulated to be in an attempt to promote cell survival until attachment is re-established [300].

In our experiments DCA treatment of HET-1A cells activated different cell death pathways depending on whether the cells remained attached or had detached from the well base. LC3-II was increased in DCA treated cells which were still attached to the well base, while significant levels of cleaved PARP were only identified in DCA treated cells which had detached (Figure 3–16). Although theoretically LC3-II levels should have been greater in the detached cells, it may be that the any increase in LC3-II upregulation in the detached (but not apoptotic) cells is overwhelmed by cells which have undergone apoptosis prior to detachment in response to DCA. However, despite the large increase in levels of cleaved PARP in the detached DCA-treated HET-1A cells, at least

some of these cells were capable of re-adhering and growing. Although increasing doses of DCA reduced viability, higher concentrations of DCA were also associated with a greater proportion of surviving cells having detached and re-adhered (Figure 3–8). These findings suggested that DCA treatment was inducing two processes in a dose dependent fashion: cell death and a reversible cell detachment.

Strengthening our hypothesis that that detachment and apoptosis in response to DCA are discreetly regulated entities in HET-1A cells was the selective loss of adhesion to ECM proteins and the selective reduction in the surface expression of ITGAV, integrin α_5 and α_6. Although integrin-ECM interactions are poorly selective, certain integrins demonstrate higher affinity for certain ECM proteins [284-285]. In particular, ITGAV is relatively selective for the ECM protein vitronectin [285-286]. Consistent with the reduction in adhesion to vitronectin, the surface expression of ITGAV was reduced in a dose dependent fashion in response to DCA (Figure 3–9 and Figure 3–12). That a second antibody directed against a second epitope of the ITGAV protein (17E6, Merck) demonstrated a similar reduction in median fluorescent intensity after DCA exposure demonstrated that this was a reduction in surface expression rather than a conformational shape change reducing the affinity of ITGAV for vitronectin [287-288]. The finding that the surface expression of ITGAV returned to baseline levels after withdrawal of the DCA stimulus strengthened the experimental finding that re-adherence of detached cells could occur after removal of DCA.

A small but significant reduction was also seen to the ECM protein laminin and consistent with this was a reduction in the surface expression of integrin α_6, a laminin receptor [285-286]. It is likely that the reduction in adhesion to laminin was less than to vitronectin after DCA treatment because adhesion to laminin is mediated through a greater number of integrin heterodimers than the relative specificity of ITGAV for vitronectin [283, 286]. Indeed, integrin α_3, an integrin which did not demonstrate a reduction in surface expression in response to DCA, also binds to laminin.

Research suggests that in some cell lines ITGAV, integrin α_5 and α_6 undergo endocytic recycling via the PNRC, while integrin α_3 and α_4 do not [326]. ITGAV has been shown to be recycled through both and fast endocytic loops [327-331]. Therefore, we next investigated whether endocytosis was involved in the DCA-induced reduction in surface expression of integrins in the HET-1A cell line. ITGAV co-localised with Rab5 and Rab11 positive vesicles suggesting that the protein was undergoing endocytic recycling. After serum starvation, a greater number of smaller Rab5 and Rab11 positive vesicles were seen with DCA stimulation than with DMSO vehicle control. In the DMSO treated cells the number of Rab vesicles decreased and the vesicular size increased consistent with an upregulation of endocytosis after serum free medium was replaced with complete medium containing DMSO [323]. Although indirect evidence, these findings suggest that endosomal processing is being impaired by DCA treatment. However, as mean

vesicular intensity remains constant, this suggests that impaired processing is not as a result of Rab dysfunction or an reduction in GTP energy [323].

While not investigated in this research, it is also possible that alterations in cell membrane cholesterol could be influencing endocytototic recycling. BAs are known to incorporate themselves into the phospholipid bi-layer of the cell membrane resulting in cholesterol depletion, increased membrane fluidity and alterations in cell signalling [114-115, 332]. However, cholesterol depletion inhibits vesicular internalisation during endocytosis, without inhibiting externalisation [333], and impairs Rab GTPase dependent endocytic recycling [334]. Therefore, this mechanism would be expected to increase the expression of surface receptors rather than reducing them.

Finally, in this research we demonstrated that vitronectin is expressed throughout the normal-BO-OAC sequence. In BO and OAC ITGAV demonstrated polarisation toward the basal region of the cells consistent with its function of binding to the basement membrane. In squamous epithelium and SqCCa ITGAV was located diffusely around the cell membrane although there appeared to be greater expression in the basal layers. The published literature has contradictory findings regarding the expression of this integrin in normal oesophageal epithelium [314, 316], although the expression of ITGAV on SqCCa has not been challenged [316]. While integrins predominantly mediate cell-ECM adhesion, they also have a role in intercellular adhesion both indirectly [335] and directly [336]. In the epidermis the role of integrin α_2 and α_3 in cell-cell adhesion has been particularly well demonstrated [336-339]. Potentially ITGAV could have a direct role in cell-cell adhesion in the oesophagus, a structure sharing a similar embryological origin to skin. This may explain the diffuse localisation of ITGAV seen in squamous epithelium.

The expression of vitronectin in the oesophagus was not investigated in this research, nor is it published in the literature. The low level of specificity of integrins for ECM and the identification that DCA modulated a number of integrins made the documentation of specific ECM proteins unnecessary in this hypothesis.

In order to validate the *in-vitro* findings we used a rat model and human oesophageal explants in conjunction with immunofluorescent staining for ITGAV. The fluorescent intensity of ITGAV was slightly higher in the upper than in the lower oesophagus of rats with unaltered gastro-intestinal anatomy. If our findings are valid, this may reflect a greater exposure of the lower oesophagus to BAs, which reduces the surface expression of ITGAV. We next used a rat model in which oesophago-jejunostomies had been performed to investigate the expression of ITGAV in epithelial cells exposed to high levels of BAs. In this model, designed to induce a BO equivalent, only ulcerations and hyperkeratinisation occurred [322]. An increase, rather than a decrease, in the expression of ITGAV was identified in these areas. While this was contradictory to our *in-vitro* findings, it could reflect a healing response in which integrin expression is upregulated in order to

allow cell migration into a wound. Upregulation of ITGAV has been demonstrated in response to wounds in skin and brain tissue [340-341]. We therefore used a tissue explant model to further investigate our hypothesis. Explanted healthy oesophageal tissue demonstrated a non-significant dose dependent reduction in the median fluorescent intensity of ITGAV after two hours treatment with DCA (Figure 3–23). This suggested that our *in-vitro* findings have an *in-vivo* correlation.

Further adding to the hypothesis that integrin modulation by BAs may have a role in the genesis of erosive oesophagitis and BO is the higher expression of ITGAV in BO and the failure of DCA to reduce expression of ITGAV in the QH cell line. BO is thought to represent an adaptive mechanism to protect the oesophagus from oesophageal refluxate. It is more resistant to the inflammatory effects of BAs. That DCA failed to induce detachment of QH cells from uncoated plastic and failed to decrease surface expression of ITGAV despite inducing apoptosis, adds further evidence that BO is more resistant to the detrimental effects of BAs in refluxate.

Finally, while the statistical model of detachment had suggested that UDCA had a role in inducing loss of adhesion, UDCA failed to induce a significant reduction in the expression of any of the studied integrins. Furthermore, although UDCA co-treatment reduced the DCA-induced loss of adhesion to the ECM vitronectin (Figure 3–9), it failed to modulate the reduction in surface expression of ITGAV (Figure 3–19). Therefore these findings remain unexplained. They may be modulated through upregulation of expression of adhesion molecules which were not studied in this research.

The modulation of cell surface integrin expression by BAs, but not acid, is a novel finding. Cell attachment to ECM is necessary for survival [298, 301, 325]. The binding of integrins to ligand stimulates pro-survival signalling [278, 342]. Without adherence, cells undergo apoptosis [298, 342]. Therefore, a reduction in surface expression of integrins is likely to reduce activation of pro-survival signalling as well as reducing the adhesive force of cells in the oesophagus.

Compounding this potential reduction in mechanical strength and pro-survival signalling is the potential for a reduction in integrin expression to perpetuate the direct toxicity caused by GORD. Dilated intercellular spaces (DIS) have been identified in patients with GORD after acid or BA exposure [112-113, 343]. The presence of DIS between epithelial cells after exposure of the oesophagus to DGOR is hypothesised to allow refluxate to penetrate deeper into the mucosa. When this occurs, baso-lateral membranes which are less resistant to H^+ become exposed, Na^+/H^+ pumps are overwhelmed and inflammatory cellular toxicity and genetic damage occurs. Even if the Na^+/H^+ pumps are successful in protecting cells, rebound alkalinisation can lead to cellular hyper-proliferation [11]. Greater penetration of acid and BAs into the oesophageal epithelium may also allow access to the basal layer stem cells, enhancing the risk of mutagenic change in these cells. As discussed in Chapter 1 and Chapter 2, some authors suggests that mutagenic changes in basal stem

cells are the origin of Barrett's cells. Furthermore, integrin expression has a role in stem cell differentiation [344].

3.6. Conclusion

The aims of this chapter were:

- To characterise the effect of BAs (with particular focus on DCA) on the adherence of HET-1A oesophageal cells to ECM components,
- To investigate whether any BA-mediated loss of adhesion was due to alterations in the expression or function of a broad range of adhesion molecules or was specific to a certain subset,
- To investigate whether any BA-mediated loss of adhesion was occurring as a result of apoptosis, or whether it was occurring through a specific mechanism independent of cell death, and,
- To investigate the potential validity of this hypothesis *in-vivo*.

The identification that DCA mediates a loss of adhesion of HET-1A cells, in a fashion that appears to be regulated discreetly from apoptosis, is an unreported phenomenon. Integrins play a crucial role in cell survival by maintaining adherence and through "outside-in" signalling. A reduction in the surface expression of integrins is therefore likely to have an effect on epithelial cell survival in the setting of GORD.

The identification of ITGAV in normal oesophageal tissue and throughout the normal-BO –OAC sequence is also a novel scientific finding. That explanted oesophageal tissue demonstrated a reduction in ITGAV expression suggests that the *in vitro* work is likely to have an *in vivo* correlation. The finding that ITGAV was modulated in HET-1A cells but not in QH cells suggests that the Barrett's cell line is resistant to this effect. This, and the greater expression of ITGAV in BO cells suggest another mechanism by which BO could demonstrate a greater resistance to the inflammatory and erosive effects of longstanding GORD.

However, the finding that UDCA did not modulate the DCA-induced reduction in surface expression of integrins or modulate the loss of adhesion suggests that it is unlikely to have a protective role in this setting.

These findings suggest that integrin modulation may have a role in the propagation of erosive oesophagitis and in the genesis of BO. This could potentially be targeted as a therapeutic strategy to treat GORD and reduce the risk of BO.

Chapter 4.

4. UDCA Induces a Discrete Gene Signature Which Has Limited Concordance With DCA or Dex

4.1. Introduction

4.1.1. Nuclear Steroid Receptors

The NSRs comprise a diverse family of receptors including the GR, mineralocorticoid, androgen, progesterone (PR) and oestrogen receptors (ER) along with the vitamin D and the "orphan steroid" receptors including the retinoic acid receptor (RXR) and other NR1 receptors (Farnesoid X receptor (FXR), PXR, LXR, PPAR, etc). NSRs exert their function in the presence of hormones (and other ligands) and are partially responsible for growth, development, homeostasis and metabolism of an organism.

The majority of inactive forms of the NSRs are located in the cellular cytoplasm as monomeric molecules associated with receptor-associated chaperone proteins. The ER and PR are exceptions to this rule as they are predominantly located in the nucleus at all times [345]. Chaperones for the cytosolic receptors comprise a diffuse group including heat shock proteins (e.g. Hsp90, Hsp70 and Hsp40), co-chaperones (Hip, Hop), and immunophilins (FKBP59, CYP40). They maintain the cytoplasmic NSR in an inactive conformation, but are also required for proper protein folding allowing a stable conformational complex competent to bind NSR ligands [346-347]. Ligand binding results in dissociation of chaperone proteins, unmasking the nuclear transport signal and dimerisation of NSRs. All are necessary for interaction of the receptor with DNA.

Classically NSRs were solely regarded as ligand dependent transcription factors, exerting their effects exclusively through direct DNA interaction, the "slow genomic" effects. The classical slow genomic effect depends on diffusion of the ligand through the cellular membrane, binding of a ligand to a cytosolic NSR, and translocation of the complex to DNA in the nucleus [348]. In the slow genomic pathways, binding of the receptor to DNA can either activate transcriptional machinery (*trans*-activation) or prevent the binding of other transcription factors to the DNA preventing transcription (direct *trans*-repression). Furthermore direct interaction of the GR with other transcription factors (AP-1 or NF-κB) in the nucleus inhibits the transcription induced by these entities (indirect *trans*-repression). Thus gene transcription may either be up or down-regulated by NSR activation [348].

However, it has also been demonstrated that NSR hormone ligands themselves may exert effects through rapid non-genomic pathways such as transmembrane receptors and secondary signalling pathways. Natural steroids such as the oestrogens or hydrocortisone have been shown to activate specific trans-membrane receptors by induction of a conformational shape changes or receptor dimerisation [348]. Other molecules, classically regarded as NSR ligands, can exert rapid effects

through incorporation into cellular membranes (phospholipids bi-layers) resulting in increased membrane fluidity.

4.1.2. The Glucocorticoid Receptor

Similar to other NSRs, the GR has a conserved DNA binding domain (DBD) and ligand binding domain (LBD). The N-terminal domain is called "activation function-1" and contains components that are responsible for activation of target genes. It is this area that is thought to interact with the components of the basal transcription machinery and other transcription factors. The central part of the receptor constitutes the DBD and the nuclear localization signal. The C-terminal portion of the receptor includes the LBD and the sequences necessary for Hsp90 binding, nuclear translocation and receptor dimerisation. The very COOH terminal portion of the receptor, "activation function-2", serves as a molecular switch that recruits co-activator proteins and activates the transcription of target genes when flipped into the active conformation by hormone binding [349].

Two predominant subtypes of the GR (α and β) are coded for by alternate splicing of the GR gene [350-351]. The two forms differ by a length of 50 amino acids at the C terminal end and by differing in their last 12 amino acids. GRβ lacks the ligand binding domain formed by the C terminal end of the protein. It is constitutively present in the nucleus and is thought to be a dominant negative transcription factor, antagonizing the effects of GRα. Pujols *et al* demonstrated that the dominant translational pathway appears to be for GRα with both RNA and protein levels of GR α being up to 300-400 fold higher than GR β. However, the relative expression of these two molecules varies greatly among cell type [352]. Relative expression of the subtypes influences the effects produced by GR activation. Fruchter *et al* demonstrated that at ratios of 1:1 and 1:10 (GR α : GR β), GRβ impairs activity of GRα in a dose dependent fashion [353]. Consistent with these findings, over-expression of GRβ has been demonstrated in steroid resistant phenotypes of disease (asthma and ulcerative colitis) [352].

In addition to the transcriptional variation specific to different isoforms, current research suggests that the precise genomic effects of GRs are modulated in a fashion dependent on the particular ligand with which the receptor interacts. Furthermore, the effects resulting from a particular ligand receptor interaction may be cell type specific as a consequence of alternative initiator sites for NSR genes existing in different cell types [354-355]. For instance, the GR is involved in induction or prevention of apoptosis depending on cell type. Diametrically opposing effects such as this are thought to be due to differing expression patterns of co-modulators for NSR that are tissue specific, affecting the promotion or inhibition of apoptosis-related genes in different ways in different tissues [356].

NSR activation may also occur in the absence of a direct ligand. For example, The GR is promiscuous with regards the number of interactions that may cause translocation or activation. Aside from direct agonists, ligand-independent activation of GR may occur as a result of, or be influenced by, cell cycle [357-358], tyrosine phosphorylation including the p38-MAPK pathway [359-360], heat or chemical stress [361], phosphatase treatment [362-363], immunophilin ligands [364] or depletion of ATP [365].

However, the GR also exerts influence through activation or inhibition of other transcription factors: *trans*-activation and *trans*-repression respectively (Figure 4–1) [236, 348]. Possible mechanisms for direct genetic *trans*-repression include binding to or recruiting nuclear receptor co-repressors, direct repression of co-activator complexes and effects on RNA polymerase II phosphorylation [350]. However, it is felt that a significant proportion of *trans*-repression is influenced indirectly through interference with transcription factors such as AP-1 and NF-κB, which are potent mediators of inflammatory genes [236].

As a result of the variety of isoforms expressed, the number of ligands which can bind the GR, the multiple mechanisms of GR activation, the wide variety of cells in which the GR is expressed and the different initiator sites for the GR, predicting the likely gene expression profile of the GR is difficult. It has been estimated that the GR directly influences approximately one hundred genes directly including both a generally modulated group of genes as well as a cell specific genes. Consequently, it is impossible to predict the response at a translational or proteomic level to the GR in the majority of cell types [350, 354, 366-367].

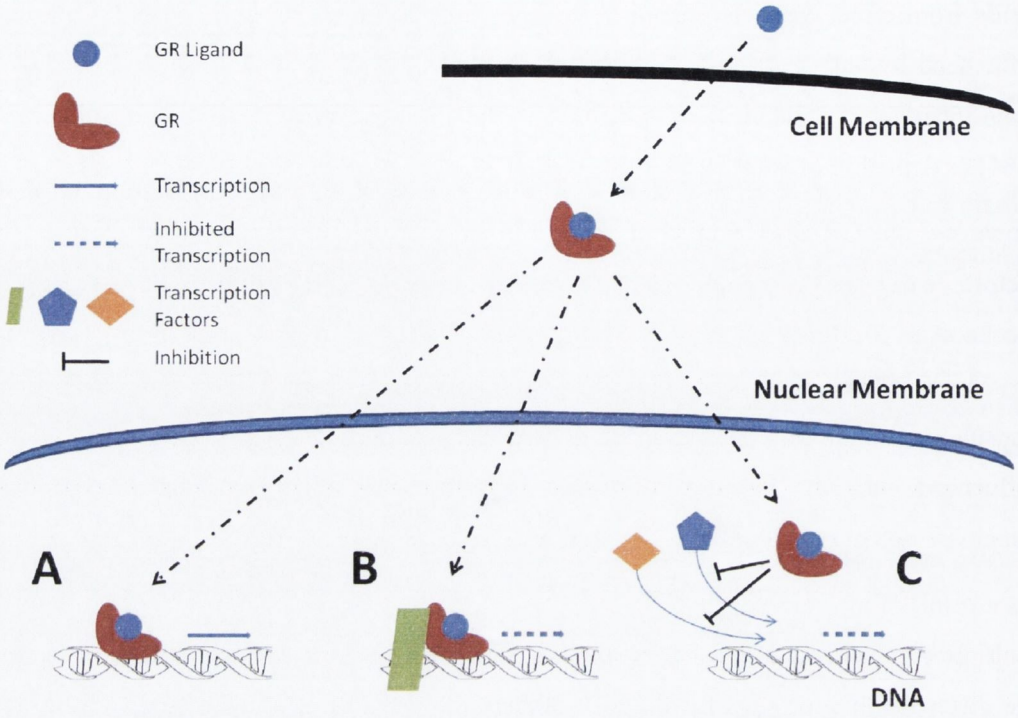

Figure 4–1: Mechanisms through which the GR exerts genomic effects. A) Direct *trans*-activation resulting in gene transcription, B) direct *trans*-repression inhibiting the trnscriptional ability of other transcription factors and C) indirect *trans*-repression of other transcription factors (e.g. AP-1 and NF-κB).

4.1.3. Expression and Physiology of the GR in Human Tissues

Quantitative RNA Polymerase Chain Reaction (PCR) has demonstrated the presence of the GR diffusely throughout the body [368]. This expression profile reflects the physiological dysfunction encountered in conditions of glucocorticoid deficiency or excess. In clinical usage, it is felt that the profound immunosuppressive properties of the GR are unlikely to be exerted through the direct interaction of the GR with a small number of anti-inflammatory genes [351]. Rather, the immunosuppressive effects are thought to be medicated through GR *trans*-repression. Conversely, the majority of the "unwanted" (adverse) effects of GCs are thought to be mediated through GR *trans*-activation.

Within the intestine limited investigation has been performed into the presence and effects of the GR. Two studies suggest that within the GI tract, GR expression varies significantly [368-369]. Lien *et al* used immunohistochemistry to evaluate the expression of GRα in intestinal cells.

Glandular epithelia such as gastric or colorectal epithelium did not demonstrate GR expression. Only low levels of expression were seen in the small intestinal and bile duct epithelium. However, strong expression was seen in hepatocytes and in pancreatic islet cells. Similarly, strong expression was seen in squamous epithelium of the oesophagus. Real Time-PCR (RT-PCR) confirmed that GRα alpha was the predominant form of the receptor in intestinal cells.

GCs are used extensively in clinical practice, predominantly for their profound immunosuppressive properties. GCs suppresses inflammation through effects on both the local tissue and inflammatory cells. However, their frequent use is associated with a multitude of side effects which manifest throughout the body. GC pathology may also result from an endogenous deficiency (Addison's disease) or excess (Cushing's disease) of GCs. These diseases manifest as a diffuse physiological phenotype mediated through GC action on numerous organ systems and metabolic functions.

4.1.4. Inflammation in the Oesophagus

Chronic inflammation is a risk factor for carcinogenesis within the gastrointestinal tract [370-372] as well as for the propagation of tumours [373]. GORD, and DGOR in particular, has been shown to upregulate inflammatory modulators in the oesophagus (For a comprehensive overview see section 1.4.4). BAs have been shown to upregulate ROS and RNS through induction of mitochondrial damage as well as through the release of arachadonic acid from the cell membrane [66, 86]. The potential production of ROS via the release of arachadonic acid may be further compounded by the ability of BAs to upregulate COX-2 expression [131]. Mutations in the p53 gene, which have been identified in one third of BO cases and over ninety percent of OAC, frequently occur as a result of oxidative damage suggesting that ROS are a likely carcinogen in OAC [122-123].

At the transcriptional level, the pro-inflammatory mediators NF-κB and IL-8 have been demonstrated to be upregulated by BAs in the OE33 cell line [85, 133]. Once BO is established, the expression of pro-inflammatory mediators such as NF-κB, IL-6, IL-8 and COX-2 becomes constitutive [133-136]. A more comprehensive review of inflammation in the oesophagus is presented in Chapter 1.

As the transcriptional effects of NF-κB can be modulated by the GR, it is possible that activation of the GR in the oesophagus could be used to modulate GORD induced inflammation in this tissue.

4.1.5. UDCA and the Glucocorticoid Receptor

BAs have recently been shown to be primary ligands for the orphan nuclear receptors PXR, LXR and FXR suggesting a hormonal function. Through interaction with these receptors, they can affect the production and metabolism of BAs and influence cholesterol metabolism [64]. Interestingly, these receptors are activated by BAs at the micromolar level. This is a thousand-fold higher concentration than that needed for natural ligands to physiologically activate the classic steroid receptors GR, ER, PR, etc. However, this micromolar concentration reflects the physiological concentration of BAs seen in the intestine (and occasionally elsewhere) [62-63]. Yet in order to activate these receptors, BAs must be able to enter a cell; unconjugated BAs can do so without a membrane transporter but conjugated BAs need membranous BA transporters which have only been shown to be present on ileal enterocytes or hepatocytes within the intestinal tract [63]. As such, the location of these transporters further reflects the homeostatic functions of the receptors.

UDCA in particular has been shown to modulate a variety of NSR activities. This secondary BA can activate PXR to upregulate CYP3A4 and while it neither binds nor activates FXR, it can inhibit receptor activation by more hydrophobic BA species [64, 374-375].

In the absence of specific GR ligands UDCA can interact with the GR and induce nuclear localization. Similar to Dex, the UDCA-GR interaction promotes dissociation of hsp90 from the GR which induces translocation [167]. It appears however that UDCA neither specifically binds to the LBD of the GR nor interferes with the specific interaction between Dex and the GR. Through sequential and progressive deletion of the C-terminal region of GR, which contains the receptor's LBD, it has been shown that at a point where UDCA still maintains its properties, Dex can no longer induce hsp90/GR dissociation, GR translocation or gene regulation [167, 169].

UDCA transforms the GR into a DNA binding species that binds to glucocorticoid response elements but the resultant effects are poorly characterized. Despite the ability of UDCA to induce translocation of the GR in a fashion similar to GCs, the gene expression profiles of the two ligand-receptor complexes differ greatly [169]. For example, the *trans*-activational potential of the GR may only be stimulated to induce expression of genes by Dex and not by UDCA [167, 171]. Where similarities exist, UDCA appears to be much less efficacious than Dex: UDCA only significantly promotes nuclear translocation of the GR in the absence of Dex, this only occurs at fold concentrations of UDCA over Dex, nuclear translocation is much slower with UDCA and the *trans*-activational potential of UDCA activated GR is much lower than that of Dex [167, 169, 171-172].

Supporting this theory is work undertaken by Miura *et al.* In their paper, they studied the interaction of the GR with DNA (after treatment with either Dex or UDCA) by studying the nuclear localization of TIF2, a co-activator for NSR that results in upregulation of DNA transcription.

Exposure to Dex resulted in co-localization of the GR with TIF2 in discreet foci within the nucleus. UDCA induced GR translocation but resulted in a diffuse nuclear pattern of the GR; one which did not overlap with the TIF2 foci. The two different distribution patterns within the nuclei suggest that UDCA-GR complex associates with different protein structures than the Dex-GR complex. If this is true, then it is unlikely that the UDCA-GR complex will have the same activation profile as the dex-GR complex [167, 169].

However, there are also direct interactions between the Dex-GR complex and other transcription factors which can inhibit the genetic effects of these molecules. *Trans*-repressive effects of the GR are largely considered to be due to protein-protein interactions between GR and other inducible transcription factors (e.g., AP-1 and NF-KB) rather than direct genomic effects [169, 172-173]. It has been shown that UDCA suppresses NF-κB-dependent transcription and the subsequent cytokine expression through direct interaction of the GR and NF-κB; in particular, via interaction with the p65 subunit [169-170].

While the precise mechanisms of the interaction between UDCA and the GR have not been satisfactorily elucidated, it presents a possible explanation for the anti-inflammatory properties of UDCA.

4.2. Aims

The anti-inflammatory effects exhibited by UDCA appear to result from two different processes. One is through modulation of pro-inflammatory signalling mechanisms that are upregulated by cell stress such as that caused by BAs. Experiments on hepatic and colonic cell lines have shown that UDCA can modulate many of the signalling pathways that BAs are known to upregulate in the oesophagus. For example, DCA has been shown to increase the expression of COX-2 in colonic cell lines through the ras/MAPK-p38 dependent pathway. UDCA inhibits this [117, 165].

The second potential anti-inflammatory mechanism of UDCA is activation of the GR. UDCA has been shown to inhibit NF-κB and AP-1 DNA binding and the upregulation of NF-κB dependent genes in colonic cell lines [166]. The ability of UDCA to induce indirect GR *trans*-repression may explain this. However, the UDCA-GR interaction appears to enhance the *trans*-repressive attributes of the GR without resulting in significant *trans*-activation [116, 167, 169-171]. Both cell line and animal models have demonstrated that the UDCA-GR interaction can inhibit apoptosis and suppress pro-inflammatory signalling such as IFN-γ induced HLA-DRA gene expression and NF-κB function, although not as effectively as GCs [167, 172]. Yet UDCA does not induce *trans*-activation [376]. This suggests that UDCA could be a GR activator with the ability to discriminate between *trans*-activation and *trans*-repression

Thus, the aims of this chapter were to:

- Investigate the expression of the GR in oesophageal tissues to determine whether this receptor could be used as a selective modulator of inflammation in the oesophagus.

- To investigate whether UDCA could be used to modulate GR translocation, *trans*-activation and *trans*-repression in oesophageal cell lines expressing the GR.

- To investigate similarities between the mRNA expression profiles induced by UDCA and Dex using microarray technology. As discussed above, expression profiles vary dramatically between cells lines and may be affected through not only direct interaction of the GR with DNA, but also through interaction with other transcription factors.

- To investigate similarities or dissimilarities between UDCA and DCA with regard to regulation of gene expression. While UDCA is a hydrophilic BA with a distinctly different inflammatory profile from DCA, it remains a BA with proven toxicity. Thus it seemed rational to investigate whether similarities existed between the two molecules with regards gene modulation.

4.3. Methods

4.3.1. Cell Lines and Culture

The HET-1A[240], QH,[320] SKGT-4,[377] OE33,[378] HCT116,[241] and HUH-7[242-243] cell lines were used for these experiments. These lines represent normal squamous epithelium of the oesophagus, non-dysplastic BO, OAC, OAC, colonic adenocarcinoma and human hepatoma cells respectively. The origin of these cells and the rationale for their use is explained in Section 9.1.1. The media used and the culture methodology have previously been explained (Sections 2.3.1 and 3.3.1).

4.3.2. Analysis of Glucocorticoid Receptor Expression by Western Blotting in Oesophageal Cells

4.3.2.1. Background

GR expression varies greatly throughout the human body. In order to investigate the potential use of UDCA in modulating inflammation via the GR in the oesophagus, it was first necessary to investigate whether this transcription factor was expressed in the cell lines to be studied. The HUH-7 cell line was used as a positive control [379].

4.3.2.2. Experimental Method

Cells were grown to 80-90% confluence in T25 cell culture flasks. Cells were lysed in RIPA buffer containing 2% SDS, with protease inhibitors, for 30 minutes on ice. A high concentration of SDS was used to ensure adequate lysis of the nuclear membrane. The lysate was aspirated and placed in a centrifuge tube prior to being sonicated briefly to ensure complete disruption of the lysate. Protein concentration was quantified using Pierce BCA kit (Thermo Fischer Scientific, Waltham, MA, USA). Lysates were loaded at approximately 20ug of protein per lane and run through a 10% SDS-PAGE gel. Subsequently the protein was transferred to PVDF membrane using a semi-dry transfer technique. After transfer, the membrane was blocked for 1 hour in 5% Marvel in TBST. The membrane was washed three times for 5 minutes with 0.1% TBST and then incubated with mouse anti-GR antibody (1:2000, BD Biosciences, Franklin Lakes, NJ, USA) in 5% marvel overnight at 4°C. The membrane was washed three times for 5 minutes in TBST and incubated with anti-mouse HRP-linked antibody (1:2000) for one hour at RT. Chemiluminescence was

performed with 4-IBPA. After development the membrane was stripped using Sodium Hydroxide and re-probed for β-actin as a loading control (See Appendix 4 for full methodology).

4.3.3. Analysis of Glucocorticoid Receptor mRNA Expression in Oesophageal Cells by RT-PCR

4.3.3.1. Background

Two predominant isoforms of GR exist: α and β. GRβ is considered a dominant negative form of the GR and high levels of expression can impair the function of GRα. Thus it was necessary to determine the relative expression of GRα and GRβ in cells to be studied.

Taqman PCR probes were used to identify the relative expression of GR mRNA in the cell lines studied. These probes consist of a fluorophore attached to the 5'-end of the oligonucleotide probe and a quencher at the 3'-end. The quencher molecule quenches the fluorescence emitted by the fluorophore. While the fluorophore and quencher are in close proximity, the fluorescence of the fluorophore in inhibited. These probes are designed to anneal to a specific DNA region (the target gene) amplified by a specific set of primers. However, as Taq polymerase extends the primer, synthesising the complementary strand, the 5' to 3' exonuclease activity of the polymerase degrades the annealed probe. This releases the fluorophore from the TaqMan probe, separating it from the quencher, allowing the fluorophore to fluoresce. Therefore, the fluorescence detected in the real-time PCR thermal cycler is directly proportional to the fluorophore released, and the amount of DNA template present in the PCR. As a result of the 5' to 3' direction of Taq DNA polymerase, the Taqman probes are often biases toward the 5' end of the cDNA strand.

4.3.3.2. Experimental Method

Cells were grown to 80 – 90% confluence in 6 well plates. mRNA was isolated using the Quiagen RNeasy Plus Mini Kit (Qiagen, Hilden, Germany). mRNA concentration was quantified using the NanoDrop 8000 (Thermo Scientific, Wilmington, DE, USA) and then equalization was performed by dilution with RNase-free water. Complementary DNA (cDNA) was generated using the Retroscript Kit (Applied Biosystems/Ambion, Austin, TX, USA). 4.5μL of cDNA was added to 5μL of TaqMan Mastermix (Applied Biosystems, Carlsbad, CA, USA) and 0.5μL of primer. A PCR primer for total GR expression (Hs00353740_m1, Applied Biosystems, Carlsbad, CA, USA) and a primer specific to GRβ (Applied Biosystems, Carlsbad, CA, USA) were used for this experiment. Real-time PCR was performed using the Applied Biosystems 7900HT Fast Real-Time

PCR System (Applied Biosystems, Carlsbad, CA, USA). GAPDH was used as the housekeeping gene in order to determine ΔΔCT values. A full protocol is provided in Appendix 4.

4.3.4. Immunohistochemical Staining of GR in Paraffin Embedded Oesophageal Biopsies.

4.3.4.1. Background

To validate the expression of the GR in cell lines, DAB (3,3'-Diaminobenzidine) immunohistochemical staining of paraffin embedded biopsy samples was used. DAB is a derivative of benzidine which is oxidized by H_2O_2 in the presence of haemoglobin to give a dark brown colour. This can be visualized using light microscopy. However, unlike immunofluorescent staining, DAB does not follow the Beer-Lambert law meaning that the intensity of the stain does not predictably correlate with the with the amount of protein present in the tissue.

4.3.4.2. Experimental Method

Paraffin embedded tissue of samples representing normal squamous epithelium, BO, OAC and SqCCa of the oesophagus was kindly provided by the department of pathology, St James's Hospital, Dublin 8, under ethics permission granted by the St James's Ethics Committee. 4μM thick sections were cut from the blocks. Deparaffinisation and dewaxing was performed by sequential passage of the sections through xylene (5 minutes X 2), 100% ethanol (5 minutes X 2), 70% ethanol (5 minutes X 2), and distilled water (5 minutes X 2). Antigen retrieval was then performed by incubation in sodium citrate at pH 6 for ten minutes in a low-pressure pressure cooker. The slides were allowed to cool to RT in fresh sodium citrate and then transferred to 0.1% PBST.

Blocking and staining were performed using the Vectastain ABC elite kit and the avidin biotin blocking kit. Briefly, endogenous peroxidise was quenched for 30 min in 0.3% H_2O_2, and washed twice in 0.1% PBST for 5 minutes. The sections were incubated with avidin for 15 minutes and biotin for 15 minutes. The slides were blocked for 30 min with diluted horse serum in a humidity chamber. Excess serum was removed by blotting the slide on a piece of tissue paper. Sections were incubated for 60 min with mouse anti-GR antibody (1:250, BD Biosciences, Franklin Lakes, NJ, USA) in a humidity chamber and then washed twice with 0.1% PBST for 5 minutes. Sections were incubated with diluted biotinylated secondary antibody solution for another 30 minutes in a humidity chamber, and again washed twice with 0.1% PBST for 5 minutes. Slides were then incubated with the VECTASTAIN® Elite ABC reagent for 30 min and washed twice with 0.1% PBST for 5 minutes. Sections were incubated in a DAB peroxidase substrate solution, until the

desired stain intensity developed. The slides were then rinsed in tap water, counterstained with haematoxylin and coverslips mounted using the Fluoromount aqueous mounting medium (Sigma, St. Louis, MO, USA). Images were acquired at 20X magnification using the Scan-Scope Digital Imager (Aperio, Vista, CA, USA). Individual staining is demonstrated in Figure 4–2.

For scoring of GR expression in oesophageal epithelium, an IHC scale was used. This is based on IHC scores used by pathology labs to quantify immunohistochemical staining of tissue sections [380-381]. The percentage of cells expressing GR was classified on a scale from 0 – 4 where 0 represents 0% of cells expressing the protein, 1 represents occasional cells, 2 represents 10%, 3 represents 10-50% and 4 represents >50%. The average intensity of staining was classified as 0 (no stain) – 3 (strong). Multiplication of the two factors resulted in an overall score of 0 – 12 for each section (Figure 4–5).

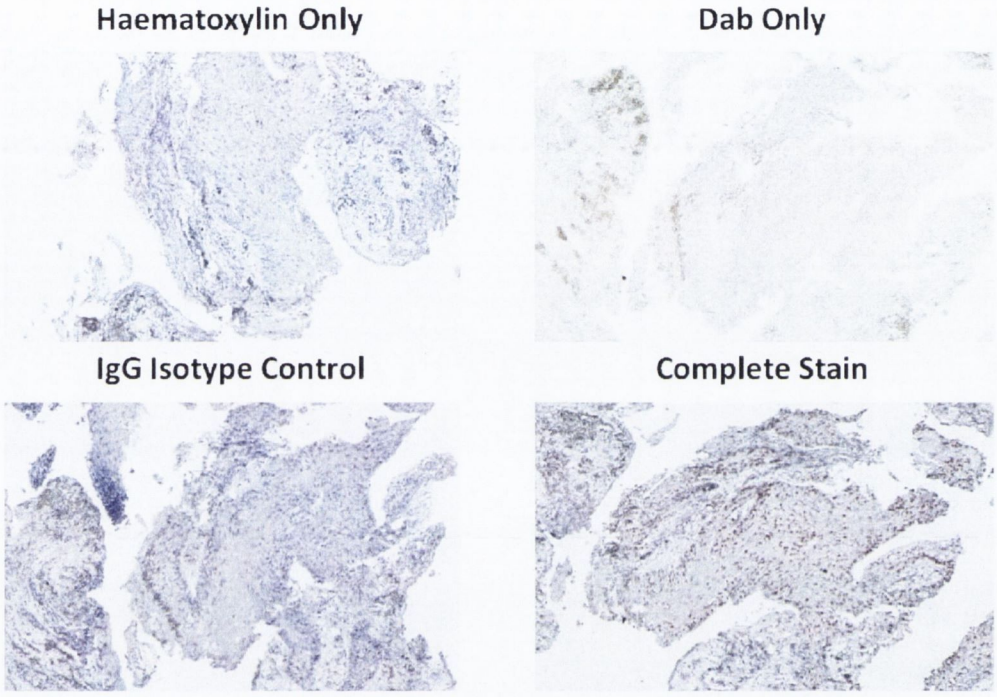

Figure 4–2: Optimization of immunohistochemical staining for the GR in oesophageal tissue. SqCCa of the oesophagus was used as a positive control. Staining of sequential sections of the paraffin block demonstrates staining with Haematoxylin only, non specific staining with Dab Only (no primary antibody) and the Mouse IgG isotype control, and specific staining of the tissue with complete staining.

4.3.5. Nuclear Translocation of the Glucocorticoid Receptor

4.3.5.1. Background

Nuclear translocation of the GR is necessary for this transcription factor to exert its genomic effects. While UDCA has been shown to induce nuclear translocation of the GR in a mechanism distinct from GCs, it was necessary to determine whether UDCA could induce GR translocation in the cell lines to be studied. Furthermore, it was necessary to determine the concentrations of UDCA which could translocate the GR and the time-course of any translocation.

To establish a model of translocation, we first optimised a high content analysis method using PFA fixed HET-1A, QH and SKGT-4 cells which had been treated with Dex for 2 hours. Cells were immunofluorescently stained for the GR and the nucleus (Figure 4–3). Images were acquired using the InCell Analyzer 1000 (GE Healthcare, Wauwatosa, WI, USA). Analysis was performed by determining nuclear and cytoplasmic intensity of the GR stain using InCell Analysis software. To establish the validity of our model and its ability to determine differences in the Nuclear:Cytoplasmic (N:C) ratio we calculated the z-factor for each of these optimization experiments.

In high-content analysis, it is necessary to establish whether the quality of an assay is sufficient to differentiate genuine results from variance in the system. One method of assessing this is the z-factor. It is calculated as follows,

$$Z = 1 - \left(\frac{3(\sigma p + \sigma n)}{\mu p - \mu n}\right),$$

where σp is the SD of the positive control (100nM Dex), σn is the SD of the negative control (untreated cells), μp is the mean of the positive control and μn is the mean of the negative control.

Z-factors cannot exceed the value of 1. A value of 1 suggests an ideal assay. Between 0.5 and 1.0 suggest an excellent assay. Values of 0 to 0.5 are of marginal use and less than 0 suggests that the overlap between the positive and negative controls is too great for the assay to be useful. In our optimization assay, the z-factors for HET-1A cells, QH cells and SKGT-4 cells were 0.91, 0.55 and 0.42 respectively. This suggested that the assay was capable of being used for high content analysis.

4.3.5.2. Experimental Method

Cells were seeded into 96 well plates at concentrations appropriate to the cell line and allowed to adhere. 24 hours later, media was replaced with serum free RPMI for the SKGT-4 cell line and with BEBM medium containing 1% FBS without supplements for the HET-1A and QH cell lines.

After overnight serum starvation the cells were treated with various concentrations of UDCA or DCA in serum free medium. At the appropriate time-points cells were fixed in 4% PFA for 15 minutes at 37°C. The PFA was then aspirated and the cells washed in PBS. The cells were then permeabilised using 0.1% triton in PBS for 5 minutes. After this, blocking was performed with 3% BSA (Sigma, St. Louis, MO, USA) in PBS for 30 minutes at RT. The BSA was aspirated and the cells incubated with mouse anti-GR antibody (1:1000, BD Biosciences, Franklin Lakes, NJ, USA) in PBS for one hour at RT. The cells were washed three times with PBS and incubated with goat anti-mouse Alexa Fluor 488 (Invitrogen, Carlsbad, CA, USA) for one hour. The cells were washed three times and incubated with Hoechst 33258 (Invitrogen, Carlsbad, CA, USA) and TRITC-phalloidin (Sigma, St. Louis, MO, USA) for 15 minutes at RT. The cells were washed three times with 200µL PBS, finally leaving 200µL PBS in each well. Image acquisition was performed using the InCell Analyzer 1000 and analysis performed using InCell Analysis software (GE Healthcare, Wauwatosa, WI, USA).

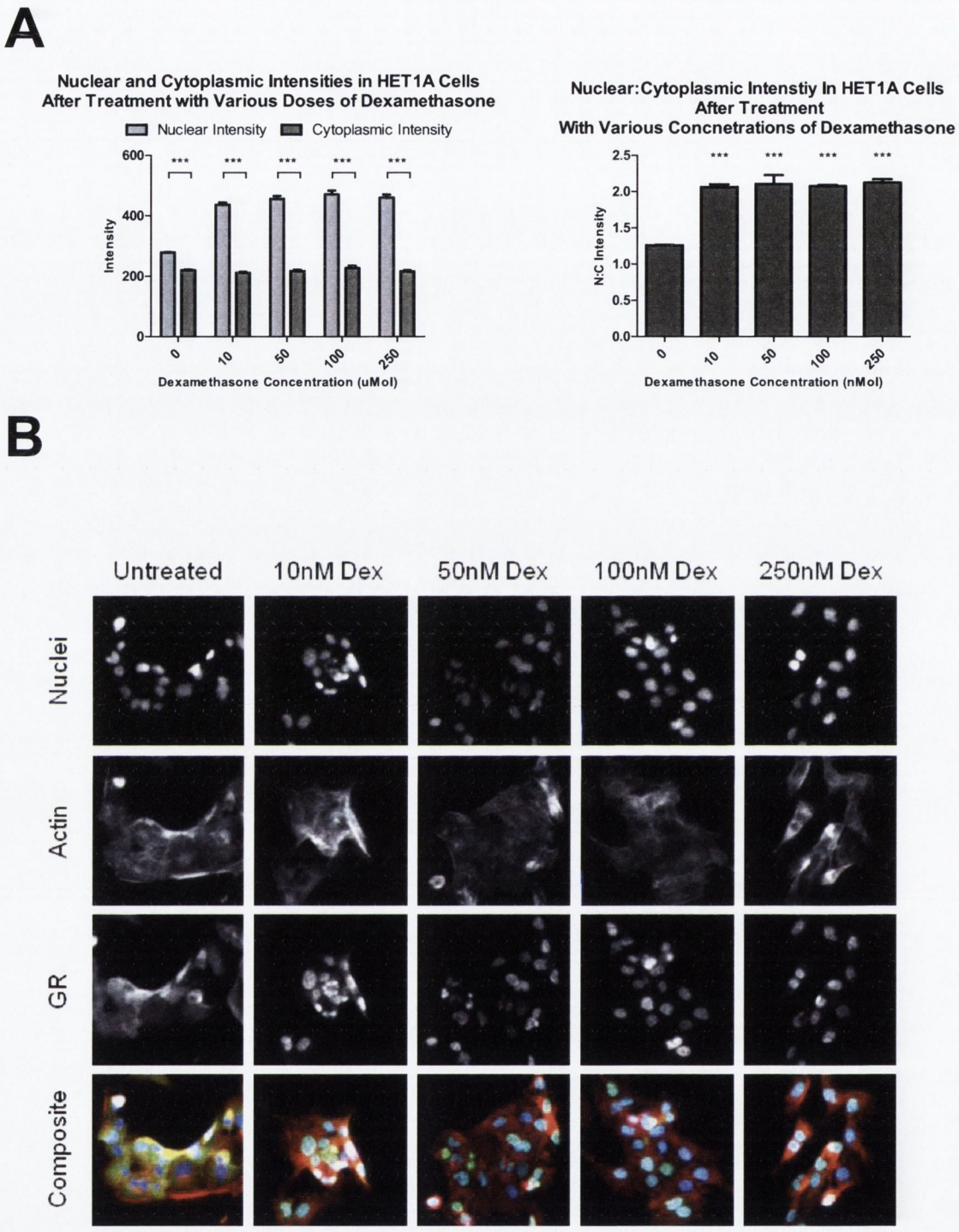

Figure 4–3: Optimization of a high content assay for nuclear translocation of the GR demonstrates that Dex (a positive control) induces translocation of the GR to the Nucleus. A) Graph Demonstrating the alterations in nuclear and cytoplasmic GR intensity and nuclear:cytoplasmic ratios in response to Dex stimulation. *** denotes $P < 0.001$. B) Images acquired using the GE InCell 1000. Hoechst; Blue. GR; Green, Phalloidin; Red.

4.3.6. GR *Trans*-activation Assay

4.3.6.1. Background

Trans-activation by the GR is a marker that the GR has not only been translocated to the nucleus but also suggests that the receptor has dimerised and is capable of binding to DNA and activating transcriptional machinery. To investigate this, the Cignal GRE Reporter Kit (SA Biosciences Corporation, Frederick, MD, USA) was used. A firefly luciferase reporter gene under the control of a minimal CMV promoter and tandem repeats of the glucocorticoid transcriptional response element (GRE) is transfected into cultured cells. Binding of the GR to the GRE results in activation of transcriptional machinery and transcription of the luciferase construct. A constitutively expressed Renilla luciferase acts as internal control for normalizing transfection efficiencies.

4.3.6.2. Experimental Method

HET-1A and SKGT-4 cells were transiently transfected with a mixture of the inducible glucocorticoid responsive firefly luciferase reporter and constitutively expressing renilla construct (40:1). A reverse transfection procedure was optimized using Fugene HD (Roche, Schweiz, Germany) as a transfection reagent at a ratio of 4:1 (Fugene HD: DNA). DNA and fugene HD were diluted in OptiMem (Invitrogen, Carlsbad, CA, USA) and this mixture was added to 96-well plates to give 100ng DNA per well. 1.5×10^4 cells in 200µl of medium was added to this mixture. After 24 h the media was changed to fresh media. 24 hours later, the cells were treated with UDCA, DCA or Dexamethasone for 16 h. After 16 h the cells were lysed using 50µl of passive lysis buffer (Promega Corporation, Madison, USA) and incubated at RT for 15 min. The lysates were then assayed for firefly and renilla luciferase activity (Promega Dual-Luciferase Reporter Assay System, Promega Corporation, Madison, USA) using a Victor Perkin Elmer luminometer.

4.3.7. Microarray Data Experiment and Analysis.

4.3.7.1. Background

Two predominant classes of gene expression microarray exist: complementary DNA (cDNA) arrays and oligonucleotide arrays. Microarrays represent a tool for comparative (cDNA) or quantitative (oligonucleotide) analysis of gene expression profiles. Oligonucleotide arrays comprise probes of 20-25mers, which in the case of Affymetrix technology, are synthesised *in situ* by photolithography onto silicon wafers. Although these probesets are much shorter than those in spotted cDNA arrays, the greater number of probesets in oligonucleotide arrays allows sufficient reproducibility to enable accurate comparison of expression levels between experiments. This provides a data set which can be used to investigate gene expression profiles induced by numerous treatments and at numerous time-points.

In oligonucleotide array experiments, mRNA is first extracted from experimental cells. After assessment and confirmation of RNA quality, the mRNA is amplified by PCR and labelled with biotin, which will subsequently allow the attachment of a fluorescent marker. The RNA is then cleaved into shorter segments. The labelled and cleaved RNA is then washed over the chip for 14 to 16 hours to allow hybridization, the binding of RNA to its complementary DNA probe. The chips are washed to remove excess RNA which has not bound to a probe, the biotin conjugated RNA labelled with a fluorescent marker (usually streptavidin phycoerythrin (PE) conjugate) and the fluorescent intensity each probe set is measured.

The probe sets on Affymetrix Genechip microarrays are designed to hybridize within the 3' end of a transcript. This is because during the preparation of amplified RNA, cDNA or complementary RNA, the generation of these oligonucleotide strands is preformed from the 3' to the 5' end of the string. This means that the expression of genes which are only partially amplified, transcribed, or reverse transcribed, will be less likely to be biased downward by virtue of the preparatory steps. For housekeeping genes, additional probe sets are included in the array that that specifically hybridize in the 5' region and middle portion of the genes transcript. This is in order to allow better data normalisation across the genechips. This also allows the ratio of signal intensities from the 3' probe set to be compared with those from the 5' probe set to calculate the 3'/5' ratio. This ratio is used to assess the integrity of the input RNA and the efficiency of first strand cDNA synthesis and/or amplification by in vitro transcription.

The Affymetrix Genechip Human Genome U133A Plus 2.0 was used for these experiments. This oligonucleotide microarray is comprised of 1.3million unique oligonucleotide sequences which represent approximately 47,000 gene transcripts and variants derived from GenBank, dbEST and RefSeq and refined through comparison with other database sets. Eleven pairs of oligonucleotide

probes are used to measure the transcription of each sequence represented and this reflects approximately 39,000 human genes.

4.3.7.2. Experimental Method

For the micro-array experiment, HET-1A, OE33 and HCT116 cells were grown to 80-90% confluence in T25 cell culture flasks. This ensured that all cell lines were in a proliferative stage of growth. The cells were washed twice with fresh medium with no supplements and then treated with 0.06% DMSO (vehicle control), 200μM UDCA, 100nM Dex (containing 0.06% DMSO) or 200μM DCA and incubated at 37°C for 12 hours. After treatment the medium was removed and RNA isolated using a RNeasy Plus Minikit (Quiagen, Germantown, MD, USA).

For quality control, RNA concentration was determined using the Nanodrop 8000 (NanoDrop products, Wilmington, DE, USA). Integrity was assessed RNA Nano Chip Assay and the Agilent Bioanalyser (Agilent Technologies, Santa Clara, CA, USA). The RNA Integrity Number (RIN) provides a numeric determination of the quality of the RNA in a sample based on ribosomal RNA integrity. Samples are classified with a number from 1 to 10. A RIN of 1 represents almost completely degraded RNA while a RIN of 10 suggests almost perfectly intact RNA. This allows direct comparison of the quality of numerous samples for analysis (See Appendix 3).

Twenty-four Affymetrix U133A Plus 2.0 genechips were used in this experiment. Technical duplicates were processed for each of the treatments (DMSO, UDCA, DCA or Dex) in each of the cell lines (HET-1A, OE33 and HCT116). Microarray processing was performed by the Core facility in the Conway Institute, University College Dublin, Dublin 4.

4.3.7.3. Analysis

Microarray datasets provide large gene lists. In the case of the U133 Plus 2.0 array, 47,000 transcript probes code for 37,000 thousand genes. Refining these lists for data mining and comparative analysis is necessary. Quality control and basic data analysis was performed using GeneSpring GX 11.5 (Agilent Technologies, Santa Clara, CA, USA).

Prior to comparisons, refining of data sets was required. Three factors were considered when refining our data sets:

- The fluorescence of a probe set (reflecting whether a gene was expressed or not), and whether a gene was expressed at a high or low level,
- the magnitude of change in gene expression (fold change) induced by treatment relative to the control group (vehicle control), and,

- reproducibility of the measurement (statistical measure of the fold change difference relative to DMSO vehicle as determined by t-tests or ANOVA).

To determine whether a gene was expressed, and at what level of expression, the intensity of the signal was evaluated. In general, intensity levels ranged from 4 to 30,000 across the array sets. A minimum cut-off intensity level of 100 in two of the four samples being analysed was used to remove mRNA that was not considered to be expressed. Specifying that a intensity level of 100 was only required in one of the two sample pairs enhanced the probability that genes with low expression profiles with significant increases, or genes with significant expression that were greatly downregulated, would not be excluded from the analysis. This cut-off was chosen by repeated preliminary analysis of the data. Genes with low levels of expression are more susceptible to intrinsic variation which can result in large fold changes and significance during further analysis. This can result in false positive changes and statistical changes where the gene is in fact either not expressed or the absolute magnitude of this change is minor. At the chosen threshold of 100, approximately 35% of genes were excluded from each dataset.

We next used a minimum fold change of 1.5 from DMSO vehicle control to further refine the data sets to genes which were modulated by treatment. This cut-off was chosen for two reasons. Firstly, it represents a lower level of real fold change that is genuinely detectable using RT-PCR [382-383]. Secondly, in the cells stimulated by Dex or UDCA, the magnitude of the fold changes observed was minor compared to that seen with DCA. Few of the probe-sets demonstrated a greater than two-fold difference from DMSO after treatment (Figure 8–3, p273). Therefore, in order to identify genes whose expression was altered by stimulation with UDCA or Dex treatment, the minimum fold change to be studied was chosen as 1.5. Statistical analysis (described below) was used to reduce the number of false positives generated by this technique.

Finally, the reproducibility of the measurement was investigated using statistical analysis (t-tests). In our experiment, using technical replicates, this analysis represented an analysis of the reproducibility of the array technology rather than an analysis of the change induced by treatment. This experimental methodology was chosen as a result of our experience during pilot experiments using RT-PCR to investigate the effects of DCA and UDCA treatment on the HET-1A cell line. While similar effects were seen between experiments, statistical significance was frequently lost. This was because the high sensitivity of RT-PCR in determining changes in gene expression led to large variance between experimental replicates.

Using t-tests (comparing treated replicates with DMSO vehicle control replicates), multiple significance levels (α = 0.05, 0.01 and 0.005) were used to investigate the validity of the genes identified during expression level and fold change analysis of the micro-array data. A cut-off of $\alpha \leq$ 0.01 was initially chosen. This was felt to be appropriate to reduce the number of false positives

generated by a less stringent cut-off ($\alpha \leq 0.05$), and to reduce the false negatives excluded by too stringent a cut-off ($\alpha \leq 0.005$). This cut-off subsequently had to be lowered to ≤ 0.05 because it was found to exclude all genes in some cell lines and in some experiments. False discovery rate correction was not used for two reasons. Firstly, because of the relatively few genes which demonstrated altered expression in the UDCA and Dex groups after the first two filtering step, especially in the OE33 and HCT116 cell lines. Secondly, the limited numbers of replicates used in this experiment (N=2) meant that only genes which were likely to be significantly altered in both replicates would be identified by the t-tests, thus reducing the false positive rate.

To determine whether particular genes were similarly or differently regulated by treatments, two analysis methods were used; direct comparisons of genes similarly up- and down-regulated by specific stimulation and clustering analysis. Direct comparisons of gene lists were performed using Venn diagrams to elucidate subgroups of genes similarly or dissimilarly modulated by different treatments.

Clustering was performed using an unsupervised technique: hierarchical Euclidian clustering methods based on average fold changes. This technique clusters genes into similarly regulated patterns of genes or patterns of treatments allowing an easily interpreted visual aid for data mining. Simultaneous clustering of both genes and treatment or cell line was performed to investigate similarities.

Ingenuity Pathway Analysis (IPA, Redwood City, CA, USA) was used to find associations between genes modulated by UDCA and Dex which were associated with the GR in the literature. IPA is a software package which allows identification of relationships between chemicals, proteins, genes, and cellular processes by searching through a repository of information which has been extracted from the currently published literature.

4.3.7.4. Array Validation

From these analyses, gene lists were constructed and genes chosen for validation. Validation was performed using RT-PCR technology. HET-1A cells were grown to 80 – 90 % confluence, were washed with serum free medium, and treated with 0.06% DMSO (vehicle control), 200μM UDCA, 100nM Dex (containing 0.06% DMSO) or 200μM DCA and incubated at 37°C for 12 hours.

After treatment, RNA was isolated using the Qiagen RNeasy Plus Mini Kit (Quiagen, Germantown, MD, USA). Normalisation, cDNA generation, and RT-PCR was performed as described above (Section 0) using the following Taqman primers (provided by Applied Biosystems):

- CTTN Hs00193322_m1
- STAM2 Hs00195241_m1

- CITED2 Hs01897804_s1
- CRIM1 Hs00212750_m1
- PRKDC Hs00179161_m1
- SERPINE1 Hs01126606_m1
- v-SKI Hs00161707_m1
- PHACTR3 Hs00294903_m1
- BIRC3 Hs00154109_m1
- NOTCH2 Hs00225747_m1
- GR (NR3C1) Hs00353740_m1
- IL-8 Hs00174103_m1
- ACTB Hs99999903_m1
- ATF3 Hs00231069_m1
- CXCL14 Hs01557413_m1
- DDIT3 Hs01090850_m1
- GDF15 Hs00171132_m1
- TRIB3 Hs01082394_m1

GAPDH (Hs99999905_m1) was used as a housekeeping gene. A full protocol is provided in Appendix 4.

The rationale for the choice of these genes is explained in detail in section 4.4.4.5

4.4. Results

4.4.1. Glucocorticoid Receptor α, but not GRβ, is Expressed in Oesophageal Cell Lines representing the Normal - BO - OAC Sequence

Using Western blotting it was demonstrated that the GR is expressed in the HET-1A, QH, SKGT-4 and OE33 cell lines representing normal oesophageal mucosa, BO and OAC (Figure 4–4). A lower level of expression was seen in the HCT116 cell line relative to the oesophageal cell lines. These findings were consistent with previously published data suggesting that the GR is significantly expressed in oesophageal epithelium but not in colonic epithelium. However, the same paper suggested that the level of expression in OAC is negligible whereas it was readily demonstrated in both the SKGT-4 and OE33 cell lines [369].

Using RT-PCR, the expression of total GR and GRβ, an endogenous dominant negative GR, was investigated in the same cell lines (Figure 4–4). Total GR expression was similar in HET-1A, SKGT-4 and OE33 cells. However, mRNA expression was significantly lower in the QH and HCT116 cell lines relative to the HET-1A cell line. GRβ mRNA expression was only intermittently detected close to 40 PCR cycles. This suggested that the GR isoform expressed in these cell lines was predominantly GRα. The mean cycle number that the GAPDH control was expressed at was 20.8 (at a threshold of 0.2) in the HET-1A cell line and total GR at 26.4 cycles. As GRβ mRNA was only intermittently detected at around 40 cycles, this suggests that the relative expression of GRα was at least 5000 fold that of GRβ in these cell lines. For this reason, the expression of GRβ is not shown in Figure 4–4.

In paraffin embedded tissue the GR was consistently demonstrated in squamous epithelium but only intermittently in Barrett's epithelium (Figure 4–5). Within squamous epithelium the strongest expression was seen in the basal layers of the epithelium and within the oesophageal glands. BO was readily identified by the columnar cells and glandular structure in which the epithelium contains numerous mucin producing goblet cells. While the epithelium in BO stained poorly for GR, in the sub-epithelium numerous cells stained positive for GR. These may reflect inflammatory cell infiltrate associated with BO [384]. Only necrotic tissue was recovered from the OAC samples provided and only two SqCCa samples (positive controls) survived processing or were not comprised solely of necrotic tissue. Within these two samples, GR was expressed within the tumour islands but not within tissue outside of this. Similar findings to BO were identified within colonic epithelium (glandular epithelium with no goblet cells); no GR was detected in the columnar epithelium but was visible in the sub-epithelial layers. Using IHC scoring of the squamous epithelium and BO samples, the expression of GR in squamous epithelium was demonstrated to be significantly greater than in BO (Figure 4–5, discussed in section 4.3.4).

These findings suggest that a modulator of the GR may be able to target normal squamous epithelium of the oesophagus without exerting an anti-inflammatory effect in BO.

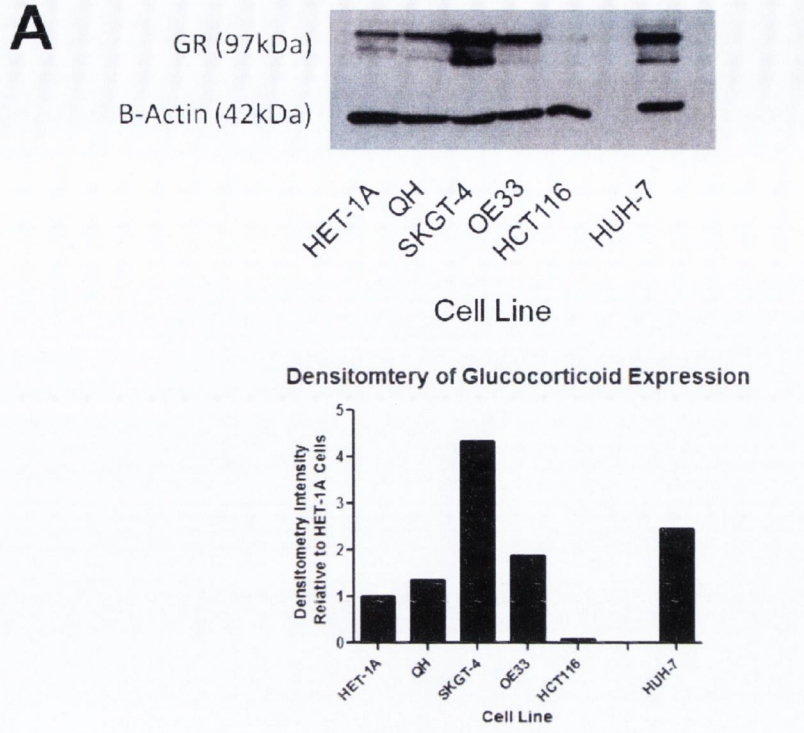

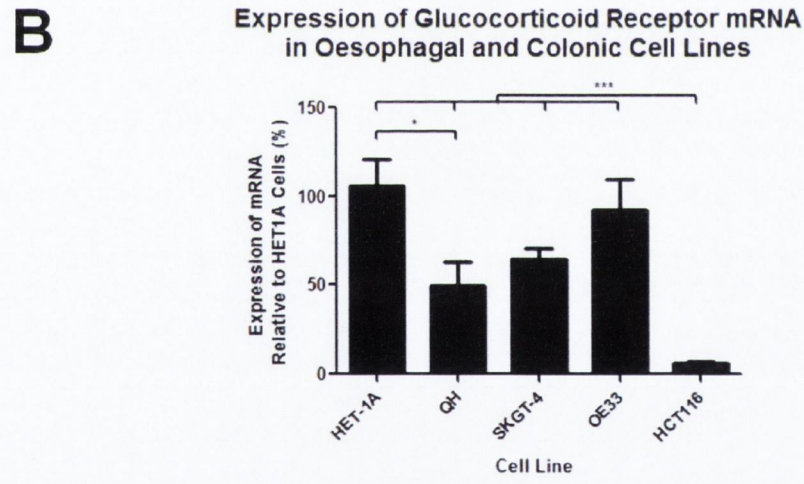

Figure 4–4: The expression of GR in oesophageal and colonic epithelium as determined by Western blotting (A) and RT-PCR (B). Untreated Cells were lysed in RIPA buffer containing 2% SDS. Protein samples were normalised and expression probed with mouse anti-GR antibody. Subsequently, the membrane was stripped and re-probed for β-Actin. Densitometry was performed on a representative example of three experiments (Shown above (A)). For the RT-PCR, untreated cell lysates were lysed and mRNA isolated using the Qiagen RNeasy Mini Kit Plus. cDNA was generated using a reverse transcription method. Primers were supplied by Applied Biosystems. Real time PCR was performed using Applied Biosystems 7900HT Fast Real-Time PCR System. Mean and SEM of n = 3 is shown and * and *** denote $p < 0.05$ and < 0.001 respectively.

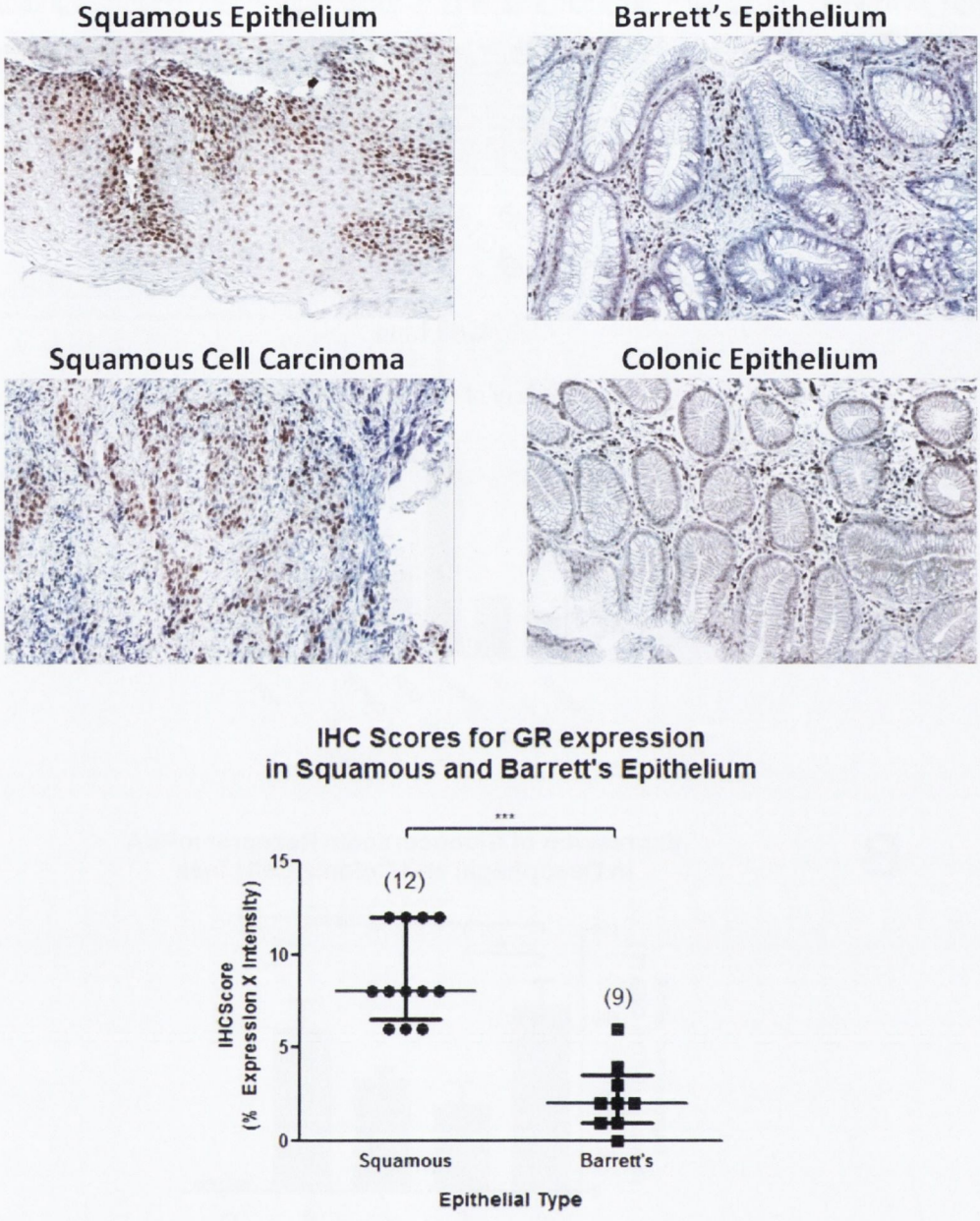

Figure 4–5: IHC staining of oesophageal and colonic tissue demonstrating expression of GR in squamous epithelium and squamous cell cancer of the oesophagus but not in BO or colonic epithelium. Columnar epithelium is readily visible in the BO and the colonic samples. Mucin producing goblet cells are readily visible in the BO sample but not in the colonic epithelium. Paraffin embedded tissue was deparaffinised and rehydrated. Only two samples of SqCCa and one sample of colonic epithelium survived processing or were fit for imaging. Semi-quantitative scoring (B) of squamous epithelium (N=12) and BO (N=9) was performed using an IHC score. Data is represented as median and inter-quartile range. Comparison was performed using Mann-Whitney U Test and *** represents $p < 0.001$.

4.4.2. UDCA Stimulation Induces Nuclear Translocation of the GR

Using immunofluorescent staining for the GR and high content analysis we next established a model that was capable of identifying nuclear translocation of the GR in response to Dex (see section 4.3.5). Subsequently, we indentified that UDCA could translocate the GR to the nucleus in a time and dose dependent fashion in the HET-1A, QH, SKGT-4, OE33 and HCT116 cell lines (Figure 4–6, Figure 4–7 and Figure 4–8)

In the dose-response experiments, the EC_{50} of UDCA was 336 μM in HET1A cells (R^2 = 0.82), 2977μM in QH cells (R^2 = 0.03), 500μM in SKGT-4 cells (R^2 = 0.85) and 223μM in HCT116 cells (R^2 = 0.18). The maximum concentration of UDCA used (1000μM) exhibited 36%, 17%, 48%, and 117% the efficacy of 100nM dexamethasone in the HET-1A, QH, SKGT-4 and HCT116 cell lines respectively (all $p < 0.05$ relative to untreated control). The EC_{50} and potency of UDCA in the OE33 cell line after two hours stimulation could not be determined. Given the poor correlation of translocation in the QH, OE33 and HCT116 cell lines (R^2 = 0.03, 0.05 and 0.18 respectively), the values calculated for the EC_{50} and efficacy must be interpreted with caution. Note that the values quoted for the R^2 differ slightly from the graphs shown in Figure 4–6. This is because to calculate the EC_{50} of the dose response curve, values were normalised to the maximum concentration of UDCA used (1000μM) rather than to 100nM Dex.

In the timecourse experiment, the relative potency of eight hours exposure to 300μM UDCA, relative to 100nM Dex, was 35.7%, 36.5%, 25.5%, 12.6% and 50.9% in the HET-1A, QH, SKGT4, OE33 and HCT116 cell lines respectively (all $p < 0.05$ relative to untreated control). Non-linear regression and curve fitting was much better in the timecourse experiment than in the 2 hour dose response experiment. The respective R^2 for the non-linear regression were 0.49, 0.57, 0.50, 0.64 and 0.45 suggesting a moderate to good fitting of the data. This may reflect that UDCA takes longer to induce nuclear translocation in the QH, OE33 and HCT116 cell lines than in the HET-1A or the SKGT-4 cell lines.

We next investigated whether DCA would exert the same effect as UDCA in translocating the GR to the nucleus (Figure 4–9, Figure 4–10 and Figure 4–11). Cells were treated as per the UDCA translocation assay in the HET-1A and SKGT-4 cell lines. In the HET-1A cell line DCA failed to translocate the GR to the nucleus. Within the SKGT-4 cell line, the GR translocated the GR to the nucleus with almost the same efficacy as UDCA. The $logEC_{50}$ for GR translocation in the SKGT-4 Cell line in response to DCA was 2.77 +/- 0.06 with an R^2 of 0.71. The efficacy of the translocation induced by 1000μM DCA was 89.1% relative to 1000μM UDCA. In the HET-1A cell line, the EC_{50} for the log(dose)-response curve and the efficacy relative to Dex were not calculated as the R^2 was 0.08.

The ability of DCA to translocate the GR to the nucleus in SKGT-4 cells but not HET-1A cells was an interesting finding and may suggest that DCA is itself capable of translocating the GR to the nucleus in a fashion similar to UDCA in cells which are more resistant to DCA induced cell death.

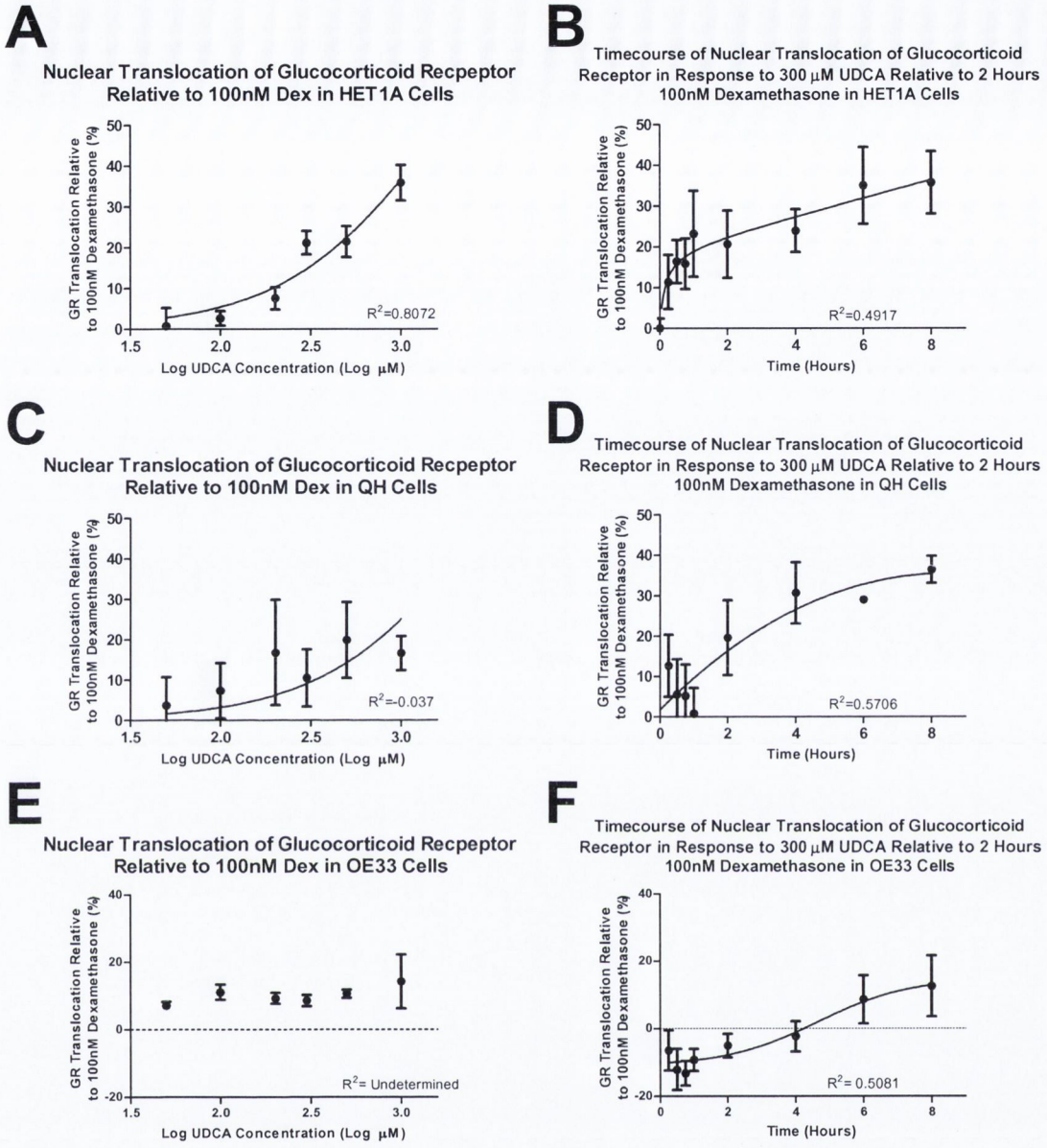

Figure 4–6: UDCA is capable of inducing nuclear translocation of the GR in a dose and time dependent fashion in the HET-1A (A, B), QH (C, D), OE33 (E, F), SKGT-4 (G, H) and HCT116 (I, J) cell lines. Cells were seeded and left to adhere overnight. Subsequently the medium was replaced with serum free medium for the OE33, SKGT-4 and HCT116 cells and with medium containing 1% FBS for the HET-1A and QH cell lines. After overnight serum starvation the cells were treated with BAs in serum free medium. At appropriate time-points the cells were fixed in 4% PFA, The cells were incubated anti-GR antibody, Hoechst 33258 and phalloidin. Image acquisition was performed using the InCell Analyzer 1000 and analysis performed using InCell Analysis software. Translocation is expressed relative to translocation induced by 100nM Dex. Non-linear regression of N:C ratio was performed with GraphPad Prism using a log(dose)-normalised response for the dose response experiment and a sigmoidal variable slope model for the timecourse model. Figures G, H, I and J are found on the next page.

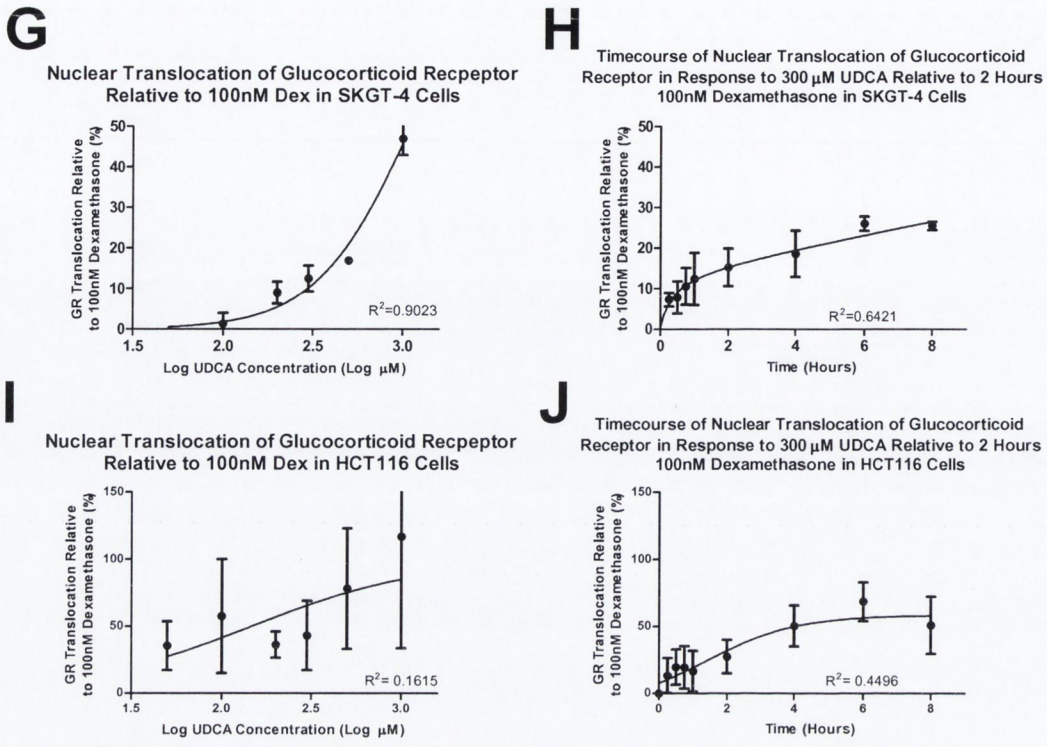

Figure 4-6 Continued: UDCA is capable of inducing nuclear translocation of the GR in a dose and time dependent fashion in the HET-1A (A, B), QH (C, D), OE33 (E, F), SKGT-4 (G, H) and HCT116 (I, J) cell lines.

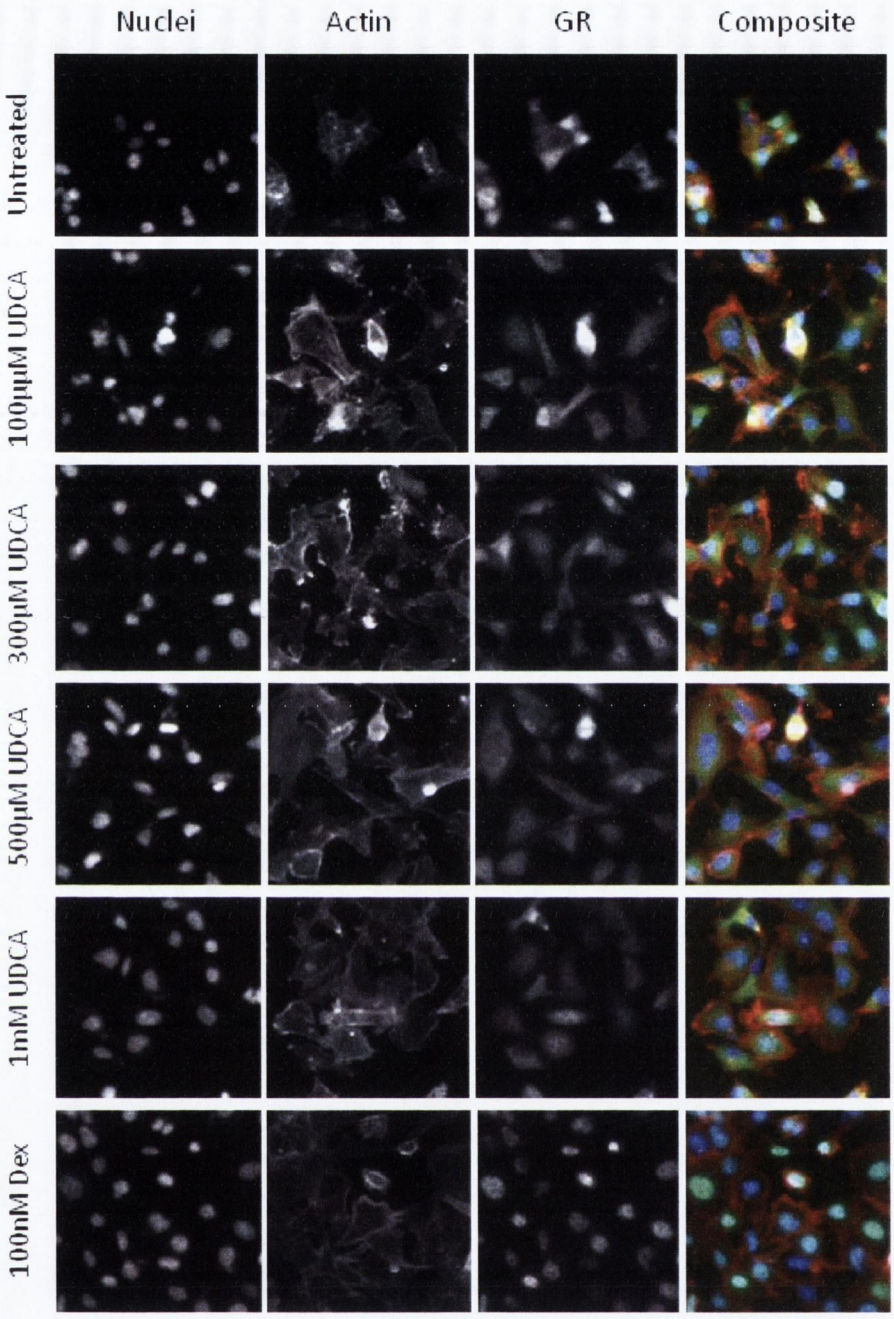

Figure 4–7: UDCA is capable of inducing translocating the GR to the nucleus in a dose dependent fashion. Images are of the HET-1A cell line. Cells were seeded and left to adhere overnight. Subsequently the medium was replaced with medium containing 1% FBS. After overnight serum starvation the cells were treated with appropriate concentrations of UDCA in serum free medium. After two hours the cells were fixed in 4% PFA, The cells were permeabilised and stained with anti-GR antibody (Green), Hoechst 33258 (Blue) and phalloidin (Red). Image acquisition was performed using the InCell Analyzer 1000. Two hours treatment with 100nM Dex was used as a positive control for translocation.

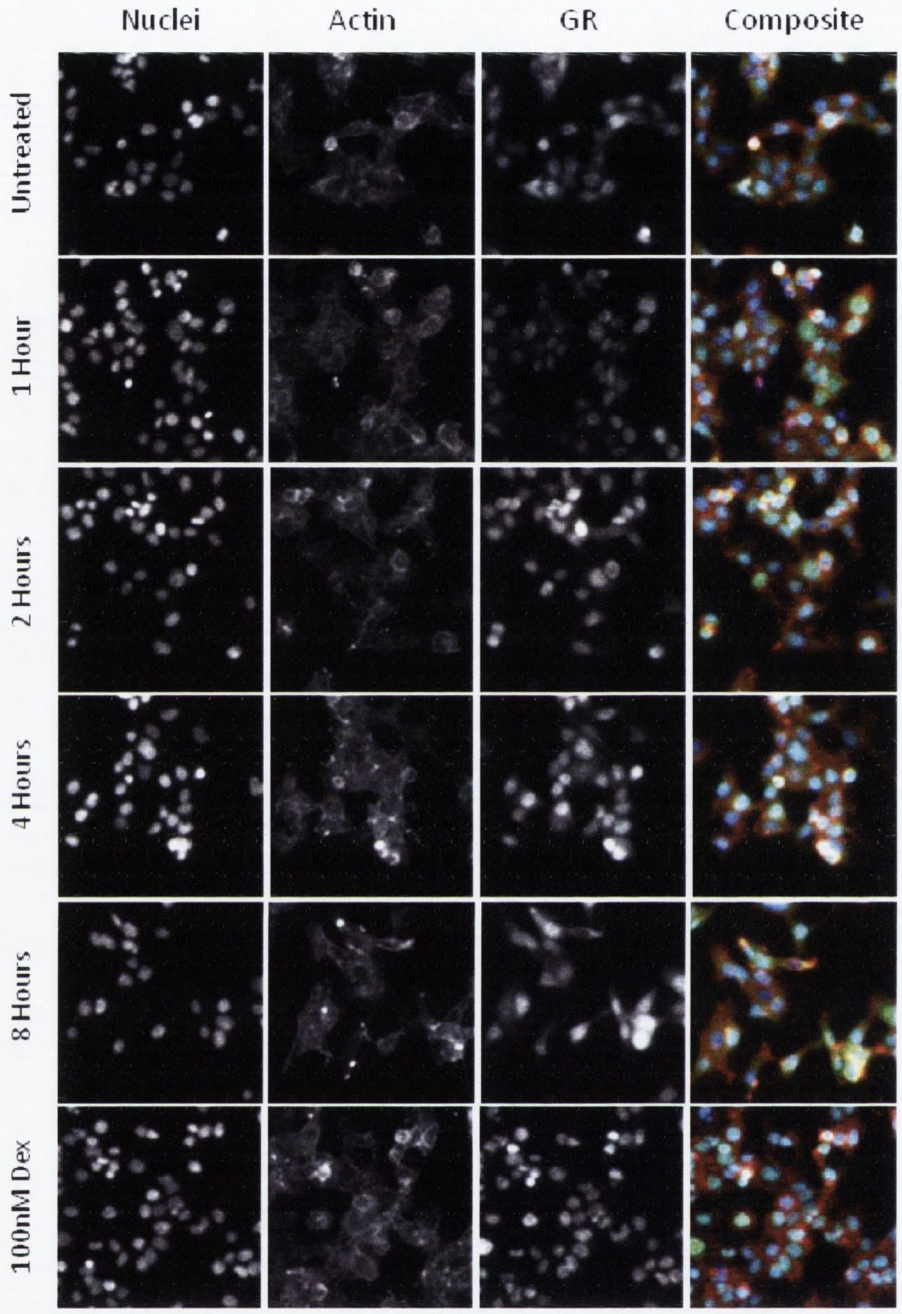

Figure 4–8: UDCA is capable of inducing translocating the GR to the nucleus in a time dependent fashion. Image shown are those of the HET-1A cell line. Cells were seeded and left to adhere overnight. Subsequently the medium was replaced with serum free medium for the SKGT-4 cell lines and with medium containing 1% FBS for the HET-1A and QH cell lines. After overnight serum starvation the cells were treated with 300μM UDCA in serum free medium. At appropriate time-points the cells were fixed in 4% PFA, The cells were incubated anti-GR antibody (Green), Hoechst 33258 (Blue) and phalloidin (Red). Image acquisition was performed using the InCell Analyzer 1000. Two hours treatment with 100nM Dex was used as a positive control for translocation.

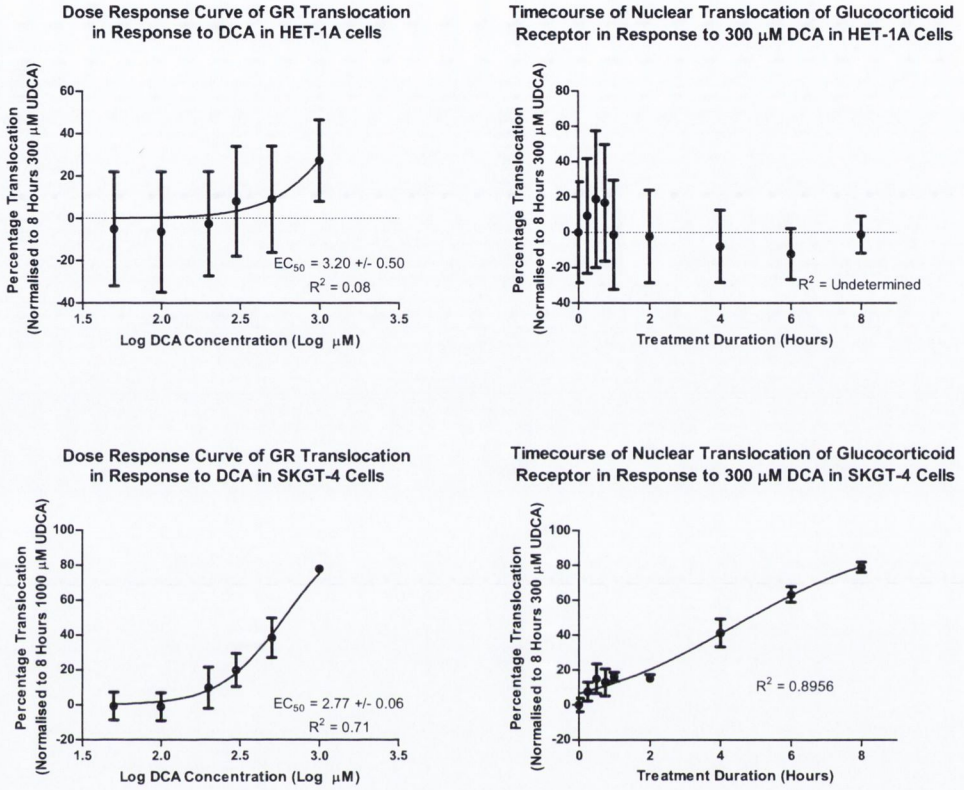

Figure 4–9: DCA translocates the GR to the nucleus in the SKGT-4 cell line (B) but not the HET-1A cell line (A). Cells were seeded and left to adhere overnight. Subsequently the medium was replaced with serum free medium for the SKGT-4 cell line and with medium containing 1% FBS for the HET-1A cell line. After overnight serum starvation the cells were treated with appropriate concentrations of DCA in serum free medium. At appropriate time-points the cells were fixed in 4% PFA, The cells were incubated anti-GR antibody (Green), Hoechst 33258 (Blue) and phalloidin (Red). Image acquisition was performed using the InCell Analyzer 1000 and analysis performed using InCell Analysis software. Two hours treatment with 100nM Dex was used as a positive control for translocation. Translocation is expressed relative to maximal translocation seen with 1000μM UDCA. Non-linear regression of N:C ratio was performed with GraphPad Prism using a log(Dose)-normalised response for the dose response experiment and a sigmoidal variable slope model for the timecourse model.

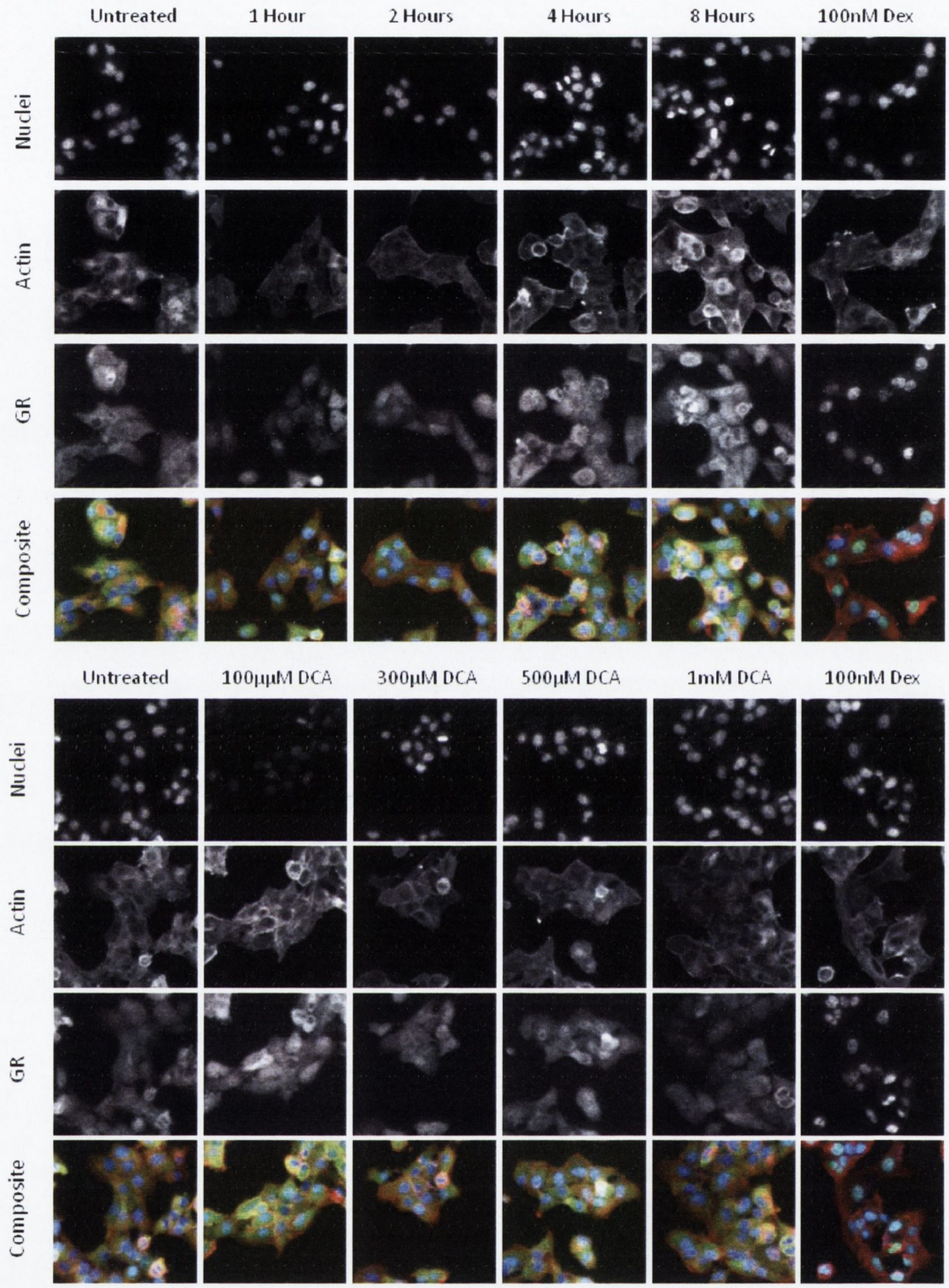

Figure 4–10: DCA does not induce nuclear translocation of the GR in a dose or time dependent fashion in HET-1A cells. Cells were seeded and left to adhere overnight. Subsequently the medium was replaced with medium containing 1% FBS. After overnight serum starvation the cells were treated with DCA in serum free medium. At appropriate time-points the cells were fixed in 4% PFA, The cells were incubated anti-GR antibody (Green), Hoechst 33258 (Blue) and phalloidin (Red). Image acquisition was performed using the InCell Analyzer 1000. Two hours treatment with 100nM Dex was used as a positive control for translocation.

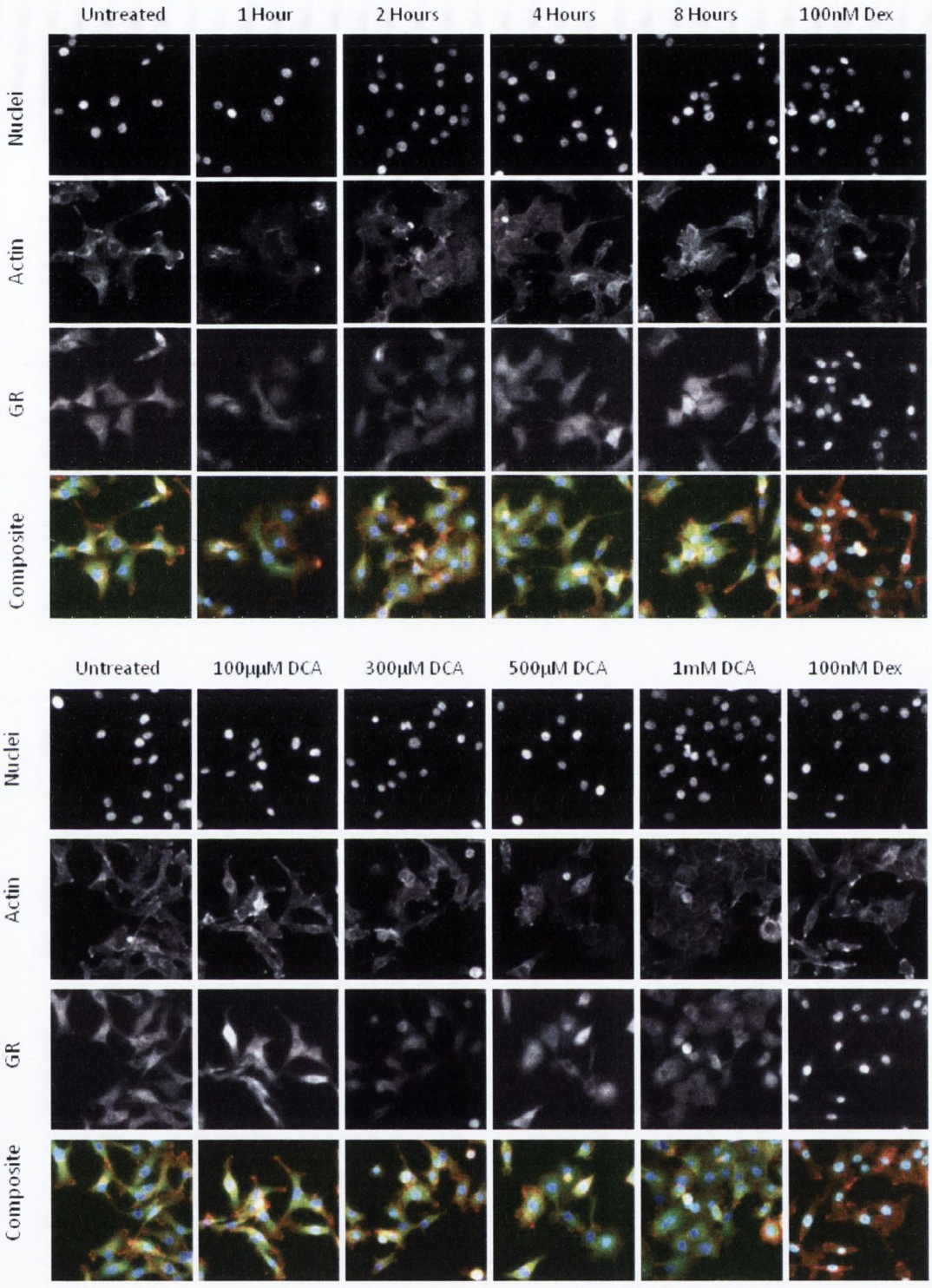

Figure 4–11: DCA induces nuclear translocation of the GR in a dose and time dependent fashion in SKGT-4 cells. Cells were seeded and left to adhere overnight. Subsequently the medium was replaced with serum free medium. After overnight serum starvation the cells were treated with DCA in serum free medium. At appropriate time-points the cells were fixed in 4% PFA, The cells were incubated anti-GR antibody (Green), Hoechst 33258 (Blue) and phalloidin (Red). Image acquisition was performed using the InCell Analyzer 1000. Two hours treatment with 100nM Dex was used as a positive control for translocation.

4.4.3. Stimulation of HET-1A and SKGT-4 Cells with UDCA Does Not Result in *Trans*-Activation of the GR.

We next investigated whether translocation of the GR in response to UDCA or DCA resulted in *trans*-activation. *Trans*-activation of the GR, resulting in transcription of GRE dependent genes, is thought to account for the majority of unwanted side effects associated with GC treatment.

In this model, a GRE dependent luciferase construct was reverse transfected into the HET-1A and SKGT-4 cell lines. After overnight treatment with DCA, UDCA or Dex, neither 300μM UDCA nor DCA induced an increase in the expression of the GRE dependent luciferase construct while Dex did so significantly (Figure 4–12).

In the SKGT-4 cell line, it is difficult to determine the significance of this result. DCA stimulation had resulted in GR translocation in a fashion similar to UDCA. As no difference was seen between the UDCA and DCA treatments, it is not possible to determine from this experiment whether DCA is activating the GR in a fashion similar to UDCA, including the failure to *trans*-activate the GR, or not.

The absence of UDCA induced *trans*-activation has been shown previously in our lab. However, it has previously been shown that UDCA exerts a *trans*-repressive effect with equal efficacy to Dex [376]. This would have been a more crucial experiment to investigate whether DCA was exerting a similar effect to UDCA in modulating the GR. However, in previous experiments in this lab it was necessary to investigate trans-repression in the HEK293 cell line as IL-8 is constitutively over-expressed in OAC cell lines making *trans*-repression induced by DCA difficult to investigate in the SKGT-4 cell line.

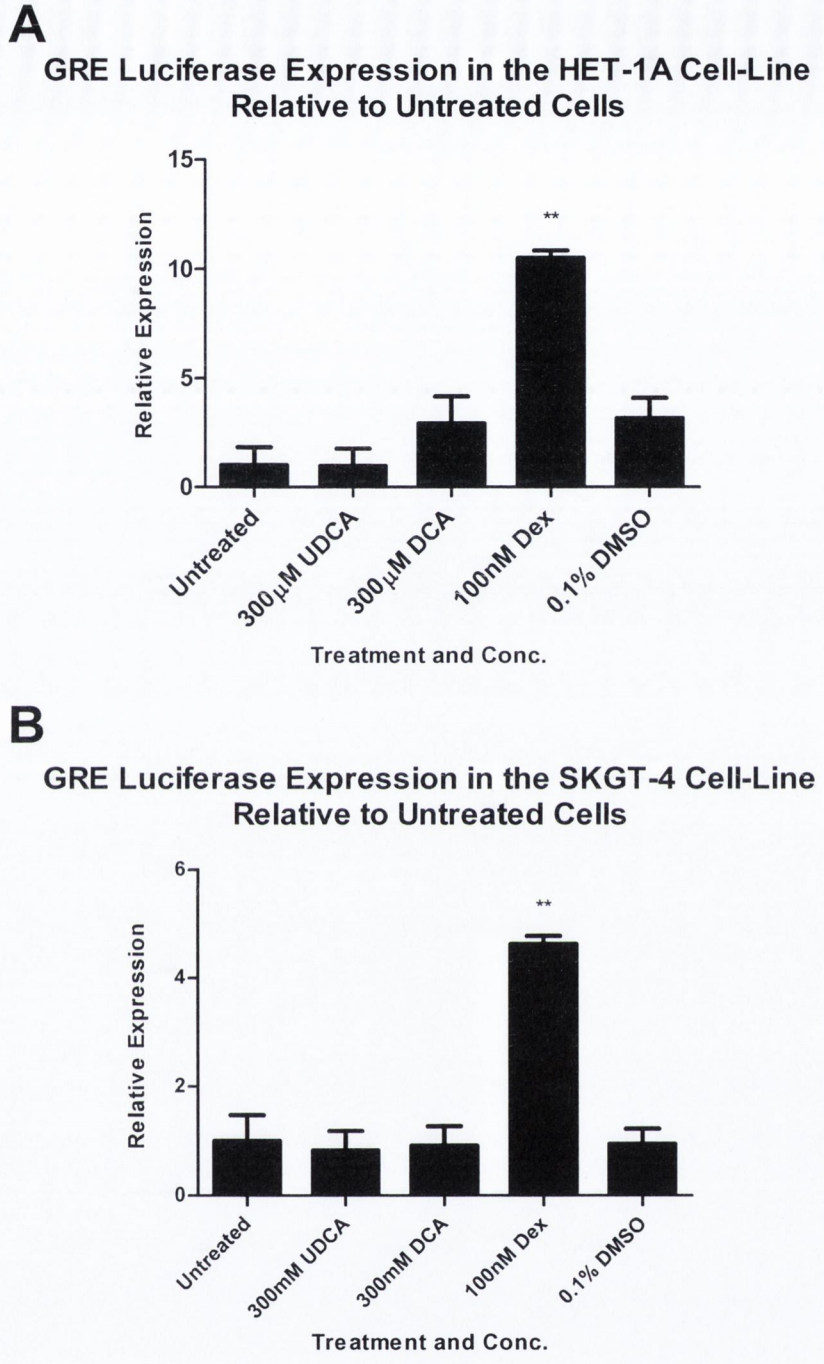

Figure 4–12: Neither UDCA nor DCA results in GR *trans*-activation in HET-1A (A) or SKGT-4 (B) cell lines. Cells were seeded and reverse transfected with a GRE luciferase construct. After 24 hours the medium was replaced with fresh medium. 24 Hours later the cells were treated with UDCA, DCA or dexamethasone for 16 hours. After treatment the cells were lysed with a passive lysis buffer and the intensity of the firefly and renilla luciferase activity determined using a Dual-Luciferase Reporter Assay system (Promega). Results were normalised to untreated cells. Data is Mean and SEM of N=3 and ** denotes $p < 0.01$ relative to untreated control.

4.4.4. The Genes Expression Profile Induced by UDCA Shares Similarities With Those Induced by Dexamethasone and DCA

Having demonstrated that the expression of the GR was greater in normal squamous epithelium than in BO, we hypothesised that UDCA may be a useful therapeutic for modulating inflammatory oesophageal disease prior to the genesis of BO, or selectively modulating inflammation in squamous epithelium without enhancing the survival of established BO. Oral administration of hydrophilic UDCA alters the endogenous BA pool, displacing more hydrophobic (more toxic) BAs and greatly increasing the proportion of the GR-modulating agent UDCA. Thus, both modulation of the BA pool and modulation of the GR by UDCA could conceivably reduce GORD induced inflammation and the risk of BO and OAC.

The transcriptional effects of the GR differ depending on the ligand used, and the cell type being stimulated. In our translocation experiments, UDCA had induced the most consistent translocation of the GR in the HET-1A cell line (Figure 4–6). Despite exhibiting a similar quantity of GR, UDCA had a less potent effect in inducing GR translocation in the OE33 cell line. Finally, in the HCT116 cell line a smaller quantity of GR was expressed but UDCA demonstrated greater efficacy at translocating the GR in this cell line compared to the HET-1A cell line. Even in the absence of translocation, it is conceivable that UDCA could potentially mediate a GR response in any of the cell lines because of the potential to exert indirect *trans*-repression. Thus, micro-array technology was used to perform a comparative investigation regarding the effects of UDCA and Dex. However, UDCA *is* a BA, albeit one with a lower toxicity profile than its more hydrophobic family members and thus, in this experiment, we also chose to compare the gene expression profile induced by UDCA with that induced by DCA.

HET-1A cells, OE33 cells and HCT116 cells were treated with 200μM DCA, 200μM UDCA or 100nM Dex for 12 hours in serum free medium. The 200μM concentration of BAs was chosen as it induced very little detachment of HET-1A cells (as demonstrated in chapter 3) and would be predicted to induce a relatively low level of cell death (as demonstrated in chapter 2), yet induced GR translocation. At this time-point, the cells were lysed and RNA isolated for the micro-array analysis. The concentration and integrity of RNA was assessed prior to processing (See Appendix 3). The Micro-arrays were processed by the Core Facility in the Conway Institute in University College Dublin using the Affymetrix Human U133 Plus 2.0 gene expression chip.

4.4.4.1. Refinement of Array Data

Refinement of the data (as described in section 4.3.7) reduced the number of genes for analysis (Table 4–1). The number of genes with significantly altered expression was greater with DCA

treatment than with UDCA or Dex treatment in all three cell lines (Table 4–1 and Appendix 3). While DCA modulated similar numbers of genes in the three cell lines, UDCA modulated a significantly greater number of genes in the HET-1A cell line than in the OE33 or HCT116 cells. Dex modulated a similar number of genes in the HET-1A and OE33 cell lines but a negligible number of genes in the HCT116 cell line. These results were partially predictable. The markedly lower levels of GR expression in the HCT116 cells explains the low number of gene modulated by Dex, and perhaps UDCA, in this cell line (Figure 4–4 and Figure 4–5). However, we expected to see a greater number of genes modulated by Dex and UDCA in the HET-1A cell line than in the OE33 cell line. This was because UDCA had not appeared to exert the same potency in translocating the GR to the nucleus in the translocation experiments (Figure 4–6).

Time	12 Hours								
Cell Line	**HET-1A**			**OE33**			**HCT116**		
Treatment	UDCA	Dex	DCA	UDCA	Dex	DCA	UDCA	Dex	DCA
Genes Present on Array	54,675	54,675	54,675	54,675	54,675	54,675	54,675	54,675	54,675
Genes with intensity > 100 in at least one pair of probe samples	21,171	22,775	24,466	19,725	20,427	22,046	19,233	19,095	19,402
Genes with 1.5 fold difference in expression from DMSO vehicle control	3,668	2,183	7,417	363	1,629	4,281	96	227	4,528
Genes with $\alpha \leq 0.01$	848	416	4,112	147	565	3,068	6	46	1,599
Genes with $\alpha \leq 0.05$	2,396	1,470	6, 689	298	1,312	4,116	37	121	3,604

Table 4–1: The effect of data refinement on the absolute numbers of genes regulated by 200μM UDCA, 100nM Dex and 200μM DCA in the HET-1A, OE33 and HCT116 cell lines after twelve hours treatment. Cells were treated for twelve hours. RNA was isolated and an oligonucleotide microarray analysis performed. Data refinement was performed by 1) Filtering by intensity $\geq$ 100 in pair of samples being investigated (vehicle or treatment), 2) A fold change $\geq$ 1.5 relative to 0.6% DMSO vehicle and 3) Statistical analysis with ANOVA with $\alpha \leq 0.01$ or $\alpha \leq 0.05$.

4.4.4.2. UDCA Shares Greater Similarities With Dex and DCA than DCA Does With Dex

To investigate similarities in gene expression changes between experimental treatments, gene lists were first compared using Venn diagrams of up and downregulated genes. Subsequently, hierarchical clustering was performed. Lists of the 25 most up or downregulated genes are presented in Appendix 3 for each treatment and each cell line.

4.4.4.2.1. Similarities in Gene Expression in the HET-1A Cell Line Induced by UDCA, Dex or DCA Treatment

In the HET-1A cell line UDCA upregulated the expression of 647 genes after twelve hours treatment at a significance level of 0.01 (Figure 4–13). The corresponding number of down-regulated genes was 201. For Dex, 291 genes were upregulated after twelve hours treatment and 125 genes were down-regulated. In the DCA group, 2057 and 2055 genes were up and downregulated respectively.

However, the number of genes similarly modulated by UDCA and Dex was much more restricted. Only 97 genes were similarly upregulated by UDCA and Dex although 33 of these were similarly upregulated by DCA, leaving a specific group of 64 genes upregulated similarly by UDCA and Dex. This corresponded to 21.9% (64/291) of the genes upregulated by Dex after twelve hours being modulated by UDCA and 9.9% (64/647) of genes upregulated by UDCA being similarly modulated by Dex. Regarding downregulated genes, 31 genes were similarly regulated by UDCA and Dex although 13 of these were similarly downregulated by DCA. This left a specific group of 18 genes downregulated similarly by UDCA and Dex. This corresponded to 14.6% (18/125) of the genes downregulated by Dex after twelve hours being modulated by UDCA and 9.4% (18/201) of genes upregulated by UDCA being modulated by Dex.

The comparison of genes similarly modulated by DCA and UDCA resulted in greater overlap between the two datasets. 250 genes were similarly upregulated by DCA and UDCA although 33 of these were similarly upregulated by Dex, leaving 217 genes specific to DCA and UDCA alone. This corresponded to 33.6% (217/647) of genes upregulated by UDCA being similarly upregulated by DCA, and 10.7% (217/2057) of genes upregulated by DCA being similarly upregulated by UDCA. For downregulated genes 86 genes were similarly downregulated by UDCA and DCA although 13 of these were similarly downregulated by Dex. This left 73 genes which were specifically downregulated by DCA and UDCA. This corresponded to 36.1% (73/201) of genes downregulated by UDCA being similarly downregulated by DCA and only 3.5% (73/2055) of genes downregulated by DCA being similarly downregulated by UDCA.

The final comparison performed was between DCA and Dex. In theory there should have been very little overlap between theses datasets. 54 genes were similarly upregulated by DCA and Dex although 33 of these were also upregulated by UDCA. 30 genes were similarly downregulated by DCA and Dex although 13 of these were similarly downregulated by UDCA. This correlated to 7.1% (21/291) of genes upregulated by Dex being similarly modulated by DCA and 1.0% (21/2057) genes upregulated by DCA being modulated similarly modulated by Dex. Among the downregulated genes 13.1% (17/125) of genes modulated by Dex were similarly modulated by DCA and 0.8% (17/2055) of genes modulated by DCA being similarly modulated by Dex.

These findings suggested that there was a greater similarity between Dex and UDCA and between UDCA and DCA than there was between Dex and DCA. The percentage of genes similarly modulated by UDCA and DCA was slightly greater than the percentage of genes similarly modulated by UDCA and Dex. However, the high percentage of Dex modulated genes similarly modulated by DCA was of concern as this unexpected. This could potentially reflect either activation of stress pathways which in turn are activating the GR indirectly, or it could simply reflect the large magnitude of difference in gene numbers between the two groups, resulting in statistical error. At the chosen α of 0.01 we would expect a false positive rate of 1%, equating to 20 genes upregulated by DCA and 20 genes which were downregulated. These figures correspond with our findings between the DCA and Dex groups. In reality it probably reflects a combination of the two sources of error.

However, while an $\alpha \leq 0.01$ was used in the HET-1A line initially, the number of genes modulated by UDCA and Dex in the OE33 and HCT116 at an $\alpha \leq 0.01$ was small (see below). In fact, in the HCT116 cell line, no genes were found to be significantly modulated by Dex or UDCA. This may represent the relative deficiency of GR in this cell line. Thus, we also investigated the overlapping gene lists in the HET-1A cell line at $\alpha \leq 0.05$ (Figure 4–14), in order to allow comparison of results with the OE33 and HCT116 cell lines.

At this cut-off, among the upregulated genes:

- 35.0% (401/1146) of genes upregulated by Dex were similarly modulated by UDCA and 21.6% (401/1858) of genes modulated by UDCA were similarly modulated by Dex.
- 30.2% (561/1858) of genes upregulated by UDCA were similarly modulated by DCA and 17.1% (561/3285) of genes modulated by DCA were similarly modulated by UDCA.
- Only 1.7% (58/3285) of genes upregulated by DCA were similarly modulated by Dex and 5.1% (58/1146) of genes modulated by Dex were similarly modulated by DCA.

Among the downregulated genes:

- 17.3% (56/324) of genes modulated by Dex were similarly modulated by UDCA and 10.4% (56/538) of genes modulated by UDCA were similarly modulated by Dex.
- 41.6% (224/538) of genes downregulated by UDCA were similarly modulated by DCA but only 6.6% (224/3404) of genes modulated by DCA were similarly modulated by UDCA.
- Only 1.5% (50/3404) of genes downregulated by DCA were similarly modulated by Dex but 15.4% (50/324) of genes downregulated by DCA were similarly modulated by Dex.

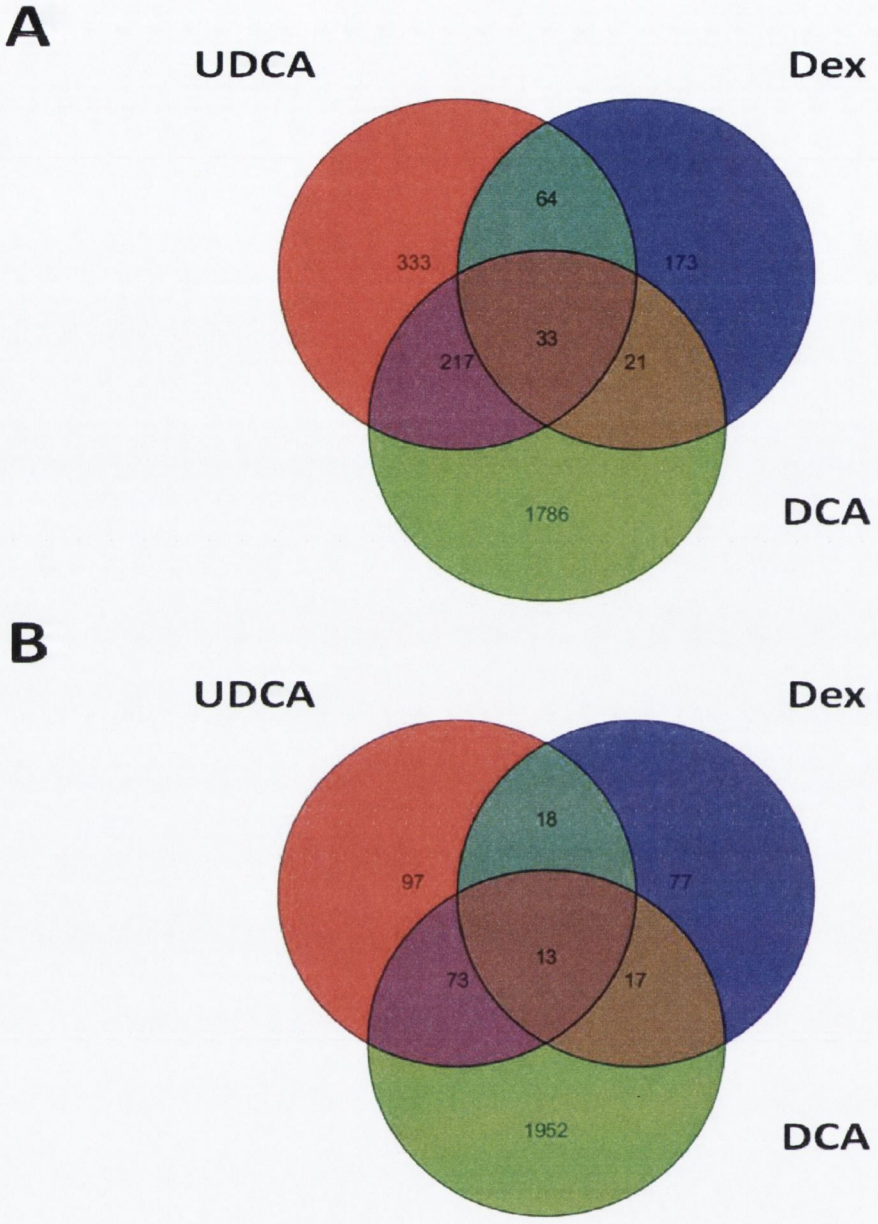

Figure 4–13: Absolute numbers of genes upregulated (A) and downregulated (B) by UDCA, Dex and DCA in the HET-1A cell lines after twelve hours treatment at $\alpha \leq 0.01$. Cells were treated for twelve hours. RNA was isolated and an oligonucleotide microarray analysis performed. After data refinement (Filtered as intensity > 100 in at least one set of replicates (treatment or control), Fold change >1.5 relative to DMSO vehicle and $\alpha \leq 0.01$), the resulting lists of genes upregulated and downregulated by treatment were compared using Venn diagrams.

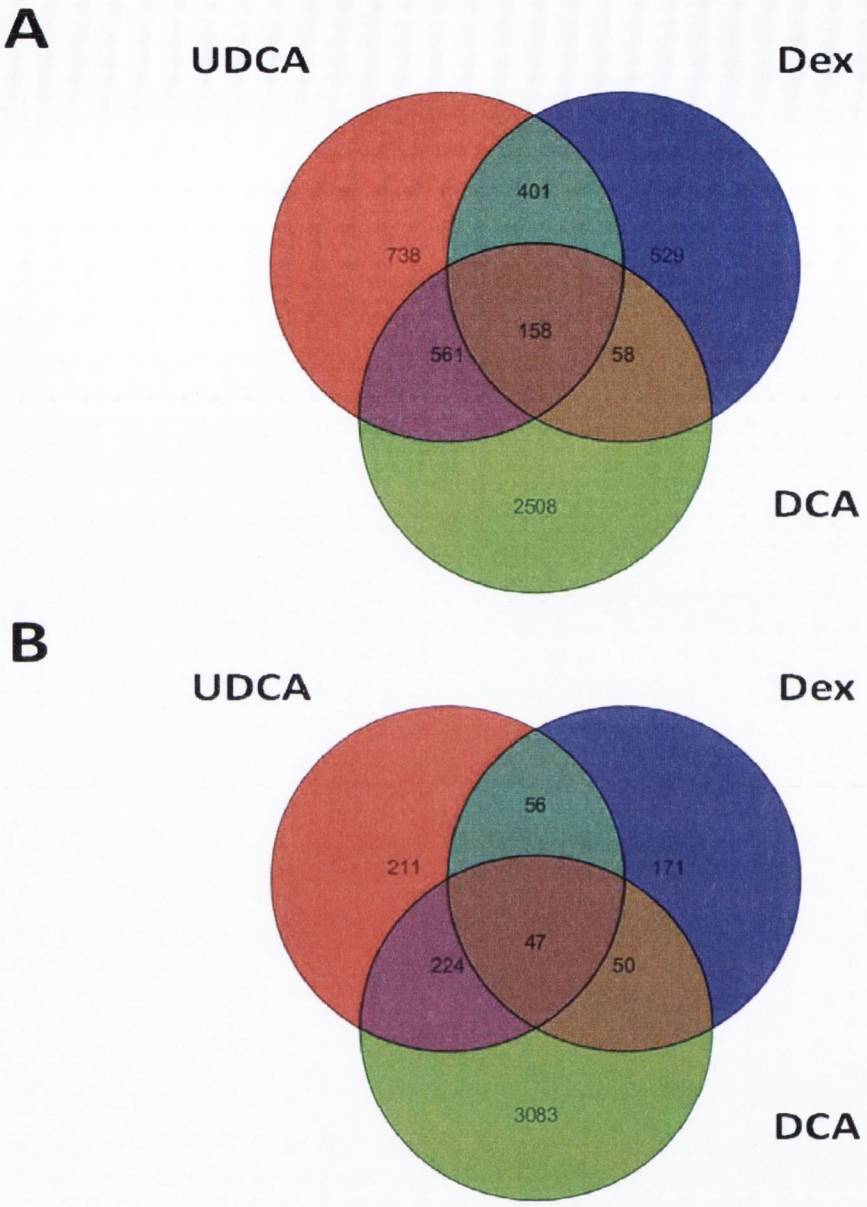

Figure 4–14: Absolute numbers of genes upregulated (A) and downregulated (B) by UDCA, Dex and DCA in the HET-1A cell lines after twelve hours treatment $\alpha \leq 0.05$. Cells were treated for twelve hours with the respective treatment. RNA was isolated and an oligonucleotide microarray analysis performed. After data refinement (Filtered as intensity > 100 in at least one set of replicates (treatment or control), Fold change >1.5 relative to DMSO vehicle and $\alpha \leq 0.05$), the resulting lists of genes upregulated and downregulated by treatment were compared using Venn diagrams.

We next used hierarchical clustering to further investigate similarities between UDCA, Dex and DCA (Figure 4–15). Hierarchical clustering was performed using a Euclidian approach based on the averages of the data at a cut-off of $\alpha \leq 0.05$. Clustering was simultaneously performed on both the genes and the treatments. This revealed that there was a large set of commonly upregulated genes and a smaller set of downregulated genes between the three treatments. DCA clustered independently of Dex and UDCA. UDCA and Dex clustered together. This suggested that the similarity between these two treatments was greater than the similarity between UDCA and DCA.

Interestingly, from among the gene clusters, a group similarly upregulated by DCA and UDCA was identified. At the bottom of the heatmap, (shown in Figure 4–16) genes including INHBE, GDF15, DDIT, TRIB3, ATF3, CHAC1, MAFF and STC2 were clustered. These genes represent a group of genes which are upregulated when the function of the ER is disrupted. This results in dysregulated protein synthesis and increased protein degradation. The adaptive response to the increased stress placed on the cell by the accumulation of mis-folded proteins is called the unfolded protein response [385]. Activation of ER stress proteins has been shown to enhance the activity of NF-κB and increase expression of IL-8. Prolonged ER stress, can result in apoptosis through unknown mechanisms [386]. These proteins have previously been identified as modulated by DCA but not by UDCA [103, 387].

Using IPA, the list of genes similarly modulated by Dex and UDCA in the HET-1A cell line (559 upregulated probesets and 103 downregulated) were investigated for direct relationships with the GR (Figure 4–17). Only 16 genes were found to be directly associated with the GR in the literature.

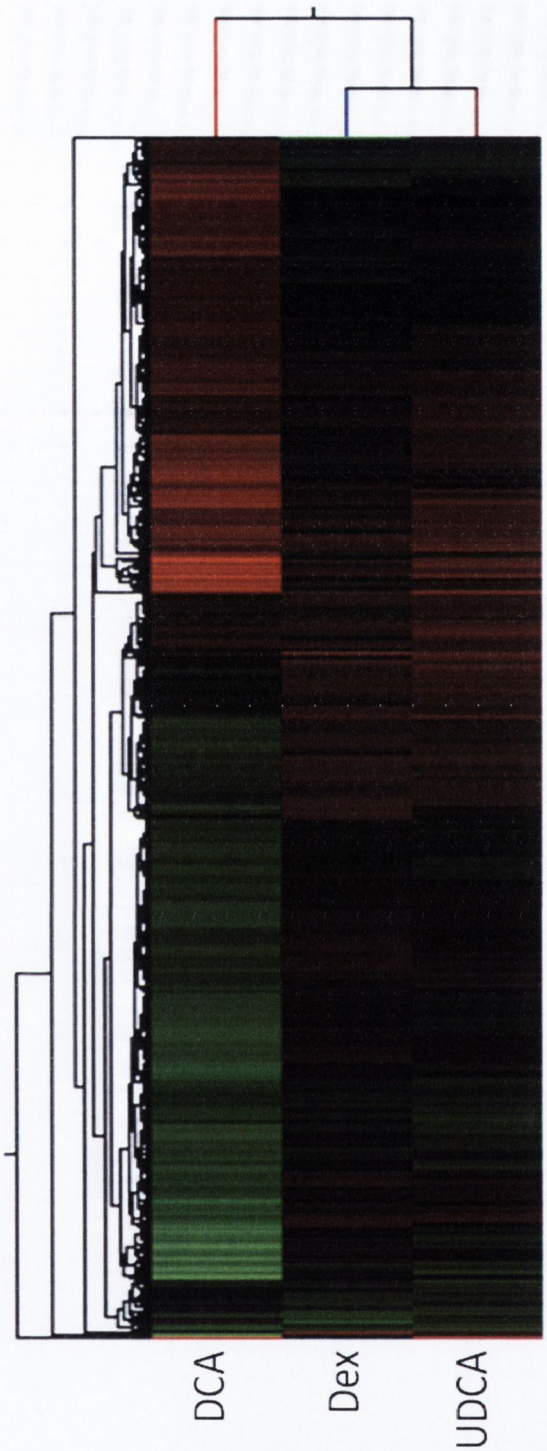

Figure 4–15: Heatmap of clustered genes produced through hierarchical clustering using Euclidian averages of probeset intensities after treatment of HET-1A cells with DCA, UDCA or Dex for 12 hours ($p \leq 0.05$). Clustering was performed using GeneSpring. DCA clusters independently of Dex or UDCA.

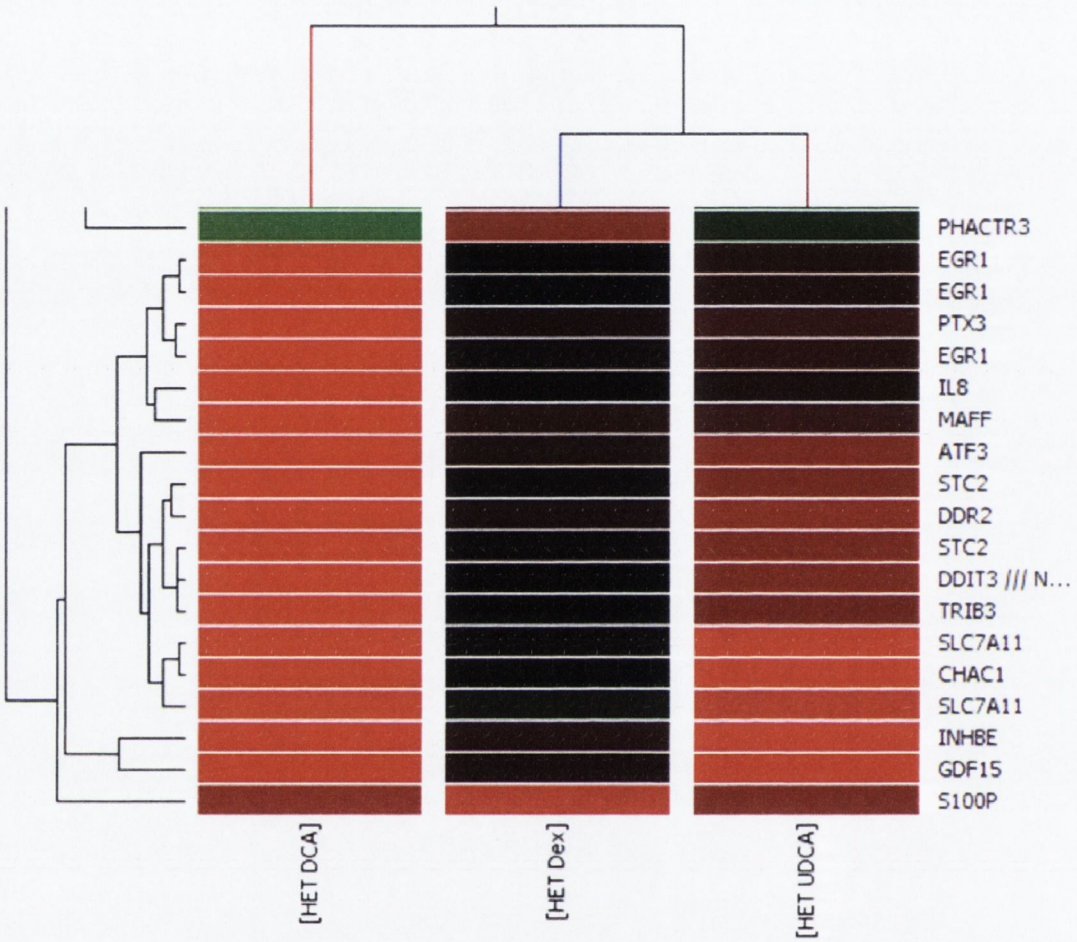

Figure 4–16: Genes associated with ER stress are similarly modulated by DCA and UDCA in the HET-1A cell line. Heatmap of clustered genes produced through hierarchical clustering using Euclidian averages of treatment of HET-1A cells with DCA, UDCA or Dex for 12 hours ($p \leq 0.05$). Clustering was performed using GeneSpring. DCA clusters independently of Dex or UDCA but there are similarities between UDCA and DCA.

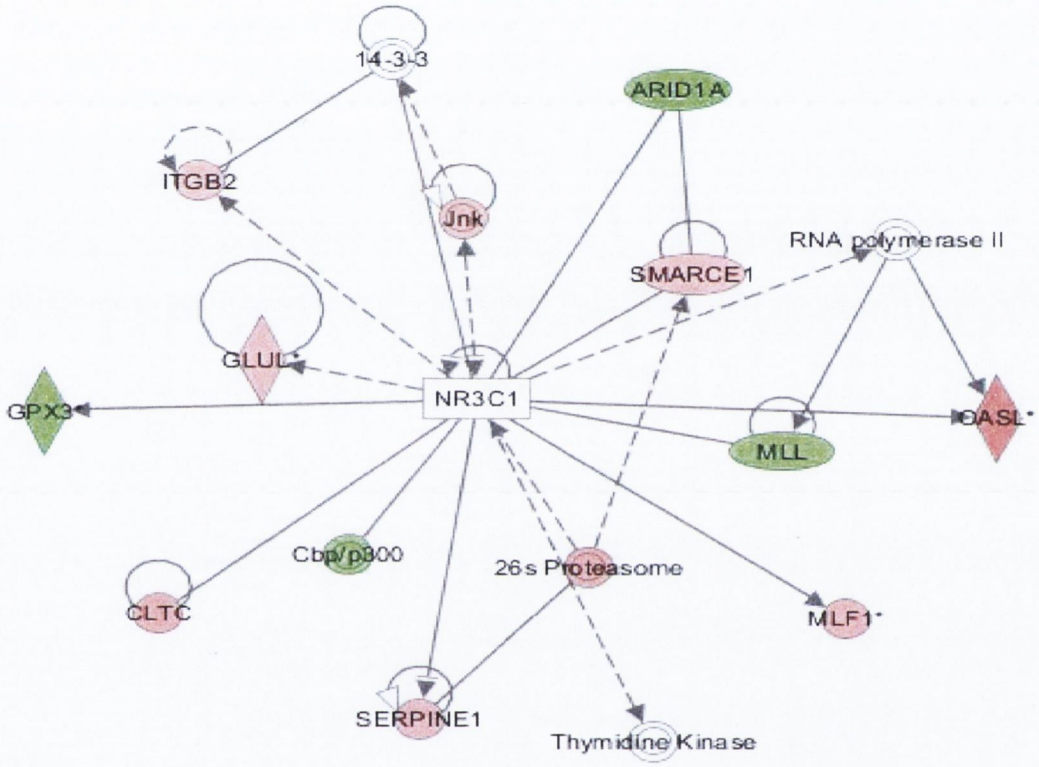

Figure 4–17: Genes modulated by both UDCA and Dex in the HET-1A cell line which are associated with the GR as determined using IPA. From among the 662 genes similarly modulated by UDCA and Dex using an $\alpha \leq 0.05$ in the HET-1A cell line, 16 were found to directly interact with the GR. Colouring represents mRNA regulation by UDCA and Dex. Red represents upregulated and green downregulated.

4.4.4.2.2. Similarities in the Modulation of Gene Expression Induced by UDCA, Dex or DCA Treatment in the OE33 Cell Line

Within the OE33 cell line, UDCA upregulated 172 genes and downregulated 126 genes when a cut-off of $\alpha \leq 0.05$ was used. The respective numbers for Dex were 878 and 434 and for DCA were 1957 and 2159 (Figure 4–18). From among these, only 18 genes were selectively upregulated by both UDCA and Dex and 7 downregulated. This corresponded to 2.1% (18/878) of genes upregulated by Dex being modulated by UDCA and 10.5% (18/172) of genes upregulated by UDCA being modulated by Dex. 1.6% of genes downregulated by Dex were modulated by UDCA and 5.6% of genes downregulated by UDCA were modulated by Dex.

84 genes were selectively upregulated by both UDCA and DCA and 63 selectively downregulated by the two. This corresponded to 48.8% (84/172) of genes upregulated by UDCA being modulated by DCA and 4.3% (84/1957) of genes modulated by DCA being modulated by UDCA. Correspondingly, 50.0% (63/126) of genes downregulated by UDCA being modulated by DCA and 2.9% (63/2159) of genes modulated by DCA were similarly modulated by UDCA.

105 genes were similarly and selectively upregulated by DCA and Dex and 30 downregulated. This corresponded to 12.0% (105/878) of genes modulated by Dex being similarly upregulated by DCA and 5.4% (105/1957) of DCA modulated genes being similarly upregulated by Dex. 6.9% (30/434) of genes modulated by Dex were similarly downregulated by DCA and 1.4% (30/2159) of DCA modulated genes being downregulated by Dex. Interestingly, IL-8 was downregulated by UDCA and Dex treatment in this cell lines whereas in the HET-1A and HCT116 cell lines, IL-8 mRNA expression was upregulated by UDCA.

Clustering demonstrated that UDCA and Dex clustered independently of DCA (Figure 4–19). However, again despite the clustering, in this cell line the greatest percentage of overlapping genes was seen between DCA and UDCA rather than between UDCA and Dex as discussed above (Figure 4–18).

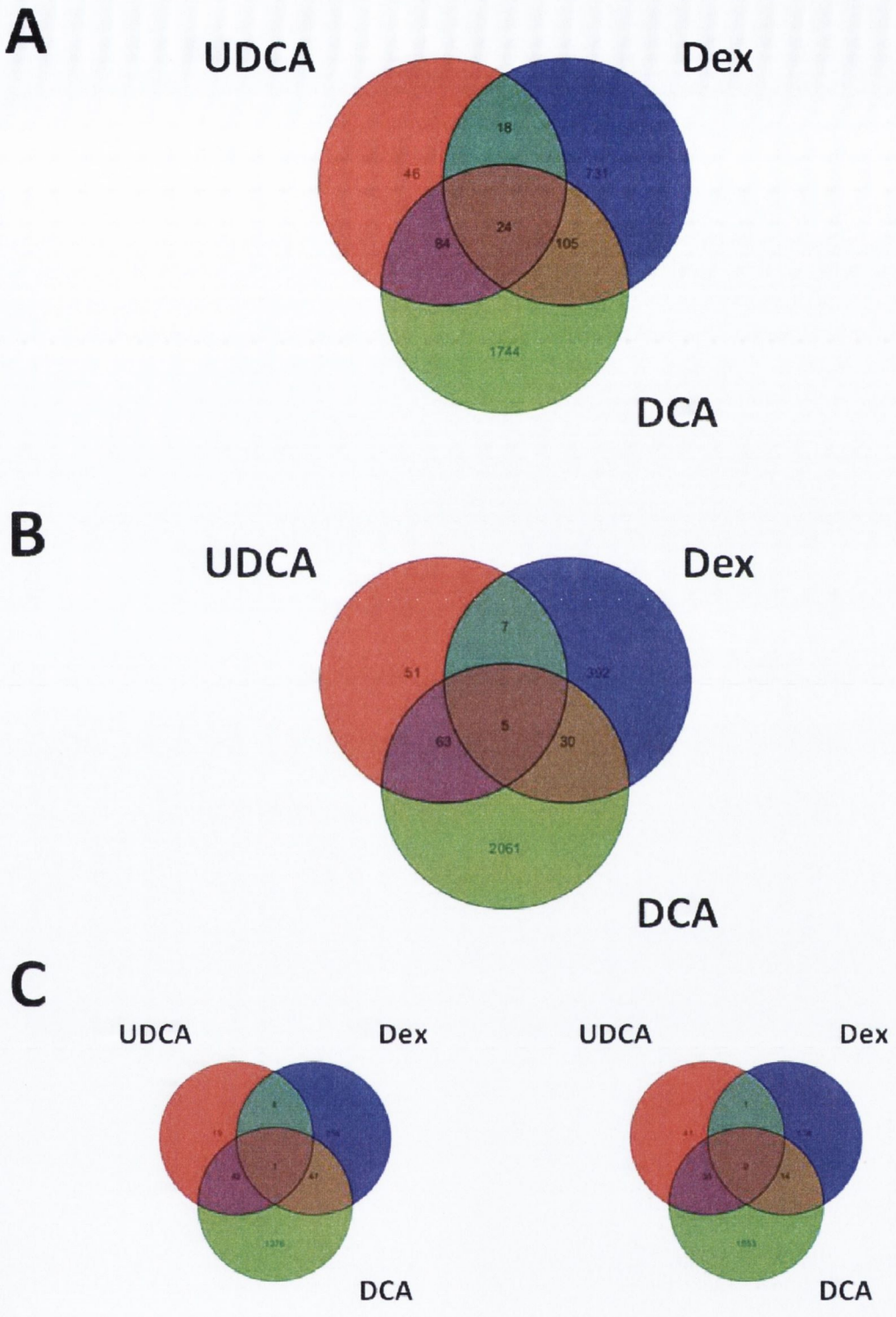

Figure 4–18: Absolute numbers of genes upregulated (A) and downregulated (B) by UDCA, Dex and DCA in the OE33 cell lines after twelve hours treatment at $\alpha \leq 0.05$ (A and B) and $\alpha \leq 0.01$ (C). Cells were treated for twelve hours with the respective stimulus. RNA was isolated and an oligonucleotide microarray analysis performed. After data refinement (Filtered as intensity > 100 in 2/4 samples, Fold change >1.5 relative to DMSO vehicle and $\alpha \leq 0.05$), the resulting lists of genes upregulated and downregulated by treatment were compared using Venn diagrams.

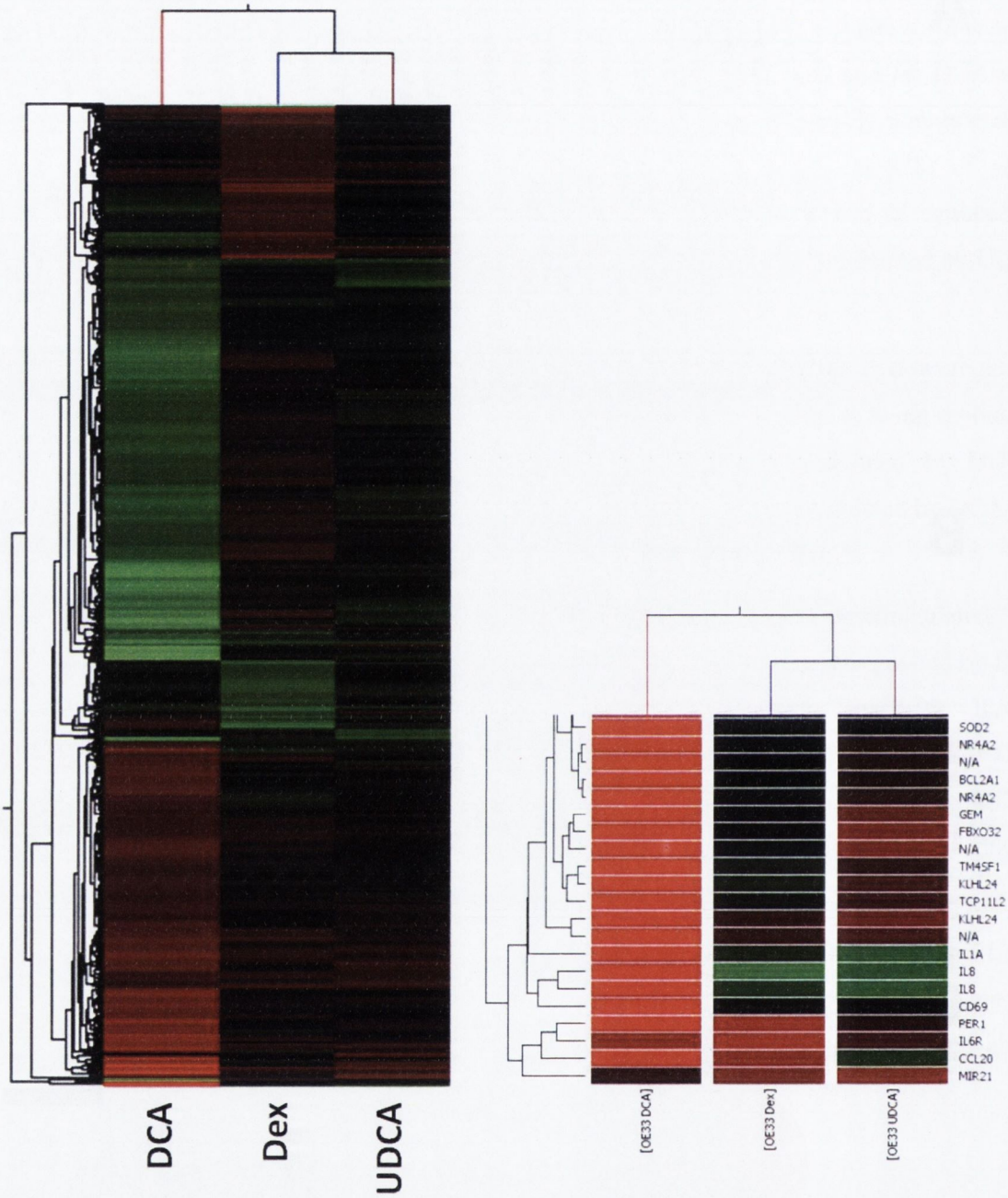

Figure 4–19: Heatmap of clustered genes produced through hierarchical clustering using Euclidian averages of probeset intensities after treatment of OE33 cells with DCA, UDCA or Dex for 12 hours ($p \leq 0.05$). Clustering was performed using GeneSpring. DCA clusters independently of Dex and UDCA.

4.4.4.2.3. Similarities in Gene Expression in the HCT116 Cell Line Induced by UDCA, Dex or DCA Treatment

Finally, in the HCT116 cell lines the response to treatment was exceptionally limited in the UDCA and the Dex groups, even at a cut-off of $\alpha \leq 0.05$ (Figure 4–20). This result was predictable for the Dex treated cells due to the relative paucity of GR expressed in this cell line. The deficit of genes modulated by UDCA could suggest that either this BA modulated its effects predominantly through the GR or that this cell line is more resistant to gene modulation by this hydrophilic BA. Only 14 genes were upregulated and 23 genes downregulated by UDCA, 14 and 107 by Dex. The DCA treatment group demonstrated similar numbers to the responses seen in the HET-1A and the OE33 cell lines, with 1423 genes being upregulated and 2181 genes being downregulated. In this experimental model no genes were identified as being commonly modulated by all three treatments and no genes were commonly modulated by Dex and UDCA. However the majority of genes upregulated by UDCA were also modulated by DCA (71.4%, 10/14) and similarly in the downregulated genes (65.2%, 15/23). Again, 14.2% (2/14) of genes upregulated by Dex were also modulated by DCA but Dex only modulated 0.1% (2/1423) of genes modulated by DCA. For the down regulated genes, the numbers were 12.1% (13/107) and 0.6% (13/2181).

Unsurprisingly, DCA clustered independently of UDCA and Dex (Figure 4–21). However, this may simply represent the paucity of genes significantly modulated by the latter two in this cell line.

The lists of genes modulated by the three treatments are shown in Appendix 3.

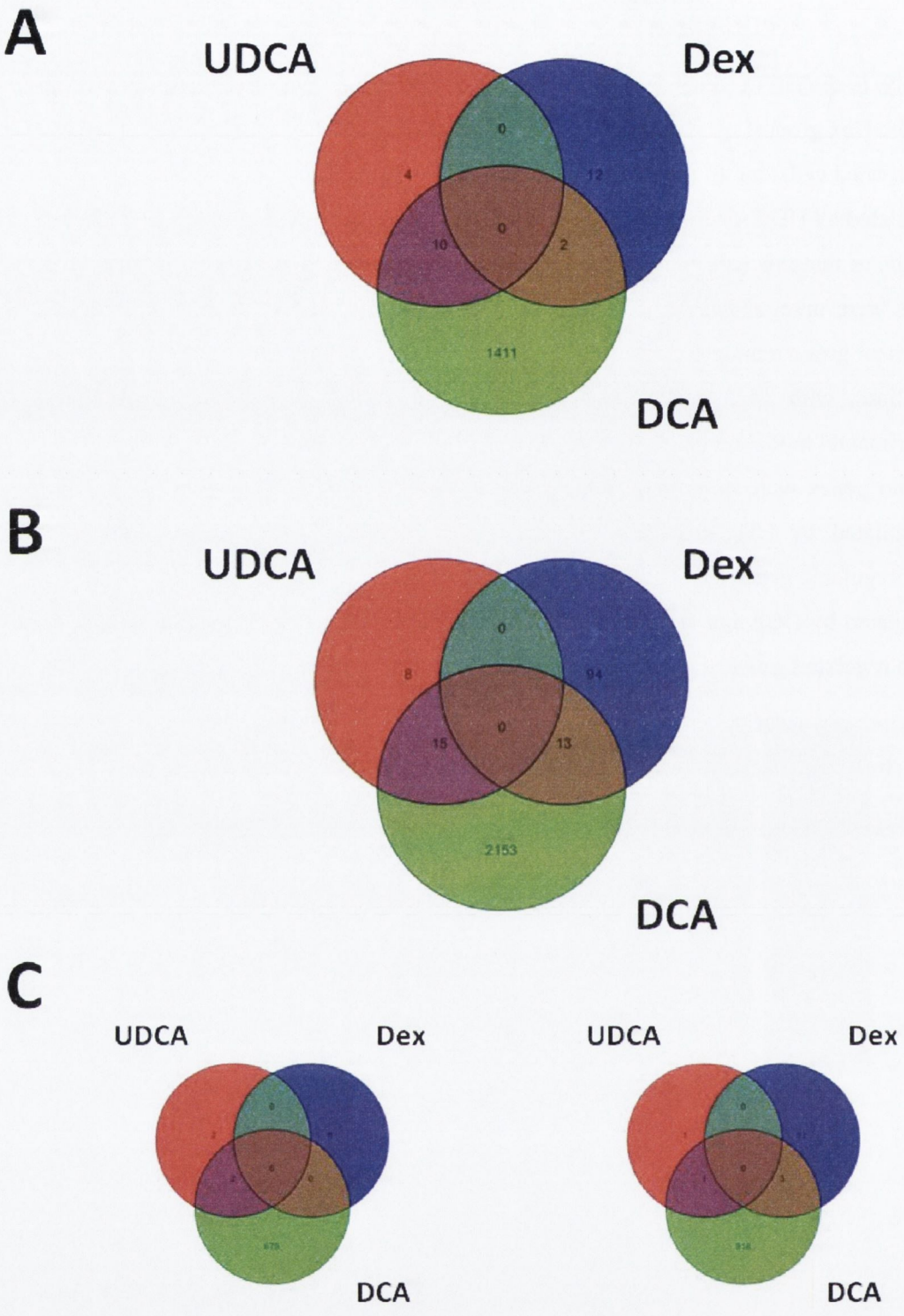

Figure 4–20: Absolute numbers of genes upregulated (A) and downregulated (B) by UDCA, Dex and DCA in the HCT116 cell lines after twelve hours treatment at $\alpha \leq 0.05$ and $\alpha \leq 0.01$ (C). Cells were treated for twelve hours. RNA was isolated and an oligonucleotide microarray analysis performed. After data refinement (Filtered as intensity > 100 in 2/4 samples, Fold change >1.5 relative to DMSO vehicle and $\alpha \leq 0.05$), the resulting lists of genes upregulated and downregulated by treatment were compared using Venn diagrams.

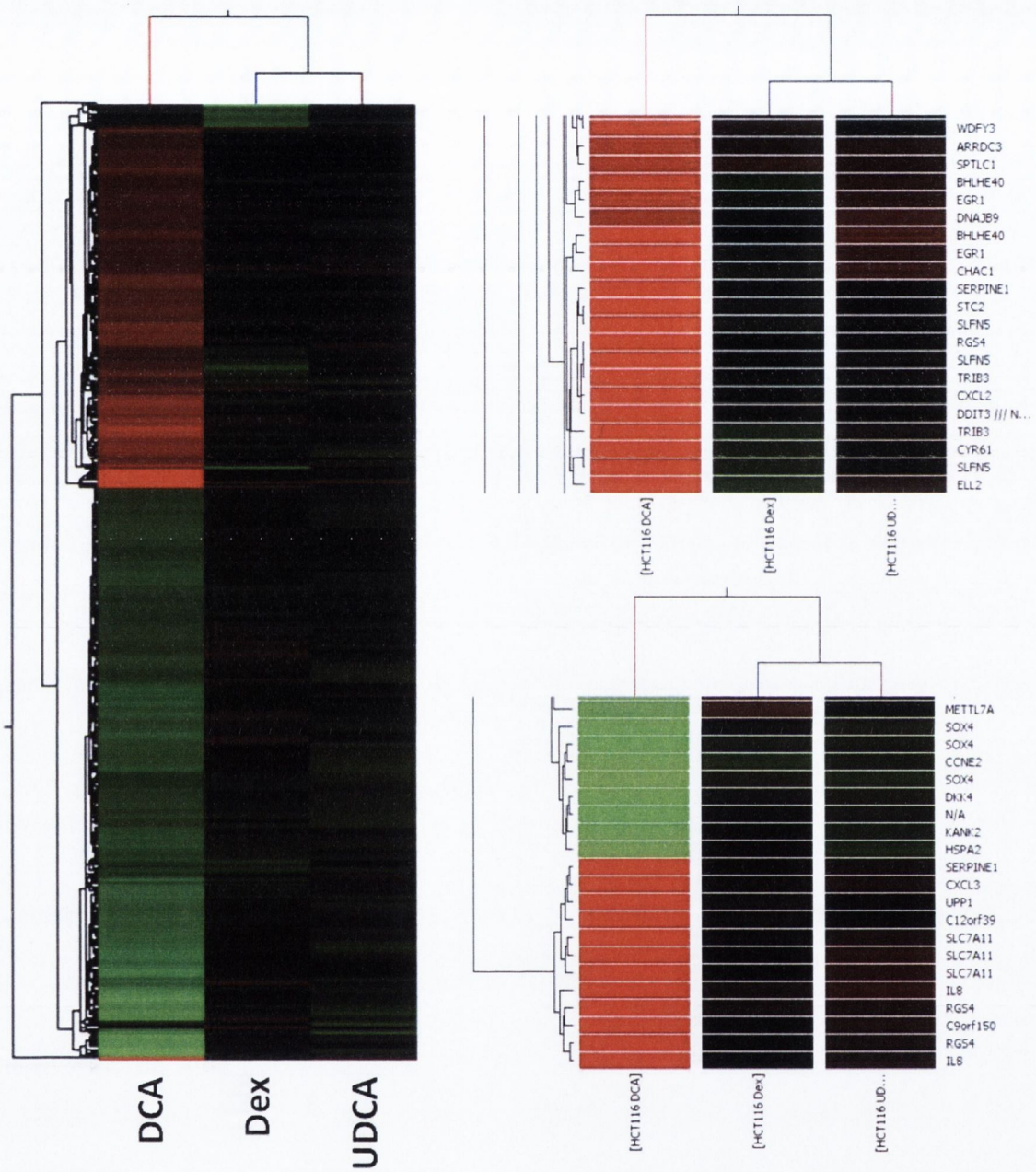

Figure 4–21: Heatmap of clustered genes produced through hierarchical clustering using Euclidian averages of probeset intensities after treatment of HCT116 cells with DCA, UDCA or Dex for 12 hours ($p \leq 0.05$). Clustering was performed using GeneSpring. DCA clusters independently of Dex or UDCA.

4.4.4.3. Similarities in Gene Expression Modulated By UDCA, Dex or DCA between the HET-1A, OE33 and HCT116 cell lines

The microarray experiment was designed to allow the identification of a set of core genes modulated similarly in the three cell lines by UDCA, Dex or DCA. Consequently we next investigated similarities between treatments among the three cell lines (Figure 4–22, Figure 4–23 and Figure 4–24). The cell line with the greatest sensitivity to the treatments was the HET-1A cell line and the treatment which modulated the greatest number of genes was consistently DCA. However while DCA modulated a similar number of genes in the three cell lines, UDCA and Dex only modulated a small number of genes in the HCT116 cell line even when the cut-off of $\alpha \leq 0.05$ was used. Lists of the genes with the greatest alteration in expression in response to treatment, in the three cell lines, are presented in Table 4–2 and Appendix 3.

Analysis demonstrated that UDCA similarly upregulated no probesets in all three cell lines and downregulated only one (Figure 4–22). However, this probeset is uncharacterised, representing no known gene. Dex only similarly upregulated two probesets in the three cell lines and downregulated 13 (Figure 4–23). DCA upregulated 308 genes across the three cell lines and downregulated 299 (Figure 4–24). For UDCA treatment, the OE33 and HCT116 cell lines clustered together suggesting greater similarity. However, given the paucity of GR in the HCT116 cell line and the low number of genes modulated by UDCA in both the HCT116 and OE33 cell lines, the clustering may simply represent the greater sensitivity of the HET-1A cell line to UDCA. For Dex, the HET-1A and OE33 cell lines clustered closer together, although the dendritic tree suggested that the gene expression profiles of the three cell lines were quite similar. This may represent the closer embryological origin of these two cell lines suggesting that they have a greater similarity regarding tissue specific GREs and adaptor proteins. However, it may also represent the relative paucity of the GR in the HCT116 cell line relative to the other two.

For DCA treatment the greatest similarity was seen between HET-1A and HCT116 cell lines. The ER stress genes shown to be upregulated by DCA in the HET-1A cell line were similarly modulated by DCA in the HCT116 cell line. However in the OE33 cell line these genes were differentially regulated (Figure 4–25).

When the HCT116 cell line was excluded from the analysis (because of the small number of genes modulated by UDCA and Dex in this cell line), 14 and 5 genes were similarly up- and down-regulated by UDCA in the HET-1A and OE33 cell lines. For Dex the respective numbers of genes were 131 and 32. For DCA 705 and 602 genes were similarly up- and down-regulated in the HET-1A and OE33 cell lines.

Genes similarly modulated by UDCA and Dex in the three cell lines are shown in Table 4–2.

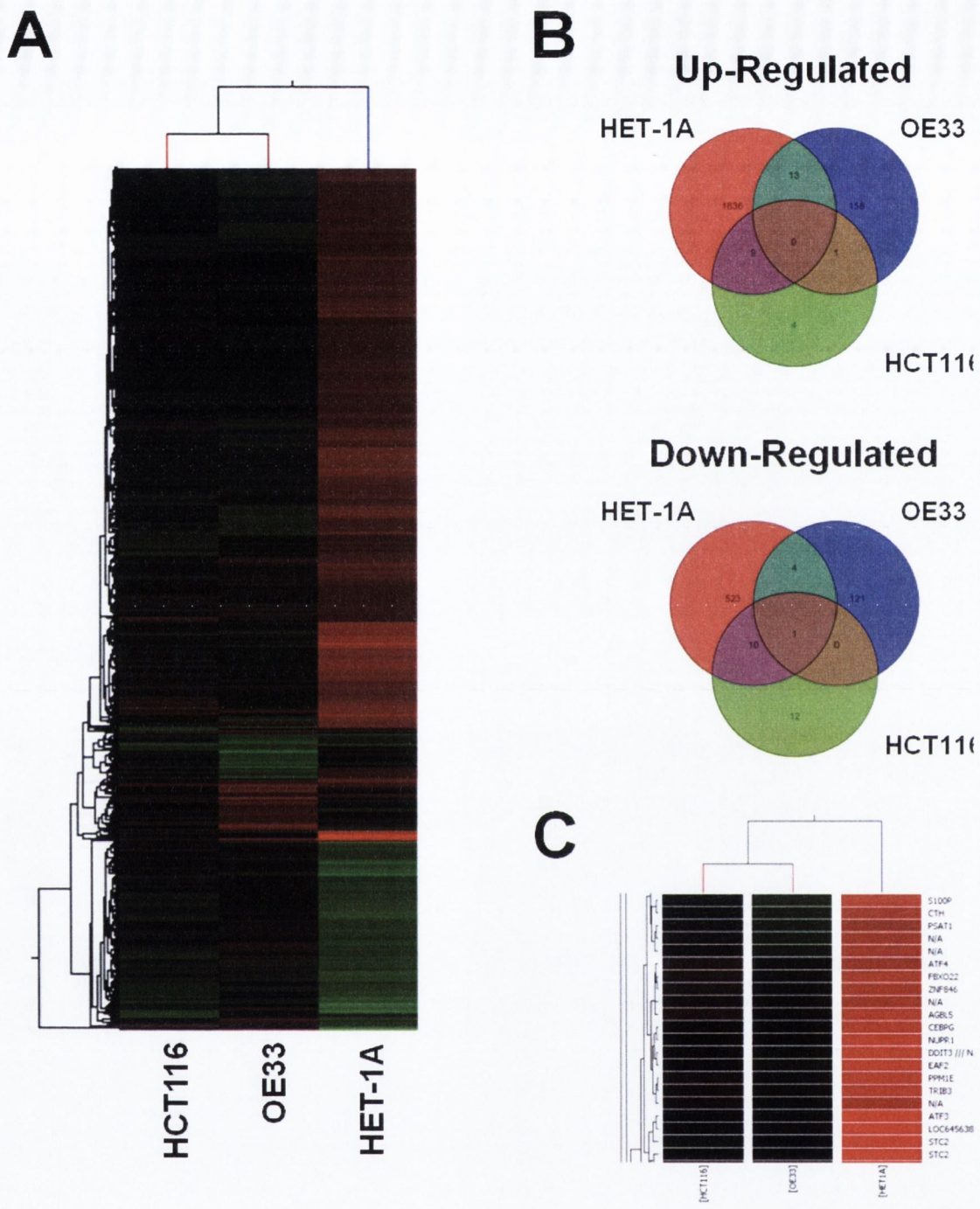

Figure 4–22: Heatmap of clustered genes after 12 hours treatment with UDCA ($p \leq 0.05$) in the HET-1A, OE33 and HCT116 cell lines. Clustering was performed in GeneSpring using hierarchical clustering of the Euclidian averages of probeset intensities. The cell lines derived from cancers (OE33 and HCT116) clustered independently of the HET-1A cell line (A). The greatest numbers of modulated genes were seen in the HET-1A cell line (B). ER stress genes were only upregulated by UDCA in the HET-1A cell line (C).

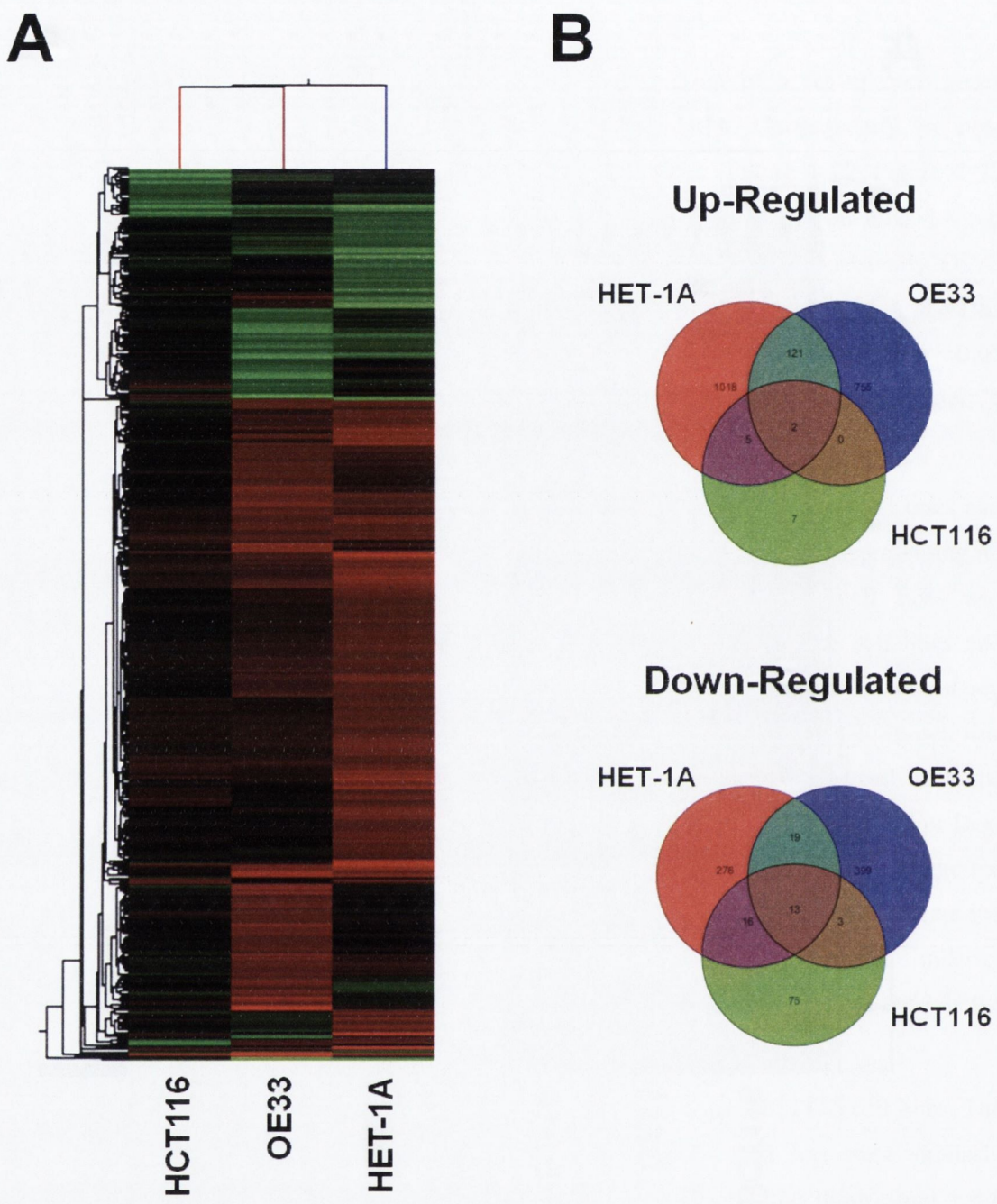

Figure 4–23: Heatmap of clustered genes after 12 hours treatment with Dex ($p \leq 0.05$) in the HET-1A, OE33 and HCT116 cell lines. Clustering was performed in GeneSpring using hierarchical clustering of Euclidian averages of probeset intensities. The cell lines derived from cancers (OE33 and HCT116) clustered independently of the HET-1A cell line although all three cell lines demonstrated greater similarity then was seen with UDCA or DCA treatment (A). The greatest numbers of modulated genes were seen in the HET-1A cell line (B). Fewer genes were modulated by Dex treatment in the HCT116 cell line than in other cell lines consistent with the relatively lower expression of the GR in this cell line.

Upregulated by UDCA in:	**Genes**
HET-1A, OE33 and HCT116	No Genes
HET-1A and OE33	EGR1, LGALS8, NRP1, TFPI, SLC30A1, RPL37A, **CTTN**, KLHL24, TMEM135, C5orf41, SLC16A6, ATP11B
HET-1A and HCT116	BHLHE40, INSIG1, DHRS3, PER2, SCD, TMEM22, TMEM39A, C2orf30
OE33 and HCT116	EGR1

Downregulated by UDCA in:	**Genes**
HET-1A, OE33 and HCT116	No Genes
HET-1A and OE33	FEN1, SAE1, UHRF1, ASF18
HET-1A and HCT116	GJA1, CENPE, AHNAK, MKI67, TGOLN2, FAM13B, AKAP12, ENAH
OE33 and HCT116	No Genes

Upregulated by Dex in:	**Genes**
HET-1A, OE33 and HCT116	AFFY_LysX_5_at, AFFY_LysX_3_at
HET-1A and OE33	SGK1, SERPINA3, RGS2, ITGB2, NEBL, MB, STX8, HOXB7, TMEM5, CSTA, XRCC4, RNASE4, PEX11A, LAMP3, ZNF673, ZNF165, ACYP2, MED6, BNIP1, TSC22D3, CASP4, EIF4E2, APOL1, SMAGP, NAPG, **BIRC3**, CFLAR, TACC2, HOPX, TPM4, LARP7, GPX7, BRAP, LOC100134128, LIAS, MTERFD2, EXOSC2, ARPP19, AGA, CD58, RAB31, MAPKSP1, SNAP29, INTS12, CCDC53, CHCHD7, ATAD4, NOL12, HCFC2, HSPC159, ZNF669, C17orf48, MRTO4, USE1, KLHL24, KRCC1, TMLHE, SCML1, C11orf1, CCNDBP1, C18orf21, SNHG12, SNHG12, REXO2, INF2, C11orf58, LZIC, C12orf45, ZFAND2A, DMKN, CYP2R1, C9orf21, FAM27E3, **PHACTR3**, MFSD8, CARD8, SNHG9, CCDC125, ZSWIM7, NAGS, C13orf1, STK32C, C11orf1, TTC17, PHF20, AASDH, TMEM151A, DAZAP2, TAF1B, LOC100130506, SDR16C5, hCG_1815491, C6orf130, RFESD, BOD1L, ZNF182, DCP2, SEPSECS, TIPRL, C10orf76
HET-1A and HCT116	METTL7A, UNC84A, KBTBD3, IMMP1L, SPTLC1
OE33 and HCT116	No Genes

Downregulated by Dex in:	**Genes**
HET-1A, OE33 and HCT116	**ACTB**, SAE1, PPP5C, STIP1, KLF22, RHBDD2
HET-1A and OE33	AP2M1, PKM2, SFRS1, LLGL1, TRAF4, RPL37A, ATP6VOE1, CYP2D6, WDTC1, EML4, SGPP1, C19orf22, MVK, NR1D2, YIF1B, ZNF598, LOC100129380, CTNND1
HET-1A and HCT116	PPP2R1A, SCD, PLD3, DCTN1, TMED2, HPCAL1, TM7SF2, MAP2K2, MVK, HNRNPUL2, UNC93B1, UCKL1, JAK1, APH1A, LMNA, LAPTM4B
OE33 and HCT116	TMED2, GULP1, MED18

Table 4–2: Lists of genes similarly regulated by UDCA and Dex in the cell lines HET-1A, OE33 and HCT116. Lists were generated from the Venn diagrams of overlapping probesets as described above. Genes with bold underlined font represent some genes which were subsequently chosen for validation experiments.

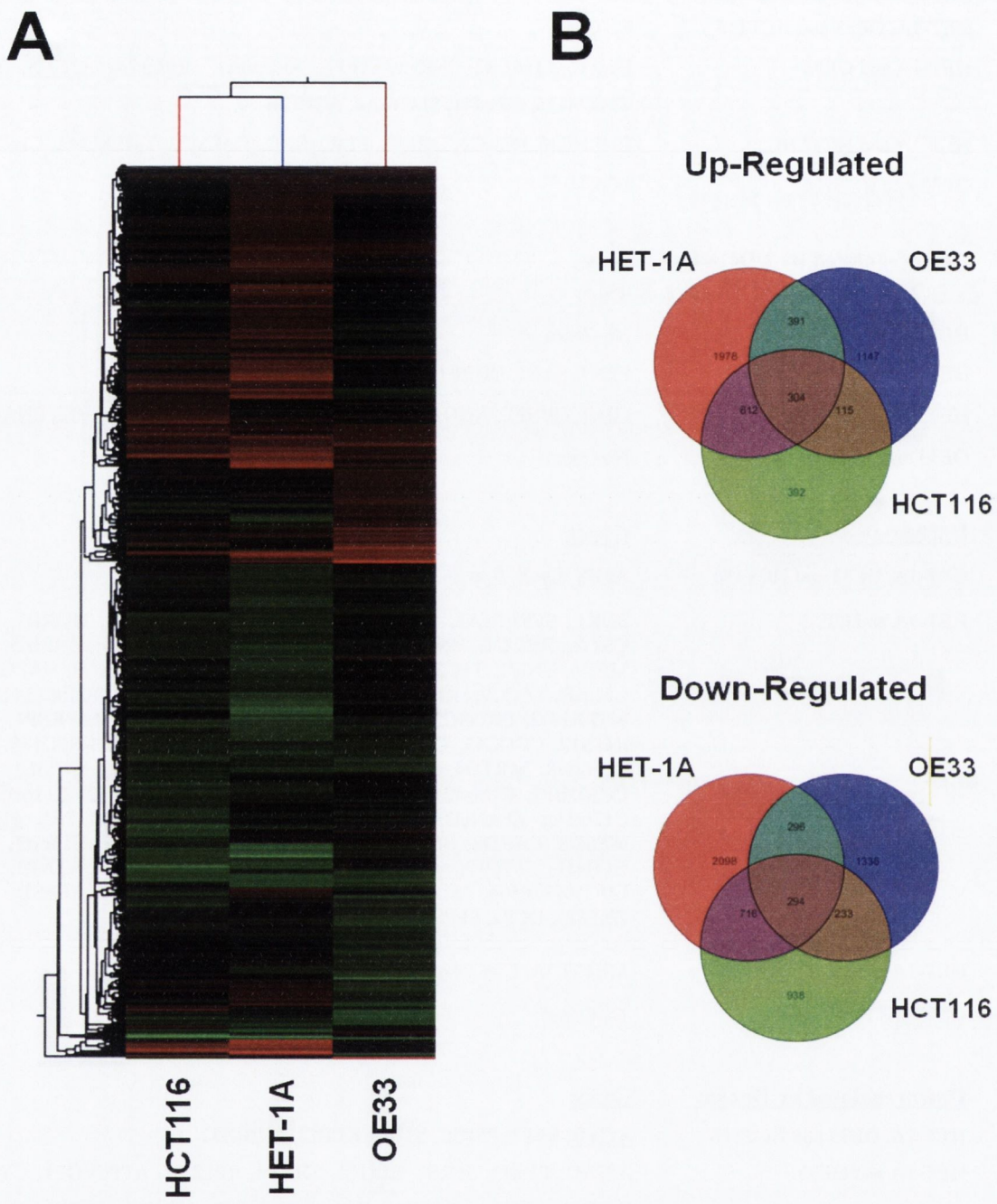

Figure 4–24: Heatmap of clustered genes after 12 hours treatment with DCA ($p \leq 0.05$) in the HET-1A, OE33 and HCT116 cell lines. Clustering was performed in GeneSpring by hierarchical clustering using Euclidian averages of probeset intensities. The HCT116 and HET-1A clustered independently of the OE33 cell line (A). The greatest numbers of modulated genes were seen in the HET-1A cell line (B).

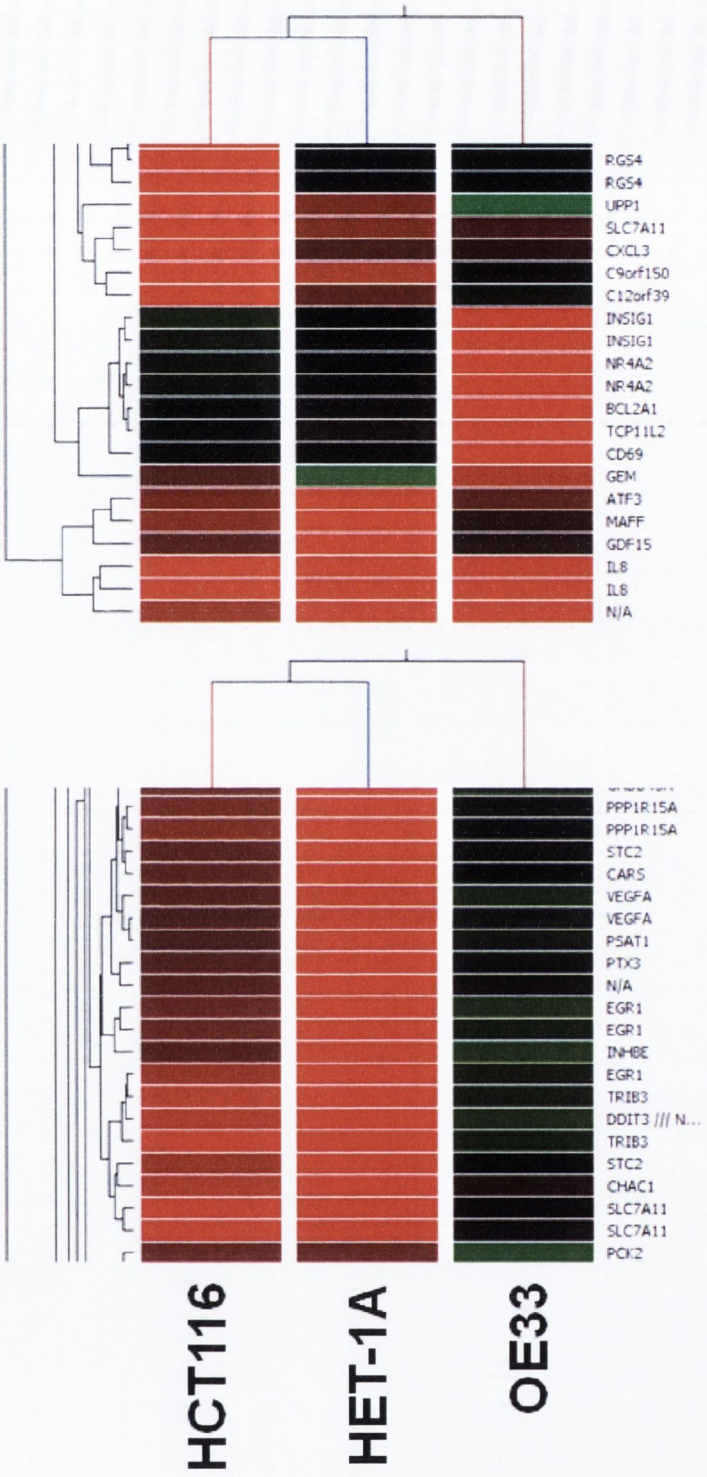

Figure 4–25: ER stress genes classically associated with DCA stimulation demonstrated differential regulation in the OE33 cell line. Genes which are classically associated with DCA stimulation include ER stress genes (ATF3, DDIT2, MAFF, TRIB3, etc) and inflammatory genes (IL-8). Similar modulation of the ER stress genes was seen in the HET-1A and the HCT116 cell lines but not in the OE33 cell line. IL-8 was upregulated by DCA in all three cell lines.

Finally, the 25 array probesets with the most altered level of expression (up and down regulated) were compared between treatments and across the cell lines (Appendix 3). IL-8 was the only gene consistently upregulated in all three cell lines by DCA treatment. Six genes were similarly modulated in the HET-1A and the HCT116 cell lines. These were IL-8, EGR1, TRIB3, STC2, DDIT3 and CHAC1 and accounted for 11/25 and 8/25 probesets in the HET-1A and HCT116 cell lines respectively. No probesets were similarly downregulated by DCA in the three cell lines. Interestingly, eight genes were similarly modulated by DCA and UDCA in the HET-1A cell lines. These were INHBE, GDF15, CHAC1, SLC7A11, DDR2, DDIT3, STC2, ATF3 and TRIB3. Many of these genes are associated with ER stress and were identified in the clustering algorithms as demonstrated in Figure 4–15. The only gene similarly regulated in this analysis by UDCA and Dex in the HET-1A cell line was S100P. This gene has recently been identified as a GC modulated gene [388].

4.4.4.4. Simultaneous Clustering Analysis of Cell lines and Treatments

Finally, clustering analysis of genes modulated by UDCA, Dex or DCA treatment in the HET-1A, OE33 and HCT116 cell lines was performed simultaneously. This analysis was based on the filtered data of mRNA expression, with 1.5 fold difference from the expression in DMSO treated cells , and at $\alpha \leq 0.05$ based on a paired t-test. Analysis demonstrated that DCA treatment in the HET-1A and the HCT116 cell line clustered independently of all other treatments. DCA treatment in the OE33 cell line clustered in a group with all other treatments. Within the branch of the dendritic tree containing the majority of treatments, UDCA and Dex in the HET-1A and the HCT116 cell line clustered closely to each other. UDCA treatment in the OE33 cell line clustered slightly more closely with the UDCA and Dex treatment in the HCT116 cell line than it did with Dex treatment in the OE33 cell line (Figure 4–26A).

These findings suggest that UDCA and Dex share a greater similarity with each other within a cell line than between cell lines. This finding was consistent with the analysis presented in sections 4.4.4.2 and 4.4.4.3. However, while DCA modulated gene expression differently in the OE33 cell line than it does in the HET-1A or the HCT116 cell line, UDCA similarly regulated a number of genes associated with DCA (Figure 4–26B).

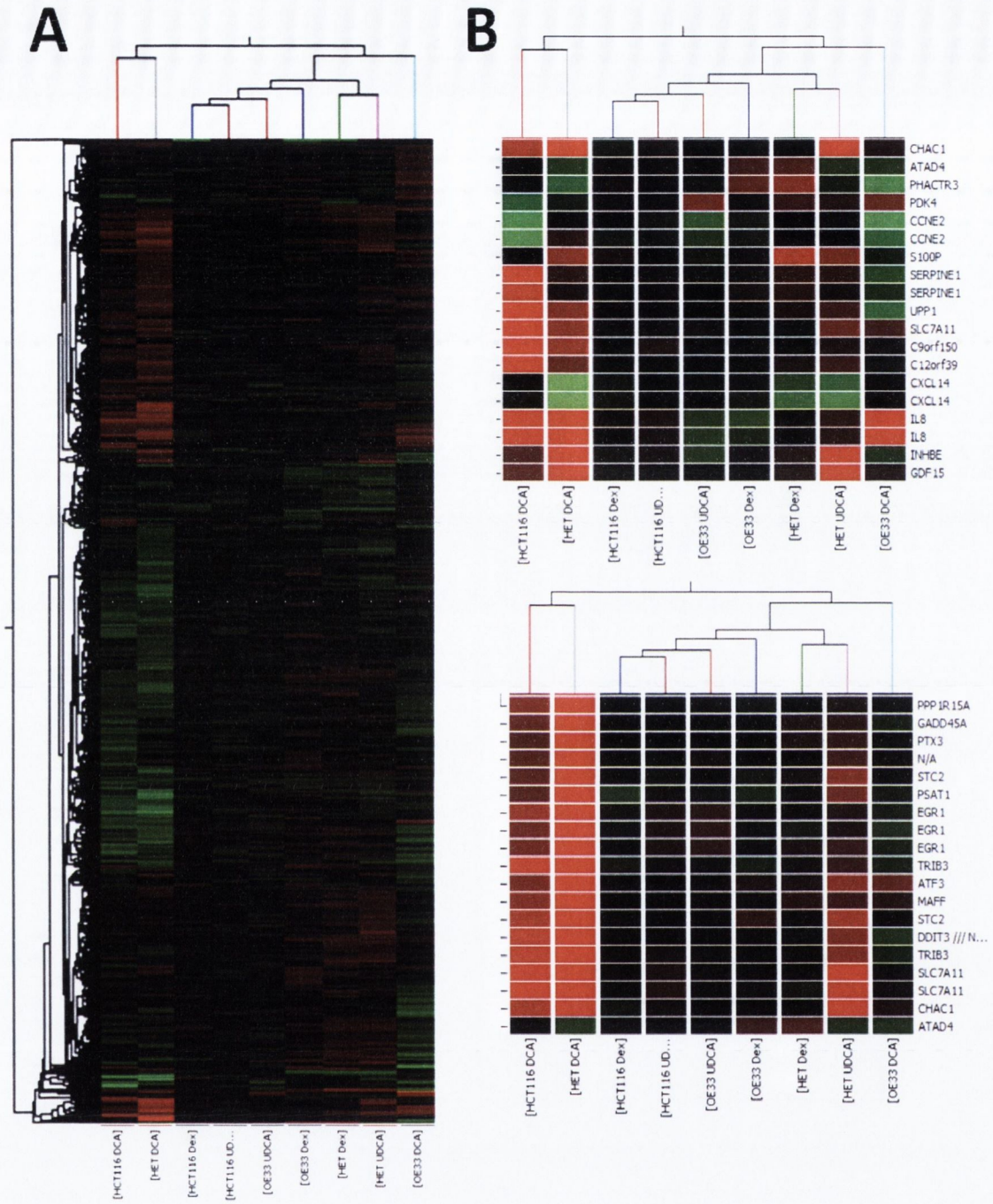

Figure 4–26: Heatmap of clustered genes after 12 hours treatment with UDCA, Dex or DCA ($p \leq 0.05$) in cell lines HET-1A, OE33 and HCT116 cell lines. A) Global clustering of Cell lines and treatments was performed in GeneSpring by hierarchical clustering using Euclidian averages of probeset intensities. B) ER stress genes classically associated with DCA stimulation demonstrate similar regulation by UDCA in the HET-1A cell line.

4.4.4.5. Validation of the Microarray

Analysis of the array demonstrated that UDCA and Dex had significant overlap in the HET-1A cell line. However the gene expression profile of UDCA had also significantly overlapped with that of DCA. Consistent with the expression of the GR in the cell lines, the number of genes modulated by UDCA or Dex in the HCT116 cell line was significantly smaller than in the HET-1A or the OE33 cell lines suggesting the possibility that UDCA may indeed be modulating gene expression through the GR (See Table 4–1). Validation of a panel of the genes modulated by UDCA, Dex and DCA was next undertaken using real time PCR of cDNA isolated in experiments performed independently of the microarray.

Genes to validate using PCR were chosen from the array data by three methods. Firstly the absolute change in gene expression induced by the treatments was studied (Appendix 3). In conjunction with this the significance of the change was assessed. Finally, genes were chosen for validation after performing a literature review. These genes were either involved in carcinogenesis, inflammation or ER stress and related to an established role in epithelial tumours (oesophageal or otherwise) or were related to the research described in earlier chapters. Further explanation of the rationale for choosing these genes and their function will be discussed below.

The following genes were chosen to be validated:

- Phosphatase and Actin Regulator 3 (PHACTR3)
- v-ski Sarcoma Viral Oncogene Homolog (avian), (SKI)
- Serpin Peptidase Inhibitor, Clade E (SERPINE1)
- Protein Kinase, DNA-Activates, Catalytic Subunit (PRKDC)
- Cysteine Rich Transmembrane BMP Regulator 1 (chordin-like) (CRIM1)
- Cbp/p300-interacting transactivator 2 (CITED2)
- Signal Transducing Adaptor Molecule 2 (STAM2)
- Cortactin (CTTN)
- Baculoviral IAP repeat-containing protein 3 (BIRC1)
- NOTCH, Drosophilia, Homolog of, 2 (NOTCH 2)
- Nuclear Receptor Subfamily 3, Group C, Member 1 (NR3C1, Glucocorticoid Receptor)
- Interleukin-8 (IL-8)
- Actin Beta (ACTB)
- Activating Transcription Factor 3 (ATF3)
- Chemokine, CXC Motif, Ligand 14 (CXCL14)
- DNA Damage Inducible Transcript 3 (DDIT3)
- Growth/Differentiation Factor 15 (GDF15)

- Tribbles, Drosophila, Homolog of, 3 (TRIB3)

As each of these genes was studied for all three treatments, this equated to 54 genes investigated for validation of the array.

4.4.4.5.1. Phosphatase and Actin Regulator 3 (PHACTR3)

PHACTR3 is expressed primarily in the brain in healthy tissues. However, upregulation of this protein has been identified in breast and lung cancers [389]. The protein contains a protein phosphatase 1 (PP1) binding sequence. PP1 is involved in numerous metabolic functions including glycogen metabolism, neuronal signalling, and actin cytoskeleton organization [390-392].

While little is known about this gene, its neuronal location and established role in glycogen metabolism suggest that it could have an association with the GR. PHACTR3 was identified as the gene with greatest increase in expression induced by Dex. Confirmation of the alteration in expression levels was seen with PCR (Appendix 3, Figure 4–27A).

4.4.4.5.2. v-ski Sarcoma Viral Oncogene Homolog (avian), (SKI)

TGFβ treatment of cells induces growth inhibition, differentiation, and apoptosis. TGFβ1 induces phosphorylation and nuclear translocation of SMAD3, where SMAD3 associates with the nuclear proto-oncogene protein SKI. Association disrupts the formation of a functional complex between the co-mediator SMADs (Co-SMADs) and R-SMADs, repressing TGFβ, activin, and bone morphogenetic protein responses.

Over-expression of SKI makes cells resistant to the growth-inhibitory effects of TGFβ1 [393]. In humans, over-expression of SKI has been seen in colorectal cancer although correlation with prognosis or invasiveness is disputed [394-395]. In the upper GI tract, over-expression of SKI has been demonstrated in diffuse gastric cancer. In SqCCa of the oesophagus, increased expression of c-SKI correlates with a greater depth of invasion and poorer survival [396-398]. Over-expression of SKI promotes the ability of TGFβ to upregulate the expression of SERPINE1, a molecule identified as modulated in our array data (see section below). Interestingly, a reduction in the expression of SKI may also be associated with carcinogenesis. The loss of a copy of c-ski increased proliferative capacity of mouse embryonic fibroblasts increases susceptibility to tumorigenesis [399]. Reduced expression of SKI induced by potent TGFβ signalling is thought to promote invasiveness and tumour metastases [400-401].

In the normal-BO-OAC sequence, high levels of SKI have been demonstrated in BO but not in normal, dysplastic BO or OAC [402].

The array data suggested a wide variance in expression of SKI after treatment with DCA, UDCA or Dex. Validation however, suggested that DCA and UDCA significantly reduced the expression of SKI in HET-1A cells while Dex had no significant effect (Figure 4–27B).

4.4.4.5.3. Serpin Peptidase Inhibitor, Clade E (SERPINE1, plasminogen activator inhibitor 1)

SERPINE1 (also known as Plasminogen Activator Inhibitor Type 1, PAI-1) is a serine protease inhibitor which was classically thought to be solely involved in thrombosis and haemostasis. It is the principal inhibitor of urokinase (uPA) and tissue plasminogen activator (tPA), the activators of plasminogen and hence the principal inhibitor of fibrinolysis. More recently, SERPINE1 has been shown to be involved in metastasis and invasion in cancer and higher levels of protein expression in tumours is associated with a poorer prognosis [403-404].

SERPINE1 modulates urokinase receptor (uPAR) and integrin mediated cell attachment to the ECM. Vitronectin appears to be the primary ECM protein through which SERPINE1 modulates cell adhesion [405]. SERPINE1 binds to vitronectin at a site which overlaps with the binding site for the uPAR and which is just adjacent to the RGD motif for integrin attachment [406-407]. Integrins and uPAR interact significantly to mediate both attachment to vitronectin and the surface expression of each other [408-409]. As a result of its higher affinity for vitronectin, SERPINE1 competitively inhibits the binding of uPAR and integrins to vitronectin [405, 410]. Furthermore, it can induce detachment of integrins and uPAR which are already bound to vitronectin [410-412]. Although loss of association between the cell adhesion molecules and ECM proteins results in internalisation of both receptors (in an endocytotic manner mediated by the low-density lipoprotein receptors), cell detachment does not occur as a result of internalization [408, 411].

The array data suggested that SERPINE1 was upregulated by all three treatments while the PCR validation demonstrated that only DCA and Dex exerted this effect (Figure 4–27C). The greater upregulation of SERPINE1 by DCA may suggest a possible mechanism as to why DCA promoted HET-1A cell detachment as described in Chapter 3.

4.4.4.5.4. Protein Kinase, DNA-Activates, Catalytic Subunit (PRKDC)

PRKDC is a serine/threonine protein kinase required for the repair of double-stranded DNA breaks and for immunoglobulin recombination in lymphocytes. Cells defective in PRKDC are hypersensitive to killing by ionizing radiation due to an inability to repair double-stranded breaks effectively [413]. PRKDC phosphorylates several transcription factors, suggesting that it functions in cell homeostasis by modulating transcription. PRKDC has been shown to phosphorylate p53 impairing the ability of MDM2 to inhibit p53-dependent *trans*-activation [414].

In colorectal cancer PRKDC levels are increased [415]. In the oesophagus, PRKDC expression has been researched as a potential marker of sensitivity to radiation. Although levels of expression of

PRKDC correlate with sensitivity to radiation in oesophageal cell lines *in vitro*, PRKDC has been shown to be heterogeneously expressed in oesophageal cancer [416-417]. Consequently, it is not felt to be a good predictor of potential response to treatment.

Array data suggested that UDCA and Dex downregulated expression of PRKDC mRNA. However, PCR demonstrated the opposite effect. DCA downregulated mRNA levels of PRKDC while UDCA and Dex had no effect (Figure 4–27D).

4.4.4.5.5. Cysteine Rich Transmembrane BMP Regulator 1 (chordin-like) (CRIM1)

The CRIM1 gene encodes a type I transmembrane protein containing six cysteine-rich repeat domains and an insulin-like growth factor-binding domain. It is thought to play a role in embryogenesis and tissue development though interactions with members of the TGFβ family, such as bone morphogenetic proteins [418-419]. However, it also appears to play a role in angiogenesis [420]. Array data suggested that DCA significantly upregulated expression of CRIM1 mRNA while UDCA and Dex downregulated the expression. PCR demonstrated that no treatment exerted a significant effect on expression of CRIM1 mRNA expression (Figure 4–27E).

4.4.4.5.6. Cbp/p300-Interacting Transactivator 2 (CITED2)

CITED2 is a protein which is classically associated with congenital cardiac defects.[421] However, this protein has also been demonstrated to variably influence apoptosis. It induces apoptosis in response to butyric acid in colonocytes and in response to TNFα in macrophages but inhibits apoptosis in response to cisplatin [422-425]. Furthermore, it has been shown to potentiate neoplastic invasion through upregulation of matrix metalloproteinases [426-427]. CITED2 has also been demonstrated to be a negative feedback regulator of NF-κB [425]. It also inhibits trans-activation of HIF1A-induced genes by competing with binding of HIF1a to p300-CH1 [428].

Data from the microarray suggested that DCA and UDCA were likely to down regulate this gene. However, DCA significantly increased mRNA expression while UDCA reduced expression. Dex exerted no significant effect in either the array or in the PCR validation (Figure 4–27F).

4.4.4.5.7. Signal Transducing Adaptor Molecule 2 (STAM2)

STAM2 is an adaptor protein involved in the downstream signalling and processing of growth factor and cytokine receptors [429]. It acts downstream of JAK kinases and is phosphorylated in response to tyrosine kinase receptor activation potentiating the effects of cytokine signalling [429-431]. However, STAMs also have a role in the processing of endosomes. Functional STAM2 is required for functional endocytosis, lysosomal degradation and receptor down-regulation [432-434]. This adaptor protein interacts with hepatocyte growth factor-regulated substrate located on the cytoplasmic surface of early endosomes and is involved in the sorting of ubiquitinated proteins

for lysosomal degradation [432]. It is also involved in ER to golgi trafficking highlighting a role of this protein in the endocytic recycling process. Over-expression of STAMs results in golgi fragmentation, a phenomenon which has previously been demonstrated in our laboratory to occur in response to DCA [435-436].

Array data suggested that DCA should upregulate expression of STAM2 mRNA while the effects of UDCA and Dex were varied. PCR demonstrated that both DCA and UDCA upregulated expression of STAM2 mRNA (Figure 4–27G). This could provide a further insight as to the mechanism behind DCA inducing golgi fragmentation as well as a potential explanation for the reduction in surface expression of ITGAV demonstrated in chapter 3.

4.4.4.5.8. Cortactin (CTTN)

CTTN is a protein that localizes within membrane ruffles in cultured cells [437-438]. It has been shown to be involved in actin polymerisation and to interact with Src and the GTPase Dynamin in clathrin coated pits [437-441]. Consequently, it is felt to exert a role in cell migration and endocytosis. Amplification of the 11q13 region has been demonstrated in breast and head and neck cancers with upregulation of CTTN being frequently identified as a consequence. In cells with 11q13 amplification, excessive post-translational modification of CTTN is seen in response to EGFR stimulation. This results in localisation of the protein to cell-matrix attachment sites, implying that CTTN may have a role in the modulation of cellular adhesion [442-443]. It has also been identified as a modulator of neoplastic invasion [444-445]. In cancers of the gastrointestinal tract including colorectal, gastric and squamous cell cancer of the oesophagus, CTTN has been shown to be a predictor of tumour aggressiveness and risk of recurrence post resection [446-449]. Although CTTN over-expression has been associated with a number of adenocarcinomas (Breast, stomach, colon) its role and presence in BO and OAC have not been investigated.

Analysis of array data had suggested that UDCA may induce an upregulation of this gene. However, this was not verified in the PCR validation (Figure 4–27H).

4.4.4.5.9. Baculoviral IAP repeat-containing protein 3 (BIRC1)

BIRC3 (also known as cIAP2) is a member of the inhibitor of apoptosis family of proteins. BIRC3 has been shown to interfere with the expression of TNF receptor associated factors and the activation of caspases [450-452]. The protein has been shown to be upregulated in response to cellular detachment, delaying the onset of anoikis [301]. While Dex significantly upregulated expression of BIRC3, as demonstrated previously in the literature in breast, ovarian and lung cells, neither UDCA nor DCA stimulation elicited this effect [453-455]. This may be because, in our experimental design of the array study, detached cells were discarded and thus excluded from the analysis (Figure 4–27I).

4.4.4.5.10. Notch, Drosophila, Homolog of, 2 (NOTCH 2)

NOTCH2 is a type 1 trans-membrane protein involved in embryogenesis and organogenesis. Mouse models have demonstrated its particular role in cardiac and liver development. NOTCH-ligand interactions can result in the activation in one of three signalling mechanisms. The classical mechanism involves repression of transcription of tissue specific transcription factors, inhibiting differentiation and maintaining the pluripotency of stem cells. However, in conjunction with different ligands, NOTCH signalling can induce cell differentiation or augment NF-κB signalling [456].

In the gastrointestinal tract, NOTCH2 expression correlates with progression through the metaplasia carcinoma sequence in the stomach [457]. However, in colonic tumours, NOTCH1 expression correlates with poor prognosis while NOTCH2 expression correlated with a better prognosis [458]. Within the oesophagus NOTCH1 and NOTCH2 have been shown to be expressed in the basal cell layer in mice. Here, they are thought to maintain the balance between stem cells and progenitor cells [456]. Hypothetically, disruption of NOTCH2 signalling could have a role in the genesis of BO by allowing erroneous differentiation of oesophageal stem cells.

Array data suggested that UDCA and Dex should reduce expression of NOTCH2 mRNA. However, PCR validation failed to confirm this finding (Figure 4–27J).

4.4.4.5.11. Nuclear Receptor Subfamily 3, Group C, Member 1 (NR3C1, GR)

The expression and function of the GR (NR3C1) has been discussed extensively elsewhere (See Sections 4.1.2 and 4.1.3). Array data and PCR validation confirmed that DCA upregulated expression of GR mRNA (Figure 4–27K).

4.4.4.5.12. Interleukin-8 (IL-8)

IL-8 is a chemokine produced by macrophages and other cell types including epithelial cells. The protein encoded by this gene is a member of the CXC chemokine family. This chemokine is one of the major mediators of a localised inflammatory response. It functions as a chemo-attractant, and is also a potent angiogenic factor. Its primary function is to recruit neutrophils to a site of inflammation.

Upregulation of IL-8 in the oesophagus has been demonstrated to occur in response to BA and low pH exposure [133, 459]. Increasing levels are seen across the normal-BO-OAC sequence with constitutive expression being seen in OAC [135].

Consistent with previously published data, DCA significantly upregulated levels of IL-8 mRNA (Figure 4–27L). However, UDCA and Dex had no effect of the expression of IL-8 mRNA.

4.4.4.5.13. Actin Beta (ACTB)

Localization of beta-actin mRNA to sites of active actin polymerization modulates cell migration during embryogenesis, differentiation, and possibly carcinogenesis.

DCA significantly reduced the expression of ACTB in both the microarray and PCR experiments. However, while the array data suggested that UDCA and Dex had a similar effect in reduction the expression of ACTB mRNA, PCR suggested that DCA downregulated, UDCA upregulated and Dex had no effect on the expression of this gene (Figure 4–27M).

4.4.4.5.14. Activating Transcription Factor 3 (ATF3)

Activating transcription factor 3 is a member of the cAMP Responsive Element-Binding (CREB) protein family of transcription factors. Two isoforms of this gene exist. The larger isoform represses transcription of genes with ATF binding elements by stabilizing the binding of inhibitory cofactors at the promoter region. The shorter isoform lacks the ability to dimerise and to bind to DNA. It is thought to stimulate transcription by sequestering inhibitory co-factors away from the promoter. The two isoforms antagonize each other's actions and therefore changes in the relative expression of the isoforms regulate transcription of ATF3 target genes [460]. In mice, the Atf3 promoter is closely localized to the Nf-κb promoter region. Atf3 appears to antagonise the transcriptional signalling of Nf-κb and toll-like receptors [461].

Transcription of the ATF3 gene has been shown to occur in response to low pH [462]. Microarray data suggested that DCA and UDCA upregulated the expression of ATF3 mRNA while Dex had no effect on the expression. PCR demonstrated that DCA upregulated mRNA expression to 70 times the level of vehicle control. UDCA upregulated the expression to five times the expression of vehicle (Figure 4–27N).

4.4.4.5.15. Chemokine, CXC Motif, Ligand 14, (CXCL14)

CXCL14 is constitutively expressed at high levels in many normal tissues including intestinal lamina propria and is thought to be primarily produced by fibroblasts [463]. However, it is reduced or absent from most neoplastic tissues [464-465]. In the presence of prostaglandin E2, CXCL14 is chemotactic for monocytes but apparently not for lymphocytes, dendritic cells, macrophages, and neutrophils. CXCL14 also inhibits angiogenesis, possibly as a result of its ability to block endothelial cell chemotaxis [466].

CXCL14 has previously been shown to be modulated in response to DCA in HET-1A cells but not in a cell line representing an oesophageal adenocarcinoma (SKGT-4) [387]. In the array data all treatments were seen to down regulate expression of CXCL14, while PCR validation demonstrated

that DCA and UDCA downregulated expression CXCL14 mRNA while Dex had no significant effect (Figure 4–27O).

4.4.4.5.16. DNA Damage-Inducible Transcript 3 (DDIT3 / CHOP)

DDIT3 acts as a dominant-negative inhibitor of the transcription factors C/EBP and LAP by forming heterodimers incapable of binding DNA [467]. DDIT3 activation occurs in response to ER stress induced by the unfolded protein response. DDIT3 deletion protects cells from ER stress by decreasing ER protein load and changing redox conditions [468]. It has been shown to bind to ATF3, forming a heterodimer incapable of binding DNA, thus allowing transcription of stress genes [469]. ATF3 is also capable of suppressing DDIT3 transcription [470].

PCR experiments validated that DCA and UDCA upregulated DDIT3 expression while Dex had no significant effect (Figure 4–27P).

4.4.4.5.17. Growth/Differentiation Factor 15 (GDF15)

GDF15 is a protein belonging to the TGF-β family which has a role in regulating inflammation and apoptosis. GDF15 has been shown to inhibit polymorphonuclear leukocyte adhesion and transmigration by inhibiting β2 integrin function through interference with activation of the small GTPase Rap1 and by directly activating the small GTPase Cdc42 [471]. Interestingly β2 integrin gene expression was upregulated by both UDCA and Dex in the HET-1A cell line in the micro-array (Figure 4–17, Table 4–2 and Appendix 3). GDF15 functions as an anti-inflammatory cytokine by directly interfering with chemokine signalling, and also appears to be a modulator of inflammation and cancer [472].

In the same paper that demonstrated that CXCL14 was upregulated in response to DCA, GDF15 was identified as similarly upregulated by DCA [387]. Array data suggested that DCA upregulated to expression of 100 times that of vehicle while UDCA increased the expression to 15 times that of vehicle. PCR demonstrated that DCA and UDCA upregulated the expression to approximately 200 and 34 times the expression seen in vehicle treatment respectively (Figure 4–27Q).

4.4.4.5.18. Tribbles, Drosophila, Homolog of, 3 (TRIB3)

TRIB3 is a negative regulator of NF-κB which exerts its effects through phosphorylation of the p65 subunit of NF-κB. This sensitizes cells to death receptor induced apoptosis [473]. It also inhibits the activity of AP1 and AKT1 [474-475]. Expression has been shown to be upregulated by NF-κB. DCA and UDCA significantly increased the expression of TRIB3 mRNA while Dex had no significant effect (Figure 4–27R).

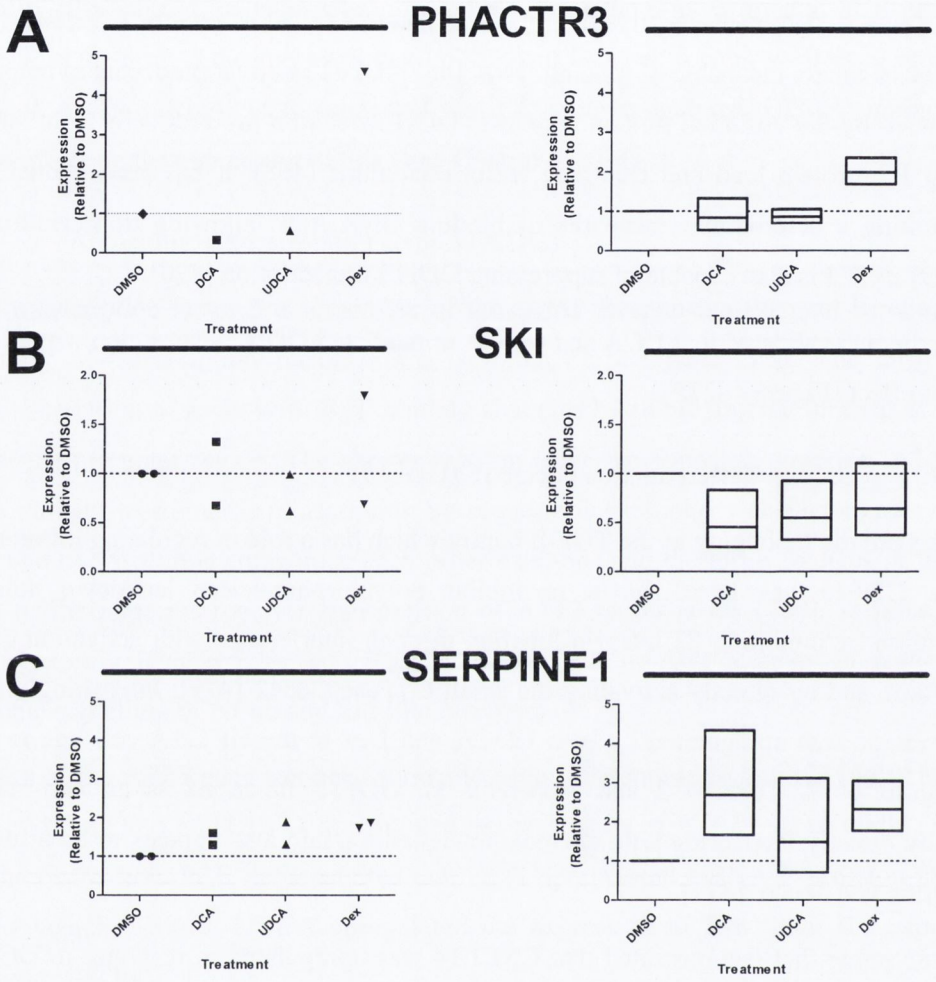

Figure 4–27: Expression levels of mRNA as determined by microarray probesets and as validated by PCR. Array data (Left) presents various numbers of data points as determined by the number of probesets representing each gene on the Affymetrix Human U133 Plus 2 gene expression chip. Intensity expression varied unpredictably between probesets. The expression of the probesets is plotted but no averaging or statistical representation is presented. The raw data of intensity measurements is presented in Appendix 3. PCR validation data (Right) of the genes chosen for validation is expressed as mean +/- 95% CI (N = 5) so that bars not crossing the line at Y=1 are considered statistically significant.

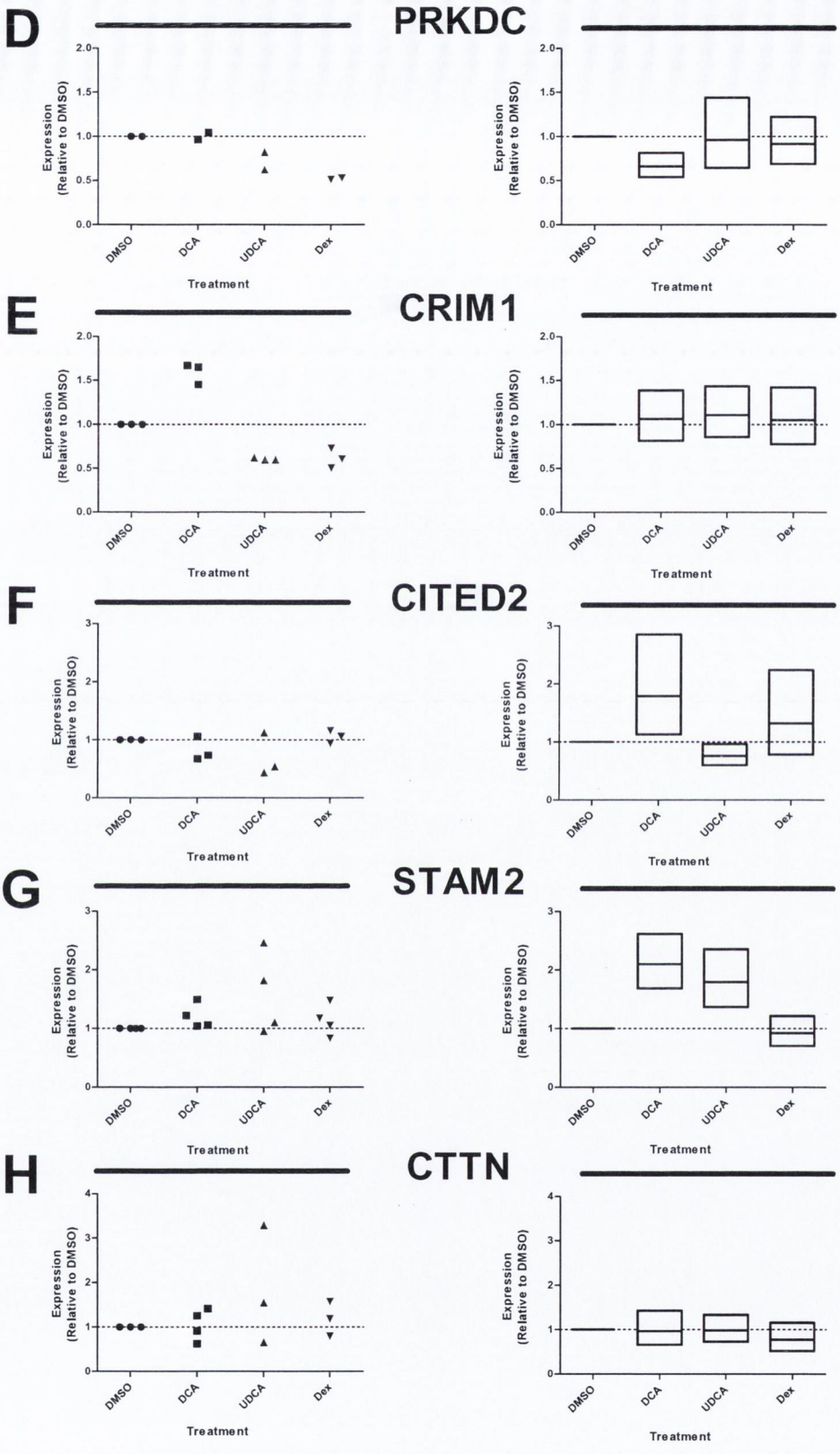
D
PRKDC
E
CRIM1
F
CITED2
G
STAM2
H
CTTN
Expression (Relative to DMSO)
Treatment
DMSO
DCA
UDCA
Dex

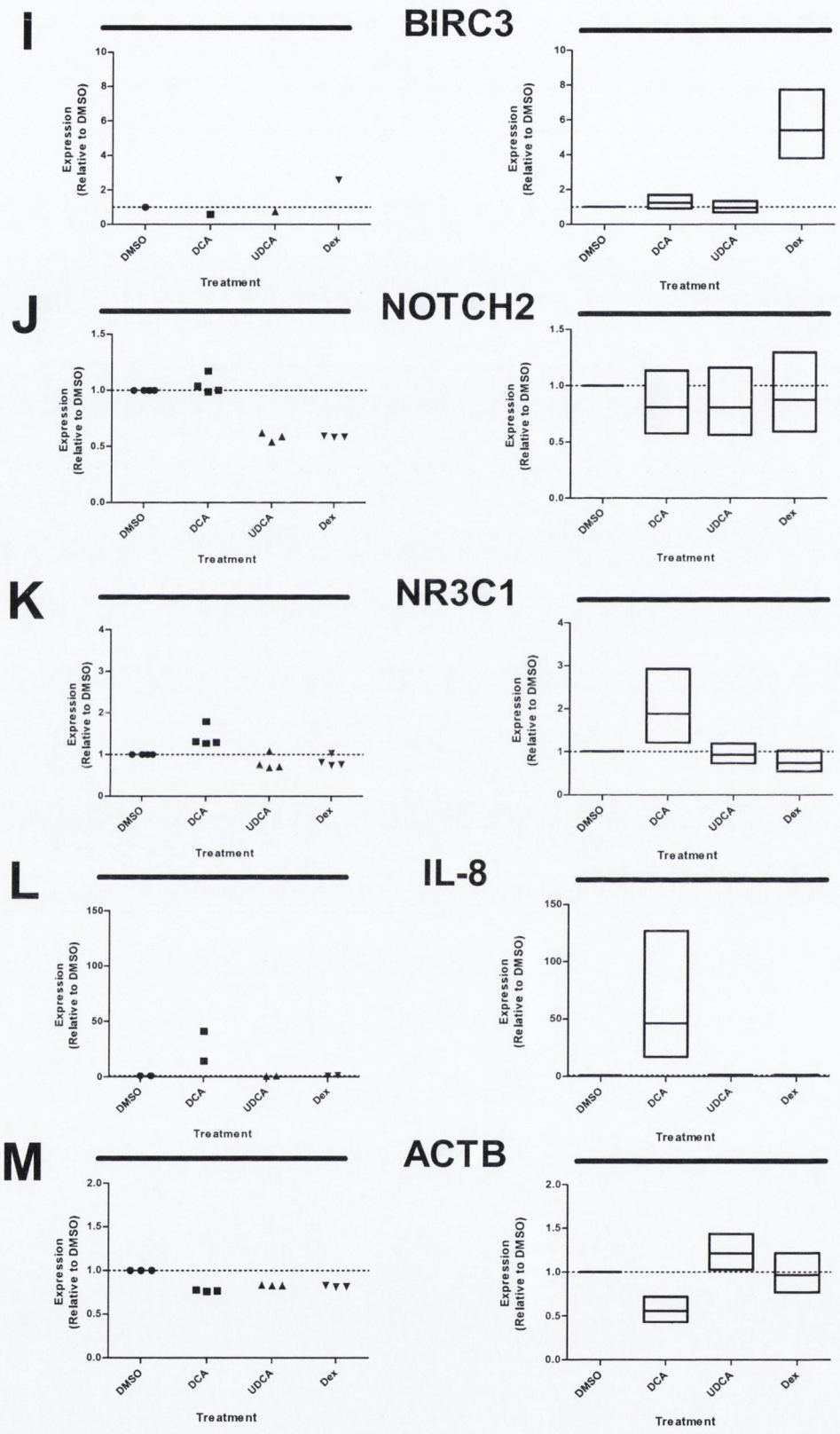
I
BIRC3
Expression (Relative to DMSO)
DMSO
DCA
UDCA
Dex
Treatment
J
NOTCH2
K
NR3C1
L
IL-8
M
ACTB

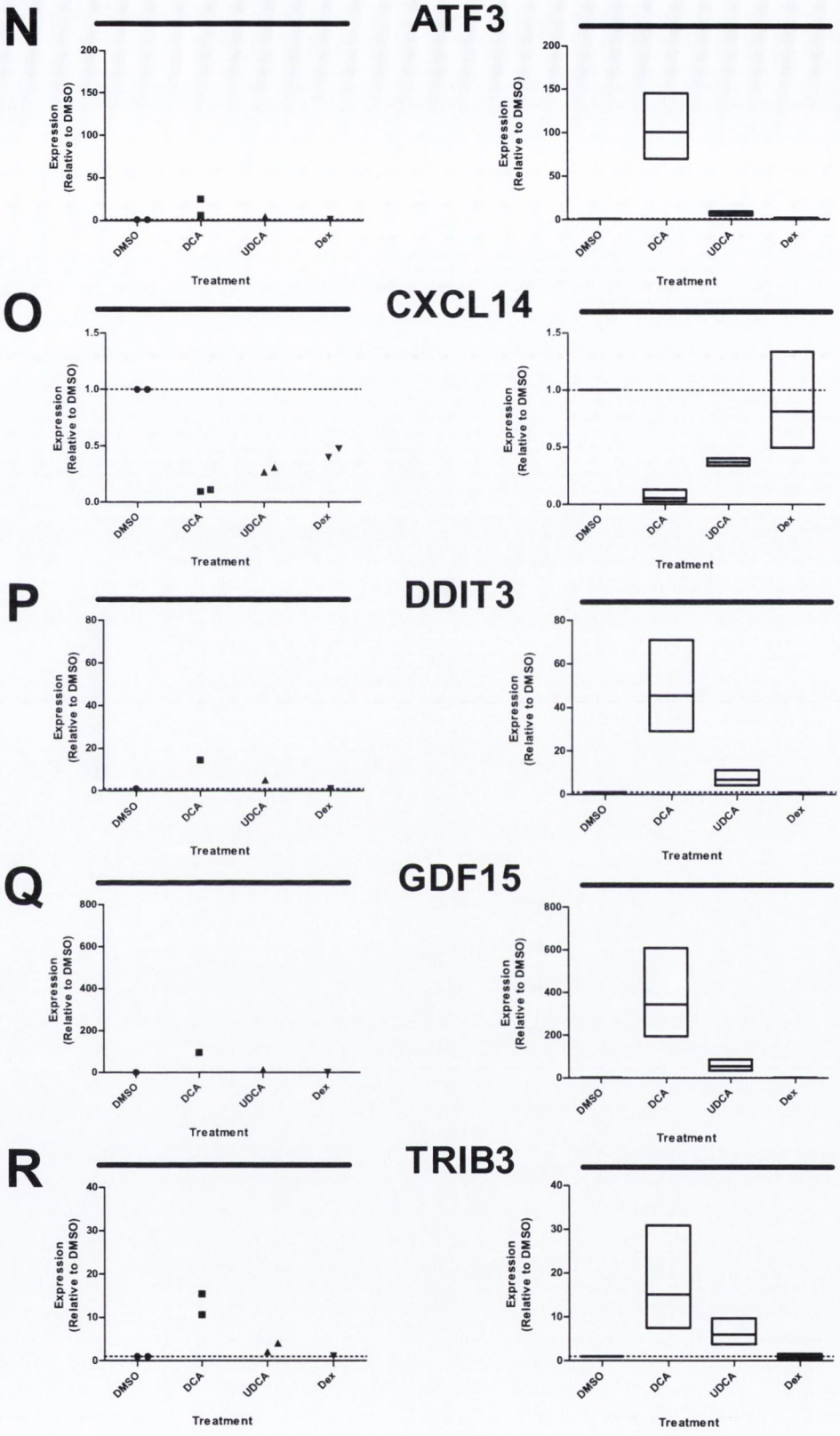
N
ATF3
Expression (Relative to DMSO)
200
150
100
50
0
DMSO
DCA
UDCA
Dex
Treatment
O
CXCL14
1.5
1.0
0.5
0.0
P
DDIT3
80
60
40
20
Q
GDF15
800
600
400
200
R
TRIB3
40
30
20
10

	DCA		UDCA		Dex	
	MA	PCR	MA	PCR	MA	PCR
PHACTR3	↓	↔	↓	↔	↑	↑
SKI	↔	↓	↔	↓	↔	↔
SERPINE1	↑	↑	↑	↔	↑	↑
PRKDC	↔	↓	↓	↔	↓	↔
CRIM1	↑	↔	↓	↔	↓	↔
CITED2	↓	↑	↓	↓	↔	↔
STAM2	↑	↑	↑	↑	↔	↔
CTTN	↔	↔	↑	↔	↔	↔
BIRC1	↔	↔	↔	↔	↑	↑
NOTCH 2	↔	↔	↓	↔	↓	↔
NR3C1	↑	↑	↔	↔	↔	↔
IL-8	↑	↑	↔	↔	↔	↔
ACTB	↓	↓	↓	↑	↓	↔
ATF3	↑	↑	↑	↑	↔	↔
CXCL14	↓	↓	↓	↓	↓	↔
DDIT3	↑	↑	↑	↑	↔	↔
GDF15	↑	↑	↑	↑	↔	↔
TRIB3	↑	↑	↑	↑	↔	↔

Table 4–3: An overview of changes in mRNA expression induced by DCA, UDCA or Dex in the microarray experiment (MA) and the changes identified using RT-PCR (PCR). Coloured boxes indicate genes in which there was correlation between the two techniques. 37/54 gene sets demonstrated similar findings between the micro-array and PCR validation.

4.4.4.6. Interpretation of the Array Validation

Cluster analysis of the microarray data had suggested that UDCA and Dex may be similarly modulating gene expression in the HET-1A cell line. Interestingly though, the similarities between gene lists appeared much greater between DCA and UDCA (Appendix 3). In order to validate the findings of the microarray data, genes were identified which could validate and further elucidate our findings. Significant similarity was identified between the array data and the PCR validation (Table 4–3). In fact, overall 37/54 genes (69%) validated. However this was primarily between DCA and UDCA.

The majority of genes identified as similarly modulated by DCA and UDCA in the array were similarly altered by UDCA and DCA in the validation data. These genes were primarily chosen from lists of the top 25 genes modulated by UDCA or DCA (Appendix 3). Interestingly, the majority of these genes can be associated with ER stress and apoptosis. ATF3, DDIT3, TRIB3, CXCL14 are all associated with ER stress [476-478]. DDIT3 may itself potentiate ER stress through a reduction in BCL-2 (increasing ROS) [479] and inducing TRIB3-mediated ER-induced cell death [480-481]. Interestingly, while GDF15 is also regarded as a marker of ER stress, levels of apoptosis are not affected by absence of this protein [482]. Furthermore, ER stress can upregulate expression of IL-8 [483].

In the array analysis UDCA and Dex had appeared to exhibit significant overlap in gene expression profiles and to cluster together. During the validation this did not appear to be the case; genes modulated by Dex were not similarly modulated by UDCA and *vice versa*. It is possible that UDCA and Dex clustered together in the array analysis simply because DCA clustered independently due to the greater fold changes in gene expression induced by this chemical. For the converse reason, the relatively small change in mRNA expression induced by UDCA and Dex, similarities between these two treatments may have been difficult to demonstrate (See Figure 8–3, Appendix 3).

Differences between the microarray data and the PCR data may also have occurred as a result of the different biases inherent to each of these technologies. The microarray data sets are biased toward representing the 3' end of the oligonucleotide string (see Section 4.3.7) while the Taqman probes are biased toward the 5' end of any cDNA because of the 5' to 3' nature of Taq polymerase (See Section 0). This means that different gene transcripts may be identified in only one of the technologies used, rather than in both, leading to different results. For the same reason, the different preparation steps used in the two experimental techniques prior to quantification are also likely to bias the results obtained by the two technologies. Yet the PCR data is, on balance, more

likely to be an accurate representation of the real alteration in gene expression for any specific gene transcript.

Finally, the differences between the array data and the PCR validation may also have been a consequence of the genes chosen for validation. Unfortunately, two of the most promising genes for validation (SAE-1 and S100P) did not have PCR primers available at the time the research was performed. Custom designed probes were not used due to time limitations.

4.4.5. UDCA Pre-Treatment Inhibits DCA-Induced Expression of IL-8

Finally, as the aim of this research was to investigate whether UDCA could modulate the inflammatory effects of DCA at a transcriptional level, we investigated whether UDCA pre-treatment could modulate IL-8 mRNA upregulation in response to DCA treatment.

Trans-repressive effects of the GR are largely considered to be due to protein-protein interactions between GR and other inducible transcription factors (e.g., AP-1 and NF-KB) rather than direct genomic effects. It has been shown that UDCA suppresses NF-κB-dependent transcription and the subsequent cytokine expression through direct interaction of the GR and NF-κB; in particular, via interaction with the p65 subunit. IL-8 (an NF-κB dependent gene) was chosen as a representative pro-inflammatory gene, involved in the normal-BO-OAC sequence transition, which was significantly upregulated in the micro-array and PCR data.

HET-1A cells were treated with 300μM DCA, with or without UDCA pre-treatment, and the expression of IL-8 mRNA was normalised to DMSO vehicle for each time-point studied. DCA induced a much greater upregulation of IL-8 mRNA expression than UDCA after 6 and 8 hours treatment. Four hours UDCA pre-treatment prior to DCA exposure significantly reduced the expression of IL-8 mRNA induced by DCA at the 6 and 8 hour time-point (Figure 4–28). This duration of pre-treatment was chosen because it had been shown to reduce apoptosis in the HET-1A cell line in earlier work.

This finding suggests that UDCA can modulate DCA induced gene expression in the HET-1A cell line. However, this finding would need to be validated further (including with GR knockdown) prior to generalising the finding.

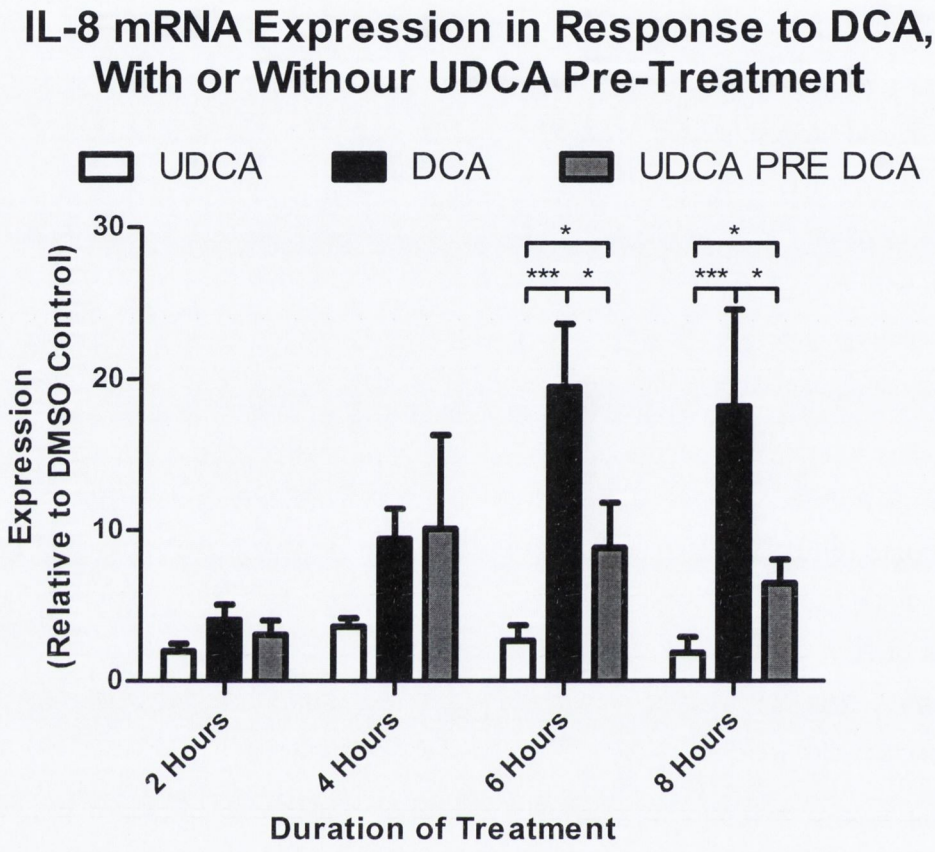

Figure 4–28: Four hours UDCA pre-treatment prior to DCA exposure in HET-1A cells reduced DCA induced expression of IL-8 mRNA. HET-1A cells were grown until 80 – 90 % confluent. Cells were either pre-treated with UDCA in fresh media or with fresh media alone for 4 hours. At T = 0, cells were exposed to DCA, UDCA or DMSO for 2, 4,6 or 8 hours. At the relevant time-point, the cells were lysed, RNA extracted and cDNA generated for RT-PCR. RT-PCR was per-formed using performed using Applied Biosystems 7900HT Fast Real-Time PCR System. Data represents Mean and SEM of N=5. * denotes $p < 0.05$ and *** denotes $p < 0.001$.

4.5. Discussion

The aetiological association between chronic inflammation and carcinogenesis has been established [370, 372]. In the oesophagus, inflammation occurs in response to the refluxate of gastric and duodenal contents. At the molecular level, both high concentrations of H^+ ions and BAs have been shown to activate pro-inflammatory pathways and generate ROS and RNS [85, 87, 133, 136, 462]. *In-vivo,* increasing exposure of the oesophagus to refluxate correlates with the degree of inflammatory cell infiltrate as well as the risk of developing BO and OAC [18, 21, 51, 187].

UDCA has been shown to activate the GR through a mechanism distinct from GCs [169, 171]. Activation of the GR by UDCA appears to dissociate *trans*-activation and *trans*-repression; it *trans*-represses with the same efficacy as Dex without inducing *trans*-activation to the same extent [376]. Thus UDCA is a dissociated steroid compound with the ability to exert anti-inflammatory effects without inducing the side effects associated with the use of GCs. Consequently, the aim of this research was to investigate the potential role of UDCA in modulating the GR in the oesophagus and to investigate the potential of this compound to act in a fashion similar to Dex.

To investigate this, we first examined the expression of the GR in oesophageal cell lines representing normal epithelium, BO and OAC. All cell lines expressed GR. The lowest level of expression was seen in the HCT116 cell line representing colorectal cancer. The GR present in all cell lines was determined to be GRα. The expression of the GR *in-vivo* was then investigated using immunohistochemical staining of paraffin embedded biopsies of normal squamous epithelium, BO, OAC, SqCCa of the oesophagus and normal colonic epithelium. The expression of the GR in squamous epithelium has already been demonstrated [369]. However, the identification of the relative absence of GR in BO is a novel finding. It suggests that activation of the GR in non-neoplastic oesophageal tissue may preferentially target normal squamous epithelium rather than metaplastic BO. This could be used as a mechanistic strategy to selectively protect normal epithelium while treating BO.

We next investigated the ability of UDCA to induce translocation of the GR to the nucleus. UDCA was found to consistently induce translocation of the GR in cell lines representing the normal-BO-OAC sequence. In the HET-1A cell line, the EC_{50} for translocation was 336μM. The efficacy of GR translocation after eight hours stimulation with 300μM UDCA (relative to 100nM Dex, a dose chosen to induce maximal GR translocation) varied considerably between the cell lines. In the HET-1A cell line the efficacy was 36%. In the QH, SKGT-4, OE33 and HCT116 cell lines, the relative efficacies were 37%, 26%, 13% and 51% respectively.

Interestingly, DCA induced nuclear translocation of the GR in the SKGT-4 cell line. The efficacy of DCA induced translocation was almost identical to that of UDCA. To date the ability of DCA to

induce nuclear translocation has not been reported. It is possible that DCA could induce GR translocation through a mechanism similar to UDCA, or that this could simply represent a stress reaction [361, 484-486]. While it was initially suggested that UDCA was the only BA with which exerted anti-apoptotic effects, it was recently demonstrated that pre-treatment with low dose hydrophobic BAs could protect against apoptosis induced by subsequent exposure to high dose hydrophobic BAs [229]. As the GR has been demonstrated to be involved in eliciting the protective effects of UDCA, it may also be that DCA could be exerting an anti-apoptotic effect through this mechanism [167, 239].

The ability of UDCA and DCA to induce *trans*-activation was next investigated. DCA was included in this experiment because it had demonstrated the ability to induce GR translocation in the SKGT-4 cell line. Neither prolonged UDCA nor prolonged DCA treatment induced *trans*-activation in the HET-1A or the SKGT-4 cell line. Thus, despite UDCA inducing translocation of the GR, trans-activation did not occur, consistent with previously published research [376]. While the ability of UDCA to *trans*-repress the effects of transcription factors such as KF-κB and AP-1 has previously been demonstrated, this effect was not investigated in this research. Confirmation that UDCA can induce *trans*-repression in oesophageal cell lines will be necessary in future experiments. However, the use of a standard IL-8 or NF-κB *trans*-repression assay is precluded in OAC cell lines due to their high constitutive NF-κB activity. An AP-1 *trans*-repression assay may be of use in future experiments to demonstrate the *trans*-repressive ability of UDCA in oesophageal cell lines. Perhaps more interesting will be the investigation as to whether DCA induces *trans*-repression in the SKGT-4 cell line in a manner similar to Dex or UDCA.

Finally, we investigated similarities between the mRNA expression profiles induced by UDCA, Dex and DCA. The HET-1A cell line was the primary cell line we wished to investigate it order to determine whether UDCA could reduce inflammation in normal squamous epithelium. The identification of an anti-inflammatory role, mediated through the GR, in a tissue which expressed the GR would suggest that UDCA could be used to prevent inflammation, thus conceivably reducing the toxicity of GORD in the oesophagus.

The GR has been shown to directly modulate the expression of a core set of approximately 100 genes. However, these appear to vary among different tissues and when different GR ligands are used [236, 354, 366-367, 487]. For this reason, the OE33 cell line was chosen for the micro-array experiment because of its embryologically similar origin to the HET-1A cell lines (i.e. oesophageal). Thus, this should have allowed a core "oesophageal" set of GR modulated genes induced by Dex, and possibly UDCA, to be identified. The HCT116 cell line was chosen because is represented a cell line in which the expression of the GR was low.

The HET-1A and OE33 cell lines demonstrated that over 100 genes were similarly modulated by Dex. This was consistent with previously published literature[236, 487]. Definition of this core set of genes should also have allowed investigation into whether any of this core set were similarly modulated by UDCA. Similarities between UDCA and Dex within a single cell line were greater than similarities of the treatments between the cell lines. The two compounds similarly upregulated 559 probesets and downregulated 103 in the HET-1A cell line. Using IPA, 16 of the genes were found to be directly associated with the GR. However, the genes similarly upregulated and downregulated by UDCA and Dex (e.g. SERPINE1, PRKDC, ACTB and NOTCH) did not validate with RT-PCR. This may simply represent the greater variance seen in the multiple RT-PCR experiments compared with the technical replicates of the array. In the OE33 cell line 42 probesets were similarly upregulated by UDCA and Dex and 12 were downregulated. Only one gene was similarly regulated by UDCA and Dex in the HET-1A and OE33 cell line (KLHL24).

In the HCT116 cell line no genes were similarly modulated by UDCA and Dex. The paucity of genes modulated by UDCA and Dex in the HCT116 cell line may be because of the low level of GR expression in this cell line. It could possible also be because of a low number of GREs in this cell line. As the GR is not expressed in normal colonic epithelium the HCT116 cell line may not be designed for stimulation by GCs. Identification of a set of genes modulated by UDCA in the (relative) absence of the GR (i.e. in the HCT116 cell line), and comparison with genes modulated in the presence of the GR would hypothetically have allowed differentiation between UDCA-mediated GR effects and UDCA effects not mediated through the GR. However, the paucity of genes modulated by UDCA in this cell line precluded this analysis.

Although UDCA and Dex demonstrated significant overlap in gene expression profiles in the HET-1A cell line, UDCA and DCA also exhibited significant similarities. DCA similarly upregulated 30.2% of those genes upregulated by UDCA and downregulated 41.6%. Clustering analysis of the array data sets consistently demonstrated that ER stress and inflammatory genes were similarly regulated by these two BAs. Validation of the array confirmed these findings. This finding may explain why UDCA reduced proliferation (and likely induced cell death) in the HET-1A cell line as demonstrated in Chapter 2. However, the relative toxicity of DCA is much greater than that of UDCA, as exhibited by the much lower levels of stress or inflammatory gene expression (e.g. ATF3, GDF15, IL-8) induced by UDCA. However numerous other genes were similarly regulated by the two BAs. One possibility is that the two BAs could also be similarly activating other pathways such as the BA dependent orphan nuclear receptors.

Therefore, UDCA, although inducing a discrete set of genes, demonstrated some similarity with gene expression profiles induced by both Dex and DCA. This was most noticeable in the HET-1A cell line (Table 4–4and Table 4–5). As the structure of UDCA exhibits similarities with both Dex

and DCA, its ability to modulate genes in a fashion similar to both DCA and Dex may reflect that UDCA exhibits structure-function effects of both. Adding validity to this hypothesis is that the overlap between DCA and Dex was smaller than between the other comparison groups. DCA consistently modulated approximately 10% of genes modulated by Dex and Dex consistently modulated less than 5% of genes whose expression was altered by DCA.

Percentage of Genes Modulated by DCA or Dex similarly modulated by UDCA

	HET-1A		OE33		HCT116	
	Up	**Down**	**Up**	**Down**	**Up**	**Down**
DCA	**17.1**	**6.6**	**4.3**	**2.9**	**<1**	**<1**
Dex	**35.0**	**17.3**	**2.1**	**1.6**	**0**	**0**

Table 4–4: Percentage of genes modulated by DCA or Dex which are similarly modulated by UDCA.

Percentage of Genes Modulated by UDCA Similarly Modulated by Dex or DCA

	HET-1A		OE33		HCT116	
	Up	**Down**	**Up**	**Down**	**Up**	**Down**
DCA	**30.2**	**41.6**	**48.8**	**50**	**71.4**	**65.2**
Dex	**21.6**	**10.4**	**10.5**	**5.6**	**0**	**0**

Table 4–5: Percentage of genes modulated by UDCA which are similarly modulated by Dex or DCA

Within the HET-1A cell line there was as much similarity between UDCA and Dex as there was between UDCA and DCA. However, RT-PCR demonstrated that similarities between UDCA and DCA were more likely to validate than similarities between UDCA and Dex. In fact, no genes similarly modulated by UDCA and Dex in the micro-array validated using RT-PCR. Numerous reasons could potentially explain this. It could reflect the smaller fold changes in gene expression seen with UDCA and Dex being more difficult to validate (Figure 8.3 in Appendix 3). Another possible explanation for the different expression profiles induced by UDCA and Dex is that UDCA simulated GR may not interact with DNA in the same way as GC-stimulated GR. Miura *et al* demonstrated that GC-stimulated GR co-localized with TIF2 (a co-activator for NSR that results in upregulation of DNA transcription) in the nucleus. However, in UDCA-stimulated cells GR

translocation occurred but induced a diffuse nuclear pattern of the GR; one which did not overlap with the TIF2 foci. This suggests that the GC-GR and the UDCA-GR complexes associate with different nuclear protein structures. Therefore, it is unlikely that the UDCA-GR complex will have a genetic profile identical to that of the Dex-GR complex [167, 169]. Yet similarities are also likely to exist. The gene S100P was identified as one of the genes most upregulated by both UDCA and Dex. This gene is regarded as GR dependent [388]. However, this gene was also upregulated by DCA undermining that it is necessarily upregulated by a selective UDCA-GR interaction.

A final reason for the poor validation of genes similarly modulated by UDCA and Dex may have been the experimental design. In the absence of a pro-inflammatory stimulant, UDCA and Dex may not have had a chance to exert a significant *trans*-repressive effect via the GR. As *trans*-repression is thought to be the predominant mechanism through which UDCA mediates its GR effects, we may not have identified this using our current experimental design, thus we may have failed to identify a significant similarity between UDCA and Dex. UDCA was certainly able to prevent the upregulation of IL-8 induced by DCA.

The research in this chapter needs further work to be undertaken in the future. Firstly, demonstration of the *trans*-repressive potential of UDCA and DCA in oesophageal cell lines needs to be demonstrated. Next, further exploration of the similarities between UDCA and Dex needs to be pursued. The genes chosen to validate the micro-array data demonstrated that the individual effects of Dex and UDCA in the HET-1A cell line were reliable. However, the genes chosen to investigate genes similarly modulated by Dex and UDCA failed to validate using RT-PCR. It would certainly be interesting to validate SAE1 and S100P as these were two of the biggest hits identified as modulated by both Dex and UDCA in the micro-array.

Finally, functional work needs to be pursued. In particular, the finding that DCA up-regulates STAM2 and SERPINE1 could be of interest to pursue. The roles of these genes (modulating ITGAV and endocytic recycling) suggest that they may influence cell adhesion. STAM2 is required for endocytic recycling and lysosomal degradation. High levels of STAM2 expression induce fragmentation of the golgi apparatus [432-435]. ITGAV, integrin α_5 and α_6 have all been shown to be recycled through a long endocytic recycling loop through the PNRC and the golgi apparatus [331, 488] and fragmentation of the organelle has been identified in the colonic cell line HCT116 after exposure to DCA [436]. SERPINE1 reduces the surface expression of ITGAV and the adhesion of ITGAV to vitronectin [406-407, 410-412]. Although SERPINE1 upregulation does not explain the reduction in the surface expression of integrins α_5 and α_6 it is certainly worthy of further study. Therefore, investigation of these genes could potentially further elucidate the mechanism through which DCA induces cell detachment (Chapter 3).

4.6. Conclusion

The aims of this chapter were to:

- Investigate the expression of the GR in oesophageal tissues,
- To investigate whether UDCA could be used to activate the GR, and,
- To investigate similarities between the mRNA expression profiles induced by UDCA and Dex and UDCA and DCA.

This research has demonstrated that UDCA modulates the GR in oesophageal cells. The identification that the GR is expressed in squamous epithelium but not BO suggests that targeting this receptor could provide a therapy which targets squamous epithelium but not BO. This research certainly demonstrates that in the absence of GR, Dex (and possibly UDCA) exerts little effect on gene expression, as exhibited by the HCT116 cell line. Thus modulation of the GR could be potentially be used to reduce inflammatory pathways in squamous epithelium, either reducing the risk of generating BO or protecting squamous epithelium from collateral damage while targeting BO for ablation.

The mRNA expression profile induced by UDCA is distinct from that induced by DCA or Dex. However, there are significant overlaps in the expressed gene profile of UDCA and Dex and UDCA and DCA. DCA and Dex demonstrate less similarity between gene expression profiles. The physical structure of UDCA (having similarities to both DCA and Dex) may explain this finding. It also suggests that the overlap in gene expression profiles between UDCA and DCA and UDCA and Dex is probably real. Therefore, UDCA may be able to modulate the GR in oesophageal cells. However, further validation and functional work will need to be undertaken in order to confirm this hypothesis.

Even if no further similarities between UDCA and Dex were validated in future experiments, UDCA does exerts less cellular stress than DCA (as demonstrated by the up-regulation of ER stress genes and pro-inflammatory genes). Therefore, oesophageal inflammation could possibly be reduced through displacement of DCA from the circulating BA pool by the oral administration of UDCA.

Chapter 5.

5. Discussion of Research and Conclusions

GORD is a prevalent disease in the western world. Up to 20% of the western population will complain of symptoms of sufficient severity to impact their quality of life [2-3]. In up to 10% of these patients BO will exist [5, 16]. This metaplastic epithelium protects the oesophagus against erosive oesophagitis and the risk of ulcers or inflammatory peptic strictures. However, it carries a risk of developing into OAC. The most current estimates place the risk at less than 0.5% per year among those with no dysplasia or LGD [489-491].

Interestingly the hereditary genetic component to these diseases is negligible [30-32]. Apart from gender, BO and OAC are archetypal environmental diseases with obesity, smoking and GORD being the predominant aetiological risk factors [8, 15, 33-38]. Smoking and obesity can addressed through behaviour modification, albeit with varying success. GORD remains only partially treated. The refluxate of GORD is predominantly comprised of acid and BAs [18, 20]. PPIs and H2RAs have effectively targeted the acid component of GORD and have successfully reduced the incidence of erosions, ulcerations and strictures and in the oesophagus [492]. However despite the success in reducing these non-malignant complications, the incidence of BO and OAC has risen steadily over the last three decades [14, 27-28].

BAs present in refluxate remain the untreated component of GORD. Increasing exposure of the oesophagus to BAs has been shown to correlate with an increasing risk of erosive oesophagitis, BO and OAC [18, 20-21]. Retrospective epidemiological studies, performed after the advent of tools to assess oesophageal BA exposure, have confirmed the independent role of BAs in the aetiology of OAC [15]. Research has shown these amphipathic molecules are pro-inflammatory, carcinogenic molecules. Even when acid is adequately suppressed by the administration of PPIs, significant levels of DGOR can continue and this puts GORD patients at risk of developing metaplastic and neoplastic complications [53-54].

5.1. The Role of BAs in Inflammation and Carcinogenesis in the Oesophagus

BAs have been identified as pro-inflammatory molecules in numerous diseases. The most well known are cholestatic diseases of the liver. In these diseases BAs have been shown to up-regulate inflammatory and apoptotic pathways. Similarly, in the oesophagus, exposure to BAs can result in significant pathology. High concentrations of BAs in the oesophagus result in micelles which have detergent properties and destroy cell membranes. Even at concentrations below the CMC, BAs damage the cell membrane, releasing phospholipids, cholesterol and arachadonic acid which results in the generation of ROS and RNS [108-111]. Individual protonated BAs may traverse the cell membrane, where they are then ionised and become trapped intracellularly. Increasing

concentrations of intracellular BA have been shown to correlate with increasing mucosal damage [110-111, 119-120]. Once intracellular, BAs activate inflammatory pathways or exert mutagenic effects [66, 86, 121]. BAs induce mitochondrial depolarization which generates ROS independently of their effects on the cell membrane [156, 195]. They can also upregulate expression of COX-2 which, as a by product of its function, produces ROS [131]. IL-8, NF-κB and downstream NF-κB dependent genes have also been shown to be induced in oesophageal cells exposed to BAs [85, 133].

Through the inflammatory mechanisms described above, BAs are also carcinogenic. The production of ROS induces oxidative DNA damage and replication errors as well as inhibiting the function of mismatch repair mechanisms [66]. The p53 mutation, found in over 90% of OAC, frequently occurs as a result of oxidative damage and highlights that inflammation and ROS are likely carcinogens in OAC [122-123]. Genotoxicity has also been demonstrated in HET-1A cells during short duration BA exposure, without a reduction in viability [88], and chromosomal damage has been identified in the OE33 and KYSE30 cell lines in response to BAs [86].

Animal models have demonstrated that BA exposure is significantly more likely to result in the genesis of columnar lined oesophagus and adenocarcinoma than acid exposure in the presence or absence of a tumour promoter [56-59]. In humans, the independent role of BAs in the aetiology of BO is well demonstrated by the finding that post-gastrectomy patients, whose oesophagi are not exposed to acid, may still develop BO even though there is minimal inflammatory injury to the oesophageal mucosal [17, 55].

Of particular concern is that highly efficacious acid suppression therapy, which significantly reduces the inflammatory consequences of GORD, may be compounding the toxicity of BAs. In animal models, acid has been shown to protect against BA-induced OAC in the presence of a tumour promoter [58]. Hypothetically, this finding could partially explain the increasing incidence of OAC during last three decades [493].

5.2. The Need for a New Therapeutic for the Treatment of GORD.

Strategies to prevent the rising incidence of OAC are limited. PPIs target the acid component of reflux but have failed to impact on the rising incidence of OAC. No therapeutic agent currently exists to counter the inflammatory and carcinogenic potential of BAs. Of more concern, the carcinogenic potential of BAs may be propagated by the use of PPIs.

Therefore, in a highly prevalent environmental disease (GORD) which carries a moderate risk of developing metaplastic complication (BO) and a low but definite risk of a neoplastic consequence (OAC), a significant risk factor remains untreated.

Furthermore, screening GORD patients for BO and OAC appears ineffective in reducing mortality. Firstly, symptomatology and the risk of oesophagitis, BO and OAC remain poorly correlated [5]. Secondly, while the risk of developing OAC in the setting of BO is 100 times that of the general population, there is no definite reduction in life expectancy or increase in mortality associated with BO [494]. Therefore, screening for BO and OAC is arguably neither cost effective nor beneficial to the patient. This presents a significant dilemma for clinicians. The prognosis of OAC is dismal and therefore PPIs are prescribed and screening for OAC is often undertaken in the setting of biopsy proven BO.

There is a need for a safe and effective therapeutic which targets BA-induced inflammation in the oesophagus. Ideally, this therapeutic could be safely prescribed in conjunction with PPIs to a large cohort of the population at the onset of GORD symptoms. This strategy could potentially be used to empirically in this prevalent disease to lower the risk of a developing a metaplastic or neoplastic complication.

5.3. UDCA

UDCA has been shown to modulate the inflammatory, apoptotic and carcinogenic effects of BAs such as DCA. There appear to be two predominant mechanisms through which UDCA is hypothesised to exert its effects.

The first is through attenuation of the pro-inflammatory signalling mechanisms that are upregulated by cell stress such as that caused by BAs. *In-vitro*, UDCA has been shown to reduce the generation of ROS induced by BAs, protect mitochondria from depolarization induced by BAs and, reduce the mutagenicity of BAs [116-117, 156-157, 165, 179, 194-195, 225, 495-496]. UDCA has also been shown to directly inhibit DCA-induced expression of COX-2 [117, 165] and to induce the production of anti-oxidants, potentially mitigating BA-induced ROS production [154-155] without up-regulating ROS itself [68].

The second potential anti-inflammatory mechanism of UDCA is activation of the GR [168-169, 171, 376]. The interaction appears to enhance the *trans*-repressive and inhibitory attributes of the GR without resulting in significant *trans*-activation [116, 167, 169-171]. GR mediated *Trans*-repression inhibits the functions of pro-inflammatory transcription factors such as NF-κB and AP-1. The activity of these transcription factors is reduced by UDCA [166]. This could not only reduce inflammation, but could also hypothetically prevent cellular apoptosis [167-168].

Yet, despite a large volume of literature suggesting an *in vitro* anti-inflammatory and anti-apoptotic role for UDCA, the findings are not ubiquitous. Some authors have argued that UDCA is pro-apoptotic or may synergise with other BAs to induce mitochondrial damage and cell death [197,

203-204, 269, 497-498]. Perhaps more concerning is that since this PhD was undertaken there has been an increase in the published literature regarding the null or harmful effects of UDCA *in vivo*. A Cochrane review published in 2009 concluded that UDCA did not increase life expectancy or reduce the risk of HCC in patients with PBC [499]. Two papers, similarly published since the beginning of this research, have suggested that high dose UDCA may even be harmful. The first suggests no benefit with treatment and an increase in the number of severe adverse events in patients receiving high dose UDCA for the treatment of PSC [500]. The second suggested an increase in the rate of colorectal cancer in ulcerative colitis patients who have PSC and who are receiving UDCA [501]. These findings highlight the potential danger of UDCA at high doses. Despite these concerning findings, low to moderate dose UDCA remains one of the accepted therapeutics for cholestatic hepatic disease and it thought to be of significant benefit in specific subsets of patients [502-503].

Therefore, based on *in-vitro* and previous *in-vivo* data, the hypothesis investigated in this PhD was that UDCA may be of therapeutic use in the modulation of BA induced inflammation and apoptosis and in the oesophagus.

5.4. UDCA Reduces DCA-Induced Apoptosis but does not Reduce the Total Magnitude of DCA-Induced Cell Death

BAs induce both inflammation and apoptosis in the oesophagus [15]. Greater exposure of the oesophagus to refluxate has been shown to correlate with a more severe inflammatory phenotype [20-22] and increasing levels of apoptosis are seen in increasingly severe inflammatory oesophageal disease [184]. Significant levels of apoptosis have been demonstrated in the oesophagi of rats who had undergone an oesophagoduodenostomy demonstrating that BAs can induce this phenotype in the absence of acid [187]. Furthermore, in this model, glutathione levels in the oesophageal cells were increased, suggesting that apoptosis, and the resulting oesophagitis, are mediated by ROS and RNS [187]. The ability of BAs to induce free radicals in oesophageal cell lines has been demonstrated [85-86, 188]. Therefore, modulation of BA-induced apoptosis is likely to reflect modulation of inflammation in normal squamous epithelium and *vice versa*.

In the first part of this research we investigated the role of UDCA in modulating cell death induced by DCA in the oesophageal cell line HET-1A. UDCA at low doses inhibited cellular proliferation while higher doses induced cell death. Consistent with the published literature, the magnitude of this effect was much less than that seen with DCA exposure. Although 300μM UDCA did not induce PARP cleavage in subsequent experiments, the micro-array experiment demonstrated that UDCA was inducing the expression of numerous ER-stress genes (GDF-15, TRIB3, DDIT3, etc) in

a fashion very similar to DCA. Thus, UDCA in this cell line may be pro-apoptotic independently of DCA, albeit at a much lower level.

UDCA pre-treatment (but not co-treatment) reduced PARP cleavage and mitochondrial depolarisation induced by DCA. PARP cleavage was the most specific marker of apoptosis used in this research and this demonstrates that UDCA pre-treatment is reducing apoptosis in these cell lines. Co-treatment of DCA with UDCA led to increased levels of these apoptotic markers above that of DCA alone. Other markers of "apoptosis" (TUNEL and AV/PI based flow cytometry) were not influenced by UDCA pre- or co-treatment. However, these are less specific markers of apoptosis; the validity of both assays for differentiating apoptosis from necrosis and autophagy has been questioned [256, 272]. These findings argue that UDCA pre-treatment, but not co-treatment, is reducing apoptosis in the oesophageal cell line HET-1A.

The demonstration that autophagy was induced by DCA added further complexity to the analysis of this data. Similar to the findings seen with PARP, DCA increased LC3-II expression in a fashion consistent with autophagy. Co-treatment with UDCA unpredictably modulated the upregulation of LC3-II while UDCA pre-treatment consistently reduced LC3-II expression after four hours DCA stimulation but increased it after twelve hours. This may suggest that UDCA pre-treatment at least transiently protects against autophagy.

However, UDCA did not attenuate the reduction in cell viability induced by DCA in any of five experimental setups, at any of nine concentration combinations investigated, or at any of the three time-points investigated. In MTT assays UDCA demonstrated a null effect, neither enhancing nor reducing DCA-induced cell death. In the nuclear count assay UDCA appeared to enhance DCA-induced cell death, although this result was called into question by the subsequent finding that BAs modulate adhesion in the HET-1A cell line.

Taken together, the findings presented in this research suggest that UDCA pre-treatment is likely to induce a reduction in DCA-induced apoptosis and autophagy, but at the expense of an increase in necrosis. To further this research, it would be interesting to repeat the explant experiments using higher concentrations of BAs in order to determine whether UDCA could protect against DCA-induced cell death in explanted human tissue. Expression of cleaved PARP, in combination with explant viability, could be used to determine the mechanism of cell death being induced by the different treatment strategies.

Based on this research, it is unknown if UDCA would be beneficial in modulating the inflammatory and apoptotic phenotype induced by DGOR *in vivo*. Although the concentrations of BAs used in this oesophageal research had little effect on the viability of explanted human tissue, the toxicity exerted by UDCA *in vitro* is consistently less than that exerted by DCA. Therefore, displacement of hydrophobic BAs by oral administration of UDCA could potentially reduce the

magnitude of the inflammatory and carcinogenic effects of DGOR. The finding that UDCA pre-treatment attenuated DCA-induced mitochondrial depolarisation infers that there would be a reduction in the quantity of ROS and RNS induced by BA exposure. Consequently, there is likely to be a reduction in pro-inflammatory signalling. As such, it can be argued that UDCA could act as a chemo-preventative agent protecting against BO and OAC. However, if the findings presented here did translate to the *in vivo* setting, it is unknown what effect a switch from apoptosis to necrosis would cause. Any reduction in apoptosis (and pro-inflammatory signalling) could be counteracted by pro-inflammatory effects of necrosis in the oesophagus.

5.5. DCA Modulates Adhesion Molecules

Based on data identified in research regarding the effect of DCA and UDCA on cell death in the HET-1A cell line, we hypothesised that both DCA and UDCA were inducing a loss of adhesion. We confirmed that DCA induces a loss of adherence in a dose dependent fashion and that cells which had become detached are capable of re-adhering to uncoated plastic. Loss of adhesion appeared predominantly specific for the ECM protein vitronectin although a smaller significant loss of adherence was seen to the ECM protein laminin. Consistent with these findings, there was a reduction in the surface expression of ITGAV and the integrins α_5 and α_6. ITGAV has specificity for vitronectin and Integrin α_6 is a laminin receptor. Surface expression of ITGAV returned to baseline levels twelve hours after the removal of the DCA stimulus consistent with the finding that detached cells were capable of re-adherence. Strengthening the hypothesis was the finding that ITGAV fluorescent intensity at the inter-cellular junctions of explanted oesophageal tissue was almost significantly reduced by exposure to DCA.

These findings were however identified at the same concentrations of DCA that were inducing cell death and up-regulating markers of apoptosis. As the process of cell death, especially apoptosis, induces a loss of adherence, it was important to demonstrate that these two effects were discrete entities. The finding that detached cells were capable of re-adhering, that loss of adhesion was specific to certain ECM proteins, and that the surface expression of only a subgroup of integrins (appropriate to the ECM proteins with reduced HET-1A adherence) were modulated by DCA argues that the loss of adhesion is not a primarily mediated by cell death.

While not directly conclusive as a mechanism through which DCA reduces the surface expression of ITGAV, we demonstrated that ITGAV co-localises with Rab5 and Rab11. Consistent our findings, ITGAV, integrin α_5 and α_6 have all been shown to be recycled through a long (Rab 11) endocytic recycling loop through the PNRC and the golgi apparatus [331, 488]. DCA treatment induced an alteration in Rab vesicle morphology consistent with impaired endocytosis. As integrins

are dynamic molecules on the cell surface constantly undergoing endocytic recycling, impairment of this process could hypothetically result in a reduction in the surface expression of these molecules. Interestingly our findings did not suggest that the impairment of endocytic recycling was due to impaired function of Rab GTPases.

The micro-array experiment suggested further possible mechanisms through with DCA may be inducing a loss of adhesion in the HET-1A cell line. One of the most interesting findings from this was that DCA significantly up regulated the expression of SERPINE1 mRNA. This protein is known to specifically modulate the adhesion of ITGAV to vitronectin [406-407, 410-412]. Although this does not explain the reduction in the surface expression of integrins α_5 and α_6, is certainly worthy of further study. STAM2 mRNA expression was also significantly up regulated by DCA exposure. STAM2 is required for functional endocytosis, lysosomal degradation and receptor down-regulation [432-434]. Excess levels of this protein have been shown to induce fragmentation of the Golgi apparatus [435]. Fragmentation of this organelle has been identified in the colonic cell line HCT116 after exposure to DCA through a mechanism involving PKCη [436].

These novel findings may hold significant relevance regarding the pathophysiology of erosive oesophagitis and BO. Not only is a loss of adhesion molecules likely to reduce the adhesive strength of squamous cells and to reduce pro-survival ("outside-in") signalling, it may also increase the susceptibility of oesophageal cells to acid reflux. H^+ toxicity associated with refluxate is known to be propagated when adhesion molecules between cells are damaged by proteases such as trypsin and pepsin [11]. Furthermore, the presence of DIS between epithelial cells after exposure of the oesophagus to DGOR has been well documented and this is hypothesised to allow refluxate to penetrate deeper into the mucosa.[112-113]. The greater penetration of acid and BAs into the oesophageal epithelium, will not only allow stimulation of nociceptors, worsening the symptoms of GORD, but also allows refluxate access to the basal layer stem cells, enhancing the risk of mutagenic change in these cells, possibly increasing the risk of BO.

As we have demonstrated that DCA modulates the surface expression of adhesion molecules, this could potentially represent a new mechanism by which DCA propagates the erosive and mutagenic properties of GORD. That QH cells resisted the effect of DCA on cell detachment and ITGAV surface expression adds further strength to the hypothesis that DCA-induced reduction in the surface expression of cell adhesion molecules may be involved in the pathogenesis of BO. However, despite suggestions that UDCA was independently modulating a loss of adhesion, and could attenuate the DCA-mediated reduction in adherence to vitronectin in the HET-1A cell line, we could find no evidence of this in adhesion assays to uncoated plastic or in studies of surface expression of the integrins. Thus, UDCA neither reduced nor enhanced the effects of DCA.

To further this research, demonstration of the reduction in surface expression of ITGAV in more oesophageal cell lines is needed. The HEEpiC cell line (Human Esophageal Epithelial Cell, a primary oesophageal cell line), would represent an ideal starting point to begin validating this work. *In-vivo* validation that GORD reduces ITGAV could be pursued using explanted tissue from patients with GORD. However, the finding that ITGAV is up-regulated in peri-ulcerated regions of rat oesophagus suggests that non ulcerated areas of the oesophagus would have to be targeted for this research. Investigation in to the role of SERPINE1 over-expression in this model could be undertaken by repeating the adhesion assays after siRNA knockdown of SERPINE1 or pharmacological inhibition of the protein using PAI-039 (tiplaxtinin). If this were to have a role this model, it could potentially be targeted as a treatment strategy to reduce symptoms of GORD as well as the metaplastic and neoplastic risk associated with this disease.

5.6. UDCA Induces a Discrete Gene Signature Which Has Limited Concordance With DCA or Dex

While UDCA had not reduced the magnitude of DCA-induced cell death or detachment in the HET-1A cell line, it appeared to reduce apoptosis. Although it is likely that multiple mechanisms of cell death were being induced by these treatments, the finding that pre-treatment with UDCA could reduce DCA-induced levels of PARP cleavage and mitochondrial depolarization suggested that UDCA could exert some of the anti-inflammatory and anti-apoptotic effects in the HET-1A cell line that are published in the literature.

We first demonstrated that the GR was present in a variety of oesophageal cell lines representing the normal-BO-OAC sequence and UDCA was capable of modulating the GR in these cell lines. Consistent with the published literature, UDCA only induced nuclear translocation of the GR at fold concentrations of UDCA over Dex, nuclear translocation was much slower with UDCA, and the *trans*-activational potential of UDCA activated GR is much lower than that of Dex [167, 169, 171-172].

One of the most interesting findings identified in this research was the novel finding that the GR was strongly expressed in the squamous epithelium of the oesophagus but not in BO. This finding demonstrated that a key target needed for UDCA to induce an anti-inflammatory effect was present in squamous epithelium of the oesophagus. The absence of this anti-inflammatory transcription factor in BO suggests that any GR-mediated effects are unlikely to affect BO to a significant degree. Consequently administration of UDCA to patients with GORD could enhance the survival of DGOR-stressed squamous epithelium. This could attenuate the selective pressure induced by GORD to favour the presence of BO in the oesophagus above squamous epithelium. If this

hypothesis were true, administration of UDCA to patients with GORD could potentially reduce the incidence and prevalence of BO in the GORD population. Similarly, the administration of UDCA to patients with BO, whether dysplastic or not, who are undergoing ablative therapy may enhance survival of squamous epithelium over that of Barrett's epithelium. This could potentially facilitate more aggressive therapy to ablate BO while protecting squamous epithelium from collateral damage. Furthermore, the presence of a GR ligand in the oesophagus during these therapies could potentially reduce the risk of post therapy complications including fibrotic (post-inflammatory) strictures.

In the final part of this research, we investigated the gene expression profile induced by UDCA and similarities between it and the gene expression profiles induced by Dex and DCA. The HET-1A cell line was the most sensitive to UDCA. Interestingly, the genes with most altered expression after UDCA treatment in the HET-1A cell line were those associated with ER stress. However, the upregulation of these ER stress genes by UDCA was much lower than the change induced by DCA. This finding was consistent with the low level of cytotoxicity demonstrated by UDCA in proliferation and viability assays.

Consistent with the published literature, Dex similarly altered the expression of approximately 100 genes in the HET-1A and OE33 cell lines. It is estimated that this number of genes represents a core set modulated by this transcription factor in any given tissue [487]. UDCA and Dex simultaneously modulated a number of genes associated with the GR in both the HET-1A and OE33 cell lines. In the HET-1A cell line, UDCA induced further alterations in the expression of genes known to be associated with GR (e.g. S100P). These findings suggest that UDCA is indeed modulating the GR.

Although UDCA induced a gene expression profile discrete to that of DCA or Dex, similarities between all three treatments also existed. While only a subset of genes induced by each treatment were similarly modulated by other treatments, the similarity between Dex and UDCA appeared as great as the similarity between DCA and UDCA. While similarities existed between DCA and Dex, it was to a much lesser extent than the similarities between the other treatments. One explanation for this may be that UDCA represents a molecule with structural similarities to both DCA and Dex and as such exerts some structure-function effects of both.

To develop this research, further validation of genes similarly modulated by UDCA and Dex needs to be undertaken. Subsequently, we would examine whether UDCA could modulate the pro-inflammatory genes similar to the reduction we have demonstrated in IL-8 upregulation (i.e. those upregulated by DCA). If UDCA were to modulate these genes in a fashion similar to how it is modulating IL-8, knockdown of the GR using SiRNA technology could elucidate whether this effect was being mediated through this transcription factor. Finally, an animal model of BA reflux

could be used to further validate this cohort of genes, potentially demonstrating that that UDCA could modulate BA-induced inflammation in the oesophagus *in vivo*.

5.7. Conclusion

Despite three decades of clinical use, the role of UDCA as a therapeutic in BA mediated inflammatory diseases is still controversial. While *in-vitro* data suggests that UDCA could potentially be a therapeutic agent to modulate diseases in which BAs induce pathology, *in-vivo* the role of this molecule remains unproven.

The aim of this PhD was to begin investigating whether UDCA could be used to modulate inflammation and cell death in the oesophagus. Our findings suggest that this molecule may have this potential. At the least, displacement of hydrophobic BAs by oral administration is likely to reduce ER stress induced by DGOR. However, micro-array data suggests that UDCA shares similarities in its gene expression profile with Dex. This suggests that it may have a role as an anti-inflammatory molecule as well. Therefore, it could potentially be used as a chemo-preventative to reduce the inflammatory consequences of reflux in patients with GORD.

An unexpected finding was also identified in this research; that DCA could modulate adhesion in an oesophageal cell line. This previously unidentified finding suggests a further mechanism through which BAs could mediate erosive oesophagitis and increase the risk of re-epithelialisation of the oesophagus with BO. Targeting this therapeutically in patients with GORD symptoms or those with erosive oesophagitis could hypothetically not only reduce symptoms of GORD (by reducing permeation of GORD deep into the oesophageal epithelial layers where nociceptive receptors are present), but could also reduce the risk of generating BO, thereby reducing the risk of OAC.

Appendix 1.

6. Appendix 1: Supplemental Data from Chapter 2

This appendix contains supplemental data for chapter 2: "The Effect of Ursodeoxycholic Acid in Modulating Deoxycholic Acid Induced Apoptosis and Cell Death in an Oesophageal Cell Line". These experiments were undertaken in order to determine whether UDCA could modulate cell death in the HET-1A cell line representing normal oesophageal epithelium.

Figures 6.1 to 6.20 demonstrate the following experiments in both the HET-1A and the HCT116 cell lines:

- No UDCA pre-treatment prior to UDCA and DCA co-treatment
- Eighteen hours UDCA pre-treatment prior to DCA treatment
- Four hours UDCA pre-treatment prior to UDCA and DCA co-treatment,
- Four and Eighteen hours UDCA pre-treatment prior to UDCA and DCA co-treatment.

In none of the experimental designs did UDCA protect against DCA induced cell death.

Figures 6.21 to 6.24 demonstrate that longer duration pre-treatment (18 hours vs. 4 hours) reduces viability in the HCT-16 cell line and demonstrates the nuclear area analysis experiments not presented in chapter 2.

6.1. List of Figures

Figure 6–1: The effect of DCA and UDCA co-treatment, with no pre-treatment, in the HET-1A cell line as determined by a nuclear count assay normalised to untreated cells. 263

Figure 6–2: The effect of DCA and UDCA co-treatment, with no pre-treatment, in the HET-1A cell line as determined by an MTT assay normalised to untreated cells..... 264

Figure 6–3: The effect of DCA and UDCA co-treatment, with no pre-treatment, in the HCT116 cell line as determined by a nuclear count assay normalised to untreated cells..... 265

Figure 6–4: The effect of DCA and UDCA co-treatment, with no pre-treatment, in the HCT116 cell line as determined by an MTT assay normalised to untreated cells..... 266

Figure 6–5: The effect of DCA, UDCA and 18 hours UDCA pre-treatment prior to DCA treatment in HET-1A cells as determined by a nuclear count assay normalised to untreated cells 267

Figure 6–6: The effect of DCA, UDCA and 18 hours UDCA pre-treatment prior to DCA treatment in HET-1A cells as determined by an MTT assay normalised to untreated cells. 268

Figure 6–7: The effect of DCA, UDCA and 18 hours UDCA pre-treatment prior to DCA treatment in HCT116 cells as determined by a nuclear count assay normalised to untreated cells 269

Figure 6–8: The effect of DCA, UDCA and 18 hours UDCA pre-treatment prior to DCA treatment in HCT116 cells as determined by an MTT assay normalised to untreated cells. 270

Figure 6–9: The effect of DCA, UDCA and 4 hours UDCA pre-treatment prior to co-treatment in HET-1A cells as determined by a nuclear count assay normalised to untreated cells 271

Figure 6–10: The effect of DCA, UDCA and 4 hours UDCA pre-treatment prior to co-treatment in HET-1A cells as determined by an MTT assay normalised to untreated cells. 272

Figure 6–11: The effect of DCA, UDCA and 4 hours UDCA pre-treatment prior to co-treatment in HCT116 cells as determined by a nuclear count assay normalised to untreated cells 273

Figure 6–12: The effect of DCA, UDCA and 4 hours UDCA pre-treatment prior to co-treatment in HCT116 cells as determined by an MTT assay normalised to untreated cells 274

Figure 6–13: The effect of DCA, UDCA and 18 hours 300μM UDCA pre-treatment prior to co-treatment with various doses of DCA in HET-1A cells as determined by a nuclear count assay normalised to untreated cells 275

Figure 6–14: The effect of DCA, UDCA and 18 hours of various concentrations of UDCA pre-treatment prior to co-treatment with 300μM DCA in HET-1A Cells as determined by a nuclear count assay normalised to untreated cells 275

Figure 6–15: The effect of DCA, UDCA and 18 hours 300μM UDCA pre-treatment prior to co-treatment with various doses of DCA in HET-1A cells as determined by an MTT assay normalised to untreated cells. 276

Figure 6–16: The effect of DCA, UDCA and 18 hours of various concentrations of UDCA pre-treatment prior to co-treatment with 300μM DCA in HET-1A Cells as determined by an MTT assay normalised to untreated cells. 276

Figure 6–17: The effect of DCA, UDCA and 18 hours 300μM UDCA pre-treatment prior to co-treatment with various doses of DCA in HCT116 cells as determined by a nuclear count assay normalised to untreated cells 277

Figure 6–18: The effect of DCA, UDCA and 18 hours of various concentrations of UDCA pre-treatment prior to co-treatment with 300μM DCA in HCT116 cells as Determined by a nuclear count assay normalised to untreated cells 277

Figure 6–19: The effect of DCA, UDCA and 18 hours 300μM UDCA pre-treatment prior to co-treatment with various doses of DCA in HCT116 cells as determined by an MTT assay normalised to untreated cells 278

Figure 6–20: The effect of DCA, UDCA and 18 hours UDCA pre-treatment prior to co-treatment in HCT116 cells as determined by an MTT assay normalised to untreated cells. 278

Figure 6–21: Bland-Altman plots of the differences between the 4 hour pre-treated matrices and the 18 hour-pre-treated matrices for cell counts and MTT assays in the HCT116 cell line 279

Figure 6–22: The effect of UDCA and DCA and 18 hours UDCA pre-treatment prior to DCA on the nuclear area of HET-1A cells 280

Figure 6–23: The effect of UDCA and DCA co-treatment and 4 hours UDCA pre-treatment prior to DCA on the nuclear area of HCT116 cells 281

Figure 6–24: The effect of UDCA and DCA and 18 hours UDCA pre-treatment prior to DCA on the nuclear area of HCT116 cells 282

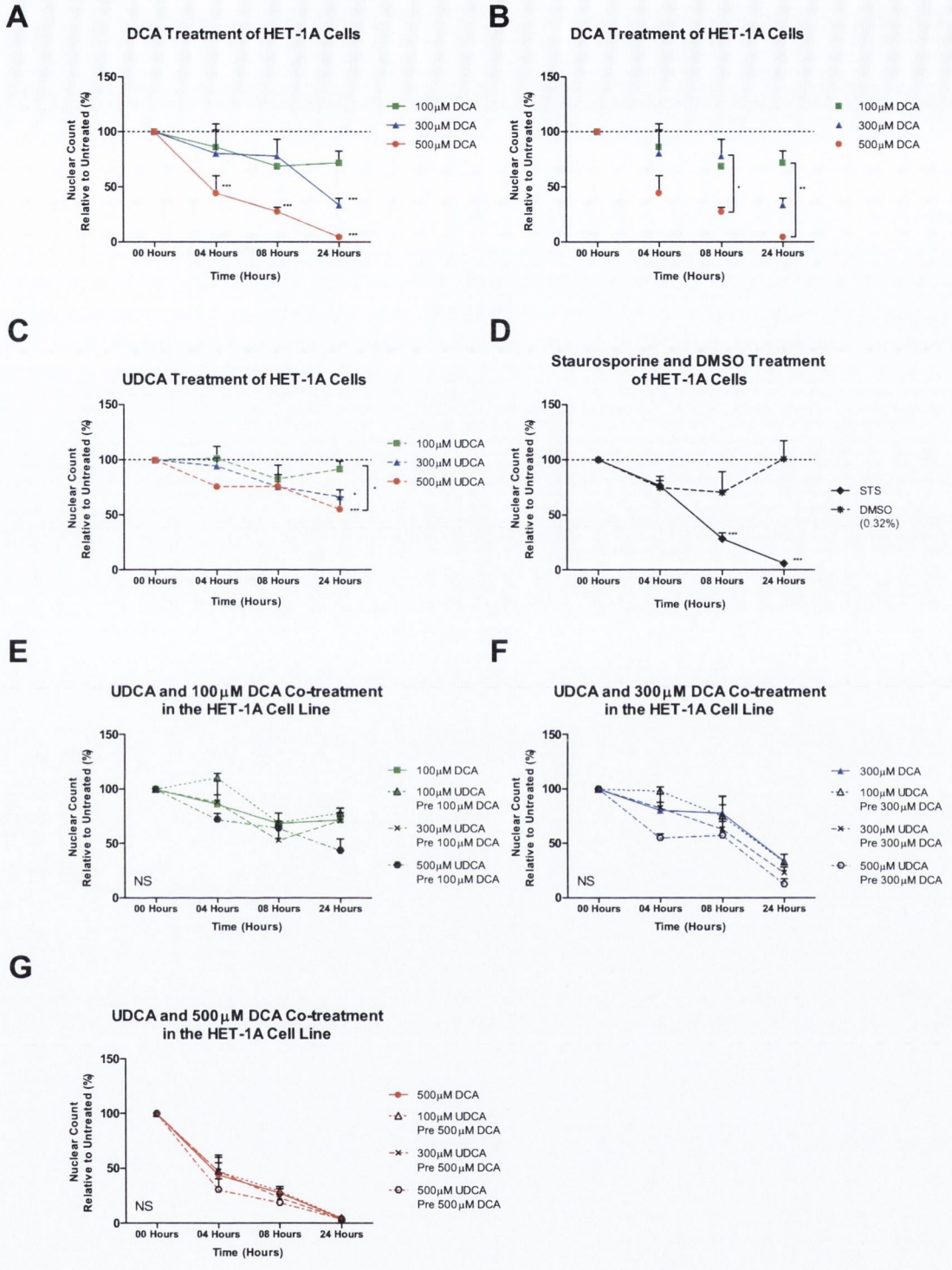

Figure 6–1: The effect of DCA and UDCA co-treatment, with no pre-treatment, in the HET-1A cell line as determined by a nuclear count assay normalised to untreated cells. DCA induced a time (A) and dose (B) dependent reduction in viability. UDCA stimulation reduced viability but to a lesser degree than DCA (C). 0.32% DMSO vehicle (equivalent to the highest vehicle concentration used) and the positive control staurosporine reduced viability at 24 hours only (D). UDCA pre-treatment prior to DCA reduced nuclear count below that of DCA alone at all concentrations studied (E - G). Results are mean and SEM of N=3. Analysis was performed using two-way ANOVA. * denotes $p < 0.05$, ** denotes $p < 0.01$ and *** denotes $p < 0.001$ compared to untreated cells. No differences were identified between co-treatment and DCA alone (E – G).

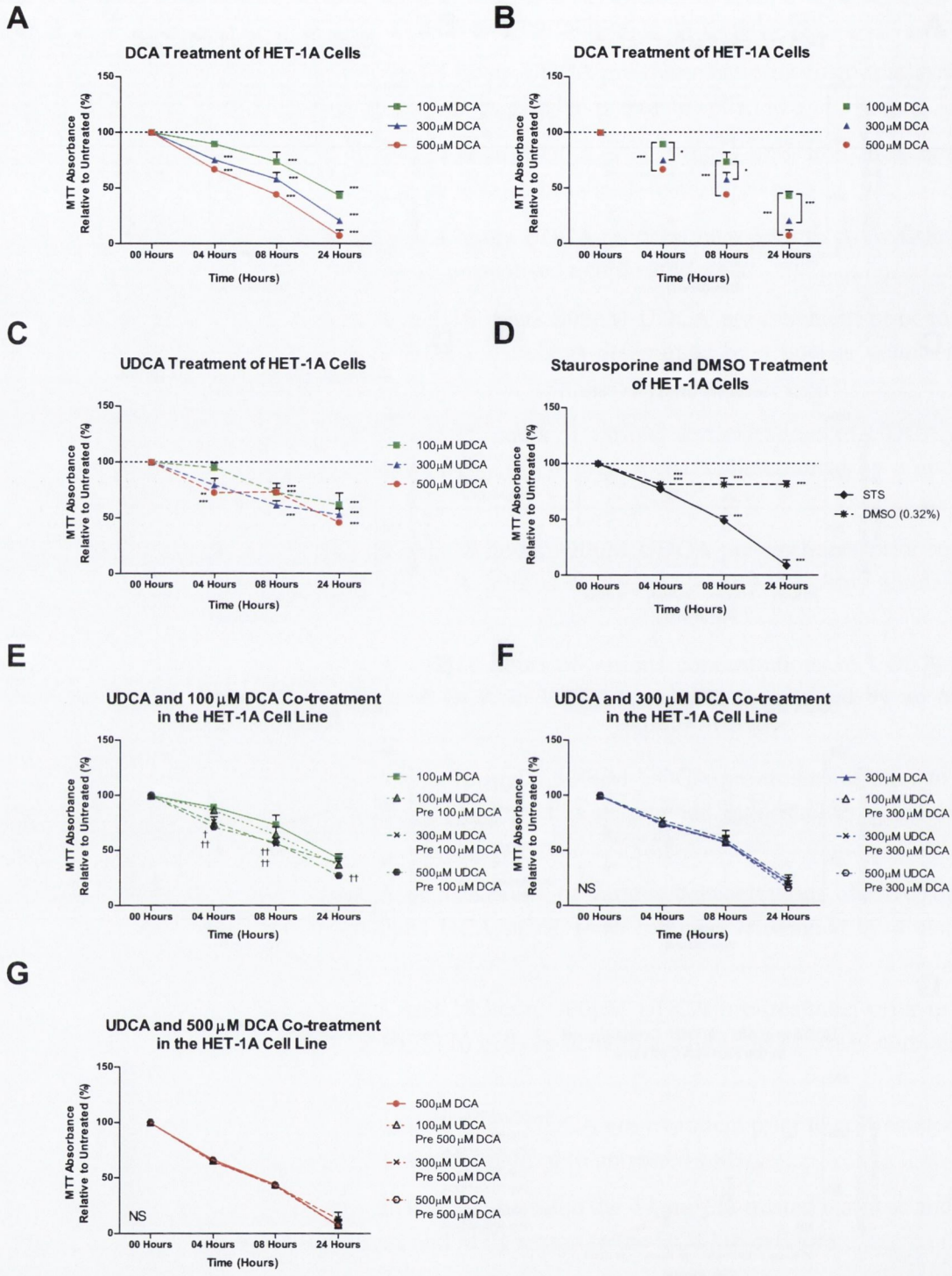

Figure 6–2: The effect of DCA and UDCA co-treatment, with no pre-treatment, in the HET-1A cell line as determined by an MTT assay normalised to untreated cells. DCA induced a time (A) and dose (B) dependent reduction in nuclear count. UDCA stimulation reduced viability but to a lesser degree than DCA (C). 0.32% DMSO vehicle, equivalent to the highest vehicle concentration used, and the positive control staurosporine, reduced viability at 24 hours only (D). UDCA pre-treatment prior to DCA reduced nuclear count below that of DCA alone at all concentrations studied (E - G). Results are mean and SEM of N=3. Analysis was performed using two-way ANOVA. */† denotes $p < 0.05$, **/†† denotes $p < 0.01$ and ***/††† denotes $p < 0.001$, * = relative to untreated (A, C, D) or different concentration of DCA (B) and † = relative to DCA alone (E – G).

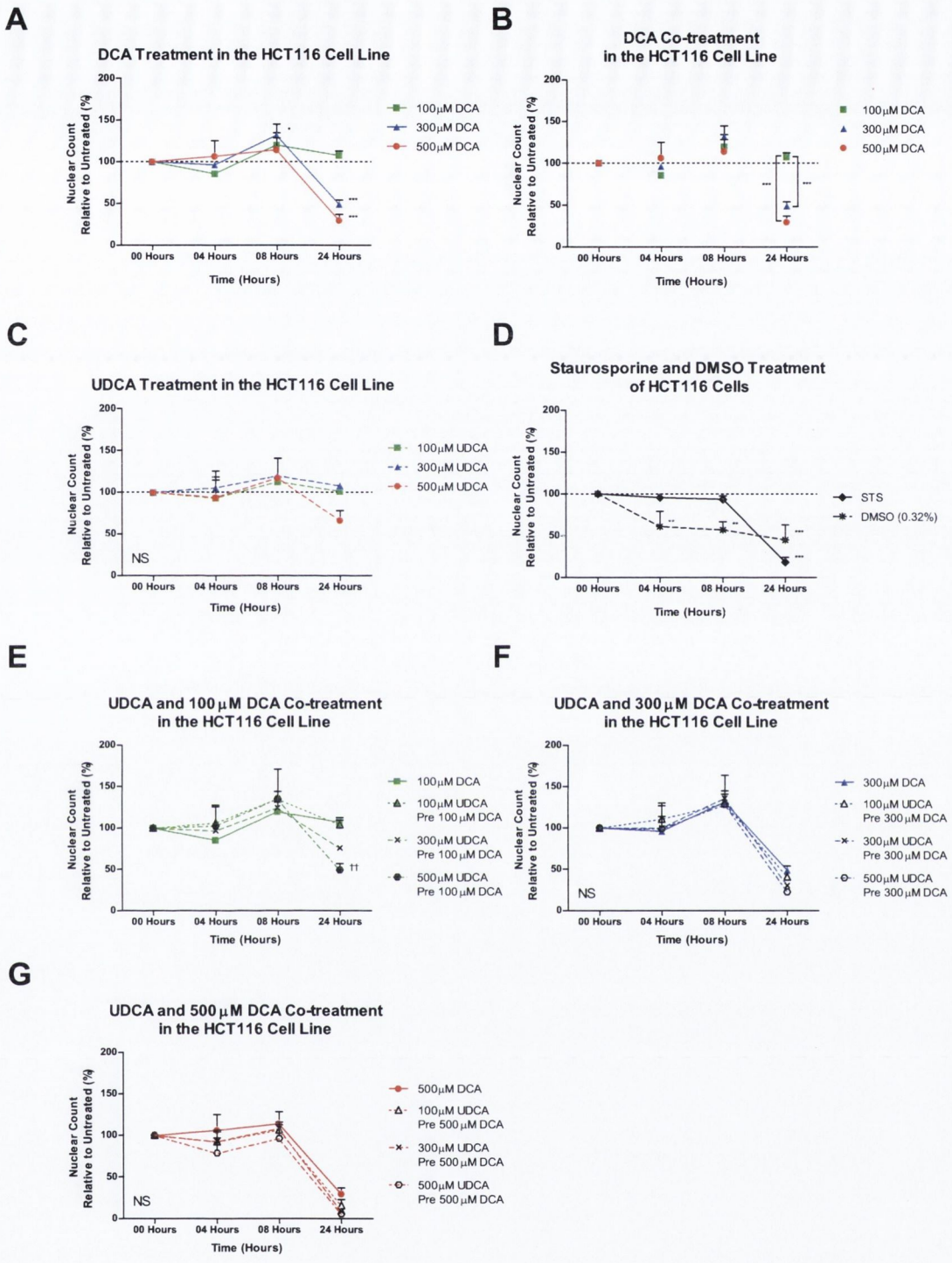

Figure 6–3: The effect of DCA and UDCA co-treatment, with no pre-treatment, in the HCT116 cell line as determined by a nuclear count assay normalised to untreated cells. DCA induced a time (A) and dose (B) dependent reduction in viability. UDCA stimulation reduced viability but to a lesser degree than DCA (C). 0.32% DMSO vehicle, equivalent to the highest vehicle concentration used, and the positive control staurosporine, reduced viability at 24 hours only (D). UDCA pre-treatment prior to DCA reduced nuclear count below that of DCA alone at all concentrations studied (E - G). Results are mean and SEM of N=3. Analysis was performed using two-way ANOVA. * denotes $p < 0.05$, **/†† denotes $p < 0.01$ and *** denotes $p < 0.001$, * = relative to untreated (A, D) or different concentration of DCA (B) and † = relative to DCA alone (E – G).

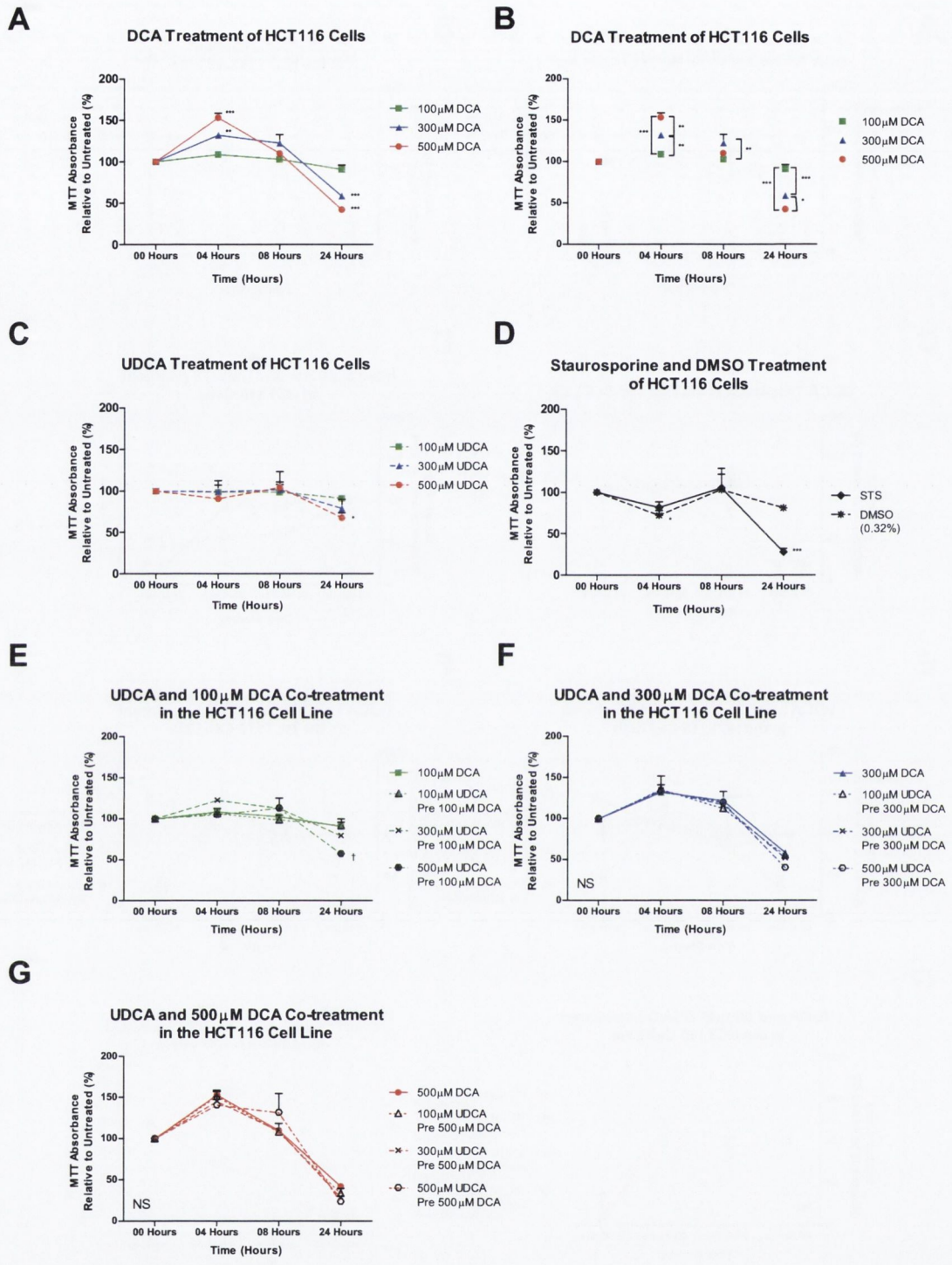

Figure 6–4: The effect of DCA and UDCA co-treatment, with no pre-treatment, in the HCT116 cell line as determined by an MTT assay normalised to untreated cells. DCA induced a time (A) and dose (B) dependent reduction in viability. UDCA stimulation reduced viability but to a lesser degree than DCA (C). 0.32% DMSO vehicle, equivalent to the highest vehicle concentration used, and the positive control staurosporine, reduced viability at 24 hours only (D). UDCA pre-treatment prior to DCA reduced nuclear count below that of DCA alone at all concentrations studied (E - G). Results are mean and SEM of N=3. Analysis was performed using two-way ANOVA. */† denotes $p < 0.05$, **/†† denotes $p < 0.01$ and ***/††† denotes $p < 0.001$, * = relative to untreated (A, C, D) or relative to different DCA concentration (B) and † = relative to DCA alone (E – G).

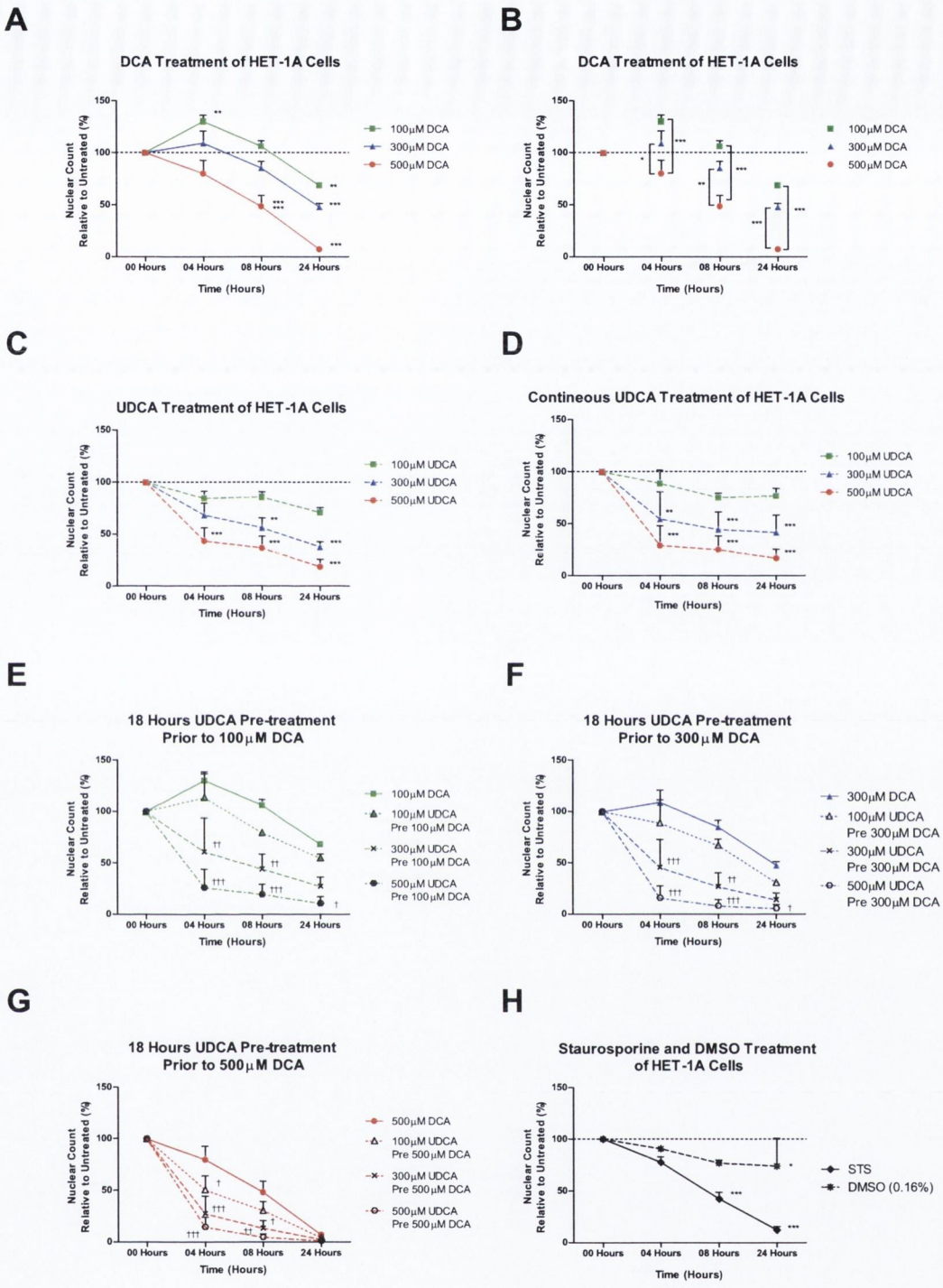

Figure 6–5: The effect of DCA, UDCA and 18 hours UDCA pre-treatment prior to DCA treatment in HET-1A cells as determined by a nuclear count assay normalised to untreated cells. DCA induced a time (A) and dose (B) dependent reduction in viability. UDCA stimulation reduced viability but to a lesser degree than DCA when treated for 24 hours (C) or for 18 hours pre-treatment followed by another 24 hours treatment (D). UDCA pre-treatment prior to DCA reduced nuclear count below that of DCA alone at all concentrations studied (E - G). The effect of 0.32% DMSO vehicle (equivalent to the highest vehicle concentration used) and the positive control staurosporine (H). Results are mean and SEM of N=3. Analysis was performed using two-way ANOVA. */† denotes $p < 0.05$, **/†† denotes $p < 0.01$ and ***/††† denotes $p < 0.001$, * = relative to untreated (A, C, D, H) or different concentration of DCA (B) and † = relative to DCA alone (E – G).

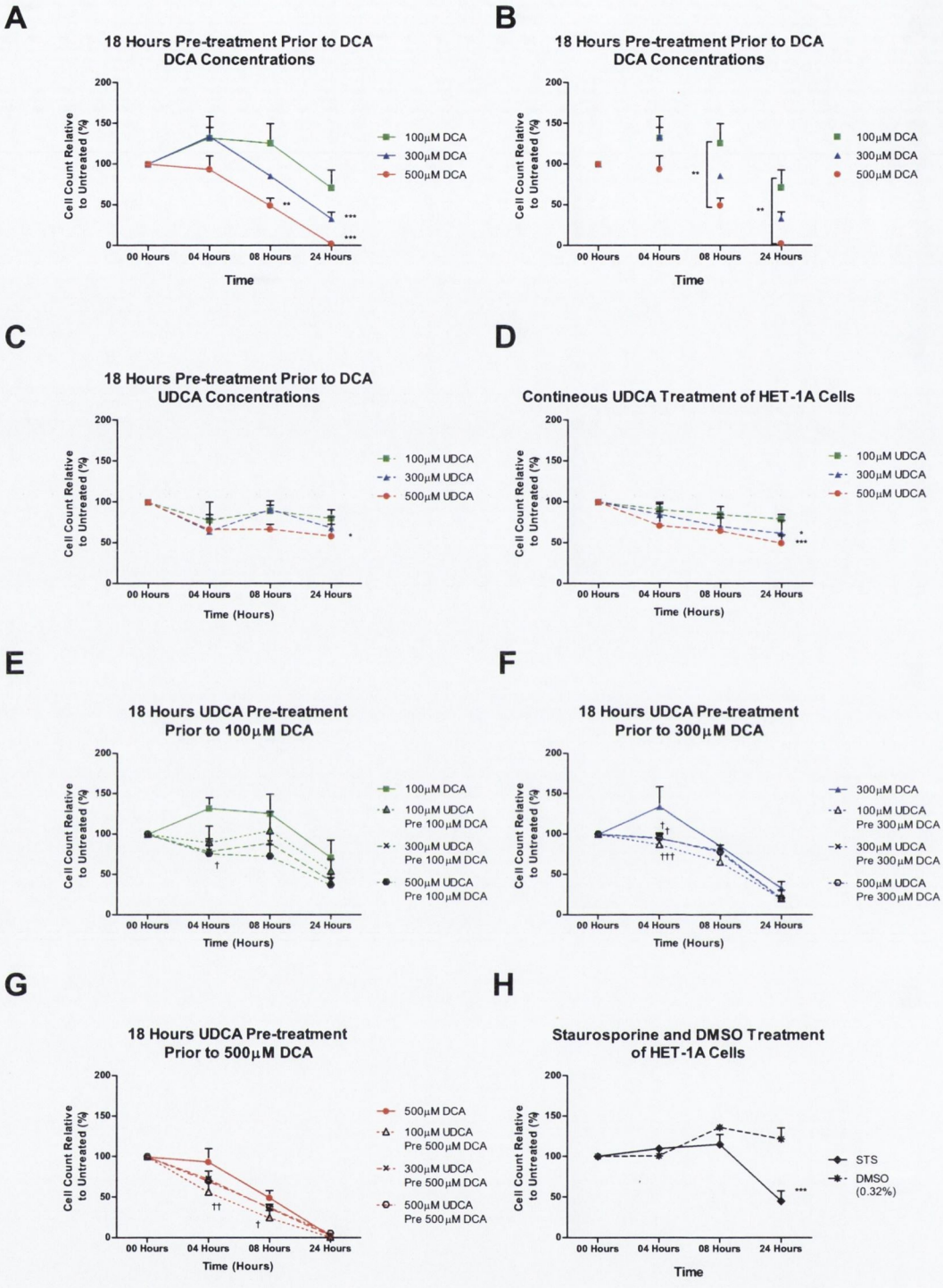

Figure 6–6: The effect of DCA, UDCA and 18 hours UDCA pre-treatment prior to DCA treatment in HET-1A cells as determined by an MTT assay normalised to untreated cells. DCA induced a time (A) and dose (B) dependent reduction in viability. UDCA stimulation reduced viability but to a lesser degree than DCA when treated for 24 hours (C) or for 18 hours pre-treatment followed by another 24 hours treatment (D). UDCA pre-treatment prior to DCA reduced nuclear count below that of DCA alone at all concentrations studied (E - G). The effect of 0.32% DMSO vehicle, equivalent to the highest vehicle concentration used, and the positive control staurosporine (H). Results are mean and SEM of N=3. Analysis was performed using two-way ANOVA. */† denotes $p < 0.05$, **/†† denotes $p < 0.01$ and ***/††† denotes $p < 0.001$, * = relative to untreated (A, C, D, H) or different concentration of DCA (B) and † = relative to DCA alone (E – G).

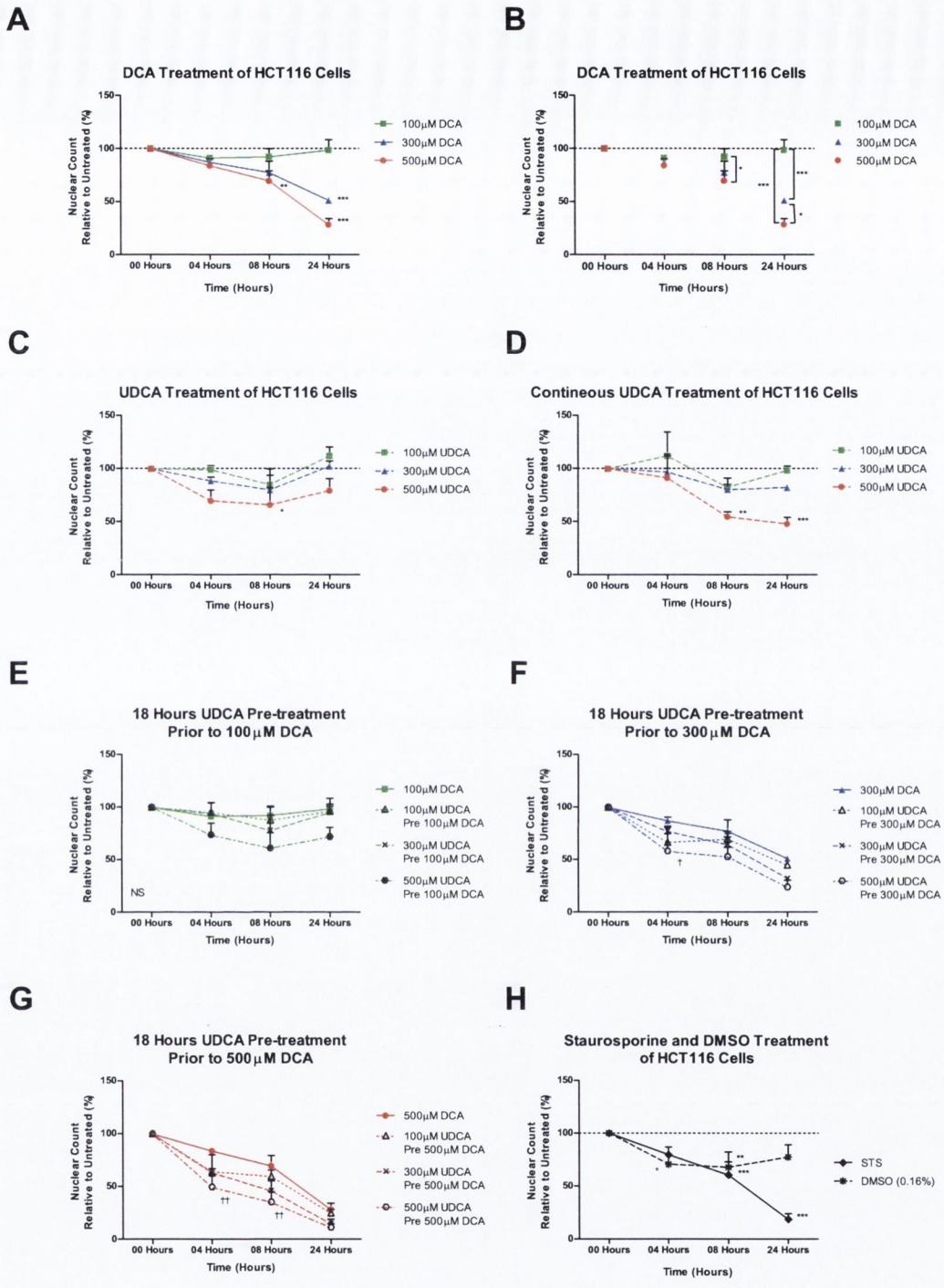

Figure 6–7: The effect of DCA, UDCA and 18 hours UDCA pre-treatment prior to DCA treatment in HCT116 cells as determined by a nuclear count assay normalised to untreated cells. DCA induced a time (A) and dose (B) dependent reduction in viability. UDCA stimulation reduced viability but to a lesser degree than DCA when treated for 24 hours (C) or for 18 hours pre-treatment followed by another 24 hours treatment (D). UDCA pre-treatment prior to DCA reduced nuclear count below that of DCA alone at all concentrations studied (E - G). The effect of 0.32% DMSO vehicle, equivalent to the highest vehicle concentration used, and the positive control staurosporine (H). Results are mean and SEM of N=3. Analysis was performed using two-way ANOVA. */† denotes $p < 0.05$, **/†† denotes $p < 0.01$ and ***/††† denotes $p < 0.001$, * = relative to untreated (A, C, D, H) or different concentration of DCA (B) and † = relative to DCA alone (E – G).

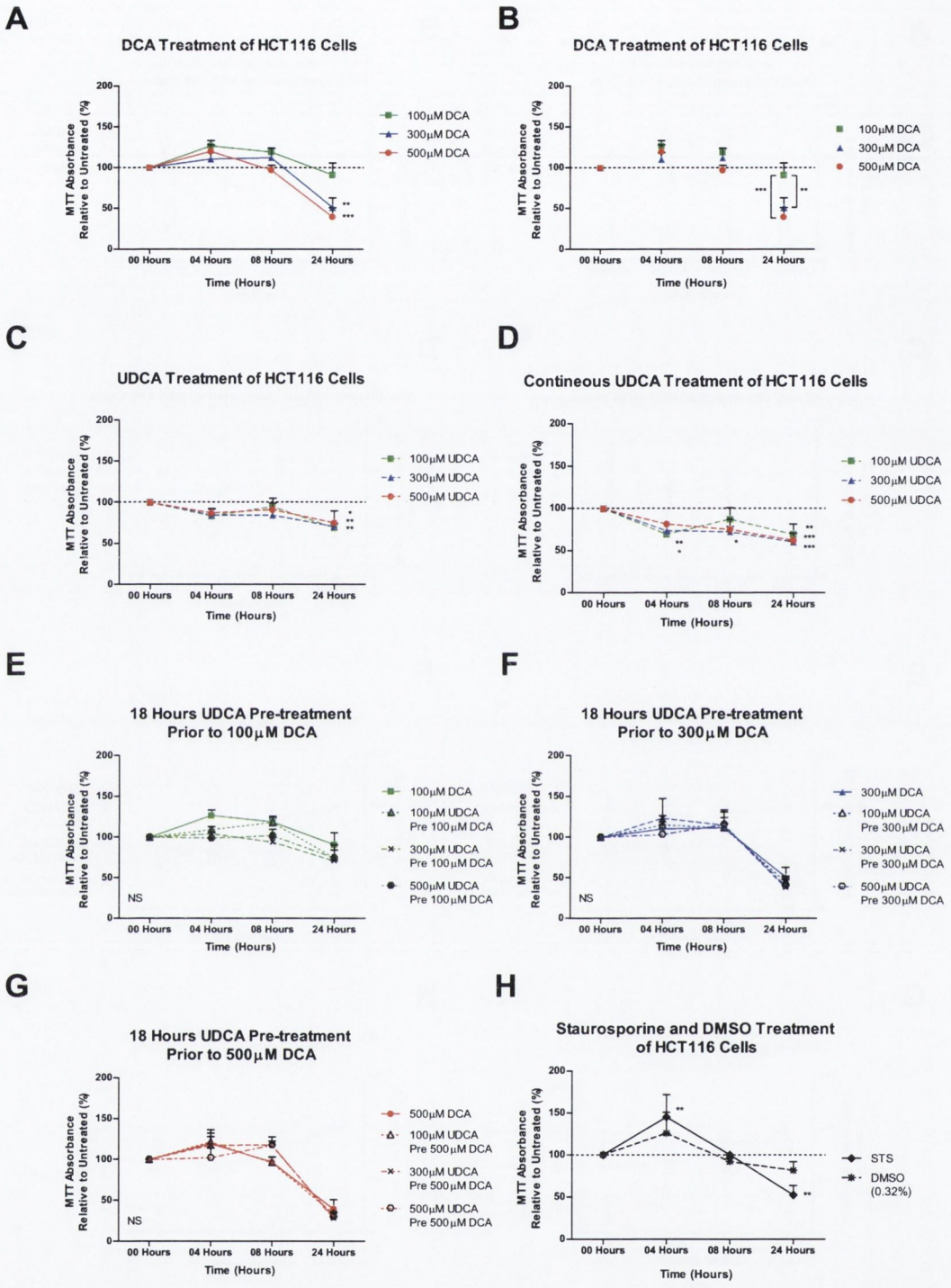

Figure 6–8: The effect of DCA, UDCA and 18 hours UDCA pre-treatment prior to DCA treatment in HCT116 cells as determined by an MTT assay normalised to untreated cells. DCA induced a time (A) and dose (B) dependent reduction in viability. UDCA stimulation reduced viability but to a lesser degree than DCA when treated for 24 hours (C) or for 18 hours pre-treatment followed by another 24 hours treatment (D). UDCA pre-treatment prior to DCA reduced nuclear count below that of DCA alone at all concentrations studied (E - G). The effect of 0.32% DMSO vehicle, equivalent to the highest vehicle concentration used, and the positive control staurosporine (H). Results are mean and SEM of N=3. Analysis was performed using two-way ANOVA. */† denotes $p < 0.05$, **/†† denotes $p < 0.01$ and ***/††† denotes $p < 0.001$, * = relative to untreated (A, C, D, H) or different concentration of DCA (B) and † = relative to DCA alone (E – G).

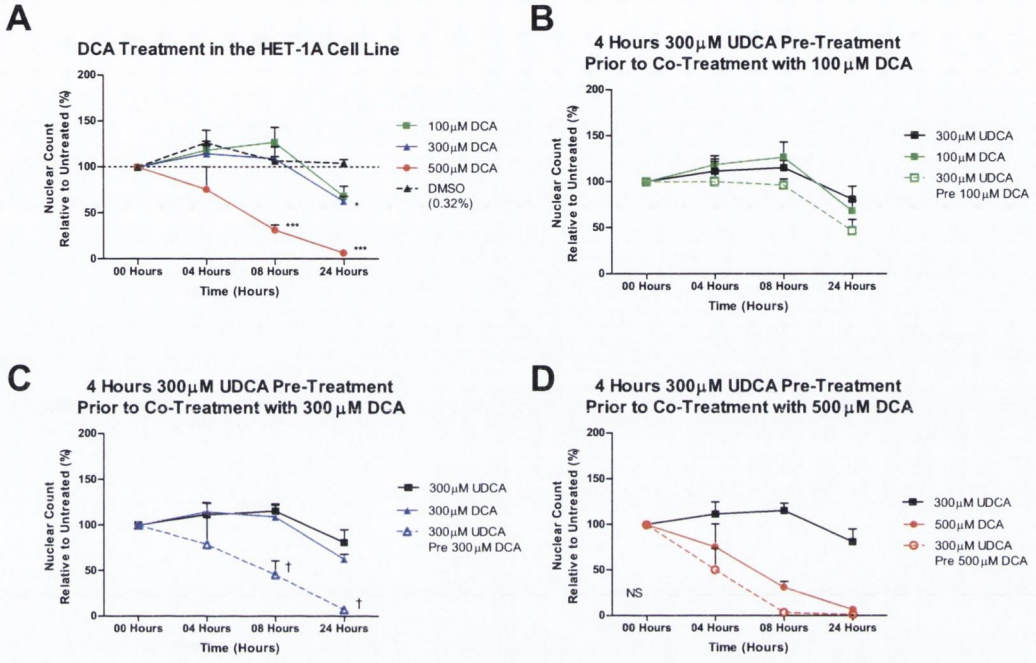

Figure 6–9: The effect of DCA, UDCA and 4 hours UDCA pre-treatment prior to co-treatment in HET-1A cells as determined by a nuclear count assay normalised to untreated cells. DCA induced a time and dose dependent reduction in viability (A). 4 hours UDCA pre-treatment followed co-treatment reduced nuclear count below that of DCA alone at all concentrations studied (B - D).Mean results and SEM of N=3. Comparative analysis was performed using two-way ANOVA. */† denotes $p < 0.05$, **/†† denotes $p < 0.01$ and ***/††† denotes $p < 0.001$, * = relative to untreated (A) and † = relative to DCA alone (B – D).

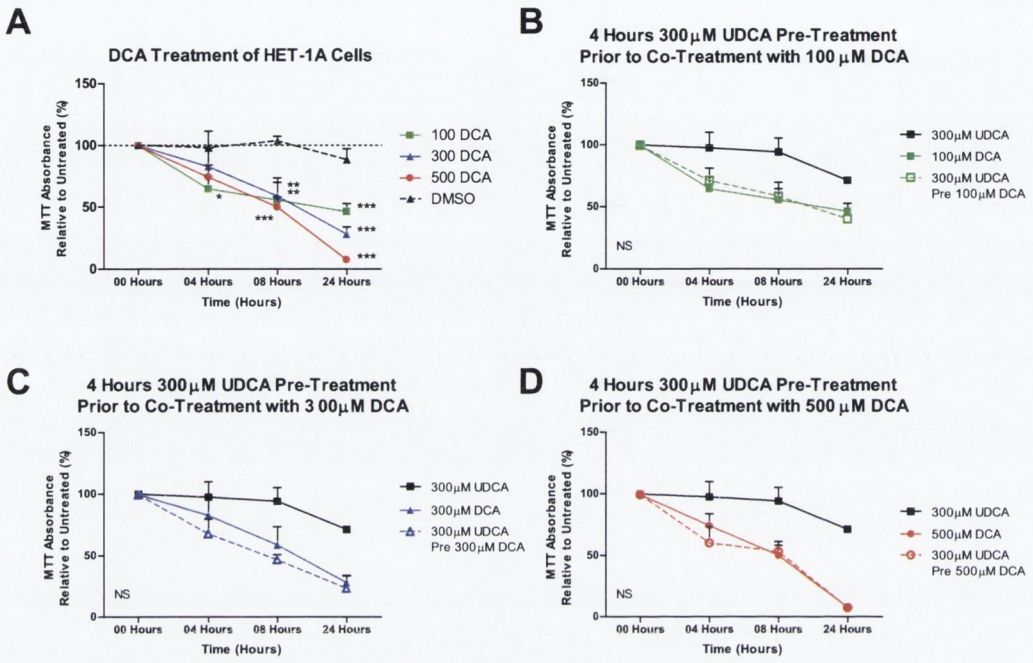

Figure 6–10: The effect of DCA, UDCA and 4 hours UDCA pre-treatment prior to co-treatment in HET-1A cells as determined by an MTT assay normalised to untreated cells. DCA induced a time and dose dependent reduction in viability (A). In this assay 4 hours UDCA pre-treatment followed co-treatment did not reduce viability below that of DCA alone (B - D). Mean results and SEM of N=3. Comparative analysis was performed using two-way ANOVA. * denotes $p < 0.05$, ** denotes $p < 0.01$ and *** denotes $p < 0.001$ compared to untreated cells (A).

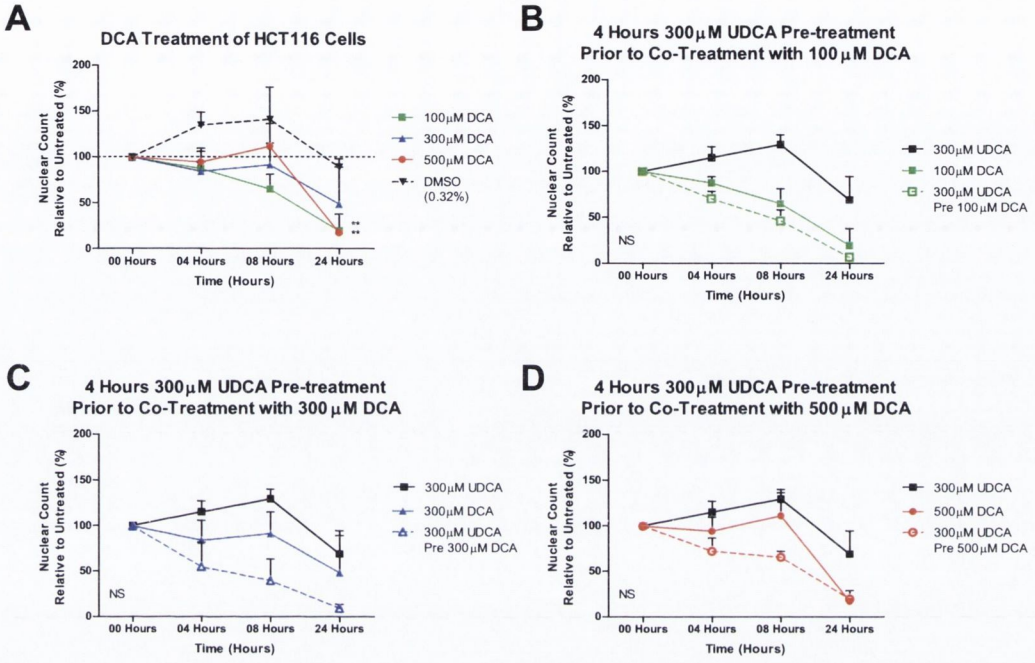

Figure 6–11: The effect of DCA, UDCA and 4 hours UDCA pre-treatment prior to co-treatment in HCT116 cells as determined by a nuclear count assay normalised to untreated cells. DCA induced a time and dose dependent reduction in nuclear count (A). In this assay 4 hours UDCA pre-treatment followed co-treatment did not significantly reduce viability below that of DCA alone (B - D). Mean results and SEM of N=3. Comparative analysis was performed using two-way ANOVA. ** denotes $p < 0.01$ compared to untreated cells (A).

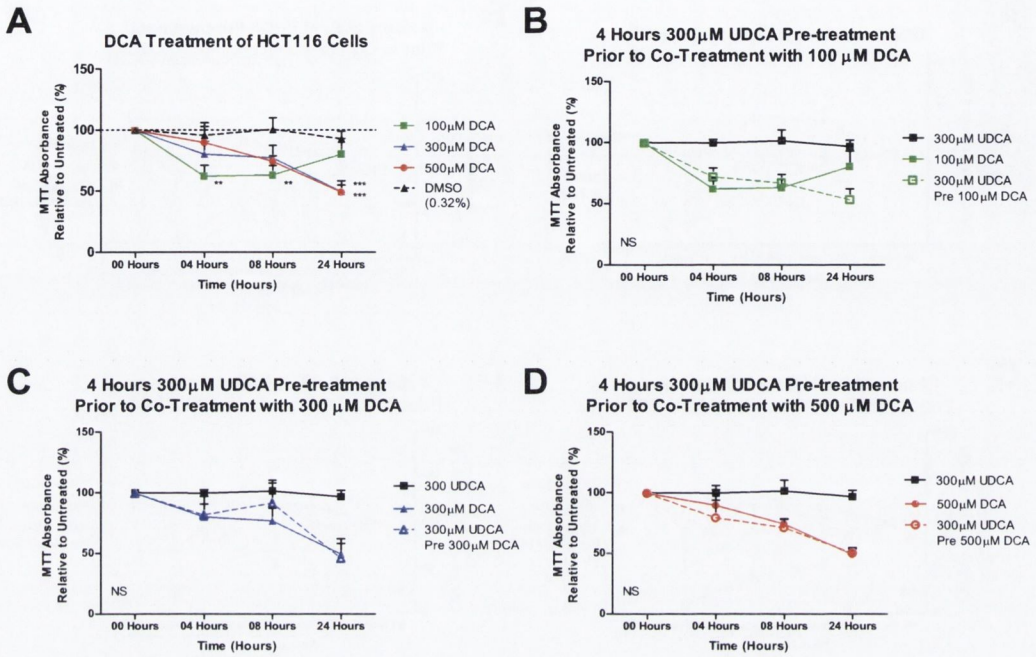

Figure 6–12: The effect of DCA, UDCA and 4 hours UDCA pre-treatment prior to co-treatment in HCT116 cells as determined by an MTT assay normalised to untreated cells. DCA induced a time and dose dependent reduction in viability (A). In this assay 4 hours UDCA pre-treatment followed co-treatment did not reduce viability below that of DCA alone (B - D). Mean results and SEM of N=3. Comparative analysis was performed using two-way ANOVA. ** denotes $p < 0.01$ and *** denotes $p < 0.001$ compared to untreated cells (A).

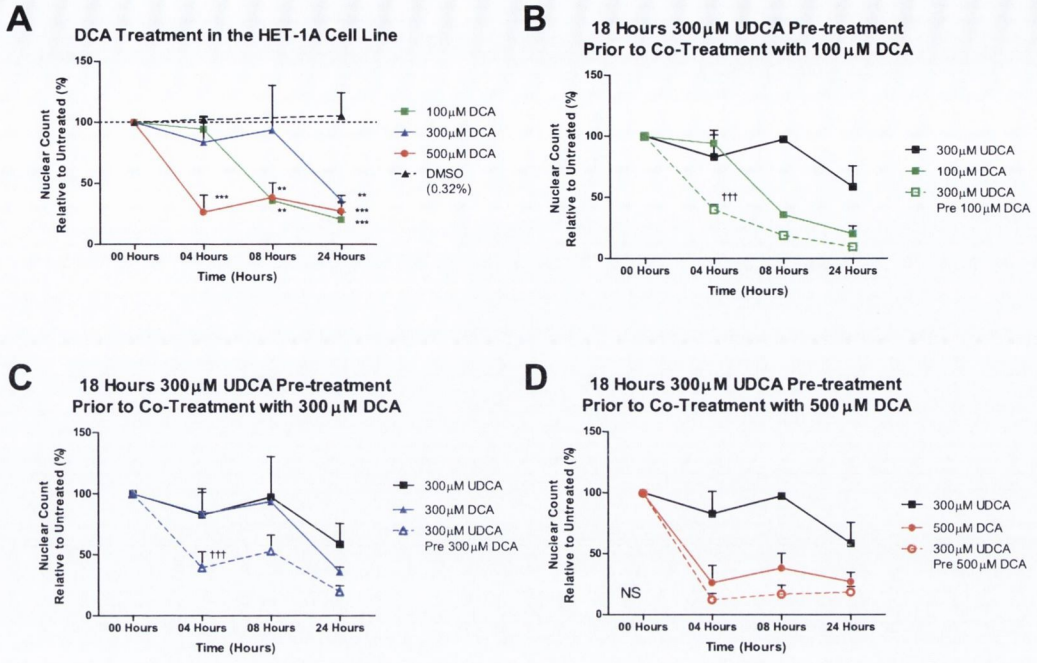

Figure 6–13: The effect of DCA, UDCA and 18 hours 300μM UDCA pre-treatment prior to co-treatment with various doses of DCA in HET-1A cells as determined by a nuclear count assay normalised to untreated cells. Mean results and SEM of N=3. Comparative analysis was performed using two-way ANOVA. */† denotes $p < 0.05$, **/†† denotes $p < 0.01$ and ***/††† denotes $p < 0.001$, * = relative to untreated (A) and † = relative to DCA alone (B – D).

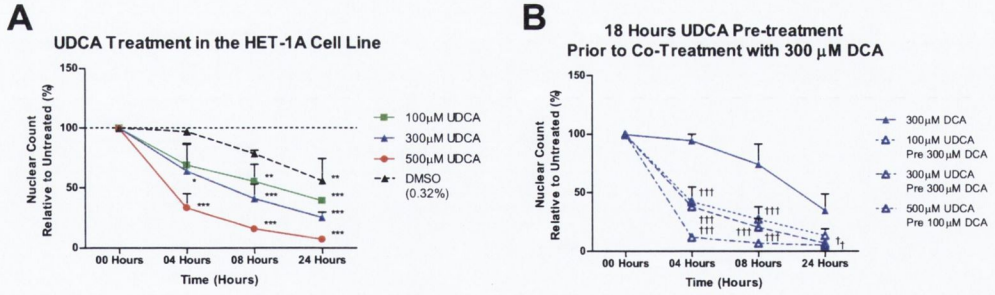

Figure 6–14: The effect of DCA, UDCA and 18 hours of various concentrations of UDCA pre-treatment prior to co-treatment with 300μM DCA in HET-1A Cells as determined by a nuclear count assay normalised to untreated cells. Mean results and SEM of N=3. Comparative analysis was performed using two-way ANOVA. */† denotes $p < 0.05$, **/†† denotes $p < 0.01$ and ***/††† denotes $p < 0.001$, * = relative to untreated (A) and † = relative to DCA alone (B).

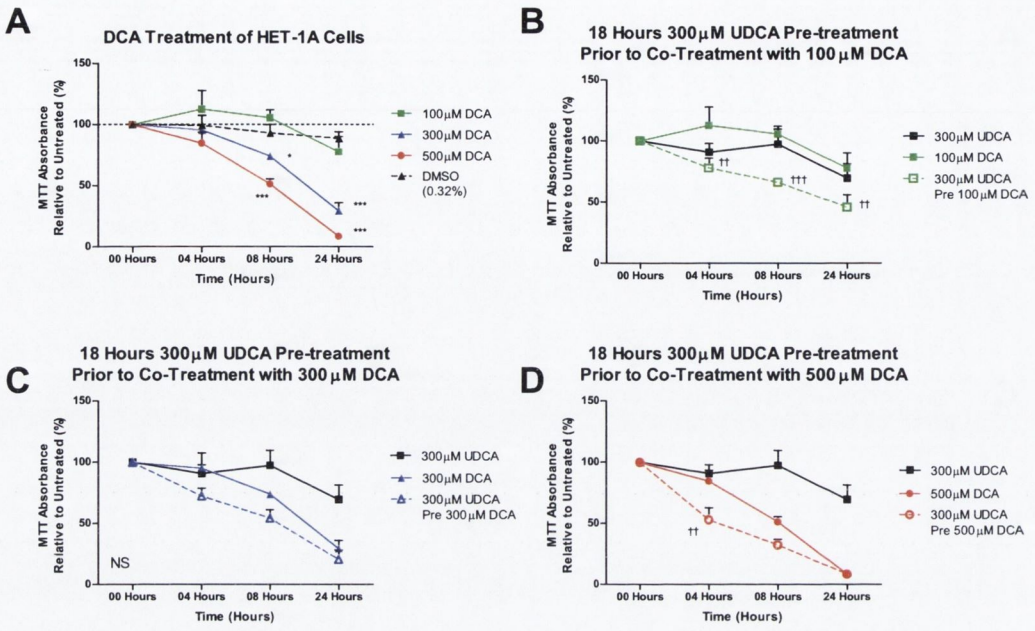

Figure 6–15: The effect of DCA, UDCA and 18 hours 300μM UDCA pre-treatment prior to co-treatment with various doses of DCA in HET-1A cells as determined by an MTT assay normalised to untreated cells. Mean results and SEM of N=3. Comparative analysis was performed using two-way ANOVA. */† denotes $p < 0.05$, **/†† denotes $p < 0.01$ and ***/††† denotes $p < 0.001$, * = relative to untreated (A) and † = relative to DCA alone (B – D).

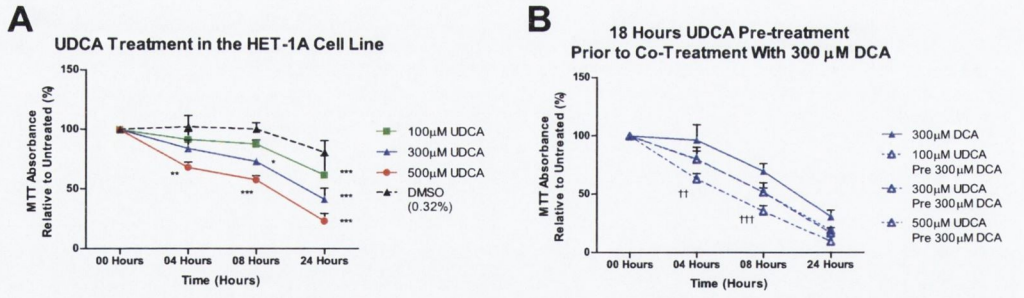

Figure 6–16: The effect of DCA, UDCA and 18 hours of various concentrations of UDCA pre-treatment prior to co-treatment with 300μM DCA in HET-1A Cells as determined by an MTT assay normalised to untreated cells. Mean results and SEM of N=3. Comparative analysis was performed using two-way ANOVA. **/†† denotes $p < 0.01$ and ***/††† denotes $p < 0.001$, * = relative to untreated (A) and † = relative to DCA alone (B).

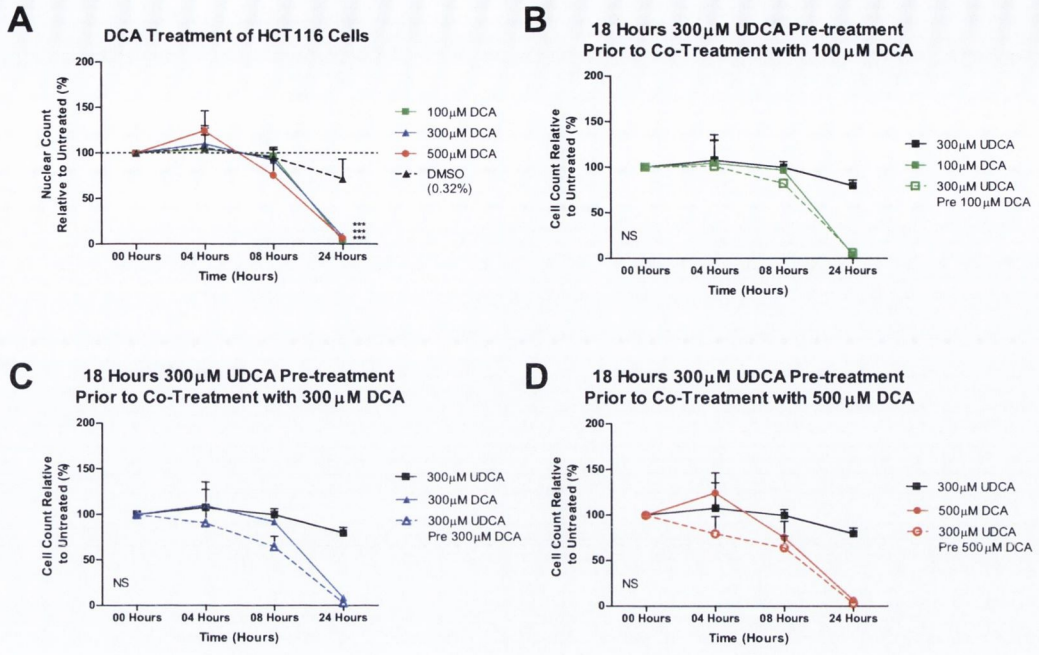

Figure 6–17: The effect of DCA, UDCA and 18 hours 300μM UDCA pre-treatment prior to co-treatment with various doses of DCA in HCT116 cells as determined by a nuclear count assay normalised to untreated cells. Mean results and SEM of N=3. Comparative analysis was performed using two-way ANOVA. *** denotes $p < 0.001$ relative to untreated cells (A).

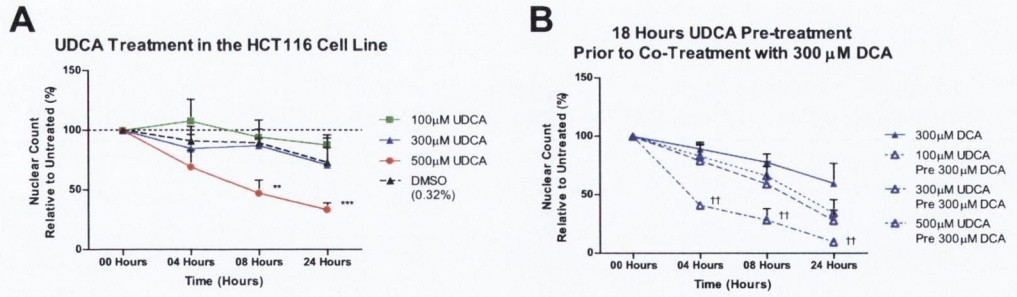

Figure 6–18: The effect of DCA, UDCA and 18 hours of various concentrations of UDCA pre-treatment prior to co-treatment with 300μM DCA in HCT116 cells as Determined by a nuclear count assay normalised to untreated cells. Mean results and SEM of N=3. Comparative analysis was performed using two-way ANOVA. **/†† denotes $p < 0.01$ and *** denotes $p < 0.001$, * = relative to untreated (A) and † = relative to DCA alone (B).

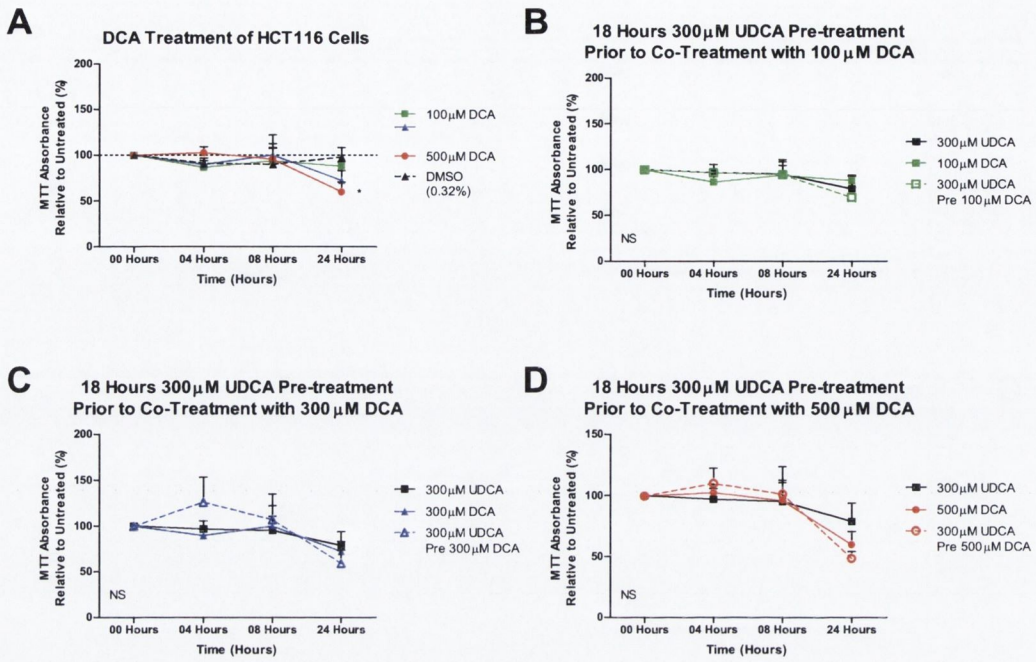

Figure 6–19: The effect of DCA, UDCA and 18 hours 300μM UDCA pre-treatment prior to co-treatment with various doses of DCA in HCT116 cells as determined by an MTT assay normalised to untreated cells. Mean results and SEM of N=3. Comparative analysis was performed using two-way ANOVA. * denotes $p < 0.05$ relative to untreated (A).

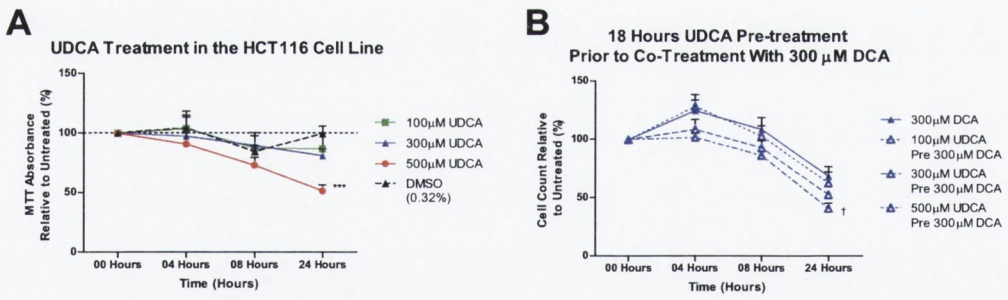

Figure 6–20: The effect of DCA, UDCA and 18 hours UDCA pre-treatment prior to co-treatment in HCT116 cells as determined by an MTT assay normalised to untreated cells. Mean results and SEM of N=3. Comparative analysis was performed using two-way ANOVA. ***denotes $p < 0.001$ compared to untreated cells (A) and † denotes $p < 0.05$ relative to DCA alone (B).

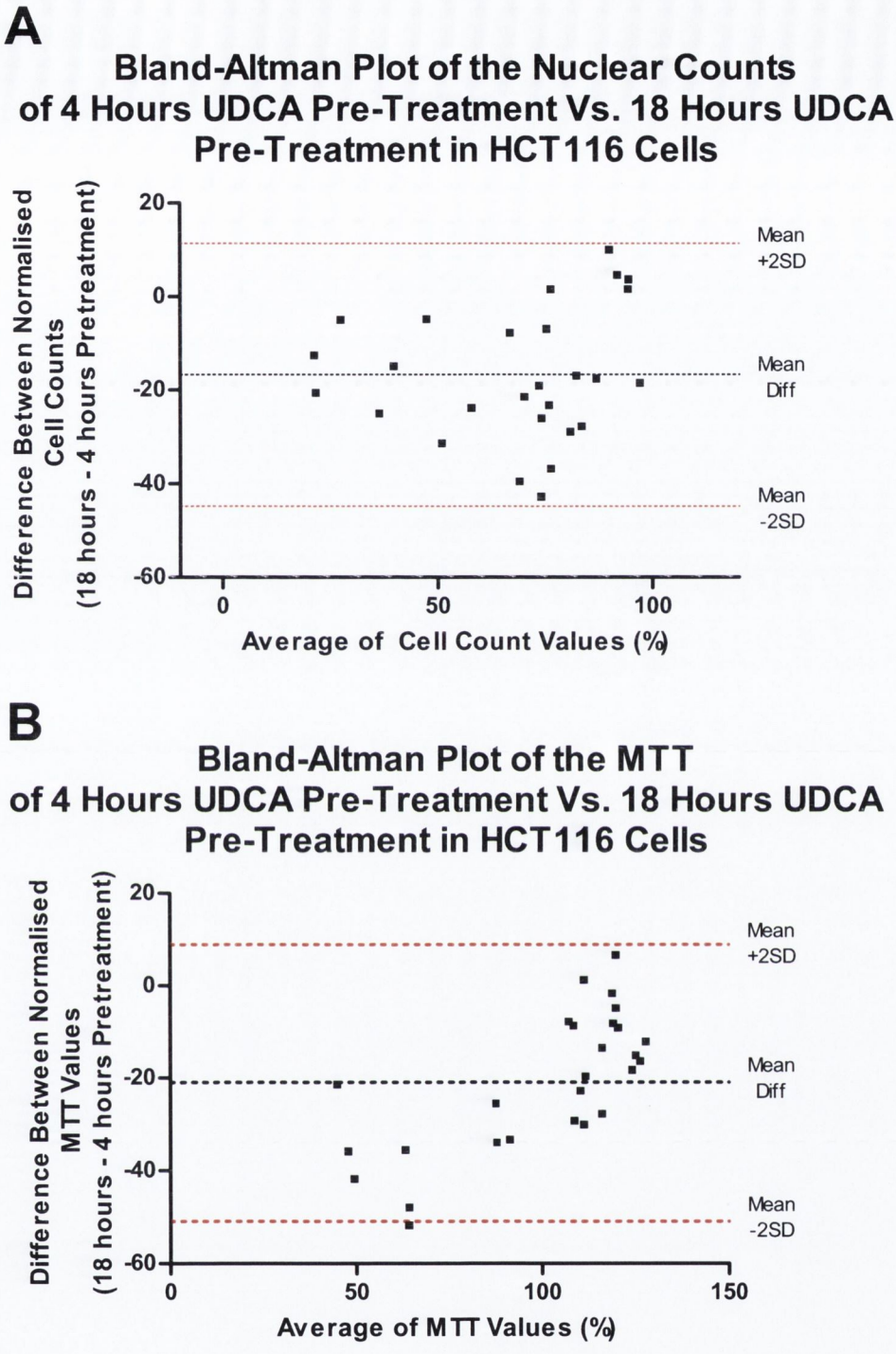

Figure 6–21: Bland-Altman plots of the differences between the 4 hour pre-treated matrices and the 18 hour-pre-treated matrices for cell counts (A) and MTT assays (B) in the HCT116 cell line. Both demonstrate that the 4 hour pre-treatment exhibits higher values on average than the 18 hour pre-treat. The mean difference for the cell count was 11.4% ($p < 0.001$, 95% CI of the difference: -5.8% to -17.1%) and the MTT 20.1% ($p < 0.0001$, 95% CI of the difference: 15.6% to 26.4%).

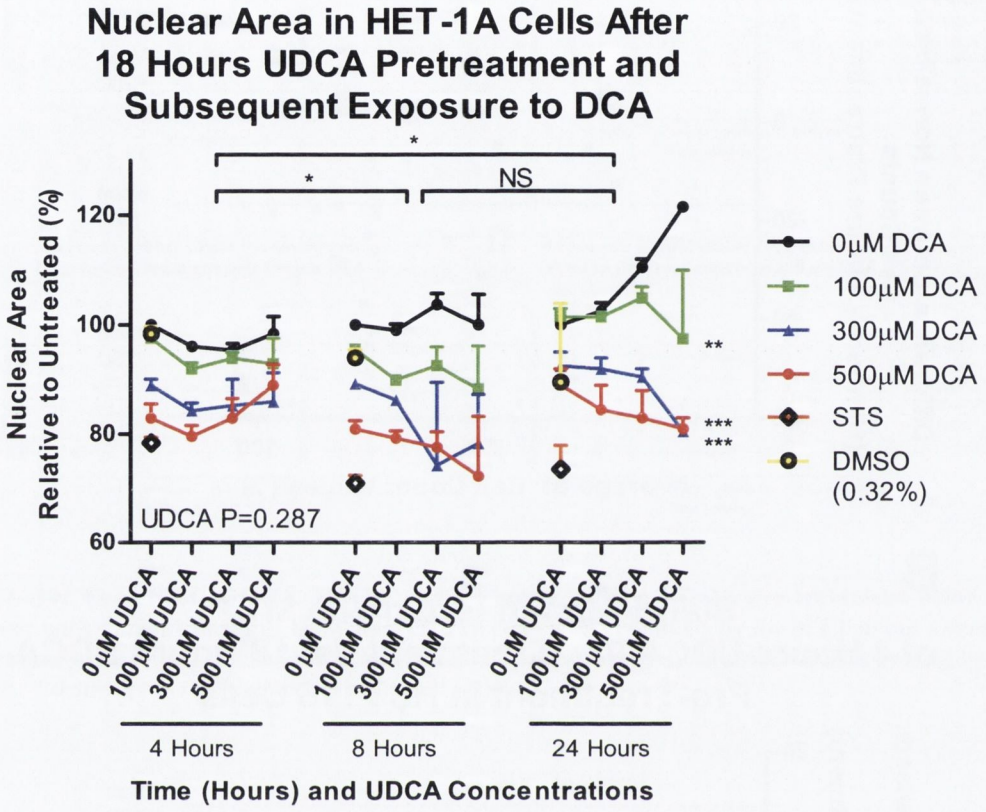

Figure 6–22: The effect of UDCA and DCA and 18 hours UDCA pre-treatment prior to DCA on the nuclear area of HET-1A cells. Mean results and SEM of N=3. Comparative analysis was performed using general linear model ANOVA. * denotes $p < 0.05$, ** denotes $p < 0.01$ and *** denotes $p < 0.001$ compared to untreated cells.

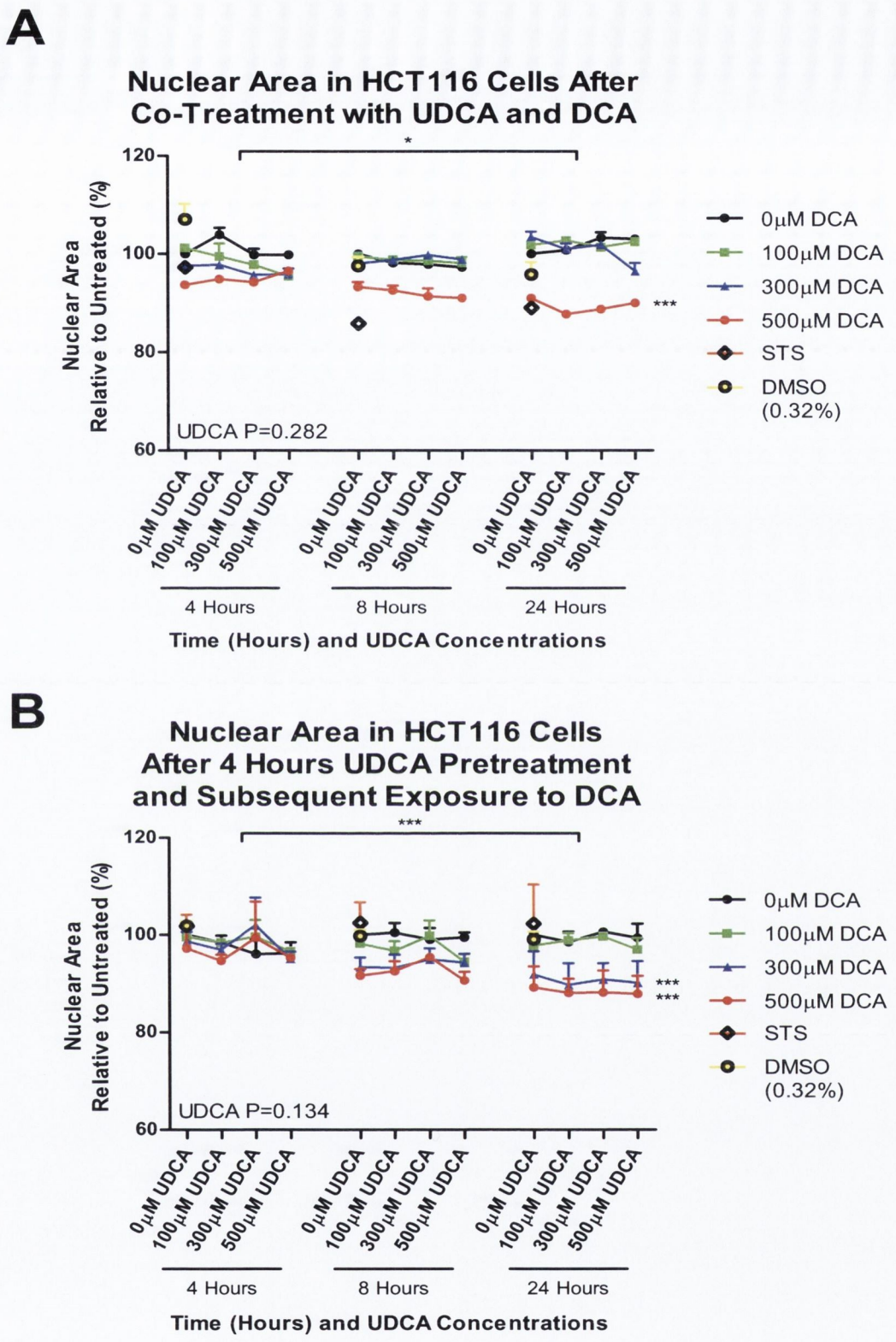

Figure 6–23: The effect of UDCA and DCA co-treatment (A) and 4 hours UDCA pre-treatment prior to DCA (B) on the nuclear area of HCT116 cells. Mean results and SEM of N=3. Comparative analysis was performed using general linear model ANOVA. * denotes $p < 0.05$ and *** denotes $p < 0.001$ compared to untreated cells.

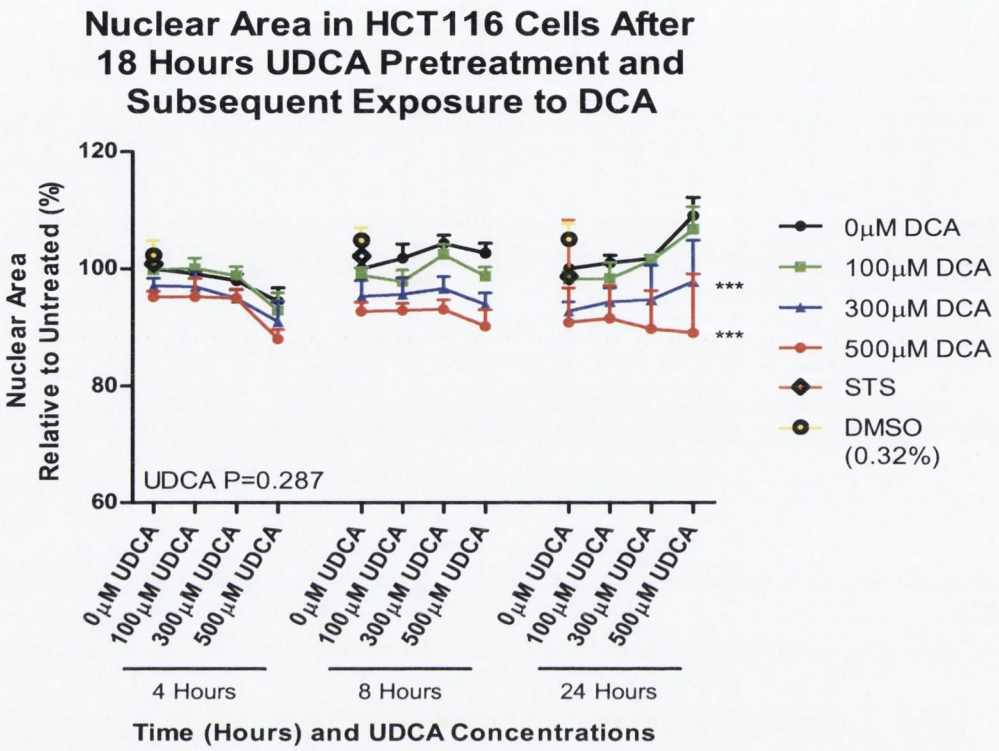

Figure 6–24: The effect of UDCA and DCA and 18 hours UDCA pre-treatment prior to DCA on the nuclear area of HCT116 cells. Mean results and SEM of N=3. Comparative analysis was performed using general linear model ANOVA. * denotes $p < 0.05$ and *** denotes $p < 0.001$ compared to untreated cells.

Appendix 2.

7. Appendix 2: Supplemental Data from Chapter 3

This appendix contains supplemental data from chapter 3 "Deoxycholic Acid Modulates Cell Adhesion in a Mechanism Discreet From Apoptosis"

7.1. List of Figures

Figure 7–1: Difference between viability as estimated by the cell count and the MTT assay is greatest at higher BA concentrations and at earlier time-points in the co-treatment experiment. . 286

Figure 7–2: Difference between viability as estimated by the cell count and the MTT assay is greatest at higher BA concentrations and at earlier time-points in the 18 hour pre-treatment experiment..... 287

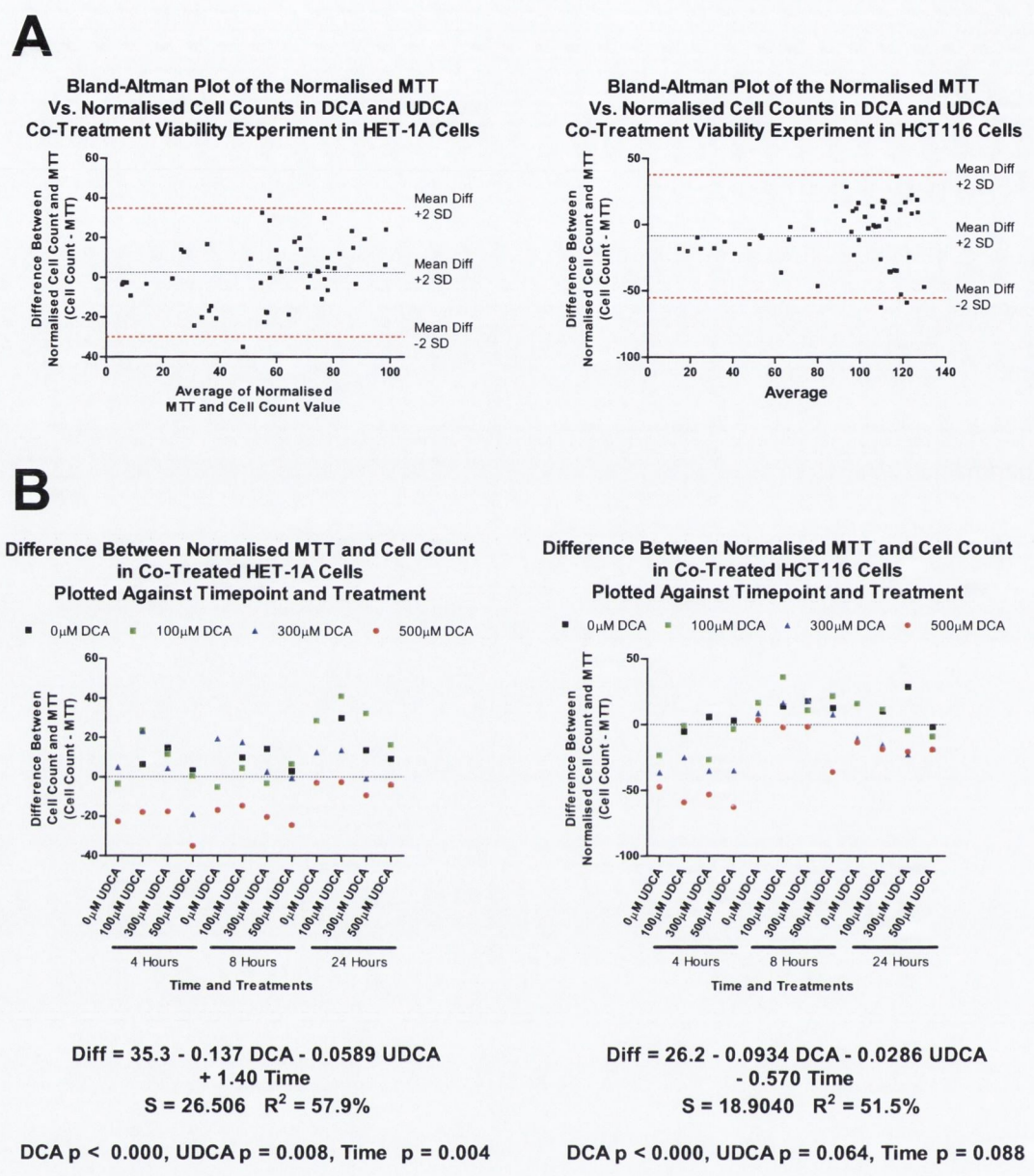

Figure 7–1: Difference between viability as estimated by the cell count and the MTT assay is greatest at higher BA concentrations and at earlier time-points in the co-treatment experiment. The mean normalised viability of the MTT experiments for each treatment was subtracted from the same treatment normalised viability as measured by the nuclear count. Data represents the difference between the mean values of the three experiments. The Bland-Altman plots demonstrate that HET-1A cells exhibit a wide variety of viabilities while the HCT116 cell line remains viable in the majority of time-points and treatments. However, the Bland-Altman plots demonstrated a large limit of agreement between the two assays as demonstrated by the red dashed lines marking +/- 2SD from the mean difference. Plotting the difference between the assays against treatment and time demonstrated a predictable pattern in the HET-1A cell line with difference being predicted by DCA concentration, UDCA concentration and time.

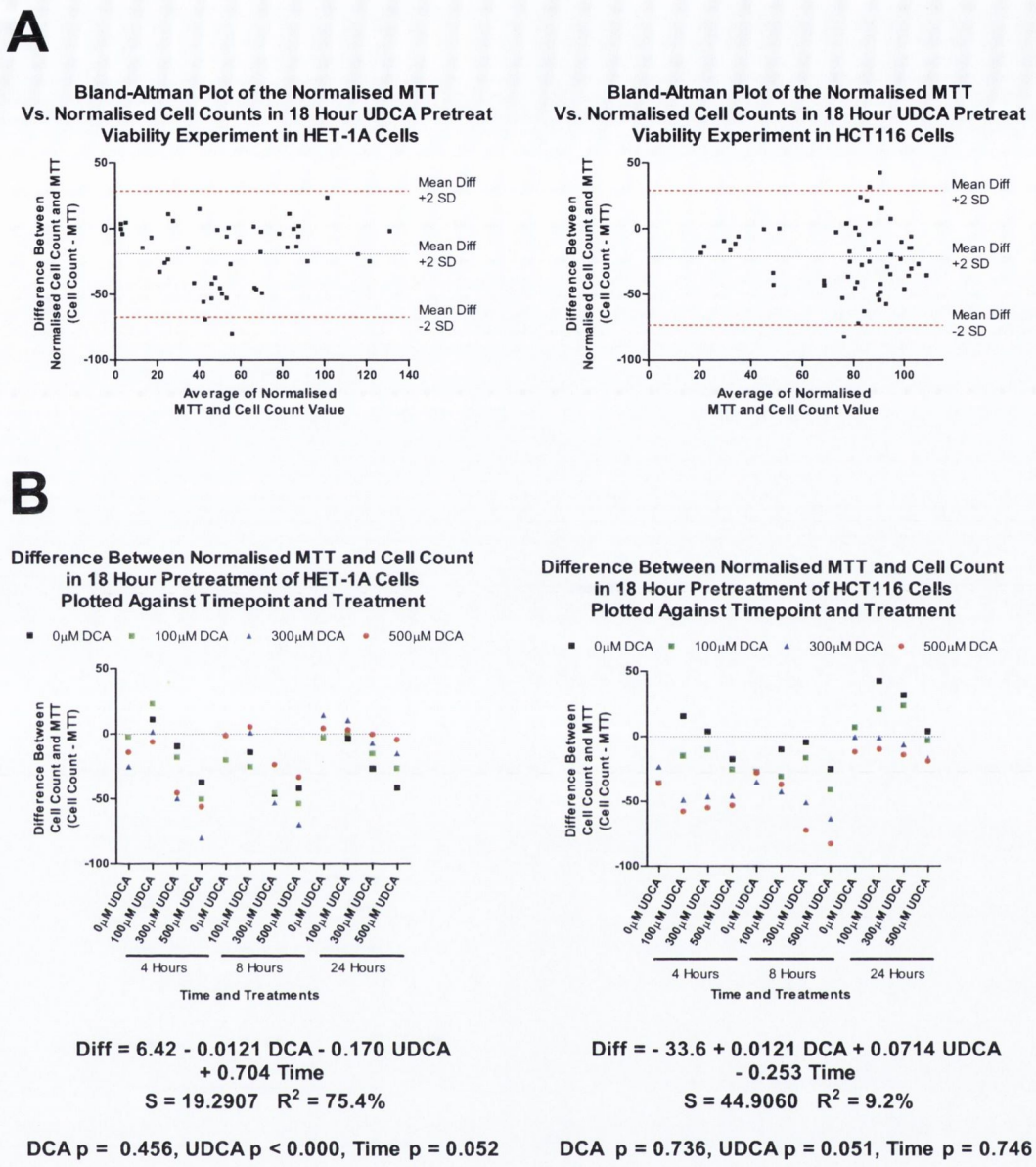

Figure 7–2: Difference between viability as estimated by the cell count and the MTT assay is greatest at higher BA concentrations and at earlier time-points in the 18 hour pre-treatment experiment. The mean normalised viability of the MTT experiments for each treatment was subtracted from the same treatment normalised viability as measured by the nuclear count. Data represents the difference between the mean values of the three experiments. The Bland-Altman plots demonstrate that HET-1A cells exhibit a wide variety of viabilities while the HCT116 cell line remains viable in the majority of time-points and treatments. However, the Bland-Altman plots demonstrated a large limit of agreement between the two assays as demonstrated by the red dashed lines marking +/- 2SD from the mean difference. Plotting the difference between the assays against treatment and time demonstrated a predictable pattern in the HET-1A cell line with difference being predicted by DCA concentration, UDCA concentration and time.

Appendix 3.

8. Appendix 3. Supplemental Data from Chapter 4.

8.1. List of Figures

Figure 8–1: Example of Control RNA ladder used to determine RINs for each RNA sample..... 293

Figure 8–2: RIN and RNA concentration of each sample processed in duplicate during the micro-array experiment. 295

Figure 8–3: Micro-array probesets available for analysis after data refinement..... 297

8.2. List of Tables

Table 8–1: List of 25 Probesets with the greatest upregulation or down-regulation in response to UDCA. Unnamed genes are probesets with no known corresponding gene..... 299

Table 8–2: List of 25 Probesets with the greatest upregulation or down-regulation in response to Dex. Unnamed genes are probesets with no known corresponding gene. 300

Table 8–3: List of 25 Probesets with the greatest upregulation or down-regulation in response to DCA. Unnamed genes are probesets with no known corresponding gene. 301

Table 8–4: Genes Up-regulated by UDCA, Dex, DCA or both UDCA and Dex in the HET-1A Cell Line 303

Table 8–5: Genes Up-regulated by UDCA and DCA, DCA and Dex, or All Three of UDCA, Dex and DCA in the HET-1A Cell Line..... 304

Table 8–6: Genes Down-regulated by UDCA, Dex, DCA or both UDCA and Dex in the HET-1A Cell Line..... 305

Table 8–7: Genes Down-regulated by UDCA and DCA, DCA and Dex, or All Three of UDCA, Dex and DCA in the HET-1A Cell Line..... 306

Table 8–8: Genes Up-regulated by UDCA, Dex, DCA or both UDCA and Dex in the OE33 Cell Line 307

Table 8–9: Genes Up-regulated by UDCA and DCA, DCA and Dex, or All Three of UDCA, Dex and DCA in the OE33 Cell Line 308

Table 8–10: Genes Down-regulated by UDCA, Dex, DCA or both UDCA and Dex in the OE33 Cell Line..... 309

Table 8–11: Genes Down-regulated by UDCA and DCA, DCA and Dex, or All Three of UDCA, Dex and DCA in the OE33 Cell Line..... 310

Table 8–12: Genes Up-regulated by UDCA, Dex, DCA or both UDCA and Dex in the HCT116 Cell Line 311

Table 8–13: Genes Up-regulated by UDCA and DCA, DCA and Dex, or All Three of UDCA, Dex and DCA in the HCT116 Cell Line 312

Table 8–14: Genes Down-regulated by UDCA, Dex, DCA or both UDCA and Dex in the HCT116 Cell Line 313

Table 8–15: Genes Down-regulated by UDCA and DCA, DCA and Dex, or All Three of UDCA, Dex and DCA in the HCT116 Cell Line 314

Table 8–16: Micro-Array Intensity Values for Probeset Pairs of Validation Genes 316

Table 8–17: Micro-Array Intensity Values for Probeset Pairs of Validation Genes 317

Table 8–18: Micro-Array Intensity Values for Probeset Pairs of Validation Genes 318

8.3. Quality and Quantity of mRNA Used for the Micro-Array Experiment

To assess the quality of RNA isolated from the HET-1A, OE33 and HCT116 cell lines after treatment with DMSO, UDCA, Dex or DCA RINs were determined using Integrity was assessed RNA Nano Chip Assay and the Agilent Bioanalyser (Agilent Technologies, Santa Clara, CA, USA). The technique has been described in section 4.3.7.

For quality control, RNA concentration was determined using the NanoDrop 8000 (NanoDrop products, Wilmington, DE, USA).

The data shown demonstrates a representative control RNA ladder and RINs and RNA concentrations as determined during quality control assessments (Figure 8–1and Figure 8–2).

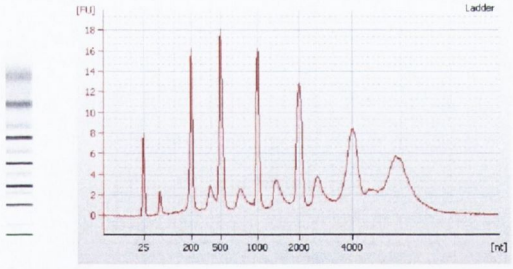

Control Ladder for the RNA Nano Chip Assay

Figure 8–1: Example of Control RNA ladder used to determine RINs for each RNA sample.

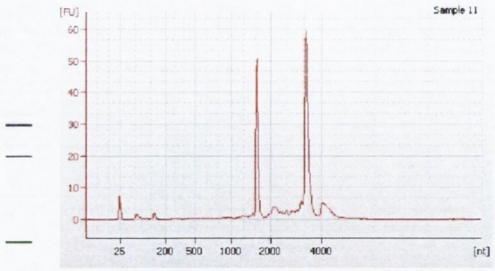

HET1A 12 Hours RESTING
RIN 9.7
RNA Concentration 179 µg/µL

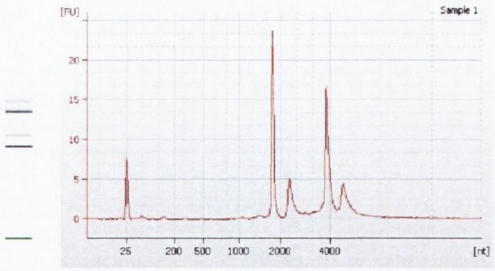

HET1A 12 Hours UDCA
RIN 9.7
RNA Concentration 88 µg/µL

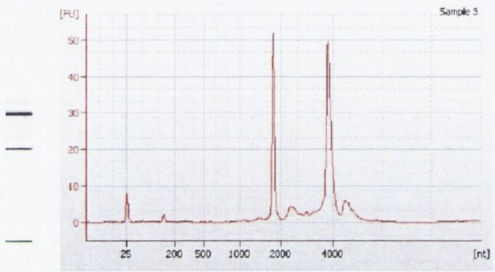

HET1A 12 Hours DCA
RIN 9.7
RNA Concentration 336 µg/µL

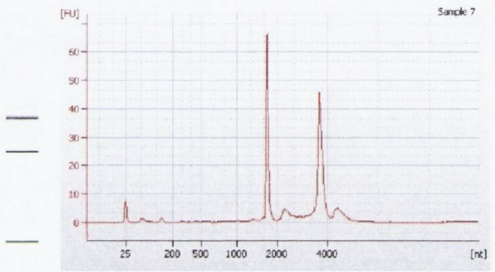

HET-1A Dex 12 Hours
RIN 9.6
RNA Concentration 268.1 µg/µL

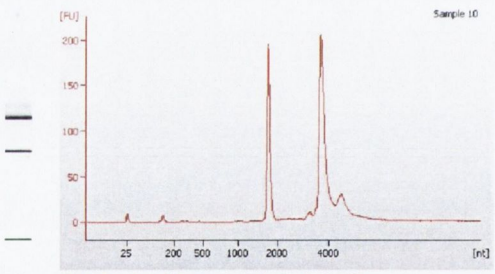

OE33 12 Hours RESTING
RIN 9.9
RNA Concentration 693 µg/µL

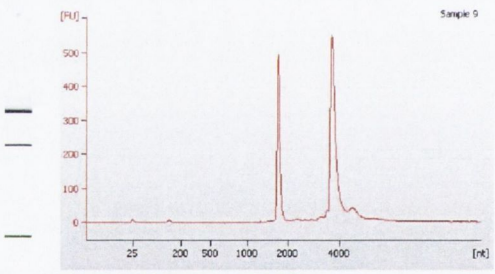

OE33 12 Hours UDCA
RIN 10
RNA Concentration 871 µg/µL

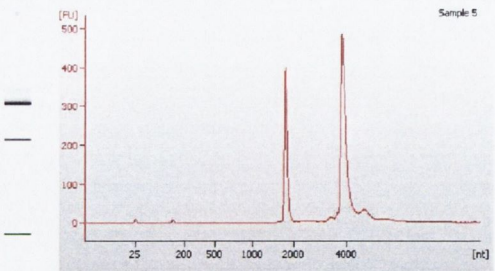

OE33 12 Hours DCA
RIN 10
RNA Concentration 822 µg/µL

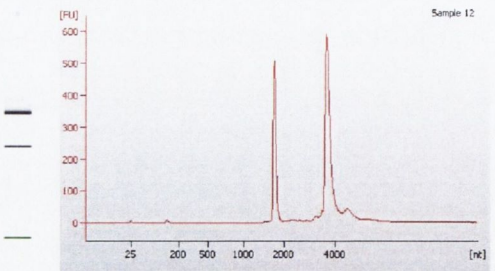

OE33 Dex 12 Hours
RIN 10
RNA Concentration 822 µg/µL

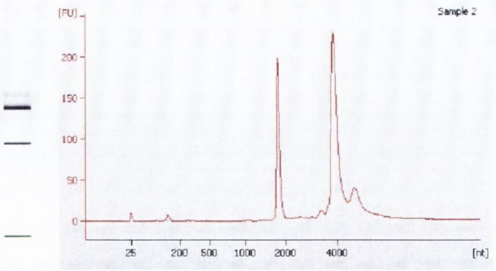

HCT116 12 Hours RESTING
RIN 10
RNA Concentration 1040 µg/µL

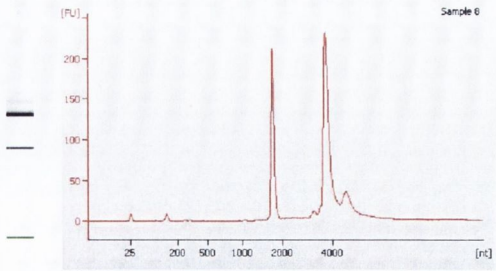

HCT116 12 Hours UDCA
RIN 10
RNA Concentration 789 µg/µL

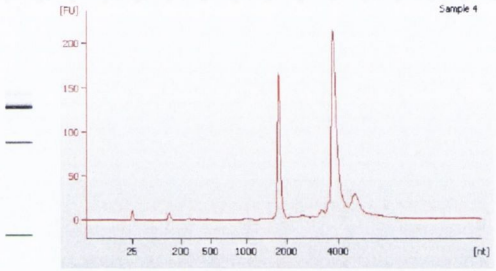

HCT116 12 Hours DCA
RIN 10
RNA Concentration 563 µg/µL

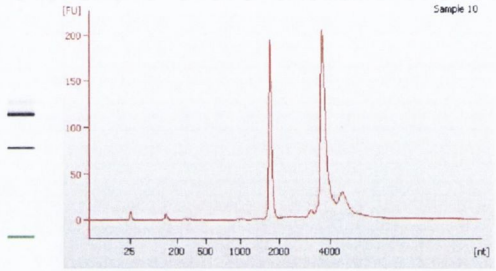

HCT116 Dex 12 Hours
RIN 10
RNA Concentration 624 µg/µL

Figure 8–2: RIN and RNA concentration of each sample processed in duplicate during the micro-array experiment.

8.4. Microarray Probesets Remaining after Data Refinement

Refinement of the microarray data reduced the numbers of probesets for subsequent comparative analysis. The data shown in Figure 8–3 represents the probesets remaining after data refinement as described in section 4.3.7. Briefly, Probesets were exclude is intensity was less than 100 in both sets. Afterwards, probesets were refined to probesets with a fold expression 1.5 above that of DMSO and to an $\alpha \leq 0.05$ relative to DMSO.

The largest fold changes relative to DMSO were seen with DCA treatment.

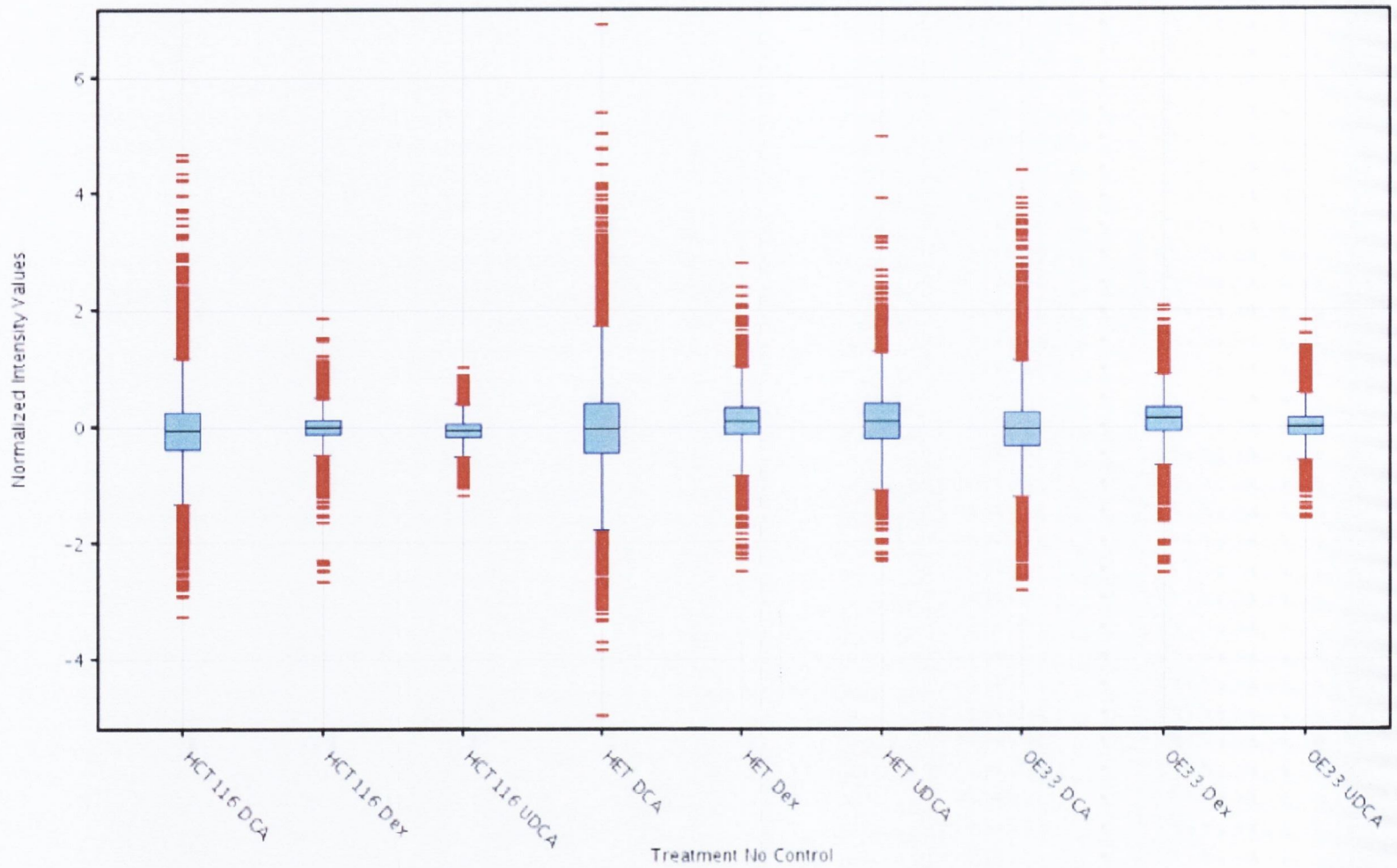

Figure 8–3: Micro-array probesets available for analysis after data refinement

8.5. Genes with the Largest Alterations in Expression induced by UDCA, Dex or DCA.

Table 8–1, Table 8–2 and Table 8–3 demonstrate the 25 genes with the greatest alteration in expression in response to UDCA, Dex or DCA treatment after 12 hours treatment.

Numerous of the probesets in the Dex treated cells demonstrate no known associated genes.

Genes Upregulated by UDCA

HET-1A			OE33			HCT116		
Gene	Log Fold Change	p-value	Gene	Log Fold Change	p-value	Gene	Log Fold Change	p-value
INHBE	28.57739	5.64E-04	PDK4	2.906856	0.005736	EGR1	1.760259	0.025458
GDF15	14.58988	0.004143	PCDH7	2.815429	0.006805	BHLHE40	1.724636	0.04334
SLC7A11	9.018328	7.27E-04		2.631741	0.004647	DHRS3	1.721233	0.013819
CHAC1	8.587502	0.001897	MIR21	2.561889	9.17E-04	IL8	1.700345	0.001586
SLC7A11	7.691288	0.001248		2.477765	0.008443	SCD	1.603246	0.044433
IL21R	7.13495	0.004931	HNRNPD	2.452153	0.011758	DNAJB9	1.574159	0.029291
FLJ35024	5.696633	0.011018	FBXO32	2.40607	0.011475	TMEM22	1.567012	0.021439
	5.300021	0.001128	GALNT5	2.371763	0.002241	TMEM39A	1.561481	0.004556
DDR2	5.270354	0.0038	BACH2	2.35751	0.013413	C4orf34	1.539655	0.02437
NR1H3	5.163504	0.015702	CBX3	2.356507	0.019534	PER2	1.51985	0.019951
STC2	5.139193	0.001293	KLHL24	2.305211	0.044501	C2orf30	1.516776	0.037945
ATF3	4.980477	0.011822	MT1F	2.304414	0.014478	INSIG1	1.513806	0.006646
STC2	4.597278	0.006463	EIF1	2.288215	4.70E-04	SCD	1.5137	0.004407
PSAT1	4.271223	3.68E-05	SLC16A6	2.283062	0.005275	DDIT4	1.512023	0.031382
S100P	4.204898	0.006613		2.179002	0.046844			
SLC16A6	4.142852	0.005675	SLC16A6	2.109109	0.049825			
TRIB3	4.132659	0.002083	SLC2A12	2.08079	0.012638			
FGF21	4.049981	0.012816	GEM	2.043877	0.006953			
LOC148189	3.931408	0.006126		2.039864	0.018143			
NUPR1	3.928657	0.004877		2.032953	0.013985			
EAF2	3.858143	0.018633	GALNT5	2.031253	0.002012			
LOC645638	3.854245	1.19E-04	FNBP4	2.014482	2.59E-04			
NRP1	3.827377	0.024526	KLHL24	1.995723	0.011718			
CEBPG	3.808169	0.010485	FBXO32	1.988312	0.028353			
	3.781105	0.006237	OPN3	1.976587	0.010026			

Genes Downregulated by UDCA

HET-1A			OE33			HCT116		
Gene	Log Fold Change	p-value	Gene	Log Fold Change	p-value	Gene	Log Fold Change	p-value
MALAT1	5.02265	0.041466	CCNE2	2.972812	0.011435	PCNX	1.852869	0.027338
MALAT1	4.369186	0.049904		2.455261	0.001023	FAM13B	1.831038	0.017671
CXCL14	3.739844	0.005681	RRM2	2.403292	5.51E-04	PDLIM5	1.804374	0.002362
MALAT1	3.695185	0.047748	MCM10	2.238239	0.013897	CENPF	1.744431	0.014856
MALAT1	3.535926	0.026571	IL8	2.035689	0.012671	PDLIM5	1.715008	0.02401
CXCL14	3.235661	0.014858	POLE2	2.027806	0.002874	GJA1	1.703376	0.023746
MBNL1	3.232083	0.035456	MCM10	2.021179	0.016643		1.703359	0.029413
ASPM	3.212945	0.028822	RRM2	1.996508	0.002159	SNHG7	1.692138	0.033501
ACTB	3.16667	0.001004	MCM10	1.98462	0.012155	MKI67	1.674157	0.029178
EPPK1	2.860454	0.001452	FABP5	1.969767	0.001087		1.644101	0.0306
TRERF1	2.839141	0.032993	TYMS	1.951205	6.76E-04	TNRC6C	1.616345	0.039055
ATP8B3	2.738437	0.036521	IL1A	1.931991	0.006791	C14orf159	1.609332	0.015657
FAM13B	2.567017	0.022166	TYMS	1.927494	0.002232	TGOLN2	1.607213	0.008665
MKI67	2.524829	0.001163	HELLS	1.916053	0.012935	NFYB	1.605123	0.03873
	2.506263	0.015959	GINS2	1.900356	0.002011	MKI67	1.564763	0.017635
BCLAF1	2.505465	0.021216	CDC7	1.90028	0.016482	AHNAK	1.550387	0.015947
	2.457882	0.001088	IL8	1.895976	0.003446	BRCC3	1.548916	0.021619
SLC16A3	2.443127	0.001303	CENPK	1.831121	0.034608		1.548266	0.035191
IRS1	2.441736	0.019113	HELLS	1.813827	0.008744	AKAP12	1.545505	0.03329
	2.432611	0.004854	CHAC2	1.811564	0.001866	CENPE	1.524091	0.046919
DHRS2	2.378299	0.001524	DTL	1.810494	5.81E-04	EPPK1	1.524051	0.024367
SPEN	2.338734	0.01225	FEN1	1.794846	0.005556		1.52364	0.041155
SAE1	2.330665	0.004215	UNG	1.793907	8.76E-04	ENAH	1.512356	0.027318
CENPE	2.32033	0.001742	MCM2	1.790359	0.002483			
AHNAK	2.320161	0.001494	AK2	1.779879	0.021113			

Table 8–1: List of 25 Probesets with the greatest upregulation or down-regulation in response to UDCA. Unnamed genes are probesets with no known corresponding gene.

Genes Upregulated by Dex

HET-1A			OE33			HCT116		
Gene	Log Fold Change	p-value	Gene	Log Fold Change	p-value	Gene	Log Fold Change	p-value
S100P	7.101088	8.36E-04		3.948284	9.37E-04		2.273459	0.044384
PHACTR3	4.601025	0.003893	KLF9	3.610304	0.001104		2.050048	0.023968
CALCA	4.204984	0.010485		3.559813	9.54E-04		1.887336	0.003279
LCN2	4.17973	6.57E-04	PER1	3.379381	0.003709	UNC84A	1.770207	0.007465
	4.17175	0.001011	GCNT3	3.19592	5.12E-04	UGCGL2	1.758202	0.047259
CSTA	4.04405	0.003175	IL6R	3.160652	5.88E-04	ING3	1.624699	0.022351
	3.952877	6.13E-04		3.061797	9.72E-04	METTL7A	1.593115	0.019529
MGC16075	3.611789	0.007119	FKBP5	3.02924	0.002749	IMMP1L	1.580958	4.40E-04
	3.457513	0.00195	AHNAK2	3.015992	0.041902	KBTBD3	1.570351	0.003727
LAMP3	3.411414	0.007594	PHACTR3	3.009652	0.003435	SPTLC1	1.554881	0.046301
	3.330688	0.012732	CCL20	2.940656	0.020665		1.548234	0.038071
	3.277921	0.007716		2.845818	9.30E-04		1.539878	0.013002
	2.815258	5.91E-04	ANGPTL4	2.836928	0.008166	HINT3	1.518083	0.005595
GNG12	2.747666	0.040542	BOD1L	2.792421	0.038806	ATP5S	1.502527	1.86E-04
	2.690582	0.006357	CAMK2N1	2.787324	0.003575			
	2.650566	0.003649	ZFR	2.752286	0.049511			
SLC7A3	2.599834	0.010693	FKBP5	2.748076	0.00317			
BIRC3	2.59846	0.003044	PPFIBP1	2.694422	0.030441			
	2.395709	0.01152	PDE9A	2.59959	0.001863			
	2.39179	0.015395		2.537583	0.005341			
	2.387252	0.035057	SLCO1B3	2.511362	0.001012			
	2.36536	0.00955	MIR21	2.493584	0.001628			
FKBP11	2.34794	0.006532	PTPN12	2.486485	0.002219			
MAOA	2.341528	0.010004	ANGPT2	2.484795	0.003161			
	2.336666	0.003459	PILRB	2.481615	0.005123			

Genes Downregulated by Dex

HET-1A			OE33			HCT116		
Gene	Log Fold Change	p-value	Gene	Log Fold Change	p-value	Gene	Log Fold Change	p-value
	5.284109	0.016843	RPL37A	6.019536	0.012577		6.242496	7.18E-04
	4.741802	0.028639		5.778359	0.002283		5.914123	3.80E-04
	4.678569	0.013635		5.212982	9.11E-04		5.335531	4.04E-04
	4.594721	0.010745		4.854082	8.83E-04		5.219642	2.20E-04
	4.316375	5.54E-04		4.839591	0.001175		5.116818	0.002427
	4.265136	0.033699		4.745367	0.006404		4.823034	3.55E-04
	4.008457	0.023997		4.642927	0.008958	TMED2	3.112157	0.028897
4	3.504505	0.005629	ATP6V0E1	4.314965	0.00516	ACTB	3.027622	0.0262
	3.378768	0.004717	RPL38	3.778504	0.010994	KIF22	2.83665	0.014975
	3.30769	0.014648	ACSL4	3.255538	0.021437	TMED2	2.774409	0.048238
	3.263014	0.007648		3.156609	0.010301	STIP1	2.702576	0.025826
RPL37A	3.251434	0.040895	YIF1B	3.123508	0.010175	SNAP23	2.269673	0.007008
ACTB	3.197373	0.002445		3.001652	0.009039	DCAKD	2.254533	0.007732
	3.03073	0.008711	ADK	2.961416	0.00545	RHBDD2	2.205557	0.021879
1///								
LOC10027221	3.020559	8.78E-04	RPL38	2.887855	0.010108	MED18	2.178259	0.003922
	2.99271	0.009474	TMEFF2	2.853598	0.030683	ADAM10	2.083417	0.043514
EIF2C1	2.743094	0.017001	GLS	2.845208	0.012335	ADAM9	2.081111	0.025055
COL12A1	2.646975	5.83E-04	TMED2	2.793556	0.04476	HNRNPH1	2.0363	0.009856
DLEU2	2.593592	2.95E-04		2.788655	0.014233	PPP5C	2.026812	0.00238
6	2.5594	0.007498	RAP2C	2.714724	0.021642	SAE1	2.011452	0.01822
ZFAND6	2.5431	0.01234		2.676178	0.0071	RAB5A	1.986325	0.040116
RHBDD2	2.535879	0.004106	ITGB5	2.64817	5.09E-04	ACTB	1.97889	0.032169
	2.525105	0.007324	CEP97	2.522339	0.011026	PPP2R1A	1.957436	0.041977
CXCL14	2.502464	0.009349	UBLCP1	2.50167	0.011357	MOSPD1	1.932184	0.014434
	2.462309	0.011989	PSPH	2.476602	0.009229	CYP51A1	1.889677	0.0254

Table 8–2: List of 25 Probesets with the greatest upregulation or down-regulation in response to Dex. Unnamed genes are probesets with no known corresponding gene.

Genes Upregulated by DCA

HET-1A			OE33			HCT116		
Gene	Log Fold Change	p-value	Gene	Log Fold Change	p-value	Gene	Log Fold Change	p-value
GDF15	95.46162	7.43E-04	CD69	18.67936	1.80E-04	C9orf150	28.01939	5.23E-04
INHBE	36.27743	3.17E-04	IL8	15.19477	1.56E-04	RGS4	21.67074	2.26E-04
MAFF	35.07697	0.001167		13.78873	0.003409	RGS4	19.8828	0.002956
IL8	34.56135	0.004547	NR4A2	12.17557	6.02E-04	IL8	19.08894	0.006092
ATF3	25.0075	7.70E-04	NR4A2	11.81169	9.78E-04	C12orf39	18.73937	3.72E-04
EGR1	19.59727	0.019069	BCL2A1	11.57141	6.62E-04	IL8	14.56391	7.43E-04
PTX3	18.01726	8.41E-06	SOD2	10.96877	0.002036	SERPINE1	14.27583	1.86E-05
TRIB3	15.39548	6.09E-04		10.75607	5.66E-04	SLC7A11	13.68918	0.002105
EGR1	14.74083	0.001905	ICAM1	10.72913	2.45E-04	CXCL3	11.82042	0.002039
STC2	14.59773	3.06E-04	FBXO32	9.957809	1.71E-04	UPP1	11.80761	4.91E-04
DDIT3	14.54132	9.13E-04	KLHL24	9.686928	0.001121	SLC7A11	10.73369	0.001657
EGR1	14.49067	4.62E-04	INSIG1	9.560369	5.78E-05	SERPINE1	10.73298	4.32E-04
	14.41066	0.001231	INSIG1	9.491711	4.69E-04	SLC7A11	10.12614	0.001461
CHAC1	13.37115	4.43E-05	TCP11L2	8.50314	4.00E-05	TRIB3	9.42966	0.002112
SLC7A11	12.90347	2.90E-04	IL8	8.426155	0.003493	RGS4	8.41406	4.02E-04
SLC3A2	12.20638	3.74E-04	ICAM1	7.966524	1.39E-04	TRIB3	8.14103	4.87E-04
SLC7A11	12.08852	0.00109	KLHL24	7.770437	0.001291	DDIT3	7.768386	0.002219
UNC5B	12.07043	4.17E-04	NR4A2	7.679092	9.32E-04	SLFN5	7.207128	0.012949
IL6	11.65883	4.51E-04	UBD	7.580849	3.39E-04	CXCL2	7.042403	0.005103
GADD45A	11.25095	3.63E-04	GEM	7.330222	0.001277	CHAC1	6.831085	0.002438
FOXJ3	11.23941	9.51E-05	KLHL24	7.091074	0.006164	SLFN5	6.552124	0.009606
DDR2	10.96104	6.11E-04	INSIG1	6.814323	1.91E-04		6.548169	0.003027
STC2	10.83817	4.34E-05	ZAK	6.669375	4.97E-04	STC2	6.419821	4.87E-04
TRIB3	10.61385	1.44E-04	TM4SF1	6.21724	4.89E-04	EGR1	6.205886	0.001536
DUSP6	10.49339	6.45E-04	KLHL24	6.183865	0.00327	ELL2	6.166528	0.009768
IL8	10.17713	3.09E-04	HBP1	6.119176	0.013335	NT5E	6.123558	0.001583

Genes Downregulated by DCA

HET-1A			OE33			HCT116		
Gene	Log Fold Change	p-value	Gene	Log Fold Change	p-value	Gene	Log Fold Change	p-value
CXCR4	26.95041	0.001292	FAM43A	7.138911	7.33E-04	SOX4	9.918746	0.001626
CXCL14	10.51629	0.001401	FAM13B	5.707318	0.002879	SOX4	7.724889	0.006647
CXCL14	9.141905	1.11E-04	ALDH1L2	5.63998	0.022187	KANK2	7.228088	3.00E-04
CXCR4	8.977458	0.003048		5.600324	2.07E-04	CCNE2	7.048328	0.008153
COL1A1	8.61316	7.08E-04		5.400554	0.004387		6.873243	0.004927
CXCR4	8.418798	0.003439	MGC16385	5.367833	0.001338	DKK4	6.778997	0.009686
TMEM19	8.37767	0.001729	CCNE2	5.252843	0.006014	HSPA2	6.731787	0.0473
TMEM107	7.513113	0.006527	MAT2A	5.159547	3.69E-04	SOX4	6.703837	6.43E-04
REEP1	7.347687	0.005319	DUSP6	5.108868	3.67E-04		6.364396	0.008717
NEURL1B	7.168158	2.59E-04	C5orf54	5.046314	0.0114	CCNE2	6.349454	0.004522
	6.939158	0.001261	RNF170	4.720758	0.001688	GJA1	6.267131	4.90E-05
MARCKSL1	6.910674	0.001224	PHOSPHO2	4.65157	5.49E-04		5.719539	0.00918
TMEM19	6.90449	0.002758	DUSP6	4.651476	6.12E-04	GPRC5B	5.660699	4.38E-05
TMEM107	6.871285	0.004324	THBD	4.564087	4.32E-05	OSGEPL1	5.596393	7.49E-04
ADM	6.778385	2.36E-05	C7orf40	4.506939	8.73E-04	PPWD1	5.49113	0.009591
GAS1	6.769722	0.004684	PHACTR3	4.50639	1.46E-04	SOX4	5.326847	0.01088
NANOS1	6.639301	0.004979	LOC729680	4.499136	8.05E-04	C1orf93	5.244075	0.00548
COL1A1	6.576711	0.005842	DUSP6	4.484277	3.59E-04	ELOVL6	5.234448	8.73E-04
SOX2	6.5073	0.007989	ZNF302	4.479859	0.0021		5.135356	0.027077
	6.39061	0.004608	THBD	4.424262	7.21E-04		5.112232	0.006358
	6.33408	0.041376	C7orf36	4.358579	0.001668	ADAM19	5.101102	9.65E-04
	6.067531	0.011024	CD3EAP	4.356209	1.02E-04		5.083004	0.011353
PDK3	5.958356	0.002013		4.353038	0.004902	FBXO9	4.93808	0.001138
RCAN3	5.836283	7.82E-04	CDC7	4.280674	0.005356	FGF18	4.870637	0.00419
CXXC5	5.817663	1.49E-04	FBXO9	4.278653	4.28E-04		4.86479	0.001136

Table 8–3: List of 25 Probesets with the greatest upregulation or down-regulation in response to DCA. Unnamed genes are probesets with no known corresponding gene.

8.6. Overlapping Gene Profiles Induced by Treatment with UDCA, Dex and DCA.

This section provides lists of Genes upregulated and downregulated by UDCA, Dex or DCA alone or simultaneously by either two or three treatments.

Table 8–4, Table 8–5, Table 8–6 and Table 8–7 demonstrate lists of the 25 genes/probesets with the largest alterations in expression of mRNA in the HET-1A cell line.

Table 8–8, Table 8–9, Table 8–10 and Table 8–11 demonstrate lists of the 25 genes/probesets with the largest alterations in expression of mRNA in the OE33 cell line.

Table 8–12, Table 8–13, Table 8–14 and Table 8–15 demonstrate lists of the 25 genes/probesets with the largest alterations in expression of mRNA in the HCT116 cell line.

Upregulated Genes in the HET-1A Cell Line

UDCA			Dex			DCA			UDCA and Dex			
GENE	PROBE ID	LOG CHANGE	GENE	PROBE ID	LOG CHANGE	GENE	PROBE ID	LOG CHANGE	GENE	PROBE ID	LOG CHANGE UDCA	LOG CHANGE Dex
	238953_at	1.78	PHACTR3	227949_at	2.202	IL8	202859_x_at	5.111	CSTA	204971_at	1.71	2.016
	241745_at	1.769	CALCA	217561_at	2.072	EGR1	227404_s_at	4.293	DPH5	224060_s_at	1.595	0.976
CTTN	214073_at	1.721	LCN2	212531_at	2.063	PTX3	206157_at	4.171	BCL2L13	223664_x_at	1.559	0.729
VTI1A	235923_at	1.632	GNG12	222834_s_at	1.458	EGR1	201693_s_at	3.882		AFFX-r2-Bs-lys-5_at	1.553	2.061
SIRT5	219185_at	1.617	BIRC3	210538_s_at	1.378	IL6	205207_at	3.543	SEPSECS	231730_at	1.537	1.115
ZNF846	1569157_s_at	1.593		1557029_at	1.255	FOXJ3	217310_s_at	3.49		AFFX-r2-Bs-lys-M_at	1.535	1.79
LOC387723	229323_at	1.539		1568643_a_at	1.224	IL8	211506_s_at	3.347		AFFX-r2-Bs-phe-5_at	1.515	1.406
WDR78	1554141_s_at	1.496	CREM	230511_at	1.218	PPP1R15A	37028_at	3.317	YKT6	217785_s_at	1.511	0.957
SDSL	228274_at	1.483	SGK1	201739_at	1.184	DUSP6	208891_at	3.244		AFFX-LysX-5_at	1.49	1.983
HIST1H2BG	210387_at	1.476		242521_at	1.151	CARS	240983_s_at	3.239	TRNT1	223814_at	1.462	0.997
DENND1A	219763_at	1.429	KBTBD3	228777_at	1.134	RAB39B	238695_s_at	3.195		235373_at	1.45	1.081
ZNF643	207219_at	1.384	FKBP11	219117_s_at	1.118	SEC24D	202375_at	3.181	FKBP1A	210187_at	1.425	0.626
MPZL1	210087_s_at	1.365	RARRES1	206392_s_at	1.11	PPP1R15A	202014_at	3.132		222376_at	1.406	1.048
LOC730631	238529_at	1.347	AASDH	235435_at	1.109	MAFF	205193_at	3.085		AFFX-LysX-M_at	1.4	1.713
NF2	217150_s_at	1.341	MUTED	226543_at	1.096	SLCO4C1	222071_s_at	3.054	TMEM116	227172_at	1.395	0.597
DCTN5	209231_s_at	1.33		AFFX-PheX-3_at	1.088		1569362_at	2.95		AFFX-PheX-5_at	1.38	1.26
WDR78	1554140_at	1.314	FCF1	219927_at	1.085	PHC3	238693_at	2.909	C12orf45	226349_at	1.378	0.763
STAM2	215044_s_at	1.302	SSH2	1554114_s_at	1.077	ARAF	230652_at	2.827		AFFX-r2-Bs-phe-M_at	1.375	1.16
FBXO4	223493_at	1.297	METTL7A	207761_s_at	1.065	ENAH	1553672_at	2.802	CAB39L	225914_s_at	1.369	0.716
IMPACT	222698_s_at	1.296	IP6K3	231179_at	1.061	CREB5	229228_at	2.798		237065_s_at	1.35	1.108
	226458_at	1.26	LOC100134	213747_at	1.042	DUSP5	209457_at	2.763	C20orf7	227160_s_at	1.343	0.997
C17orf39	220058_at	1.259	KIAA1704	229078_s_at	1.031	PHLDA1	225842_at	2.754	C11orf71	222743_s_at	1.341	0.62
LOC81691	208107_s_at	1.257	KIAA1704	226429_at	1.022	FRY	214319_at	2.742	SEPSECS	1553167_a_at	1.33	0.983
LOC81691	215215_s_at	1.248	C6orf35	218453_s_at	1.018		237593_at	2.731	C6orf52	236504_x_at	1.317	1.073
USP45	224441_s_at	1.24	TEPP	240119_at	1.015	ETV5	230102_at	2.73	DUS4L	205761_s_at	1.312	0.741

Table 8–4: Genes Up-regulated by UDCA, Dex, DCA or both UDCA and Dex in the HET-1A Cell Line

Upregulated Genes in the HET-1A Cell Line

UDCA and DCA				DCA and Dex				UDCA and Dex and DCA				
GENE	PROBE ID	LOG CHANGE UDCA	LOG CHANGE DCA	GENE	PROBE ID	LOG CHANGE UDCA	LOG CHANGE DCA	GENE	PROBE ID	LOG CHANGE UDCA	LOG CHANGE Dex	LOG CHANGE DCA
INHBE	210587_at	4.837	5.181	C5orf26	225698_at	2.836	0.794	S100P	204351_at	2.072	2.828	2.261
GDF15	221577_x_at	3.867	6.577	NEDD9	202149_at	2.708	1.163	NUPR1	209230_s_at	1.974	0.998	2.567
SLC7A11	209921_at	3.173	3.69		235556_at	2.43	0.685	EAF2	219551_at	1.948	0.675	2.02
CHAC1	219270_at	3.102	3.741	FNIP1	228250_at	2.316	0.85	LOC645638	229566_at	1.946	1.135	1.308
SLC7A11	217678_at	2.943	3.596	SNHG12	223774_at	2.298	0.94		228661_s_at	1.919	0.887	1.271
IL21R	221658_s_at	2.835	2.578	C7orf40	225699_at	1.954	0.593	FBXO22	219638_at	1.82	0.764	1.624
FLJ35024	1558212_at	2.51	1.83	IL18	206295_at	1.938	0.768		230527_at	1.814	1.143	1.689
	243813_at	2.406	1.769	SNHG12	223773_s_at	1.912	0.636	ASNS	205047_s_at	1.706	0.716	2.049
DDR2	225442_at	2.398	3.454	ANKRD1	206029_at	1.809	0.694	NAPG	210048_at	1.684	0.935	1.254
DDIT3	209383_at	2.368	3.862	CHD2	1554014_at	1.737	0.683	CLIP4	219944_at	1.664	0.616	1.362
STC2	203439_s_at	2.362	3.868	CHD2	1554015_a_at	1.734	0.629	GOSR2	210009_s_at	1.657	0.951	0.657
ATF3	202672_s_at	2.316	4.644	MTPAP	229676_at	1.661	0.992	SELI	1555274_a_at	1.656	0.676	2.064
STC2	203438_at	2.201	3.438	NUPL1	204435_at	1.575	0.797	C14orf50	237654_at	1.548	0.659	0.766
PSAT1	220892_s_at	2.095	2.93	Sep-13	1569973_at	1.531	0.656	TXNL4B	222748_s_at	1.522	1.077	1.159
SLC16A6	230748_at	2.051	2.195	CUL1	238509_at	1.527	0.676	DNAJC18	227166_at	1.521	0.675	1.068
TRIB3	218145_at	2.047	3.944	ATF1	1565269_s_at	1.523	0.761	LIPT1	205571_at	1.52	0.987	1.271
FGF21	221433_at	2.018	1.03	BTG1	200920_s_at	1.469	0.812	C12orf4	218374_s_at	1.497	0.64	1.351
LOC148189	235191_at	1.975	2.259	ESRP1	225846_at	1.459	0.722	PTK2	241453_at	1.489	1.006	0.699
NRP1	210510_s_at	1.936	0.729	TXNDC9	1554047_at	1.308	0.693	SHMT2	214095_at	1.488	0.657	1.941
CEBPG	204203_at	1.929	2.706	MAP2	225540_at	1.306	0.638	RHEBL1	1570253_a_at	1.487	0.899	1.128
PLAC1	219702_at	1.896	2.661		231576_at	1.255	1.736	OASL	205660_at	1.473	0.69	2.156
AGBL5	238889_at	1.888	1.049	USP53	230083_at	1.219	0.651	LOC399959	225381_at	1.469	0.702	1.361
SCD	211162_x_at	1.875	1.834	SLC25A37	222528_s_at	1.136	0.898	EIF5	208290_s_at	1.437	0.728	2.27
LIPG	219181_at	1.859	2.677		221788_at	1.12	0.641	RWDD2A	213555_at	1.435	0.861	1.243
CTH	206085_s_at	1.843	3.007	UGCG	204881_s_at	1.109	0.603	ETV5	203349_s_at	1.417	0.806	3.243

Table 8–5: Genes Up-regulated by UDCA and DCA, DCA and Dex, or All Three of UDCA, Dex and DCA in the HET-1A Cell Line

Down-regulated Genes in the HET-1A Cell Line

UDCA			Dex			DCA			UDCA and Dex			
GENE	PROBE ID	LOG CHANGE	GENE	PROBE ID	LOG CHANGE	GENE	PROBE ID	LOG CHANGE	GENE	PROBE ID	LOG CHANGE UDCA	LOG CHANGE Dex
MALAT1	223940_x_at	-2.127	NCRNA0008	234989_at	-1.809	COL1A1	1556499_s_a	-3.107	ACTB	AFFX-HSAC	-1.663	-1.677
MALAT1	1558678_s_a	-1.886	COL12A1	231879_at	-1.404	TMEM19	226860_at	-3.067	SPEN	201996_s_at	-1.226	-1.29
MALAT1	224567_x_at	-1.822	LOC100190	235060_at	-1.356	TMEM107	224496_s_at	-2.909	SAE1	1555618_s_a	-1.221	-0.917
MBNL1	201151_s_at	-1.692	ZFAND6	239757_at	-1.347	REEP1	204364_s_at	-2.877		230746_s_at	-1.181	-0.599
	M10098_5_a	-1.326	ANKHD1	233292_s_at	-1.162	TMEM19	229126_at	-2.788	HUWE1	236294_at	-1.148	-0.686
BCLAF1	201083_s_at	-1.325		231205_at	-1.151	TMEM107	224495_at	-2.781	ARID1B	225181_at	-1.131	-0.739
PAPOLA	212720_at	-1.213	ACTBL3	210926_at	-1.147	NANOS1	228523_at	-2.731	NDE1	222625_s_at	-1.106	-0.722
PKP2	207717_s_at	-1.203	C1orf199	225786_at	-1.116	SOX2	228038_at	-2.702		224549_x_at	-1.096	-1.134
CITED2	209357_at	-1.183	NAPA	208751_at	-1.057		1554007_at	-2.676	EIF2C1	222576_s_at	-1.045	-1.456
TEAD1	214600_at	-1.179	HNRNPM	224373_s_at	-1.035		242127_at	-2.601	PEG10	212092_at	-1.024	-0.948
PHACTR2	244774_at	-1.147		237895_at	-1.025	PDK3	206348_s_at	-2.575	RHBDD2	232053_x_at	-0.941	-1.342
IRS1	242979_at	-1.144		244753_at	-1.023	CXXC5	224516_s_at	-2.54	LAPTM4B	1554679_a_a	-0.938	-1.062
LGALS8	208935_s_at	-1.132		241460_at	-1.01	OLFM1	213131_at	-2.538	ENO1	217294_s_at	-0.91	-0.679
C1orf63	209006_s_at	-1.121	FLNA	213746_s_at	-1.009	TMEM14A	218477_at	-2.494	LMNA	1554600_s_a	-0.904	-0.785
CDCA2	236957_at	-1.087	SFXN1	232055_at	-0.999	REEP1	204365_s_at	-2.489	KIF22	216969_s_at	-0.884	-0.883
VGLL3	220327_at	-1.055	LOC641298	1557987_at	-0.978	WRB	202749_at	-2.465	BCL9L	228065_at	-0.884	-0.719
	213686_at	-1.048	CRIM1	228496_s_at	-0.973	ANKRD36B	220940_at	-2.443	UCKL1	232675_s_at	-0.883	-0.924
WSB1	210561_s_at	-1.018		232134_at	-0.973	C1orf93	231835_at	-2.437	RPL37A	214041_x_at	-0.882	-1.701
HIVEP3	235122_at	-1.005	CD24	208650_s_at	-0.952	TXNIP	201010_s_at	-2.434	NOTCH2	212377_s_at	-0.878	-0.762
PTPN11	209895_at	-0.985	PRKDC	208694_at	-0.95	TNFAIP8L1	227420_at	-2.411	SPTBN1	200672_x_at	-0.86	-1.045
BCLAF1	201084_s_at	-0.981		230099_at	-0.943	CTHRC1	225681_at	-2.407	APH1A	1554417_s_a	-0.842	-0.65
IQGAP1	210840_s_at	-0.944	ZBTB20	235308_at	-0.933	RHOB	212099_at	-2.383	ACTB	AFFX-HSAC	-0.815	-1.016
SERPINB9	209723_at	-0.924	IRS1	235392_at	-0.932	FLJ90757	1566557_at	-2.342	LMNA	203411_s_at	-0.8	-0.627
PRPF4B	211090_s_at	-0.921	FASN	212218_s_at	-0.929	CXXC5	233955_x_at	-2.334	AKAP12	227529_s_at	-0.8	-0.792
ERC1	1563947_a_a	-0.92		239331_at	-0.922	BRI3BP	231810_at	-2.32	MYH10	212372_at	-0.796	-0.665

Table 8–6: Genes Down-regulated by UDCA, Dex, DCA or both UDCA and Dex in the HET-1A Cell Line

Down-regulated Genes in the HET-1A Cell Line

UDCA and DCA				DCA and Dex				UDCA and Dex and DCA				
GENE	PROBE ID	LOG CHANGE UDCA	LOG CHANGE DCA	GENE	PROBE ID	LOG CHANGE UDCA	LOG CHANGE DCA	GENE	PROBE ID	LOG CHANGE UDCA	LOG CHANGE Dex	LOG CHANGE DCA
MALAT1	226675_s_at	-2.328	-0.722		242471_at	-1.706	-2.106	CXCL14	222484_s_at	-1.903	-1.323	-9.142
ASPM	232238_at	-1.684	-1.68		1559391_s_a	-1.581	-0.79	CXCL14	218002_s_at	-1.694	-1.068	-10.52
EPPK1	232164_s_at	-1.516	-2.16	DLEU2	1556821_x_	-1.375	-1.955	TRERF1	238520_at	-1.505	-0.625	-4.913
ATP8B3	1554704_at	-1.453	-0.967		217482_at	-1.336	-1.268	MKI67	212020_s_at	-1.336	-1.112	-2.235
FAM13B	218518_at	-1.36	-0.815		242121_at	-1.3	-1.937		242890_at	-1.297	-0.882	-2.751
IRS1	238933_at	-1.288	-0.641		232889_at	-1.215	-1.594	SLC16A3	202855_s_at	-1.289	-0.977	-1.987
	213484_at	-1.283	-0.959	ATP6V0E1	214149_s_at	-1.171	-0.801	AHNAK	211986_at	-1.214	-0.834	-1.909
DHRS2	214079_at	-1.25	-2.061	LOC727820	227383_at	-1.153	-1.194		244354_at	-1.137	-0.655	-2.101
CENPE	205046_at	-1.214	-1.811		232541_at	-1.049	-1.1	FUS	1565717_s_a	-1.131	-0.624	-1.58
TNRC6B	238468_at	-1.161	-1.019		217164_at	-1.04	-1.884		230085_at	-1.114	-0.651	-4.576
MKI67	212023_s_at	-1.16	-1.138	LOC649305	1568780_at	-1	-1.354		1559156_at	-1.105	-1.756	-4.137
ADM	202912_at	-1.156	-2.761	LARP1	212193_s_at	-0.973	-0.702	SOX4	201417_at	-1.054	-0.811	-2.057
ATAD4	219127_at	-1.143	-1.057	STOX2	231969_at	-0.939	-1.029	HIPK2	225368_at	-1.035	-0.692	-1.847
ZFHX4	241700_at	-1.138	-1.236		240247_at	-0.908	-0.992	GNAI2	201040_at	-1.028	-0.925	-2.066
NEURL1B	225355_at	-1.132	-2.842	GFRA1	227550_at	-0.888	-0.89	SFRS1	201742_x_at	-0.997	-1.127	-1.782
LBH	221011_s_at	-1.128	-1.905	AP2M1	200613_at	-0.855	-0.672	DAPK1	203139_at	-0.98	-0.693	-1.646
MXD4	210778_s_at	-1.105	-1.751		238142_at	-0.839	-0.992	CHD4	201183_s_at	-0.949	-0.662	-1.856
NDRG2	214279_s_at	-1.096	-1.119	NOTCH2NL	214722_at	-0.827	-0.815	NID1	202007_at	-0.946	-0.598	-1.794
MID1	203637_s_at	-1.091	-1.189	COL1A1	202310_s_at	-0.82	-2.717	FAT3	236029_at	-0.918	-0.815	-2.647
NR2F2	209120_at	-1.085	-1.662	AHNAK2	212992_at	-0.816	-1.336	STRBP	229513_at	-0.918	-0.967	-3.477
CXCR4	209201_x_at	-1.083	-3.074	SFPQ	221768_at	-0.815	-0.785	MSI2	225238_at	-0.894	-0.688	-1.804
CXCR4	211919_s_at	-1.083	-3.166	SFRS4	242837_at	-0.803	-0.665	GYS1	201673_s_at	-0.879	-0.641	-3.194
ZNF451	1556060_a_a	-1.081	-1.935		1563431_x_	-0.801	-0.69		222111_at	-0.868	-0.589	-1.558
MKI67	212021_s_at	-1.06	-0.649	PKM2	201251_at	-0.795	-0.814		241726_at	-0.867	-0.934	-2.552
NOS1	239132_at	-1.056	-1.683	MLEC	200617_at	-0.778	-0.679	DIDO1	227335_at	-0.853	-0.785	-2.067

Table 8–7: Genes Down-regulated by UDCA and DCA, DCA and Dex, or All Three of UDCA, Dex and DCA in the HET-1A Cell Line

Up-regulated Genes in the OE33 Cell Line

UDCA			Dex			DCA			UDCA and Dex			
GENE	PROBE ID	LOG CHANGE	GENE	PROBE ID	LOG CHANGE	GENE	PROBE ID	LOG CHANGE	GENE	PROBE ID	ANGE UDCA	LOG CHANGE Dex
MT1F	213629_x_at	1.2044	KLF9	203542_s_at	1.85212	CD69	209795_at	4.223373	MIR21	224917_at	1.357208	1.318221
	242343_x_at	1.028473	FKBP5	224840_at	1.598956	IL8	211506_s_at	3.925503	GOLGA8A	208798_x_at	0.945499	1.005712
	238142_at	1.023577	AHNAK2	1558378_a_:	1.592633		240655_at	3.785418	NCRNA0008	224566_at	0.905756	0.906363
EGR1	201693_s_at	0.940273	PHACTR3	227949_at	1.589597	NR4A2	216248_s_at	3.605917	PCBP2	213517_at	0.869764	0.619707
IL1RL1	207526_s_at	0.907689	ANGPTL4	223333_s_at	1.504329	NR4A2	204622_x_at	3.562143	LOC1001288	1555392_at	0.857322	0.738251
SYNE1	209447_at	0.858993	BOD1L	235009_at	1.481516	BCL2A1	205681_at	3.532492	PILRB	225321_s_at	0.824823	1.311279
RALGPS2	232112_at	0.854883	CAMK2N1	228302_x_at	1.478881	SOD2	215078_at	3.45533	N4BP2L2	221899_at	0.781968	0.613046
EGR1	201694_s_at	0.819627	ZFR	213286_at	1.46063		1569362_at	3.427079		1558154_at	0.758844	1.003876
EGR1	227404_s_at	0.794443	FKBP5	224856_at	1.458422	ICAM1	202638_s_at	3.423461		1560297_at	0.745499	0.787465
SLC30A1	212907_at	0.79115	PPFIBP1	214374_s_at	1.429976	INSIG1	201626_at	3.257066	BRWD2	229694_at	0.714249	0.704356
ZNF207	1556035_s_:	0.780427	PDE9A	205593_s_at	1.378284	INSIG1	201627_s_at	3.246668	GART	230097_at	0.697614	0.785671
	241991_at	0.770761	SLCO1B3	206354_at	1.32847	TCP11L2	1553861_at	3.087996	LOC1001328	1557996_at	0.693023	0.79089
OPN3	224392_s_at	0.761956	PTPN12	216915_s_at	1.314107	IL8	202859_x_at	3.074874	CAPRIN2	218456_at	0.685593	0.869284
MERTK	206028_s_at	0.758536	ANGPT2	205572_at	1.313127	ICAM1	202637_s_at	2.99395	C17orf91	214696_at	0.681917	0.797053
C17orf42	238295_at	0.749486	ESCO1	235645_at	1.290149	NR4A2	204621_s_at	2.940936	PABPC1L	226670_s_at	0.660001	0.996825
LOC653498	209403_at	0.739141	RGS2	202388_at	1.222179	GABBR1 /// L	205890_s_at	2.92236	NCRNA0008	224565_at	0.64423	0.640317
TPM1	238688_at	0.739113		242389_at	1.22181	KLHL24	242088_at	2.826004	DLG1	230229_at	0.594076	0.6112
N4BP2L2	214748_at	0.730946	BATF	205965_at	1.216566	INSIG1	201625_s_at	2.76857	TRIO	209013_x_at	0.586605	0.751649
POLR2J2	1552621_at	0.70976	FRMD3	230645_at	1.204571	ZAK	1555259_at	2.737552				
ZNF207	228157_at	0.708745	TP53I3	210609_s_at	1.200215	TM4SF1	215033_at	2.636274				
MT1F	217165_x_at	0.695555	ANGPTL4	221009_s_at	1.187156	HBP1	207361_at	2.613338				
RALGPS2	242458_at	0.693039	HRASLS2	221122_at	1.179702	ID2 /// ID2B	213931_at	2.60348				
MT1X	208581_x_at	0.67707	TSC22D3	208763_s_at	1.173144	NFKBIA	201502_s_at	2.529199				
THRB	228716_at	0.676367		241359_at	1.144642	LATS2	230348_at	2.522531				
MT1X	204326_x_at	0.675656	SAA1	208607_s_at	1.133628	CYP1B1	202437_s_at	2.519429				

Table 8–8: Genes Up-regulated by UDCA, Dex, DCA or both UDCA and Dex in the OE33 Cell Line

Up-regulated Genes in the OE33 Cell Line

UDCA and DCA				DCA and Dex				UDCA and Dex and DCA				
GENE	PROBE ID	LOG CHANGE UDCA	LOG CHANGE DCA	GENE	PROBE ID	LOG CHANGE UDCA	LOG CHANGE Dex	GENE	PROBE ID	LOG CHANGE UDCA	LOG CHANGE Dex	LOG CHANGE DCA
PDK4	225207_at	1.53946	1.604618	PER1	202861_at	1.756759	2.367165	CBX3	1555920_at	1.23665	0.874934	0.946256
PCDH7	228640_at	1.493355	0.804563	GCNT3	219508_at	1.676231	1.382505		241769_at	1.123668	0.825913	1.785404
	222168_at	1.396017	1.70102	CCL20	205476_at	1.556138	2.300887	KLHL24	221985_at	0.996912	0.772915	2.957996
	225328_at	1.30904	2.589723	YPEL2	229060_at	1.145941	1.457746		235094_at	0.973238	0.697749	0.739155
HNRNPD	213359_at	1.294049	2.242589	KLF9	203543_s_at	1.079119	0.836408	TSC22D4	1554501_at	0.932701	0.794222	1.345353
FBXO32	225803_at	1.266679	3.315828	CEBPD	203973_s_at	1.068766	0.772054	CFLAR	239629_at	0.862647	0.86359	0.71668
GALNT5	237183_at	1.24596	1.212583	PTGER4	204897_at	1.059459	1.054823		232290_at	0.848011	0.721871	1.694942
BACH2	221234_s_at	1.237264	1.624724	ATXN1	203231_s_at	1.017849	0.806082	PRDM1	228964_at	0.825294	0.608843	2.456161
KLHL24	221986_s_at	1.204899	3.276039	RBM39	227223_at	0.966757	0.884467	IL6R	205945_at	0.79479	1.660222	1.422286
EIF1	212225_at	1.194223	0.993189	ABHD2	228490_at	0.95602	1.741167	SPG7	230885_at	0.79145	0.619343	1.355565
SLC16A6	230748_at	1.19097	1.083354	MALAT1	224558_s_at	0.943647	1.10678	HNRNPL	221860_at	0.789909	0.794687	0.871212
SLC16A6	207038_at	1.076634	0.858386	WASF2	224563_at	0.908115	0.751648	GABARAPL	211458_s_at	0.739624	0.700082	2.301925
SLC2A12	244353_s_at	1.057132	1.197057	PER1	36829_at	0.887347	1.491872	EDN1	222802_at	0.730526	0.767525	2.103601
GEM	204472_at	1.031309	2.873857	IL6R	226333_at	0.86765	1.15059		229434_at	0.729535	0.591591	1.076246
GALNT5	240390_at	1.02237	1.563623	EDN1	218995_s_at	0.846284	1.455035	UFM1	242669_at	0.726548	0.632758	0.802504
FNBP4	212232_at	1.010409	0.925169	C6orf106	205457_at	0.839607	0.710422	RNASE4	213397_x_at	0.724068	0.631598	1.701171
FBXO32	241763_s_at	0.991544	1.338845	SEC14L1	202082_s_at	0.832579	0.849168		242725_at	0.720244	0.651346	0.816774
OPN3	219032_x_at	0.983011	0.872532	BIRC3	210538_s_at	0.820484	1.715526	MYOF	217518_at	0.711565	0.598106	0.628021
CTTN	214782_at	0.982285	1.920446	ATXN3	205415_s_at	0.814446	0.72117	ANKRD12	212286_at	0.692795	0.890642	1.099796
	225239_at	0.981303	2.268057	MKI67	212022_s_at	0.81251	0.593071	SNHG12	228990_at	0.661636	0.869661	0.825918
CTTN	214073_at	0.980101	1.236588	TUBB2A	204141_at	0.806351	0.761981	TBRG1	226318_at	0.638737	0.755754	0.722405
TP53INP1	225912_at	0.97919	1.336748	ARPP19	214553_s_at	0.790537	0.814298	CDKN1C	213348_at	0.636337	0.690597	0.783939
GRHL3	232116_at	0.967065	1.406998		239228_at	0.788865	0.712873	RUFY3	213939_s_at	0.621047	0.600977	1.039398
SERPINB9	242814_at	0.93193	1.553589	ZBTB46	227329_at	0.784073	1.258017	CCNL2	222999_s_at	0.616175	0.821469	0.741081
LGALS8	210732_s_at	0.918198	0.988785	ABHD2	225337_at	0.776728	0.967256					

Table 8–9: Genes Up-regulated by UDCA and DCA, DCA and Dex, or All Three of UDCA, Dex and DCA in the OE33 Cell Line

Down-regulated Genes in the OE33 Cell Line

UDCA			Dex			DCA			UDCA and Dex			
GENE	PROBE ID	LOG CHANGE	GENE	PROBE ID	LOG CHANGE	GENE	PROBE ID	LOG CHANGE	GENE	PROBE ID	LOG CHANGE UDCA	LOG CHANGE Dex
FABP5	202345_s_at	-0.97802	RPL37A	214041_x_at	-2.58965	FAM43A	227410_at	-2.8357	IL8	211506_s_at	-1.02552	-0.66661
TYMS	202589_at	-0.96437	ATP6V0E1	214149_s_at	-2.10935	FAM13B	218518_at	-2.51281	IL8	202859_x_at	-0.92294	-1.25993
IL1A	210118_s_at	-0.95009	RPL38	221943_x_at	-1.91782	ALDH1L2	231202_at	-2.49569	CENPK	222848_at	-0.87273	-1.22285
TYMS	1554696_s_a	-0.94673	ACSL4	202422_s_at	-1.7029		242140_at	-2.48551	LSM5	202904_s_at	-0.74134	-0.63886
HELLS	227350_at	-0.93814		217211_at	-1.65838		232569_at	-2.43311	SAE1	1555618_s_a	-0.70122	-0.76354
HELLS	223556_at	-0.85904	YIF1B	231211_s_at	-1.64317	MGC16385	1552330_at	-2.42434	MAD2L1	203362_s_at	-0.64976	-1.05053
MCM2	202107_s_at	-0.84025		213813_x_at	-1.58576	MAT2A	200768_s_at	-2.36724	HPS3	231121_at	-0.61931	-0.94336
AK2	212174_at	-0.83178	ADK	204120_s_at	-1.56629	DUSP6	208892_s_at	-2.353				
SPC25	209891_at	-0.82597	RPL38	202028_s_at	-1.53	C5orf54	220770_s_at	-2.33523				
CDCA7	224428_s_at	-0.80736	TMEFF2	224321_at	-1.51278	RNF170	226104_at	-2.23902				
	242890_at	-0.77302	GLS	221510_s_at	-1.50853	PHOSPHO2	230434_at	-2.21772				
AK2	205996_s_at	-0.76642	TMED2	204426_at	-1.4821	DUSP6	208891_at	-2.21769				
DLEU2	216870_x_at	-0.75627		216246_at	-1.47957	THBD	203887_s_at	-2.19033				
UNC5B	226899_at	-0.7464	RAP2C	218668_s_at	-1.44081	PHACTR3	227949_at	-2.17197				
SCML1	218793_s_at	-0.74429		214001_x_at	-1.42017	LOC729680	228977_at	-2.16965				
SUB1	221727_at	-0.7433	ITGB5	214021_x_at	-1.405	DUSP6	208893_s_at	-2.16488				
MCM6	201930_at	-0.74104	CEP97	235918_x_at	-1.33476	ZNF302	218490_s_at	-2.16345				
SNRPA1	206055_s_at	-0.73824	ATE1	225497_at	-1.29145	THBD	203888_at	-2.14544				
PTGS2	204748_at	-0.7377	MANSC1	220945_x_at	-1.2908	C7orf36	223433_at	-2.12386				
DNA2	213647_at	-0.73603	PRKAA1	225984_at	-1.24222	CD3EAP	205264_at	-2.12307				
SMEK2	222270_at	-0.73421	KIAA0776	212633_at	-1.22732		236489_at	-2.12202				
PCIF1	222044_at	-0.73295	ITGB8	226189_at	-1.1945	FBXO9	1566509_s_a	-2.09716				
CHEK1	238075_at	-0.71411	SLMO2	217851_s_at	-1.19266	C17orf86	221621_at	-2.06575				
NAP1L1	1556121_at	-0.70967	RP2	205191_at	-1.19108	SNAI2	213139_at	-2.04067				
DHFR	202532_s_at	-0.70504	EIF1AX	201016_at	-1.18741	TMEM177	218897_at	-2.03759				

Table 8–10: Genes Down-regulated by UDCA, Dex, DCA or both UDCA and Dex in the OE33 Cell Line

Down-regulated Genes in the OE33 Cell Line

UDCA and DCA				DCA and Dex				UDCA and Dex and DCA				
GENE	PROBE ID	LOG CHANGE UDCA	LOG CHANGE DCA	GENE	PROBE ID	LOG CHANGE DCA	LOG CHANGE Dex	GENE	PROBE ID	LOG CHANGE UDCA	LOG CHANGE Dex	LOG CHANGE DCA
CCNE2	205034_at	-1.57183	-2.3931	UBLCP1	243916_x_at	-1.32289	-0.63627	ACN9	218981_at	-0.74829	-1.14134	-0.77689
	213930_at	-1.29588	-1.2188	B3GALNT1	211379_x_at	-1.07563	-2.01086	TTF2	204407_at	-0.69419	-0.96334	-1.21671
RRM2	201890_at	-1.26501	-0.79802	TUBE1	226181_at	-1.04579	-1.21165	GART	210005_at	-0.68588	-0.64839	-1.10682
MCM10	222962_s_at	-1.16236	-1.60049	OTUD6B	222825_at	-1.02444	-0.9024	PSPH	205194_at	-0.63034	-1.30836	-1.5405
POLE2	205909_at	-1.01992	-1.61911	PACRGL	235554_x_at	-1.00879	-2.02979	POLE3	208828_at	-0.6209	-0.65357	-0.72922
MCM10	220651_s_at	-1.0152	-1.2049	PHF6	225501_at	-1.00466	-0.79804					
RRM2	209773_s_at	-0.99748	-0.81571	DBR1	234295_at	-0.91543	-1.73405					
MCM10	223570_at	-0.98886	-1.20414	FTSJD1	222811_at	-0.91489	-0.81515					
GINS2	221521_s_at	-0.92627	-0.73478	ZNF468	214751_at	-0.90811	-1.04976					
CDC7	204510_at	-0.92621	-2.09784	C5orf44	236526_x_at	-0.8682	-0.91463					
CHAC2	235117_at	-0.85724	-1.63036	KLHL20	204176_at	-0.84603	-0.81687					
DTL	218585_s_at	-0.85638	-0.63136	ABHD3	213017_at	-0.8414	-0.635					
FEN1	204768_s_at	-0.84386	-0.71197	PHLDA1	218000_s_at	-0.83891	-1.15981					
UNG	202330_s_at	-0.84311	-1.06685	TRIB3	1555788_a_at	-0.80436	-0.72534					
C7orf40	225699_at	-0.81845	-2.17215	MANEA	219003_s_at	-0.74595	-0.91621					
FEN1	204767_s_at	-0.79489	-0.7301	C10orf97	218297_at	-0.72847	-1.34371					
LUC7L	1557067_s_at	-0.78412	-1.31117	ALG13	222808_at	-0.70604	-0.93383					
C1orf53	1558508_a_at	-0.76771	-0.85023	PHLDA1	217996_at	-0.70142	-0.73751					
PCNA	201202_at	-0.76654	-0.67261	LPAR1	204036_at	-0.68293	-0.71086					
AK2	212175_s_at	-0.75852	-0.78504	ALG10	1552306_at	-0.67385	-1.73443					
KRR1	203203_s_at	-0.74195	-0.77582	PHLDA1	217997_at	-0.67375	-2.02024					
	228955_at	-0.7339	-1.17849	CSGALNACT1	218871_x_at	-0.6496	-0.76636					
LOC100129(	236075_s_at	-0.72573	-0.74524		1558801_at	-0.64157	-1.74451					
UHRF1	225655_at	-0.72266	-1.58986	RAD51AP1	204146_at	-0.61603	-0.63794					
SFRS7	201129_at	-0.72261	-1.43104	NIPSNAP3A	224436_s_at	-0.60444	-1.40725					

Table 8–11: Genes Down-regulated by UDCA and DCA, DCA and Dex, or All Three of UDCA, Dex and DCA in the OE33 Cell Line

Up-regulated Genes in the HCT116 Cell Line

UDCA			Dex			DCA			UDCA and Dex			
GENE	PROBE ID	LOG CHANGE	GENE	PROBE ID	LOG CHANGE	GENE	PROBE ID	LOG CHANGE	GENE	PROBE ID	LOG CHANGE UDCA	LOG CHANGE Dex
DHRS3	202481_at	1.721233		AFFX-LysX-	2.273459	C9orf150	227443_at	28.01939				
SCD	211162_x_at	1.603246		AFFX-LysX-	2.050048	RGS4	204337_at	21.67074				
INSIG1	201625_s_at	1.513806		239302_s_at	1.887336	RGS4	204338_s_at	19.8828				
SCD	211708_s_at	1.5137	UNC84A	214169_at	1.770207	IL8	211506_s_at	19.08894				
			UGCGL2	235749_at	1.758202	C12orf39	229778_at	18.73937				
			ING3	231863_at	1.624699	SERPINE1	202627_s_at	14.27583				
			METTL7A	207761_s_at	1.593115	SLC7A11	217678_at	13.68918				
			IMMP1L	230556_at	1.580958	CXCL3	207850_at	11.82042				
			KBTBD3	228777_at	1.570351	UPP1	203234_at	11.80761				
				1569114_at	1.548234	SLC7A11	207528_s_at	10.73369				
				235429_at	1.539878	SERPINE1	202628_s_at	10.73298				
			ATP5S	213995_at	1.502527	SLC7A11	209921_at	10.12614				
						TRIB3	1555788_a_:	9.42966				
						RGS4	204339_s_at	8.41406				
						TRIB3	218145_at	8.14103				
						DDIT3 /// NF	209383_at	7.768386				
						SLFN5	1553055_a_:	7.207128				
						CXCL2	209774_x_at	7.042403				
						CHAC1	219270_at	6.831085				
						SLFN5	1557078_at	6.552124				
							242228_at	6.548169				
						STC2	203439_s_at	6.419821				
						EGR1	201693_s_at	6.205886				
						ELL2	214446_at	6.166528				
						NT5E	1553994_at	6.123558				

Table 8–12: Genes Up-regulated by UDCA, Dex, DCA or both UDCA and Dex in the HCT116 Cell Line

Up-regulated Genes in the HCT116 Cell Line

UDCA and DCA				DCA and Dex				UDCA and Dex and DCA				
GENE	PROBE ID	LOG CHANGE UDCA	LOG CHANGE DCA	GENE	PROBE ID	LOG CHANGE UDCA	LOG CHANGE DCA	GENE	PROBE ID	LOG CHANGE UDCA	LOG CHANGE Dex	LOG CHANGE DCA
EGR1	227404_s_at	1.760259	4.184574	SPTLC1	1554053_at	1.554881	3.96579					
BHLHE40	201170_s_at	1.724636	5.437502	HINT3	228697_at	1.518083	1.516992					
IL8	202859_x_at	1.700345	14.56391									
DNAJB9	202842_s_at	1.574159	3.243553									
TMEM22	219569_s_at	1.567012	2.270718									
TMEM39A	222690_s_at	1.561481	2.523274									
C4orf34	224990_at	1.539655	2.920692									
PER2	205251_at	1.51985	3.129195									
C2orf30	224628_at	1.516776	1.503106									
DDIT4	202887_s_at	1.512023	5.074414									

Table 8–13: Genes Up-regulated by UDCA and DCA, DCA and Dex, or All Three of UDCA, Dex and DCA in the HCT116 Cell Line

Down-regulated Genes in the HCT116 Cell Line

UDCA			Dex			DCA			UDCA and Dex			
GENE	PROBE ID	LOG CHANGE	GENE	PROBE ID	LOG CHANGE	GENE	PROBE ID	LOG CHANGE	GENE	PROBE ID	LOG CHANGE UDCA	LOG CHANGE Dex
CENPF	209172_s_at	-1.74443	TMED2	204426_at	-3.11216	SOX4	201416_at	-9.91875				
SNHG7	229050_s_at	-1.69214	ACTB	X00351_5_a	-3.02762	SOX4	213668_s_at	-7.72489				
TNRC6C	222820_at	-1.61635	KIF22	216969_s_at	-2.83665	KANK2	218418_s_at	-7.22809				
TGOLN2	212043_at	-1.60721	TMED2	204427_s_at	-2.77441	CCNE2	211814_s_at	-7.04833				
AHNAK	211986_at	-1.55039	STIP1	212009_s_at	-2.70258		238956_at	-6.87324				
	235612_at	-1.54827	SNAP23	214544_s_at	-2.26967	DKK4	206619_at	-6.779				
AKAP12	227529_s_at	-1.54551	RHBDD2	232053_x_at	-2.20556	HSPA2	211538_s_at	-6.73179				
ENAH	228310_at	-1.51236	MED18	219730_at	-2.17826	SOX4	201417_at	-6.70384				
			ADAM10	214895_s_at	-2.08342		236219_at	-6.3644				
			ADAM9	1555326_a_a	-2.08111	CCNE2	205034_at	-6.34945				
			PPP5C	201979_s_at	-2.02681		227533_at	-5.71954				
			SAE1	1555618_s_a	-2.01145	GPRC5B	203632_s_at	-5.6607				
			RAB5A	206113_s_at	-1.98632	OSGEPL1	230032_at	-5.59639				
			ACTB	X00351_M	-1.97889	PPWD1	213483_at	-5.49113				
			PPP2R1A	200695_at	-1.95744	SOX4	201418_s_at	-5.32685				
			MOSPD1	1557455_s_a	-1.93218	C1orf93	231835_at	-5.24408				
			CYP51A1	216607_s_at	-1.88968	ELOVL6	227491_at	-5.23445				
			JAK1	1552610_a_a	-1.86333		228717_at	-5.13536				
			UCKL1	232675_s_at	-1.85269		220915_s_at	-5.11223				
			CCNG2	211559_s_at	-1.84694	ADAM19	209765_at	-5.1011				
			LAPTM4B	1554679_a_a	-1.84477		228479_at	-5.083				
			DCTN1	201082_s_at	-1.83286	FBXO9	212987_at	-4.93808				
			PICALM	215236_s_at	-1.82176	FGF18	231382_at	-4.87064				
			RPAP3	1557984_s_a	-1.7931		228955_at	-4.86479				
			ECT2	234992_x_at	-1.7876	C5orf13	201310_s_at	-4.85005				

Table 8–14: Genes Down-regulated by UDCA, Dex, DCA or both UDCA and Dex in the HCT116 Cell Line

Down-regulated Genes in the HCT116 Cell Line

UDCA and DCA				DCA and Dex				UDCA and Dex and DCA				
GENE	PROBE ID	LOG CHANGE UDCA	LOG CHANGE DCA	GENE	PROBE ID	LOG CHANGE UDCA	LOG CHANGE DCA	GENE	PROBE ID	LOG CHANGE UDCA	LOG CHANGE Dex	LOG CHANGE DCA
PCNX	229287_at	-1.85287	-3.69782	DCAKD	221224_s_at	-2.25453	-1.61248					
FAM13B	218518_at	-1.83104	-3.02074	HNRNPH1	213470_s_at	-2.0363	-1.6327					
PDLIM5	213684_s_at	-1.80437	-2.99582	MVK	215649_s_at	-1.88777	-1.80291					
PDLIM5	221994_at	-1.71501	-2.88634	NDRG2	214279_s_at	-1.87385	-2.93286					
GJA1	201667_at	-1.70338	-6.26713	MVD	203027_s_at	-1.85539	-2.08275					
	237435_at	-1.70336	-2.62888	TFDP1	204147_s_at	-1.75407	-1.65667					
MKI67	212023_s_at	-1.67416	-3.1237	RBBP4	217301_x_at	-1.57424	-1.81549					
	228959_at	-1.6441	-2.49443	SLC37A4	217289_s_at	-1.56976	-1.50163					
C14orf159	218298_s_at	-1.60933	-3.1127	NT5DC2	218051_s_at	-1.56445	-1.68785					
NFYB	218129_s_at	-1.60512	-1.56566	CYB5B	201633_s_at	-1.546	-2.21204					
MKI67	212021_s_at	-1.56476	-1.76056	TM7SF2	210130_s_at	-1.52263	-2.21547					
BRCC3	231913_s_at	-1.54892	-1.55681	RETSAT	1566472_s_a	-1.51536	-1.63219					
CENPE	205046_at	-1.52409	-2.44457	HMG20B	209113_s_at	-1.50997	-1.51506					
EPPK1	232165_at	-1.52405	-2.70307									
	242890_at	-1.52364	-2.72812									

Table 8–15: Genes Down-regulated by UDCA and DCA, DCA and Dex, or All Three of UDCA, Dex and DCA in the HCT116 Cell Line

8.7. Intensity Values of Probeset Pairs for Genes Chosen for Validation

Probeset	Gene	Intensity		p-Value	Intensity		p-Value	Intensity		p-Value
		Control	DCA		Control	UDCA		Control	Dex	
Probeset 1	PHACTR3	172.65	61.66	0.003	135.97	78.8	0.03	154.04	657.33	0.004
		195.98	59.6		156.28	90.35		159.82	792.84	
Probeset 1	SKI	1000.4	646.37	0.021	801.76	509.56	0.002	116.21	225.21	0.038
		1020.75	723.28		838.18	511.1		145.14	242.51	
Probeset 2	SKI	120.69	217.69	0.326	100.51	100.13	0.981	930.38	681.71	0.012
		161.04	156.8		124.48	123.93		977.61	640.21	
Probeset 1	SERPINE1	258.75	474.13	0.043	187	395.71	0.015	253.18	466.15	0.013
		275.78	390.23		210.98	357.97		275.39	526.22	
Probeset 2	SERPINE1	155.93	226.04	0.079	115.04	160.21	0.037	128.88	226.16	0.033
		170.24	198.5		128.44	161.5		150.48	258.52	
Probeset 1	PRKDC	2209.84	1921.36	0.702	1854.89	951.26	0.111	2222.03	1245.66	0.035
		2034.99	2187.25		1718.25	1322.4		2052.27	980.37	
Probeset 2	PRKDC	828.74	928.15	0.585	632.12	549.47	0.041	693.06	362.24	0.006
		832.45	811		681.9	535.18		724.21	395.51	
Probeset 1	CRIM1	1948.98	2921.6	0.028	1921.55	981.32	0.053	1450.88	1180.76	0.054
		1904.16	3467.84		1718.9	1219.91		1582.37	1044.34	
Probeset 2	CRIM1	1486.12	2822.44	0.03	1151.2	666.07	0.079	1050.4	695.08	0.118
		1727.01	2546.12		1285.38	863.36		884.77	499.98	
Probeset 3	CRIM1	1047.39	1409.75	0.023	932.97	415.71	0.162	2165.5	1251.26	0.035
		943.72	1482.27		791.75	644.12		2150.26	965.68	
Probeset 1	CITED2	323.23	279.99	0.117	270.56	148.07	0.02	360.78	429.77	0.54
		389.15	245.47		308.17	165.99		421.45	400.87	
Probeset 2	CITED2	1254.91	767.91	0.031	935.71	352.03	0.038	1093.42	1047.29	0.522
		1159.24	863.74		946.48	488.05		998.74	928.46	
Probeset 3	CITED2	129.12	143.75	0.252	109.17	141.58	0.431	131.58	117.3	0.522
		134.8	135.75		113.37	111.13		108.64	164.21	
Probeset 1	STAM2	846.09	1019.25	0.029	54.41	115.55	0.065	639.9	802.14	0.753
		793.67	988		75.04	117.05		653.13	584.15	
Probeset 2	STAM2	242.48	384.72	0.013	628.3	491.94	0.788	201.96	286.21	0.067
		251.5	353.59		613.93	963.75		223.36	345.61	
Probeset 3	STAM2	518.68	550.47	0.379	174.53	525.8	0.031	417.12	513.51	0.042
		500.63	514.14		190.63	384.56		427.96	481.46	
Probeset 4	STAM2	156.53	173.98	0.675	339.03	347.58	0.469	129.02	109.64	0.121
		142.38	142.59		363.78	326.22		118.9	98.6	

Table 8–16: Micro-Array Intensity Values for Probeset Pairs of Validation Genes

Probeset	Gene	Intensity		p-Value	Intensity		p-Value	Intensity		p-Value
		Control	DCA		Control	UDCA		Control	Dex	
Probeset 1	CTTN	312.59	278.92	0.094	168.86	657	0.01	1741.47	1432.02	0.008
		295.09	277.78		191.79	535.82		1806.1	1411.56	
Probeset 2	CTTN	215.68	301.95	0.103	238.03	359.28	0.002	180.4	264.87	0.051
		235.09	264.43		231.65	369.31		191.86	325.49	
Probeset 3	CTTN	97.97	158.04	0.067	1584.06	1054.76	0.001	274.23	322.71	0.07
		112.71	139.35		1616.83	1070.64		290.16	349.21	
Probeset 4	CTTN	1879.14	1166.56	0.001						
		1904.85	1193.51							
Probeset 1	BIRC3	413.83	271.19	0.039	341.45	254.78	0.065	382.27	1067.08	0.003
		414.53	218.5		355.78	289.41		419.42	1014.51	
Probeset 1	NOTCH2	424.17	444	0.549	1492.59	843.83	0.004	1697.6	964.93	0.003
		397.11	409		1415.53	876.53		1599.75	964.49	
Probeset 2	NOTCH2	1607.68	1615.17	0.698	337.11	200.45	0.03	382.63	212.79	0.013
		1580.99	1537.28		288.62	188.58		339.43	216.16	
Probeset 3	NOTCH2	1789.05	1823.09	0.979	1438.08	685.23	0.035	1558.87	957.76	0.005
		1697	1670.45		1387.6	862.45		1572.84	890.64	
Probeset 4	NOTCH2	107.99	139.18	0.254						
		131.9	140.47							
Probeset 1	NR3C1	2877.08	3873.47	0.033	2882.26	1893.34	0.03	3322.96	2520.71	0.001
		2749.07	3535.06		2911.8	2151.28		3273.3	2514	
Probeset 2	NR3C1	1887.88	3390.36	0.002	631.85	780.04	0.603	741.83	721.37	0.655
		1830.13	3278.27		609.36	587.71		751.71	833.65	
Probeset 3	NR3C1	3340.21	4421.3	0.013	2455.54	1615.75	0.024	3013.51	2206.67	0.006
		3309.44	4172.64		2342.22	1781.46		2883.13	2197.82	
Probeset 4	NR3C1	737.2	1007.25	0.062	1444.32	1008.62	0.073	1692.71	1427.13	0.039
		760.19	893.05		1440.81	1182.22		1659.64	1319.49	
Probeset 1	IL8	29.38	730.69	0.005						
		19.48	935.4							
Probeset 2	IL8	35.81	365.5	0						
		33.9	344							

Table 8–17: Micro-Array Intensity Values for Probeset Pairs of Validation Genes

Probeset	Gene	Intensity		p-Value	Intensity		p-Value	Intensity		p-Value
		Control	DCA		Control	UDCA		Control	Dex	
Probeset 1	ACTB	14026.95	11707.77	0.032	12600.28	3788.94	0.001	14524.66	4735.21	0.002
		13590.98	10976.7		11801.07	3913.61		14115.8	4235.31	
Probeset 2	ACTB	14434.18	11851.09	0.027	13095.99	7336.52	0.001	14347.23	7070.17	0
		14094.52	11057.81		12563.78	7247.95		14186.28	7039.26	
Probeset 3	ACTB	18081.14	12975.84	0.017	15976.8	11669.56	0.037	16825.42	12575.85	0.029
		17374.81	13821.74		15773	12916.34		16554.46	11177.92	
Probeset 4	ACTB	19905.97	15075.44	0.003	17914.88	14677.83	0.024	16825.42	12575.85	0.029
		19346.63	15092.65		16981.92	14366.41		16554.46	11177.92	
Probeset 5	ACTB	19624.59	14328.05	0.011	17354.2	14647.02	0.012	18907.67	15140.19	0.014
		18914.55	14977.25		17180.13	14073.38		18034.44	15120.8	
Probeset 6	ACTB	19462.91	14611.11	0.01	17287.39	14812.2	0.019	18729.08	15433.73	0.007
		18938.87	15237.17		17181.76	14107.62		18177.96	15260.28	
Probeset 1	ATF3	76.07	2067.19	0.001	64.37	405.47	0.012	78.86	118.32	0.069
		90.93	2092.48		74.92	295.04		88.74	148.3	
Probeset 2	ATF3	125.43	662.78	0.003						
		103.47	710.99							
Probeset 1	CXCL14	7277.27	773.63	0.001	6629.36	2432.88	0.015	7674.1	3485.77	0.012
		7694.11	654.44		7042.78	1833.03		8105.74	4058.24	
Probeset 2	CXCL14	6044.14	659.7	0	5362.72	1607.79	0.006	6207.29	2261.45	0.009
		5835.92	639.77		5535.48	1320.09		6167.96	2703.46	
Probeset 1	DDIT3	290.94	4133.41	0.001	208.01	1145.22	0.016	211.68	220.99	0.222
		254.12	3782.09		166.4	805.82		176.96	238.43	
Probeset 1	GDF15	90.54	7362.83	0.001	75.29	1108.28	0.004	109.61	135.83	0.104
		71.77	8042.82		59.48	860.1		97.96	175.48	
Probeset 1	TRIB3	357.6	5084.18	0.001	276.98	1088.53	0.002	283.29	304.21	0.151
		348.09	5803.03		284.4	1235.95		283.15	340.39	
Probeset 2	TRIB3	107.95	1182.74	0	64.65	136.62	0.013			
		108.75	1118.14		57.36	121.08				

Table 8–18: Micro-Array Intensity Values for Probeset Pairs of Validation Genes

Appendix 4.

9. Appendix 4: Protocols, Reagents and Equipment Used

This appendix presents the protocols for cell culture and passage, Western Blotting, immunofluorescent staining of cell lines and paraffin embedded tissue, DAB staining of paraffin embedded tissue and a protocol for RT-PCR.

The Western blotting protocols were provided by Dr Michael Freely and are reproduced with permission.

9.1. Cell Lines, Cell Culture and Cell Passage

9.1.1. Cell lines

Multiple cell lines were used for this research. Each has been described in the relevant chapter in the methods section. The rationale for their use has been explained in specific experimental sections.

For the majority of experiments investigating the effects of DCA and UDCA on oesophageal epithelium, the HET-1A [240] cell line was used. This cell line, derived from the oesophagus of a 25 year old black male represents the only cell line available for study of oesophageal squamous epithelium. One primary cell line exists to study squamous epithelium of the oesophagus however its ability to propagate and passage is limited and therefore it is only used for validation experiments when required. It was not used in this research. Although the protective role of UDCA has been well established in hepatocellular and colorectal cell lines, these are distinctly different from the oesophagus. The oesophageal epithelium is squamous where the rest of the GI tract is columnar epithelium. The hepatic cells are of mesenchymal origin where the oesophageal cells are epithelial in origin. Thus, in order to strengthen our findings, it was necessary to use cell lines in which UDCA had an established protective role.

The HUH-7 [242-243] cell line was chosen as is represents a model in which the protective effects of UDCA have been most frequently demonstrated and validated. In this research it was used to demonstrate that the techniques used were capable of reproducing the findings of other laboratories. It also acted as a positive control for the expression of the GR.

The HCT116 [241] cell line was used because it represented an epithelial cell line derived from the gastro-intestinal tract and one in which the protective effects of UDCA have been demonstrated, although with less reproducibility than the HUH-7 cell line.

The origin of other cell lines used in this research are shown below (See. They were used as positive controls or for direct comparisons in different experiments to highlight the differences between cell lines of different embryological origins.

Cell Line	Origin	Immortilized	Medium
HET-1A	Healthy oesophagus of a 25year old black male	Yes (SV40)	BEBM with supplements
HCT116	Adult male colorectal adenocarcinoma	No	McCoy's 5A medium with 10% FCS
HUH-7	Adult male (Japanese), well differentiated hepatocellular carcinoma	No	Dulbecco's minimal essential medium with 10% FCS
SKGT-4	Male, OAC derived from BO	No	RPMI1640 with 10% FCS.
OE33	Female, OAC derived from BO	No	RPMI1640 with 10% FCS.
KYSE410	Adult male (Japanese) poorly differentiated squamous cell carcinoma of the oesophagus	No	RPMI1640 with 10% FCS.
QH	Adult male, Non-dysplastic BO	Yes (hTERT)	BEBM with supplements and 10% FCS

Table 9–1: Cell Lines used in this research, Their origin and Growth Medium.

9.1.2. Cell Culture and Cell Passage

a) Warm medium, trypsin, soybean trypsin inhibitor, PBS and HBSS in the water-bath at 37°C incubator for at least 30 min prior to doing cell culture

b) Clean out the laminar airflow hood with 70% IMS prior to working. Wipe all surfaces. Spray all surfaces of bottles/pipettes/ flasks etc to avoid bringing contamination into the hood. Also spray your gloves. Clean white Labcoat must be worn at all times when using the Hood.

Protocol

a) Examine the flask of cultured cells under the inverted microscope to check for contamination, cell density, etc. Cells should be split at no greater that 80 – 90% confluent.

b) Remove the old (spent) media.

c) Wash the monolayer with twice with 3mls PBS (SKGT4, OE33, HUH-7 and HCT116) or HBSS (HET-1A and QH). Let the PBS sit on the cells for at least 30 seconds during each wash to remove as much extracellular proteins as possible.

d) Remove the PBS or HBSS and add 1 ml of 0.25% w/v trypsin solution (1X) (SKGT4, OE33, HUH-7 and HCT116) or trypsin/HBSS (HET-1A and QH).

e) Incubate for ~3 minutes, then check flask under inverted microscope to make sure cells are detached from the bottom of the flask.

f) Add 5mls of complete medium (SKGT4, OE33, HUH-7 and HCT116) or 1ml soybean trypsin inhibitor (HET-1A and QH) to inhibit trypsin. The FCS in the medium contains trypsin inhibitor.

g) Transfer the cell suspension to a sterile 15 ml conical centrifuge tube.

h) Spin the cells down at 1,100 rpm for 3 minutes in a tabletop centrifuge.

i) Discard the supernatant carefully, so as not to disturb the cell pellet. Break up the pellet by tapping the tube.

j) Re-suspend the cells in ~5mls of fresh complete media.

k) Count cells for seeding, or split cells by adding 1ml (depending on splitting ratio*) of suspended cells to new flask containing 10 ml of fresh medium.

l) Replace the flask in the incubator.

9.1.3. Freezing Cells for Storage

a) Follow protocol for splitting cells up to step i.

b) Re-suspend the cells in pre-warmed freezing mix (FCS + 5% DMSO) by adding drop-wise to the broken up pellet

- A T25 is frozen down to 1 cryovial (add 1 ml freezing mix and put into 1 cryovial)

- A T75cm flask can be frozen down into 3 cryovials (add 3mls of freezing mix then aliquot 1 ml into each cryovial).

- A T 175 can be frozen down to 6 or 7 cryovials (add 6 or 7mls freezing mix and aliquot 1 ml into cryovial).

9.2. Sodium Dodecyl Sulphate Polyacrylamide Gel Electrophoresis (SDS-PAGE) (based on the Atto gel electrophoresis system)

©Michael Freeley, Dept. of Biochemistry, RCSI, Dublin. Written: 9th August 2005

(a) Rinse electrophoresis plates with ethanol.

(b) Attach rubber gaskets to notched plates, add the plain glass plate and fasten the green clips to each side.

(c) Add a comb between the plates and mark the glass 1 cm down from the bottom of the comb.

Remove comb and prepare acrylamide *resolving gel* in the following order as shown (the above resolving gel is enough for two complete gel plates).

Component	**Volume**	
	10% Gel	**15% Gel**
dH_20	7.9 ml	4.6 ml
30 % Acrylamide	6.7 ml	10.0 ml
1.5 M Tris-HCl (pH 8.8)	5.0 ml	5.0 ml
10 % w/v SDS	200 µl	200 µl
10 % w/v APS	200 µl	200 µl
TEMED	8 µl	8 µl

(d) Quickly mix the resolving gel solution and pour between the glass plates up to the 1 cm mark.

(e) Overlay the resolving gel with 1 ml of isopropanol.

(f) Allow the gel to set for approximately 40 minutes at RT.

(g) Remove isopropanol and wash the top of the gel with dH_20.

(h) Remove any excess water with paper towel.

(i) Prepare *stacking gel* in the following order as shown.

Component	Volume
dH_20	3.4 ml
30 % Acrylamide	0.83 ml
1.0 M Tris-HCl (pH 6.8)	0.63 ml
10 % w/v SDS	50 µl
10 % w/v APS	50 µl
TEMED	5 µl

(j) Mix the stacking gel quickly and pipette between glass plates until solution reaches the top of the plate.

(k) Add combs (be careful to exclude any air bubbles from stacking gel).

(l) Allow stacking gel to set for approximately 40 minutes at RT.

(m) Remove the green clips and rubber gaskets and place the glass plates into the electrophoresis rig (the shorter, notched glass plates should be facing each other on the inside of the electrophoresis rig). Fasten the plates with the clear plastic holders.

(n) Prepare 1X SDS-PAGE running buffer (= 80mls of 5X SDS-PAGE running buffer and 320mls dH_20) and pour the running buffer into the electrophoresis rig and between the glass plates in the centre of the electrophoresis rig.

(o) Remove combs carefully (you can mark the bottom of wells with a marker before you remove the combs as it makes them easier to see), straighten any crooked wells with a gel-loading tip and wash each well by pipetting up and down.

(p) Load protein samples (approx 20µl) and molecular weight markers (approx 5 – 10 ul) (both of these must be boiled previously for 5mins) into the wells.

(q) Attach the leads and run gel at 200V and 40mAmps until the blue dye reaches the bottom the gel (approximately 1.5 hours).

Solutions required

30 % Acrylamide (Sigma catalogue A3699)

Store at 4°C

10 % w/v Ammonium Persulphate (10 % APS) (Sigma catalogue A3678)

Dissolve 0.1g APS in 1 ml dH_20

Store at 4°C

10 % APS must be prepared fresh weekly!

1.5 M Tris-HCl (pH 8.8) (Sigma catalogue T-1503)

Dissolve 90.825g Trizma in 400 ml dH_20

Adjust pH to 8.8 with HCl and add dH_20 to 500 ml

Store at RT

1.0 M Tris-HCl (pH 6.8) (Sigma catalogue T-1503)

Dissolve 60.55g Trizma in 400 ml dH_20

Adjust pH to 6.8 with HCl and add dH_20 to 500 ml

Store at room temperature

10 % w/v SDS (Sigma catalogue L-5750)

Dissolve 10g of SDS in 100 ml dH_20

Wear a face mask when weighing out as the powder creates lots of dust and is toxic (Consult MSDS)

TEMED (Sigma catalogue T-9281)

Store in the fume-hood as TEMED is pungent. Add TEMED to the resolving/stacking gel in the fume-hood

Isopropanol (Sigma catalogue l9516)

Store in the fume-hood or in solvent cupboard

5X SDS-PAGE running buffer

15.1 g TRIZMA (Sigma catalogue T-1503)

94 g Glycine (Sigma catalogue G-8898)

50 mls of 10 % w/v SDS

dH_20 to 1 litre

Dilute to 1X before use with dH_20 (=80 mls of 5X buffer and 320 mls dH_20)

Molecular weight markers (Sigma catalogue SDS-6H)

Reconstitute powder with SDS-PAGE sample buffer according to the instructions and aliquot 5-10 uL into tubes and store at -20 degrees.

SDS-PAGE sample buffer (1X)

Combine: 1.51 g Trizma

20 ml Glycerol

35 ml dH_20

Adjust the pH to 6.8 with HCl and then add:

4g SDS powder (Sigma catalogue L-5750) (*Caution when weighing*!)

0.002g bromophenol blue (Sigma catalogue B-0126)

Add distilled water to 180ml. Store at room temperature.

Important: Add fresh DTT to 100mM final concentration immediately before use!

9.3. Western blotting (based on the Atto semi-dry technique)

© Michael Freeley, Dept. of Biochemistry, RCSI, Dublin. Written: 30th August 2005

a) While the SDS-PAGE gel is running cut 4 sets of filter paper (10 sheets in each set) and 2 pieces of PVDF membrane (6.5 cm x 9.2 cm for both filter paper and PVDF).

b) Activate the PVDF membrane by soaking in methanol for 30 seconds and then place it in Western blot transfer buffer.

c) When the SDS-PAGE gel has run, prise apart the plates, remove the stacking gel with a scalpel and discard the stacking gel.

d) On the Atto Western blot transfer system, soak 1 set of filter papers in Western blot transfer buffer and place on the bottom of the rig.

e) Place the activated PVDF membrane on top of the filter papers and add more Western blot transfer buffer on top.

f) Take the SDS-PAGE gel, immerse it in Western blot transfer buffer briefly and place it on top of the PVDF membrane (exclude any air bubbles).

g) Complete the sandwich by adding 1 set of filter papers (previously soaked in Western blot transfer buffer) on top of the SDS-PAGE gel.

h) Remove any excess transfer buffer on the bottom of the rig with paper towel

i) Lower the top piece of the transfer system onto the sandwich, connect the leads and run at 100 V and 100 mAmps per gel sandwich for 1 hour (the system can accommodate two gel sandwiches).

The following procedure to detect antigens on the PVDF membrane with antibodies is described below and is a general protocol. Each antibody may have specific incubation conditions and buffers so consult the antibody data sheet as they may not be the same as described below.

(10) Remove filter papers on top of gel sandwich and also remove SDS-PAGE gel and discard it.

(11) Cut off molecular weight marker lane with a scalpel and incubate with Coomassie stain solution for 5 minutes. De-stain with Coomassie de-staining solution.

(12) Mark any relevant lanes on the PVDF membrane with a pencil and incubate with Western blot blocking buffer for 1 hour at room temperature on a shaker. *From this point on, do not let the PVDF membrane go dry!*

(13) Wash the PVDF membrane three times with Western blot wash buffer (5 minutes washes) at RT.

(14) Incubate PVDF membrane with primary antibody (diluted according to manufacturer's instructions) in Western blot blocking buffer overnight at 4°C with gentle agitation.

(15) Wash the PVDF membrane three times with Western blot wash buffer (5 minutes washes) at RT

(16) Incubate PVDF membrane with HRP-labelled secondary antibody (diluted according to manufacturer's instructions) in Western blot blocking buffer for 1-2 hours at room temperature with gentle agitation.

(17) Wash the PVDF membrane three times with Western blot wash buffer (5 minutes washes) at RT.

Prepare fresh HRP development solution (this is enough for two PVDF membranes):

12mls of 100mM Tris-HCl (pH 8.5)

3.6µl of 30% H_2O_2

30µl of 250mM luminol

133µl of 90mM 4-IBPA

(18) Take the PVDF membranes and place them on cling film, add the HRP development solution and incubate for 60 seconds.

(19) Drain off the solution, transfer the PVDF membranes to fresh cling film, and cover the front of the PVDF membrane with cling film.

(20) Tape the wrapped PVDF membrane to the film cassette and immediately expose the PVDF membrane with X-ray film in the darkroom for various times (30 seconds exposure is a good starting point and note that the signal fades with time). Place film in the X-ray developer.

Solutions Needed

Western blot transfer buffer

48 mM Trizma Base, 39 mM Glycine, 0.04 w/v SDS and 20 % Methanol

5.8 g Trizma base (Sigma catalogue T-1503)

2.9 g Glycine (Sigma catalogue G-8898)

0.37 g of SDS powder (Sigma catalogue L-5750) or 8 mls 10 % w/v SDS

200 ml Methanol

dH_20 to 1 L

Coomassie stain solution

2.5 g Coomassie brilliant blue G-250 (Bio-Rad; catalogue number 161-0406)

450 ml dH_20

450 ml Methanol

100 ml glacial acetic acid

Store at room temperature

Coomassie destaining solution

450 ml dH_20

450 ml Methanol

100 ml glacial acetic acid

Store at room temperature

Western blot blocking buffer

5 % w/v milk powder (Marvel) in Western blot wash buffer (TBS-T)

Western blot wash buffer

1X TBS with 0.1% v/v Tween-20 (TBS-T)

To make 10X TBS:

24.2g Trizma base (Sigma catalogue T-1503)

80g NaCl (Sigma catalogue S-7653)

900 ml dH_20

pH solution to 7.6 with HCl

Add dH_20 to 1L.

Store at room temperature and dilute to 1X with dH_20 before use

HRP development solution

13mls of 100mM Tris-HCl (pH 8.5)

3.6µL □l of 30 % H_2O_2 (BDH labs catalogue number 285194F)

120µL of 250mM luminol (Sigma catalogue 09253, dissolved in DMSO)

53.2µL of 90mM p-Coumaric acid (Sigma catalogue C9008, dissolved in DMSO)

9.4. Immunofluorescence Staining Protocol (PFA fixation)

© Michael Freeley, Dept. of Biochemistry, RCSI, Dublin. Written: 11th June 2004

a) After treatment of cells, remove treatment medium and add 4% PFA

b) Incubate at 37°C for 15 minutes

c) Remove PFA and wash twice with PBS

d) Permeabalise cells with 0.1% Triton PBS for 5 minutes at RT

e) Wash cells twice with PBS

f) Epitope block with 5% BSA in PBS for 30 minutes at RT.

g) Wash cells three times in PBS for 5 minutes.

h) Incubate cells with primary antibody in 5% BSA in PBS. The concentration of antibody and duration of treatment needed will have to be determined by optimization studies. For short durations incubation can be performed at RT. For longer durations incubate at 4°C.

i) Wash three times with PBS to remove unbound antibody

j) Incubate with secondary antibody at appropriate concentration for at least one hour at RT in the dark.

k) Wash three times with PBS for 5 minutes.

l) Incubate for 30 minutes with Hoechst (1:2000) or Phalloidin (1:2000) if staining of the nucleus of actin cytoskeleton is required.

m) Wash three times with PBS for 5 minutes.

n) For 96-well plates, leave 200µ PBS in each well. For chamber-slides, remove plastic covering, add two drops of fluoromount (Sigma, stored at 4°C) and cover with a cover-slip. Dry excess anti-fade medium off the edges of the slide by capillary action with some paper towel. The slides can then be analysed immediately or alternatively stored at 4°C in the dark and analysed at a later date.

Reagents required:

Fixation solution (4 % w/v paraformaldehyde)

4 g of paraformaldehyde (Sigma)

Add 100mls of PBS with a magnetic stirrer bar.

Add a few drops of NaOH and heat/dissolve to 60°C in the fume hood (keep the cap of the beaker loose).

Once dissolved, let cool to room temperature and pH the solution to 7.4.

4% PFA can be aliquotted and storet at -20°C.

10 X PBS (Phosphate Buffered Saline): *Use at 1 X final concentration*

80 g NaCl

2.0 g KCl

2.4 g KH_2PO_4

14.4 g Na_2HPO_4

900 ml of distilled water

Dissolve completely and pH the solution to 7.4 by adding conc. HCl

Add distilled water to 1000 ml

NB: To dilute to 1X PBS, add 100 mls of 10 X PBS stock to 900 ml distilled water and mix well.

Permeabilisation buffer: 0.1 % v/v Triton X100 in 1X PBS

Blocking buffer: 5 % BSA (Sigma) in 1X PBS

9.5. Immunofluorescent Staining of Paraffin Embedded Tissue.

Preparation of Slides

a) Paraffin blocks were chilled to -20°C

b) Blocks were mounted on Microtome (Leica Microsystems) and 4uM sections cut

c) The sections were places in cold distilled water containing a drop of ethanol

d) Sections were subsequently moved to a water-bath and placed on poly-L-lysine coated slides (Superfrost Plus, Thermo-scientific)

e) The slides were placed in a drying rack and incubated overnight at 60°C.

Staining Protocol

a) 4μM thick paraffin embedded biopsy sections on slides were rehydrated as by sequential immersion in Xylene (sigma) for 5 minutes X2, 100% ethanol (Sigma) for 5 minutes X 2, 70% ethanol for 5 minutes X2 and distilled water for 5 minutes X2.

b) Antigen retrieval was performed as follows

   i. The slides were placed in a slide rack and placed in sodium citrate buffer (pH 6) treated for 10 minutes in a low-pressure pressure-cooker.

   ii. After 10 minutes, the sections were transferred to fresh warm sodium citrate buffer and allowed to cool to RT (30 minutes).

   iii. The sections were transferred to 0.1% PBST.

c) Blocking was performed with 5% normal goat serum (Sigma) in PBS for one hour at RT.

d) The tissue was then incubated with primary antibody in 5% normal goat serum in PBS overnight at 4°C in a humidity chamber.

e) The tissue was washed twice for 5 minutes in baths of 0.1% Tween 20 in PBS

f) The slide was then incubated with secondary antibody in 5% normal goat serum in PBS for one hour at RT in a humidity chamber.

g) The tissue was washed twice for 5 minutes in baths of PBST to remove excess secondary antibody.

h) The tissue was then incubated with Hoechst (1:2000) for 30 minutes at RT in a humidity chamber

i) Coverslips were mounted using aqueous mounting medium (Sigma).

Solutions Needed

Sodium Citrate Buffer

(10mM Sodium Citrate, 0.05% Tween 20, pH 6.0):

2.94 g Tri-sodium citrate (dihydrate) (Sigma)
Add 1000mL of distilled Water and mix to dissolve.
Adjust pH to 6 with 1M HCl
Add 0.5mL of Tween 20 (Sigma)
Store at RT.

Blocking Buffer: 5% Normal Goat serum (Sigma) in PBS

9.6. Protocol for Real Time Polymerase Chain Reaction

TaqMan probes were used for RT-PCR experiments. These probes consist of a fluorophore attached to the 5'-end of the oligonucleotide probe and a quencher at the 3'-end. The quencher molecule quenches the fluorescence emitted by the fluorophore. While the fluorophore and quencher are in close proximity, the fluorescence of the fluorophore in inhibited. These probes are designed to anneal to a specific DNA region (the target gene) amplified by a specific set of primers. However, as Taq polymerase extends the primer, synthesising the nascent strand, the 5' to 3' exonuclease activity of the polymerase degrades the annealed probe. This releases the fluorophore from the TaqMan probe, separating it from the quencher, allowing the fluorophore to fluoresce. Therefore, the fluorescence detected in the real-time PCR thermal cycler is directly proportional to the fluorophore released, and the amount of DNA template present in the PCR.

The following methodology was used:

a) RNA was isolated from treated cells using the RNeasy Plus Minikit (Qiagen) following the protocol provided with the kit.

b) RNA concentration was determined using the Nanodrop 8000 (Thermo Scientific).

c) RNA concentrations were normalised by dilution with RNase free water using the formula:

$$V_1 \times C_1 = V_2 \times C_2$$ where V = volume and C = concentration.

d) cDNA was reverse transcribed from RNA using the RETROscript® Kit (Ambion).

e) cDNA was diluted to provide a volume sufficient for the number of genes to be investigated

f) 4.5µL of diluted cDNA was added to 5µL of Taqman Mastermix (Applied Biosystems) and to 0.5µL of RT-PCR primer (Applied Biosystems) in a 384 well plate. All genes and treatments were run in triplicate wells.

g) RT-PCR was performed using the Applied Biosystems 7900HT Fast Real-Time PCR System (Applied Biosystems), using the following conditions:

   a. Step 1: hold at 50°C for 2 minutes

   b. Step 2: hold at 95°C for 10mins;

   c. Step 3: 40 cycles of 95°C for 15secs followed by 60°C for 1 min.

h) Threshold determination was set to 0.2 as this threshold was above the baseline activity and was within the log-linear (exponential) phase of the reaction. This allowed ΔΔCT values to be calculated using the housekeeping gene GAPDH. A housekeeping gene is a

constitutive gene whose expression remains relatively constant between treatments and can thus be used to normalize data between treatment groups.

i) ΔΔCT values were used to determine the changes in gene expression induced by treatments. ΔΔCT is the change in target gene expression induced by a treatment relative to an untreated control. The ΔΔCT values were calculated as follows:

   a. The CT value (cycle number at which the log-linear curve crossed the threshold value) was determined for each of the triplicate replicates of the GAPDH probeset and the target gene probeset.

   b. The CT values for the GAPDH probesets were averaged.

   c. The average CT of the GAPDH probe was subtracted from each of the untreated target gene's CT to provide ΔCT (the difference in cycle number between the housekeeping gene and the target gene). The mean ΔCT of the untreated gene of interest was then determined.

   d. The average CT of the GAPDH probe was subtracted from each of the treated target gene's CT to provide ΔCT (the difference in cycle number between the housekeeping gene and the treated target gene). The mean ΔCT of the treated gene of interest was then determined.

   e. Subtracting the untreated ΔCT from the treated ΔCT generated ΔΔCT (The difference in threshold cycle number between the treated and untreated gene). However, this is a log value. Therefore, taking the expression of the untreated gene as 1 (the expression of the gene in the untreated cells), the absolute fold difference between the gene expression in the treated cells and the untreated cells could be calculated using the formula $2^{(-\Delta\Delta CT)}$.

A full protocol for determining ΔΔCT and the standard error associated with this technique can be found at:
http://www3.appliedbiosystems.com/cms/groups/mcb_support/documents/generaldocuments/cms_040980.pdf

9.7. Reagents and Suppliers

CHEMICAL	CATELOG REF	SUPPLIER
4-iodophenylboronic acid	471933	Sigma (St. Louis, MO, USA)
Acrylamide	A3449	Sigma (St. Louis, MO, USA)
Ammonium Persulphate	A3678	Sigma (St. Louis, MO, USA)
Annexin V	IQP-120F	IQ Products (Groningen, Netherlands)
Bovine Serum Albumin	A9418	Sigma (St. Louis, MO, USA)
Calcein AM	80011	Biotium (Hayward, CA, USA)
Crystal Violet	C3886	Sigma (St. Louis, MO, USA)
Deoxycholic Acid	D2510	Sigma (St. Louis, MO, USA)
Dexamethasone	D1756	Sigma (St. Louis, MO, USA)
Diaminobenzidine	D8001	Sigma (St. Louis, MO, USA)
Dimethyl Sulphoxide 99.5%	D8418	Sigma (St. Louis, MO, USA)
Ethanol	E7023	Sigma (St. Louis, MO, USA)
Fluoromount	F4680	Sigma (St. Louis, MO, USA)
Hank's Buffered Saline Solution	H9269	Sigma (St. Louis, MO, USA)
Hematoxylin	H9627	Sigma (St. Louis, MO, USA)
Hoechst 33258	H3569	Invitrogen (Carlsbad, CA, USA)
Hoechst 33342	H3570	Invitrogen (Carlsbad, CA, USA)
Hydrogen Peroxide	H3410	Sigma (St. Louis, MO, USA)
Leupeptin	INHIB1	Sigma (St. Louis, MO, USA)
Luminol	09253	Sigma (St. Louis, MO, USA)
Methanol	494437	Sigma (St. Louis, MO, USA)
Methylthiazolyldiphenyl-tetrazolium bromide	M2128	Sigma (St. Louis, MO, USA)
N,N,N′,N′-Tetramethylethylenediamine	T9281	Sigma (St. Louis, MO, USA)
Paraformaldehyde	P6148	Sigma (St. Louis, MO, USA)
Phalloidin TRITC	P1951	Sigma (St. Louis, MO, USA)
phenylmethanesulfonylfluoride	P7626	Sigma (St. Louis, MO, USA)
Phosphate Buffered Saline	PBS1	Sigma (St. Louis, MO, USA)
Poly-l-lysine	P4707	Sigma (St. Louis, MO, USA)
Propidium Iodide	P4864	Sigma (St. Louis, MO, USA)
PVDF membrane	P2813	Sigma (St. Louis, MO, USA)
Sodium Deoxycholate	D6750	Sigma (St. Louis, MO, USA)
Sodium Dodecyl Sulphate	L4390	Sigma (St. Louis, MO, USA)
Sodium Orthovanadate	S6508	Sigma (St. Louis, MO, USA)
Sodium phosphate monobasic dihydrate	71500	Sigma (St. Louis, MO, USA)
Taurochenodeoxycholic Acid	T6260	Sigma (St. Louis, MO, USA)
tetramethylrhodamine methyl ester	T668	Sigma (St. Louis, MO, USA)
Triton X	T8787	Sigma (St. Louis, MO, USA)
Tween 20	P2287	Sigma (St. Louis, MO, USA)
Ursodeoxycholic Acid	U5127	Sigma (St. Louis, MO, USA)
Ursodeoxycholic Sodium	672305	EMD Chemicals (Gibbstown, NJ, USA)

KITS	CATELOG REF	SUPPLIER
Apo-Direct Apoptosis Kit	556381	BD Biosciences (Franklin Lakes, NJ, USA)
Avidin/Biotin blocking kit	SP-2001	Vector Laboratories (Burlingame, CA, USA)
Millicoat™ ECM screening kit	ECM205	Millipore (Billerica, MA, USA)
Pierce BCA Protein Assay Kit	23227	Thermo Fischer Scientific (Waltham, MA, USA)
RETROscript Kit	AM1710	Applied Biosystems
Rneasy Plus Minikit	74134	Quiagen (Germantown, MD, USA).
Vestastain Elite ABC Kit	PK-6102	Vector Laboratories (Burlingame, CA, USA)
LDH Cytotoxicity Assay Kit	10008882	Caymen Chemical Company (Ann Arbour, MI, USA)

MEDIA	CATELOG REF	SUPPLIER
Bronchial Epithelium Based Medium (BEBM)	CC-3170	Lonza (Allendale, NJ, USA)
Dublecco's Modifies Eagle Medium (DMEM)	21331020	Gibco (Billings, MT, USA)
Fetal Bovine Serum (FBS)	12664025	Gibco (Billings, MT, USA)
McCoy's 5A Medium	36600021	Gibco (Billings, MT, USA)
RPMI 1640	31870082	Gibco (Billings, MT, USA)
Soybean Trypsin Inhibitor (SBTI)	17075029	Gibco (Billings, MT, USA)
Trypsin with EDTA	R001100	Gibco (Billings, MT, USA)

ANTIBODIES	SPECIES	CATELOG REF	CLONE	SUPPLIER
AlexaFluor goat anti-mouse 488	Goat	A-11001		Invitrogen (Carlsbad, CA, USA)
AlexaFluor goat anti-rabbit 488	Goat	A-11008		Invitrogen (Carlsbad, CA, USA)
AlexaFluor goat anti-rabbit 546	Goat	A-11003		Invitrogen (Carlsbad, CA, USA)
Glucocorticoid Antibody	Mouse	611227	41/GR	BD Biosciences (Franklin Lakes, NJ, USA)
HRP-linked Anti-Mouse IgG		7076		Cell Signaling Technology, Inc. (Danvers, MA, USA)
HRP-linked Anti-Rabbit IgG		7074		Cell Signaling Technology, Inc. (Danvers, MA, USA)
Integrin α_3 Antibody	Mouse	556025	C3 II.1	BD Biosciences (Franklin Lakes, NJ, USA)
Integrin α_4 Antibody	Mouse	555503	9F10	BD Biosciences (Franklin Lakes, NJ, USA)
Integrin α_5 Antibody	Mouse	555617	IIA1	BD Biosciences (Franklin Lakes, NJ, USA)
Integrin α_6 Antibody	Mouse	555736	GoH3	BD Biosciences (Franklin Lakes, NJ, USA)
Integrin α_v Antibody	Mouse	611013	21/CD51	BD Biosciences (Franklin Lakes, NJ, USA)
Integrin α_v Antibody	Mouse	407286	17E6	Merck (Whitehouse Station, NJ, USA)
Integrin α_v Antibody	Mouse	SC-9969	P2W7	Santa Cruz Biotechnology Inc (Santa Cruz, Ca, USA)
LC3 Antibody	Mouse	5F10		Nanotools, Teningen, Germany
Mouse IgG_1 Isotype Control Antibody	Mouse	A10630		Zymed Laboratories (San Francisco, CA, USA)
PARP (Cleaved, p85)	Rabbit	G734		Promega (Madison, WI, USA)
Rab11 Antibody	Rabbit	71-5300		Zymed Laboratories (San Francisco, CA, USA)
Rab5 Antibody	Rabbit	SC-68344	H-288	Santa Cruz Biotechnology Inc (Santa Cruz, Ca, USA)

9.9. Equipment and Suppliers

EQUIPMENT	MODEL	SUPPLIER
Flow Cytometer	Cyan ADP 9 Colour	Beckman Coulter, Brea, CA, USA
Plate Reader	Elx800	BioTek, Winooski, VT, USA
Fluorometer	Victor	Perkin Elmer, Waltham, MA, USA
Slide Scanner	Scanscope	Aperio, Vista, CA, USA
Developer	Curex CP1000	Agfa, Mortsel, Belgium
Haemacytometer	Bright-Line Haemacytometer	Hausser Scientific, Horsham, P.A., USA
Centrifuge	Eppendorf 5810 R	Eppendorf, Hamburg, Germany
Microtome		Leica Microsystems, Wetzlar, Germany
Electrophoresis Power Supply	Consort E865	Consort, Turnhout, Belgium
High Content Analysis Platform	InCell 1000	GE Heatlhcare, Waukesha, WI, USA
Time Lapse Light Microscope	IncuCyte live cell imaging system	Essen Biosystems, Ann Arbour, MI, USA
Confocal Microscope	Zeiss LSM510	Herts, UK

10. References

1. Dent, J., et al., *Symptom evaluation in reflux disease: workshop background, processes, terminology, recommendations, and discussion outputs.* Gut, 2004. **53**(suppl_4): p. iv1-24.

2. Wahlqvist, P., M.C. Reilly, and A. Barkun, *Systematic review: the impact of gastro-oesophageal reflux disease on work productivity.* Alimentary Pharmacology & Therapeutics, 2006. **24**(2): p. 259-272.

3. Dent, J., et al., *Epidemiology of gastro-oesophageal reflux disease: a systematic review.* Gut, 2005. **54**(5): p. 710-717.

4. Moayyedi, P. and N.J. Talley, *Gastro-oesophageal reflux disease.* The Lancet, 2006. **367**(9528): p. 2086-2100.

5. Ronkainen, J., et al., *High prevalence of gastroesophageal reflux symptoms and esophagitis with or without symptoms in the general adult Swedish population: a Kalixanda study report.* Scand J Gastroenterol, 2005. **40**(3): p. 275-85.

6. Narayani, R.I., M.P. Burton, and G.S. Young, *Utility of esophageal biopsy in the diagnosis of nonerosive reflux disease.* Diseases of the Esophagus, 2003. **16**(3): p. 187-192.

7. DeVault, K.R., *Review article: the role of acid suppression in patients with non-erosive reflux disease or functional heartburn.* Aliment Pharmacol Ther, 2006. **23 Suppl 1**: p. 33-9.

8. Spechler, S.J., *Barrett's Esophagus.* N Engl J Med, 2002. **346**(11): p. 836-842.

9. Atherfold, P.A. and J.A. Jankowski, *Molecular biology of Barrett's cancer.* Best Practice & Research Clinical Gastroenterology, 2006. **20**(5): p. 813-827.

10. Fitzgerald, R.C., *Molecular basis of Barrett's oesophagus and oesophageal adenocarcinoma.* Gut, 2006. **55**(12): p. 1810-1820.

11. Guillem, P.G., *How to Make a Barrett Esophagus: Pathophysiology of Columnar Metaplasia of the Esophagus.* Digestive Diseases and Sciences, 2005. **50**(3): p. 415-424.

12. Wright, N.A., *Migration of the ductular elements of gut-associated glands gives clues to the histogenesis of structures associated with responses to acid hypersecretory state: the origins of "gastric metaplasia" in the duodenum of the specialized mucosa of barrett's esophagus and of pseudopyloric metaplasia.* Yale J Biol Med, 1996. **69**(2): p. 147-53.

13. Wang, X., et al., *Residual Embryonic Cells as Precursors of a Barrett's-like Metaplasia.* Cell, 2011. **145**(7): p. 1023-35.

14. van Soest, E.M., et al., *Increasing incidence of Barrett's oesophagus in the general population.* Gut, 2005. **54**(8): p. 1062-6.

15. Koek, G.H., et al., *Multivariate analysis of the association of acid and duodeno-gastro-oesophageal reflux exposure with the presence of oesophagitis, the severity of oesophagitis and Barrett's oesophagus.* Gut, 2008. **57**(8): p. 1056-1064.

16. Ronkainen, J., et al., *Prevalence of Barrett's Esophagus in the General Population: An Endoscopic Study.* Gastroenterology, 2005. **129**(6): p. 1825-1831.

17. Champion, G., et al., *Duodenogastroesophageal reflux: Relationship to pH and importance in Barrett's esophagus.* Gastroenterology, 1994. **107**(3): p. 747-754.

18. Gotley, D.C., et al., *Composition of gastro-oesophageal refluxate.* Gut, 1991. **32**(10): p. 1093-1099.

19. Kauer, W.K., et al., *Mixed reflux of gastric and duodenal juices is more harmful to the esophagus than gastric juice alone. The need for surgical therapy re-emphasized.* Ann Surg, 1995. **222**(4): p. 525-31; discussion 531-3.

20. Kauer, W.K.H., et al., *Composition and concentration of bile acid reflux into the esophagus of patients with gastroesophageal reflux disease.* Surgery, 1997. **122**(5): p. 874-881.

21. Nehra, D., et al., *Assessment of combined bile acid and pH profiles using an automated sampling device in gastro-oesophageal reflux disease.* Br J Surg, 1998. **85**(1): p. 134-7.

22. Nehra, D., et al., *Toxic bile acids in gastro-oesophageal reflux disease: influence of gastric acidity.* Gut, 1999. **44**(5): p. 598-602.

23. Enzinger, P.C. and R.J. Mayer, *Esophageal Cancer.* N Engl J Med, 2003. **349**(23): p. 2241-2252.

24. Lagergren, J., *Adenocarcinoma of oesophagus: what exactly is the size of the problem and who is at risk?* Gut, 2005. **54 Suppl 1**: p. i1-5.

25. Menon, D., et al., *Endoscopic treatments for Barrett's esophagus: a systematic review of safety and effectiveness compared to esophagectomy.* Bmc Gastroenterology, 2010. **10**(1): p. 111.

26. Schembre, D.B., et al., *Treatment of Barrett's esophagus with early neoplasia: a comparison of endoscopic therapy and esophagectomy.* Gastrointestinal endoscopy, 2008. **67**(4): p. 595-601.

27. Bollschweiler, E., et al., *Demographic variations in the rising incidence of esophageal adenocarcinoma in white males.* Cancer, 2001. **92**(3): p. 549-55.

28. Brown, L.M., S.S. Devesa, and W.H. Chow, *Incidence of adenocarcinoma of the esophagus among white Americans by sex, stage, and age.* J Natl Cancer Inst, 2008. **100**(16): p. 1184-7.

29. Pohl, H. and H.G. Welch, *The role of overdiagnosis and reclassification in the marked increase of esophageal adenocarcinoma incidence.* J Natl Cancer Inst, 2005. **97**(2): p. 142-6.

30. Dhillon, P.K., et al., *Family history of cancer and risk of esophageal and gastric cancers in the United States.* Int J Cancer, 2001. **93**(1): p. 148-52.

31. Lagergren, J., et al., *Heredity and risk of cancer of the esophagus and gastric cardia.* Cancer Epidemiol Biomarkers Prev, 2000. **9**(7): p. 757-60.

32. Zhang, Z.F., et al., *Adenocarcinomas of the esophagus and gastric cardia: medical conditions, tobacco, alcohol, and socioeconomic factors.* Cancer Epidemiol Biomarkers Prev, 1996. **5**(10): p. 761-8.

33. Lagergren, J., et al., *Symptomatic gastroesophageal reflux as a risk factor for esophageal adenocarcinoma.* N Engl J Med, 1999. **340**(11): p. 825-31.

34. Chow, W.H., et al., *Body mass index and risk of adenocarcinomas of the esophagus and gastric cardia.* J Natl Cancer Inst, 1998. **90**(2): p. 150-5.

35. Merry, A.H., et al., *Body mass index, height and risk of adenocarcinoma of the oesophagus and gastric cardia: a prospective cohort study.* Gut, 2007. **56**(11): p. 1503-11.

36. Gammon, M.D., et al., *Tobacco, alcohol, and socioeconomic status and adenocarcinomas of the esophagus and gastric cardia.* J Natl Cancer Inst, 1997. **89**(17): p. 1277-84.

37. Freedman, J., et al., *Association between cholecystectomy and adenocarcinoma of the esophagus.* Gastroenterology, 2001. **121**(3): p. 548-53.

38. Pera, M., et al., *Epidemiology of esophageal adenocarcinoma.* J Surg Oncol, 2005. **92**(3): p. 151-9.

39. Dulai, G.S., et al., *Preoperative prevalence of Barrett's esophagus in esophageal adenocarcinoma: a systematic review.* Gastroenterology, 2002. **122**(1): p. 26-33.

40. Fox, M. and I. Forgacs, *Gastro-oesophageal reflux disease.* BMJ, 2006. **332**(7533): p. 88-93.

41. Schoeman, M.N., et al., *Mechanisms of gastroesophageal reflux in ambulant healthy human subjects.* Gastroenterology, 1995. **108**(1): p. 83-91.

42. Oh, D.S., et al., *The impact of reflux composition on mucosal injury and esophageal function.* Journal of Gastrointestinal Surgery, 2006. **10**(6): p. 787-796.

43. C. P. Barham, D.C.G.A.M.D.A., *Oesophageal acid clearance in patients with severe reflux oesophagitis.* British Journal of Surgery, 1995. **82**(3): p. 333-337.

44. Sifrim, D., et al., *Transient lower esophageal sphincter relaxations and esophageal body muscular contractile response in reflux esophagitis.* Dig Dis Sci, 2000. **45**(7): p. 1293-300.

45. Koek, G.H., et al., *Oesophageal clearance of acid and bile: a combined radionuclide, pH, and Bilitec study.* Gut, 2004. **53**(1): p. 21-26.

46. Cuomo, R., et al., *Analysis of Ambulatory Duodenogastroesophageal Reflux Monitoring.* Digestive Diseases and Sciences, 2000. **45**(12): p. 2463-2469.

47. Vaezi, M.F., R.G. Lacamera, and J.E. Richter, *Validation studies of Bilitec 2000: an ambulatory duodenogastric reflux monitoring system.* Am J Physiol Gastrointest Liver Physiol, 1994. **267**(6): p. G1050-1057.

48. Vaezi, M.F. and J.E. Richter, *Fiberoptic sensor for bilirubin.* Am J Surg, 1995. **170**(3): p. 310-2.

49. Barrett, M.W., et al., *Detection of bile reflux: in vivo validation of the Bilitec fibreoptic system.* Dis Esophagus, 2000. **13**(1): p. 44-50.

50. Koek, G.H., et al., *The role of acid and duodenal gastroesophageal reflux in symptomatic GERD.* Am J Gastroenterol, 2001. **96**(7): p. 2033-40.

51. Vaezi, M.F. and J.E. Richter, *Role of acid and duodenogastroesophageal reflux in gastroesophageal reflux disease.* Gastroenterology, 1996. **111**(5): p. 1192-1199.

52. Wilmer, A., et al., *Duodenogastroesophageal reflux and esophageal mucosal injury in mechanically ventilated patients.* Gastroenterology, 1999. **116**(6): p. 1293-9.

53. Monaco, L., et al., *Prevalence of bile reflux in gastroesophageal reflux disease patients not responsive to proton pump inhibitors.* World J Gastroenterol, 2009. **15**(3): p. 334-8.

54. Tack, J., et al., *Gastroesophageal reflux disease poorly responsive to single-dose proton pump inhibitors in patients without Barrett's esophagus: acid reflux, bile reflux, or both?* Am J Gastroenterol, 2004. **99**(6): p. 981-8.

55. Sears, R.J., G.L. Champion, and J.E. Richter, *Characteristics of distal partial gastrectomy patients with esophageal symptoms of duodenogastric reflux.* Am J Gastroenterol, 1995. **90**(2): p. 211-5.

56. Attwood, S.E., et al., *Duodenoesophageal reflux and the development of esophageal adenocarcinoma in rats.* Surgery, 1992. **111**(5): p. 503-10.

57. Fein, M., et al., *Duodenoesophageal reflux induces esophageal adenocarcinoma without exogenous carcinogen.* J Gastrointest Surg, 1998. **2**(3): p. 260-8.

58. Ireland, A.P., et al., *Gastric juice protects against the development of esophageal adenocarcinoma in the rat.* Ann Surg, 1996. **224**(3): p. 358-70; discussion 370-1.

59. Miwa, K., et al., *Duodenal reflux through the pylorus induces gastric adenocarcinoma in the rat.* Carcinogenesis, 1992. **13**(12): p. 2313-6.

60. Kawamata, Y., et al., *A G Protein-coupled Receptor Responsive to Bile Acids.* J. Biol. Chem., 2003. **278**(11): p. 9435-9440.

61. Maruyama, T., et al., *Identification of membrane-type receptor for bile acids (M-BAR).* Biochemical and Biophysical Research Communications, 2002. **298**(5): p. 714-719.

62. Parks, D.J., et al., *Bile Acids: Natural Ligands for an Orphan Nuclear Receptor.* Science, 1999. **284**(5418): p. 1365-1368.

63. Chiang, J.Y.L., *Bile Acid Regulation of Gene Expression: Roles of Nuclear Hormone Receptors.* Endocr Rev, 2002. **23**(4): p. 443-463.

64. Scotti, E., et al., *Lipid sensing and lipid sensors.* Cellular and Molecular Life Sciences (CMLS), 2007. **64**(19): p. 2477-2491.

65. Lew, J.-L., et al., *The Farnesoid X Receptor Controls Gene Expression in a Ligand- and Promoter-selective Fashion.* J. Biol. Chem., 2004. **279**(10): p. 8856-8861.

66. Bernstein, H., et al., *Bile acids as carcinogens in human gastrointestinal cancers.* Mutation Research/Reviews in Mutation Research, 2005. **589**(1): p. 47-65.

67. Debruyne, P.R., et al., *The role of bile acids in carcinogenesis.* Mutation Research-Fundamental and Molecular Mechanisms of Mutagenesis, 2001. **480**: p. 359-369.

68. Lechner, S., et al., *Bile acids mimic oxidative stress induced upregulation of thioredoxin reductase in colon cancer cell lines.* Carcinogenesis, 2002. **23**(8): p. 1281-1288.

69. Lee, F.Y., et al., *FXR, a multipurpose nuclear receptor.* Trends in Biochemical Sciences, 2006. **31**(10): p. 572-580.

70. Wang, H., et al., *Endogenous Bile Acids Are Ligands for the Nuclear Receptor FXR/BAR.* Molecular Cell, 1999. **3**(5): p. 543-553.

71. Maruyama, T., et al., *Identification of membrane-type receptor for bile acids (M-BAR).* Biochem Biophys Res Commun, 2002. **298**(5): p. 714-9.

72. Hofmann, A.F. and K.J. Mysels, *Bile acid solubility and precipitation in vitro and in vivo: the role of conjugation, pH, and Ca2+ ions.* J Lipid Res, 1992. **33**(5): p. 617-26.

73. Lillemoe, K.D., L.F. Johnson, and J.W. Harmon, *Role of the components of the gastroduodenal contents in experimental acid esophagitis.* Surgery, 1982. **92**(2): p. 276-84.

74. Lillemoe, K.D., L.F. Johnson, and J.W. Harmon, *Alkaline esophagitis: a comparison of the ability of components of gastroduodenal contents to injure the rabbit esophagus.* Gastroenterology, 1983. **85**(3): p. 621-8.

75. Fini, A., G. Feroci, and A. Roda, *Acidity in bile acid systems.* Polyhedron, 2002. **21**(14-15): p. 1421-1427.

76. Fini, A. and A. Roda, *Chemical properties of bile acids. IV. Acidity constants of glycine-conjugated bile acids.* J Lipid Res, 1987. **28**(7): p. 755-9.

77. Cabral, D.J., J.A. Hamilton, and D.M. Small, *The ionization behavior of bile acids in different aqueous environments.* J Lipid Res, 1986. **27**(3): p. 334-43.

78. Patel, T., S.F. Bronk, and G.J. Gores, *Increases of intracellular magnesium promote glycodeoxycholate-induced apoptosis in rat hepatocytes.* The Journal of Clinical Investigation, 1994. **94**(6): p. 2183-2192.

79. Qiao, L., et al., *Deoxycholic acid (DCA) causes ligand-independent activation of epidermal growth factor receptor (EGFR) and FAS receptor in primary hepatocytes: inhibition of EGFR/mitogen-activated protein kinase-signaling module enhances DCA-induced apoptosis.* Mol Biol Cell, 2001. **12**(9): p. 2629-45.

80. Kwo, P., et al., *Nuclear serine protease activity contributes to bile acid-induced apoptosis in hepatocytes.* Am J Physiol Gastrointest Liver Physiol, 1995. **268**(4): p. G613-621.

81. Spivey, J.R., S.F. Bronk, and G.J. Gores, *Glycochenodeoxycholate-induced lethal hepatocellular injury in rat hepatocytes. Role of ATP depletion and cytosolic free calcium.* The Journal of Clinical Investigation, 1993. **92**(1): p. 17-24.

82. Botla, R., et al., *Ursodeoxycholate (UDCA) inhibits the mitochondrial membrane permeability transition induced by glycochenodeoxycholate: a mechanism of UDCA cytoprotection.* J Pharmacol Exp Ther, 1995. **272**(2): p. 930-938.

83. Krahenbuhl, S., et al., *Ursodeoxycholate protects oxidative mitochondrial metabolism from bile acid toxicity: dose-response study in isolated rat liver mitochondria.* Hepatology, 1994. **20**(6): p. 1595-601.

84. Zhang, G., et al., *Multiple Cyclin Kinase Inhibitors Promote Bile Acid-induced Apoptosis and Autophagy in Primary Hepatocytes via p53-CD95-dependent Signaling.* Journal of Biological Chemistry, 2008. **283**(36): p. 24343-24358.

85. Jenkins, G.J.S., et al., *The bile acid deoxycholic acid has a non-linear dose response for DNA damage and possibly NF-{kappa}B activation in oesophageal cells, with a mechanism of action involving ROS.* Mutagenesis, 2008: p. gen029.

86. Jenkins, G.J.S., et al., *Deoxycholic acid at neutral and acid pH, is genotoxic to oesophageal cells through the induction of ROS: the potential role of anti-oxidants in Barrett's oesophagus.* Carcinogenesis, 2007. **28**(1): p. 136-142.

87. Dvorak, K., et al., *Bile acids in combination with low pH induce oxidative stress and oxidative DNA damage: relevance to the pathogenesis of Barrett's oesophagus.* Gut, 2007. **56**(6): p. 763-771.

88. Jolly, A.J., C.P. Wild, and L.J. Hardie, *Acid and bile salts induce DNA damage in human oesophageal cell lines.* Mutagenesis, 2004. **19**(4): p. 319-324.

89. Green, D.R. and G. Kroemer, *The pathophysiology of mitochondrial cell death.* Science, 2004. **305**(5684): p. 626-9.

90. Vieira, H.L. and G. Kroemer, *Pathophysiology of mitochondrial cell death control.* Cell Mol Life Sci, 1999. **56**(11-12): p. 971-6.

91. Youle, R.J. and A. Strasser, *The BCL-2 protein family: opposing activities that mediate cell death.* Nat Rev Mol Cell Biol, 2008. **9**(1): p. 47-59.

92. Wang, Z.-B., Y.-Q. Liu, and Y.-F. Cui, *Pathways to caspase activation.* Cell Biology International, 2005. **29**(7): p. 489-496.

93. Wolf, B.B. and D.R. Green, *Suicidal Tendencies: Apoptotic Cell Death by Caspase Family Proteinases.* Journal of Biological Chemistry, 1999. **274**(29): p. 20049-20052.

94. Chao, D.T. and S.J. Korsmeyer, *BCL-2 FAMILY: Regulators of Cell Death.* Annual Review of Immunology, 2003. **16**(1): p. 395-419.

95. Cory, S. and J.M. Adams, *The Bcl2 family: regulators of the cellular life-or-death switch.* Nat Rev Cancer, 2002. **2**(9): p. 647-656.

96. Schulze-Osthoff, K., et al., *Apoptosis signaling by death receptors.* European Journal of Biochemistry, 1998. **254**(3): p. 439-459.

97. Tafani, M., et al., *Cytochrome c Release upon Fas Receptor Activation Depends on Translocation of Full-length Bid and the Induction of the Mitochondrial Permeability Transition.* Journal of Biological Chemistry, 2002. **277**(12): p. 10073-10082.

98. Krammer, P.H., *The CD95(APO-1/Fas)/CD95L system.* Toxicol Lett, 1998. **102-103**: p. 131-7.

99. Li, S., et al., *Relief of Extrinsic Pathway Inhibition by the Bid-dependent Mitochondrial Release of Smac in Fas-mediated Hepatocyte Apoptosis.* Journal of Biological Chemistry, 2002. **277**(30): p. 26912-26920.

100. Szegezdi, E., et al., *Bcl-2 family on guard at the ER.* Am J Physiol Cell Physiol, 2009. **296**(5): p. C941-53.

101. Heath-Engel, H.M., N.C. Chang, and G.C. Shore, *The endoplasmic reticulum in apoptosis and autophagy: role of the BCL-2 protein family.* Oncogene, 2008. **27**(50): p. 6419-33.

102. Tsuchiya, S., et al., *Involvement of endoplasmic reticulum in glycochenodeoxycholic acid-induced apoptosis in rat hepatocytes.* Toxicology Letters, 2006. **166**(2): p. 140-149.

103. Bernstein, H., et al., *Activation of the promoters of genes associated with DNA damage, oxidative stress, ER stress and protein malfolding by the bile salt, deoxycholate.* Toxicology Letters, 1999. **108**(1): p. 37-46.

104. Combettes, L., et al., *Release of calcium from the endoplasmic reticulum by bile acids in rat liver cells.* Journal of Biological Chemistry, 1988. **263**(5): p. 2299-2303.

105. Ziegler, U. and P. Groscurth, *Morphological Features of Cell Death.* Physiology, 2004. **19**(3): p. 124-128.

106. Rello, S., et al., *Morphological criteria to distinguish cell death induced by apoptotic and necrotic treatments.* Apoptosis, 2005. **10**(1): p. 201-208.

107. Klionsky, D.J., et al., *Guidelines for the use and interpretation of assays for monitoring autophagy in higher eukaryotes.* Autophagy, 2008. **4**(2): p. 151-75.

108. Duane, W.C. and D.M. Wiegand, *Mechanism by which bile salt disrupts the gastric mucosal barrier in the dog.* J Clin Invest, 1980. **66**(5): p. 1044-9.

109. Tanaka, K. and D. Fromm, *Effects of bile acid and salicylate on isolated surface and glandular cells of rabbit stomach.* Surgery, 1983. **93**(5): p. 660-3.

110. Schweitzer, E.J., et al., *Lipid solubilization during bile salt-induced esophageal mucosal barrier disruption in the rabbit.* J Lab Clin Med, 1987. **110**(2): p. 172-9.

111. Schweitzer, E.J., et al., *Bile acid efflux precedes mucosal barrier disruption in the rabbit esophagus.* Am J Physiol, 1984. **247**(5 Pt 1): p. G480-5.

112. van Malenstein, H., R. Farre, and D. Sifrim, *Esophageal Dilated Intercellular Spaces (DIS) and Nonerosive Reflux Disease.* Am J Gastroenterol, 2008. **103**(4): p. 1021-1028.

113. Farre, R., et al., *Short exposure of oesophageal mucosa to bile acids, both in acidic and weakly acidic conditions, can impair mucosal integrity and provoke dilated intercellular spaces.* Gut, 2008: p. gut.2007.141804.

114. Jean-Louis, S., et al., *Deoxycholic acid induces intracellular signaling through membrane perturbations.* J Biol Chem, 2006. **281**(21): p. 14948-60.

115. Guldutuna, S., et al., *Molecular aspects of membrane stabilization by ursodeoxycholate [see comment].* Gastroenterology, 1993. **104**(6): p. 1736-44.

116. Im, E. and J.D. Martinez, *Ursodeoxycholic acid (UDCA) can inhibit deoxycholic acid (DCA)-induced apoptosis via modulation of EGFR/Raf-1/ERK signaling in human colon cancer cells.* Journal of Nutrition, 2004. **134**(2): p. 483-486.

117. Khare, S., et al., *Ursodeoxycholic acid inhibits Ras mutations, wild-type Ras activation, and cyclooxygenase-2 expression in colon cancer.* Cancer Research, 2003. **63**(13): p. 3517-3523.

118. Souza, R.F., et al., *Acid exposure activates the mitogen-activated protein kinase pathways in Barrett's esophagus.* Gastroenterology, 2002. **122**(2): p. 299-307.

119. Batzri, S., et al., *Bile acid accumulation in gastric mucosal cells.* Proc Soc Exp Biol Med, 1991. **197**(4): p. 393-9.

120. Schweitzer, E.J., et al., *Bile acid accumulation by rabbit esophageal mucosa.* Dig Dis Sci, 1986. **31**(10): p. 1105-13.

121. Liu, T., et al., *Regulation of Cdx2 expression by promoter methylation, and effects of Cdx2 transfection on morphology and gene expression of human esophageal epithelial cells.* Carcinogenesis, 2007. **28**(2): p. 488-496.

122. Jenkins, G.J.S., et al., *The detection of mutations induced in vitro in the human p53 gene by hydrogen peroxide with the restriction site mutation (RSM) assay.* Mutation Research/Genetic Toxicology and Environmental Mutagenesis, 2001. **498**(1-2): p. 135-144.

123. Jenkins, G.J.S., et al., *Restriction enzymes in the analysis of genetic alterations responsible for cancer progression.* British Journal of Surgery, 2002. **89**(1): p. 8-20.

124. Moons, L.M., et al., *The homeodomain protein CDX2 is an early marker of Barrett's oesophagus.* J Clin Pathol, 2004. **57**(10): p. 1063-8.

125. Kazumori, H., et al., *Bile acids directly augment caudal related homeobox gene Cdx2 expression in oesophageal keratinocytes in Barrett's epithelium.* Gut, 2006. **55**(1): p. 16-25.

126. Wong, N.A., et al., *CDX1 is an important molecular mediator of Barrett's metaplasia.* Proc Natl Acad Sci U S A, 2005. **102**(21): p. 7565-70.

127. Eda, A., et al., *Aberrant expression of CDX2 in Barrett's epithelium and inflammatory esophageal mucosa.* J Gastroenterol, 2003. **38**(1): p. 14-22.

128. Hu, Y., et al., *Pathogenesis of Barrett Esophagus: Deoxycholic Acid Up-Regulates Goblet-Specific Gene MUC2 in Concert With CDX2 in Human Esophageal Cells.* Arch Surg, 2007. **142**(6): p. 540-545.

129. Hu, Y., et al., *The Pathogenesis of Barrett's Esophagus: Secondary Bile Acids Upregulate Intestinal Differentiation Factor CDX2 Expression in Esophageal Cells.* Journal of Gastrointestinal Surgery, 2007. **11**(7): p. 827-834.

130. Burnat, G., et al., *Bile acids induce overexpression of homeobox gene CDX-2 and vascular endothelial growth factor (VEGF) in human Barrett's esophageal mucosa and adenocarcinoma cell line.* Scand J Gastroenterol, 2007. **42**(12): p. 1460-5.

131. Zhang, F., et al., *Duodenal reflux induces cyclooxygenase-2 in the esophageal mucosa of rats: Evidence for involvement of bile acids.* Gastroenterology, 2001. **121**(6): p. 1391-1399.

132. Tselepis, C., et al., *Upregulation of the oncogene c-myc in Barrett's adenocarcinoma: induction of c-myc by acidified bile acid in vitro.* Gut, 2003. **52**(2): p. 174-180.

133. Jenkins, G.J.S., et al., *The bile acid deoxycholic acid (DCA) at neutral pH activates NF-{kappa}B and induces IL-8 expression in oesophageal cells in vitro.* Carcinogenesis, 2004. **25**(3): p. 317-323.

134. Abdel-Latif, M.M.M., et al., *NF-kappa B activation in Esophageal adenocarcinoma - Relationship to Barrett's metaplasia, survival, and response to neoadjuvant chemoradiotherapy.* Annals of Surgery, 2004. **239**(4): p. 491-500.

135. O'Riordan, J.M., et al., *Proinflammatory cytokine and nuclear factor kappa-B expression along the inflammation-metaplasia-dysplasia-adenocarcinoma sequence in the esophagus.* American Journal of Gastroenterology, 2005. **100**(6): p. 1257-1264.

136. Dvorak, K., et al., *Activation of the Interleukin-6/STAT3 Antiapoptotic Pathway in Esophageal Cells by Bile Acids and Low pH: Relevance to Barrett's Esophagus.* Clin Cancer Res, 2007. **13**(18): p. 5305-5313.

137. Bailey, T., et al., *Altered cadherin and catenin complexes in the Barrett's esophagus-dysplasia-adenocarcinoma sequence: correlation with disease progression and dedifferentiation.* Am J Pathol, 1998. **152**(1): p. 135-44.

138. Tselepis, C., et al., *Tumour necrosis factor-alpha in Barrett's oesophagus: a potential novel mechanism of action.* Oncogene, 2002. **21**(39): p. 6071-81.

139. Onwuegbusi, B.A., et al., *Impaired transforming growth factor beta signalling in Barrett's carcinogenesis due to frequent SMAD4 inactivation.* Gut, 2006. **55**(6): p. 764-74.

140. Jankowski, J.A., et al., *Molecular Evolution of the Metaplasia-Dysplasia-Adenocarcinoma Sequence in the Esophagus.* Am J Pathol, 1999. **154**(4): p. 965-973.

141. Jenkins, G.J.S., et al., *Early p53 mutations in nondysplastic Barrett's tissue detected by the restriction site mutation (RSM) methodology.* Br J Cancer, 2003. **88**(8): p. 1271-1276.

142. Roman, S., et al., *Downregulation of p63 upon exposure to bile salts and acid in normal and cancer esophageal cells in culture.* Am J Physiol Gastrointest Liver Physiol, 2007. **293**(1): p. G45-53.

143. Pohler, E., et al., *The Barrett's antigen anterior gradient-2 silences the p53 transcriptional response to DNA damage.* Mol Cell Proteomics, 2004. **3**(6): p. 534-47.

144. Fracchia, M., et al., *Biliary lipid composition in cholesterol microlithiasis.* Gut, 2001. **48**(5): p. 702-706.

145. Ruppin, D.C., G.M. Murphy, and R.H. Dowling, *Gall stone disease without gall stones--bile acid and bile lipid metabolism after complete gall stone dissolution.* Gut, 1986. **27**(5): p. 559-566.

146. Martinez-Diez, M.C., et al., *Comparison of the effects of bile acids on cell viability and DNA synthesis by rat hepatocytes in primary culture.* Biochimica et Biophysica Acta (BBA) - Molecular Basis of Disease, 2000. **1500**(2): p. 153-160.

147. Lazaridis, K.N., G.J. Gores, and K.D. Lindor, *Ursodeoxycholic acid 'mechanisms of action and clinical use in hepatobiliary disorders'.* J Hepatol, 2001. **35**(1): p. 134-46.

148. Alberts, D.S., et al., *Phase III trial of ursodeoxycholic acid to prevent colorectal adenoma recurrence.* Journal of the National Cancer Institute, 2005. **97**(11): p. 846-853.

149. Loddenkemper, C., et al., *Prevention of colitis-associated carcinogenesis in a mouse model by diet supplementation with ursodeoxycholic acid.* International Journal of Cancer, 2006. **118**(11): p. 2750-2757.

150. Pardi, D.S., et al., *Ursodeoxycholic acid as a chemopreventive agent in patients with ulcerative colitis and primary sclerosing cholangitis.* Gastroenterology, 2003. **124**(4): p. 889-893.

151. Bozikas, A., et al., *The effect of oral administration of ursodeoxycholic acid and high-dose proton pump inhibitors on the histology of Barrett's esophagus.* Dis Esophagus, 2008. **21**(4): p. 346-54.

152. Stiehl, A., C. Benz, and P. Sauer, *Mechanism of hepatoprotective action of bile salts in liver disease.* Gastroenterol Clin North Am, 1999. **28**(1): p. 195-209, viii.

153. Trauner, M. and I.W. Graziadei, *Review article: mechanisms of action and therapeutic applications of ursodeoxycholic acid in chronic liver diseases.* Aliment Pharmacol Ther, 1999. **13**(8): p. 979-96.

154. Arisawa, S., et al., *Ursodeoxycholic acid induces glutathione synthesis through activation of PI3K/Akt pathway in HepG2 cells.* Biochemical Pharmacology, 2009. **77**(5): p. 858-866.

155. Mitsuyoshi, H., et al., *Ursodeoxycholic Acid Protects Hepatocytes against Oxidative Injury via Induction of Antioxidants.* Biochemical and Biophysical Research Communications, 1999. **263**(2): p. 537-542.

156. Rodrigues, C.M., et al., *Ursodeoxycholic acid may inhibit deoxycholic acid-induced apoptosis by modulating mitochondrial transmembrane potential and reactive oxygen species production.* Mol Med, 1998. **4**(3): p. 165-78.

157. Azzaroli, F., et al., *Ursodeoxycholic acid diminishes Fas-ligand-induced apoptosis in mouse hepatocytes.* Hepatology, 2002. **36**(1): p. 49-54.

158. Qiao, L., et al., *Inhibition of the MAPK and PI3K pathways enhances UDCA-induced apoptosis in primary rodent hepatocytes.* Hepatology, 2002. **35**(4): p. 779-89.

159. Arnoult, D., et al., *Mitochondrial release of apoptosis-inducing factor occurs downstream of cytochrome c release in response to several proapoptotic stimuli.* J Cell Biol, 2002. **159**(6): p. 923-9.

160. Shi, S.R., et al., *Antigen retrieval technique utilizing citrate buffer or urea solution for immunohistochemical demonstration of androgen receptor in formalin- fixed paraffin sections.* J. Histochem. Cytochem., 1993. **41**(11): p. 1599-1604.

161. Rodrigues, C.M.P., et al., *Ursodeoxycholic acid may inhibit deoxycholic acid-induced apoptosis by modulating mitochondrial transmembrane potential and reactive oxygen species production.* Molecular Medicine, 1998. **4**(3): p. 165-178.

162. Sola, S., et al., *Game and players: Mitochondrial apoptosis and the therapeutic potential of ursodeoxycholic acid.* Current Issues in Molecular Biology, 2007. **9**: p. 123-138.

163. Piazza, F., et al., *Competition in liver transport between chenodeoxycholic acid and ursodeoxycholic acid as a mechanism for ursodeoxycholic acid and its amidates' protection of liver damage induced by chenodeoxycholic acid.* Dig Liver Dis, 2000. **32**(4): p. 318-28.

164. Amaral, J.D., et al., *p53 Is a Key Molecular Target of Ursodeoxycholic Acid in Regulating Apoptosis.* J. Biol. Chem., 2007. **282**(47): p. 34250-34259.

165. Khare, S., et al., *Ursodeoxycholic acid suppresses Cox-2 expression in colon cancer: roles of Ras, p38, and CCAAT/enhancer-binding protein.* Nutr Cancer, 2008. **60**(3): p. 389-400.

166. Shah, S.A., et al., *Ursodeoxycholic acid inhibits interleukin 1 beta [corrected] and deoxycholic acid-induced activation of NF-kappaB and AP-1 in human colon cancer cells.* Int J Cancer, 2006. **118**(3): p. 532-9.

167. Sola, S., et al., *Nuclear translocation of UDCA by the glucocorticoid receptor is required to reduce TGF-beta 1-induced apoptosis in rat hepatocytes.* Hepatology, 2005. **42**(4): p. 925-934.

168. Weitzel, C., et al., *Ursodeoxycholic acid induced activation of the glucocorticoid receptor in primary rat hepatocytes.* European Journal of Gastroenterology & Hepatology, 2005. **17**(2): p. 169-177.

169. Miura, T., et al., *Functional modulation of the glucocorticoid receptor and suppression of NF-kappa B-dependent transcription by ursodeoxycholic acid.* Journal of Biological Chemistry, 2001. **276**(50): p. 47371-47378.

170. Sola, S., et al., *Modulation of hepatocyte apoptosis: Cross-talk between bile acids and nuclear steroid receptors.* Current Medicinal Chemistry, 2006. **13**(25): p. 3039-3051.

171. Tanaka, H., et al., *Ligand-independent activation of the glucocorticoid receptor by ursodeoxycholic acid. Repression of IFN-gamma-induced MHC class II gene expression via a glucocorticoid receptor-dependent pathway.* J Immunol, 1996. **156**(4): p. 1601-1608.

172. Ray, A. and K.E. Prefontaine, *Physical association and functional antagonism between the p65 subunit of transcription factor NF-kappa B and the glucocorticoid receptor.* Proc Natl Acad Sci U S A, 1994. **91**(2): p. 752-6.

173. Mukaida, N., et al., *Novel mechanism of glucocorticoid-mediated gene repression. Nuclear factor-kappa B is target for glucocorticoid-mediated interleukin 8 gene repression.* J. Biol. Chem., 1994. **269**(18): p. 13289-13295.

174. Chiang, J., Y. L., *Regulation of bile acid synthesis: pathways, nuclear receptors, and mechanisms.* Journal of Hepatology, 2004. **40**(3): p. 539-551.

175. Fuchs, M., *Bile Acid Regulation of Hepatic Physiology: III. Regulation of bile acid synthesis: past progress and future challenges.* Am J Physiol Gastrointest Liver Physiol, 2003. **284**(4): p. G551-557.

176. Javitt, N., *Bile acid synthesis from cholesterol: regulatory and auxiliary pathways.* FASEB J., 1994. **8**(15): p. 1308-1311.

177. Chiang, J.Y.L., *Bile acids: regulation of synthesis.* J. Lipid Res., 2009. **50**(10): p. 1955-1966.

178. Bramlett, K.S., S. Yao, and T.P. Burris, *Correlation of Farnesoid X Receptor Coactivator Recruitment and Cholesterol 7[alpha]-Hydroxylase Gene Repression by Bile Acids.* Molecular Genetics and Metabolism, 2000. **71**(4): p. 609-615.

179. Benz, C., et al., *Effect of tauroursodeoxycholic acid on bile-acid-induced apoptosis and cytolysis in rat hepatocytes.* Journal of Hepatology, 1998. **28**(1): p. 99-106.

180. Benz, C., et al., *Effect of tauroursodeoxycholic acid on bile acid-induced apoptosis in primary human hepatocytes.* Eur J Clin Invest, 2000. **30**(3): p. 203-9.

181. Castro, R.E., et al., *Differential regulation of cyclin D1 and cell death by bile acids in primary rat hepatocytes.* Am J Physiol Gastrointest Liver Physiol, 2007. **293**(1): p. G327-34.

182. Shiraki, K., et al., *Different effects of bile acids, ursodeoxycholic acid and deoxycholic acid, on cell growth and cell death in human colonic adenocarcinoma cells.* Int J Mol Med, 2005. **16**(4): p. 729-33.

183. Tsagarakis, N.J., et al., *A concentration-dependent effect of ursodeoxycholate on apoptosis and caspases activities of HepG2 hepatocellular carcinoma cells.* European Journal of Pharmacology, 2010. **640**(1-3): p. 1-7.

184. Wetscher, G.J., et al., *Reflux-induced apoptosis of the esophageal mucosa is inhibited in Barrett's epithelium.* Am J Surg, 1998. **176**(6): p. 569-73.

185. Zhang, R., et al., *Bile salts inhibit growth and induce apoptosis of human esophageal cancer cell line.* World J Gastroenterol, 2005. **11**(33): p. 5109-16.

186. Zhang, R., et al., *Bile salts inhibit growth and induce apoptosis of culture human normal esophageal mucosal epithelial cells.* World J Gastroenterol, 2005. **11**(41): p. 6466-71.

187. Katada, N., et al., *Duodenoesophageal Reflux Induces Apoptosis in Rat Esophageal Epithelium.* Digestive Diseases and Sciences, 1999. **44**(2): p. 301-310.

188. Wetscher, G.J., et al., *Esophagitis in Sprague-Dawley rats is mediated by free radicals.* Dig Dis Sci, 1995. **40**(6): p. 1297-305.

189. Koga, H., et al., *Nuclear DNA fragmentation and expression of Bcl-2 in primary biliary cirrhosis.* Hepatology, 1997. **25**(5): p. 1077-84.

190. Harada, K., et al., *Enhanced apoptosis relates to bile duct loss in primary biliary cirrhosis.* Hepatology, 1997. **26**(6): p. 1399-405.

191. Graham, A.M., et al., *Bile duct cells in primary biliary cirrhosis are 'primed' for apoptosis.* Eur J Gastroenterol Hepatol, 1998. **10**(7): p. 553-7.

192. Tinmouth, J., et al., *Apoptosis of biliary epithelial cells in primary biliary cirrhosis and primary sclerosing cholangitis.* Liver, 2002. **22**(3): p. 228-34.

193. Neuman, M.G., et al., *An electron microscopic and morphometric study of ursodeoxycholic effect in primary biliary cirrhosis.* Liver, 2002. **22**(3): p. 235-44.

194. Rodrigues, C.M., et al., *A novel role for ursodeoxycholic acid in inhibiting apoptosis by modulating mitochondrial membrane perturbation.* J Clin Invest, 1998. **101**(12): p. 2790-9.

195. Rodrigues, C.M., et al., *Ursodeoxycholic acid prevents cytochrome c release in apoptosis by inhibiting mitochondrial membrane depolarization and channel formation.* Cell Death Differ, 1999. **6**(9): p. 842-54.

196. Sola, S., et al., *Ursodeoxycholic acid modulates E2F-1 and p53 expression through a caspase-independent mechanism in transforming growth factor beta1-induced apoptosis of rat hepatocytes.* J Biol Chem, 2003. **278**(49): p. 48831-8.

197. Rolo, A.P., et al., *Bile acids affect liver mitochondrial bioenergetics: possible relevance for cholestasis therapy.* Toxicol Sci, 2000. **57**(1): p. 177-85.

198. Oyama, K., et al., *Reduction of hepatocarcinogenesis by ursodeoxycholic acid in rats.* Carcinogenesis, 2002. **23**(5): p. 885-892.

199. Liu, H., et al., *Mechanism of apoptotic effects induced selectively by ursodeoxycholic acid on human hepatoma cell lines.* World J Gastroenterol, 2007. **13**(11): p. 1652-8.

200. Yui, S., R. Kanamoto, and T. Saeki, *Deoxycholic acid can induce apoptosis in the human colon cancer cell line HCT116 in the absence of Bax.* Nutr Cancer, 2008. **60**(1): p. 91-6.

201. Yui, S., et al., *Characteristics of apoptosis in HCT116 colon cancer cells induced by deoxycholic acid.* J Biochem, 2005. **138**(2): p. 151-7.

202. Krahenbuhl, S., et al., *Toxicity of bile acids on the electron transport chain of isolated rat liver mitochondria.* Hepatology, 1994. **19**(2): p. 471-9.

203. Rolo, A.P., et al., *Role of mitochondrial dysfunction in combined bile acid-induced cytotoxicity: the switch between apoptosis and necrosis.* Toxicol Sci, 2004. **79**(1): p. 196-204.

204. Rolo, A.P., C.M. Palmeira, and K.B. Wallace, *Mitochondrially mediated synergistic cell killing by bile acids.* Biochimica et Biophysica Acta (BBA) - Molecular Basis of Disease, 2003. **1637**(1): p. 127-132.

205. Pinkoski, M.J., et al., *Fas and Fas ligand in gut and liver.* Am J Physiol Gastrointest Liver Physiol, 2000. **278**(3): p. G354-366.

206. Barnhart, B., E. Alappat, and M. Peter, *The CD95 type I/type II model.* Seminars in Immunology, 2003. **15**(3): p. 185-193.

207. Gupta, S., *Molecular signaling in death receptor and mitochondrial pathways of apoptosis (Review).* Int J Oncol, 2003. **22**(1): p. 15-20.

208. Khosravi-Far, R. and M.D. Esposti, *Death receptor signals to mitochondria.* Cancer Biol Ther, 2004. **3**(11): p. 1051-7.

209. Jin, Z. and W.S. El-Deiry, *Overview of cell death signaling pathways.* Cancer Biol Ther, 2005. **4**(2): p. 139-63.

210. Faubion, W.A., et al., *Toxic bile salts induce rodent hepatocyte apoptosis via direct activation of Fas.* The Journal of Clinical Investigation, 1999. **103**(1): p. 137-145.

211. Wachs, F.P., et al., *Bile salt-induced apoptosis in human colon cancer cell lines involves the mitochondrial transmembrane potential but not the CD95 (Fas/Apo-1) receptor.* Int J Colorectal Dis, 2005. **20**(2): p. 103-13.

212. Sodeman, T., et al., *Bile salts mediate hepatocyte apoptosis by increasing cell surface trafficking of Fas.* Am J Physiol Gastrointest Liver Physiol, 2000. **278**(6): p. G992-999.

213. Naran, S., et al., *Bile Salts Differentially Sensitize Esophageal Squamous Cells to CD95 (Fas/Apo-1 Receptor) Mediated Apoptosis.* Journal of Surgical Research, 2010(1095-8673 (Electronic)).

214. Takikawa, Y., et al., *The Bile Acid-Activated Phosphatidylinositol 3-Kinase Pathway Inhibits Fas Apoptosis Upstream of Bid in Rodent Hepatocytes.* Gastroenterology, 2001. **120**(7): p. 1810-1817.

215. Reinehr, R., D. Graf, and D. Haussinger, *Bile salt-induced hepatocyte apoptosis involves epidermal growth factor receptor-dependent CD95 tyrosine phosphorylation.* Gastroenterology, 2003. **125**(3): p. 839-53.

216. Schlottmann, K., et al., *Characterization of Bile Salt-induced Apoptosis in Colon Cancer Cell Lines.* Cancer Res, 2000. **60**(15): p. 4270-4276.

217. Chipuk, J.E. and D.R. Green, *Dissecting p53-dependent apoptosis.* Cell Death Differ, 2006. **13**(6): p. 994-1002.

218. Haupt, S., et al., *Apoptosis - the p53 network.* J Cell Sci, 2003. **116**(20): p. 4077-4085.

219. Zuckerman, V., et al., *Tumour suppression by p53: the importance of apoptosis and cellular senescence.* The Journal of Pathology, 2009. **219**(1): p. 3-15.

220. Looby, E., et al., *Deoxycholate induces COX-2 expression via Erk1/2-, p38-MAPK and AP-1-dependent mechanisms in esophageal cancer cells.* Bmc Cancer, 2009. **9**(1): p. 190.

221. Qiao, D., E.D. Stratagouleas, and J.D. Martinez, *Activation and role of mitogen-activated protein kinases in deoxycholic acid-induced apoptosis.* Carcinogenesis, 2001. **22**(1): p. 35-41.

222. McMillan, L., et al., *Opposing effects of butyrate and bile acids on apoptosis of human colon adenoma cells: differential activation of PKC and MAP kinases.* Br J Cancer, 2003. **88**(5): p. 748-53.

223. Rust, C., et al., *The Bile Acid Taurochenodeoxycholate Activates a Phosphatidylinositol 3-Kinase-dependent Survival Signaling Cascade.* Journal of Biological Chemistry, 2000. **275**(26): p. 20210-20216.

224. Marzioni, M., et al., *Ca2+-dependent cytoprotective effects of ursodeoxycholic and tauroursodeoxycholic acid on the biliary epithelium in a rat model of cholestasis and loss of bile ducts.* Am J Pathol, 2006. **168**(2): p. 398-409.

225. Im, E., et al., *Ursodeoxycholic acid can suppress deoxycholic acid-induced apoptosis by stimulating Akt/PKB-dependent survival signaling.* Nutr Cancer, 2005. **51**(1): p. 110-6.

226. Schoemaker, M., et al., *Tauroursodeoxycholic acid protects rat hepatocytes from bile acid-induced apoptosis via activation of survival pathways.* Hepatology, 2004. **39**(6): p. 1563-1573.

227. Gupta, S., et al., *Deoxycholic Acid Activates the c-Jun N-terminal Kinase Pathway via FAS Receptor Activation in Primary Hepatocytes.* Journal of Biological Chemistry, 2004. **279**(7): p. 5821-5828.

228. Yang, J.I., et al., *Bile acid-induced TGR5-dependent c-Jun-N terminal kinase activation leads to enhanced caspase 8 activation in hepatocytes.* Biochemical and Biophysical Research Communications, 2007. **361**(1): p. 156-161.

229. Yui, S., R. Kanamoto, and T. Saeki, *Biphasic regulation of cell death and survival by hydrophobic bile acids in HCT116 cells.* Nutr Cancer, 2009. **61**(3): p. 374-80.

230. Giltiay, N.V., et al., *Ceramide- and ERK-dependent pathway for the activation of CCAAT/enhancer binding protein by interleukin-1{beta} in hepatocytes.* J. Lipid Res., 2005. **46**(11): p. 2497-2505.

231. Datta, S.R., et al., *Akt Phosphorylation of BAD Couples Survival Signals to the Cell-Intrinsic Death Machinery.* Cell, 1997. **91**(2): p. 231-241.

232. Díaz-Meco, M.T., et al., *The Product of par-4, a Gene Induced during Apoptosis, Interacts Selectively with the Atypical Isoforms of Protein Kinase C.* Cell, 1996. **86**(5): p. 777-786.

233. Utanohara, S., et al., *The effect of ursodeoxycholic acid on glycochenodeoxycholic acid-induced apoptosis in rat hepatocytes.* Toxicology, 2005. **214**(1-2): p. 77-86.

234. Helmberg, A., et al., *Glucocorticoid-induced apoptosis of human leukemic cells is caused by the repressive function of the glucocorticoid receptor.* EMBO J, 1995. **14**(3): p. 452-60.

235. Herr, I., et al., *Regulation of differential pro- and anti-apoptotic signaling by glucocorticoids.* Apoptosis, 2007. **12**(2): p. 271-291.

236. Karin, M., *New Twists in Gene Regulation by Glucocorticoid Receptor: Is DNA Binding Dispensable?* Cell, 1998. **93**(4): p. 487-490.

237. Garside, H., et al., *Glucocorticoid ligands specify different interactions with NF-kappaB by allosteric effects on the glucocorticoid receptor DNA binding domain.* J Biol Chem, 2004. **279**(48): p. 50050-9.

238. De Bosscher, K., et al., *Glucocorticoid-mediated repression of nuclear factor-κBdependent transcription involves direct interference with transactivation.* Proceedings of the National Academy of Sciences of the United States of America, 1997. **94**(25): p. 13504-13509.

239. Sola, S., et al., *Modulation of nuclear steroid receptors by ursodeoxycholic acid inhibits TGF-beta1-induced E2F-1/p53-mediated apoptosis of rat hepatocytes.* Biochemistry, 2004. **43**(26): p. 8429-38.

240. Stoner, G.D., et al., *Establishment and Characterization of SV40 T-Antigen Immortalized Human Esophageal Epithelial Cells.* Cancer Research, 1991. **51**(1): p. 365-371.

241. Brattain, M.G., et al., *Heterogeneity of Malignant Cells from a Human Colonic Carcinoma.* Cancer Research, 1981. **41**(5): p. 1751-1756.

242. Nakabayashi, H., et al., *Growth of Human Hepatoma Cell Lines with Differentiated Functions in Chemically Defined Medium.* Cancer Research, 1982. **42**(9): p. 3858-3863.

243. Nakabayashi, H., et al., *Phenotypical stability of a human hepatoma cell line, HuH-7, in long-term culture with chemically defined medium.* Gann, 1984. **75**(2): p. 151-8.

244. Golias, C., A. Charalabopoulos, and K. Charalabopoulos, *Cell proliferation and cell cycle control: a mini review.* International Journal of Clinical Practice, 2004. **58**: p. 1134-1141.

245. Samali, A., et al., *Cell stress and cell death.* Int J Cell Biol, 2010. **2010**: p. 245803.

246. Hotchkiss, R.S., et al., *Cell Death.* New England Journal of Medicine, 2009. **361**(16): p. 1570-1583.

247. Galluzzi, L., et al., *Guidelines for the use and interpretation of assays for monitoring cell death in higher eukaryotes.* Cell Death Differ, 2009. **16**(8): p. 1093-1107.

248. Okamoto, A., et al., *Overexpression of Human Cyclin D1 Reduces the Transforming Growth Factor β (TGF-β) Type II Receptor and Growth Inhibition by TGF-β 1 in an Immortalized Human Esophageal Epithelial Cell Line.* Proceedings of the National Academy of Sciences of the United States of America, 1994. **91**(24): p. 11576-11580.

249. Mosmann, T., *Rapid colorimetric assay for cellular growth and survival: Application to proliferation and cytotoxicity assays.* Journal of Immunological Methods, 1983. **65**(1-2): p. 55-63.

250. Bernas, T. and J. Dobrucki, *Mitochondrial and nonmitochondrial reduction of MTT: interaction of MTT with TMRE, JC-1, and NAO mitochondrial fluorescent probes.* Cytometry, 2002. **47**(4): p. 236-42.

251. Berridge, M.V. and A.S. Tan, *Characterization of the cellular reduction of 3-(4,5-dimethylthiazol-2-yl)-2,5-diphenyltetrazolium bromide (MTT): subcellular localization, substrate dependence, and involvement of mitochondrial electron transport in MTT reduction.* Arch Biochem Biophys, 1993. **303**(2): p. 474-82.

252. Pradelli, L., M. Bénéteau, and J.-E. Ricci, *Mitochondrial control of caspase-dependent and -independent cell death.* Cellular and Molecular Life Sciences, 2010. **67**(10): p. 1589-1597.

253. van Engeland, M., et al., *Annexin V-affinity assay: a review on an apoptosis detection system based on phosphatidylserine exposure.* Cytometry, 1998. **31**(1): p. 1-9.

254. Overbeeke, R., et al., *Early Features of Apoptosis Detected by Four Different Flow Cytometry Assays.* Apoptosis, 1998. **3**(2): p. 115-121.

255. Vermes, I., C. Haanen, and C. Reutelingsperger, *Flow cytometry of apoptotic cell death.* Journal of Immunological Methods, 2000. **243**(1-2): p. 167-190.

256. Grasl-Kraupp, B., et al., *In situ detection of fragmented DNA (TUNEL assay) fails to discriminate among apoptosis, necrosis, and autolytic cell death: a cautionary note.* Hepatology, 1995. **21**(5): p. 1465-8.

257. Negoescu, A., et al., *Importance of DNA fragmentation in apoptosis with regard to TUNEL specificity.* Biomed Pharmacother, 1998. **52**(6): p. 252-8.

258. Negoescu, A., et al., *In situ apoptotic cell labeling by the TUNEL method: improvement and evaluation on cell preparations.* J Histochem Cytochem, 1996. **44**(9): p. 959-68.

259. Altman, D.G. and J.M. Bland, *Measurement in Medicine: The Analysis of Method Comparison Studies.* Journal of the Royal Statistical Society. Series D (The Statistician), 1983. **32**(3): p. 307-317.

260. Bland, M. and D. Altman, *Statistical Methods For Assessing Agreement Between Two Methods of Clinical Measurement.* The Lancet, 1986. **327**(8476): p. 307-310.

261. Croagh, D., et al., *Identification of candidate murine esophageal stem cells using a combination of cell kinetic studies and cell surface markers.* Stem Cells, 2007. **25**(2): p. 313-8.

262. Seery, J. and F. Watt, *Asymmetric stem-cell divisions define the architecture of human oesophageal epithelium.* Current Biology, 2000. **10**(22): p. 1447–1450.

263. Seery, J.P., *Stem cells of the oesophageal epithelium.* J Cell Sci, 2002. **115**(Pt 9): p. 1783-9.

264. Chang, C.L., et al., *Retinoic acid-induced glandular differentiation of the oesophagus.* Gut, 2007. **56**(7): p. 906-17.

265. Coad, R.A., et al., *On the histogenesis of Barrett's oesophagus and its associated squamous islands: a three-dimensional study of their morphological relationship with native oesophageal gland ducts.* J Pathol, 2005. **206**(4): p. 388-94.

266. Leedham, S.J., et al., *Individual crypt genetic heterogeneity and the origin of metaplastic glandular epithelium in human Barrett's oesophagus.* Gut, 2008. **57**(8): p. 1041-8.

267. Souza, R.F., et al., *Gastroesophageal Reflux Might Cause Esophagitis Through a Cytokine-Mediated Mechanism Rather Than Caustic Acid Injury.* Gastroenterology, 2009. **137**(5): p. 1776-1784.

268. Choi, Y.H., et al., *Apoptosis and modulation of cell cycle control by synthetic derivatives of ursodeoxycholic acid and chenodeoxycholic acid in human prostate cancer cells.* Cancer Letters, 2003. **199**(2): p. 157-167.

269. Fimognari, C., et al., *Micronuclei induction, cell cycle delay and apoptosis as markers of cellular stress caused by ursodeoxycholic acid in human lymphocytes.* Mutation Research/Genetic Toxicology and Environmental Mutagenesis, 2001. **495**(1-2): p. 1-9.

270. Bacsó, Z., R.B. Everson, and J.F. Eliason, *The DNA of Annexin V-binding Apoptotic Cells Is Highly Fragmented.* Cancer Research, 2000. **60**(16): p. 4623-4628.

271. Godard, T., et al., *Early detection of staurosporine-induced apoptosis by comet and annexin V assays.* Histochem Cell Biol, 1999. **112**(2): p. 155-61.

272. Darzynkiewicz, Z., et al., *Cytometry in cell necrobiology: Analysis of apoptosis and accidental cell death (necrosis).* Cytometry, 1997. **27**(1): p. 1-20.

273. Rolo, A.P., C.M. Palmeira, and K.B. Wallace, *Interactions of combined bile acids on hepatocyte viability: cytoprotection or synergism.* Toxicology Letters, 2002. **126**(3): p. 197-203.

274. Gumbiner, B.M., *Cell Adhesion: The Molecular Basis of Tissue Architecture and Morphogenesis.* Cell, 1996. **84**(3): p. 345-357.

275. Hynes, R.O., *Cell adhesion: old and new questions.* Trends in Cell Biology, 1999. **9**(12): p. M33-M37.

276. Joseph-Silverstein, J. and R.L. Silverstein, *Cell adhesion molecules: an overview.* Cancer Invest, 1998. **16**(3): p. 176-82.

277. Streuli, C.H., *Integrins and cell-fate determination.* J Cell Sci, 2009. **122**(2): p. 171-177.

278. Giancotti, F.G. and E. Ruoslahti, *Integrin Signaling.* Science, 1999. **285**(5430): p. 1028-1033.

279. Cavallaro, U. and E. Dejana, *Adhesion molecule signalling: not always a sticky business.* Nat Rev Mol Cell Biol, 2011. **12**(3): p. 189-197.

280. Koistinen, P. and J. Heino, *The Selective Regulation of αVβ1 Integrin Expression Is Based on the Hierarchical Formation of αV-containing Heterodimers.* Journal of Biological Chemistry, 2002. **277**(27): p. 24835-24841.

281. Heino, J., et al., *Regulation of cell adhesion receptors by transforming growth factor-beta. Concomitant regulation of integrins that share a common beta 1 subunit.* Journal of Biological Chemistry, 1989. **264**(1): p. 380-388.

282. Sheppard, D., et al., *Transforming growth factor beta differentially regulates expression of integrin subunits in guinea pig airway epithelial cells.* Journal of Biological Chemistry, 1992. **267**(24): p. 17409-17414.

283. Hynes, R.O., *Integrins: Bidirectional, Allosteric Signaling Machines.* Cell, 2002. **110**(6): p. 673-687.

284. Ruoslahti, E. and M. Pierschbacher, *New perspectives in cell adhesion: RGD and integrins.* Science, 1987. **238**(4826): p. 491-497.

285. Barczyk, M., S. Carracedo, and D. Gullberg, *Integrins.* Cell Tissue Res, 2010. **339**(1): p. 269-80.

286. Humphries, J.D., A. Byron, and M.J. Humphries, *Integrin ligands at a glance.* Journal of Cell Science, 2006. **119**(19): p. 3901-3903.

287. Carman, C.V. and T.A. Springer, *Integrin avidity regulation: are changes in affinity and conformation underemphasized?* Current Opinion in Cell Biology, 2003. **15**(5): p. 547-556.

288. Hughes, P.E. and M. Pfaff, *Integrin affinity modulation.* Trends in Cell Biology, 1998. **8**(9): p. 359-364.

289. Askari, J.A., et al., *Linking integrin conformation to function.* Journal of Cell Science, 2009. **122**(2): p. 165-170.

290. Takagi, J., et al., *Global Conformational Rearrangements in Integrin Extracellular Domains in Outside-In and Inside-Out Signaling.* Cell, 2002. **110**(5): p. 599-611.

291. Honda, S., et al., *Integrin-linked kinase associated with integrin activation.* Blood, 2009. **113**(21): p. 5304-5313.

292. Stupack, D.G. and D.A. Cheresh, *Get a ligand, get a life: integrins, signaling and cell survival.* Journal of Cell Science, 2002. **115**(19): p. 3729-3738.

293. Wong, N.C., et al., *αv Integrins mediate adhesion and migration of breast carcinoma cell lines.* Clinical and Experimental Metastasis, 1998. **16**(1): p. 50-61.

294. Chen, Q., et al., *CNTO 95, a fully human anti αv integrin antibody, inhibits cell signaling, migration, invasion, and spontaneous metastasis of human breast cancer cells.* Clinical and Experimental Metastasis, 2008. **25**(2): p. 139-148.

295. Cooper, C.R., C.H. Chay, and K.J. Pienta, *The role of alpha(v)beta(3) in prostate cancer progression.* Neoplasia, 2002. **4**(3): p. 191-4.

296. Shahan, T.A., et al., *Regulation of Tumor Cell Chemotaxis by Type IV Collagen Is Mediated by a Ca2+-dependent Mechanism Requiring CD47 and the Integrin αVβ3.* Journal of Biological Chemistry, 2000. **275**(7): p. 4796-4802.

297. Kumar, C., *Integrin αvβ3 as a Therapeutic Target for Blocking Tumor-Induced Angiogenesis.* Current Drug Targets, 2003. **4**(2): p. 123.

298. Frisch, S.M. and E. Ruoslahti, *Integrins and anoikis.* Current Opinion in Cell Biology, 1997. **9**(5): p. 701-706.

299. Frisch, S. and H. Francis, *Disruption of epithelial cell-matrix interactions induces apoptosis.* The Journal of Cell Biology, 1994. **124**(4): p. 619-626.

300. Fung, C., et al., *Induction of Autophagy during Extracellular Matrix Detachment Promotes Cell Survival.* Mol. Biol. Cell, 2008. **19**(3): p. 797-806.

301. Liu, Z., et al., *Detachment-induced upregulation of XIAP and cIAP2 delays anoikis of intestinal epithelial cells.* Oncogene, 2006. **25**(59): p. 7680-90.

302. Kirfel, G., et al., *Cell migration: mechanisms of rear detachment and the formation of migration tracks.* European Journal of Cell Biology, 2004. **83**(11-12): p. 717-724.

303. Nakamura, T.Y., et al., *Detachment of cultured cells from the substratum induced by the neutrophil-derived oxidant NH2Cl: synergistic role of phosphotyrosine and intracellular Ca2+ concentration.* The Journal of Cell Biology, 1995. **131**(2): p. 509-524.

304. Kocí, L., et al., *Detachment-mediated resistance to TRAIL-induced apoptosis is associated with stimulation of the PI3K/Akt pathway in fetal and adenocarcinoma epithelial colon cells.* Cytokine, 2011. **55**(1): p. 34-39.

305. Rolli, M., et al., *Activated integrin αvβ3 cooperates with metalloproteinase MMP-9 in regulating migration of metastatic breast cancer cells.* Proceedings of the National Academy of Sciences, 2003. **100**(16): p. 9482-9487.

306. van Zijl, F., G. Krupitza, and W. Mikulits, *Initial steps of metastasis: Cell invasion and endothelial transmigration.* Mutat Res, 2011.

307. Odrljin, T.M., et al., *Integrin {alpha}v{beta}3-Mediated Endocytosis of Immobilized Fibrinogen by A549 Lung Alveolar Epithelial Cells.* Am. J. Respir. Cell Mol. Biol., 2001. **24**(1): p. 12-21.

308. Grant, B.D. and J.G. Donaldson, *Pathways and mechanisms of endocytic recycling.* Nature Reviews Molecular Cell Biology, 2009. **10**(9): p. 597-608.

309. Maxfield, F.R. and T.E. McGraw, *Endocytic recycling.* Nature Reviews Molecular Cell Biology, 2004. **5**(2): p. 121-132.

310. Jones, M.C., P.T. Caswell, and J.C. Norman, *Endocytic recycling pathways: emerging regulators of cell migration.* Current Opinion in Cell Biology, 2006. **18**(5): p. 549-557.

311. Caswell, P.T., et al., *Rab25 Associates with Alpha5Beta1 Integrin to Promote Invasive Migration in 3D Microenvironments.* Developmental cell, 2007. **13**(4): p. 496-510.

312. Lucie, S., et al., *Clustering and Internalization of Integrin [alpha]v[beta]3 With a Tetrameric RGD-synthetic Peptide.* Mol Ther, 2009. **17**(5): p. 837-843.

313. Caswell, P. and J. Norman, *Endocytic transport of integrins during cell migration and invasion.* Trends in Cell Biology, 2008. **18**(6): p. 257-263.

314. Dobson, H., et al., *Cell adhesion molecules in oesophageal epithelium.* Gut, 1994. **35**(10): p. 1343-1347.

315. Nair, K.S., R. Naidoo, and R. Chetty, *Expression of cell adhesion molecules in oesophageal carcinoma and its prognostic value.* Journal of Clinical Pathology, 2005. **58**(4): p. 343-351.

316. Miller, S.E. and R.B. Veale, *Environmental modulation of alpha(v), alpha(2) and beta(1) integrin subunit expression in human oesophageal squamous cell carcinomas.* Cell Biol Int, 2001. **25**(1): p. 61-9.

317. Townsend, P.A., et al., *An antisense oligonucleotide targeting the αV integrin gene inhibits adhesion and induces apoptosis in breast cancer cells.* European journal of cancer (Oxford, England : 1990), 2000. **36**(3): p. 397-409.

318. Jin, H. and J. Varner, *Integrins: roles in cancer development and as treatment targets.* Br J Cancer, 2004. **90**(3): p. 561-5.

319. Grob, D., *Proteolytic Enzymes:1. The Control of Their Activity.* The Journal of general physiology, 1946. **29**(4): p. 219-47.

320. Palanca-Wessels, M.C.A., et al., *Extended lifespan of Barrett's esophagus epithelium transduced with the human telomerase catalytic subunit: a useful in vitro model.* Carcinogenesis, 2003. **24**(7): p. 1183-1190.

321. Altorki, N., et al., *Characterization of cell lines established from human gastric-esophageal adenocarcinomas: Biologic phenotype and invasion potential.* Cancer, 1993. **72**(3): p. 649-657.

322. Murphy, J.O., et al., *Neither Antioxidants nor COX-2 Inhibition Protect Against Esophageal Inflammation in an Experimental Model of Severe Reflux.* The Journal of surgical research, 2007. **142**(1): p. 20-27.

323. Rink, J., et al., *Rab conversion as a mechanism of progression from early to late endosomes.* Cell, 2005. **122**(5): p. 735-49.

324. Stenmark, H., et al., *Inhibition of rab5 GTPase activity stimulates membrane fusion in endocytosis.* EMBO J, 1994. **13**(6): p. 1287-96.

325. Gilmore, A.P., *Anoikis.* Cell Death Differ, 2005. **12**(S2): p. 1473-1477.

326. Bretscher, M.S., *Circulating integrins: alpha 5 beta 1, alpha 6 beta 4 and Mac-1, but not alpha 3 beta 1, alpha 4 beta 1 or LFA-1.* EMBO J, 1992. **11**(2): p. 405-10.

327. Pellinen, T. and J. Ivaska, *Integrin traffic.* Journal of Cell Science, 2006. **119**(18): p. 3723-3731.

328. Roberts, M., et al., *PDGF-regulated rab4-dependent recycling of [alpha]v[beta]3 integrin from early endosomes is necessary for cell adhesion and spreading.* Current Biology, 2001. **11**(18): p. 1392-1402.

329. Panetti, T.S. and P.J. McKeown-Longo, *The alpha v beta 5 integrin receptor regulates receptor-mediated endocytosis of vitronectin.* Journal of Biological Chemistry, 1993. **268**(16): p. 11492-11495.

330. Pierini, L.M., et al., *Oriented endocytic recycling of α5β1 in motile neutrophils.* Blood, 2000. **95**(8): p. 2471-2480.

331. Roberts, M.S., et al., *Protein kinase B/Akt acts via glycogen synthase kinase 3 to regulate recycling of alpha v beta 3 and alpha 5 beta 1 integrins.* Molecular and cellular biology, 2004. **24**(4): p. 1505-15.

332. Annaba, F., et al., *Modulation of ileal bile acid transporter (ASBT) activity by depletion of plasma membrane cholesterol: association with lipid rafts.* American Journal of Physiology - Gastrointestinal and Liver Physiology, 2008. **294**(2): p. G489-G497.

333. Subtil, A., et al., *Acute cholesterol depletion inhibits clathrin-coated pit budding.* Proceedings of the National Academy of Sciences, 1999. **96**(12): p. 6775-6780.

334. Chen, H., et al., *Cholesterol Level Regulates Endosome Motility via Rab Proteins.* Biophysical Journal, 2008. **94**(4): p. 1508-1520.

335. Martinez-Rico, C., et al., *Integrins stimulate E-cadherin-mediated intercellular adhesion by regulating Src-kinase activation and actomyosin contractility.* Journal of Cell Science, 2010.

336. Symington, B.E., Y. Takada, and W.G. Carter, *Interaction of integrins alpha 3 beta 1 and alpha 2 beta 1: potential role in keratinocyte intercellular adhesion.* The Journal of Cell Biology, 1993. **120**(2): p. 523-535.

337. Carter, W.G., et al., *The role of integrins alpha 2 beta 1 and alpha 3 beta 1 in cell-cell and cell-substrate adhesion of human epidermal cells.* J Cell Biol, 1990. **110**(4): p. 1387-404.

338. Larjava, H., et al., *Novel function for beta 1 integrins in keratinocyte cell-cell interactions.* J Cell Biol, 1990. **110**(3): p. 803-15.

339. Tenchini, M.L., et al., *Evidence against a major role for integrins in calcium-dependent intercellular adhesion of epidermal keratinocytes.* Cell Adhes Commun, 1993. **1**(1): p. 55-66.

340. Noszczyk, B.H., et al., *Integrin expression in the dermis during scar formation in humans.* Experimental Dermatology, 2002. **11**(4): p. 311-318.

341. Ellison, J.A., et al., *Osteopontin and its Integrin Receptor αvβ3 Are Upregulated During Formation of the Glial Scar After Focal Stroke • Editorial Comment.* Stroke, 1998. **29**(8): p. 1698-1707.

342. Reginato, M.J., et al., *Integrins and EGFR coordinately regulate the pro-apoptotic protein Bim to prevent anoikis.* Nat Cell Biol, 2003. **5**(8): p. 733-740.

343. Farré, R., et al., *Acid and weakly acidic solutions impair mucosal integrity of distal exposed and proximal non-exposed human oesophagus.* Gut, 2010. **59**(2): p. 164-169.

344. Du, J., et al., *Integrin activation and internalization on soft ECM as a mechanism of induction of stem cell differentiation by ECM elasticity.* Proceedings of the National Academy of Sciences, 2011.

345. Mangelsdorf, D.J. and R.M. Evans, *The RXR heterodimers and orphan receptors.* Cell, 1995. **83**(6): p. 841-50.

346. Pratt, W.B., *The hsp90-based chaperone system: involvement in signal transduction from a variety of hormone and growth factor receptors.* Proc Soc Exp Biol Med, 1998. **217**(4): p. 420-34.

347. Pratt, W.B. and D.O. Toft, *Regulation of signaling protein function and trafficking by the hsp90/hsp70-based chaperone machinery.* Exp Biol Med (Maywood), 2003. **228**(2): p. 111-33.

348. Falkenstein, E., et al., *Multiple Actions of Steroid Hormones---A Focus on Rapid, Nongenomic Effects.* Pharmacol Rev, 2000. **52**(4): p. 513-556.

349. Kumar, R. and E.B. Thompson, *The structure of the nuclear hormone receptors.* Steroids, 1999. **64**(5): p. 310-9.

350. Ito, K., K.F. Chung, and I.M. Adcock, *Update on glucocorticoid action and resistance.* Journal of Allergy and Clinical Immunology, 2006. **117**(3): p. 522-543.

351. van der Laan, S. and O.C. Meijer, *Pharmacology of glucocorticoids: Beyond receptors.* European Journal of Pharmacology, 2008. **585**(2-3): p. 483-491.

352. Pujols, L., et al., *Expression of glucocorticoid receptor alpha - and beta -isoforms in human cells and tissues.* Am J Physiol Cell Physiol, 2002. **283**(4): p. C1324-1331.

353. Fruchter, O., et al., *The Human Glucocorticoid Receptor (GR) Isoform {beta} Differentially Suppresses GR{alpha}-Induced Transactivation Stimulated by Synthetic Glucocorticoids.* J Clin Endocrinol Metab, 2005. **90**(6): p. 3505-3509.

354. So, A.Y.-L., et al., *Determinants of Cell- and Gene-Specific Transcriptional Regulation by the Glucocorticoid Receptor.* PLoS Genetics, 2007. **3**(6): p. e94.

355. McCormick, J.A., et al., *5'-heterogeneity of glucocorticoid receptor messenger RNA is tissue specific: differential regulation of variant transcripts by early-life events.* Mol Endocrinol, 2000. **14**(4): p. 506-17.

356. Bastian, L.S. and S.K. Nordeen, *Concerted stimulation of transcription by glucocorticoid receptors and basal transcription factors: limited transcriptional synergism suggests mediation by coactivators/adaptors.* Mol Endocrinol, 1991. **5**(5): p. 619-27.

357. Hsu, S.C. and D.B. DeFranco, *Selectivity of cell cycle regulation of glucocorticoid receptor function.* J Biol Chem, 1995. **270**(7): p. 3359-64.

358. Hu, J.M., J.E. Bodwell, and A. Munck, *Cell cycle-dependent glucocorticoid receptor phosphorylation and activity.* Mol Endocrinol, 1994. **8**(12): p. 1709-13.

359. Gradin, K., et al., *A tyrosine kinase-dependent pathway regulates ligand-dependent activation of the dioxin receptor in human keratinocytes.* J Biol Chem, 1994. **269**(38): p. 23800-7.

360. Irusen, E., et al., *p38 Mitogen-activated protein kinase-induced glucocorticoid receptor phosphorylation reduces its activity: role in steroid-insensitive asthma.* J Allergy Clin Immunol, 2002. **109**(4): p. 649-57.

361. Sanchez, E.R., et al., *Potentiation of glucocorticoid receptor-mediated gene expression by heat and chemical shock.* Mol Endocrinol, 1994. **8**(4): p. 408-21.

362. DeFranco, D.B., et al., *Protein phosphatase types 1 and/or 2A regulate nucleocytoplasmic shuttling of glucocorticoid receptors.* Mol Endocrinol, 1991. **5**(9): p. 1215-28.

363. Somers, J.P. and D.B. DeFranco, *Effects of okadaic acid, a protein phosphatase inhibitor, on glucocorticoid receptor-mediated enhancement.* Mol Endocrinol, 1992. **6**(1): p. 26-34.

364. Tai, P.K., et al., *Association of a 59-kilodalton immunophilin with the glucocorticoid receptor complex.* Science, 1992. **256**(5061): p. 1315-8.

365. Hu, L.M., et al., *Glucocorticoid receptors in ATP-depleted cells. Dephosphorylation, loss of hormone binding, HSP90 dissociation, and ATP-dependent cycling.* J Biol Chem, 1994. **269**(9): p. 6571-7.

366. Rogatsky, I., et al., *Target-specific utilization of transcriptional regulatory surfaces by the glucocorticoid receptor.* Proceedings of the National Academy of Sciences of the United States of America, 2003. **100**(24): p. 13845-13850.

367. Wang, J.-C., et al., *Chromatin immunoprecipitation (ChIP) scanning identifies primary glucocorticoid receptor target genes.* Proceedings of the National Academy of Sciences of the United States of America, 2004. **101**(44): p. 15603-15608.

368. Bookout, A., et al. *Tissue-Specific Expression Patterns of Nuclear Receptors* 2005 15th October 2011]; Available from: www.nursa.org/10.1621/datasets.02001.

369. Lien, H.C., et al., *Differential expression of glucocorticoid receptor in carcinomas of the human digestive system.* Histopathology, 2008. **52**(3): p. 314-24.

370. Hong, S., et al., *Connection between inflammation and carcinogenesis in gastrointestinal tract: focus on TGF-beta signaling.* World J Gastroenterol, 2010. **16**(17): p. 2080-93.

371. Macarthur, M., G.L. Hold, and E.M. El-Omar, *Inflammation and Cancer II. Role of chronic inflammation and cytokine gene polymorphisms in the pathogenesis of gastrointestinal malignancy.* American Journal of Physiology - Gastrointestinal and Liver Physiology, 2004. **286**(4): p. G515-G520.

372. Quante, M. and T.C. Wang, *Inflammation and Stem Cells in Gastrointestinal Carcinogenesis.* Physiology, 2008. **23**(6): p. 350-359.

373. Coussens, L.M. and Z. Werb, *Inflammation and cancer.* Nature, 2002. **420**(6917): p. 860-867.

374. Howard, W.R., et al., *Catabolites of cholesterol synthesis pathways and forskolin as activators of the farnesoid X-activated nuclear receptor.* Toxicol Appl Pharmacol, 2000. **163**(2): p. 195-202.

375. Makishima, M., et al., *Identification of a nuclear receptor for bile acids.* Science, 1999. **284**(5418): p. 1362-5.

376. Sharma, R., et al., *Ursodeoxycholic Acid Amides As Novel Glucocorticoid Receptor Modulators.* Journal of Medicinal Chemistry, 2010. **54**(1): p. 122-130.

377. Altorki, N., et al., *Characterization of cell lines established from human gastric-esophageal adenocarcinomas. Biologic phenotype and invasion potential.* Cancer, 1993. **72**(3): p. 649-57.

378. Rockett, J.C., et al., *Five newly established oesophageal carcinoma cell lines: phenotypic and immunological characterization.* Br J Cancer, 1997. **75**(2): p. 258-63.

379. Wu, J., et al., *Repression of p65 Transcriptional Activation by the Glucocorticoid Receptor in the Absence of Receptor-Coactivator Interactions.* Molecular Endocrinology, 2004. **18**(1): p. 53-62.

380. Shiao, Y.-H., et al., *Genetic and Immunohistochemical Analyses of p53 Independently Predict Regional Metastasis of Gastric Cancers.* Cancer Epidemiology Biomarkers & Prevention, 2000. **9**(6): p. 631-633.

381. Charafe-Jauffret, E., et al., *Immunophenotypic analysis of inflammatory breast cancers: identification of an 'inflammatory signature'.* J Pathol, 2004. **202**(3): p. 265-73.

382. Karlen, Y., et al., *Statistical significance of quantitative PCR.* BMC Bioinformatics, 2007. **8**(1): p. 131.

383. Cikos, S., A. Bukovska, and J. Koppel, *Relative quantification of mRNA: comparison of methods currently used for real-time PCR data analysis.* BMC Molecular Biology, 2007. **8**(1): p. 113.

384. Moons, L.M.G., et al., *Barrett's oesophagus is characterized by a predominantly humoral inflammatory response.* The Journal of Pathology, 2005. **207**(3): p. 269-276.

385. Lai, E., T. Teodoro, and A. Volchuk, *Endoplasmic Reticulum Stress: Signaling the Unfolded Protein Response.* Physiology, 2007. **22**(3): p. 193-201.

386. Xu, C., B. Bailly-Maitre, and J.C. Reed, *Endoplasmic reticulum stress: cell life and death decisions.* The Journal of Clinical Investigation, 2005. **115**(10): p. 2656-2664.

387. Duggan, S.P., et al., *An integrative genomic approach in oesophageal cells identifies TRB3 as a bile acid responsive gene, downregulated in Barrett's oesophagus, which regulates NF-κB activation and cytokine levels.* Carcinogenesis, 2010. **31**(5): p. 936-945.

388. Tothova, V., et al., *Glucocorticoid receptor-mediated transcriptional activation of S100P gene coding for cancer-related calcium-binding protein.* Journal of Cellular Biochemistry, 2011: p. n/a-n/a.

389. Sagara, J., et al., *Scapinin, a Putative Protein Phosphatase-1 Regulatory Subunit Associated with the Nuclear Nonchromatin Structure.* Journal of Biological Chemistry, 2003. **278**(46): p. 45611-45619.

390. Ceulemans, H. and M. Bollen, *Functional diversity of protein phosphatase-1, a cellular economizer and reset button.* Physiol Rev, 2004. **84**(1): p. 1-39.

391. Cohen, P.T., *Protein phosphatase 1--targeted in many directions.* J Cell Sci, 2002. **115**(Pt 2): p. 241-56.

392. Fernandez, A., et al., *Protein phosphatase type-1, not type-2A, modulates actin microfilament integrity and myosin light chain phosphorylation in living nonmuscle cells.* J Cell Biol, 1990. **111**(1): p. 103-12.

393. Deheuninck, J. and K. Luo, *Ski and SnoN, potent negative regulators of TGF-beta signaling.* Cell Res, 2009. **19**(1): p. 47-57.

394. Bravou, V., et al., *TGF-beta repressors SnoN and Ski are implicated in human colorectal carcinogenesis.* Cell Oncol, 2009. **31**(1): p. 41-51.

395. Buess, M., et al., *Amplification of SKI is a prognostic marker in early colorectal cancer.* Neoplasia, 2004. **6**(3): p. 207-12.

396. Nakao, T., et al., *Expression of thrombospondin-1 and Ski are prognostic factors in advanced gastric cancer.* Int J Clin Oncol, 2011. **16**(2): p. 145-52.

397. Kiyono, K., et al., *c-Ski overexpression promotes tumor growth and angiogenesis through inhibition of transforming growth factor-beta signaling in diffuse-type gastric carcinoma.* Cancer Sci, 2009. **100**(10): p. 1809-16.

398. Fukuchi, M., et al., *Increased expression of c-Ski as a co-repressor in transforming growth factor-beta signaling correlates with progression of esophageal squamous cell carcinoma.* Int J Cancer, 2004. **108**(6): p. 818-24.

399. Shinagawa, T., et al., *Increased susceptibility to tumorigenesis of ski-deficient heterozygous mice.* Oncogene, 2001. **20**(56): p. 8100-8.

400. Le Scolan, E., et al., *Transforming growth factor-beta suppresses the ability of Ski to inhibit tumor metastasis by inducing its degradation.* Cancer Res, 2008. **68**(9): p. 3277-85.

401. Wang, P., et al., *Dual role of Ski in pancreatic cancer cells: tumor-promoting versus metastasis-suppressive function.* Carcinogenesis, 2009. **30**(9): p. 1497-506.

402. Villanacci, V., et al., *Ski/SnoN expression in the sequence metaplasia-dysplasia-adenocarcinoma of Barrett's esophagus.* Hum Pathol, 2008. **39**(3): p. 403-9.

403. Foekens, J.A., et al., *The Urokinase System of Plasminogen Activation and Prognosis in 2780 Breast Cancer Patients.* Cancer Research, 2000. **60**(3): p. 636-643.

404. Ruf, W. and B.M. Mueller, *Thrombin generation and the pathogenesis of cancer.* Semin Thromb Hemost, 2006. **32 Suppl 1**: p. 61-8.

405. Stefansson, S. and D.A. Lawrence, *The serpin PAI-1 inhibits cell migration by blocking integrin [alpha]v[beta]3 binding to vitronectin.* Nature, 1996. **383**(6599): p. 441-443.

406. Liang, O.D., et al., *Ligand binding regions in the receptor for urokinase-type plasminogen activator.* J Biol Chem, 2001. **276**(31): p. 28946-53.

407. Okumura, Y., et al., *Kinetic analysis of the interaction between vitronectin and the urokinase receptor.* J Biol Chem, 2002. **277**(11): p. 9395-404.

408. Rodenburg, K.W., et al., *Binding of urokinase-type plasminogen activator-plasminogen activator inhibitor-1 complex to the endocytosis receptors alpha2-macroglobulin receptor/low-density lipoprotein receptor-related protein and very-low-density lipoprotein receptor involves basic residues in the inhibitor.* Biochem J, 1998. **329 (Pt 1)**: p. 55-63.

409. Sidenius, N., et al., *Urokinase regulates vitronectin binding by controlling urokinase receptor oligomerization.* J Biol Chem, 2002. **277**(31): p. 27982-90.

410. Deng, G., et al., *Is plasminogen activator inhibitor-1 the molecular switch that governs urokinase receptor-mediated cell adhesion and release?* The Journal of Cell Biology, 1996. **134**(6): p. 1563-1571.

411. Czekay, R.P. and D.J. Loskutoff, *Plasminogen activator inhibitors regulate cell adhesion through a uPAR-dependent mechanism.* J Cell Physiol, 2009. **220**(3): p. 655-63.

412. Czekay, R.-P., et al., *Plasminogen activator inhibitor-1 detaches cells from extracellular matrices by inactivating integrins.* The Journal of Cell Biology, 2003. **160**(5): p. 781-791.

413. Anderson, C.W. and S.P. Lees-Miller, *The nuclear serine/threonine protein kinase DNA-PK.* Crit Rev Eukaryot Gene Expr, 1992. **2**(4): p. 283-314.

414. Shieh, S.Y., et al., *DNA damage-induced phosphorylation of p53 alleviates inhibition by MDM2.* Cell, 1997. **91**(3): p. 325-34.

415. Hosoi, Y., et al., *Up-regulation of DNA-dependent protein kinase activity and Sp1 in colorectal cancer.* Int J Oncol, 2004. **25**(2): p. 461-8.

416. Zhao, H.J., et al., *DNA-dependent protein kinase activity correlates with Ku70 expression and radiation sensitivity in esophageal cancer cell lines.* Clin Cancer Res, 2000. **6**(3): p. 1073-8.

417. Tonotsuka, N., et al., *Heterogeneous expression of DNA-dependent protein kinase in esophageal cancer and normal epithelium.* Int J Mol Med, 2006. **18**(3): p. 441-7.

418. Wilkinson, L., et al., *CRIM1 regulates the rate of processing and delivery of bone morphogenetic proteins to the cell surface.* J Biol Chem, 2003. **278**(36): p. 34181-8.

419. Kolle, G., et al., *CRIM1, a novel gene encoding a cysteine-rich repeat protein, is developmentally regulated and implicated in vertebrate CNS development and organogenesis.* Mech Dev, 2000. **90**(2): p. 181-93.

420. Glienke, J., et al., *CRIM1 is involved in endothelial cell capillary formation in vitro and is expressed in blood vessels in vivo.* Mech Dev, 2002. **119**(2): p. 165-75.

421. Sperling, S., et al., *Identification and functional analysis of CITED2 mutations in patients with congenital heart defects.* Hum Mutat, 2005. **26**(6): p. 575-82.

422. Wu, Z.Z., H.P. Lu, and C.C. Chao, *Identification and functional analysis of genes which confer resistance to cisplatin in tumor cells.* Biochem Pharmacol, 2010. **80**(2): p. 262-76.

423. Wu, Z.Z., N.K. Sun, and C.C. Chao, *Knockdown of CITED2 using short-hairpin RNA sensitizes cancer cells to cisplatin through stabilization of p53 and enhancement of p53-dependent apoptosis.* J Cell Physiol, 2010.

424. Yoshida, T., et al., *CITED2 is activated in ulcerative colitis and induces p53-dependent apoptosis in response to butyric acid.* J Gastroenterol, 2011. **46**(3): p. 339-49.

425. Lou, X., et al., *Negative feedback regulation of NF-kappaB action by CITED2 in the nucleus.* J Immunol, 2011. **186**(1): p. 539-48.

426. Bai, L. and J.L. Merchant, *A role for CITED2, a CBP/p300 interacting protein, in colon cancer cell invasion.* FEBS Lett, 2007. **581**(30): p. 5904-10.

427. Chou, Y.T., et al., *Cited2 modulates TGF-beta-mediated upregulation of MMP9.* Oncogene, 2006. **25**(40): p. 5547-60.

428. Bhattacharya, S., et al., *Functional role of p35srj, a novel p300/CBP binding protein, during transactivation by HIF-1.* Genes & Development, 1999. **13**(1): p. 64-75.

429. Pandey, A., et al., *Identification of a Novel Immunoreceptor Tyrosine-based Activation Motif-containing Molecule, STAM2, by Mass Spectrometry and Its Involvement in Growth Factor and Cytokine Receptor Signaling Pathways.* Journal of Biological Chemistry, 2000. **275**(49): p. 38633-38639.

430. Stuible, M., et al., *PTP1B Targets the Endosomal Sorting Machinery.* Journal of Biological Chemistry, 2010. **285**(31): p. 23899-23907.

431. Endo, K., et al., *STAM2, a new member of the STAM family, binding to the Janus kinases.* FEBS Letters, 2000. **477**(1-2): p. 55-61.

432. Mizuno, E., et al., *Association with Hrs Is Required for the Early Endosomal Localization, Stability, and Function of STAM.* Journal of Biochemistry, 2004. **135**(3): p. 385-396.

433. Bache, K.G., et al., *STAM and Hrs Are Subunits of a Multivalent Ubiquitin-binding Complex on Early Endosomes.* Journal of Biological Chemistry, 2003. **278**(14): p. 12513-12521.

434. Lu, Q., et al., *TSG101 interaction with HRS mediates endosomal trafficking and receptor down-regulation.* Proceedings of the National Academy of Sciences, 2003. **100**(13): p. 7626-7631.

435. Rismanchi, N., R. Puertollano, and C. Blackstone, *STAM adaptor proteins interact with COPII complexes and function in ER-to-Golgi trafficking.* Traffic, 2009. **10**(2): p. 201-17.

436. Byrne, A.-M., et al., *Bile acids modulate the Golgi membrane fission process via a protein kinase Cη and protein kinase D-dependent pathway in colonic epithelial cells.* Carcinogenesis, 2010. **31**(4): p. 737-744.

437. McNiven, M.A., et al., *Regulated Interactions between Dynamin and the Actin-Binding Protein Cortactin Modulate Cell Shape.* The Journal of Cell Biology, 2000. **151**(1): p. 187-198.

438. Wu, H. and J.T. Parsons, *Cortactin, an 80/85-kilodalton pp60src substrate, is a filamentous actin-binding protein enriched in the cell cortex.* The Journal of Cell Biology, 1993. **120**(6): p. 1417-1426.

439. Cao, H., et al., *Cortactin Is a Component of Clathrin-Coated Pits and Participates in Receptor-Mediated Endocytosis.* Mol. Cell. Biol., 2003. **23**(6): p. 2162-2170.

440. Weed, S.A., et al., *Cortactin Localization to Sites of Actin Assembly in Lamellipodia Requires Interactions with F-Actin and the Arp2/3 Complex.* The Journal of Cell Biology, 2000. **151**(1): p. 29-40.

441. Uruno, T., et al., *Activation of Arp2/3 complex-mediated actin polymerization by cortactin.* Nat Cell Biol, 2001. **3**(3): p. 259-266.

442. Schuuring, E., et al., *Identification and cloning of two overexpressed genes, U21B31/PRAD1 and EMS1, within the amplified chromosome 11q13 region in human carcinomas.* Oncogene, 1992. **7**(2): p. 355-61.

443. van Damme, H., et al., *The redistribution of cortactin into cell-matrix contact sites in human carcinoma cells with 11q13 amplification is associated with both overexpression and post-translational modification.* J Biol Chem, 1997. **272**(11): p. 7374-80.

444. Kelley, L.C., et al., *Cortactin phosphorylated by ERK1/2 localizes to sites of dynamic actin regulation and is required for carcinoma lamellipodia persistence.* PLoS One, 2010. **5**(11): p. e13847.

445. Mader, C.C., et al., *An EGFR-Src-Arg-cortactin pathway mediates functional maturation of invadopodia and breast cancer cell invasion.* Cancer Res, 2011. **71**(5): p. 1730-41.

446. Hsu, K.F., et al., *Cortactin, fascin, and survivin expression associated with clinicopathological parameters in esophageal squamous cell carcinoma.* Dis Esophagus, 2009. **22**(5): p. 402-8.

447. Hsu, N.Y., et al., *Cortactin overexpression in the esophageal squamous cell carcinoma and its involvement in the carcinogenesis.* Dis Esophagus, 2008. **21**(5): p. 402-8.

448. Lee, Y.Y., et al., *Expression of survivin and cortactin in colorectal adenocarcinoma: association with clinicopathological parameters.* Dis Markers, 2009. **26**(1): p. 9-18.

449. Wang, X., et al., *VEGF and cortactin expression are independent predictors of tumor recurrence following curative resection of gastric cancer.* J Surg Oncol, 2010. **102**(4): p. 325-30.

450. Deveraux, Q.L., et al., *IAPs block apoptotic events induced by caspase-8 and cytochrome c by direct inhibition of distinct caspases.* EMBO J, 1998. **17**(8): p. 2215-23.

451. Li, X., Y. Yang, and J.D. Ashwell, *TNF-RII and c-IAP1 mediate ubiquitination and degradation of TRAF2.* Nature, 2002. **416**(6878): p. 345-7.

452. Roy, N., et al., *The c-IAP-1 and c-IAP-2 proteins are direct inhibitors of specific caspases.* EMBO J, 1997. **16**(23): p. 6914-25.

453. Kim, Y.S., et al., *Dexamethasone inhibits TRAIL- and anti-cancer drugs-induced cell death in A549 cells through inducing NF-kappaB-independent cIAP2 expression.* Cancer Res Treat, 2004. **36**(5): p. 330-7.

454. Messmer, U.K., et al., *Dexamethasone inhibits TNF-alpha-induced apoptosis and IAP protein downregulation in MCF-7 cells.* Br J Pharmacol, 2001. **133**(4): p. 467-76.

455. Runnebaum, I.B. and A. Bruning, *Glucocorticoids inhibit cell death in ovarian cancer and up-regulate caspase inhibitor cIAP2.* Clin Cancer Res, 2005. **11**(17): p. 6325-32.

456. Katoh, M., *Notch signaling in gastrointestinal tract (review).* Int J Oncol, 2007. **30**(1): p. 247-51.

457. Sun, Y., et al., *Differential Notch1 and Notch2 expression and frequent activation of Notch signaling in gastric cancers.* Arch Pathol Lab Med, 2011. **135**(4): p. 451-8.

458. Chu, D., et al., *Notch1 and Notch2 have opposite prognostic effects on patients with colorectal cancer.* Ann Oncol, 2011.

459. Fitzgerald, R.C., et al., *Diversity in the oesophageal phenotypic response to gastro-oesophageal reflux: immunological determinants.* Gut, 2002. **50**(4): p. 451-9.

460. Chen, B.P., et al., *ATF3 and ATF3 delta Zip. Transcriptional repression versus activation by alternatively spliced isoforms.* Journal of Biological Chemistry, 1994. **269**(22): p. 15819-15826.

461. Gilchrist, M., et al., *Systems biology approaches identify ATF3 as a negative regulator of Toll-like receptor 4.* Nature, 2006. **441**(7090): p. 173-178.

462. Duggan, S.P., et al., *Low pH induces co-ordinate regulation of gene expression in oesophageal cells.* Carcinogenesis, 2006. **27**(2): p. 319-327.

463. Kurth, I., et al., *Monocyte Selectivity and Tissue Localization Suggests a Role for Breast and Kidney–Expressed Chemokine (Brak) in Macrophage Development.* The Journal of Experimental Medicine, 2001. **194**(6): p. 855-862.

464. Hromas, R., et al., *Cloning of BRAK, a Novel Divergent CXC Chemokine Preferentially Expressed in Normal versus Malignant Cells.* Biochemical and Biophysical Research Communications, 1999. **255**(3): p. 703-706.

465. Frederick, M.J., et al., *In Vivo Expression of the Novel CXC Chemokine BRAK in Normal and Cancerous Human Tissue.* The American Journal of Pathology, 2000. **156**(6): p. 1937-1950.

466. Shellenberger, T.D., et al., *BRAK/CXCL14 Is a Potent Inhibitor of Angiogenesis and a Chemotactic Factor for Immature Dendritic Cells.* Cancer Research, 2004. **64**(22): p. 8262-8270.

467. Ron, D. and J.F. Habener, *CHOP, a novel developmentally regulated nuclear protein that dimerizes with transcription factors C/EBP and LAP and functions as a dominant-negative inhibitor of gene transcription.* Genes & Development, 1992. **6**(3): p. 439-453.

468. Marciniak, S.J., et al., *CHOP induces death by promoting protein synthesis and oxidation in the stressed endoplasmic reticulum.* Genes & Development, 2004. **18**(24): p. 3066-3077.

469. Chen, B., C. Wolfgang, and T. Hai, *Analysis of ATF3, a transcription factor induced by physiological stresses and modulated by gadd153/Chop10.* Mol. Cell. Biol., 1996. **16**(3): p. 1157-1168.

470. Wolfgang, C., et al., *gadd153/Chop10, a potential target gene of the transcriptional repressor ATF3.* Mol. Cell. Biol., 1997. **17**(11): p. 6700-6707.

471. Kempf, T., et al., *GDF-15 is an inhibitor of leukocyte integrin activation required for survival after myocardial infarction in mice.* Nat Med, 2011. **17**(5): p. 581-588.

472. Breit, S.N., et al., *The TGF-β superfamily cytokine, MIC-1/GDF15: A pleotrophic cytokine with roles in inflammation, cancer and metabolism.* Growth Factors. **0**(0): p. null.

473. Wu, M., et al., *SINK Is a p65-interacting Negative Regulator of NF-κB-dependent Transcription.* Journal of Biological Chemistry, 2003. **278**(29): p. 27072-27079.

474. Kiss-Toth, E., et al., *Human Tribbles, a Protein Family Controlling Mitogen-activated Protein Kinase Cascades.* Journal of Biological Chemistry, 2004. **279**(41): p. 42703-42708.

475. Du, K., et al., *TRB3: A tribbles Homolog That Inhibits Akt/PKB Activation by Insulin in Liver.* Science, 2003. **300**(5625): p. 1574-1577.

476. Koh, I.-u., et al., *AdipoR2 is transcriptionally regulated by ER stress-inducible ATF3 in HepG2 human hepatocyte cells.* FEBS Journal, 2010. **277**(10): p. 2304-2317.

477. Peterson, F.C., et al., *Structural Determinants Involved in the Regulation of CXCL14/BRAK Expression by the 26 S Proteasome.* Journal of Molecular Biology, 2006. **363**(4): p. 813-822.

478. Kadowaki, H., H. Nishitoh, and H. Ichijo, *Survival and apoptosis signals in ER stress: the role of protein kinases.* Journal of Chemical Neuroanatomy, 2004. **28**(1-2): p. 93-100.

479. McCullough, K.D., et al., *Gadd153 sensitizes cells to endoplasmic reticulum stress by down-regulating Bcl2 and perturbing the cellular redox state.* Mol Cell Biol, 2001. **21**(4): p. 1249-59.

480. Ohoka, N., et al., *Anaphase-promoting complex/cyclosome-cdh1 mediates the ubiquitination and degradation of TRB3.* Biochemical and Biophysical Research Communications, 2010. **392**(3): p. 289-294.

481. Ohoka, N., et al., *TRB3, a novel ER stress-inducible gene, is induced via ATF4-CHOP pathway and is involved in cell death.* EMBO J, 2005. **24**(6): p. 1243-1255.

482. Hsiao, E.C., et al., *Characterization of Growth-Differentiation Factor 15, a Transforming Growth Factor beta Superfamily Member Induced following Liver Injury.* Mol. Cell. Biol., 2000. **20**(10): p. 3742-3751.

483. Park, S.-H., et al., *Endoplasmic Reticulum Stress-activated C/EBP Homologous Protein Enhances Nuclear Factor-κB Signals via Repression of Peroxisome Proliferator-activated Receptor γ.* Journal of Biological Chemistry, 2010. **285**(46): p. 35330-35339.

484. Adzic, M., et al., *Acute or chronic stress induce cell compartment-specific phosphorylation of glucocorticoid receptor and alter its transcriptional activity in Wistar rat brain.* Journal of Endocrinology, 2009. **202**(1): p. 87-97.

485. Ji, J.Y., H. Jing, and S.L. Diamond, *Shear stress causes nuclear localization of endothelial glucocorticoid receptor and expression from the GRE promoter.* Circ Res, 2003. **92**(3): p. 279-85.

486. Sanchez, E.R., *Heat shock induces translocation to the nucleus of the unliganded glucocorticoid receptor.* J Biol Chem, 1992. **267**(1): p. 17-20.

487. Adcock, I.M., K. Ito, and P.J. Barnes, *Glucocorticoids: Effects on Gene Transcription.* Proc Am Thorac Soc, 2004. **1**(3): p. 247-254.

488. Caswell, P.T. and J.C. Norman, *Integrin Trafficking and the Control of Cell Migration.* Traffic, 2006. **7**(1): p. 14-21.

489. Desai, T.K. and N. Samala, *The Incidence of Esophageal Adenocarcinoma Among Patients With Nondysplastic Barrett's Esophagus Has Been Overestimated.* Clinical

gastroenterology and hepatology : the official clinical practice journal of the American Gastroenterological Association, 2011. **9**(4): p. 363-364.

490. Schouten, L.J., et al., *Total Cancer Incidence and Overall Mortality Are Not Increased Among Patients With Barrett's Esophagus.* Clinical gastroenterology and hepatology : the official clinical practice journal of the American Gastroenterological Association, 2011. **9**(9): p. 754-761.

491. Wani, S., *Population-Based Estimates of Cancer and Mortality in Barrett's Esophagus: Implications for the Future.* Clinical gastroenterology and hepatology : the official clinical practice journal of the American Gastroenterological Association, 2011. **9**(9): p. 723-724.

492. DeVault, K.R. and D.O. Castell, *Updated Guidelines for the Diagnosis and Treatment of Gastroesophageal Reflux Disease.* Am J Gastroenterol, 2005. **100**(1): p. 190-200.

493. Stamp, D.H., *Bile acids aided by acid suppression therapy may be associated with the development of esophageal cancers in westernized societies.* Medical Hypotheses, 2006. **66**(1): p. 154-157.

494. Reid, B.J., et al., *Barrett's oesophagus and oesophageal adenocarcinoma: time for a new synthesis.* Nat Rev Cancer, 2010. **10**(2): p. 87-101.

495. Akare, S., et al., *Ursodeoxycholic acid modulates histone acetylation and induces differentiation and senescence.* Int J Cancer, 2006. **119**(12): p. 2958-69.

496. Lim, S.C., et al., *Ursodeoxycholic acid switches oxaliplatin-induced necrosis to apoptosis by inhibiting reactive oxygen species production and activating p53-caspase 8 pathway in HepG2 hepatocellular carcinoma.* Int J Cancer, 2010. **126**(7): p. 1582-95.

497. Ikegami, T., et al., *Enhancement of DNA topoisomerase I inhibitor-induced apoptosis by ursodeoxycholic acid.* Molecular Cancer Therapeutics, 2006. **5**(1): p. 68-79.

498. Castelli, M., J.J. Reiners, and D. Kessel, *A mechanism for the proapoptotic activity of ursodeoxycholic acid: effects on Bcl-2 conformation.* Cell Death Differ, 2004. **11**(8): p. 906-14.

499. Gong, Y., et al., *Ursodeoxycholic acid for primary biliary cirrhosis.* Cochrane Database Syst Rev, 2008(3): p. CD000551.

500. Lindor, K.D., et al., *High-dose ursodeoxycholic acid for the treatment of primary sclerosing cholangitis.* Hepatology, 2009. **50**(3): p. 808-14.

501. Eaton, J.E., et al., *High-Dose Ursodeoxycholic Acid Is Associated With the Development of Colorectal Neoplasia in Patients With Ulcerative Colitis and Primary Sclerosing Cholangitis.* Am J Gastroenterol, 2011. **106**(9): p. 1638-1645.

502. Corpechot, C., et al., *The effect of ursodeoxycholic acid therapy on the natural course of primary biliary cirrhosis.* Gastroenterology, 2005. **128**(2): p. 297-303.

503. Parés, A., L. Caballería, and J. Rodés, *Excellent Long-Term Survival in Patients With Primary Biliary Cirrhosis and Biochemical Response to Ursodeoxycholic Acid.* Gastroenterology, 2006. **130**(3): p. 715-720.